ANGLIA RUSKIN UNIVERSITY

FACULTY OF SCIENCE AND ENGINEERING

ARTIFICIAL SWEETENERS NEGATIVELY IMPACT GUT EPITHELIUM AND MICROFLORA

APARNA SHIL

A thesis in partial fulfilment of the requirements of Anglia Ruskin University for the degree of DOCTOR OF PHILOSOPHY

Submitted: January 2020

Acknowledgements

I would like to pay my respect to almighty God for giving me the spirit to reach this point. I want to express love and respect to my Mother who was proud when I started pursuing a PhD. Because of her Dementia, she cannot recognise me anymore, however, her face is a source of great encouragement and motivation.

This piece of work should be an inspiration for women who continue their journey facing enormous seen and unseen obstacles!

I would like to show my heartfelt gratitude to my supervisor Dr. Havovi Chichger for her guidance, support and encouragement throughout the study period. I also thank my other supervisors Dr. Linda King and Dr. Benjamin Evans for their suggestions and comments.

In addition, thanks go to Plamen for being a force of positivity in the tissue culture lab. I thank Niaz for some technical assistance.

Special thanks to Himel for always being beside me with motivations and sincerity. Janay for being an amazing friend and for influencing with her great positivity and dynamism.

Finally, I would like to thank my husband for being patient and having faith in me. Also, my brothers, my sister, and my nieces for their encouragement, patience and support.

ANGLIA RUSKIN UNIVERSITY

ABSTRACT

FACULTY OF SCIENCE AND ENGINEERING

DOCTOR OF PHILOSOPHY

ARTIFICIAL SWEETENERS NEGATIVELY IMPACT GUT EPITHELIUM AND MICROFLORA

APARNA SHIL

January 2020

Artificial sweeteners (AS) are synthetic sugar substitutes which are commonly consumed in the diet for their low-calorie profile. Recent studies have indicated considerable health risks; consumption of AS linked to metabolic derangements and gut microflora perturbations. Despite these studies, there is still limited data on how AS affects intestinal epithelium or impacts the commensal microbiota to cause pathogenicity. Furthermore, it is not well-understood whether the orphan G-protein coupled receptor (T1R2/3), which binds AS, is responsible for these health risks. The current *in vitro* study sought to investigate the role of commonly consumed AS on: intestinal epithelial cell function, gut bacterial metabolism and pathogenicity, and gut epithelium-microbiota interactions, using models of the intestinal epithelium (Caco-2) and microflora (*Escherichia coli* NCTC10418 and *Enterococcus faecalis* ATCC19433).

To address these aims, Caco-2 and model gut bacteria (MGB) were exposed to different concentrations of the AS; saccharin, sucralose, aspartame and neotame; and various *in vitro* studies were performed. Saccharin, aspartame and neotame decreased cell viability at physiological concentrations, whilst all increased permeability across the intestinal epithelial monolayer at either physiological or sub-physiological concentrations. Interestingly, these damaging effects were mediated through a T1R2/3-independent pathway. In the MGB studied, AS exposure had no impact on metabolic parameters, but increased pathogenicity of *E. coli* as measured by biofilm formation. Furthermore, AS differentially increased adhesion and invasion of MGB into Caco-2 cells, which is indicative of a pathogenic response. Interestingly, inhibition of sweet sensing attenuated these pathogenic effects.

These findings suggest that AS negatively impact gut physiology by directly damaging the intestinal epithelium and by increasing the pathogenicity of MGB. These outputs are linked with inflammation and potential development of metabolic diseases such as diabetes. Further investigations are, however, needed to utilise these findings to prevent AS-induced intestinal damage. Since AS consumption is so high in the population, understanding how this food additive affects gut health and how these damaging effects can be ameliorated is vital.

Keywords: Artificial sweetener; microbiota; dysbiosis; epithelial cells, metabolic disease.

Articles published during PhD studies

Published articles

Harrington, E.O., Braza, J., Shil, A., and Chichger, H. (2020). Extracellular vesicles released from p18 overexpressing pulmonary endothelial cells are barrier protective – Potential implications for acute respiratory distress syndrome. *Pulmonary Circulation* Accepted – in publication.

Shil, A., Olusanya, O., Ghufoor, Z., Forson, B., Marks, J., and Chichger, H. (2020). Artificial sweeteners disrupt tight junctions and barrier function in the intestinal epithelium through activation of the sweet taste receptor, T1R3. *Nutrients.* Accepted – under revision.

Shil, A., Roberts, J., and Chichger, H. (2020). Opposing effect of two different green tea extracts on oxidative stress, mitochondrial function, and cell viability in HepG2 cells. *PLOS ONE* – under revision.

Rahman, M. M., Himel, M. K., Mubassara, S., Islam, M. F., and Shil, **A.** (2019). *In vitro* antioxidant studies uncover potential in leaf and bark extracts of *Artocarpus chaplasha* Roxb. *Int. J. Sustain. Agril. Tech*. 15(5): pp. 01-08. http://gscience.gurpukur.com/journal/page-01-08-in-vitro-antioxidant-studies-uncover-potential-in-leaf-and-bark-extracts-of-artocarpus-chaplasha-roxb/

Harrington, E.O., Vang, A., Braza, J., Shil, A. and Chichger, H. (2017). Activation of the sweet taste receptor, T1R3, by the artificial sweetener sucralose regulates the pulmonary endothelium. *American Journal of Physiology-Lung Cellular and Molecular Physiology*, [e-journal] 314 (1), pp.L165-L176. ajplung.00490.2016.

Shil, A. and Chichger, H. The effect of artificial sweeteners on metabolic and pathogenic characteristics of two model gut bacteria, *E. coli* NCTC10418 and *E. faecalis* ATCC19433. manuscript in preparation

Published abstracts

Shil, A, King, L., Evans, B., and Chichger, H. (2019). Artificial sweeteners increase the pathogenic effect of model gut bacteria on the intestinal epithelium. *Proc Physiol Soc*. C054.

Shil, A., Forson, B and Chichger, H., (2018). Differential effect of artificial sweeteners on intestinal epithelial cells. *Diabetic Medicine.* **35**, PC39

Shil, A. and Chichger, H., (2017). The differential effect of artificial sweeteners on the intestinal epithelium. *Proc Physiol Soc* **39,** PC54. http://www.physoc.org/proceedings/abstract/Proc%20Physiol%20Soc%2039PC54

Table of Contents

List of figures

Chapter 1 General Introduction

Chapter 2 Effect of artificial sweeteners on intestinal epithelial cells

Chapter 4 Effect of artificial sweeteners on gut microflora and epithelial cell co-culture model

Chapter 8 Appendices

List of tables

Abbreviations

µg Microgram
µM Micromolar
a.u. Absorbance unit
Ace-K Acesulfame potassium
ADI Accepted daily intake
ANOVA Analysis of variance
AS Artificial Sweeteners
AV Annexin V
BC Before Christ
BHI Brain Heart Infusion
BW Body weight
Caco-2 Human colon adenocarcinoma cells
CCK-8 Cell counting kit 8
Cm Centimetre
CO_2 Carbon dioxide
CV Crystal violet
CytC Cytochrome C
DAPI 4′,6-diamidino-2-phenylindole
dH_2O Distilled water
DiOC6 3,3'-Dihexyloxacarbocyanine Iodide
DMSO Dimethyl sulfoxide
DNA Deoxyribonucleic acid
e.g. For example
EC50 Half maximal effective concentration
EDTA Ethylenediaminetetraacetate
ELISA Enzyme linked immunosorbent assay
ELISA Enzyme-linked immunosorbent assay
EMEM Eagle’s Minimal Essential medium
FBS Foetal Bovine Serum
FD FITC-Dextran
g Gram
GI Gastrointestinal
GLP Glucagon-like peptide
GLP-1 Glucagon-like peptide-1
GLP-2 Glucagon-like peptide-2
GLUT 2 Glucose transporter 2

GLUT Facilitative glucose transporter

GM Gut microflora

GPCR G protein-coupled receptors

h Hour

H_2O_2 Hydrogen peroxide

HDL High-density lipopolysaccharide

HPA Hypothalamic-pituitary-adrenal

i.e., That is

IBD Irritable bowel disease

IBF Intestinal barrier function

IEC Intestinal epithelial cell

JAM Junctional adhesion molecules

Kcal Kilocalorie

kg Kilogram

LPS Lipopolysaccharides

MD Metabolic disease

mg Milligram

MGB Model gut bacteria

MJ Megajoule

ml Millilitre

Mm Hg Millimetre of mercury (unit of pressure)

mM Millimolar

MW Molecular weight

NA Nutrient agar

NB Nutrient broth

nm Nanometre

NO Nitric oxide

NOD Nucleotide binding oligomerization domain

^{o}C Degree centigrade (unit of temperature)

PBS Phosphate buffered saline

PI Propidium iodide

PKC Protein kinase C

PLCβ2 Phospholipase C β2

PPR Pattern-recognition receptors

PS Phosphatidyl Serine

PYY Peptide tyrosine tyrosine

RNA Ribonucleic acid

ROS Reactive oxygen species

rpm Revolutions per minute

RT Room temperature

S.E.M. Standard error of mean

SCFA Short-chain fatty acids

SDS Sodium dodecyl sulfate

SGLT Sodium-dependent glucose co-transporter

siRNA Silencing RNA

STR Sweet taste receptor

T1D Type 1 diabetes

T1R Family of taste-specific class C type 1 G-protein-coupled receptor

T2D Type 2 diabetes

TEER Transepithelial electrical resistance

TJ Tight Junctions

TLR Toll-like receptor

TNF- α tumour necrosis factor α

TX-100 Triton X-100

UK The United Kingdom

US The United States

ZnSO4 Zinc sulphate

ZO Zonula occludin

Declaration

The reported work in this thesis was performed under the supervision of Dr. Havovi Chichger at Tissue culture and Microbiology laboratory of Anglia Ruskin University, Cambridge campus. All the presented results, unless otherwise mentioned, are the sole work of the author, as is the composition of this thesis.

Dated: 31 January 2020 Signed Aparna Shil

1 General introduction

1.1 Metabolic Diseases

Metabolic diseases (MD) are physiological disorders that perturb normal metabolic processes on a cellular level and are associated with increased risk for the development of diabetes and obesity (Lai et al., 2014). Hanefeld and Leonhardt described metabolic syndrome in 1981 suggesting that genetic and environmental factors such as diet and physical activity lead to diseases like type 2 diabetes mellitus (T2D), hyperinsulinemia, obesity, hypertension, hyperlipidemia, gout and thrombophilia which are included in the umbrella term 'metabolic syndrome' (reviewed by Sarafidis and Nilsson, 2006). More recently, metabolic syndrome was defined as the combination of diabetes, hypertension and obesity (NHS, UK, 2019). The increasing incidence of MD and its strain on the healthcare service worldwide demand investigations in every aspect including the predisposing factors (fig.1.1.1).

The actual understanding of metabolic syndrome was made in the early 1970s (reviewed by Sarafidis and Nilsson, 2006) however diabetes, one of the biggest contributors to metabolic syndrome, has a history dating back to ~1550 BC (Diabetes UK, 2019). In the 5th century, two types of diabetes were identified; one being associated with 'wealthy, heavy people' which we now believe to be T2D (Frank, 1957). However, type 1 and type 2 diabetes were only formally differentiated by research in 1936, which discovered that T2D was a result of insulin resistance rather than a deficiency (Himsworth, 1936). Initial investigations blamed pancreatic dysfunction (Halter and Porte, 1978), however, as research progressed our understanding of the responsible mechanisms became complex. Strong links between obesity and T2D have been found over the past few decades indicating that adipose dysfunction also plays a role in the pathophysiology of T2D (Esposito and Giugliano, 2004). Adipose dysfunction leads to dysfunctional hormone signalling and the production of pro-inflammatory cytokines representing a state of chronic inflammation. This, in turn, is associated with metabolic syndrome and the development of a plethora of MD (reviewed in Schuster, 2010) (fig.1.1.1).

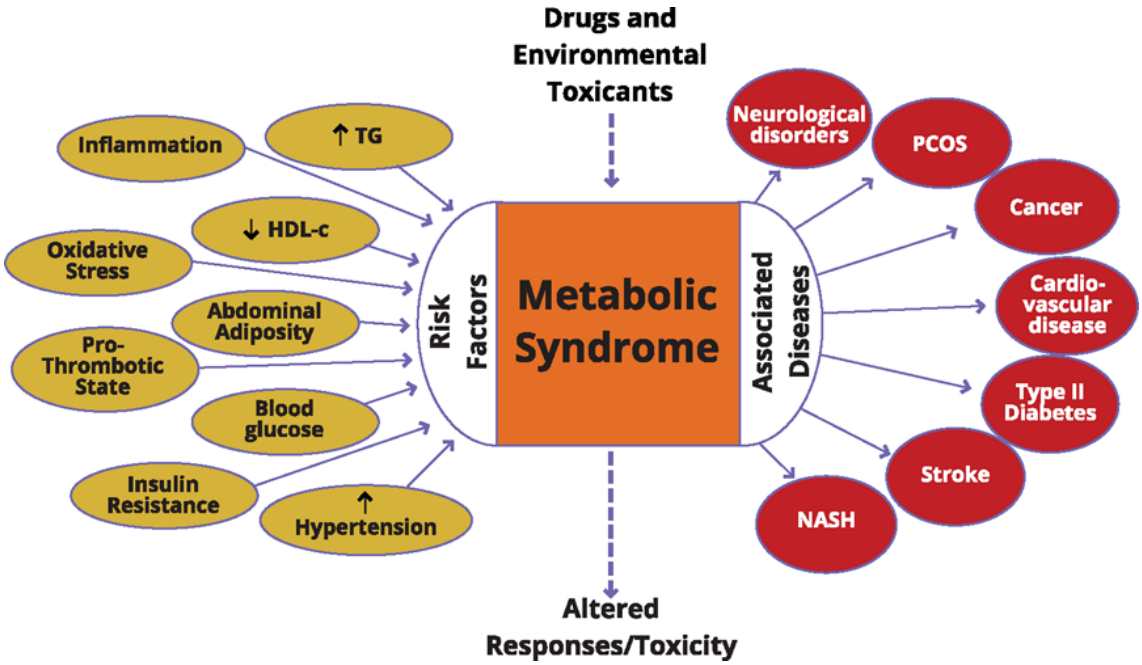

Figure 1.1.1: Risk factors associated with metabolic syndrome and the diseases.

The individual risk factors for the occurrence and escalation of the metabolic syndrome are complex, however, there are general links among the risk factors and the diseases. In fact, there are important pathways that regulate the metabolism, and understanding the biological mechanisms and taking multidisciplinary approach could help to prevent and treat these diseases. TG = triglycerides; HDL-c = high-density lipoprotein cholesterol; PCOS = polycystic ovary syndrome; NASH = nonalcoholic steatohepatitis. Figure adapted from Mendrick *et al*. (2017).

Diabetes is responsible for 1.5 million deaths worldwide and is estimated to be the 7th leading reason for global death by 2030 (Nettleton et al., 2016). In 2015 global prevalence of diabetes was 8.8% (415 million) of the total population, estimated to increase to 10.4% (642 million) by 2040 (IDF diabetes atlas). Further research is vital to reduce the huge toll on human health and healthcare providers.

Chronic inflammation triggers metabolic syndrome by causing obesity, T2D, and cardiovascular diseases (Toubal et al., 2013). Worldwide, chronic inflammation-mediated MD are responsible for 3 in 5 deaths (Pahwa et al., 2019). Metabolic disorders and inflammatory stress are interlinked, with one condition enhancing the development or exacerbating others. For example, obese patients with metabolic syndrome also develop T2D due to persistent, low-grade inflammation seen in obesity (reviewed in Schuster, 2010; Esposito and Giugliano, 2004). Emerging research indicates that gut microflora (GM) dysbiosis and impaired IBF result in metabolic endotoxaemia which is closely related to inflammation, insulin resistance, and cardiovascular events in patients with T2D (fig.1.1.2) (Fukui, 2016). Impaired IBF is characterised by increased epithelial permeability allowing entry of antigens resulting in metabolic endotoxaemia (König et al., 2016). Also, high-fat, high-sugar diets increase intestinal permeability resulting in inflammation, leading to MD such as T2D (Fukui, 2016). Moreover, food additives such as emulsifiers was shown to cause gut barrier leak leading to metabolic syndrome (Chassaing et al., 2017). Therefore,

IBF is a primary site that regulate the metabolic disease development via inflammation (fig.1.1.2) and understanding the role of dietary components is timely.

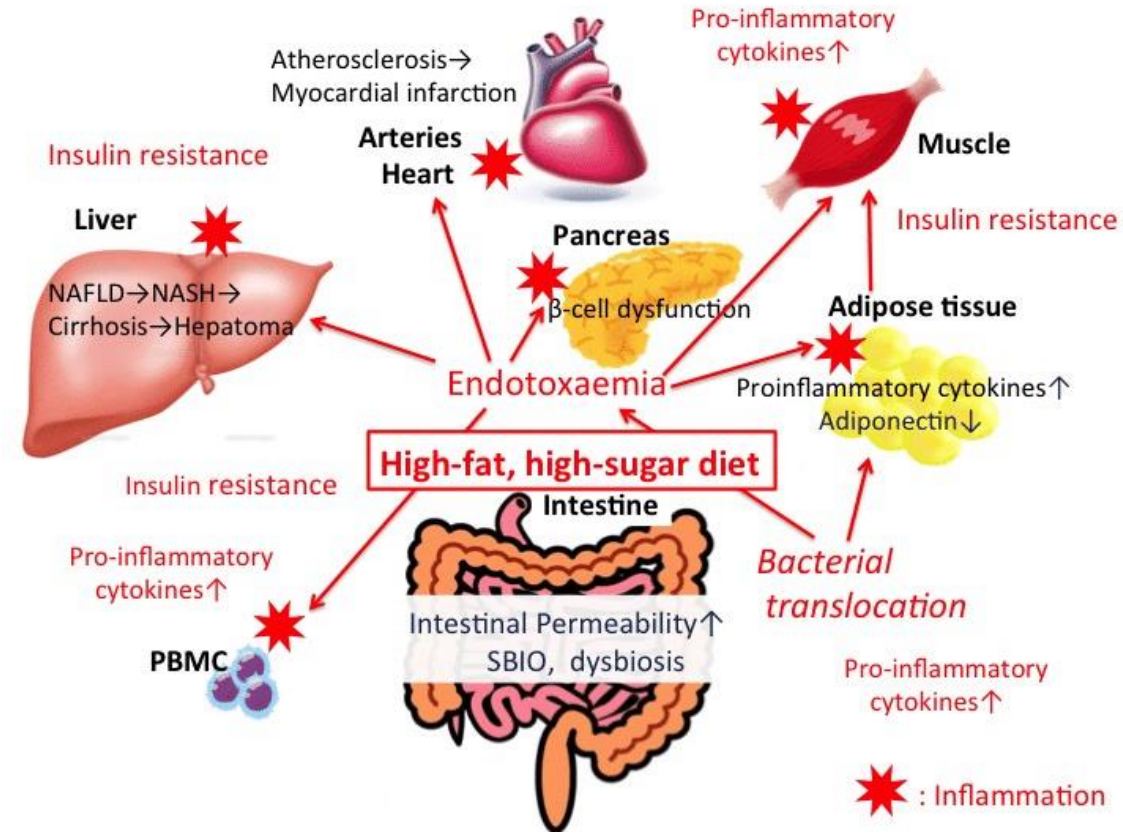

Figure 1.1.2: Interactions of gut microflora dysbiosis, intestinal permeability and endotoxaemia to the progression of metabolic diseases.

Increased Intestinal epithelial barrier permeability along with gut microflora dysbiosis allows antigenic substances in the lamina propria provoking low-grade inflammation in various tissues. This eventually leads to insulin resistance on type 2 diabetes. In obese patients, fat cell chronic inflammation in the adipose tissue causes pro-inflammatory cytokinemia. Inflammation and insulin resistance ultimately impair the insulin signalling and cause β-cell dysfunction. Similarly, inflammatory changes in the blood vessels and liver lead to ischemic heart disease and chronic liver disease, respectively. NAFLD= non-alcoholic fatty liver disease, NASH= non-alcoholic steatohepatitis, SBIO= small intestinal bacterial overgrowth, PBMC= peripheral blood mononuclear cells. Figure adapted from Fukui, 2016.

1.1.1 Risk factors of metabolic diseases

Genetic factors influence the development of MD. Locke *et al*. (2015) conducted a genome-wide association study (GWAS) and meta-analysis of body mass index in obesity-mediated metabolic disorders. They identified 150 genetic variants associated with obesity risk via insulin secretion/activity, energy metabolism, adipogenesis, and lipid biology (Locke et al., 2015). Weiss *et al*. (1984) reviewed the relationship of genetic factors and prevalence of MD, finding that people originated from Amerindian and their hybrids are prone to diabetes due to genetic configuration and environmental condition. Amerindians had a three- to fivefold greater prevalence of diabetes than the mixed ancestry. In addition, females are more susceptible to MD and pregnancy might trigger the diseases. Although the genetic

component was not defined, the review clearly showed a direct relationship between Amerindian ancestry and metabolic disease prevalence (Weiss et al., 1984).

Other than genetics, factors like lifestyle, diet, inflammation, microbiome, environmental and drug intake affects the development of MD. A sedentary lifestyle influences MD development greatly by increasing adipose tissue size, lowering high-density lipopolysaccharide (HDL) cholesterol levels, increasing triglyceride in the blood, glucose concentration and blood pressure, all of which are associated with the onset of cardiovascular disease (Eckel et al., 2010). Lipodystrophy (both genetic and acquired) and obesity are also associated with MD development and insulin resistance (Cornier et al., 2008). Impaired glucose tolerance doubles the threat of developing T2D (Goldberg and Mather 2012). Among these factors, diet has an independent and rapid impact on intestinal epithelial cell (IEC), GM composition and function, thereby modulating inflammation and disease development (Sonnenburg and Bäckhed, 2016; Lewis et al., 2015).

Inflammation in the liver, intestine, and adipose are major sites that lead to inflammation mediated MD (Mendrick et al., 2018). Furthermore, the microbiome also plays a major role in inflammation (Lewis et al., 2015). Association between the fecal microflora and MD was demonstrated using meta-GWAS (Korem et al., 2015). The role of the microbiome has been discussed in-depth (section-3.1.1). Therefore, it is important to recognise the modulatory factors of these metabolic conditions, especially the effect of different dietary components and how they impact inflammatory responses and therefore metabolic health.

1.1.2 Role of diet on metabolic disease

The link between MD and diet is widely accepted (Sonnenburg and Bäckhed, 2016). Diet is a key modulator of IBF, as the intestine is exposed to dietary components. Diet has regulatory effect on intestinal permeability by directly affecting IEC function, and indirectly via GM modulation. A study showed that high-fat diet in rodents significantly increased paracellular permeability immediately although the effect was reversible (Hamilton et al., 2015). Also, the high-fat diet reduced interleukin-10 expression, and decreased the abundance of Clostridia (Hamilton et al., 2015).

Dietary effect on loss of IBF through bacterial translocation was also reported in rats by Deitch *et al*. (1995). Rats exposed to parenteral nutrition solution had significantly higher intestinal barrier dysfunction therefore greater translocation of *E. coli* in comparison to animals on elemental- or chow-fed diet (Deitch et al., 1995).

Interestingly, diet can be as effective as high concentration of steroids in subsidence of small intestinal Crohn's disease (SICD) (Sanderson et al., 1987a). An elemental diet for six weeks improved intestinal permeability of fourteen children suffering from SICD (Sanderson et al., 1987b). The elemental diet not only increased barrier integrity but also improved other relevant disease indices such as ESR, body weight and disease activity score.

These studies provide an understanding of gut pathophysiology in diet-induced diseases and indicate its potential contribution in intestinal barrier impairment that lead to metabolic disorders.

1.2 Intestinal barrier function

1.2.1 Role of barrier in absorption

Maintenance of a healthy intestinal barrier is important for efficient absorption of essential molecules whilst preventing the ingress of harmful antigenic particles (König et al., 2016; Hollander, 1999). The intestinal barrier is composed of specialised epithelial cells that play an enormous role in protection and absorption. A single layer of columnar epithelial cells divides the lamina propria and the external environment in the intestinal lumen (fig.1.1.3). They are tightly adhered by tight junction (TJ) proteins and other intercellular junctional complexes to regulate paracellular permeability, crucial for IBF (König et al., 2016). The paracellular space is controlled by TJ proteins that control movement of water, nutrients and electrolytes into the lamina propria of the intestine (Madara and Pappenheimer, 1987). Besides, some specific water-soluble compounds that pass the epithelial barrier by the activity of protein carriers or through transport channels, most of the hydrophilic compounds rely on the paracellular space for movement into the lamina (Hollander, 1999). Impaired IBF plays an important role in the formation of various disorders such as inflammatory bowel diseases (IBD), irritable bowel syndrome, obesity, diabetes, celiac disease (König et al., 2016; Ulluwishewa et al., 2011; Damci et al., 2003).

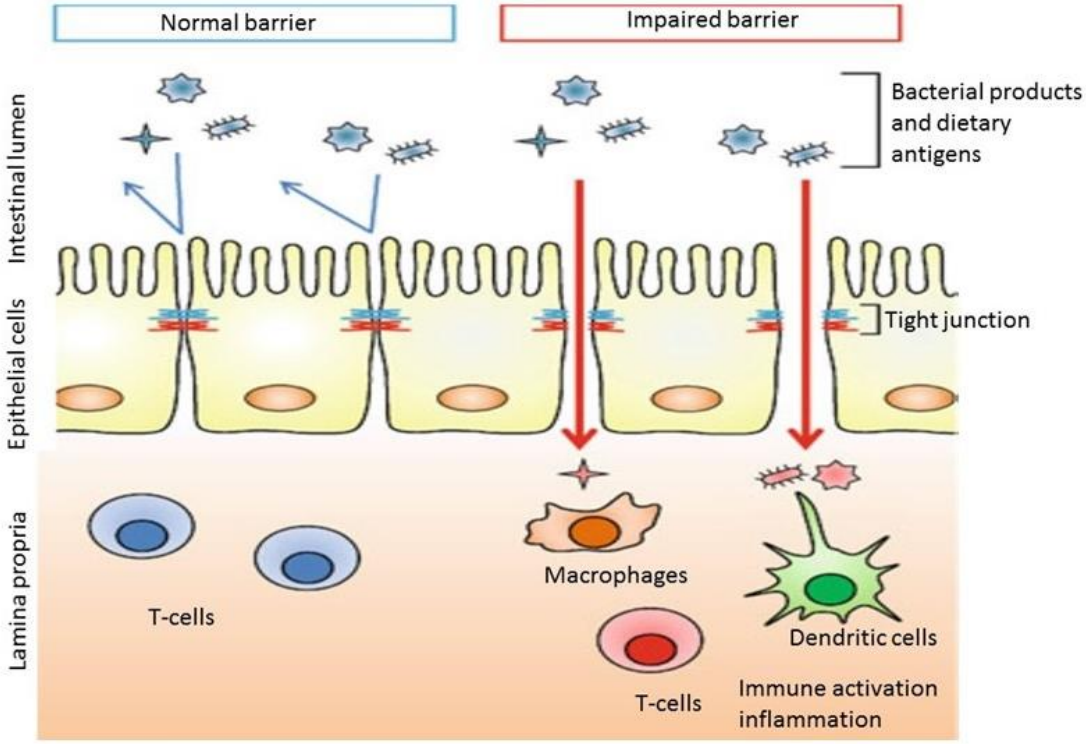

Figure 1.1.3: Barrier function of intestinal tight junctions.

The intestinal epithelial cells inhibit noxious macromolecules to penetrate in normal condition. But when epithelium is impaired, luminal bacteria, toxins, antigens can pass causing the activation of mucosal immune cells and inflammation. Figure adapted from Suzuki, (2013).

1.2.2 Tight junctions

Intestinal permeability is mediated by tight junction proteins (TJ) in intestinal cells (enterocytes), which form homotypic interactions between adjacent epithelial cells. The TJ comprises of over 50 proteins (Ulluwishewa et al., 2011), the key ones are occludins, claudins and junctional adhesion molecules (JAM) (König et al., 2016; Furuse, 2010; Mitic et al., 2000) (fig.1.1.4). Expression of these proteins at the cell surface is mediated by intracellular trafficking whilst activity can be regulated by signalling proteins such as protein kinase C (PKC), mitogen-activated protein kinases, the Rho family of small GTPases and myosin light chain kinases (Fredriksson et al, 2015; Fletcher et al., 2014; Ulluwishewa et al., 2011; Findley and Koval, 2009).

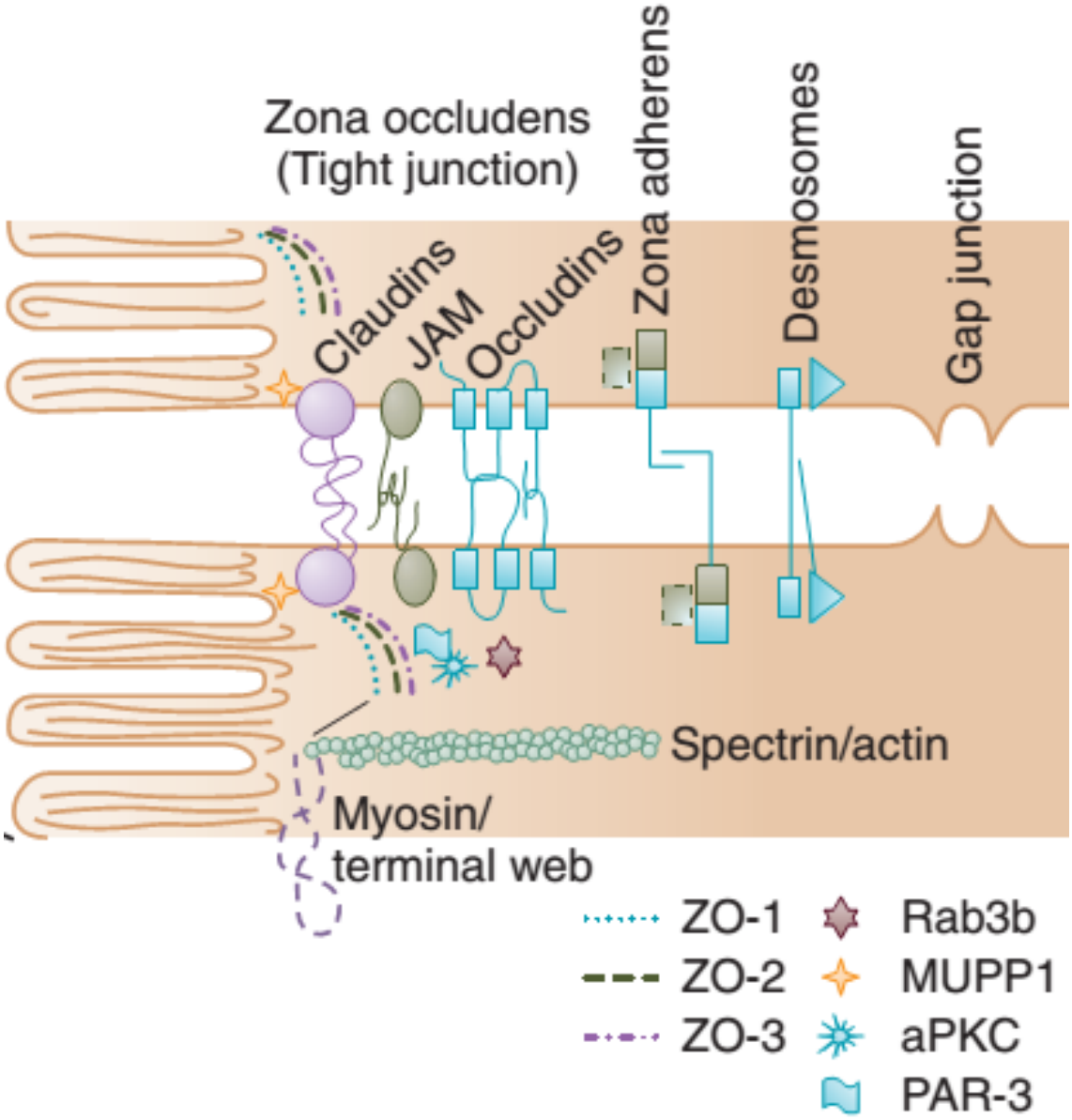

Figure 1.1.4: The tight junction in paracellular pathway is composed of proteins like occludins, claudins and junctional adhesion molecules (JAMs).

These proteins are linked to the cytoskeleton via scaffolding proteins like zonula occludens proteins, multi-PDZ domain protein-1 (MUPP1). Other proteins involved are Ras-related protein (Rab3b), atypical protein kinase C (aPKC) and protease activated receptor 3 (PAR-3) (Venkatasubramanian et al. 2015).

Protein kinases are crucial mediators of fundamental intracellular signal transductions, transport and barrier permeability of the gastrointestinal epithelium (Farhadi et al., 2006; Song et al., 2001). PKC is a diverse subfamily of serine/threonine kinases that are categorised into 12 isoforms (Farhadi et al., 2006). These isoenzymes are classified into three subtypes depending on their sequence homology, sensitivity to activators and cofactors (Farhadi et al., 2006; Song et al., 2001; Davidson et al., 1994). In the intestinal epithelium, activation of PKC isoforms is linked with an increase in paracellular permeability through actin polymerisation, with pan-inhibition of PKC promoting the recovery of TJs from

lecithin-induced leak (Sawai et al., 2002; Fasano et al., 1995). Conversely, studies show that TJ proteins interact with PKC isoforms to initiate assembly of the TJ complex, resulting in enhanced barrier function (Gonzalez-Mariscal et al., 2008; Stuart and Nigam, 1995; Harhaj and Antonetti, 2004). However, the precise mechanisms of PKC regulation are not fully understood.

1.2.3 The intestinal barrier and microflora

The GI mucosa is the interface between the internal structure and the external environment. This IEC monolayer is exposed to diverse antigenic substances from food and gut microflora. The importance of commensal microbiota for intestinal epithelium function was demonstrated in germ-free mice that experienced a significant reduction in mucosal layer thickness and antimicrobial product levels (Nagai et al., 2016).

IECs recognise microorganisms through pattern-recognition receptors (PRRs), such as Toll-like receptors (TLR) and nucleotide binding oligomerization domain (NOD) 1 and 2. Paneth cell along with NOD2 produce α-defensins when they sense bacterial invasion. A damaged NOD2 function has been linked to gut microbial dysbiosis leading to Crohn's disease development (Nagai et al., 2016).

The bacterial endotoxin lipopolysaccharide (LPS) enhances intestinal layer function at a moderate concentration (Petersson et al., 2010), however excess can cause inflammation and lead to septic shock (Patterson and Watson, 2017; Beutler and Rietschel, 2003). The IEC secretes alkaline phosphatase enzyme to detoxify LPS, thereby preventing inflammation and shock (Bates et al., 2007). In addition, TLR-5, another bacterial component was demonstrated to reduce host's ability of controlling intestinal microbial community by decreasing innate immunity (Vijay-Kumar et al., 2010). Gut bacterial flagellin acts as ligand for TLR-5, and the component defend against infection and lack of TLR-5 is correlated to metabolic changes that cause serious dysbiosis and metabolic disease development. Microbiota transplantation from TLR-5 deficient mice to germ-free mice demonstrated these implications (Vijay-Kumar et al., 2010).

Microbial metabolites also influence IBF. Microbial metabolites, especially short-chain fatty acids (SCFA) (e.g., acetate, butyrate and propionate) are important for barrier function and disease prevention. Other gut microbial metabolites (e.g., indole, lactate) influence IEC proliferation and barrier function (Nagai et al., 2016). Therefore, GM and their metabolic products play a significant role in host health and wellbeing through epithelial barrier function.

1.3 Regulation of intestinal barrier by diet and gut microbiota

Diet have direct effect on intestinal barrier. Dietary components have demonstrated effects on the expression and distribution of TJ leading to intestinal permeability (Ulluwishewa et al., 2011). Diet also influences the microbiota surrounding the intestinal epithelium. Within the intestinal tract, there are more than a hundred trillion microbes such as bacteria, fungi, protozoa, and archaea (Ley et al., 2006); referred to as gut 'microbiota' or 'normal flora' (Fukuda and Ohno, 2014). Recent studies demonstrate crosstalk between GM and IBF (Nettleton et al., 2016; Wells et al., 2011). ~60% of human GM is bacteria, comprising of at least 1000 species but diversity is limited (Schuijt et al., 2013) (fig.1.1.5).

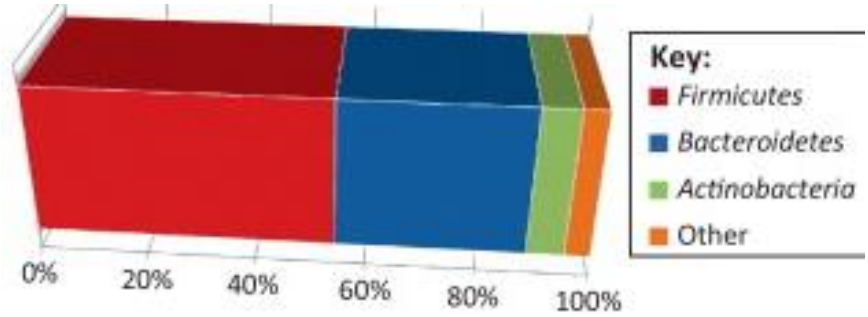

Figure 1.1.5: Major groups of intestinal microbiota.

Around 80% of the intestinal microbiota can be classified into three phyla: Firmicutes, Bacteroides, and Actinobacteria, although interindividual and interpopulation differences in gut microbiomes exist (Yatsunenko et al., 2012). Other bacterial phyla include the Proteobacteria, including various pathogenic or inflammatory groups, and the Verrucomicrobia, the latter one solely represented by the mucus-utilizing *Akkermansia* spp. Figure adapted from (Schuijt et al., 2013).

Of the ~28 phyla identified so far, only four phyla, Firmicutes, Bacteroidetes, Actinobacteria and Proteobacteria, make up the most of the GM (Nettleton et al., 2016; Fukuda and Ohno, 2014).

B. thetaiotaomicron, B. vulgatus, B. distasonis, B. fragilis are the four key species of intestinal *Bacteroides*, predominantly found following the consumption of a high-protein and -animal fat diet, whilst *Prevotella* enterotype are frequently identified in hosts consuming a high-carbohydrate diet (Fukuda and Ohno, 2014; Sears, 2005). Diet low in plant fibre and high in sugar and saturated fat causes major changes in the bacterial phyla and decrease their diversity significantly (Nettleton et al., 2016).

Wu et al. (2011) found that eating energy rich high-fat, low-fibre or low-calorie, low-fat, high-fibre diets rapidly changed GM composition and function. Despite changes, the key composition and overall classification of the individual's microflora was unaltered (Wu et al., 2011). Such fast changes in response to diet might be explained by the fact that microbes can double their population within an hour (Myhrvold et al., 2015). Also, gut epithelial cell turnover time is two to five days (Van Der Flier and Clevers, 2009). However, long-term

dietary behaviours remain the major influence in shaping the individual's GM (Wu et al., 2011; Muegge et al., 2011; De Filippo et al., 2010).

1.3.1 Formation and development of gut microbiota

The sterile condition in the uterus means that mammalian foetuses acquire their microbiome during and after birth. The GI tract undergoes rapid microbial colonisation in infants, eventually becoming a unique ecosystem. Delivery mode, mother's health, hygiene, gestation period, and breast feeding are important factors for microbial composition. During the early stage of life, the facultative anaerobes are predominant in the gut whilst Bacteroidetes and Firmicutes overtake eventually (Nagai et al., 2016). The infant GM demonstrates dynamic changes, greater degree of variability among individuals and are less stable. By the age of 2.5 to 3 years, the composition, diversity and functional capacity of the child microbiota resemble those of adults (Rodriguez, 2015; Koenig et al., 2011). The adult GM is relatively stable until ~70 years, however, life events may perturb the composition (Biagi et al., 2010).

1.3.2 The influence of diet on gut microbiota

The regular diet is one of the most important factors that shapes GM. De Filippo *et al*., (2010) compared intestinal microbiota of a rural village in Burkina Faso with an urban area in Italy, finding higher microbial diversity in children in Burkina Faso. The African diet rich in complex carbohydrate and fibre, whilst low in fat and animal protein created distinct differences in phyla composition in comparison to the European diet rich in processed sugars and fat whilst low in fibre. Similarly, adult diets rich in animal protein and saturated fats were shown to increase enterotype *Bacteroides,* whilst diets rich in complex carbohydrates increased Enterotype, *Prevotella* (Wu et al., 2011). These indicates the importance of diet in shaping intestinal microbiota.

Dietary habit also influences the composition and function of the gut microbiota (Makki et al., 2018; David et al., 2014). Short-term exposure to a diet composed entirely of either plant or animal products have the capacity to alter gut microbial community structure, implying the potential rapid effect of human dietary lifestyles on gut microflora (David et al., 2014). The 'western or omnivorous diet' contain refined carbohydrates, simple sugars and saturated fats that enhances negative alterations in microbiota leading to metabolic disorders (Tomasello et al., 2016). Oppositely, dietary fibres directly interact with gut microbial metabolism and impacts their ecology, thereby influencing host physiology and health (Makki et al., 2018). For example, adherence to the Mediterranean diet that includes high-level of cereals, fruit, vegetables, and legumes, have health benefits (De Filippis et al., 2016). Study on a 12-month long Mediterranean diet intervention in European elderly subjects demonstrated specific positive alterations of the gut microbiota and reduced frailty

(Ghosh et al., 2019). Mediterranean diet lowered several markers of frailty and inflammation, as well as improved cognitive function of the subjects. The diet also enriched the bacterial taxa in the keystone interaction positions of the microbiome ecosystem but not the peripheral frailty-associated taxa. Additionally, the diet-modulated microbial metabolism produced more short/branch-chained fatty acids whilst less secondary bile acids, p-cresols, ethanol and carbon dioxide, which helps frailty (Ghosh et al., 2020). The study highlighted the importance of dietary intervention in promoting healthier ageing via the gut microbiota modulation, which implies the role of diet on GM composition and function.

Similar protective health advantages were demonstrated when vegan diets were compared to vegetarian and omnivorous diets (Wu et al., 2016). Comparing the dietary intake, gut microbiota composition and the plasma metabolome using 16S rRNA-tagged sequencing along with plasma and urinary metabolomic platforms, Wu *et al.* (2016) showed the distinct difference in GM composition and metabolites of the healthy human vegans and omnivores in an urban USA environment. Vegan gut profile displays distinct microbiota than that of omnivores, although not always significantly different from that of vegetarians (Glick-Bauer and Yeh, 2014). The vegan diet reduce abundance of pathobionts whilst increase abundance of probionts, thereby lower the levels of inflammation (Tomasello et al., 2016; Kim et al., 2013). The vegan diet for one month could potentially decrease the disease activity of rheumatoid arthritis patients by changing the GM profile (Peltonen et al., 1997). In a study on patients with metabolic syndrome (n = 6), Kim *et al.* (2013) also showed that adherence to strict vegetarian diet for a month improved health along with reduction of Firmicutes-to-Bacteroides ratio. Without altering the enterotypes, the strict vegetarian diet led to a decrease in the pathobionts (e.g., Enterobacteriaceae) and an increase in commensals (e.g., *Bacteroides fragilis*). Therefore, the above-mentioned findings show that different dietary patterns hugely influence the GM which eventually impact host health.Beside the complete diet, food additives also impact the composition and function of gut bacteria. Food additives are employed for many reasons, such as to increase taste, aesthetic and possible food storage time (Nagai et al., 2016). Dietary emulsifiers have an enormous effect on GM. The US FDA approved two food emulsifiers, Carboxymethyl Cellulase and Polysorbate 80, as safe for health. However, their acceptable daily intake levels caused a reduction of the colonic mucin layer in wild-type mice (Chassaing et al., 2015). Research showed that emulsifiers alter GM composition, increasing mucolytic bacteria abundance whilst decreasing Bacteroidetes, resulting in reduced SCFA production. Several studies have demonstrated the relation between emulsifiers and metabolic syndrome development (Chassaing et al., 2015). Artificial sweeteners (AS), widely used for reducing energy intake, are another food additive linked with microbiota-modulating effect (Nagai et al., 2016). Several epidemiological studies have demonstrated

the correlation between AS consumption and the development of glucose intolerance and type 2 diabetes (Suez et al., 2014; Nettleton et al., 2016).

1.4 Artificial sweeteners

1.4.1 Sugar and sugar substitutes

Sugar from refined cane and beet are not only expensive but also high in calorie, which has been linked with obesity-mediated metabolic disorders in Western countries (Cordain et al., 2005). Diet that include sugar more than 22.5 g per 100 g or 27 g per portion of food is regarded as high-sugar diet (NHS, UK). High-carbohydrate diet containing more free sugars, specifically, more than 30 g of free sugar in the daily reference intake of 90 g total sugar, can cause weight gain and other health issues (NHS, UK). Continued exposure of the intestinal tract to a high-fat or high-carbohydrate (with free sugars) diet is associated with gastric permeability; where the intestinal barrier breaks down and becomes leaky (Payne et al., 2012; Frazier et al., 2011; Stenman et al., 2013; Damci et al., 2003; Watts et al., 2005). Sustained gastric permeability results in the entry of bacteria and/or antigens into the circulation, causing systemic inflammatory response, sepsis and multiple organ failure (Liu et al., 2005; Ukleja et al., 2010) (fig.1.1.3).

As blood sugar level is a key contributor to metabolic syndrome (NHS, UK, 2019), food science has incorporated AS into food to provide sweetness without the effects of sugar (Anton et al., 2010). AS are synthetic sugar substitutes, used as food additives to provide the sweet taste in low-calorie foods (Suez et al., 2015; Payne et al., 2012) (fig.1.1.6).

Chemicals eliciting sweet taste perception, namely glucose, other carbohydrates like fructose, AS and proteins like monellin and thaumatin vary largely in terms of their chemical structures (fig.1.1.6) (Keast et al., 2004). In addition, they differ in the receptor-binding mechanism and taste signal transduction mechanism, but all of them generate sweet taste perception (Keast et al., 2004; Zhao et al., 2003). AS listed in table 1.1.1 are many times sweeter than table sugar and are widely used in various food substances to reduce the energy consumption in food and beverages, and therefore, used for the present study.

Table 1.1. 1: Artificial sweeteners used in the study with sweetness level compared to sucrose.

Information adapted from Rolfes *et al.* (2014) and Gardner *et al.* (2012) unless mentioned otherwise.

Commercial name	Artificial sweetener	'Sweetness' relative to sucrose (the table sugar)	Energy (Kcal/g) (Whitehouse et al., 2008)	Concentration stimulate T1R2/T1R3 (Li et al., 2002)	ADI (mg/kg bw) EFSA/ FDA	Representative amount of AS in 12-ounce Soda, (mg)	Amount of AS in a packet[$] (mg)	No. of packets equal to ADI[#]
Sweet n low	Saccharin	300-450	0	1 mM	0-5 / 15	8*	40	8.5
Splenda	Sucralose	600	0	1 mM	0-15 / 5	68	11	30
Equal	Aspartame	160-200	4	2.5 mM	0-40 / 50	187	40	68
E961	Neotame	7000-13000	0	0.1 mM	2 / 0.3	No consumer product in the UK		

*blended with aspartame; [$] equivalent to 2 teaspoon sugar; [#] FDA approved ADI for 150-pound (68 kg) person; Bw=body weight, ADI=acceptable daily intake, T1R2/T1R3–the sweet taste receptor. FDA=Food and Drug Administration (USA), EFSA=European Food Safety Authority.
Represent the amount of sweetener if the product is exclusively sweetened with one sweetener. Very frequently more than one sweetener is used in soda or other products. Usually this information is proprietary and unavailable to the public; the exception is saccharin. The amount of saccharin must be listed in the ingredient list. The maximum amount is 12 mg/ounce fluid.

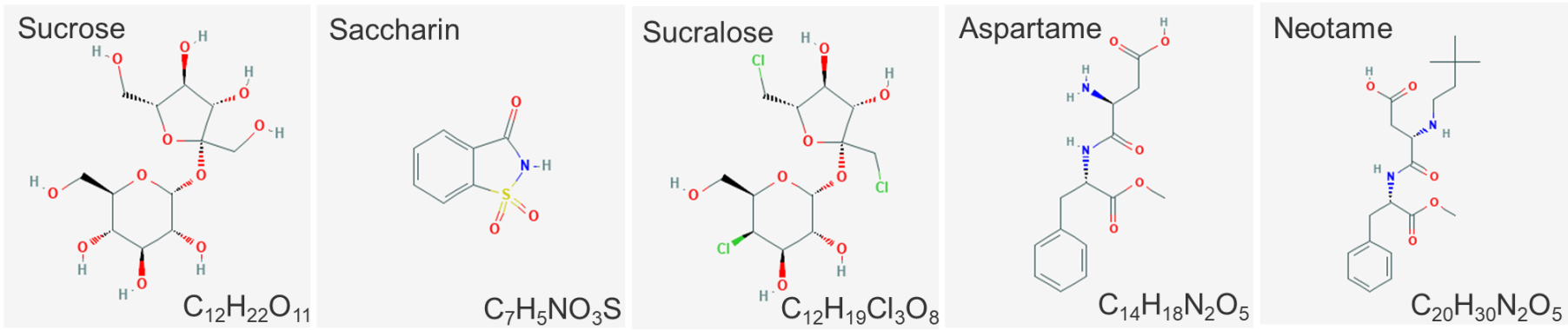

Figure 1.1.6: Structure of sucrose and the artificial sweeteners used in the study.

The panels represent the name, molecular structure and chemical formula of the AS. Figures adapted from PubChem, 2019.

Eating a healthy and balanced diet is one of the important ways of preventing MD (NHS, UK, 2019). People often select AS to reduce calorie intake and blood sugar level (Gardner et al., 2012; de La Peña, 2010). In fact, AS is useful for diabetics to get sweet taste perception (Johnston et al., 2013; Gardner et al., 2012). The use of AS is not limited to food and beverages but extended to pharmaceutical and cosmetic industries (Whitehouse et al., 2008). Therefore, the use of AS is popular and its global market still growing. The world consumption of AS is estimated to be ~159,000 metric tons with a market value of USD $2 billion (Praveena et al., 2019). However, the effect of AS remains controversial, and the physiological effect of AS needs to investigate further.

1.4.2 The sweet taste receptor

Sweet taste modality takes place by the activity of two genes (T1R2 and T1R3) of the T1R family. T1R2 was identified by sequencing a deducted cDNA library obtained from rat taste tissue in 1999. It has a distinct expression pattern and was more enriched in the circumvallate taste buds (reviewed by Li, 2009). The T1R3 was identified in human genome in 2001, which was recognised as the *sac* (a locus related to sweet taste sensitivity) gene in mice. Studies on transgenic mice introducing T1R3 gene from a taster to a non-taster individual confirmed that T1R3 in human is the *sac* gene in mice (reviewed by Li, 2009).

Similar to sugar, AS stimulate the sweet taste receptors T1R2/T1R3; G-protein coupled receptors which, when stimulated, are expressed at the plasma membrane (Elliott et al., 2011). Among the various receptors, T1R2 and T1R3 in combination are activated by sweet taste molecules (Assadi-Porter et al., 2010; Zhao et al., 2003). T1R has three main domains; the extracellular Venus-flytrap domain (VFD), the cysteine-rich domain (CRD) and the transmembrane domain (TMD) (Jiang et al., 2005). The VFD is a clam shell-shaped structure in the amino-terminal domain and is linked with the heptahelical spanning C-terminal TMD by the CRD (Fernstrom et al., 2012; Jiang et al., 2005) (fig.1.1.7). After the TMD, there is a short intracellular carboxyl-terminal tail (Jiang et al., 2005).

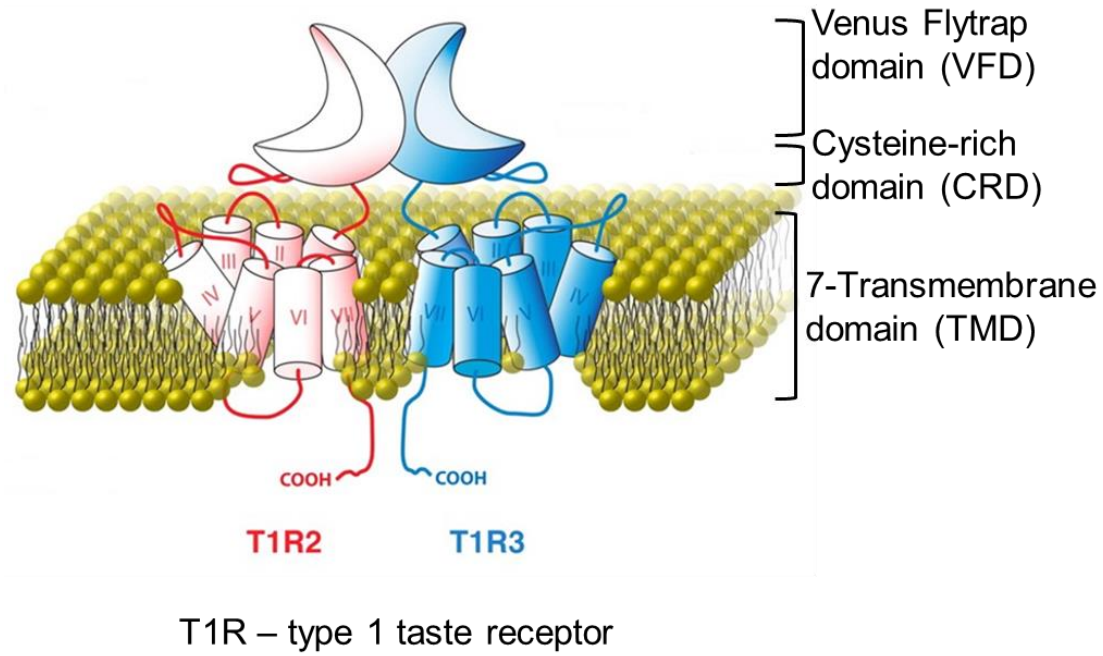

Figure 1.1.7: The heterodimeric sweet taste receptor, T1R2 and T1R3.

The receptor composed of three distinct interlinked domains and is partially embedded in the intracellular region with a short carboxyl-terminal tail. Figure adapted from Fernstrom *et al*., 2012.

The sweet taste perception only occurs if the molecule can stimulate the relevant receptor T1R2/R3 (Keast, 2003). Selective elimination of T1R subunits abolishes the detection and perception of sweet taste modality. By incorporating the human T1R2-receptor in mice, Zhao *et al*. (2003) demonstrated a humanized sweet taste preference in the animals. Besides, engineered animals expressing a modified opioid-receptor in sweet cells showed strong attraction to a synthetic opiate. The study showed that sweet cells trigger behavioural outputs, however, the nature of the receptors determine the animal's tastant selectivity (Zhao et al., 2003). Similarly, Damak *et al*. (2003) demonstrated that mice lacking T1R3 showed no preference for AS. However, the mice had not abolished behavioural and nerve responses to sugars completely, rather they showed lessened responses to sweet molecules. Their study suggested that taste cells could have T1R3-independent sweet responsive receptors and/or pathway (Damak et al., 2003).

1.4.3 AS consumption and gut physiology

Health-conscious individuals or those trying to lose weight usually consume AS as a sugar substitute (Anton et al., 2010). However, the irony is that research in AS showed links to the development of glucose intolerance (Suez et al., 2014).

The effect of AS on health via promoting hunger and unbalancing energy has been greatly debated. Research suggests that AS might cause metabolic disturbances because they are not physiologically inert (Wal et al., 2019). As mentioned, AS stimulate the gut sweet taste receptor (STR), which can interact with biochemical pathways, causing incretin release. The

receptors can alter appetite signalling and emptying rate through changes in osmotic load (Mattes and Popkin, 2008). Furthermore, taste receptor activation can stimulate the glucagon-like peptide, GLP-1 release (Jang et al., 2007). Activation of these pathways might modify glucose absorption, which in turn might participate in glucose intolerance (Shirazi-Beechey et al., 2014). Moreover, these compounds delay gastric emptying, and alter brain responses indicating possibilities for negative impact on health (Meyer-Gerspach et al., 2016). Therefore, AS consumption can directly impact intestinal epithelium and lead to MD development (fig.1.1.8).

Moreover, AS have been demonstrated to alter GM diversity (Nettleton et al., 2016), thereby unbalancing the symbiotic conditions (Suez et al., 2014). An imbalance of microflora (dysbiosis) makes the host prone to a variety of MD including obesity, insulin resistance, cardiovascular diseases and diabetes (Nettleton et al., 2016; Fukuda and Ohno, 2014; Muegge et al, 2011; Suez et al., 2014). However, the role of AS on bacterial pathogenicity of GM is unknown. Alterations in the GM is also associated with intestinal barrier permeability (fig.1.1.8). The barrier leak allows antigenic substances such as LPS to cross the intestinal lining, resulting in inflammation and metabolic endotoxaemia (Konig et al., 2016). This indicates people already suffering from glucose intolerance or obesity, consuming AS to control sugar level, could exacerbate their situation by triggering altered biochemical pathways (Pepino, 2015).

In addition, high-fat and high-carbohydrate diet alters TJ expression and distribution (Ulluwishewa et al., 2011). TJ alterations are linked to intestinal paracellular permeability; many studies link intestinal permeability and MD, but, minimal literature on the effect of AS on intestinal permeability (Cani et al., 2008). Kimmich *et al*. (1988) showed that saccharin (25 -130 mM) had a minimal effect on active transport of sugar from the lumen of chick IEC to the intracellular space, however, it inhibits passive transport from the basolateral boundary. Saccharin mediated inhibition of efflux allowed active system creating a concentration gradient of sugar. In addition, saccharin restricted transport of sugar to the IEC and into circulation by compromising the epithelial cells capacity to form sugar gradients (Kimmich et al., 1988).

Furthermore, the investigators demonstrated the inhibitory effect of 20 mM saccharin on ATP driven increase in sodium ion (Na+) permeability in exogenous IEC from three-week old chickens. This conserved the IEC capacity for sodium dependent sugar transport. 10 mM saccharin showed partial protection (Kimmich et al., 1989). On the other hand, saccharin, but not sucralose and aspartame, increased the paracellular permeability of IEC cell model Caco-2 (Santos et al., 2018). Saccharin decreased the transepithelial electrical resistance of the Caco-2 cells in a dose-dependent manner, and 10 mM caused highest reduction. In addition, saccharin exposure reduced the TJ protein, claudin-1, without

affecting the other TJ such as JAM-A, occludin-1 and ZO-1 protein content (Santos et al., 2018). Decrease in claudin-1 protein could have negative effect on the monolayer permeability.

As noted, the literature on the role of AS on intestinal permeability is limited. The above-mentioned studies show differential results; saccharin inhibited passive sodium dependent sugar transport in chick IEC (Kimmich et al., 1988) while saccharin increased paracellular permeability and decreased TEER in IEC model (Santos et al., 2018). However, the downstream metabolic effect of AS consumption remained elusive. Therefore, further investigations are important to understand how AS impact IEC, GM, and the intestinal epithelium– GM axis.

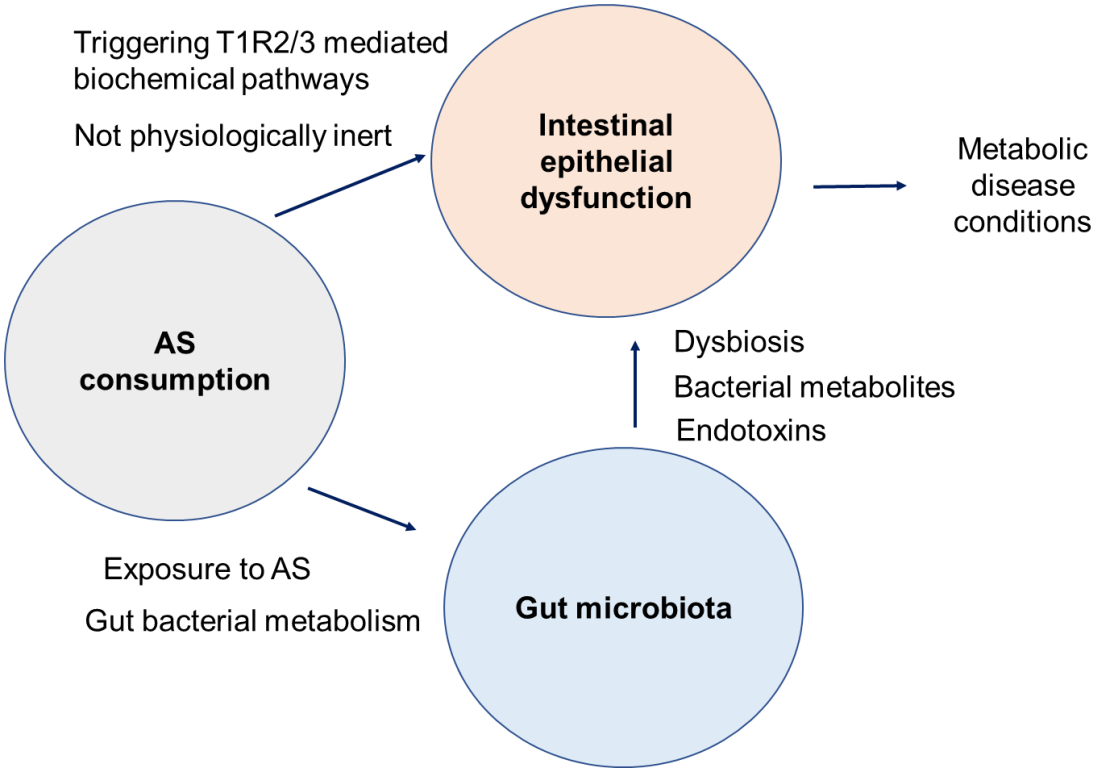

Figure 1.1.8: Schematic figure showing the artificial sweetener consumption and link to metabolic disease conditions.

AS consumption can directly affect the intestinal epithelial cell function or via gut microbiota activity, thereby leading to epithelial barrier dysfunction which is a crucial reason for metabolic disease development.

1.4.4 Metabolism of AS in the intestine

The capacity to metabolise AS has remained controversial. AS are thought to stimulate sweetness via GLUT2 up-regulation in the intestine similar in mechanism to glucose (Price et al., 1970). However, AS might enhance natural sugar uptake (Price et al., 1970), cause glucose intolerance (Suez et al., 2014), and stimulate hunger thereby affecting metabolic pathways (Payne et al., 2012).

Studies are available regarding changes in microflora following AS consumption in terms of abundance, composition, and diversity, but research on GM associated metabolism of AS is limited. Several gut bacteria were reported to have the capability to convert cyclamates into cyclohexylamine (Renwick, 1985), the derivative is more toxic than cyclamate, and metabolism of cyclohyxylamine differs in individual hosts at different times (Coates and Walker, 1992).

In addition, saccharin also changes the metabolic activity of GM. In rats, saccharin inhibited β-glucuronidase activity and proteolysis, and enhanced carbohydrate and protein accumulation, leading to enlargement of rat caecum. However, these metabolic changes were found when consumption was higher than 'acceptable' daily intake (Coates and Walker, 1992), leading to a lack of clarity, thereby urging further investigations.

1.4.5 Co-culture model for host-microbiota interactions

IEC are frontline participants interacting with GM, responsible for the initiation and regulation of intestinal epithelial response. The *in vitro* co-cultivation of model gut bacteria and IEC represents a common approach to mimic the host responses to certain food component. Considering the intrinsic limitations and complexities of studying different area of the GI tract *in vivo*, Marzorati *et al*. (2014) developed a device named Host-Microbiota Interaction (HMI) module to study the eukaryote-prokaryote interplay *in vitro*. The HMI module allows relevant conditions of the GI tract, representing a GM community to be co-cultivated microaerophilically with human IEC up to 48 hours. The device might contribute to the mechanistic understanding of indirect GM-host interactions in the GI tract (Marzorati et al., 2014).

In vitro models simulate gut microbial processes and represent enticing alternatives to rapidly test hypothesis since they are cheap, flexible, scalable and offer improved throughput (reviewed by Fritz et al., 2013). Compared to *in vivo* samples, downstream high-resolution molecular analyses of *in vitro* samples are simpler. An ideal *in vitro* model of host-microbiota interactions is presented in fig.1.1.9.

Obviously, findings from co-culture model cannot be directly compared to *in vivo* conditions. But the co-culture model like Caco-2 and model gut bacteria, represents benefits for simplicity and reproducibility (reviewed by Fritz et al., 2013). Also pursuing the role of a dietary component such as AS in a co-culture model provides molecular mechanisms for future studies which might be unmanageable to address *in vivo*.

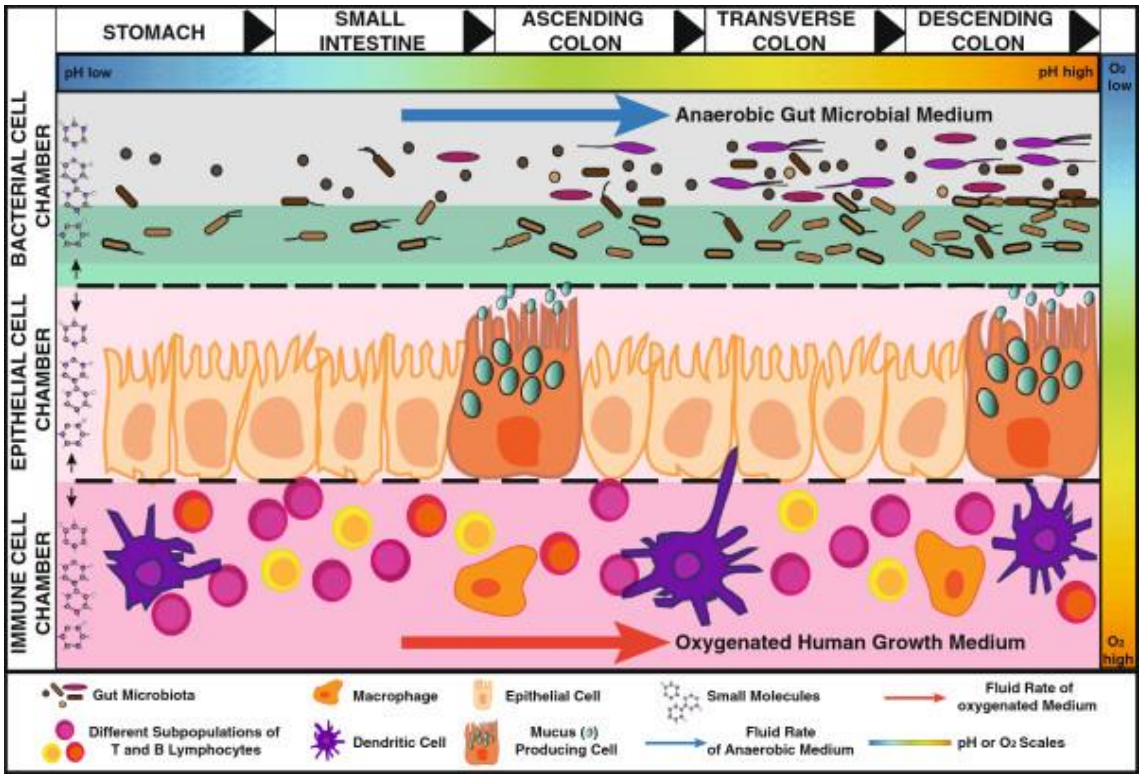

Figure 1.1.9: Conceptualization of an ideal *in vitro* model of gastrointestinal host-microbiota interactions.

The co-culture model should include separate chambers for microbial, human epithelial and human immune cell culture. The chambers should be separated by semipermeable membranes, thereby preventing microbes to overtake human cells while permitting molecular crosstalk between them. Figure taken from Fritz *et al*. 2013.

1.4.6 Inhibition of the sweet taste receptor

STR activity is blocked by sweet taste inhibitors (Assadi-Porter et al., 2010; Jiang et al., 2005). Lactisole is a common inhibitor (Assadi-Porter et al., 2010) that suppresses the sweet taste of substrates like table sugar, intensively sweet proteins such as thaumatin and monellin, and ASs (Jiang et al., 2005). Lactisole is composed of a carboxyl group and a hydrophobic phenoxyl group, and this molecular structure is important for suppression of the STR (Jiang et al., 2005; Xu et al., 2004).

In addition to Lactisole, zinc is a potent sweet taste inhibitor which suppresses the sweet taste perception of a number of sweeteners namely glucose, fructose, sucrose, maltose and AS such as sucralose, acesulfame K, aspartame, saccharin (Keast, 2003; Iwasaki and Sato, 1986). Although the mechanism of inhibition by zinc ions is unclear, several studies demonstrated that zinc sulphate ($ZnSO_4$) inhibits perceived ‘sweetness’ of compounds in a dose-dependent manner (Keast et al., 2004).

Moreover, use of taste receptor siRNA, knockout cell line (Wauson et al., 2012) or knockout mice could be other options to investigate the role of the receptor in sweet sense mediated biochemical mechanisms.

Aims and hypothesis

The broad research objective for the PhD is to develop our understanding of the molecular mechanisms regulating key gut microbiota and gastric permeability in populations consuming a normal or high concentration of artificial sweeteners in their diet.

The hypothesis for the PhD is that **artificial sweeteners negatively impact gut health through damage to the epithelium, increased pathogenicity of two key microbiota, and disruption of the interplay between the epithelium and the microbiota**. Studies will focus on the role of sweet taste sensors to address this hypothesis.

The overall impact of this research is to demonstrate the effect of AS in the diet and how they can promote gut leak and pathogenicity of key microflora bacteria. Research into this area will extend our knowledge of the role of diet components, and particularly additives such as sweeteners, in regulating gut physiology. These findings can impact our understanding of the link between diet, microbiota and the molecular mechanisms leading to metabolic diseases such as diabetes.

The PhD project will be studied via four specific aims:

Aim I: to understand the role of artificial sweeteners (AS) on an *in vitro* model of the intestinal epithelium;

Aim II: to assess whether AS affect metabolism and pathogenicity of model gut bacteria;

Aim III: to establish whether AS exposure has an impact on the interactions between the model gut microflora and intestinal epithelium using a co-culture model;

Aim IV: to determine whether the effect of AS on the intestinal epithelium and model gut microflora is mediated through sweet taste sensors.

2 Effect of artificial sweeteners on intestinal epithelial cells

2.1 Introduction

2.1.1 Intestinal epithelium

The gut constitutes the most critical organ for host communication with the environment, representing the major ground for intricate interactions between host genes and the extrinsic immunological impact on the body (Brandtzaeg, 2011). The intestinal epithelium is the single layer that separates the gut lumen from the underlying lamina propria of the gastrointestinal (GI) tract. These proliferative epithelial cells carry out the rapid renewal of the intestinal epithelium and form many specialized cell types. Epithelial cells undergo a renewal process of cell division, maturation and migration every 4-5 days (fig.2.1.1) (Bischoff et al., 2014; Van Der Flier and Clevers, 2009). The stem cells residing at the crypt of the epithelial invaginations continuously carry out this process of renewal and replace the older cells. The new cells, along with their maturation, migrate toward and out of the crypt, eventually apoptosis and are shed into the intestinal lumen (Yen and Wright, 2006; Weiser, 1973). Therefore, the intestinal epithelial layer remains the same, while renewed continuously by new cells.

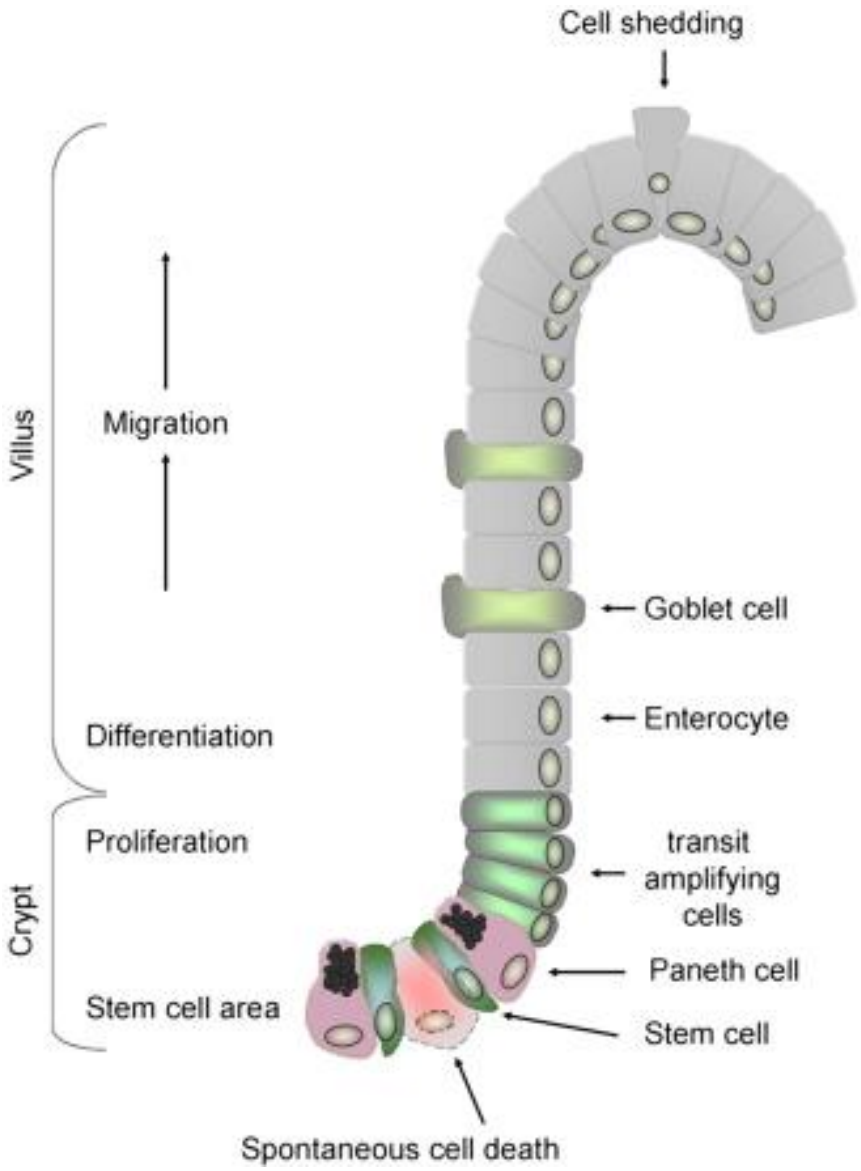

Figure 2.1.1: The succession of intestinal epithelial cells.

The life span of intestinal epithelial cells is 4-5 days. This life cycle is determined by the duration between cell migration from their origin at the crypt base to the villus tip, from where they are shed into the lumen. Figure adapted from Gunther *et al*., 2013.

Among the different types of renewable intestinal epithelial cells (IEC), more than 80% are the absorptive enterocytes (Van der Flier and Clevers, 2009). Enterocytes are the most abundant IEC that play the major function of the maintenance of epithelial barrier integrity (Groschwitz and Hogan, 2009). The other important types of cells include the Goblet cells which produce mucus and peptide (fig.2.1.2), Paneth cells secreting antimicrobial peptides, Microfold cells (M cells) responsible for antigen delivery and secretive enteroendocrine cells which produce various bioactive molecules, such as, hormones (Van der Flier and Clevers, 2009; Yen and Wright, 2006; Turner, 2009; Trier, 1963). However, some studies overruled these functional partitioning and appreciated the role of different cells performing the same function and vice versa (Geibel, 2005; Singh et al., 2005; reviewed by Binder et al., 2005). The intestinal epithelial layer, therefore, plays a vital role in the food digestion, nutrient

absorption and protection; appropriate maintenance and function of this layer are pivotal for good health while dysfunction can cause various diseases (Kong et al., 2018).

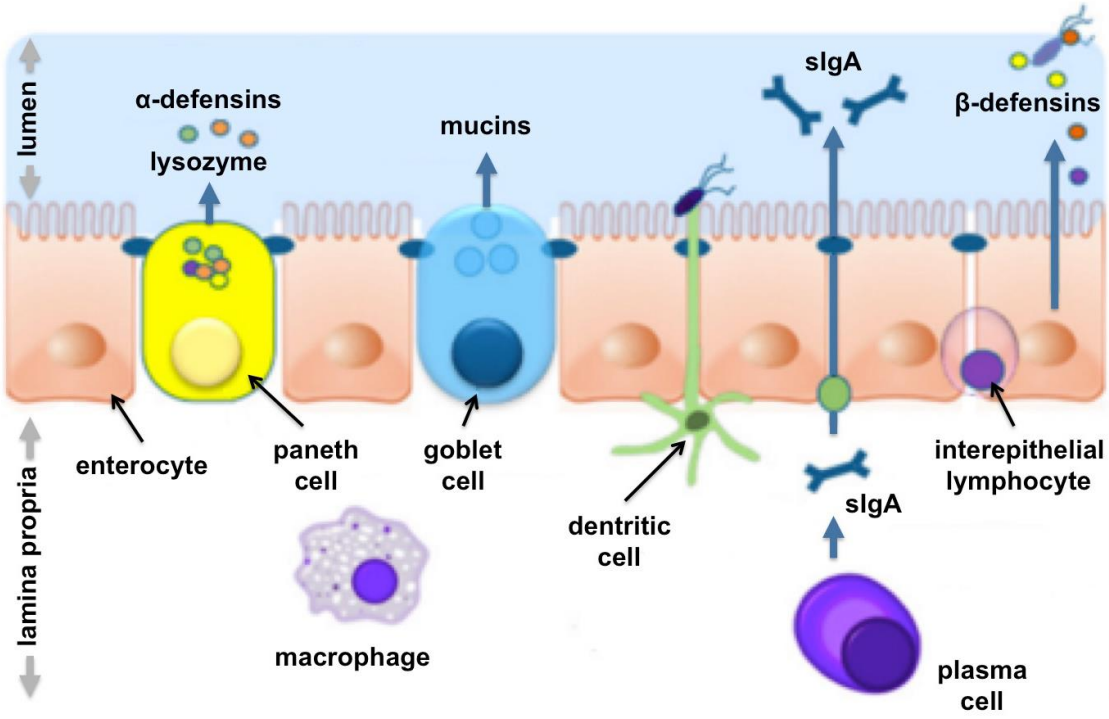

Figure 2.1.2: Different cells in the intestinal epithelia.

The single epithelial layer separates the intestinal lumen and the lamina propria. Intestinal stem cells differentiate into different types of intestinal epithelial cells such as enterocytes, enteroendocrine cells, goblet cells and Paneth cells. Enterocytes perform the absorption and transportation. Goblet cells secrete mucin which is heavily glycosylated and polymerized into an enormous net-like structure and plays a key role in keeping intestinal microbes at a distance from the epithelial surface. Paneth cells secrete antimicrobial peptides in the mucosa reflecting its central role in immunity and protection against pathogens. B cell activation and proliferation leads to antigen-specific secretory immunoglobulin A (sIgA) production in the gut associated lymphocytes via T-cell dependent pathways. Figure adapted from Bischoff *et al*., 2014.

2.1.2 Intestinal epithelial layer and permeability

The intestinal epithelial layer plays a dual role by regulating the nutrient and fluid uptake, as well as maintaining barrier and tolerance to the adjacent residing microflora. The selective nature of this barrier is fundamentally important for absorption while resisting the permeation of potentially hazardous substances present in the lumen. This selective function in the IEC layer is called ‘intestinal permeability’ (Brandtzaeg, 2011).

This term, in the clinical studies, refers to the IBF and has been defined as “the ability of medium and large-sized water-soluble compounds to passively traverse the intestinal epithelial layer through paracellular tight-junctional areas” (Ma et al., 2012). As such, the relative leakage of hydrophilic probes across the intestinal barrier regulated by the TJs or paracellular pathways are used for measuring intestinal epithelial permeability. Therefore, markers of permeability, whether for *in vitro* or *in vivo* studies, need to be water-soluble and

passively absorbed, chemically inert and atoxic, not metabolised and easily measurable (Ma et al., 2012).

2.1.3 Paracellular leak and related diseases

As a critical interface connecting the host to the surrounding environment, any barrier breach could be the initial point in the pathogenesis of many intestinal or extra-intestinal inflammatory disorders. Intestinal leak could also occur as a side effect of many disease processes, making the host susceptible to severe complications. Breakdown of the barrier can be implicated in various diseases including type 1 diabetes (T1D), irritable bowel disease (IBD), Crohn's disease, coeliac disease, food allergy, sepsis, asthma and many more (Liu et al., 2007). Understanding the significance of the intestinal barrier in the pathophysiology of disease processes is, therefore, crucial to find out preventive and therapeutic measures.

Increased intestinal barrier permeability to antigenic compounds is the hallmark of inflammatory responses related to metabolic disease conditions. Leakage can occur between (paracellular) or through (transcytosis) epithelial cells however there is no concrete research to show that these leakage pathways are linked (Armstrong et al., 2012).

Increased gastric and intestinal permeability are linked to metabolic disease development such as insulitis and diabetes (Meddings et al., 1999). BB diabetes-prone (BBdp) and control, diabetes-resistant (BBc) rats were maintained on either a control or hydrolyzed casein diet for 175 days. Their weight gain, gastrointestinal permeability and diabetes development was assessed in relation to age. While no difference was recorded for the weight gain among the control and diabetes prone rat groups, development of diabetes varied. The control groups did not have diabetes on 100-day age, however, 80% of the BBdp rats maintained on regular diet developed diabetes. On the other hand, only 20% of the BBdp rats maintained on the hydrolyzed casein diet showed incidence of diabetes. Moreover, within 50 days of age, the gastric and small intestinal permeability was significantly increased in the diabetes prone rats. Although, the small intestinal permeability was normalised in the BBdp rats around 100 days of age, however, the gastric permeability remained in the rats by this time point (Meddings et al., 1999). These findings suggest that increased permeability have an early role for the development of several immunological diseases.

Similar studies were conducted on healthy (n=161) and type 2 diabetic (n=130) individuals by Cox *et al*. (2017) to examine relationships between intestinal permeability and T2D. Their study showed that known cardiometabolic risk factors such as higher average BMI, a predominance of dyslipidemia, impaired glucose control and low-grade inflammation were significantly different between the T2D and control groups. The intestinal permeability risk

score was assessed by measuring the combination of circulating LPS, LPS-binding protein, and intestinal fatty acid binding protein, and the findings supported that intestinal permeability has association with risk for T2D (Cox et al., 2017).

Furthermore, intestinal barrier permeability is associated with chronic inflammatory gastrointestinal diseases, such as IBD (Suenaert et al., 2002) and coeliac disease (Vogelsang et al., 1998). Also, increased small intestinal permeability is common in patients with T1D (Damci et al., 2003). In addition, impaired intestinal barrier provokes immune system function that affects other organs by causing diseases like IgA nephropathy, multiple sclerosis in the brain, non-alcoholic hepatic steatohepatitis (Turner, 2009). Dysfunction of the intestinal barrier is also linked to many extra-intestinal and systemic disorders. Farhadi *et al*. (2003) reviewed the incidence of increased intestinal permeability in critically ill patients suffering from health issues like multiple traumas, extensive burn, shock, acute pancreatitis. Abnormal IBF was also linked to dermatologic disorders including eczema, psoriasis, urticaria-angioedema and dermatitis herpetiformis (Hamilton et al., 1985) and several rheumatological disorders (Farhadi et al., 2003). Furthermore, ingress of the antigenic substances promotes systemic inflammatory response syndrome, which can lead to multiple organ failure (Ulluwishewa et al., 2011). Beside the loss of TJ integrity, damage and apoptosis of the IEC can cause intestinal barrier dysfunction. Discernment toward the commensal microbiota and the dietary components and protection against pathogens require intact mechanisms of the intestinal epithelial barrier.

Different food components can influence the breakdown of IBF through affecting cell viability, apoptosis, or by affecting the TJ expression and distribution. Glucose, the most common ingredient in the diet, is known as an absorption enhancer. Also, a significant portion of intestinal glucose absorption takes place via TJs, but not by transcellular active transport. Glucose was demonstrated to increase the intestinal intercellular permeability by changing the distribution of the TJ in Caco-2 cell line (Lerner and Matthias, 2015).

There is a need to study the regulation of intestinal permeability to develop therapeutic intervention for these conditions. Given the complexity of *in vivo* models (Harrison et al., 2004), it is useful to use *in vitro* cell models of the intestinal epithelium to establish the effect of different components.

2.1.4 Factors affecting intestinal barrier function

The mammalian host defence mechanisms evolved with successful confrontations with external factors, and the immune system have been modulated and being shaped depending on the gut microbial pressure and extrinsic (including dietary) impact. The major determinant of the homeostasis is therefore the transport via intestinal barrier (Brandtzaeg, 2011). Many factors influence and modulate the intestinal epithelial barrier. Multiple defence mechanisms regulate its function (fig.2.1.3), although the mechanisms of the permeation control have not yet been fully understood. The defence relies mainly on the function of the epithelial (the mucus layer and epithelial cells) and the immunological (the epithelial secretions and immune cells) barrier (Pijls et al., 2013a; Pijls et al., 2013b). The structural element of these cells, TJs, the intraepithelial pathways altogether have a regulatory role on the intestinal permeability (Farhadi et al., 2003). Also, both hereditary and environmental factors, and their combination effect, modulate the intestinal permeability. Hereditary factors include the epithelial and mucosal immune system, and the environmental factors include diet, infectious agents, drugs and toxins. The other factors that belong to the transition of the hereditary and environmental factors include food allergy, bacterial flora, inflammatory reactions and stress (Farhadi et al., 2003).

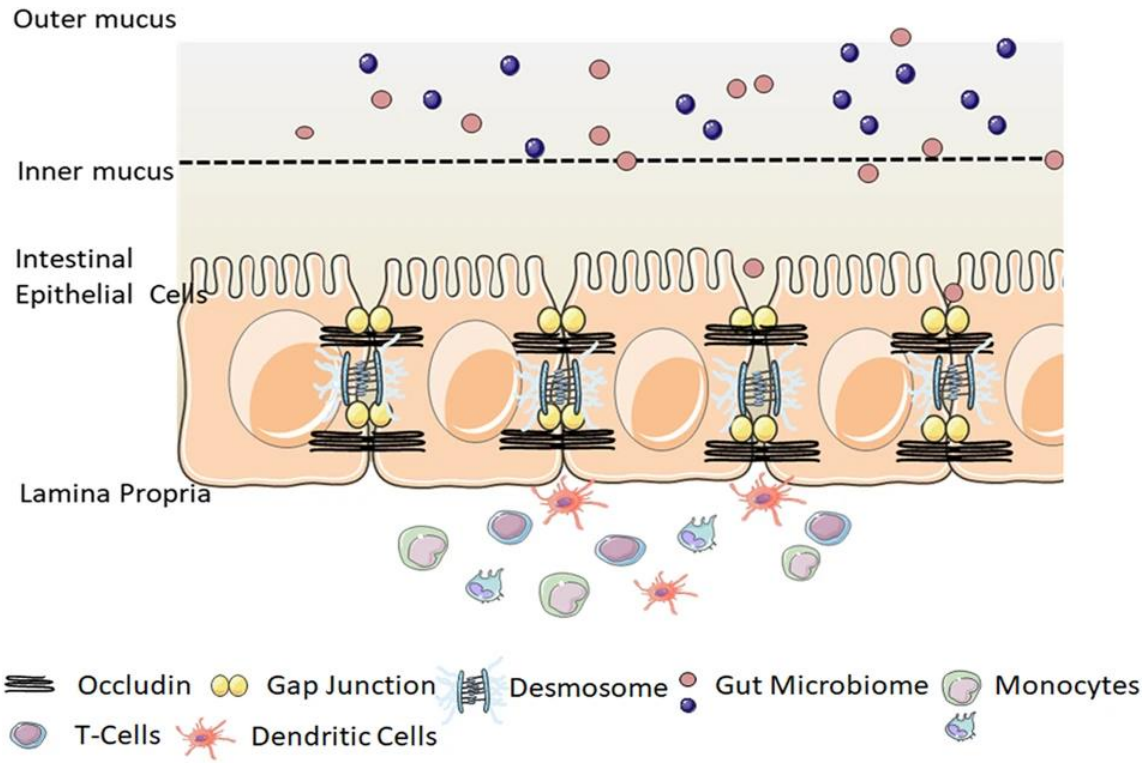

Figure 2.1.3: The intestinal epithelial defense system.

The primary layer of defence in the gut system is the mucus layer, which act as a chemical barrier to critically limit the contact between the microflora and epithelial cells. The second level is the single-layer intestinal lining that consists of different epithelial cells (fig.2.1.1), and act as a physical barrier. The appropriate connections between the epithelial cells are facilitated by many tight junction proteins that seal the paracellular pathway and conduct selective gate and fence functions. The next level is the lamina propria which is a thin layer of connective tissue and play critical role in promoting strong communication between the microflora and the immune cells. Immune cells that belongs to the intestinal epithelial system also function in close relation with the intestinal epithelial cells to maintain intestinal homeostasis and to resist unwanted external substances. Figure adapted from Chelakkot *et al*., 2018.

2.1.4.1 Role of cell-cell junction molecules

The intercellular junctional complex is a crucial regulator for the maintenance of intestinal barrier integrity. The TJ are the multifunctional complex that helps to maintain the barrier by forming a seal between (sealing the paracellular space between) adjacent epithelial cells (fig.2.1.3). TJ types and their role has already been described in general introduction (section-1.2.1). However, the TJs are a dynamic structure and their expression and function are influenced by the external stimuli, such as the components in the diet, microbiota, microbial metabolites (Armstrong et al., 2012).

2.1.4.2 Intracellular mediators

Intracellular mediators, such as nitric oxide (NO), play various roles in regulating intestinal permeability. NO modulates both the epithelial cells and the microcirculation, appearing as a significant regulator of the normal physiology of the GI tract (Farhadi et al., 2003). Constitutive NO synthase-derived low-level of NO help to reduce the consequence of acute

inflammation, while the inducible form of nitric oxide synthase-derived NO overproduction is associated with prolonged inflammatory conditions as in sepsis and IBD (Alican and Kubes, 1996). The mechanism of NO overproduction mediated intestinal barrier dysfunction is complex. Both *in vivo* and *in vitro* studies indicate that increased induced NO synthase activity is linked to LPS as well as other inflammatory cytokines and other mediators (Forsythe et al., 2002).

2.1.4.3 Inflammation (mast cells, microflora/LPS, cytokines)

Mast cells are a keystone in modulation of intestinal permeability. Mast cell mediators are involved in the impaired intestinal barrier associated pathogenesis induced by food allergy, psychological stress and intestinal inflammatory processes. Santos *et al.* (2001a,b) showed that mast cells play an important role in colonic epithelial barrier function. Comparing the mast cell deficient (Ws/Ws) and positive (+/+) rats, they have demonstrated that chronic stress significantly increased epithelial barrier leak in mast cell positive mice compared with non-stressed controls, but not in mast cell deficient ones. The study suggested that mast cells are required for expression of stress induced epithelial transport abnormalities in the rat colon.

Interactions between the commensal microflora and intestinal epithelium affect the barrier permeability. Garcia-Lafuente *et al.* (2001) demonstrated that bacterial colonization could modify the intestinal barrier permeability. Colonization of some bacteria such as *Escherichia coli*, *Klebsiella pneumoniae* and *Streptococcus viridans* significantly increased intestinal permeability in the rat, while *Lactobacillus brevis* had the opposite effect, reduced permeability (Garcia-Lafuente et al., 2001). *Bacteroides fragilis* did not have any effect on the rat intestinal permeability. However, it remained unclear whether the permeability changes were through direct bacterial actions or host immune system response.

LPS is the most prominent endotoxin in the gut environment (Moreira et al., 2012). Considering the number of GM, the amount of LPS in the enteric reservoir can reach ≥ 1g (Berg, 1996). The level of LPS in the gut reservoir vary depending on diet and other factors, a high fat meal consumption can cause postprandial increase in LPS levels of healthy men between 33 and 50 g in comparison to fasted individuals (Moreira et al., 2012). Bacterial endotoxin LPS play an essential role in the intestinal epithelial barrier permeability (Patterson and Watson, 2017). Although the physiological effects of LPS in the IBF remained unclear, however, studies indicate it causes intestinal injury, enhances overproduction of NO and promotes bacterial translocation (Forsythe et al., 2002).

Guo *et al.* (2013) demonstrated the effect of different concentrations of LPS (0 to 1 ng/mL) on the intestinal epithelial barrier function using *in vitro* (Caco-2 cell monolayer) and *in vivo* (mouse intestinal perfusion) intestinal epithelial model system. They showed that LPS at high concentrations in the mucosal surface do not affect TJ-mediated IBF. At concentrations

1 and 50 µg/ml in the apical surface, LPS had no effect on the Caco-2 cell transepithelial resistance or inulin flux (Guo et al., 2013). The increase in intestinal TJ-permeability was mediated by an intracellular mechanism involving an increase in TLR-4 expression in the enterocyte membrane, thereby increasing the co-localization of the membrane-associated protein CD14. *In vivo*, clinically relevant plasma concentrations of LPS (intraperitoneal injection of 0.1 mg/kg) also caused a time-dependent increase in intestinal permeability (Guo et al., 2013). Moreover, Mathan *et al*. (1988) challenged conventional and specific pathogen free (SPF) mice with subcutaneous C5LPS (LPS from *Salmonella typhimurium* strain C5) concentrations ranging from 0.5 to 200 µg. Their study showed no change in both type of mice at concentrations less than 10 µg. However, 100% conventionalized mice challenged with 50 and 100 µg LPS produced an intestinal microvascular lesion leading to fluid exudation into the lumen of the intestine and diarrhoea. On the other hand, challenging SPF mice with 50 µg LPS caused vascular damage in a few blood vessels in lamina propria but did not develop diarrhoea. However, only 200 µg LPS in SPF mice caused fluid accumulation and bacterial growth enhancement (Mathan et al., 1988). Taken together, these studies suggest that LPS-mediated injury takes place at high concentrations. Also, Mathan *et al.* (1988) challenged mice with subcutaneous LPS injection and produced injury at concentrations ranging from 50 and 200 µg, prompting the study of higher levels of LPS for this *in vitro* study.

2.1.4.4 Diet

Diet influences the intestinal barrier permeability by regulating the TJs and the GM. Intestinal microbiota can ferment undigested dietary components to affect the barrier integrity. For instance, butyrate production by the colonic bacteria facilitates TJ assembly and enhance the barrier integrity (Peng et al., 2007). Diet also modulates the GM with direct and indirect regulatory effect on barrier function, as discussed in the main introduction (section-1.3).

In addition to bacteria, dietary components directly regulate the expression and distribution of the TJ proteins, thereby affecting the permeability. Drago *et al.* (2006) demonstrated gliadin (a glycoprotein present in wheat) induced increased barrier permeability due to downregulation of the TJs, ZO-1 and occludin. Both IEC6 and Caco-2 cells released zonulin in the cell medium when exposed to gliadin, with subsequent zonulin binding to cell surface, cell cytoskeleton rearrangement, drop of occludin-ZO1 protein-protein interaction, resulting in an increase in monolayer permeability. Similarly, *ex vivo* intestinal samples from human coeliac patients in remission expressed a sustained luminal zonulin release when exposed to gliadin, causing cytoskeletal rearrangement and ZO-1 reorganization and showed an increase in intestinal permeability. In both cases, pretreatment with the zonulin antagonist prevented the gliadin-mediated increased permeability (Drago et al., 2006). Thus, food

components have direct effect on the TJ expression and distribution, thereby regulating the intestinal permeability.

Although most food components were not studied in detail for their effect on permeability, however, some studies mentioned the effect of diet components on enterocyte transepithelial electrical resistance (TEER), TJ expression and distribution, and eventual effect on intestinal permeability. More than 300 food-derived substances were screened for their effect on the intestinal permeability without having any cytotoxic effect on the Caco-2 cell model (Konishi, 2003). So, effect of AS as a dietary component on the IEC function needs to be investigated.

Surfactants are the known modulators of TJ permeability. Sucrose monoester fatty acid, a food-grade surfactant, was demonstrated to decrease TEER of Caco-2 cell monolayer resulting increased TJ permeability for a major egg white allergen, ovomucoid. The surfactant exposure induced shortening of microvilli, actin disbandment and structural separation of the TJs, thereby facilitating the paracellular uptake of food allergens (Mine and Zhang, 2003). In addition, synthetic surfactants that are used as food additives were reported to imbalance the GM (Csáki, 2011).

Moreover, the trace elements also influence intestinal permeability. For example, dietary zinc has a critical contribution in maintaining the membrane function and in regulating inflammatory cell infiltration (Finamore et al., 2008). Zinc deficiency decreased TEER and altered/disorganized TJ expression and localization in Caco-2 cells. These changes led to the disruption of membrane barrier integrity, resulting in increased migration of neutrophils associated with severe inflammation.

There are many other dietary components such as proteins, amino acids, polysaccharides, fatty acids and flavonoids, which have been associated with modulation of TJ and therefore IBF (Ulluwishewa et al., 2011). Other factors which are non-dietary, such as heredity, oxidative stress, psychological stress, exercise, aging and apoptosis, use of drugs and toxins, have also been identified to play essential roles in regulating intestinal barrier permeability (Farhadi et al., 2003). These factors are interdependent and intricately related, changes/response from one signal therefore influence the others and mediate the intestinal epithelial barrier function.

2.1.5 Importance of artificial sweeteners

There are many types of research that study the beneficial effects of AS. These sweeteners contribute little to no calories in comparison to approximately 25 calories in a teaspoon of sugar (NHS, UK). For the diabetes patients, AS made it possible to enjoy the sweetness of food products, since AS do not raise the blood glucose level (FDA, 2014). Also, some research findings demonstrate their preventive role in tooth decay (Washburn and

Christensen, 2012). However, long-term consumption of AS has been linked to numerous health problems and conditions related to MD (Ruiz-Ojeda et al., 2019; Suez et al., 2014), therefore, further studies are needed to investigate their impact on health.

2.1.6 The sweet taste receptor - T1R2/T1R3

T1R2/T1R3 acts as the intestinal sweet taste sensor and these taste elements are expressed in intestinal L- and K-enteroendocrine cells (Shirazi-Beechey et al., 2014; Moran et al., 2010). The T1R2/T1R3 heterodimer is stimulated by simple sugars (glucose, fructose and sucrose) acting at hundred millimolar range concentrations (300 mM, Li et al., 2002) and AS (acesulfame-K, sucralose and saccharin) at very low millimolar concentrations (Li et al. 2002). The concentration of AS (used in the study) that stimulate the STR are given in table 1.1.1.

Moran *et al*., (2010) demonstrated the co-expression of T1R2, T1R3 and gustducin in the enteroendocrine cells of piglet intestine. The endocrine cells secrete gut hormones, glucagon-like peptides (GLP-1, GLP-2) and glucose-dependent insulinotropic peptide (GIP) in response to dietary carbohydrates. In addition, type 1 G-protein-coupled receptors (T1R) and gustducin are co-expressed with those hormones, indicating the ability of enteroendocrine cells to express these taste elements (Shirazi-Beechey et al., 2014; Moran et al., 2010). GLP-1 and GIP enhance insulin secretion while GLP-2 increases intestinal growth and glucose absorption (Shirazi-Beechey et al., 2014). Stimulation of the STR and gustducin can also activate the signalling pathways leading to up-regulation of the active glucose transporter SGLT1. Moran *et al*. (2010) demonstrated, in rodent models, that supplementation of AS enhances feed palatability by increasing glucose absorption capacity in the gut. Piglets' were fed with AS combination (saccharin and neohesperidin dihydrochalcone), which enhanced Na+/glucose co-transporter (SGLT1) expression and intestinal glucose transport function (Moran et al., 2010).

Several studies have indicated the co-localisation of taste receptors with GLP-1, GIP, Peptide tyrosine tyrosine (PYY) and cholecystokinin. Investigations on T1R3 knockout models of mice have confirmed impaired glucose-stimulated incretin secretion (Jang et al., 2007). Steinert *et al*. (2011) researched healthy human subjects to assess the GI satiety peptides, glucose homeostasis and appetite feelings in response to sweetness-matched carbohydrate sugars and AS intake. Their findings showed that glucose in comparison with water stimulated GLP-1 and PYY release and reduced ghrelin secretion, as well as affected (although insignificantly) appetite with increased satiety and fullness. On the other hand, the equisweet AS intake compared to water did not affect GI peptide secretion with negligible effects on appetite (Steinert et al., 2011). Nonetheless, the cell culture-based co-

culture experiments only mimic the human physiology, whereas, *in vivo*, the regulatory interface of the GI tract is way more complex and regulated by multiple factors.

At high concentration, Glucose-mediated (30–100 mm glucose) activation range of the heterologous T1R2/R3 expression system coincides with the mechanism of apical GLUT2 insertion in the intestine (Li et al. 2002; Mace et al. 2007). Apical GLUT2, therefore, imparts the major pathway of absorption at high concentration of glucose, while AS can rapidly induce apical GLUT2 insertion at low glucose concentration (20 mm) (Mace et al. 2007). Apical GLUT2 insertion is the outcome of PKC-βII activation which is stimulated through a T1R2/R3–α-gustducin–PLC-β2 pathway (fig.2.1.4) and simple sugars and AS act synergistically in this stimulation (Helliwell et al., 2003). These imply that AS although not contributing directly to calorie intake but do stimulate the biochemical pathways like glucose.

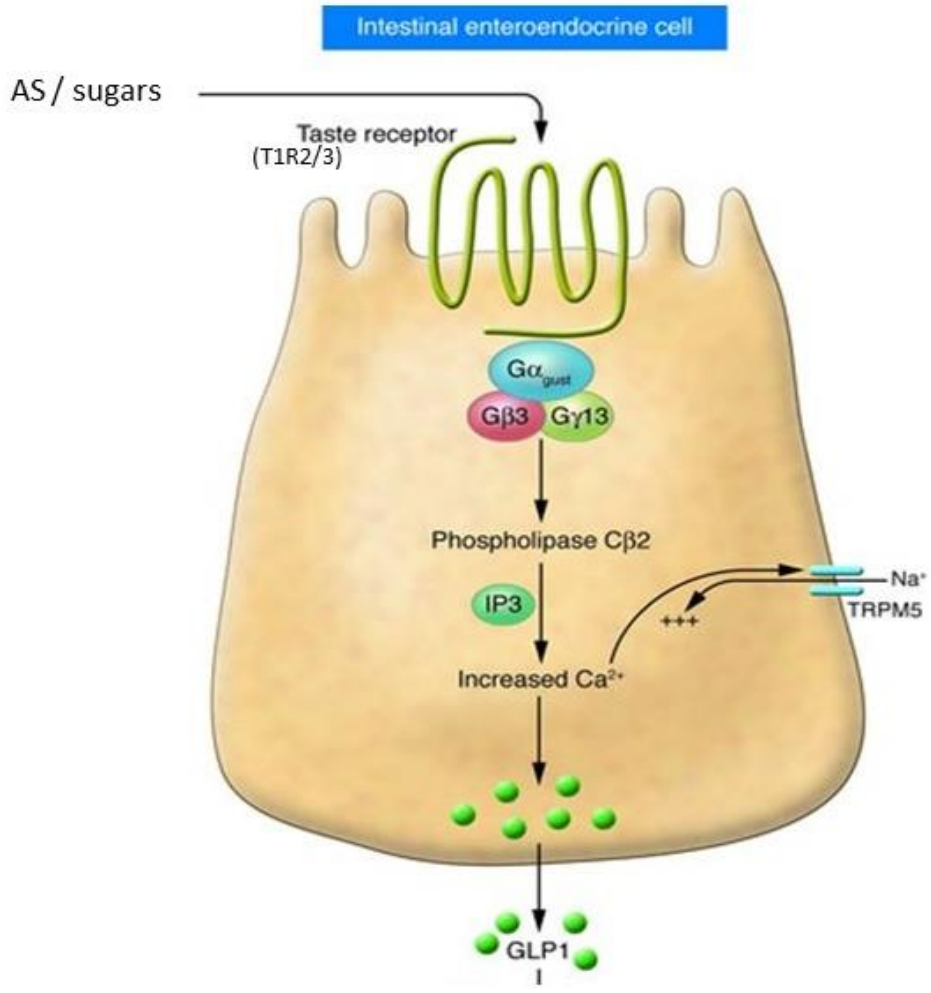

Figure 2.1.4: Signalling by a sweet taste receptor.

Sweet molecule (like sugar) binds to a sweet taste receptor (T1R2/T1R3) which initiates the sweet taste signal transduction pathway via G-proteins (α, β, and γ). Phospholipase beta2 is involved, and sodium and calcium ions play a role. IP3- inositol triphosphate, TRPM5- transient receptor potential cation channel subfamily M member 5. Figure adapted from (Cummings and Overduin, 2007).

AS are commonly used in foods, beverages, pharmaceuticals and cosmetics (Suez et al., 2014). According to global AS market reports, saccharin, sucralose, aspartame, neotame, acesulfame potassium, and cyclamate are the widely accepted AS that will have a predicted global market of USD 3 billion by the end of the year 2025 (Research and markets, 2019). For the current study, four of the above-mentioned AS were taken under consideration; all of them are approved as safe by the US Food and Drug Administration (FDA, 2006).

Saccharin is the oldest AS (Lawrence, 2003), it is heat-stable and non- metabolised in the GI tract, thus excreted unchanged in the faeces. Sucralose is also thermally stable and excreted with the faeces without being metabolized. It has a disaccharide structure like sucrose (fig.1.1.6), although three hydroxyl groups are replaced by chlorine which results in structural resemblance with an organochlorine chemical compound Dichlorodiphenyltrichloroethane (DDT). It is the closest to sucrose in taste (Roberts et al., 2000). Conversely, aspartame which is an ingredient of approximately 6,000 foods and beverages sold worldwide (PubChem database, 2019), is unstable, changes in temperature and pH changes its structure. In addition, upon ingestion, aspartame breaks down into the comprising compounds phenylalanine, aspartic acid and methanol (Wal et al., 2019). Phenylalanine plays an important role in amino acid metabolism and protein structuring as well as in neurotransmitter regulation (Humphries et al., 2008), thereby indicating hazards to health. Since aspartame decomposes in liquids during storage and contains phenylalanine, it is the most controversially discussed AS in scientific literature. Nonetheless, based on toxicological and clinical studies, both FDA and European Union consider aspartame as safe for consumption (Scheurer et al., 2009).

Neotame is one of the most recent sweeteners which is a dipeptide AS composed of N-(3,3-dimethylbutyl)-L-aspartic acid and methyl L-phenylalanate units linked by a peptide bond. Whilst closely related to aspartame in structure (derived from aspartame), neotame has an additional branched hydrocarbon chain (3,3-dimethylbutyraldehyde) attached by replacing -NH3 group of aspartames by a -NH-alkyl group at the specific region (fig.1.1.6) (O'Donnell, 2006). It is 7000 to 13000 times sweeter than sucrose (BeMiller, 2018; FDA, 2018). The ability of stimulating sweet taste perception by aspartyl-based dipeptide compounds are based on their conformation ("L-shaped" conformation). Neotame demonstrates well-oriented hydrophobic and hydrophilic regions in its solid-state conformation which could be responsible for the intense sweetness of this dipeptide compound (Prakash et al., 1999). Like aspartame, neotame is metabolized to mainly de-esterified neotame, and other compounds namely N-(3, 3 dimethylbutyl)- L aspartic acid and a beta-glucuronide conjugate of 3, 3-dimethylbutanoic acid (O'Donnell, 2006; Duffy and Anderson, 1998).

Similarly, eight available AS including saccharin, sucralose, aspartame and neotame, and five steviol glycosides were determined from 24 samples using high-performance liquid

chromatography and tandem mass spectrometry with electrospray ionization (Kubica et al., 2015). The samples belonged to carbonated and non-carbonated soft drinks and carbonated beverages bought from the local shops in Poland with special attention to ensure diversity to determine the EU-authorised high-potency sweeteners. Samples (18 of 24) were labelled with steviol glycosides, but not for aspartame or saccharin. However, carbonated alcoholic drink 1 contained aspartame and saccharin at a concentration 65.56 ± 0.60 mg/L and 5.95 ± 0.34 mg/L, respectively, while carbonated alcoholic drink 2 contained only aspartame (9.88 ± 0.17 mg/L) but no saccharin (Kubica et al., 2015). Also, de Queiroz *et al*. (2015) demonstrated the amount of AS in 11 foods and beverages using HPLC. They showed that light tomato and barbecue sauce contain an amount of acesulfame-K (115.8 ± 9.0 and 198.9 ± 30.8, respectively) which is above the legal limit of AS concentration to be used. Taken together, the above findings suggest that the concentration of AS present in different food substances in market are higher than the approved AS concentration to use.

2.1.7 Intestinal epithelial cell models

There are several transformed continuously growing IEC lines that are often used as IEC model such as Caco-2, HT29, T84. These *in vitro* differentiated human IEC monolayers are suitable for testing the intestinal processes like absorption and active and passive transport (Meunier et al., 1995).

The Caco-2 cell line is enterocyte-based colon carcinoma cells which undergoes spontaneous enterocytic differentiation in culture. Once Caco-2 cells reach confluence, they form domes, thereby enabling transepithelial ion transport. Differentiated Caco-2 cells demonstrate well-defined brush border on the apical surface and have the TJ proteins. Also, they demonstrate the typical properties of the absorptive enterocytes, including expression of the enzyme activities/markers and transport systems, therefore represent an appropriate model for the co-culture studies (Darfeuille-Michaud et al., 1990). Importantly, this cell line represents the similar level of alkaline phosphatase, sucrase-isomaltase, and aminopeptidase activities like primary enterocytes (Lea, 2015). Having all the other properties in place, Caco-2 cells lack the ability to produce mucin, but TJ expression made them a good model for studying barrier function.

The mucin secreting HT29 resembles the goblet cells, develop confluent monolayer, as well as demonstrate the TJ formation. However, HT29 do not perform spontaneous differentiation under standard culture conditions, although differentiation can be induced by adding or substituting various chemicals from the culture media. Also, HT29 can form enterocyte-like cells and goblet cells provided with appropriate induction (Huet et al., 1987). Moreover, Caco-2 cells express a higher degree of functional TJ complexes than HT29

(Lea, 2015). Another cell line, T84, differentiate spontaneously after confluence in culture; however, their brush border is not as well defined as the Caco-2, neither do the cells express the microvillus membrane hydrolases (Meunier et al., 1995).

There are thus a range of potential cell types which can be utilised for *in vitro* studies. As the current study considered the effect of artificial sweeteners on IECs focusing on barrier function, Caco-2 was found to be particularly suitable.

2.1.8 Examples of Caco-2 study with food components

Many studies have utilised Caco-2 cells to mimic physiologic conditions. Due to their similarities with absorptive enterocytes, Caco-2 cell has been widely accepted as a primary tool for absorption studies of dietary components and pharmaceutical preparations. The Caco-2 cell line was used as *in vitro* digestion model for screening foods and food combinations for iron bioavailability before definitive human trials were used (Mahler et al., 2009). They also reported that the qualitative assessment of iron bioavailability from Caco-2 model correlated tightly with human data.

Yu *et al*. (2013) also used Caco-2 model to investigate the effect of potential absorption enhancers (glucose, sodium cholate, ethanol, menthol, EDTA, and SDS) on the paracellular permeability of macromolecules. The tested enhancers increased the permeability of Caco-2 cells by affecting the TJs; changing the distribution of ZO-1, claudin-1, occludin, and E-cadherin. Ethanol at high concentrations (≥40%) also damaged epithelial barrier function by a direct cytotoxic effect. Lower concentrations of ethanol (0 to 10%) were demonstrated to have a dose-dependent decrease in cell epithelial resistance and an increase in paracellular permeability. Also, ethanol caused a progressive disruption of the TJ protein ZO-1, as well as disassembly and displacement of perijunctional actin and myosin filaments (Ma et al., 1999). Similar to ethanol, many alcoholic beverages and fermented foods can also contain acetaldehyde as an additive which disrupts junctional interactions, leading to decreased TEER and increased TJ-permeability (Sheth et al., 2007).

Vors *et al*. (2012) demonstrated the *in vitro* lipolysis of four dietary emulsions and used Caco-2 cell monolayer to assess the absorption and metabolism. The emulsions (with emulsifier either lecithin or sodium caseinate) were broken down with gastric and pancreatic enzymes and cells were exposed to the diluted (1:20) lipolysis media. They observed similar levels of gastric and duodenal lipolysis, which agreed with previous *in vivo* findings of Carrière *et al*. (2000). So, Vors *et al*. (2012) emphasised the possibility of Caco-2 model in lipid metabolism for assessing different dietary emulsions digested by gastrointestinal lipases.

Taken together, these literatures demonstrate the strong impact of dietary components on barrier function in the intestinal epithelium, and the importance of IEC model, Caco-2 cells.

Food compounds which are highly consumed by the public should therefore be investigated in detail to understand their impact on the gut epithelium.

2.1.9 AS consumption and changes in energy metabolism

AS replaces sugar, however, AS might have paradoxical impact on intestinal physiology. There are several postulated claims that undermine the weight management effect of AS (reviewed by Rogers, 2018). For example, the sweet taste confusion hypothesis notes that AS provide sweet taste but no calorie which might impair energy intake and body weight regulation (Swithers, 2013). Also, AS stimulates the sweet taste receptor and triggers the downstream signalling whilst there are no sweet molecules (Mathur et al., 2020; Cornier, 2008). AS results in insulin release due to their sweet taste which might lead to decreased receptor activity because of insulin resistance (Mathur et al., 2020).

While AS activate the STR, but partially stimulate the food reward pathway, and have no activity on the post-ingestion pathway since they lack calorie. These variations in downstream pathways in comparison to sugar may increase hunger, food craving and caloric consumption (Stice et al., 2008). These alterations might cause improper energy absorption and deposition leading to weight gain (Frisch, 2016). The blood glucose control of previously AS non-consumer healthy human subjects (n = 7) were examined upon AS exposure. Four out of seven volunteers at 5 to 7 days showed worse glucose tolerance of AS exposure in comparison to first 4 days, demonstrating the heterogeneity in the GM that makes some people more vulnerable after AS exposure than others (Suez et al., 2014).

Another hypothesis claims that consumption of sweet enhances a sweet tooth (sweet tooth hypothesis); so, encourage increased intake of high-calorie foods and beverages which can ultimately contribute in weight gain (reviewed by Rogers, 2018). Consumption of AS increase appetite and motivate to eat more compared to controls (reviewed by Pearlman et al., 2017). Also, because of changes in downstream effects on digestion, absorption and metabolism, AS do not induce satiety in the same way that sugar does (Swithers, 2015). In addition, sucralose stimulated gut hormone release, such as GLP-1 and GIP, are lower than that of glucose indicating AS can cause faster gastric emptying and decreased satiety (Wu et al., 2012). These literature supports the AS interference with basic learned physiology of the gut.

The conscious overcompensation hypothesis claims that consumers might consciously overcompensate for ‘calories saved’ by intaking AS, resulting in an overall increase in energy intake (Mattes and Popkin, 2008). This hypothesis can be supported by the literature showing AS containing beverage consuming healthy males (n = 30) had similar daily energy intake due to conscious overcompensation during subsequent meals (Tey et al., 2017). Porikos et al. (1977) more clearly showed this conscious decision of overcompensation

phenomenon in obese patients (n=8). Patients' energy intake was similar or slightly higher than with AS diet when they were aware of consuming AS-containing foods. Interestingly, a 25% decrease in caloric intake in comparison to conventional diet was observed when the diet was secretly changed to AS-containing products (Porikos et al., 1977). Although these claims are yet to prove, however, effects of AS on glucose intolerance, the activation of T1R2/T1R3, and perturbations of the GM composition remain controversial (reviewed by Ruiz-Ojeda et al., 2019).

The gut peptides also play important role in regulating digestion, absorption, disposal and intestinal epithelial integrity. These functions are initiated by a range of G protein-coupled receptors (GPCR) and mediated by direct or indirect effects on the target cells. Brubaker and Drucker (2004) exemplified the effect of specific GPCR glucagon-like peptides-1 and 2 (GLP-1 and GLP-2) on regulation of signalling to cell proliferation and apoptosis. GLP-1 promotes pancreatic β-cell survival via multiple intracellular pathways, including activation of Akt. Similarly, GLP-2 was demonstrated to confer resistance to cellular damage and enhance proliferation in different cells (Brubaker and Drucker, 2002). *In vivo*, animal models demonstrated proliferative and antiapoptotic effects upon GLP-1 and GLP-2 administration (Drucker, 2003). GLP-1 promoted β-cell expansion and resisted injury in diabetes models (Buteau, 2008; Li et al., 2003), while GLP-2 administration promoted the IEC regeneration and resisted apoptosis in intestinal disorders, suggesting the contribution of these peptides in protection and regeneration of particular cell types (Brubaker and Drucker, 2004).

AS, like natural sugars, were also demonstrated to promote the secretion of GLP-1, GLP-2 and glucose-dependent insulinotropic peptide (GIP). GLP-1 and GIP play an important role in insulin secretion, while GLP-2 promotes IEC proliferation as well as glucose absorption (Shirazi-Beechey et al., 2014). Studies on rodent models have demonstrated that AS inclusion in the diet enhances the Na+/glucose co-transporter (SGLT1) and increase glucose absorption in the gut. AS were regularly added in the piglet's diet to enhance the palatability of food. This has been supported by the findings on piglets, where animals maintained on food with AS supplementation (saccharin and neohesperidin dihydrochalcone combination) showed enhanced SGLT1 expression and intestinal glucose absorption. They also demonstrated the co-expression of GLP-1, GLP-2 and GIP with the T1R receptors (T1R2/T1R3) and gustducin expression in enteroendocrine cells of the piglet intestine.

Chemicals eliciting sweet taste perception such as glucose, other carbohydrates like fructose, AS and proteins like monellin and thaumatin vary largely in their chemical structures (fig.1.1.6) (Keast et al., 2004). In addition, they differ in receptor-binding mechanism and taste signal transduction mechanism (fig.2.1.5), but all of them generate sweet taste perception to different degrees (Keast et al., 2004; Zhao et al., 2003). Details about AS was mentioned in the general introduction (section-1.4).

Both sugar and AS stimulates the sweet taste perception via STR. So, if the sucrose mediated negative effects on health is via sweet taste sensing, it is likely that AS consumption could also cause similar effect. Nevertheless, the receptor has different binding sites for different sweeteners and inhibitors. Sucralose binds to both T1R2/T1R3 whilst aspartame and neotame bind to VFT domain of T1R2, however, if sweetener-binding fails to activate the receptor, sweetness perception (the downstream signalling cascade) does not occur (Brown and Rother, 2012). Therefore, further studies are needed to investigate the mechanisms of AS stimulated sweet sensing.

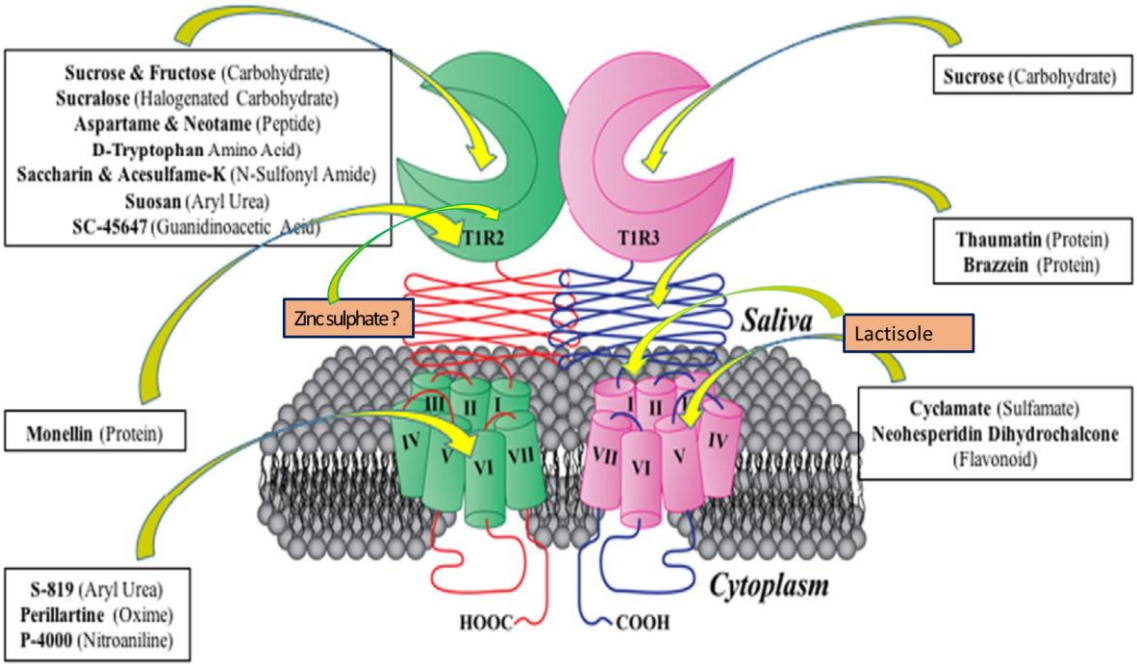

Figure 2.1.5: Binding site of different sweeteners and inhibitors to the human sweet taste receptor (T1R2/T1R3).

There are six agonist binding sites identified so far by different docking experiments, and the sweeteners represent specific binding nature. Similarly, the sweet taste inhibitors also have specific binding site to deactivate the stimulation. Figure adapted from DuBois, 2016.

2.1.10 Sweet taste sensing and permeability

AS were reported to induce glucose intolerance by altering the conformation and function of the GM (Suez et al, 2014). In mice, AS-intake was linked with dysbiosis which was confirmed by antibiotic treatment; antibiotics (200 mg/ml ciprofloxacin and 1000 mg/ml metronidazole for Gram-negative, and 500 mg/ml vancomycin for Gram-negative bacteria) killed the commensal microbiota and abrogated the metabolic effects (Suez et al, 2014), however, AS-mediated changes in gut bacteria remain largely unknown.

In addition, Palmnäs *et al*. (2014) demonstrated the effect of aspartame doses in rats (equivalent to 5-7 mg/day, approximately 2-3 diet cola for human subjects). After 8-week exposure, aspartame increased the fasting glucose level, caused insulin intolerance and

deranged GM with an increase in abundance of *Enterobacteriaceae* and *Clostridium leptum*. In a human study, 4-day food intake of American adults was assessed and the relationship between AS (especially aspartame and acesulfame potassium) intake and microflora was demonstrated (Nettleton et al., 2016). No differences in the abundance of bacteria were noted between the AS consumers and non-consumers but a higher microbial diversity was observed in those consuming AS. These studies indicate that AS consumption causes bacterial diversity which may exert a regulatory metabolic change in the host such as increased endotoxin (such as LPS) in the gut. The endotoxin could be directly diffused into the circulatory system due to intestinal paracellular permeability or through absorption by enterocytes (Moreira et al., 2012). Moreover, changes in GM, increased intestinal permeability and metabolic endotoxemia possibly play a role in the development of a chronic low-grade inflammatory state in the host that contributes to the development of obesity and associated chronic MD.

Furthermore, LPS-mediated low-grade inflammation has been demonstrated to induce insulin resistance in adolescents (mean age 15.5 ± 0.8 year) (Herder et al., 2007). In addition, small intestinal bacterial overgrowth (SIBO) was linked to increased intestinal permeability in humans with non-alcoholic fatty liver disease (NAFLD) (Miele et al., 2009). Their study showed that NAFLD patients with increased gut permeability had a prevalence of SIBO (88.8%) greater than double ($p<0.001$) that of patients with normal permeability (29.4%). Moreover, subjects with SIBO had increased intestinal permeability ($p<0.05$) and significant increase of metabolic syndrome ($p<0.001$) (Miele et al., 2009) (fig.1.1.2). Therefore, AS alters GM which could play important role in development of MD, however, the mechanisms needs further investigations.

Nonetheless, whilst the effect of AS on epithelial layer permeability has not been studied, a link between the taste receptor and endothelial barrier permeability has been established (Harrington et al., 2017). However, there are many differences between endothelial and epithelial permeability mechanisms. Furthermore, the AS sucralose was reported to play a role in the translocation and activation of the PKC substrate, myristoylated alanine-rich C-kinase (MARCK), in MIN6 cells (Nakagawa et al., 2009). PKC activation has been linked to the disruption of TJ protein complexes, via activation of the ERK1/2-MAPK pathway in human corneal epithelial cells (Lei et al., 2014). Therefore, it stands to reason that a similar effect may be seen with the intestinal epithelial layer which may lead to increased permeability. Perhaps PKC is a key signalling molecule in sweetener-mediated regulation of junctional complexes, but differences in the complexes between epithelial and endothelial cells cause opposing effects in permeability.

2.1.11 Cell apoptosis

Homeostasis in multicellular organisms is maintained through an active and complex molecular programme termed apoptosis. This is primarily responsible for physiological cell death. Programmed cell death is a vital component of the physiological processes allowing the organism to properly regulate morphogenesis, tissue remodelling, development and functioning of the immune system, atrophy, embryonic development and overall protection from dangerous cells that threaten homeostasis (Elmore, 2007; Hengartner, 2000; Thompson, 1995; Krammer et al., 1994). Inappropriate apoptosis in humans can contribute to various disorders including neurodegenerative diseases, cancer, viral infections, autoimmune diseases and other degenerative diseases. Cell's decision to signal apoptosis follows multiple independent pathways driven by a number of proteins (appendix table-A8.10), and can be initiated and/or influenced by a wide variety of regulatory factors including environmental, physiological and pathological factors within or outside cells (Strasser et al., 2000; Kerr et al., 1972) (fig.2.1.6).

Membrane asymmetry is an early characteristic of apoptosis; phospholipid phosphatidylserine (PS) translocates from the phospholipid bilayer of the inner cell surface to the external surface (Rysavy et al., 2014). The cells also undergo cytoplasmic blebbing and vacuolization, condensation of the chromatin material and nucleosomal fragmentation (Nandi et al., 2010). In the second stage, these apoptotic bodies are either shed off or absorbed by other cells, where they experience various changes and are eventually being degraded by the ingesting cell-derived lysosomal enzymes (Kerr et al., 1972).

IECs continuously proliferate and differentiate in the small intestine (fig.2.1.1) (Kim et al., 1998). For the maintenance of a sufficient number of enterocytes, apoptosis spontaneously occurs to counterbalance proliferation and maintain the survival and generation of cells (Hockenbery, 1995; Potten, 1992). Other than internal decision, external mechanical and chemical damage can induce cell apoptosis (Van Engeland et al., 1998). For example, oxidative stress from reactive oxygen species (ROS), such as hydrogen peroxide (H_2O_2), triggers apoptosis in mammalian cells (Lee et al., 2000).

Two broad pathways play a role in activation of the apoptosis mechanisms (Sanz et al., 2008) (fig.2.1.6). The extrinsic pathway is mediated by the external cell signals such as nutrient loss, X-rays, heat, hormones, and lethal factors. Conversely, the intrinsic pathway is triggered by internal cellular death signals such as removal of growth factors, DNA damage, mitochondrial damage, oxidative stress, and scarcity of energy generation (Sanz et al., 2008). Details of apoptosis pathway were mentioned in appendix A (section-8.1.7).

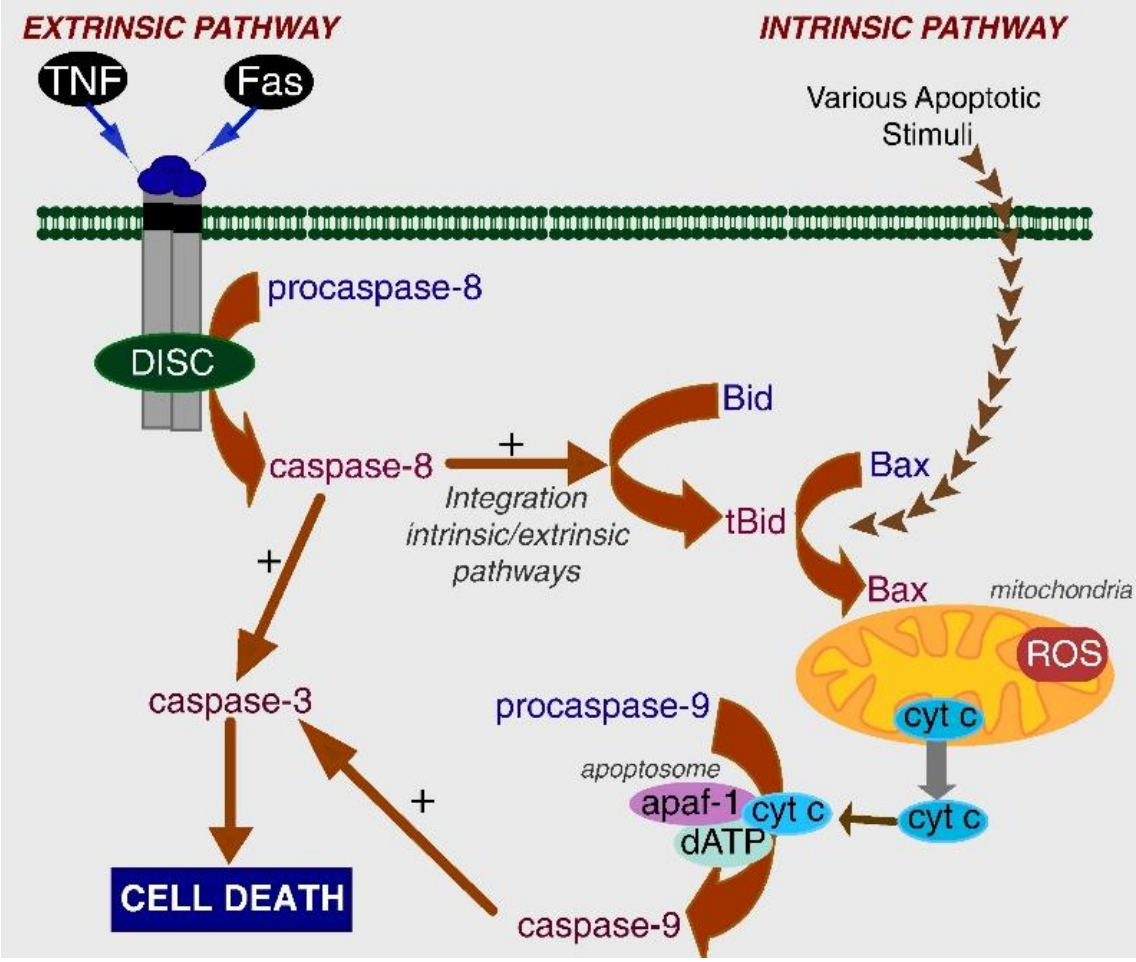

Figure 2.1.6: Diagram outlining the extrinsic and intrinsic pathways of apoptosis.

Both extrinsic (death receptor) pathway and intrinsic (mitochondrial) pathways join to a common pathway involving the caspase-3 proteinase activation and the apoptosome formation leading to execution of cell death. TNF, tumour necrosis factor; Fas, fatty acid synthetase; DISC, death-inducing signalling complex; ROS, reactive oxygen species; apaf-1, apoptotic protease activating factor; Bax, BCL2 associated X protein; Bid, BH3 interacting domain death agonist; cyt, cytochrome; ATP, adenosine triphosphate. Figure adapted from Marí *et al.*, 2013.

Previous studies have described that AS reduce epithelial cell viability and induce DNA damage (van Eyk, 2014). The study showed the effects of five AS on the morphology, cell proliferation and DNA in cells by epithelial cells lines such as HT-29 and HEK-293. Cells were exposed to sodium cyclamate, sodium saccharin, sucralose and acesulfame-K (0–50 mM) and aspartame (0–35 mM) over 24, 48 and 72 hours and colon cells were demonstrated to show cell morphology alteration, viability reduction and DNA fragmentation (van Eyk, 2014). Horio *et al*., (2014) demonstrated aspartame-induced apoptosis in PC12 cells, with cyt c content higher in the cytosol of aspartame-treated cells in comparison to control cells. The study observed that low concentrations of aspartame (0-8 µg/ml) induced cytotoxicity, whilst trace amounts (~1 ng/ml concentration) induced apoptosis-related DNA fragmentation in the PC12 cells. Therefore, AS can affect several biochemical processes of IEC that can exert negative impact on gut health, so further studies on AS effect of gut physiology is timely.

2.1.12 Sweet taste inhibitors

Inhibitors of the STR have been studied to investigate the interference of taste mechanisms. Lactisole was identified as a human-specific sweet taste inhibitor by experimenting its effect on HEK293 cells and human/mouse T1R2 and T1R3 clones in the presence of sucrose, cyclamate and acesulfame K (Jiang et al., 2005) and T1R3 transmembrane domain of the STR subunit was reported as the Lactisole binding site (fig.2.1.5) in human (Fernstrom et al., 2012; Assadi-Porter et al., 2010; Xu et al., 2004). In another experiment, Lactisole was shown to inhibit the effect of several sweeteners such as acesulfame K, sucralose and glycyrrhizin on T1R-mediated insulin secretion of MIN6 cells; it was reported that Lactisole reduced the cytoplasmic calcium ion concentration induced by sucralose and acesulfame K but intracellular cAMP remained unaffected by it (Hamano et al., 2015). Lactisole is thus a useful tool to study AS-stimulated T1R receptor inhibition.

While Lactisole is specific sweet taste inhibitor for humans, $ZnSO_4$ was reported to inhibit the sweet taste perception of a wide range of sweet molecules without showing binding specificity (Keast, 2003). For example, $ZnSO_4$ was reported to block the augmented contraction effect of saccharin in bladder cells (Elliot et al., 2011). It is possible that $ZnSO_4$ may interact with the extracellular component of the STR (fig.1.5) to inhibit the sweet taste stimulated nerve response in mice and sweet taste perception in humans (Elliot et al., 2011; Keast et al., 2004). Interestingly, zinc has been reported to improve the maintenance of the intestinal barrier integrity (Ulluwishewa et al., 2011). Caco-2 cells cultured in a media deficient of zinc demonstrated decreased TEER as well as alterations in the expression and localization of the TJ proteins ZO-1 and occludin (Finamore et al., 2008). These indicates that zinc not only inhibits sweet taste perception but also plays an important role in intestinal barrier integrity. So, sweet taste signalling inhibition with this inhibitor might be linked with improved intestinal barrier integrity, and therefore, is a suitable sweet taste inhibitor to study.

Rationale of chapter 2

AS are indigestible, but IEC are directly exposed to the synthetic AS components in the diet. Therefore, assessing their effect on cell viability and understanding the mechanisms are important to indicate the effect of AS on the intestine. Moreover, morphological observations can suggest AS-mediated physical injury, and whether the apoptosis pathway is involved via nuclear fragmentation or mitochondrial changes. In addition, cell viability interferes with monolayer permeability, also dietary components directly interfere with permeability through a variety of mechanisms including stress fibre formation (Banan et al., 2001). Consequently, it was important to study the stress fibres due to AS exposure. Nonetheless, AS stimulates sweet taste perception like natural sweeteners, so their role on AS-mediated changes in cells were important to investigate, with an aim to find a remedy of the AS effect via receptor inhibition.

Aims and objectives

The objective of this chapter is to determine the effect of different physiologically relevant concentrations of the four AS on the IEC model, Caco-2.

The hypothesis of the current chapter is that **artificial sweeteners have negative effect on an *in vitro* model of the intestinal epithelium**. To address the hypothesis, the aims of the chapter are –

- To understand whether AS interfere with IEC viability and to identify whether cell death is via apoptosis
- To observe whether AS cause morphological changes of the cell
- To ascertain whether AS cause cell monolayer permeability
- To evaluate whether the effect of AS on IECs is via the sweet taste receptor

2.2 Materials and methods

2.2.1 Chemicals and supplies

Cell culture flasks and 96-well plates were purchased from Corning Life Sciences (Lowell, MA). EMEM (Eagle's Minimal Essential medium) was purchased from ATCC® 30-2003 (American Type Culture Collection). Caco-2 cells, non-essential amino acids, Foetal Bovine Serum (FBS), Trypsin EDTA (Ethylenediaminetetraacetate) (0.25 % (w/v) Trypsin/0.53 mM EDTA), Dimethyl sulfoxide (DMSO), Penicillin/Streptomycin solution, lipopolysaccharide (LPS), Lactisole and Cell counting kit 8 (CCK-8) were purchased from Sigma (USA). The AV apoptosis assay kit was purchased from BD Pharmingen (San Diego). Phosphate Buffered Saline (PBS) was obtained from Gibco (Life Technologies, Sigma).

The artificial sweeteners (AS) saccharin, sucralose, aspartame and neotame were purchased from Sigma-Aldrich. Sterile, non-treated polystyrene 96-well plates were purchased from CytoOne (USA) and Transwell plates, and flat-bottom 24-well plate from Corning (USA). Black 96-well plates for indirect ELISA were bought from ThermoScientific (USA). Fluorescein Isothiocyanate (FITC) conjugated Dextran (FD) proteins 4000 and FD 20000 were also purchased from Sigma-Aldrich, the primary (goat polyclonal IgG, both extracellular and intracellular) and secondary (donkey anti-goat IgG-FITC) antibody for the indirect ELISA were supplied by Santa Cruz Biotech, UK. The FITC Annexin V (AV) apoptosis detection kit was purchased from BD-Pharmingen™, EU. Other chemicals namely Bovine Serum Albumin, paraformaldehyde, Triton X-100 are from Sigma. DAPI (ProLong® Gold) was purchased from Thermo Fisher Scientific (UK), Phalloidin (Phalloidin-iFluor™ 594 Conjugate) was from Cayman Chemical and DiOC6 was from Sigma-Aldrich. Zinc sulphate ($ZnSO_4$), and the carbohydrates, glucose, fructose and sucrose, were supplied by Sigma.

The AS concentrations were determined considering the amount available in the food and beverages, and in a sachet, as well as the achievable amount depending on the FDA approved ADI (table 1.1.1). A chewing gum can contain as low as 0.01 mg/kg of AS (Rasouli and Akbari-Adergani, 2016) whilst a soda can contain 0.5 µM (Franz, 2010) to 2 mM (Gardner et al., 2012), indicating that the intestine can be exposed to a range of concentrations. Considering the amount of AS in a sachet (e.g., 40 mg aspartame) and ADI of number of packets (e.g., 68 for aspartame) (table 1.1.1) shows that intestine can be exposed to a very high concentration of AS. If the ADI amount (AS sachet X number of packets) is equally split into 5 portions, the amounts of saccharin (0.068 g), sucralose (0.066 g) and aspartame (0.520 g) (Gardner et al., 2012) are greater than the amounts used to prepare 50 mM of the AS in the study (table-A8.3). Also, previous studies used a range of neotame concentrations such as 0.75 mg/kg in CD-1 mice (Chi et al., 2018) and 10 to 50

mg/kg with a very high concentration of 500 mg/kg neotame in pigs (Zhu et al., 2016). Considering 0.081 as the conversion factor between human and mouse (Nair and Jacob, 2016), the equivalent concentration for human is around 0.06 mg/kg bw/day which is also greater than the amount of neotame used in the present study (table A8.3). Zinc sulphate concentrations were previously used by Keast *et al*. (2003).

2.2.2 Cell cultures

Caco-2 cells were grown in an incubator (Thermo Scientific, HERA Cell 150i CO_2 incubator) at 37 ˚C in an atmospheric condition of above 90% humidity along with 95% O_2 and 5% CO_2 gas. The cells were cultured in different flasks (size and amount of chemicals for different surface in table-A8.1) depending on cell numbers containing EMEM with 10% FBS and 1% antibiotic (penicillin/streptomycin) solution. In addition, cells were grown in two other tissue culture media (DMEM and RPMI) and tested their growth for 3 days (fig.A8.1).

Cell maintenance

Cells were fed by replacing the used medium with the pre-warmed (37 ˚C) fresh medium. Once grown to confluence (70 – 80 %), cells were split 1:3 or 1:6 depending on necessity of the experiments (fig.2.2.1).

Cell passaging and cell freezing were performed using standard tissue culture techniques (appendix A8.1.2). Trypsin was used to detach cells from the flasks, and cells were cryopreserved in freezing medium (90% complete EMEM and 10% DMSO).

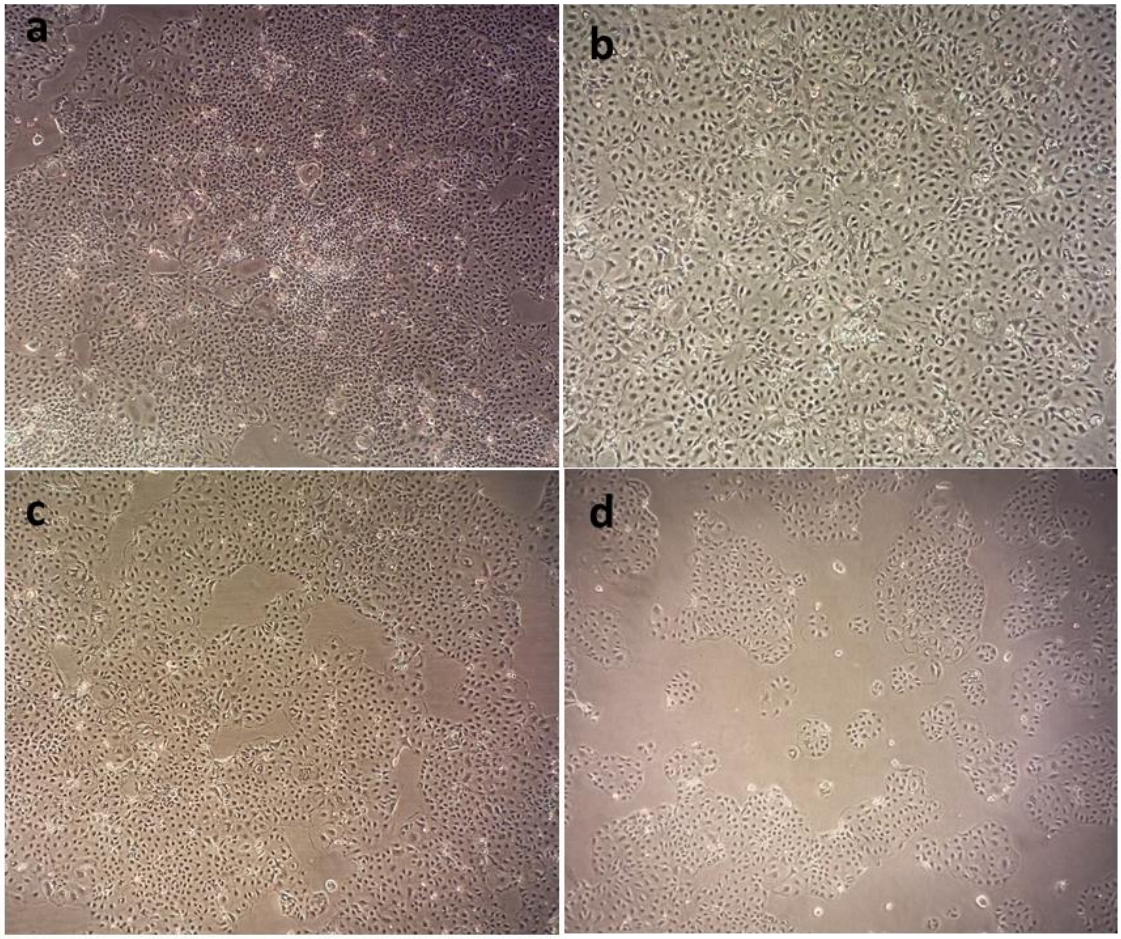

Figure 2.2.1: Caco-2 cells of different density.

Cells were grown in EMEM medium supplemented with FBS and antibiotics. Panel shows very high to low density cells; confluence was considered as over confluent (a), confluent (b), about 80% (c), and about 70% confluent in the study. Images were collected using phone from the microscopic view (×40 magnification).

Cell counting

Caco-2 cell count was performed using haemocytometer, 10 µl cell suspension was placed to the counting chamber and the four quadrants were counted under inverted microscope (fig.2.2.2) (an example calculation appendix, A8.1.2.3).

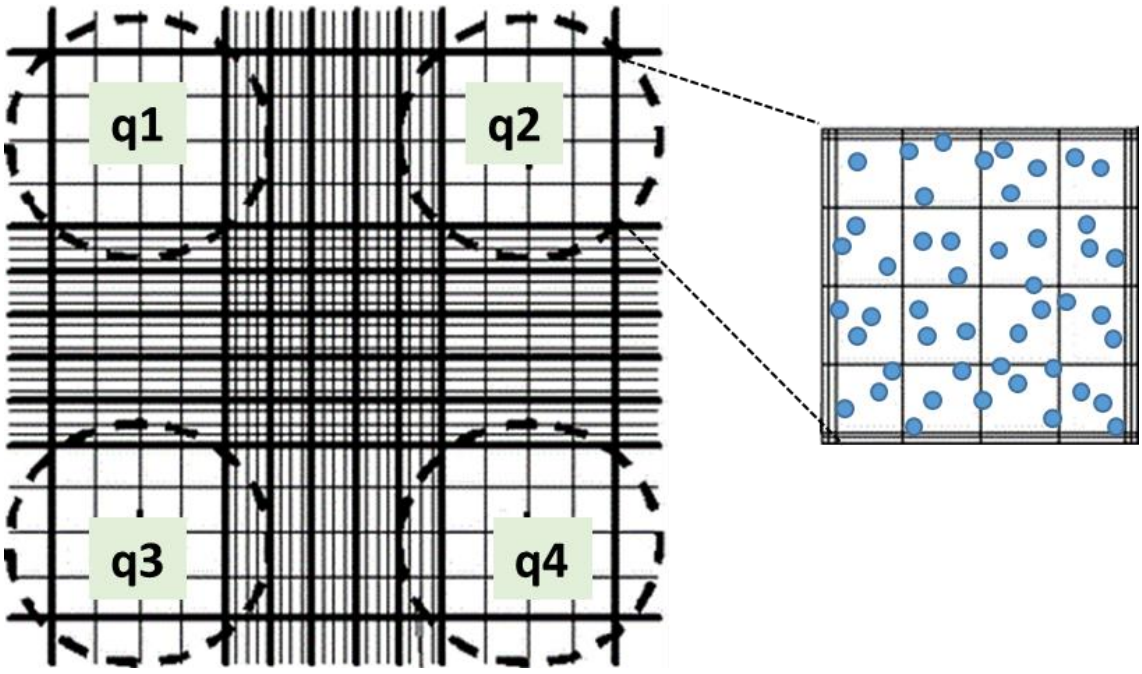

Figure 2.2.2: Caco-2 cell count using haemocytometer.

Cells in the four quadrants (q1, q2, q3, and q4) were counted using inverted microscope. The cells in the inner side of the surrounding quadrant wall were taken under consideration. Figure taken from Louis and Siegel, 2011, and modified.

Cell density (cells/ml) = average cell count [(q1 + q2 + q3 + q4)] × 10,000.

Total number of cell count was performed for individual flasks.

2.2.3 Cell viability assay

2.2.3.1 Protocol determination

Cell viability was measured by CCK-8 assay (fig.2.2.3). The assay relies on the formation of formazan from a water-soluble tetrazolium salt by dehydrogenases. The amount of formazan produced by the biochemical activity of living cells is directly proportional to the number of cells (Held, 2009).

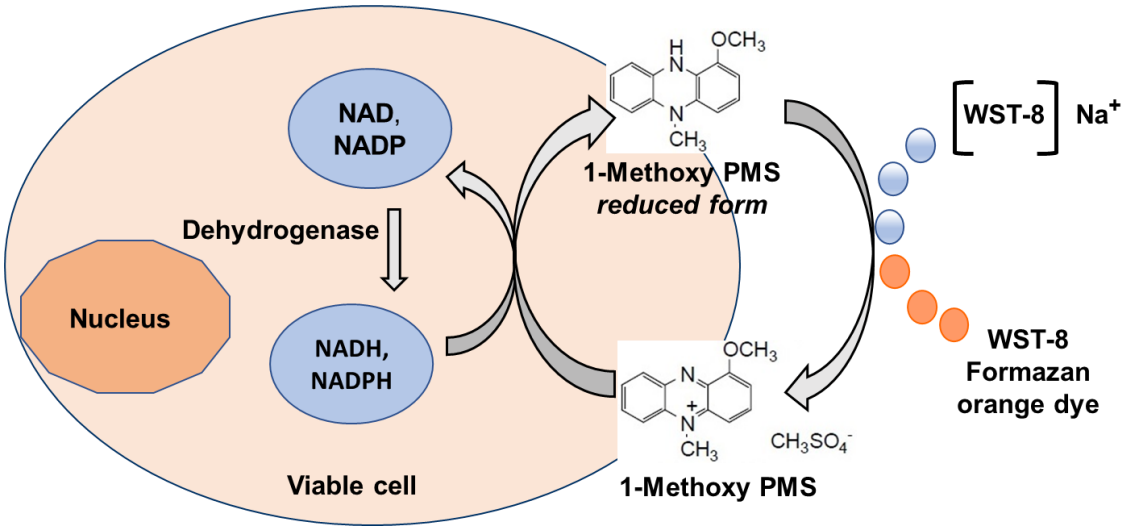

Figure 2.2.3: Schematic presentation of the principle of Cell Counting Kit 8 assay.

Cell viability is measured as absorbance. Due to the activities of the living cells, substrates (tetrazolium salt, WST-8) are reduced by dehydrogenases and formazan is produced. 1-Methoxy PMS (1-Methoxy5-methyphenazinium methyl sulfate) acts as electron mediator between NADH and other electron acceptors. Formazan dye is soluble in tissue culture medium, therefore is proportional to the dehydrogenase activity. So, the absorbance represents the number of living cells. Figure information adapted from Held, 2009.

Caco-2 cells were plated on a 96-well plate at a density of 3×10^5, 1×10^5, to 1×10^2 and incubated for 24-, 48-, and 72-hours. Example of cell number calculation using serial dilution of the initial concentration was shown (fig.A8.2). Used media was replaced with fresh media to neutralize any effect of medium colour and CCK-8 reagent was added (1:10). The plates were incubated for up to 4 hours and absorbance (450 nm) was measured every 1 hour using a precision microplate reader (Tecan Sunrise^{TM}) with Magellan software.

Data was calculated using a media-only control (blank) to neutralize the medium effect. For example, sample absorbance was (b - a); where media only absorbance was 'a', and treatment absorbance was 'b'.

2.2.3.2. Caco-2 cell viability assay with treatments

Caco-2 cells were maintained on a 96-well plate ($1x10^4$ cells/well) with 100 µl of EMEM media. After 48-hour, the used medium was replaced with EMEM supplemented with different concentrations of treatments and incubated for 24 hours. The effect of different concentrations (calculation in Appendix A) of bacterial endotoxin, LPS; AS saccharin, sucralose, aspartame and neotame; the sweet taste inhibitor $ZnSO_4$ and Lactisole; or vehicle were observed. Cells were incubated for 2 hours with CCK-8 (1:10) and absorbance was measured at 450 nm (Tecan Sunrise^{TM}).

LPS stock solution (5 mg/ml) was prepared in ddH_2O, and the used concentrations were prepared using serial dilution (fig.A8.2), an example calculation is given in table-A8.2.

The calculations for the concentrations of the saccharin, sucralose, aspartame and neotame are given in table-A8.3. Control experiments (without cells) were run in parallel with the

CCK-8 assay with AS to assess any nonspecific binding. The without cell absorbance was deducted from the with cell absorbance to calculate the effect of AS on Caco-2 cell viability. $ZnSO_{4.}$ was dissolved in distilled de-ionized water and an example calculation for the different concentrations were shown in table-A8.4.

Lactisole was dissolved in Ethanol (EtOH, 100%), and the used concentrations were prepared in EMEM and calculations are shown in table-A8.5. Given the established cytotoxic effect of the vehicle for Lactisole, ethanol (Tong et al., 2013), Lactisole was also studied with a different vehicle, DMSO (Dimethylsulfoxide). Examples of calculations for Lactisole alone, and Lactisole with AS concentrations in DMSO are shown in table-A8.5 and table-A8.6, respectively. The without cell control experiment was performed with all the concentrations of Lactisole (both DMSO and ethanol) using no cells to observe the effect chemicals with CCK-8 reagents. These 'without cell' experimental data were subtracted from the 'with cell' experimental data when calculated the absorbance of cell viability.

2.2.3.3. Apoptosis Assay

The proportion of apoptotic cells was assessed using the AV apoptosis assay (BD Biosciences, BD Pharmingen, San Diego) following the manufacturer's protocol with minor modifications. This assay relies on the binding of AV with the externalised phosphatidylserine (fig.2.2.4).

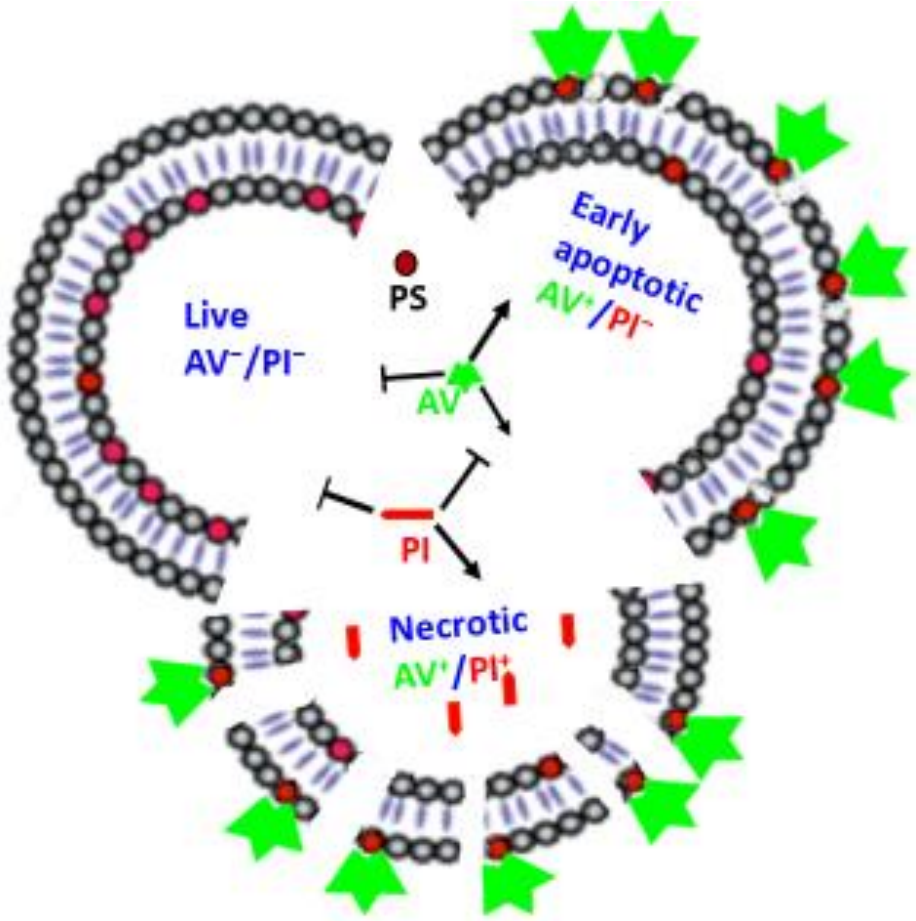

Figure 2.2.4: Schematic representation of the apoptosis process causing loss of membrane lipid asymmetry.

Healthy cells have an asymmetric lipid bilayer composition. The Phosphatidylserine (PS) molecules are embedded in the inner leaflet of the membrane facing to the cytosol. These PS residues become exposed at the outer membrane during apoptosis. FITC-labelled Annexin V (AV) has high affinity to the PS bodies and readily binds with them. Instead, Propidium iodide (PI) intercalates between DNA bases. Viable cells exclude PI with their intact cell membrane, damaged and dead cells allow PI binding with DNA. Therefore, viable cells are both AV and PI negative, apoptotic cells are AV positive and PI negative, while necrotic cells are both AV and PI positive. The lipid bilayer was taken from web source (stmichaelshospitalresearch.ca), and the image was made following the information from BD Biosciences.

Caco-2 cells were grown in T25 flasks until 60% confluence and exposed to different concentrations (0.1 µM - 10 mM) of AS saccharin, sucralose, aspartame, and neotame or H_2O_2 or vehicle for 24 hours. Both floating and adhered cells were harvested and washed (ice-cold PBS, X2) by centrifuging at 1000 rpm for 10 mins.

The binding buffer supplied in the kit was diluted (1:10) in ddH_2O. The cell pellet was re-suspended in 100 µl binding buffer at a concentration of $1X10^5$ cells/ml. Binding buffer (1X, 400 µl), AV and Propidium Iodide (PI) (5 µl each) was added followed by a 5 second vortex and incubation in dark, at RT, to allow effective double staining of the cells. After 15 minutes of incubation, the cells were analysed within an hour by flow cytometry (BD Accuri™ C6, BD Biosciences) using BD Pharmingen software (fig.2.2.5).

10,000 events were counted for each sample. Control cytometry plots (BD Pharmingen template) were used to gate the cells and exclude debris from the counted cells. The template for the AV Apoptosis Detection Kit from the BD Biosciences also included a forward scatter (FSC) vs. side scatter (SSC) plot (fig.2.2.5.i). The flow cytometry analysis then separated the cells into four quadrants; live, early apoptotic, late apoptotic/ necrotic, and dead, as shown in figure 2.2.5.ii. Early apoptotic cells were quantified by counting only AV positive cells, whereas dead cells were measured as both AV and PI positive cells. The percentage of events in each quadrant was collected for further analysis. The scattering of cells (forward and side) were measured and converted to relative percentage change from the control.

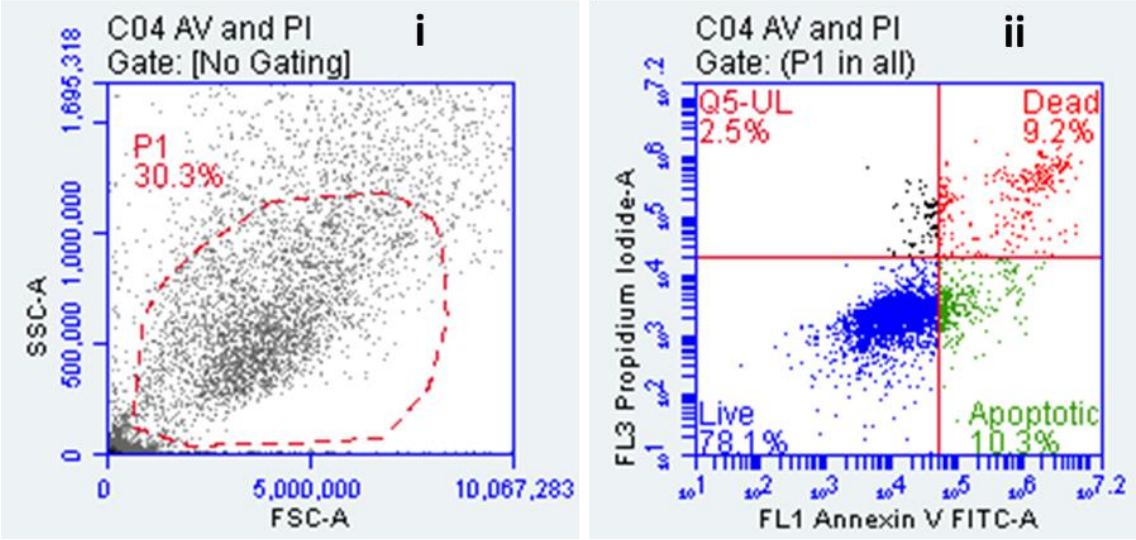

Figure 2.2.5: Determination of the counted cells for the flow cytometry (i) and different stages of cell death (ii) using BD Biosciences template.

Panel i shows the exclusion of the low forward scattering and side scattering events from the cell sample by drawing a gate, which might have cell debris. Here, 30.3% cells were counted. Quadrants in panel ii represent A) Both Annexin V(AV)-and PI-negative quadrant where live cells were recorded, B) AV-positive/PI negative quadrant where apoptotic cells were counted, C) AV-negative/PI-positive quadrant where late apoptotic/necrotic cells were noted, and D) Both AV-and PI-positive quadrant where dead cells were measured. Here, the example figure shows 78.1%, 10.3%, 2.5%, and 9.2% cells in quadrants A, B, C, and D, respectively.

2.2.4. Fluorescence Microscopy

To determine the potential modulatory effects of AS on IECs, cell nucleus, filamentous actin (F-actin) and mitochondria were observed using fluorescence microscopy (example fig.2.2.6). Caco-2 cell nuclei were stained with Prolong® Gold antifade reagent with 4′,6-diamidino-2-phenylindole (PG-DAPI) which is a blue-fluorescent DNA stain. Stress fibre were stained with Phalloidin-iFluorTM 594 Conjugate which is a high-affinity F-actin probe, and mitochondria were stained with 3,3'-Dihexyloxacarbocyanine Iodide (DiOC6), a green-

fluorescent dye selective for the mitochondria. The stain preparation is mentioned in appendix A (8.1.6).

Cells were seeded at $2x10^4$ cells/well of 96-well plate with 100 µl of media and incubated for 24 hours. The media was replaced with 100 µl of EMEM containing 10 mM of saccharin, sucralose, aspartame, neotame, 100 µg/ml of LPS or vehicle (H_2O). After 24 hours, the cells were rinsed (PBS X2), fixed (4% paraformaldehyde in PBS) for 30 minutes at room temperature (RT), rinsed (PBS X2) and permeabilized for 5 minutes with 0.1% Triton X-100 (TX-100) in PBS at RT. After washing (PBS X2), cells were stained with Phalloidin (100 µl) for 60 minutes at RT in dark. The cells were rinsed (PBS X2) and stained with 100 µl DiOC6 in PBS (1:1000) for 10 minutes at RT in dark. After rinsing (PBS X2), the cells were dyed with Prolong Gold-DAPI in PBS for 15 minutes in dark at RT. The cell monolayers were rinsed with PBS and covered with 100 µl of PBS and examined under fluorescence using the Zoe imager (exposure details in appendix table-A8.8).

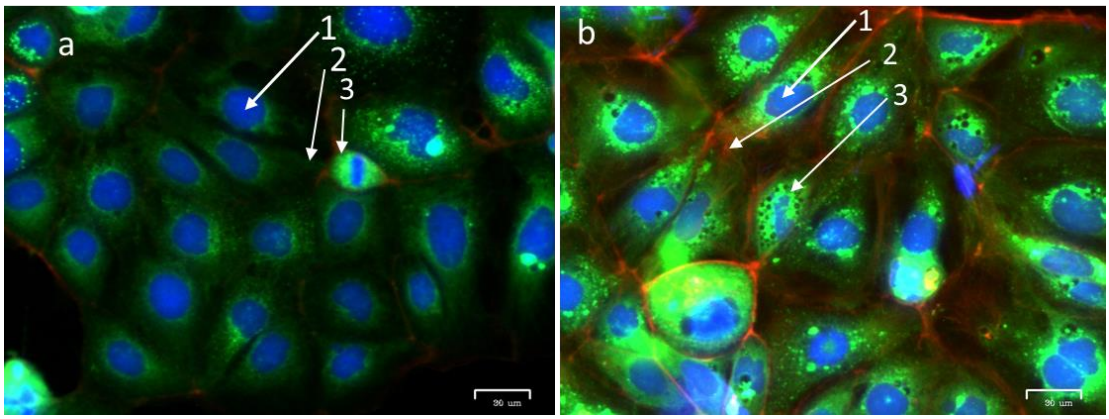

Figure 2.2.6: Fluorescence microscopy of Caco-2 cells for nucleus, stress fibre and mitochondria.

Panel a and b represent unstressed and stressed Caco-2 cells, respectively. The merged image demonstrates the nuclei (1) stained with Prolong® Gold-DAPI (blue), the F-actins (2) stained using phalloidin-iFluorTM 594 Conjugate (red), and the mitochondria (3) stained with DiOC6 (green). Scale bar = 30 µM.

2.2.5. FITC-Dextran permeability assay

The permeability of the Caco-2 cell monolayer was assessed using the FITC-Dextran permeability assay (Monaghan-Benson and Wittchen, 2011, with modifications). FITC Dextran proteins FD4 (MW 4000 Da) and FD20 (MW 20000 Da) were used for the assay, preparation of FD stock solution is mentioned in appendix A (8.1.4.4).

Caco-2 cells were plated onto filters in a 12-well Transwell plate at a cell density of $2 x10^4$ cells/well. 500 µl and 1.5 ml EMEM was added in upper and lower/basolateral chamber of the wells, respectively (fig.2.2.7). After 24-hour incubation, used media was aspirated gently and replaced with EMEM supplemented with LPS concentrations. At 24 hour, 100 µl

medium from insert chamber was aspirated and 100 µl of FITC-labelled Dextran was added (5 mg/ml) with care for light sensitivity of FD. 100 µl from each of insert- and base-chambers were collected at 60-, 180-, and 360- seconds in 96-well plate and immediately wrapped with aluminium foil.

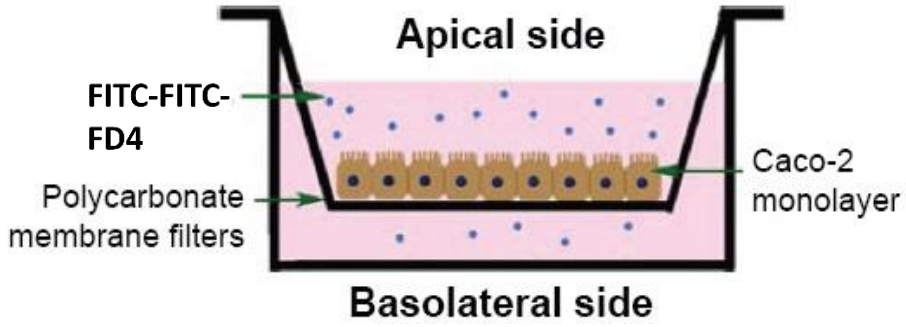

Figure 2.2.7: Schematic presentation of FITC-dextran assay to assess permeability.

If the cell monolayer is impaired, FITC can go across the cell monolayer to the basolateral compartment. Figure adapted from Fang et al., 2010).

To optimise the FITC-Dextran permeability assay, conditions such as cell number, incubation duration, and time for FD permeation were tested. The first experiment was performed using $2x10^4$ cells as described. For the second and third type, $5x10^4$ and $1x10^5$ cells, respectively were incubated for 48 hours before exposing to LPS. After FD addition, $5x10^4$ cells was maintained like before, but $1x10^5$ cells were incubated for 1 hour before sample collection. Also, 100 µl of samples were collected from both the basolateral and insert compartment into 96-well plate.

Plates were read using fluorescent plate reader (PerkinElmer 2030 Manager, Victor X3, UK) at excitation and emission wavelengths of 485 and 535 nm, respectively using HC FITC-Dextran protocol. Data was calculated as below,

Permeability (%) was calculated by dividing fluorescence of lower compartment with fluorescence of upper compartment; it was normalised with control as 100%, [(sample / control) × 100], for each sample.

2.2.6 Determination of sweet taste receptor protein level

Indirect whole cell ELISA was performed to measure the level of STR, T1R3 protein in response to LPS and AS (protocol modified from Xiao et al., 2003). The mechanism of which is shown in (fig.2.2.8).

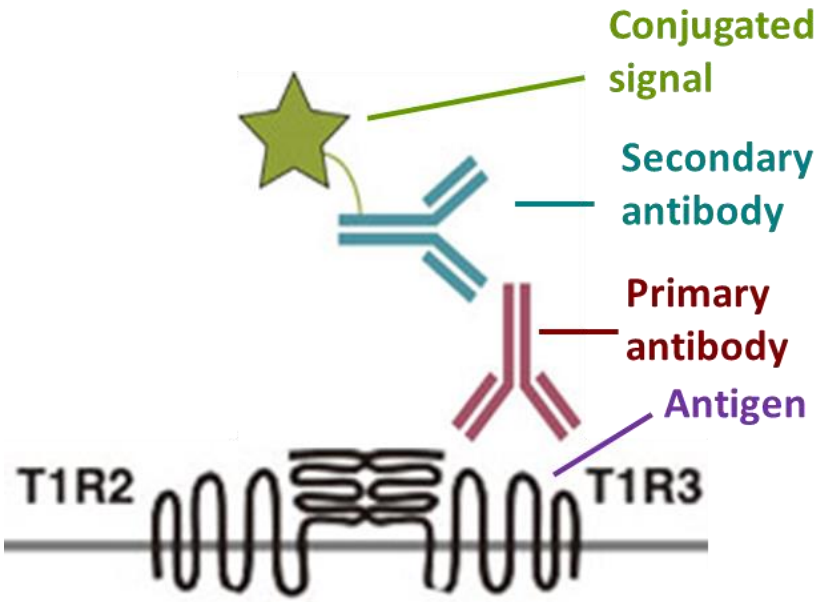

Figure 2.2.8: Schematic presentation of whole-cell ELISA.

When sweet taste receptors are expressed in cells, primary antibodies bind to them. Then the secondary antibody with fluorescent tags binds with the primary antibody and gives fluorescent signal when plates are read.

Caco-2 cells were plated at 1×10^4 cells/well with 50 µl complete EMEM media onto 96-well plates. After 24 hours, cells were treated with LPS (table-A8.2) or AS (table-A8.3) or vehicle (dH_2O).

Cells were fixed with 1% Paraformaldehyde (PFA) (50 µl/well) at RT for 10 minutes. The wells were rinsed gently with PBS (twice) and incubated with 2% BSA-PBS (200µl) at 37 ^oC for 1 hour to block non-specific binding.

For intracellular receptors cells were permeabilised with 0.1% TX-100 for 10 minutes at RT. Cells were directly incubated with 2% BSA for the non-permeabilised ELISA for extracellular ELISA.

The wells were rinsed (dH_2O X3), primary antibody (PA) (50 µl/well) was added and incubated at 37^oC for 2-hours. The PA was prepared using anti-T1R3 antibody (either N20 or V20 specific to the intracellular and extracellular domain respectively), at a 1:50 ratio in 1% BSA-PBS (control 1% BSA-PBS without PA).

The wells were rinsed (dH_2O X3) and the secondary antibody (SA) was applied (50 µl/well) and incubated at 37 ^oC for 1 hour. The fluorescent-tagged SA (donkey anti-goat FITC) was prepared in 1% BSA-PBS (1:200) (control 1% BSA-PBS without SA). Care was taken to handle the light sensitive FITC in the dark.

After 1 hour, plates were rinsed (dH_2O X3), wrapped in foil and fluorescence (r.f.u.) was measured at excitation 485 nm and emission 535 nm using PerkinElmer.

2.2.7 Data analysis

All the quantitative data in the study were collected as Excel (Microsoft Office) files. Excel processed data were analysed using appropriate statistics on GraphPad Prism 7.0. Calculation of data for each experiment are mentioned in the corresponding method section. The outliers were tested using the z-score calculation [Z = {(test result – average of all test results)/ standard deviation of all test results}]. For two groups, the variance in data sets was analysed using the non-parametric test followed by the appropriate T-test. For three or more groups, variance was assessed by using ordinary one-way ANOVA with Kruskal-Wallis test followed by Dunn's or Holm-Sidak's multiple comparison test. For more than two groups of data with more than one variant, difference was analysed using two-way ANOVA followed by appropriate method for statistical hypothesis testing such as Sidak's or Dunnet's multiple comparison test. For all other data sets, differences among the means were tested for significance by ANOVA with different multiple comparison test. Significance was reached when $p<0.05$. The replication number was presented in the legend for each experiment.

2.3 Results

2.3.1 Caco-2 cell viability assay

2.3.1.1 Method evaluation

To examine AS effect on IEC viability, CCK-8 assay (method fig.2.3.1) was performed on Caco-2 cells after 24-hour exposure to the AS. The appropriate cell number, cell maintenance period, and right incubation duration with CCK-8 reagent were pre-determined. The viability of low-density cells (1×10^2 and 3×10^2 cells/well) were almost undetectable after 24- and 48-hour incubation, and absorbance were low after 72 hours (<0.5 a.u.). Conversely, the higher density cell dilutions (1×10^5 and 3×10^5 cells/well) showed linear growth at 24 and 48 hours but plateau at 72 hours.

After CCK-8 addition, 1-hour incubation gave low absorbance (0.34±0.08) while 3-hour presented 0.85±0.18. Higher number of cells (3×10^5) at 2-hour gave absorbance 1.5±0.29, 1.6±0.18, and 1.2±0.11, while the lower cell numbers (3×10^2) gave 0.05±0.03, 0.07±0.03, and 0.11±0.06 at 24, 28, and 72 hours, respectively (fig.2.3.1.i). These do not appropriately reflect the expected absorbance trend, indicating the potential for CCK-8 saturation which would result in a lack of sensitivity.

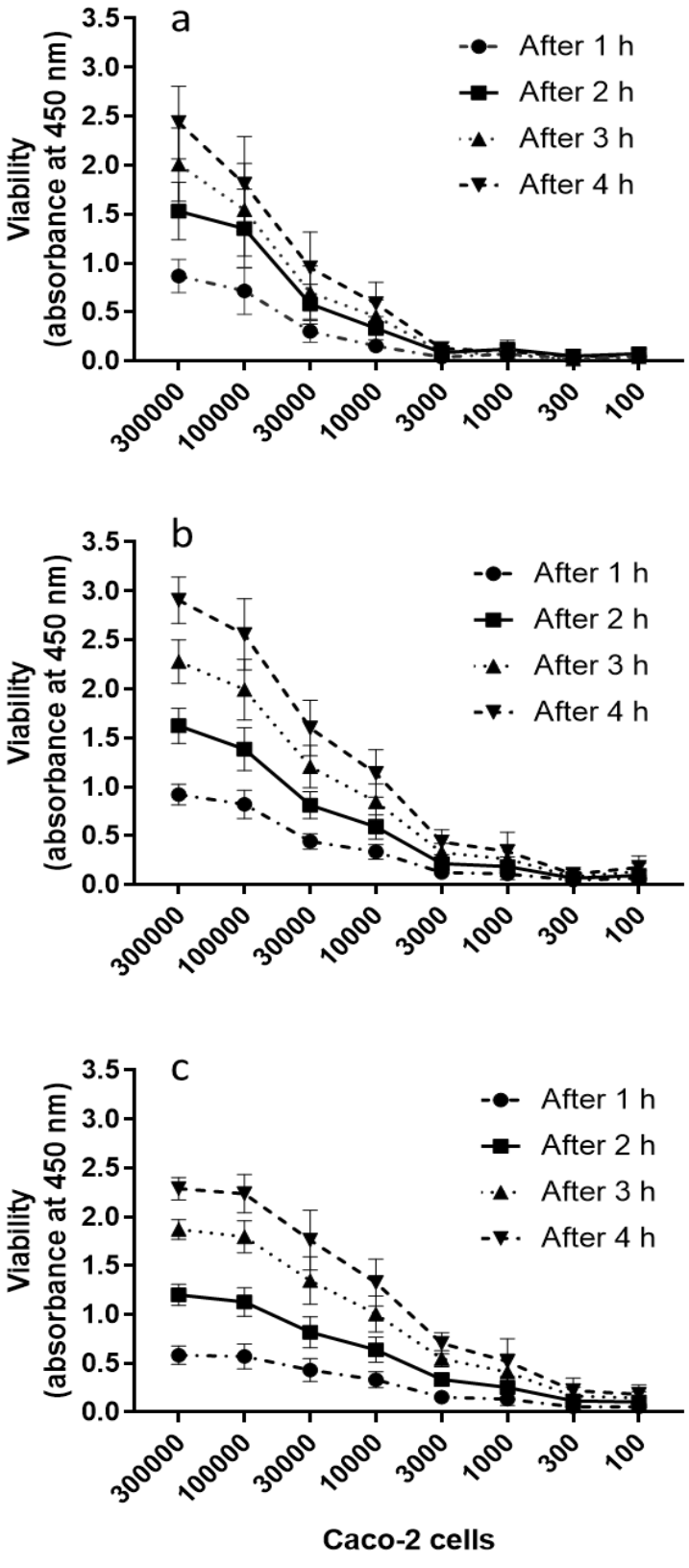

Figure 2.3.1: Caco-2 cell viability assay.

(i) Different number of cells were seeded on 96-well plate, incubated for 24 (a), 48 (b), and 72 (c) hour, and CCK-8 assay was performed. For each time point the plates were incubated for 1 to 4 hour after CCK-8 addition, and viability was measured as absorbance at 450 nm using multiplate reader (Tecan Sunrise™) with Magellan software. Data are presented as the mean ± S.E.M., n=8.

3×10^4 cells/well density showed a linear relationship, however, the absorbance readings at 1×10^4 cell density represented better consistency (remained >1 a.u.), indicating their suitability for detection with a plate reader (Berova et al., 2007). In addition, 48- and 72-hour, with different CCK-8 incubation times, gave similar values. So, 48-hour cell maintenance and 2-hour incubation with CCK-8 reagent gave the most appropriate absorbance (Berova et al., 2007) (fig.2.3.1).

At 48-hour, 1×10^4 and 3×10^4 cells showed absorbance 0.59±0.12 and 0.81±0.14, respectively (fig.2.3.1.ii), however, the absorbance for 3×10^4 cells were near the marginal level of consideration (fig.2.3.1.ii.b). So, cell number from $1x10^4$ to less than 3×10^4 per well was appropriate for further experiments.

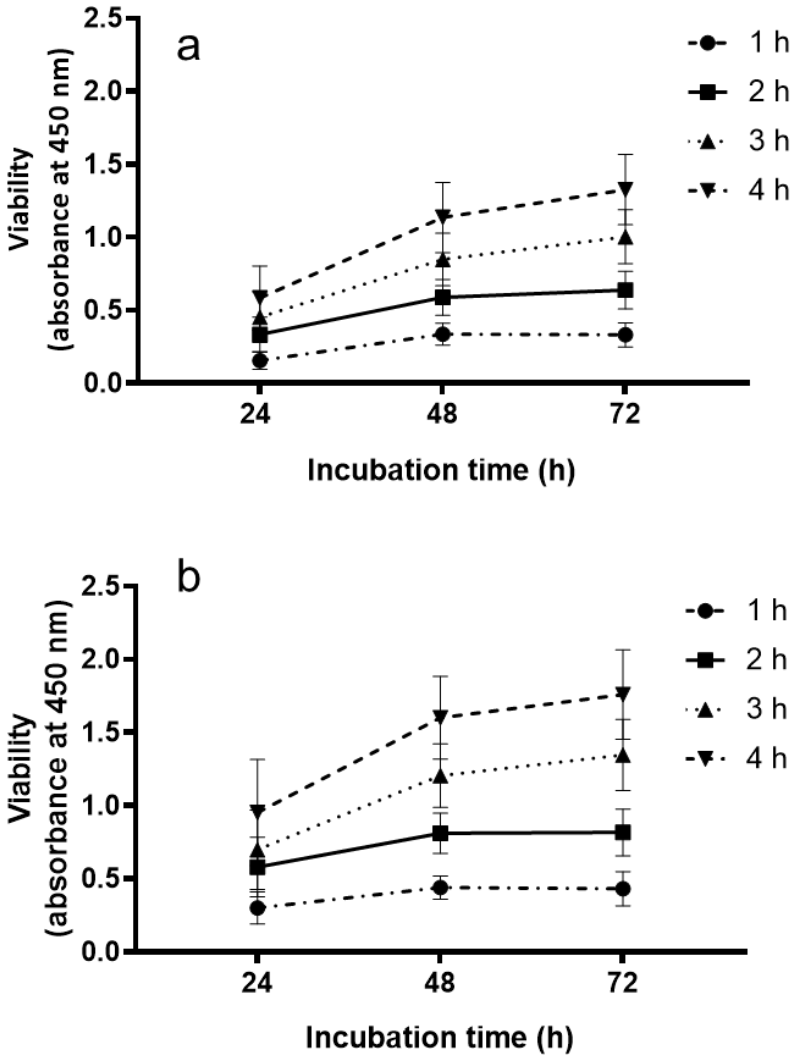

Figure 2.3.1: Caco-2 cell viability assay for method evaluation.
(ii) Cells were seeded on 96-well plates at 1×10^4 cells (a) and 3×10^4 cells (b) per well, and incubated for 24-, 48- and 72-hours. CCK-8 assay reagent was added and incubated for 1 to 4 hours, and cell viability was measured as absorbance at 450 nm using multiplate reader (Tecan Sunrise™) with Magellan software. Data are presented as the mean ± S.E.M., n=8.

2.3.1.2 Effect of Lipopolysaccharide cell viability

Since LPS is the most prominent endotoxin in the gut environment (Moreira et al., 2012) and linked to barrier function (Wang et al., 2015), its effect on Caco-2 cell viability was measured to establish a positive control and injury model. LPS-mediated injury takes place at high concentration of the endotoxin (Mathan et al., 1988), therefore, a range of concentrations up to 100 µg/ml were chosen. Cell viability was unaffected for concentrations ranging from 0.01 to 5 µg/ml (fig.2.3.2). Higher concentrations (>10 µg/ml) reduced cell viability and a dramatic decline was observed at 100 µg/ml (by 0.2 a.u.) indicating a decrease in cell viability.

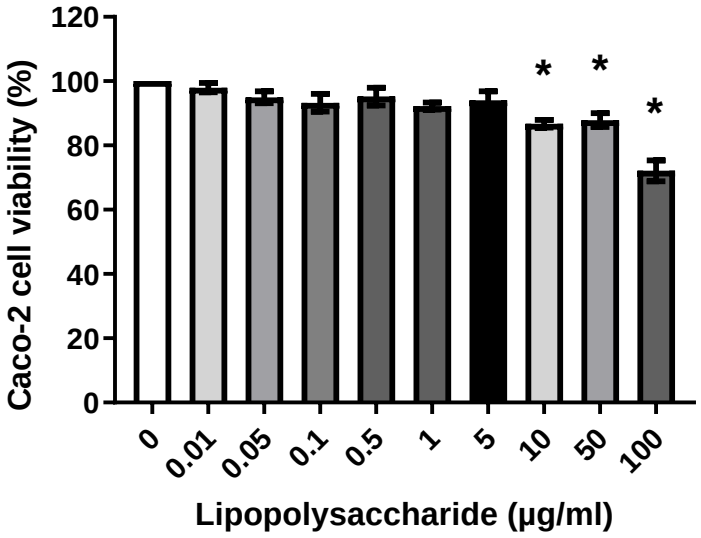

Figure 2.3.2: Effect of LPS on the viability of Caco-2 cells.

Cells were seeded in 96-well plate (1×10^4 cells/well) and maintained at standard tissue culture condition for 48 hours. Cells were exposed to different concentrations of LPS or vehicle (water) for 24 hours and CCK-8 assay was performed. The cell viability was measured as absorbance at 450 nm using Tecan Sunrise™ multiplate reader. Data are analysed using nonparametric test followed by Dunn's multiple comparisons test and presented as the mean ± S.E.M., n=10. *p<0.05 versus 0 µg/ml LPS.

2.3.1.3 Cytotoxic effect of artificial sweeteners

Intestinal barrier function (IBF) is affected by the viability of IECs. The AS or their components may have cytotoxic effect on the IECs. So, Caco-2 cells were exposed to a range of concentrations (0.01 µM to 50 mM) of saccharin, sucralose, aspartame and neotame to assess their effect. To determine any non-specific interaction of CCK-8 with the sweeteners, the control experiment without cell was also performed (fig.2.3.3b). The control experiment explained the high absorbance reading at 50 mM of saccharin. Data showing

cell viability effects of AS have been calculated by subtracting values from the control experiment.

At low concentrations (0-100 µM), the sweeteners did not affect cell viability (fig.2.3.3 – 2.3.7). A significant effect of saccharin (fig.2.3.3), sucralose (fig.2.3.4), aspartame (fig.2.3.5) and neotame (fig.2.3.6) on Caco-2 cell viability was observed at higher concentrations (10 and 50 mM).

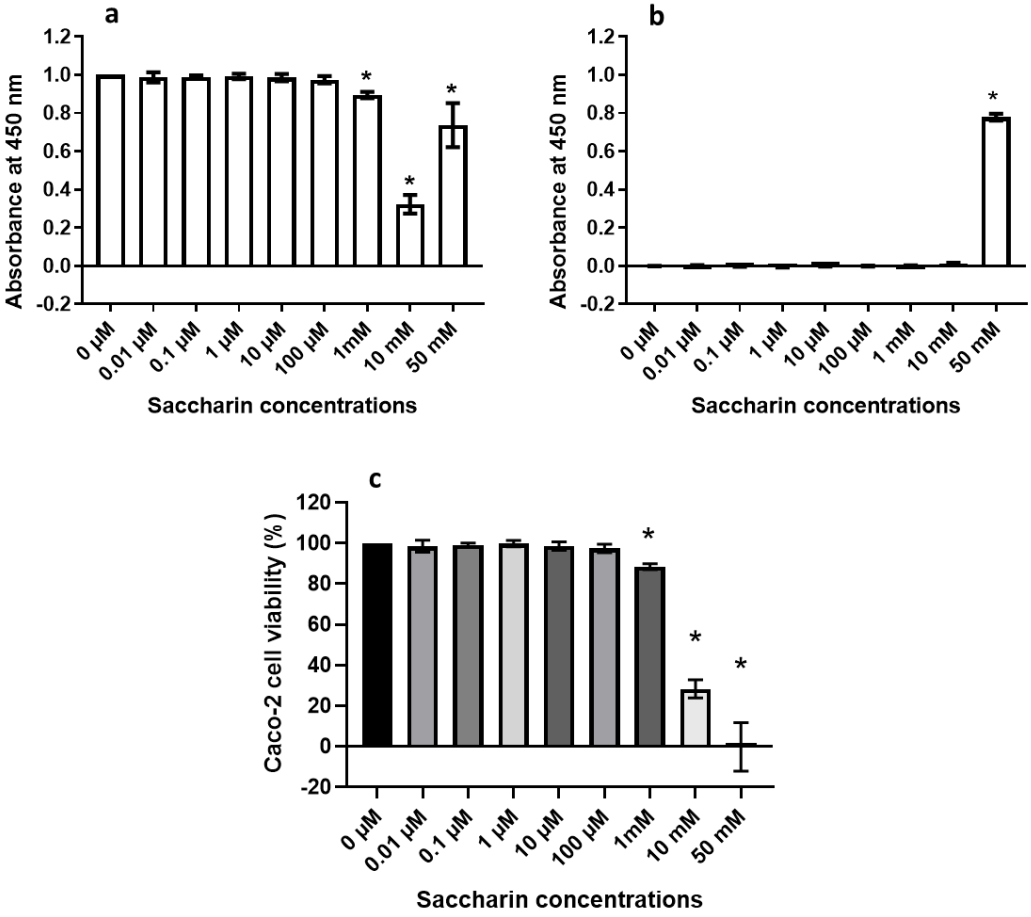

Figure 2.3.3: Effect of saccharin concentrations on the viability of Caco-2 cells.

Caco-2 cells ($1x10^4$ cells/well) were maintained for 48 hours and exposed to increasing concentrations of saccharin or vehicle and viability was assessed by CCK-8 assay read at 450 nm. The sweetener concentrations and CCK-8 reagent were incubated in the same condition in presence of Caco-2 cells (a) to see the effect on viability, or without cells (b) to assess non-specific binding of the reagent with AS. The final data (c) were calculated by subtracting the without cell (b) data from with cell data (a) and converted into percentage. Data were calculated using Kruskal-Wallis test followed by uncorrected Dunn's multiple comparison test and presented as the mean ± S.E.M., n=8 (a and c), n=4 (b). *p<0.05 versus 0 µM/ml saccharin.

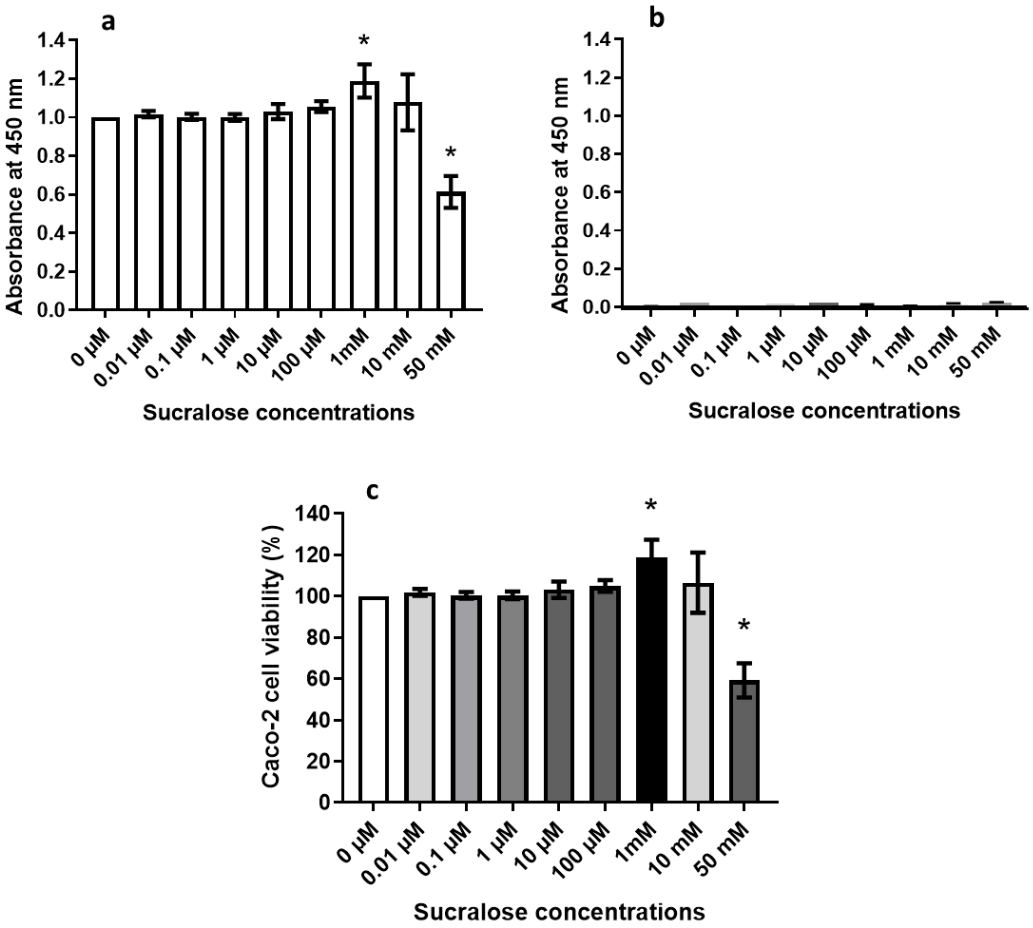

Figure 2.3.4: Cytotoxic effect of sucralose on the intestinal epithelial cells.

Caco-2 ($1x10^4$ cells/well) were maintained for 48 hours and exposed to different concentrations of sucralose or vehicle, CCK-8 viability assay was performed, and viability was measured as absorbance at 450 nm. Panels represent absorbance of treated Caco-2 cells (a), control experiment for non-specific bindings of sucralose and CCK-8 reagent (b), and final viability data (c). Viability (%) (c) was calculated by deducting control absorbance (b) from the initial absorbance (a), and normalising with control. Data were analysed using Kruskal-Wallis test followed by uncorrected Dunn's multiple comparison test and presented as the mean ± S.E.M., n=8 (a and c), n=4 (b). *$p<0.05$ versus 0 µM/ml sucralose.

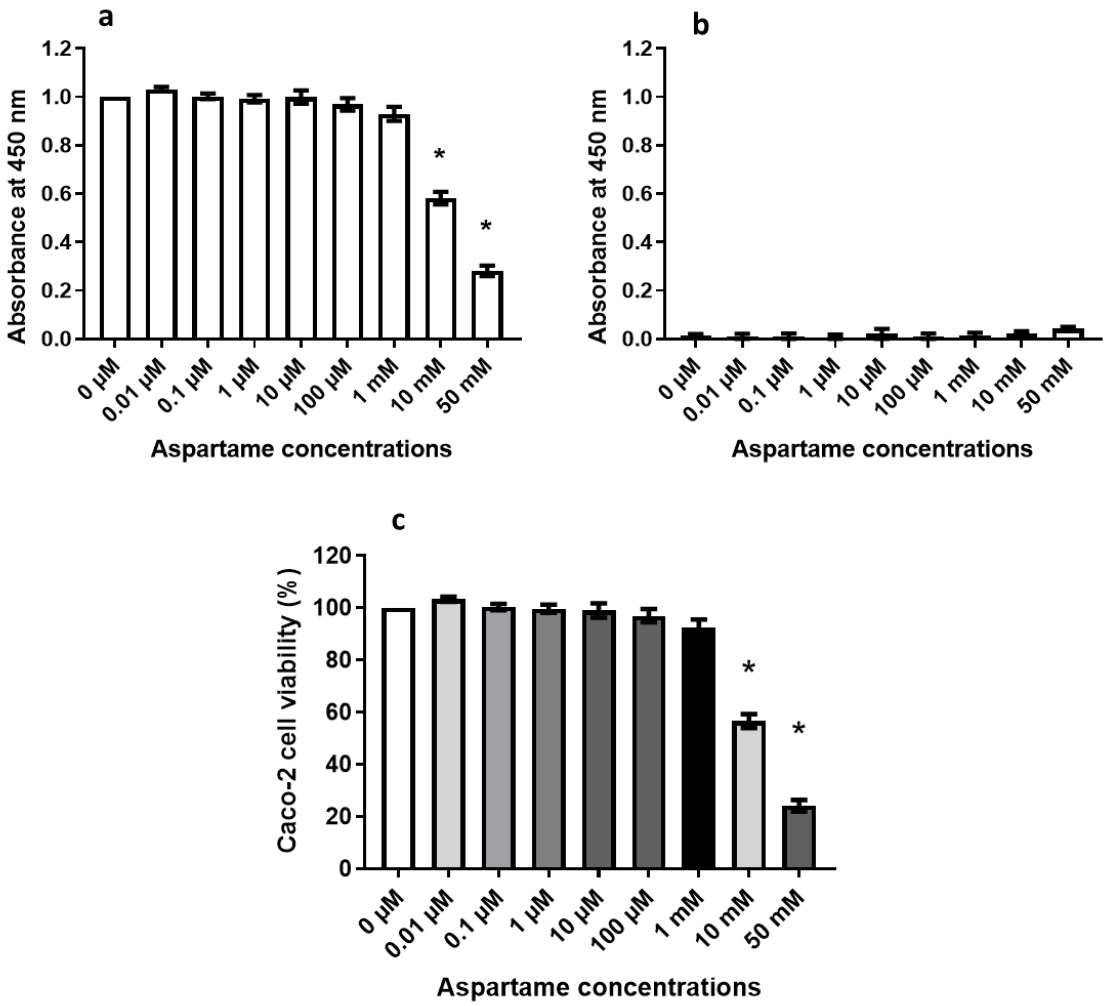

Figure 2.3.5: Effect of aspartame on Caco-2 cell viability.

Cells ($1x10^4$ cells/well) in 96-well plates were maintained for 48 hours and exposed to different concentrations of aspartame or vehicle for 24 hours and CCK-8 assay was performed. Panels represent absorbance of treated Caco-2 cells (a), control experiment for non-specific bindings of aspartame and CCK-8 reagent (b), and final viability data (c). Cell viability (c) was calculated by deducting control absorbance (b) from the initial absorbance (a), and normalising with control as 100%. Data were analysed using Kruskal-Wallis test followed by uncorrected Dunn's multiple comparison test and presented as the mean ± S.E.M., n=8 (a and c), n=4 (b). *$p<0.05$ versus 0 µM/ml aspartame.

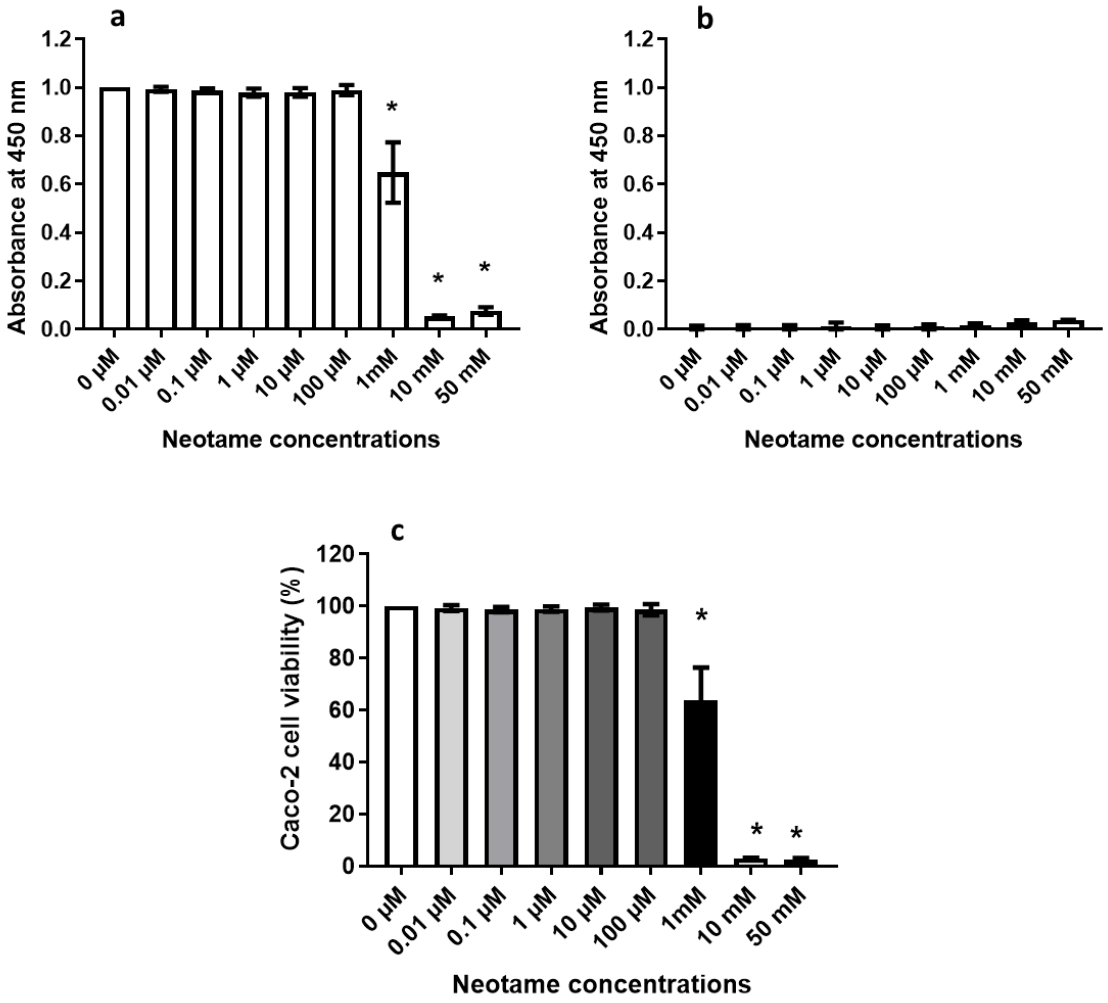

Figure 2.3.6: Cytotoxic effect of neotame on intestinal epithelial cell viability.

Caco-2 cells were seeded at $1x10^4$ cells/well of 96-well plate, maintained for 48 hours and were exposed to different concentrations of neotame for 24 hours. CCK-8 assay was performed, and cell viability was measured as absorbance at 450 nm. Panels represent absorbance of (a) treated cells, (b) controls of neotame concentrations and CCK-8 reagent, and (c) represents the final viability. The final viability percentage (c) were obtained by deducting the control absorbance (b) from initial absorbance (a) and normalised with vehicle. Data were analysed using Kruskal-Wallis test followed by uncorrected Dunn's multiple comparison test and presented as the mean ± S.E.M., n=8 (a and c), n=4 (b). *p<0.05 versus 0 µM/ml neotame.

The Caco-2 cell viability was not impaired at sub-physiological concentrations (0.01 to 100 µM) of the AS. Sucralose showed the least toxicity since cell viability was >50% in the studied concentration range. The relative EC50 values of the AS are listed in fig.2.3.7. EC50 is the half-maximal effective concentration of a toxicant that induce a response halfway between the baseline and the maximum level (Liu et al., 1999). Here, absolute EC50 could not be estimated, however, the relative EC50 (Appendix A, table-A8.7) was noted in comparison to control as 100% (Sebaugh, 2011). Neotame caused 50% viability decrease at lowest concentration (2.2 mM), followed by aspartame (15 mM) and saccharin (5.4 mM) (fig.2.3.7).

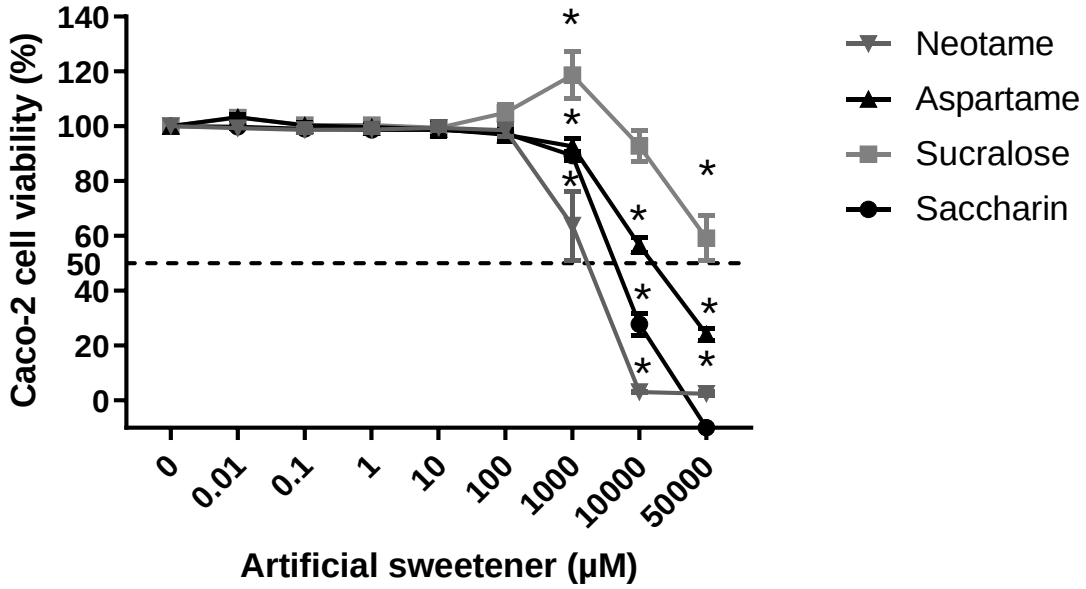

Figure 2.3.7: Effect of AS on viability of intestinal epithelial cells.

Caco-2 cells were plated at $1x10^4$ cells/well in 96-well plates with 100 µl EMEM and maintained for 24 hours. Cells were exposed to increasing concentrations of saccharin or sucralose or aspartame or neotame or vehicle (medium), and cell viability was assessed by CCK-8 assay read as absorbance at 450 nm. Final viability (%) was calculated by deducting the absorbance of AS and CCK-8 reagent from the absorbance of cell, AS and CCK-8, and normalised with the vehicle. Data were tested for outliers (Z-score), analysed using Kruskal-Wallis test followed by Uncorrected Dunn's test and presented as the mean ± S.E.M., n=8. *p<0.05 versus 0 µM/ml AS.

2.3.1.4 Cytotoxic effect of sweet taste inhibitor

Given the effect of activators of the STR, AS, on Caco-2 cell viability, the next experiment sought to understand the effect of the inhibitor of the STR, $ZnSO_4$ and Lactisole.

2.3.1.4.1 Zinc sulphate

$ZnSO_4$ is a potential inhibitor of the STR, which inhibits the sweet taste perception of a range of sweet molecules including AS (Keast, 2003). Therefore, the effect of $ZnSO_4$ on Caco-2 cell viability was next assessed to check its suitability for the later experiments with STR inhibition. $ZnSO_4$ significantly affected Caco-2 cell viability at very high concentrations (10 mM and 50 mM). Cell viability was unaffected at concentrations ranging from 0.1 to 1 mM; the highest cell viability was measured at 1 µM (1.01 a.u.) although absorbance was above 0.93 a.u. for all concentrations up to 1 mM. The effect of $ZnSO_4$ on Caco-2 cell viability was presented in fig.2.3.8.

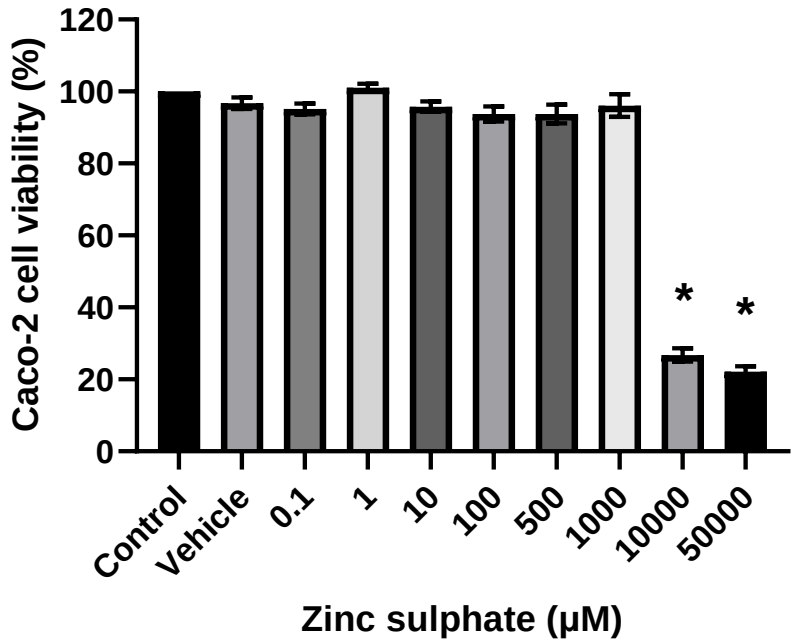

Figure 2.3.8: Effect of Zinc sulphate on intestinal epithelial cell viability.

Caco-2 cells ($1x10^4$ cells/well) were maintained for 48 hours and exposed to different concentrations of $ZnSO_4$ or vehicle for 24 hours. CCK-8 assay was performed, and viability was measured as absorbance at 450 nm using multiplate reader (Tecan Sunrise™). The cell viability was not affected by $ZnSO_4$ doses of 0.1 – 1 mM. Data normalised with control as 100%, analysed using Kruskal-Wallis test followed by Dunn's multiple comparison test, no outliers found (ROUT; Q=1%), and presented as the mean ± S.E.M., n=6. *p<0.05 versus 0 µg/ml $ZnSO_4$.

$ZnSO_4$ inhibits sweet taste perception at concentration ≥25 mM (Keast, 2003), while it significantly decreased cell viability at 10 mM concentration. Also, $ZnSO_4$ is a non-specific sweet taste inhibitor (DuBois, 2016), therefore, more specific sweet taste inhibitor was tested.

2.3.1.4.2 Lactisole

Lactisole (sodium salt of ±2-(4-methoxyphenoxy)propanoic acid) is a broad-acting sweet antagonist that decrease the sweet intensity of 12 of 15 sweeteners (Jiang et al., 2005; Schiffman et al., 1999). Also, it is a selective sweetness inhibitor and is not equally effective to inhibit sweet perception of all sweeteners (Keast et al., 2004; Schiffman et al., 1999). So, in the next set of experiment, effect of Lactisole on Caco-2 cell viability was tested.

Lactisole (vehicle ethanol) significantly decreased the Caco-2 cell viability (fig.2.3.9) at concentrations from 3 mM. Caco-2 cell viability dropped below 40% at concentrations starting from 1 mM.

The non-specific binding of the Lactisole and ethanol was tested, and the absorbance was around 0.2 a.u. (fig.2.3.9.b). So, the viability reduction is the effect of either Lactisole or vehicle. Lactisole was reported to inhibit the sweet taste perception at ≈4 mM in MIN6 cells (Hamano et al., 2015). In addition, ethanol itself has cytotoxic effect on IECs including the

Caco-2 cell line, the cell viability was demonstrated to decrease significantly after exposure to concentrations >5% for 4 hours (Tong et al., 2013). Therefore, Lactisole was tested for another more intense vehicle, DMSO (CaymanChem, USA).

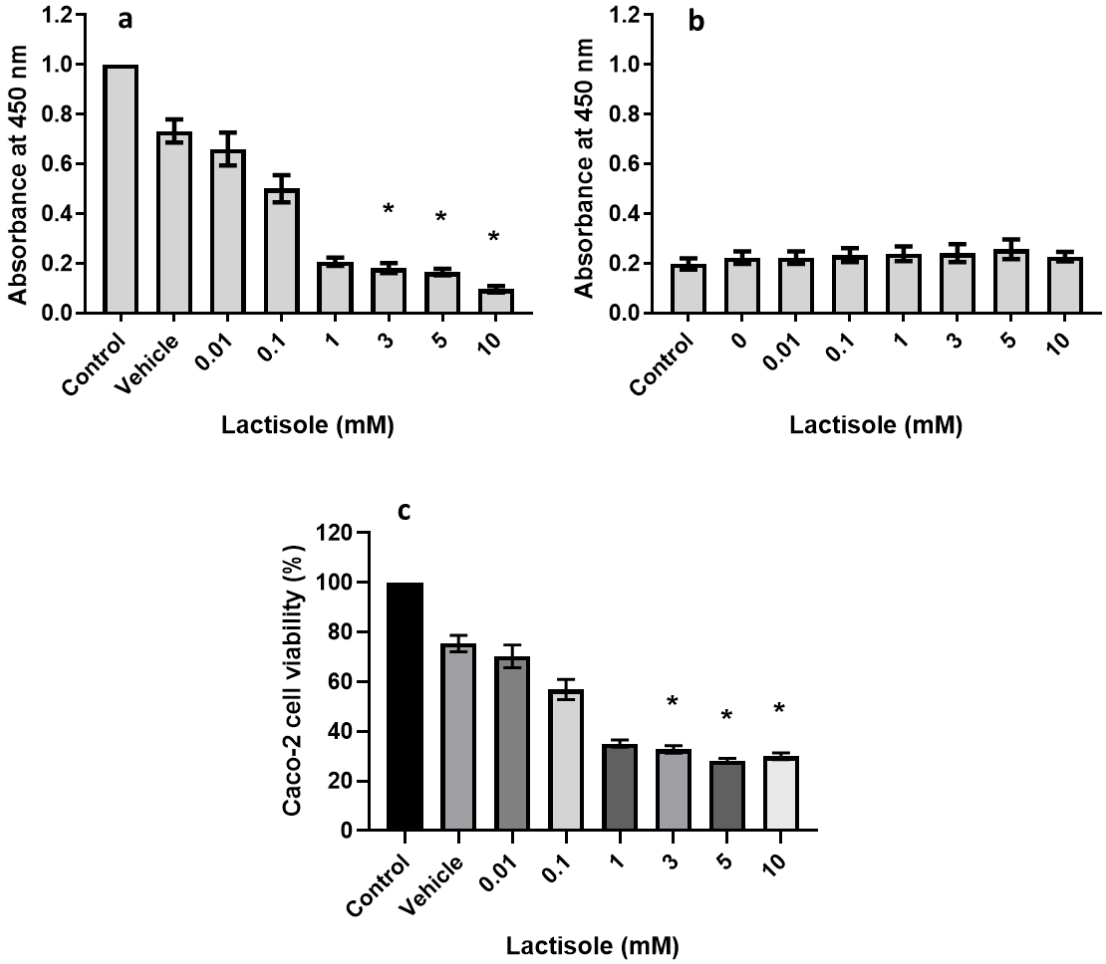

Figure 2.3.9: Effect of Lactisole (vehicle ethanol) on Caco-2 cell viability.

Cells were plated at 1×10^4 cells/well of 96-well plate and exposed to different concentrations of Lactisole in ethanol or vehicle for 24 hours. Cell viability was assessed by CCK-8 assay and absorbance at 450 nm was measured (Tecan Sunrise). (a) absorbance of Caco-2 cell, media and CCK-8; (b) absorbance of media and CCK-8, and (c) viability percentage was calculated by deducting b from a, and normalised with control (100%). Data were analysed using Kruskal-Wallis test followed by Dunn's test, and presented as Mean ±S.E.M., n=6 (a, c), 4 (b). *$p<0.05$ versus vehicle.

DMSO is a widely used vehicle for chemicals not soluble in water such as Lactisole (Brayton, 1986). Since ethanol showed high level of Caco-2 cell death in the experimental condition, Lactisole was dissolved in DMSO and viability was assessed using CCK-8 assay. Lactisole significantly reduced cell viability at concentrations ≥5 mM in comparison to vehicle (fig.2.3.10a,c). Cell viability was unaffected at 0.1 mM, while reduced to about one-third and one-fifth at concentrations 1 and 3 mM, respectively. No considerable non-specific binding of Lactisole and CCK-8 was detected from the absorbance measurement (fig.2.3.10b).

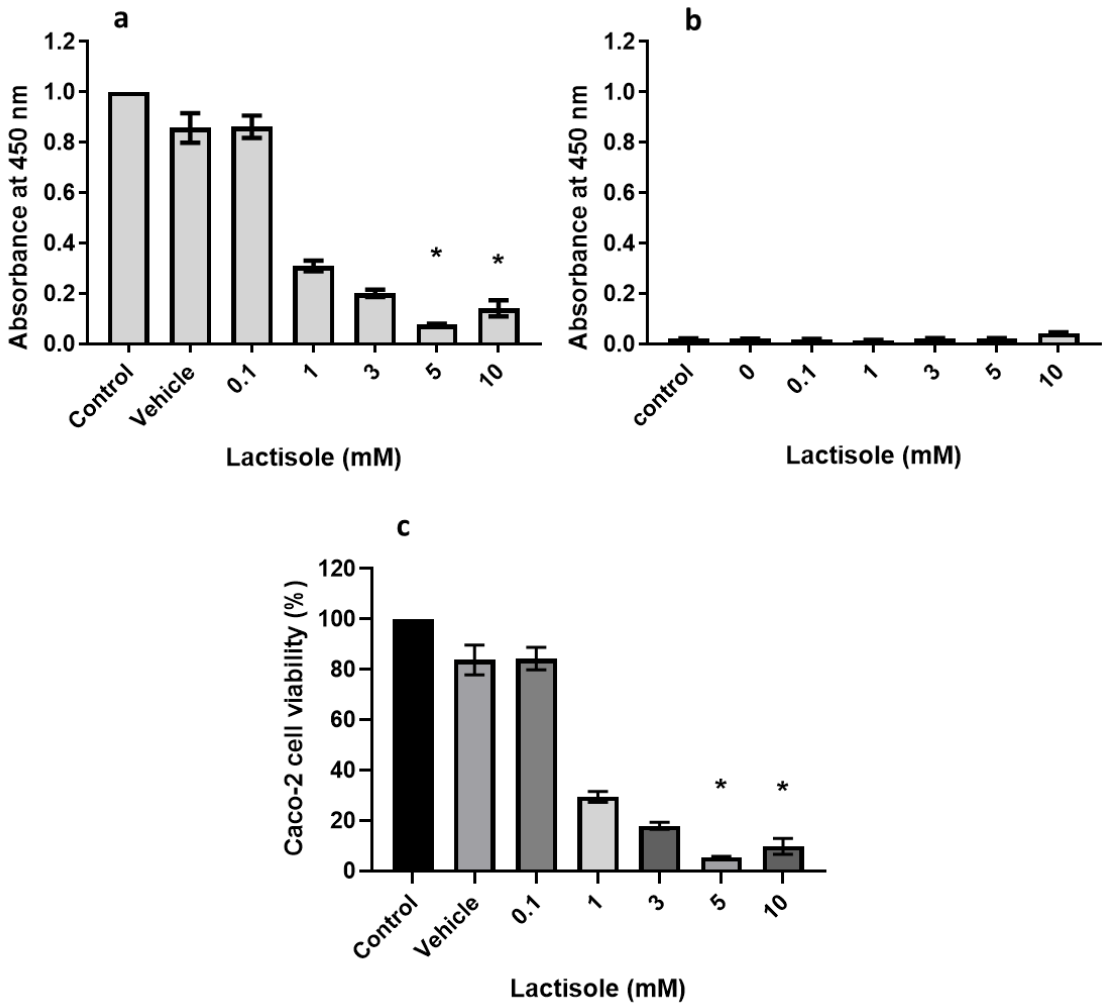

Figure 2.3.10: Effect of Lactisole (vehicle DMSO) on Caco-2 cell viability.

1×10^4 cells/well were seeded on 96-well plate and exposed to different concentrations of Lactisole in DMSO or vehicle for 24 hours. CCK-8 assay was performed, and viability was measured as absorbance at 450 nm (Tecan Sunrise). (a) absorbance of Caco-2 cell, media and CCK-8; (b) absorbance of media and CCK-8, and (c) viability percentage calculated by deducting b from a, and normalised with control (100%). Data were analysed using Kruskal-Wallis test followed by Dunn's test, and presented as Mean ±S.E.M., n=5 (a, c), 4 (b). *p<0.05 versus vehicle.

Lactisole did not affect Caco-2 cell viability at 0.1 mM, and at concentration 3 mM, it reduced cell viability, however, the effect was insignificant. In addition, all the AS except sucralose significantly reduced Caco-2 cell viability at 50 mM. So, the next set of experiment was performed to see the additive effect of the AS and Lactisole (in DMSO) on Caco-2 cell viability.

2.3.1.5 Additive effect of AS and Lactisole

CCK-8 assay was performed to assess the additive effect of AS and Lactisole on Caco-2 cells viability. If the viability reduction is via the STR, then addition of the inhibitor, Lactisole would reduce the deleterious effect.

The results of the CCK-8 assay confirmed that at 0.1 mM of AS and Lactisole, cell viability was unaffected for all the sweeteners. 10 mM of AS alone significantly reduced viability for all cases, and highest reduction was noted for neotame (fig.2.3.14). At 3 mM Lactisole, the vehicle decreased viability ≈50%, and addition of 0.1 mM AS did not give much difference compared to vehicle. However, the viability dropped to nearly 10% for treating cells with 10 mM AS and 3 mM Lactisole (fig.2.3.14). For saccharin (fig.2.3.11), sucralose (fig.2.3.12), and aspartame (fig.2.3.13), the viability reduction exacerbated (≈15%) for adding 3 mM Lactisole compared to AS alone.

Taken together, these findings suggest that AS at 10 mM negatively affect IEC viability, and 3 mM Lactisole augmented the decrease whilst Lactisole concentration interfere with sweet taste perception around 4 mM (Hamano et al., 2015). As there was a cytotoxic effect of DMSO on mammalian cells (Nasrallah et al., 2008), so use of other vehicle such as dimethyl formamide (20 mg/ml; CaymanChem, USA) or siRNA or T1R3 knockout cells (Wauson et al., 2012) could be other options for further studies.

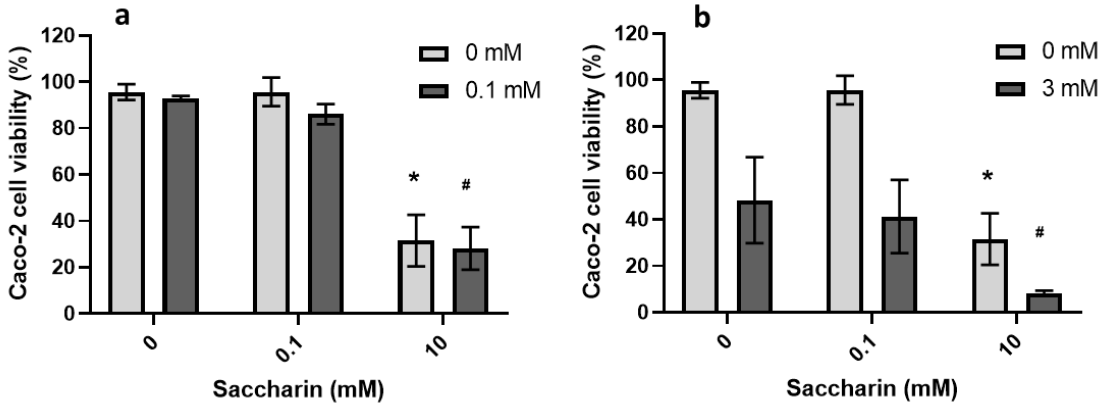

Figure 2.3.11: Cytotoxic effect of saccharin and Lactisole on the viability of Caco-2 cells.

Caco-2 cells were plated at 1×10^4 cells/well of 96-well plate and maintained for 48 hours at 37 °C with 5% CO_2. Cells were exposed to concentrations of saccharin in presence of 0.1 mM (a) or 3 mM (b) of Lactisole for 24 hour and CCK-8 assay was performed. 0.1 mM Lactisole affected cell viability in combination with 100 µM of Saccharin, but high concentration of the sweetener and Lactisole (10 mM Saccharin and 3 mM Lactisole) almost killed the cells. Data are analysed using two-way ANOVA with Dunnett's multiple comparisons test and presented as the mean ± S.E.M., n=5. *p<0.05 versus 0 µM saccharin. #p<0.05 versus 0 mM Lactisole.

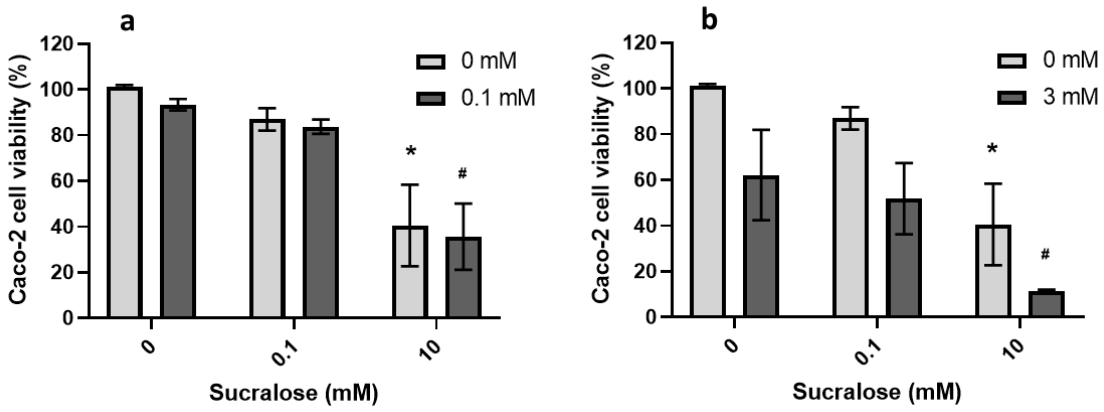

Figure 2.3.12: Cytotoxic effect of sucralose and Lactisole on Caco-2 cell viability.

Caco-2 cells were plated at 1×10^4 cells/well of 96-well plate and maintained for 48 hours at 37 °C with 5% CO_2. Cells were exposed to two concentrations of sucralose in presence of 0.1 mM (a) or 3 mM (b) of Lactisole for 24 hour and CCK-8 assay was performed. 0.1 mM Lactisole along with 100 µM of sucralose did not affect the viability significantly (a), but high concentration (10 mM) of the sweetener sharply reduced absorbance while addition of Lactisole (10 mM sucralose and 3 mM Lactisole) presented the lowest absorbance (b). Data are analysed using two-way ANOVA with Dunnett's multiple comparisons test and presented as the mean ± S.E.M., n=5. *p<0.05 versus 0 µM sucralose. #p<0.05 versus 0 mM Lactisole.

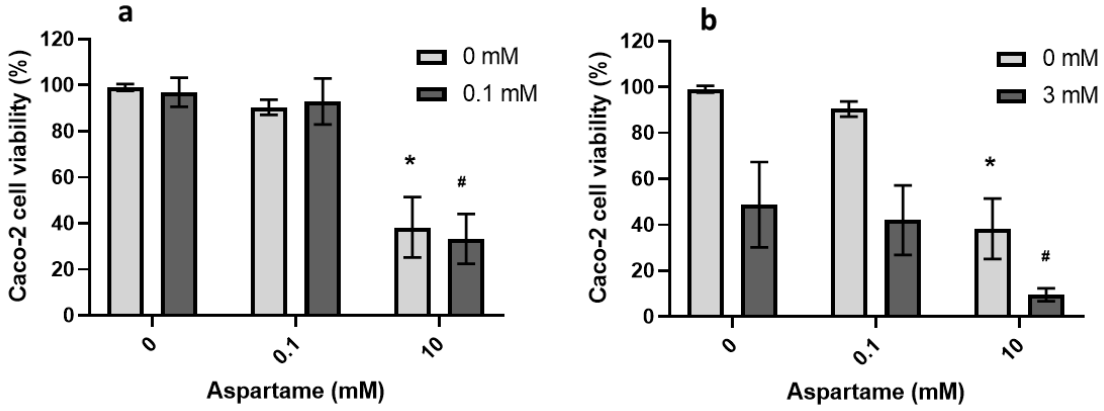

Figure 2.3.13: Additive effect of aspartame and Lactisole on Caco-2 cell viability.

1×10^4 cells/well in 96-well plate were maintained for 48 hours at 37 °C with 5% CO_2. Cells were exposed to aspartame in presence of vehicle or 0.1 mM (a) or 3 mM (b) of Lactisole for 24 hour and the CCK-8 assay was performed. Cell viability was measured as absorbance at 450 nm (Tecan Sunrise™). 10 mM Aspartame affected cell viability at both concentrations (0.1 and 3 mM) of Lactisole, however 10 mM Aspartame and 3 mM Lactisole dose reduced the cell viability drastically. Data are analysed using two-way ANOVA with Dunnett's multiple comparisons test and presented as the mean ± S.E.M., n=5. *p<0.05 versus 0 µM aspartame. #p<0.05 versus 0 mM Lactisole.

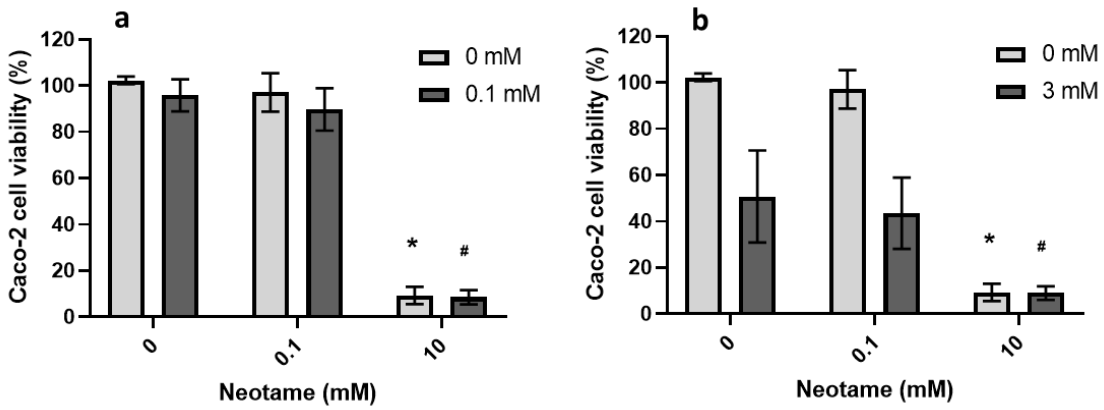

Figure 2.3.14: Cytotoxic effect of neotame and Lactisole on intestinal epithelial cell viability.

Caco-2 cells were seeded at 1 × 10^4 cells/well in 96-well plate and maintained for 48 hours at 37 °C with 5% CO_2. Cells were exposed to concentrations of neotame in presence of vehicle or 0.1 mM (a) or 3 mM (b) of Lactisole for 24 hour and the CCK-8 assay was performed to measure cell viability as absorbance at 450 nm (Tecan Sunrise™). 10 mM Neotame reduced viability of the cells in all cases. High concentration of Lactisole also decreased cell viability more than half. Data are analysed using two-way ANOVA with Dunnett's multiple comparisons test and presented as the mean ± S.E.M., n=5 *p<0.05 versus 0 µM neotame. #p<0.05 versus 0 mM Lactisole.

2.3.2 Effect of AS on Caco-2 cell apoptosis and morphology

The distinctive morphological characteristics of apoptosis are very conservative and solely dependent on the cell type and the apoptotic inducer (Kerr et al., 1972). The cell viability was significantly affected at high concentration (≥1 mM) of AS except sucralose (fig.2.3.7), therefore changes in cell morphology and apoptosis in response to AS exposure was next to assess.

Caco-2 cells were exposed to different concentrations of the four AS for 24 hours. Brightfield microscopy was performed to observe cell morphology and AV-PI flow cytometric analysis was performed to assess apoptosis.

The intact cells showed completely healthy nuclei, cobble stone-like structure and edges; by contrast the 0.8 µM H_2O_2-treated cells have lost adherence and usual morphology while the percentage of cell death was obvious (fig.2.3.15).

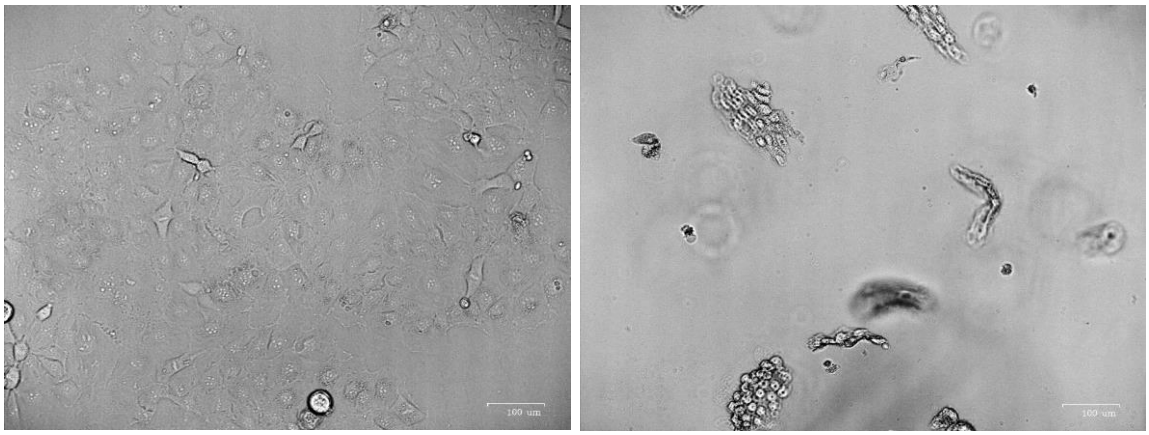

Figure 2.3.15: Caco-2 cell morphology.

Cells were exposed to vehicle (left) or H_2O_2 (right) for 24 hours and observed using brightfield microscopy (Zoe imager).

AS negatively affected Caco-2 cell morphology in a concentration-dependent manner. Cells showed more flat appearance and became less well defined with rising concentration. They displayed higher degree of shrinkage, membrane disorientation and more floating cells in relation to the increasing concentrations of AS. AS increased Caco-2 cell adherence loss with increasing concentration, 10 mM of saccharin (fig.2.3.16) and neotame (fig.2.3.19) showed highest amount of adherence loss. Also, 10 mM of sucralose and aspartame, both increased gaps among cell islands at high concentrations of 1 and 10 mM (fig.2.3.17, and fig.2.3.18, respectively).

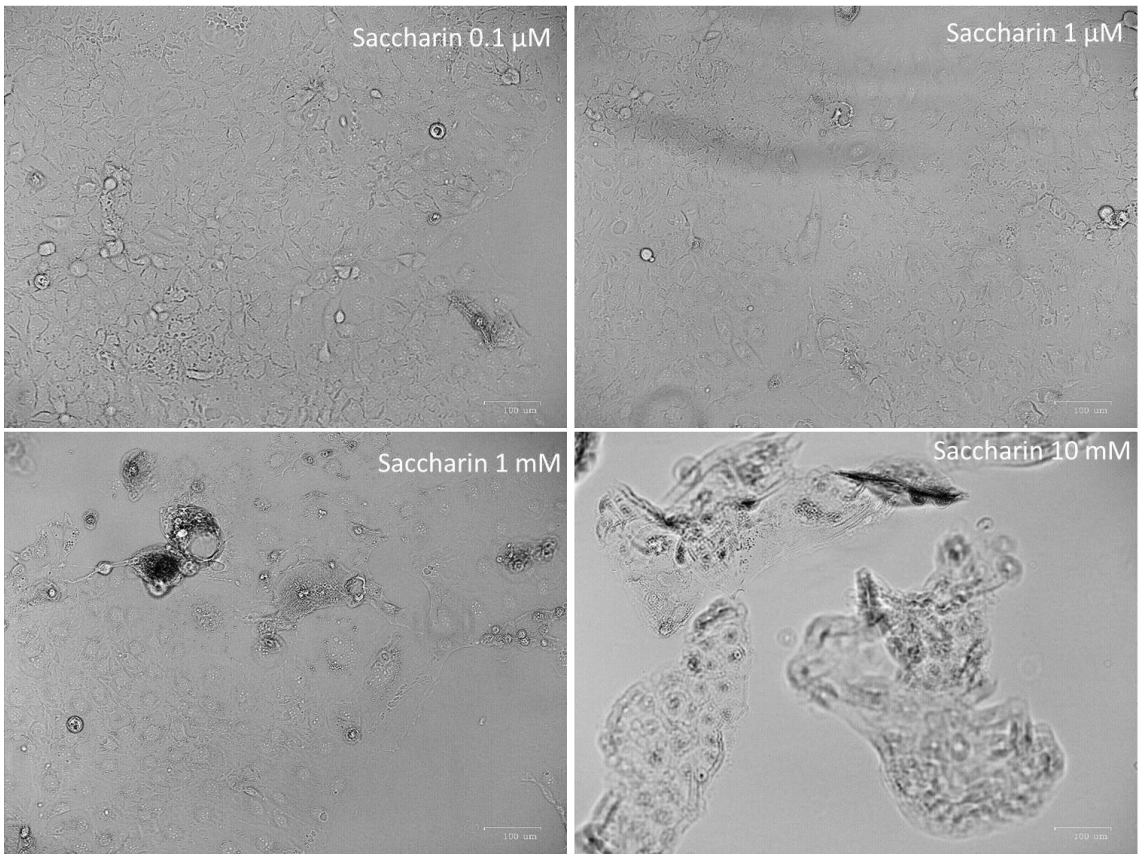

Figure 2.3.16: Effect of saccharin on the Caco-2 cell morphology.

Caco-2 cells were grown on 24-well plate until approximately 80% confluence. Cells were exposed to different concentrations of saccharin for 24 hours. Cells were observed for changes in cell adherence, shape and edges under brightfield microscopy using the Zoe imager. Negative morphological changes such as loss of adherence and rounding were observed from low to high concentration. Panel represents the concentrations of saccharin 0.1 µM(a), 1 µM(b), 1 mM(c), and 10 mM(d).

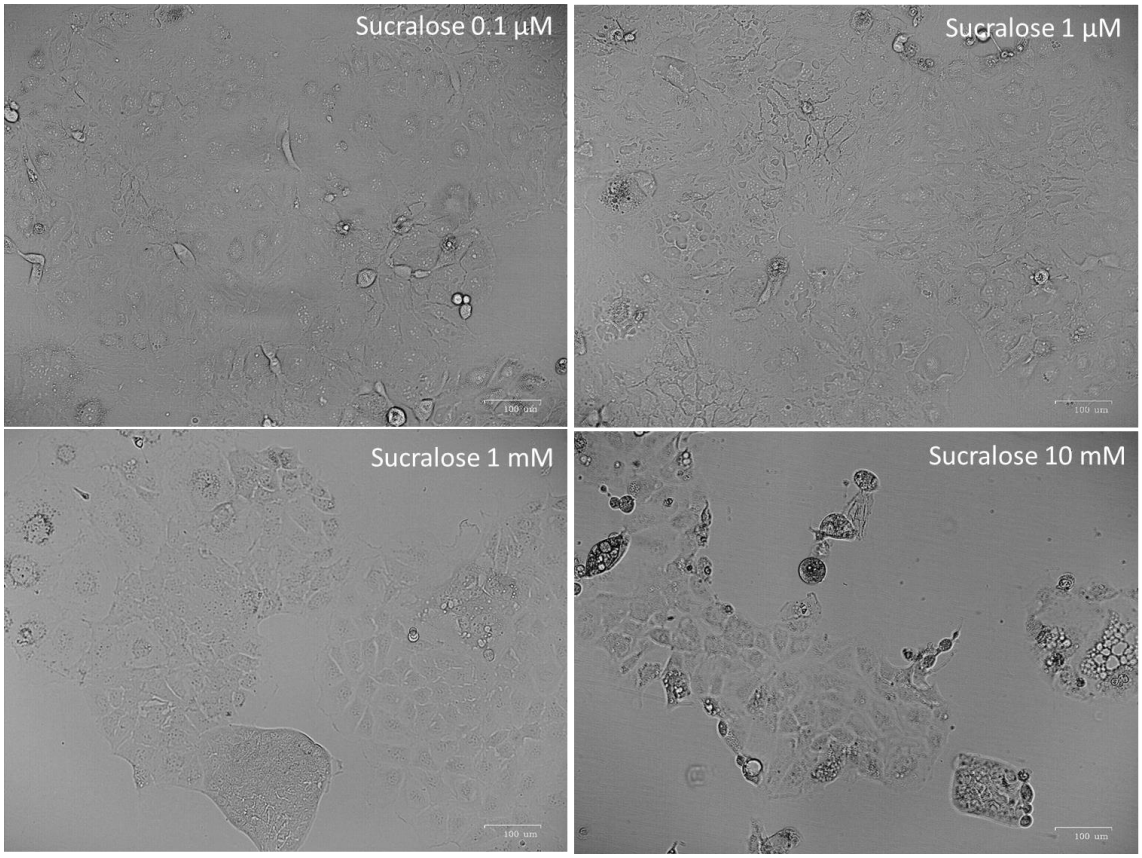

Figure 2.3.17: Effect of sucralose on the Caco-2 cell morphology.

Cells were maintained in EMEM on 24-well plate until about 80% confluence and exposed to different concentrations of sucralose for 24 hours. Cells were observed for morphological changes such as adherence, shape and edges using brightfield microscopy (Zoe imager). Higher concentration (10 mM) made cells more stretched especially in the edges and increased gaps among cell islands. Also, the vacuoles were greater in number from lower to higher concentrations of sucralose. Panel represents the concentrations of sucralose 0.1 µM(a), 1 µM(b), 1 mM(c), and 10 mM(d).

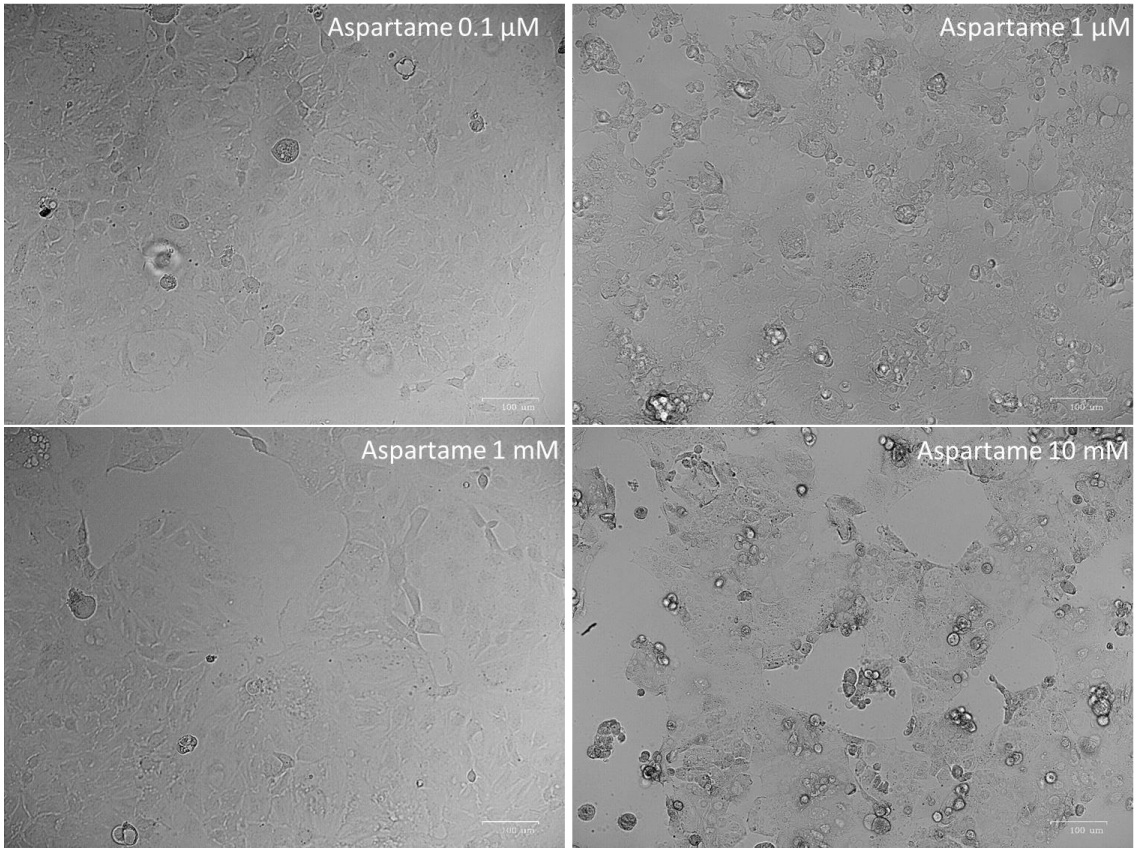

Figure 2.3.18: Effect of aspartame on the Caco-2 cell morphology.

Cells were maintained on 24-well plate until about 80% confluence and exposed to different concentrations of aspartame for 24 hours. Cells were observed for morphological changes such as adherence, shape and edges under brightfield microscopy using the Zoe imager. Higher concentration of aspartame (10 mM) increased gaps among cell islands, with an increasing stretch on cells in the edges. Also, the number of floating cells were increased with increasing concentration of aspartame. Panel represents morphology of Caco-2 cells at aspartame concentrations 0.1 µM(a), 1 µM(b), 1 mM(c), and 10 mM(d).

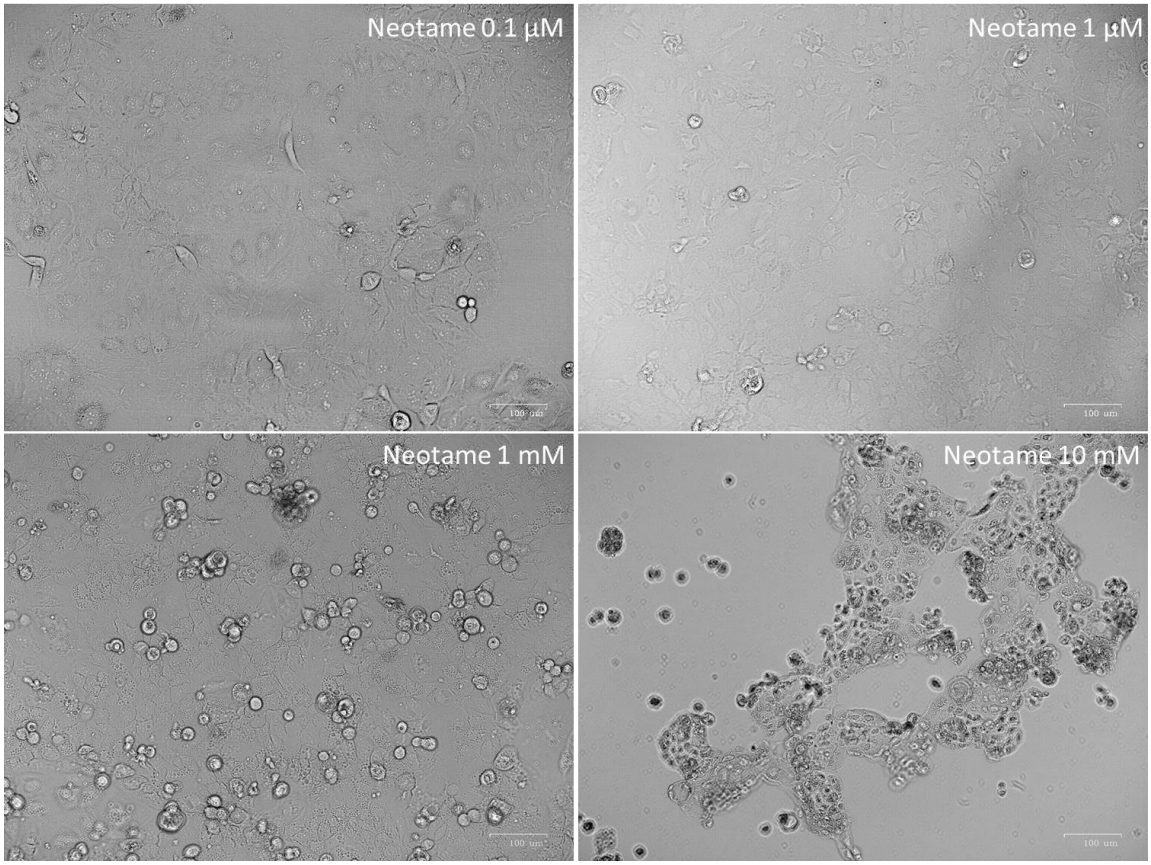

Figure 2.3.19: Effect of neotame on the Caco-2 cell morphology.

Cells were maintained in 24-well plate until about 80% confluence and were exposed to different concentrations of neotame for 24 hours. Cells were observed for morphological changes such as adherence, shape and edges using brightfield microscopy (Zoe imager). Neotame (10 mM) caused loss of adherence and shape, also the number of floating cells were higher at 1 mM. Furthermore, vacuoles inside cells were increased with the increasing concentration of neotame. Panel represents the morphology of Caco-2 cells at neotame concentrations 0.1 µM(a), 1 µM(b), 1 mM(c), and 10 mM(d).

Figure 2.3.20 represents the average percentage of necrotic (late apoptotic), dead, live and apoptotic cells found from untreated, LPS- and H_2O_2-treated Caco-2 cells. H_2O_2 is a well-known apoptosis inducer (Xiang et al., 2016), therefore was used as a positive control for the study. Caco-2 cells were exposed to a range of H_2O_2 concentrations (fig.A.8.3), and 0.8 mM was used for the further experiments with AS considering the findings (highest cell death, 62%). The effect of LPS on cell apoptosis was tested to verify the findings from the viability assay, among the tested concentrations, 100 µg/ml was found to cause significant apoptosis (fig.A.8.4), and therefore, used in the later experiments with AS. The percentage of late apoptotic (necrotic) cells were very low for all cases, and therefore, was not included for the results.

The positive control H_2O_2 caused 74% cell death (fig.2.3.20). The LPS increased cell death only 5%. The number of live cells was 69% for the control, which reduced by 10% for LPS exposure and dropped by 15% for H_2O_2 exposure. In addition, the number of apoptotic cells increased significantly (16%) for the LPS exposure of the cells. Therefore, LPS at high

concentration (100 µg/ml) cause Caco-2 cell apoptosis, and at the same duration (24-hour) of exposure 0.8 mM H_2O_2 cause cell death possibly via apoptosis.

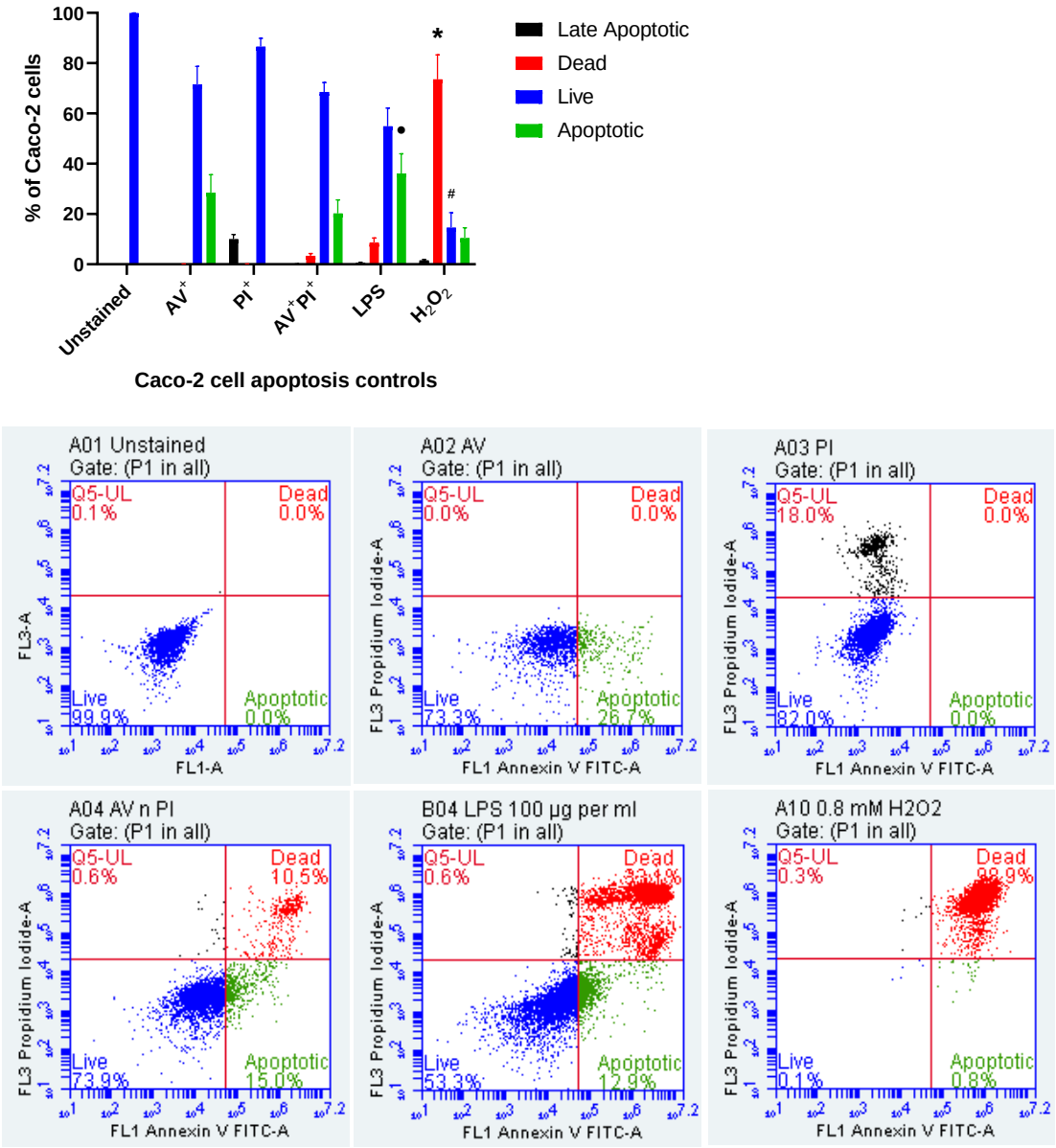

Figure 2.3.20: Detection of apoptosis in Caco-2 cells.

Caco-2 cells were maintained in T25 flasks with complete EMEM. At approximately 65% confluence, cells were treated with LPS (100 µg/ml) or H_2O_2 (0.8 mM) or vehicle for 24 hours. Untreated Caco-2 cells were stained with (BD Biosciences) only annexin-V-fluoresceinisothiocyanate (AV), only Propidium Iodide (PI) and both, and LPS- or H_2O_2- treated cells were stained with both AV and PI. Flow cytometric analysis of the untreated and treated cells were done using the BD Accuri Flow cytometer with the software Annexin V BD template-FITC. Green fluorescent apoptotic cells were monitored in the FL1 channel (530 nm), whereas red fluorescent necrotic and dead cells were measured in the FL3 channel (670 nm). The plots are representing the fluorescence of cell staining for AV (apoptotic cells, FL1) versus the fluorescence of the cell staining for PI (necrotic and dead cells, FL3). In each of the quadrats, dots with AV-/PI-(Blue), AV+/PI-(green), AV-/PI+(black) and AV+/PI+(red) represent live healthy, early apoptotic, late apoptotic, and dead cells, respectively. Panel a represents untreated cells; unstained (a01), only AV stained (a02), only PI stained (a03) and both AV and PI stained (a04), panel b04 and a10 represents effects of LPS and H_2O_2 on cells, respectively. Variation was determined using Two-way ANOVA followed by Dunnett's multiple comparisons test, and are presented as the mean ± S.E.M., n=5-6. *$p<0.05$ of dead, #$p<0.05$ of live, and •$p<0.05$ of apoptotic cells versus control.

Compared with the vehicle-treated cell that exhibited natural death, the high concentrations (1 and 10 mM) of all tested AS demonstrated significant amount of cell death AV^+/PI^+ (dead cells) after 24-hour exposure (fig.2.3.21). Sucralose at 100 µM and 1 mM reduced the percentage of live cells (fig.3.22.b) and increased apoptotic cells (fig.2.3.23.b), the other concentrations of sucralose insignificantly reduced live cells and increased apoptotic cell percentage. Saccharin at 0.1 µM slightly increased living cells (fig.2.3.22.a) while reducing apoptotic cell percentage (fig.2.3.23.a). Above 10% cell death was observed for all the AS at 1 mM (fig.2.3.21). At 10 mM, cell death was increased by only 1% for saccharin and aspartame, however, neotame caused highest cell death (37%) (fig.2.3.21).

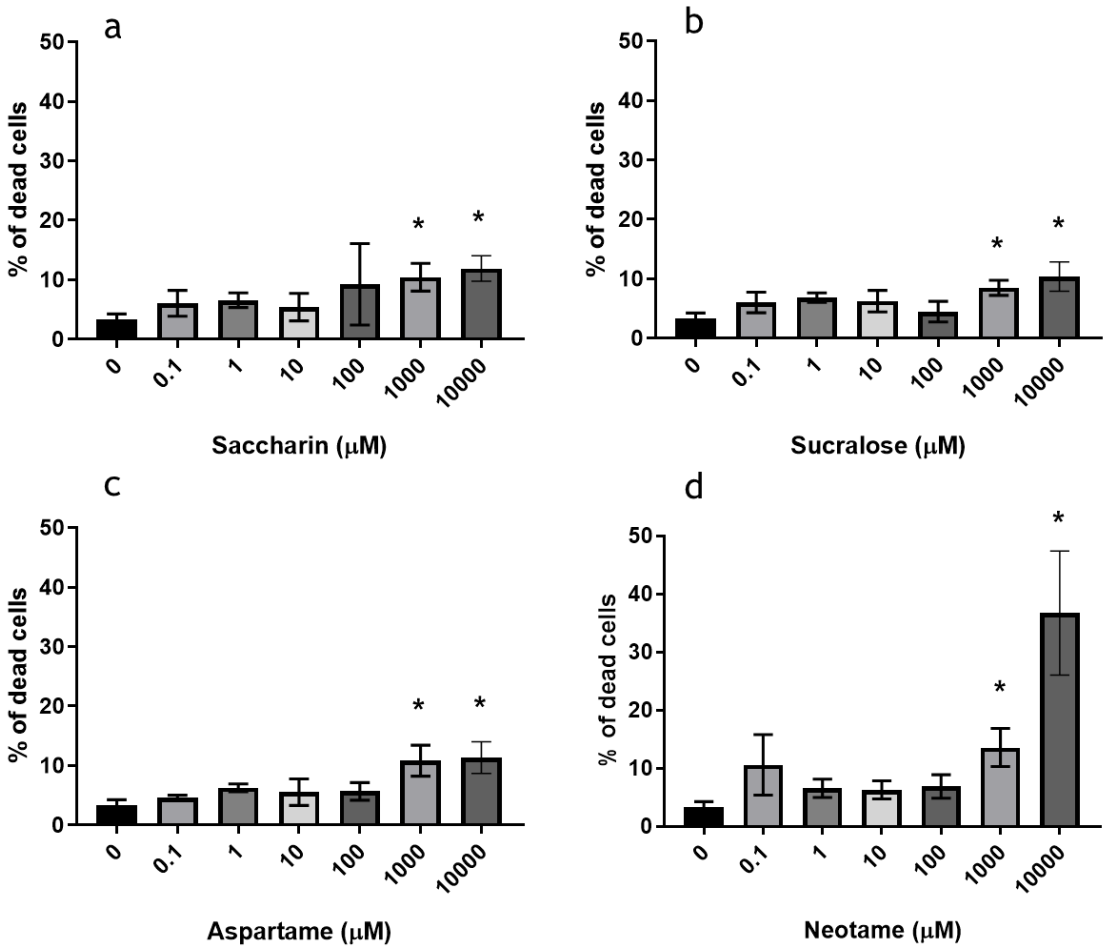

Figure 2.3.21: Dead percentage of Caco-2 cells from flow cytometric analysis after AS- or vehicle-exposure.

Panels represent the effect of saccharin (a), sucralose (b), aspartame (c), and neotame (d). Data are analysed using one-way ANOVA with uncorrected Dunn's test and are presented as the mean and S.E.M., n=6-8. *p<0.05 versus 0 µM of AS.

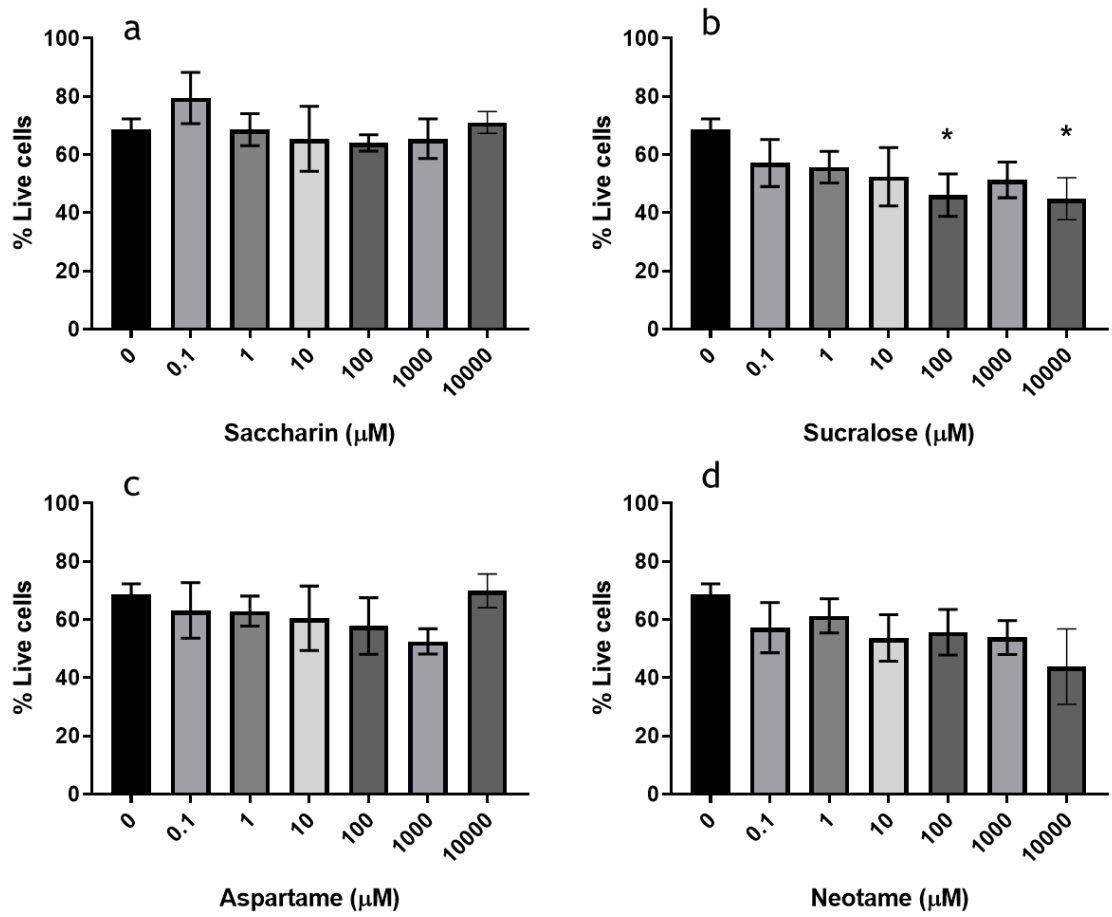

Figure 2.3.22: Percentage of live Caco-2 cells after AS- or vehicle-exposure.

Cells were exposed to different concentrations of four AS, Annexin V apoptosis assay was performed (BD Biosciences) and analysed using flow cytometry. Panels represent the effect of saccharin (a), sucralose (b), aspartame (c), and neotame (d). Data are analysed using one-way ANOVA with uncorrected Dunn's test and are presented as the mean and S.E.M., n=6-8. *p<0.05 versus 0 μM of AS.

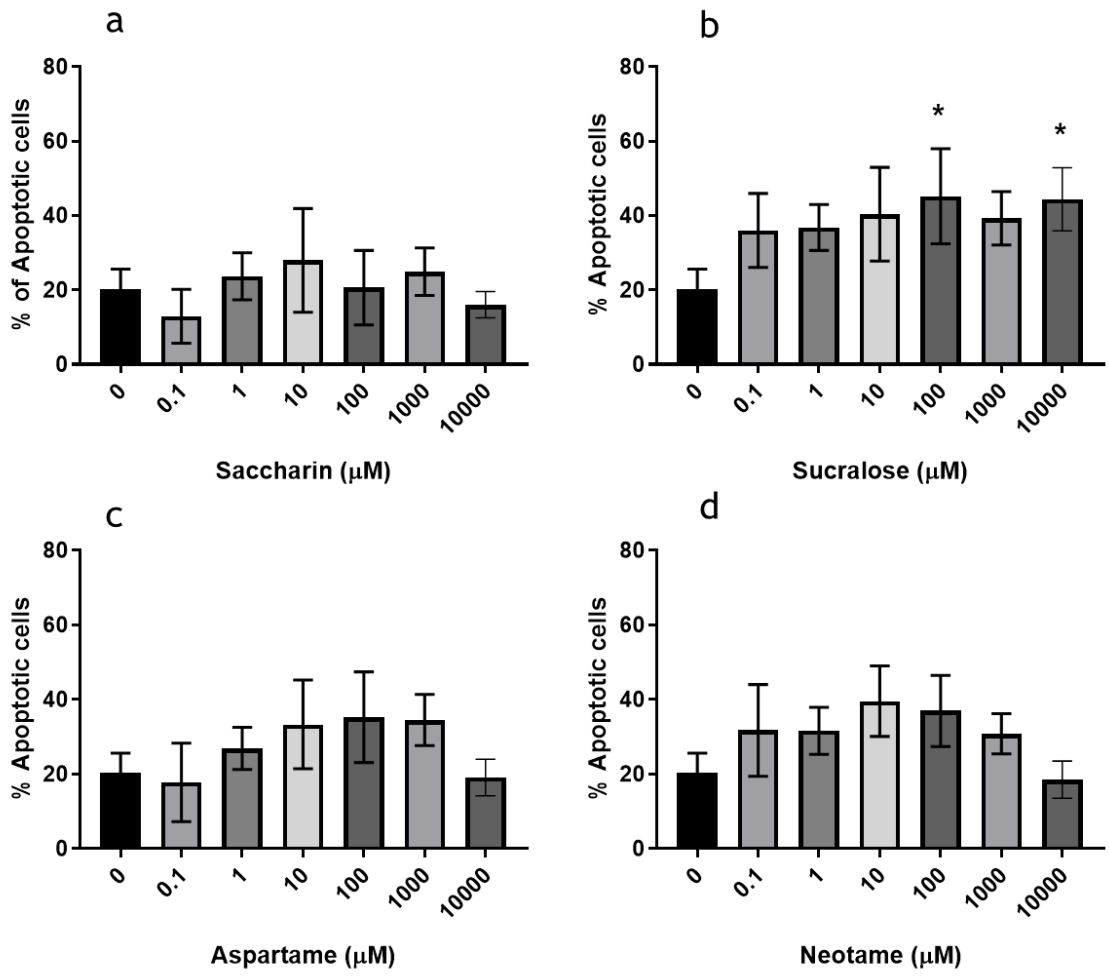

Figure 2.3.23: Quantitative apoptotic measurement of Caco-2 cells induced by AS. Approximately 65% confluent cells were exposed to different concentrations of the four AS or vehicle, stained with FITC-conjugated annexin V and analysed using flow cytometry (BD Biosciences). Panels represent the effect of saccharin (a), sucralose (b), aspartame (c), and neotame (d). Data are analysed using one-way ANOVA with uncorrected Dunn's test and are presented as the mean and S.E.M., n=6-8. *p<0.05 versus 0 μM of AS.

2.3.2.1 Effect of AS on Caco-2 cell nuclei

Apoptosis induces extensive morphological and biochemical changes. The main morphological changes include cell and nuclear shrinkage, chromatin condensation, formation of apoptotic bodies and phagocytosis by neighbouring cells (Kerr et al., 1972). The apoptosis findings suggest significant cell death due to AS exposure, and the highest death was found at 10 mM (fig.2.3.21), while apoptosis findings were not as anticipated (fig.2.3.23), the morphological changes in the nuclei was observed.

AS-mediated changes in cell and nuclei were observed using Zoe imager. The cell nuclei showed a great variability in morphology, size, and morphological features and size of organelles compared to vehicle-exposed controls (fig.2.3.24 to 2.3.26). The AS- and LPS-treated cells remained attached to the flask showed changes in cell border, distribution, and vacuolisation. Changes in cell shape with more stretching in the AS-treated cells were observed, and most cell shrinkage were found in the neotame-treated cells (fig.2.3.26 e,f).

High density of nuclear volume with loose chromatin structure was observed in control cells (fig.2.3.24 a,b). The 100 µg/ml LPS-treated cells demonstrated more flattened cells with less well-defined borders. In addition, LPS exposure caused nuclear condensations with irregular bordering, deep invaginations and blebbing (fig.2.3.24 c,d). Similar morphology was observed in the AS-treated cells and nuclei (fig.2.3.25, 2.3.26). Slightly curved nuclear border was observed for many nuclei in the sucralose-exposed cells (fig.2.3.25.d). There observed some small, round, blackish structures in the cytoplasm, the number of these small vacuoles were increased in the saccharin and aspartame treated cells (figure 2.3.25.c and 2.3.26.c). Nonetheless, intense vacuolisation in the cytoplasm was observed for neotame exposure (fig.2.3.26.e).

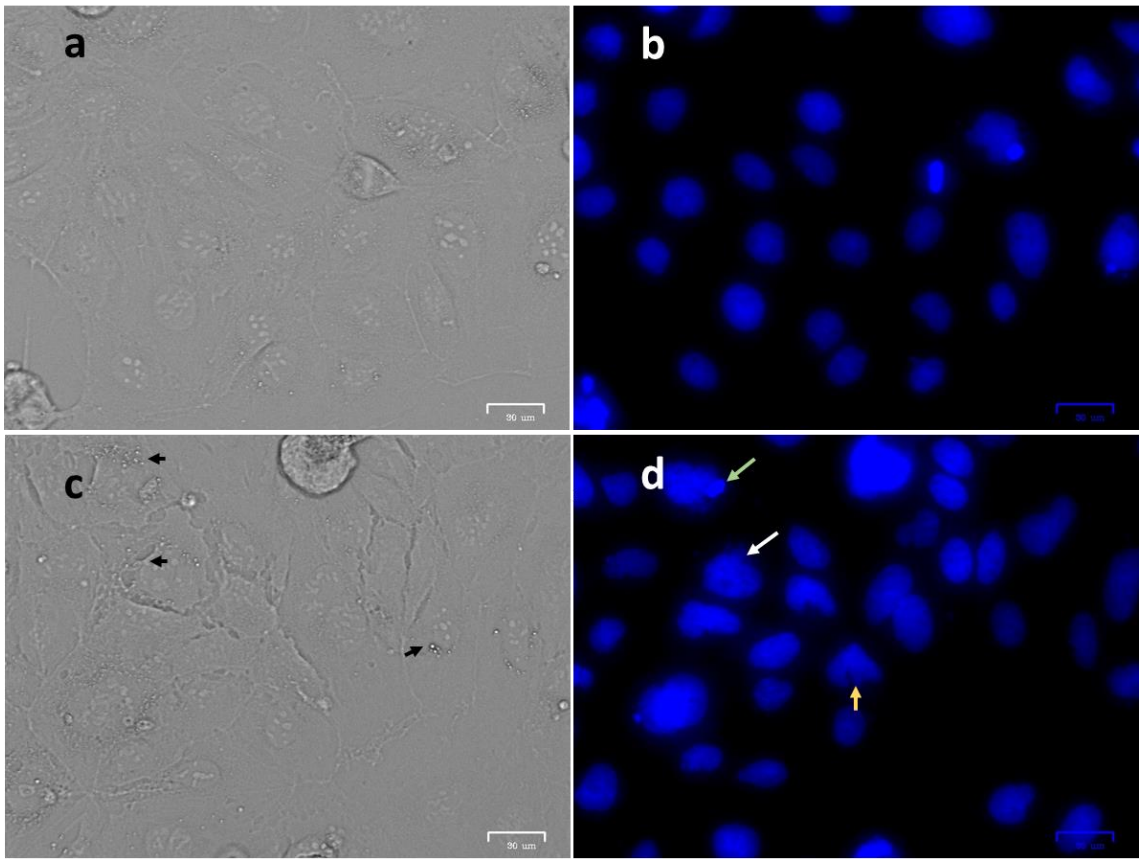

Figure 2.3.23: Morphology of Caco-2 cells after 24-hour LPS exposure.

Cells were seeded at 2×10^4 cells per well of the 24-well plate for 24 hours and treated with LPS or vehicle for 24 hours. Cells were fixed and stained with Prolong® Gold-DAPI (4′,6-diamidino-2-phenylindole) to visualize nucleus, and images were taken using Zoe imager. Panels represent brightfield (a,c) and DAPI stained (b,d) images of vehicle (a, b) and LPS (c, d) exposed cells. Unexposed cells showed high density of nucleus, nuclear bordering was regular and without intense vacuolization in the cytoplasm. The LPS-treated nuclei (d) showed condensed (white arrow), heavily convoluted nuclei with invaginations (yellow arrow), and active membrane blebbing (green arrow). There were more small vesicles in the LPS-exposed cells (c) than control cells (a). Scale = 30 µm.

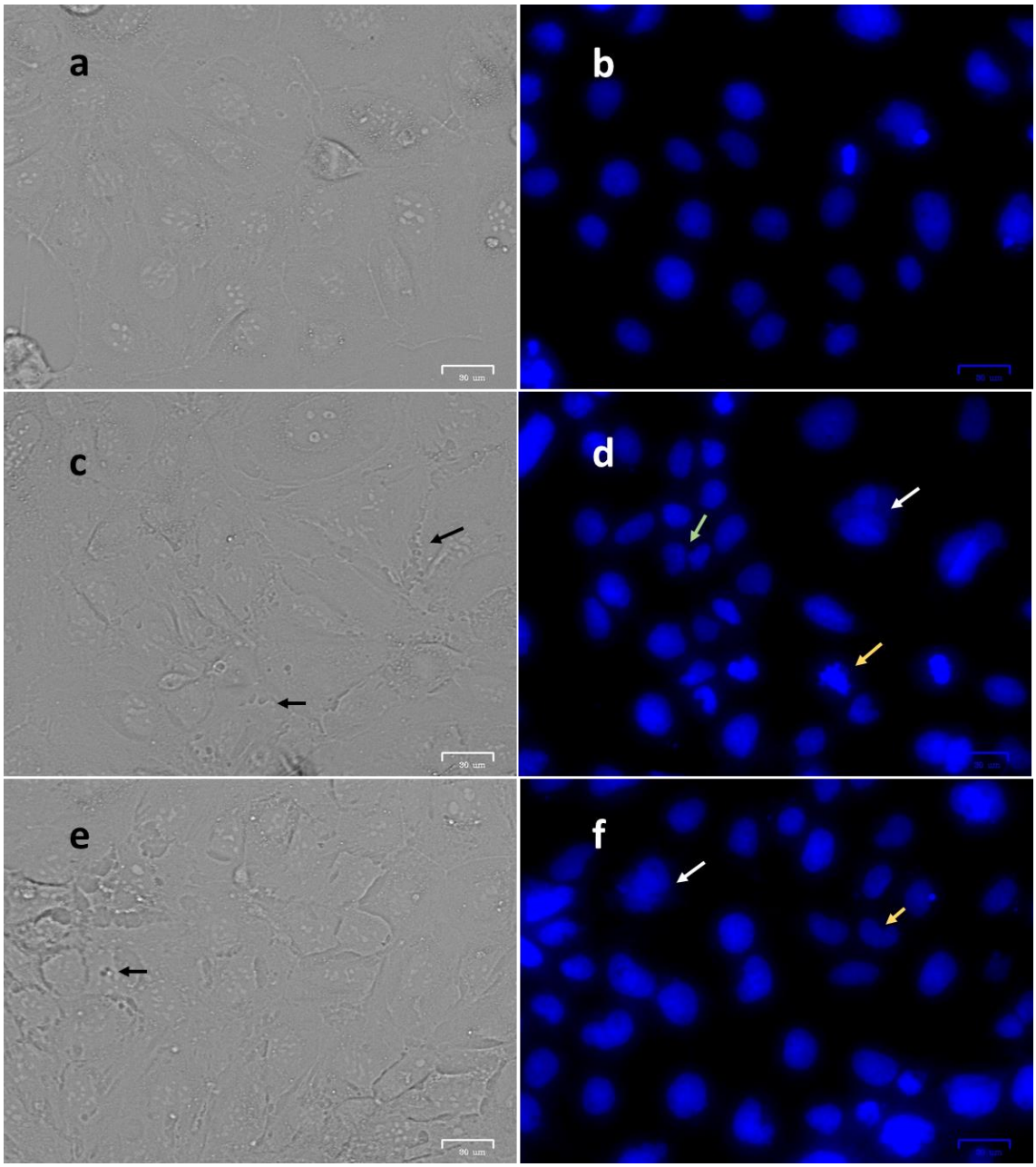

Figure 2.3.24: Effect of saccharin and sucralose on Caco-2 cell morphology after 24-hour exposure.

Cells were seeded at 2×10^4 cells/well of the 24-well plate for 24 hours and treated with 10 mM of saccharin or sucralose or vehicle. Cells were stained with Prolong® Gold-DAPI (4′,6-diamidino-2-phenylindole) to visualize nucleus, and observed using Zoe imager, scale = 30 µm. Panels represent brightfield and DAPI (blue) images of vehicle (a, b), saccharin (c, d) and sucralose (e, f) exposed cells. Unexposed cells showed high density in the nucleus with regular nuclear bordering. No intense vacuolization was observed in the cytoplasm of control cells. Small vacuoles (black arrows) and numerous black spots are visible in the sweetener-treated cells. Saccharin (d) caused disorganised nuclei with condensation (white arrow), heavily convoluted nuclei with invaginations (yellow arrow), and active membrane blebbing (green arrow). Nuclear condensation was also observed in the sucralose-exposed cells (f), and nuclei showed slight curvature in appearance.

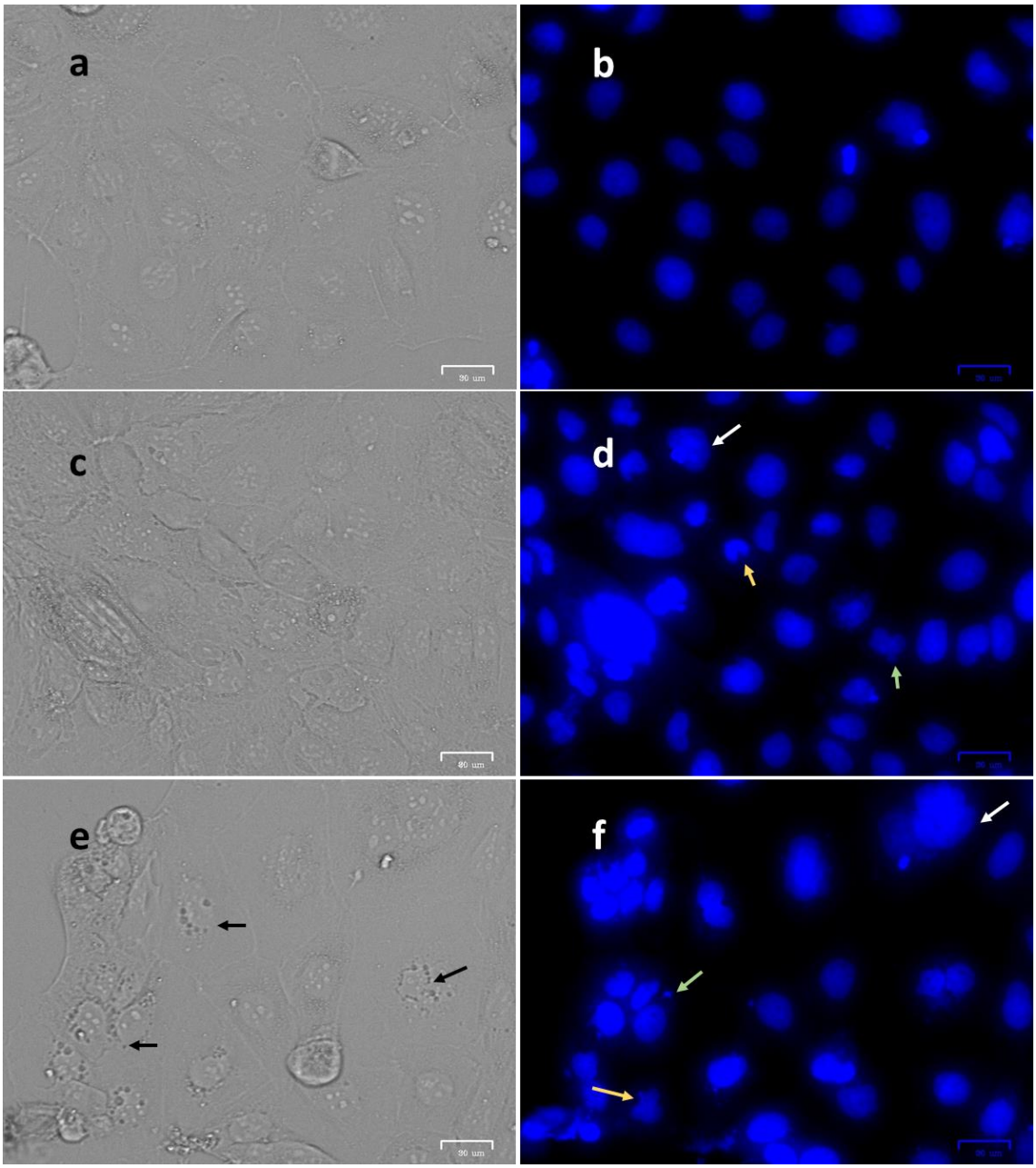

Figure 2.3.25: Effect of AS on the Caco-2 cell morphology after 24-hour exposure.

Cells were maintained on the 24-well plate and treated with 10 mM of aspartame and neotame or vehicle for 24 hours. Cells were stained Prolong® Gold-DAPI (4′,6-diamidino-2-phenylindole) and observed using Zoe imager. Panels represent brightfield and DAPI (blue) images of vehicle (a, b), aspartame (c, d) and neotame (e, f) exposed cells. Unexposed cells showed organised nuclei with smooth, regular nuclear bordering. The aspartame-treated (d) cells demonstrated different-sized nuclei with condensation (white arrow), heavily convoluted nuclei with invaginations (yellow arrow), and blebbing (green arrow). Similar nuclear changes were observed in the neotame-treated cells with more disorganised nuclei. There were numerous small vacuoles in the neotame-exposed cells (e) in comparison to the control cells (a). Scale = 30 µm.

However, DNA degradation might not be the only phenomena or play the major role in apoptotic cell death. Schulze-Osthoff *et al*. (1994) demonstrated apoptosis in enucleated cells (with cytochalasin B), indicating that DNA degradation and nuclear signalling are not the must to induce apoptotic cell death. Therefore, other cellular machineries that play role in cell apoptosis such as mitochondria were studied.

2.3.2.2 Effect of AS on cell mitochondria

Mitochondrial arrangements play an important role in cell function and apoptosis. Early stages of apoptotic cell death have been linked to dramatic alterations in mitochondrial morphology (Karbowski and Youle, 2003). Mitochondria undergo extensive fragmentation during apoptosis before activation of different cell death promoting protease enzymes (such as caspase family) (Youle and Karbowski, 2005). Since AS affected cell nuclei, mitochondria were also likely to be affected. So, mitochondria were stained (DiOC6) and morphological changes such as size, motion, and shape were observed using fluorescent microscopy (Zoe imager).

Compared to control, LPS caused mitochondria interconnected and elongated with lots of small and large vacuoles across the threads (fig.2.3.27.b). Some cells demonstrated perinuclear mitochondria and the cristae were merged. Saccharin caused mitochondrial elongation with small vacuoles in some cells. Perinuclear mitochondria with clusters were also visible along with disorganised ones (fig.2.3.28.c). In addition, sucralose did not affect mitochondrial arrangement much in comparison to control, although there were some clusters. Also, few stretched and interconnected mitochondria were visible in the sucralose-treated cells (fig.2.3.28.d). Nonetheless, short spheres were observed with perinuclear distribution. Aspartame caused some clustered mitochondria; few vacuoles were present, and the nuclei were surrounded by merged mitochondria (fig.2.3.29.e). Nevertheless, neotame caused massive changes in mitochondrial size and distribution. They became smaller and showed interrupted perinuclear arrangement. Moreover, enormous small vacuoles were observed in the mitochondria with fragmentation and merging (fig.2.3.29.f).

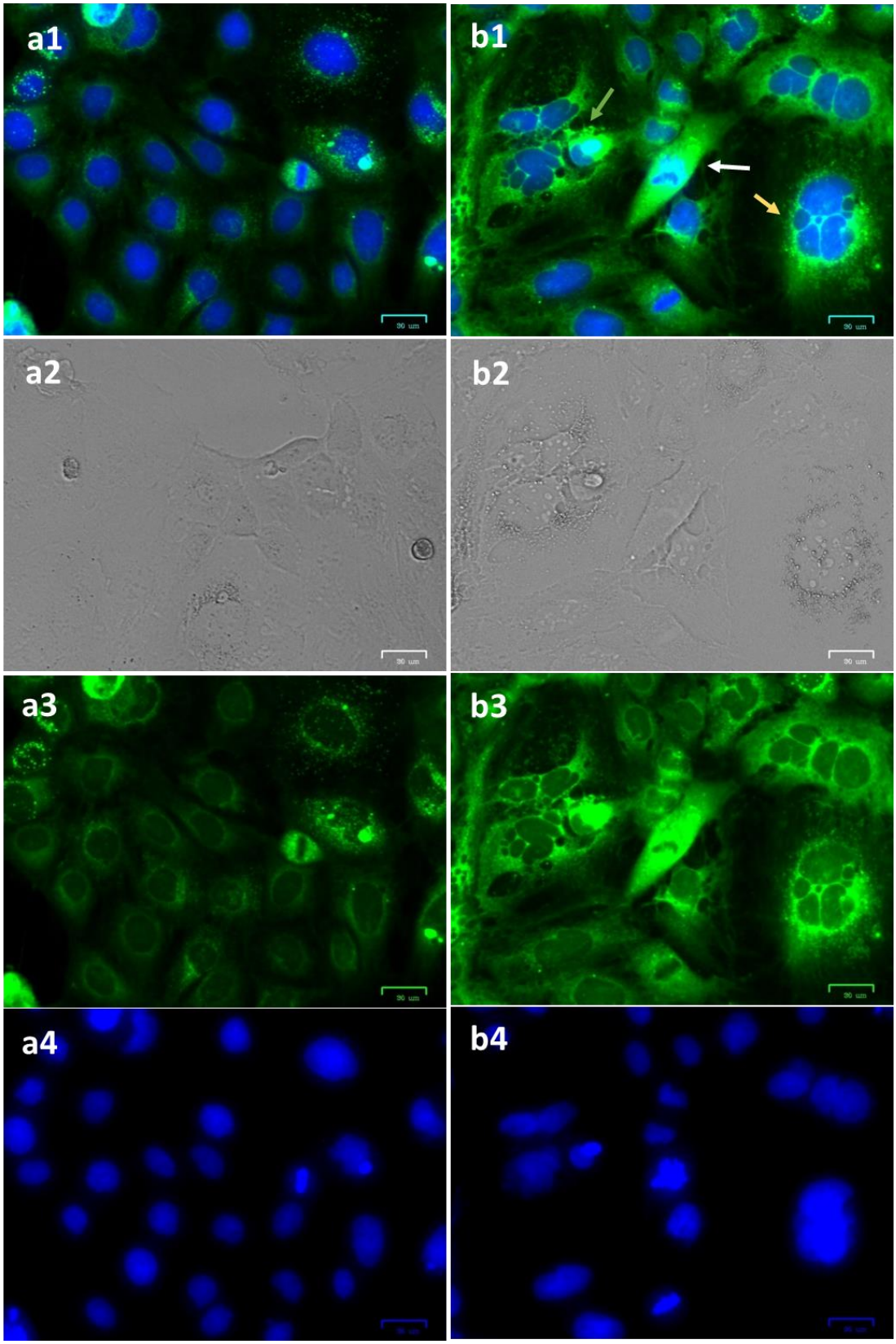

Figure 2.3.26: Changes in cell mitochondrial morphology by LPS exposure.

Caco-2 cells were exposed to 100 µg/ml of LPS or vehicle for 24 hours. Mitochondria were stained with DiOC6 (3,3'-Dihexyloxacarbocyanine Iodide) (green), and nuclei were stained using Prolong® Gold-DAPI (4′,6-diamidino-2-phenylindole) (blue) and visualized by fluorescence microscopy (Zoe imager). Panel a and b represent control and LPS-treated cells, respectively. Mitochondria are elongated and interconnected (white arrow), disorganized (green arrow), cluster perinuclearly (yellow arrow) in panel b1 compared to typical morphology of control (a1). 1, 2, 3 and 4 indicates merge, brightfield, DiOC6, and DAPI images, respectively. Scale = 30 µm.

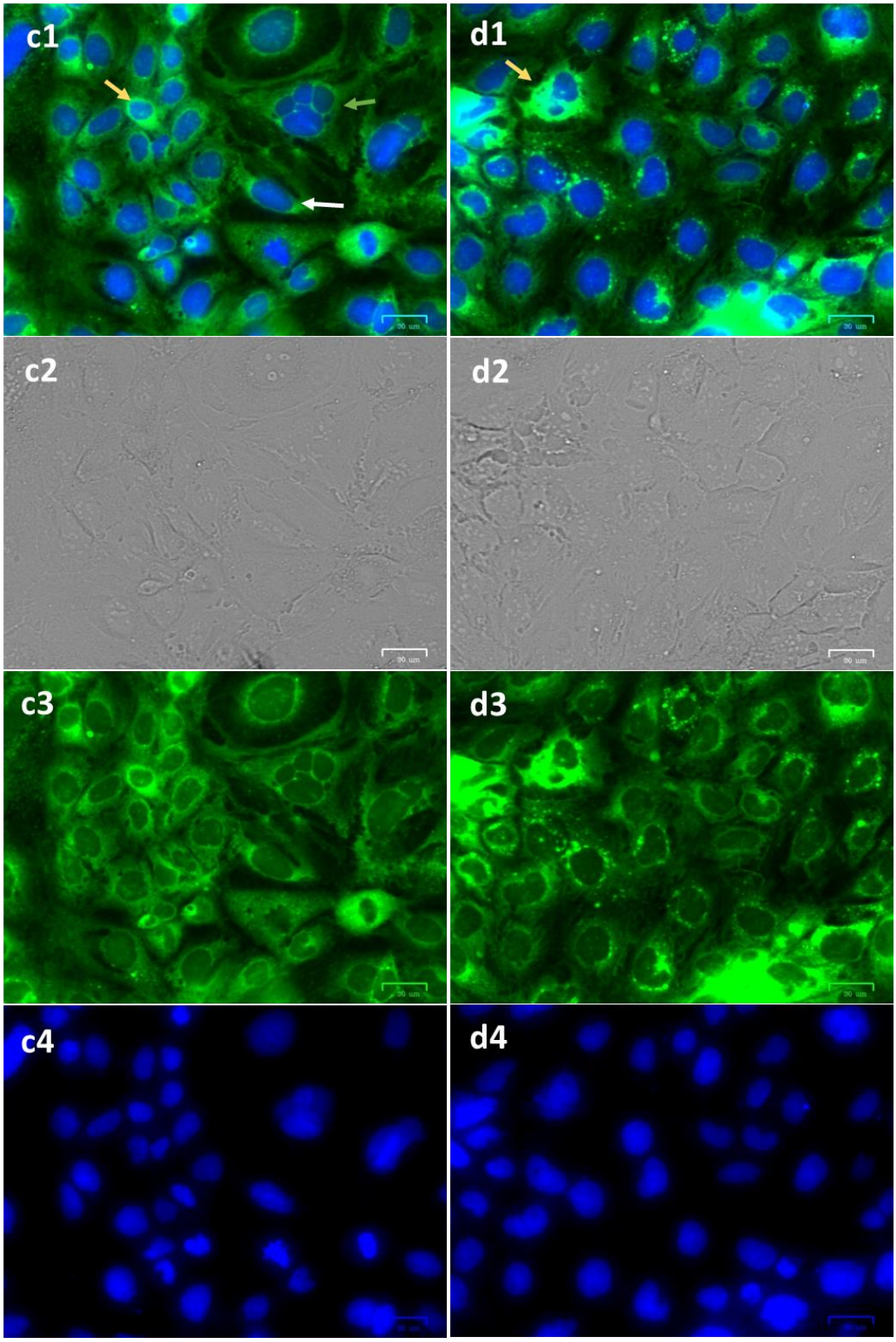

Figure 2.3.27: Effect of saccharin and sucralose on mitochondria.

Caco-2 cells were exposed to 10 mM of AS for 24 hours. Mitochondria and nuclei were stained with DiOC6 (3,3'-Dihexyloxacarbocyanine Iodide) (green) and Prolong® Gold-DAPI (4′,6-diamidino-2-phenylindole) (blue), respectively, and visualized by fluorescence microscope (Zoe imager). Panel c and d represent saccharin- and sucralose-treated cells, typical morphological features are shown in vehicle-treated cells (figure 3.27.a). Mitochondria are elongated and interconnected (white arrow), disorganized (green arrow) and clustered perinuclearly (yellow arrow) in panel c1 and d1. 1, 2, 3 and 4 indicates merge, brightfield, DiOC6 and DAPI images, respectively. Scale = 30 µm.

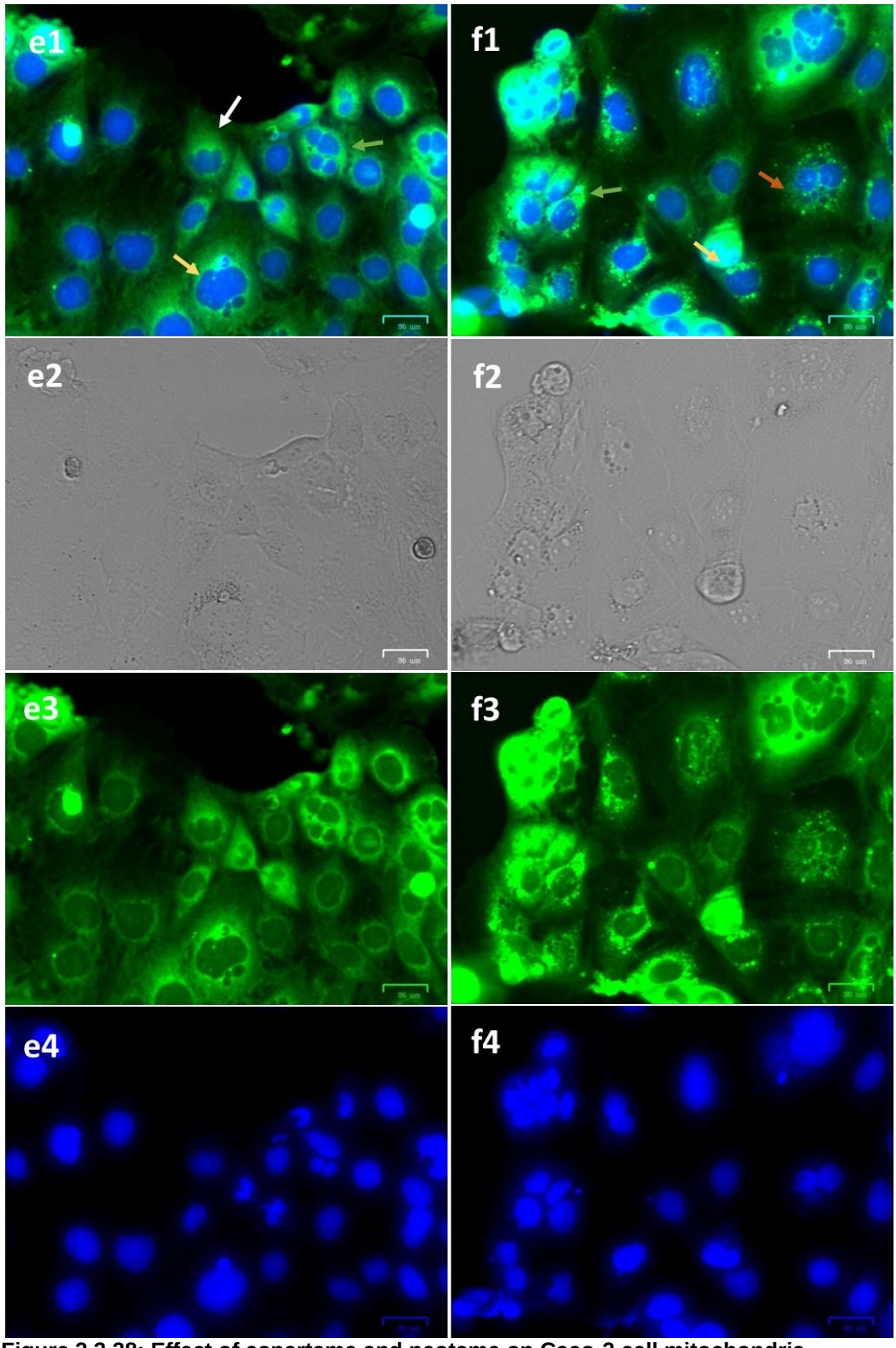

Figure 2.3.28: Effect of aspartame and neotame on Caco-2 cell mitochondria.

Caco-2 cells were exposed to 10 mM of AS for 24 hours. Mitochondria and nuclei were stained with DiOC6 (3,3'-Dihexyloxacarbocyanine Iodide) (green) and Prolong® Gold-DAPI (4′,6-diamidino-2-phenylindole) (blue), respectively, and visualized by fluorescence microscope (Zoe imager). Panel 'e' represent the aspartame and 'f' represent the neotame-exposed cells. Typical morphological features are shown in vehicle-treated cells (figure 3.27a). Mitochondria were elongated and interconnected (white arrow), disorganized (green arrow) and clustered perinuclearly (yellow arrow) in panel e1 and f1. 1, 2, 3 and 4 indicate images obtained from merge, brightfield, DiOC6 and DAPI, respectively. Scale = 30 µm.

2.3.3 FITC-Dextran permeability assay

Several agents that alter actin cytoskeleton are also responsible for an increased TJ-mediated permeability of IECs (Narai et al., 1997), so the effect of AS on the monolayer permeability was measured using FITC-Dextran permeability assay. The flux of the solute fluorescent marker FD from apical to basolateral compartment was measured to assess paracellular permeability (fig.2.3.30).

2.3.3.1 Method validation

FD is a metabolically inert, water-soluble molecule that is frequently used in microcirculation and cell permeability research (Svensjö et al., 1978; Rutili and Arfors, 1976). Both FD4 and FD20 proteins were used to investigate the concentrations of LPS causing Caco-2 cell monolayer permeability. 100 µg/ml of LPS caused Caco-2 cell viability reduction (fig.2.3.2) and increased apoptosis (fig.2.3.20); decrease in cell viability might increase monolayer permeability, therefore, lower concentrations (<100 µg/ml) were used for the permeability assay.

In addition, three different cell numbers and different incubation durations were employed to optimise the experiment. For $1x10^4$ cells, 1 µg/ml LPS showed significant permeability at 60- and 180-seconds (fig.2.3.30.a). At 50 µg/ml LPS for the same number of cells, significant permeability was observed at 60-, 180-, and 360-seconds (fig.2.3.30.a). Also, FD20 showed significant permeation at 60- and 360-seconds for 0.1 µg/ml LPS, and at 60 second for highest concentration of LPS (50 µg/ml), however, FD20 did not show significant permeability at 1 and 10 µg/ml of LPS (fig.2.3.30.b).

No consistent significance was observed for $5x10^4$ cells at tested timepoints for both FD4 and FD20 (fig.2.3.30.c,d). The incubation duration was 48 hours for $5x10^4$ cells before FD addition which might have caused cell overgrowth. This leads to overlapping of cells inhibiting any permeation. Although there was significant permeation of FD4 at 60 second (0.01 µg/ml LPS), however, no significance was found for any other concentration or timepoint (fig.2.3.30.c). FD20 also permeated across $5x10^4$ cells significantly at 180 second for 0.01 and 0.1 µg/ml LPS but no permeability was observed for the higher concentrations at any timepoint (fig.2.3.30.d). Likewise, $1x10^5$ cells and 1-hour incubation after FITC-dextran addition, a similar level of fluorescence was measured for all LPS concentrations for both FD4 and FD20 and no significance was found (fig.2.3.30.e,f).

Taken together, the above findings suggest that $2x10^4$ cells, 1 µg/ml LPS, and FD4 represent better conditions for the further permeability study with AS. Although 50 µg/ml LPS caused permeation of FD4 at all timepoints, however, this concentration might have additive effect on Caco-2 cells along with AS.

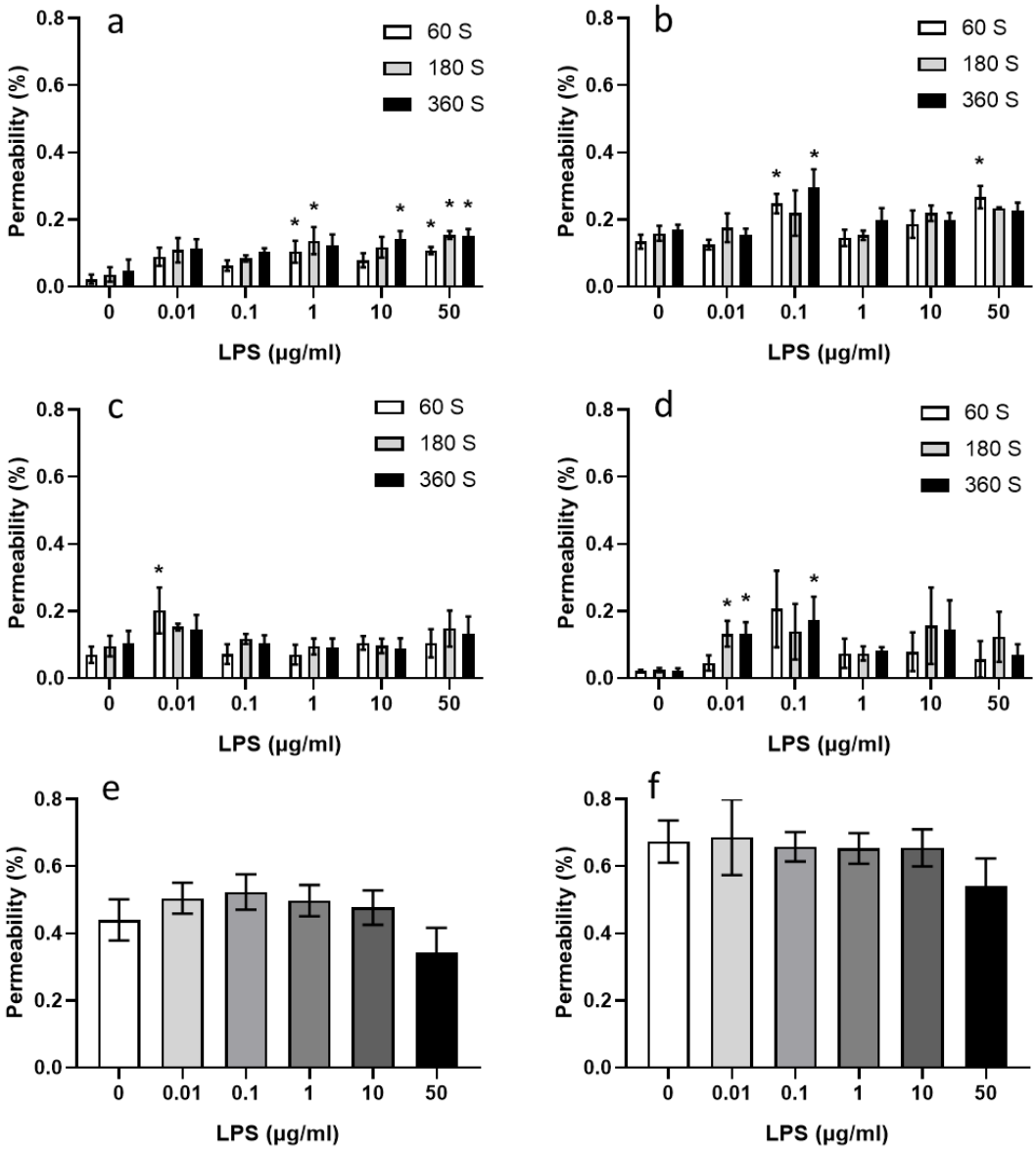

Figure 2.3. 29: FITC-Dextran permeability assay.

Caco-2 cells were seeded at $2x10^4$ (a, b), $5x10^4$ (c, d), and $1x10^5$ (e, f) on Transwell plate inserts for different timepoints and sampling was done differently. Fluorescein isothiocyanate-Dextran proteins 4000 or 20000 (FD4 and FD20, respectively) were used as soluble fluorescent marker. Panel a, c, and e represent FD4, and b, d, f represent FD20 permeation. $2x10^4$ cells (a and b) were maintained for 24 hours and exposed to lipopolysaccharide concentrations for 24 hours, FD4 (a) or FD20 (b) were added in the upper compartment of transwell plate (5 µg/ml). 100 µl sample was collected from both insert and base compartment and poured into 96-well plate at 60-, 180-, and 360-seconds. Plates were read at excitation and emission wavelengths of 485 – 535 nm (FITC HC protocol) using PerkinElmer (Victor X3). The same method was used for $5x10^4$ cells (c and d), however cells were maintained for 48 hours before LPS exposure. In panel e and f, $1x10^5$ cells were plated and treated like $5x10^4$ cells however FD proteins could permeate for 1 hour at 37 °C. Data were calculated as base/insert ratio of the fluorescence and analysed using Uncorrected Dunn's test. Data are presented as the mean ± S.E.M., n=3-4, *p<0.05 versus 0 µg/ml of LPS.

2.3.3.2 Effect of AS on intestinal epithelial cell monolayer permeability

All the AS were found to interfere with the permeability of the Caco-2 cell monolayer. FITC-dextran concentration was increased in the lower compartment of the Transwell plate after 180- (fig.2.3.31) and 360-second (fig.2.3.32) of incubation. Saccharin and sucralose increased permeability at 1 mM (fig.2.3.31 a and b, respectively), while aspartame and neotame increased at 100 µM (fig.2.3.31 c and d, respectively) at 180 second permeation time. Moreover, saccharin caused leak at 10, 100 and 1000 µM concentrations when incubated for 360 seconds (fig.2.3.32.a). Aspartame also caused leak at 0.1 and 1 mM for 360 second incubation (fig.2.3.32.c), however, neither sucralose nor neotame caused any significance in permeability at this timepoint (fig.2.3.32.b and d).

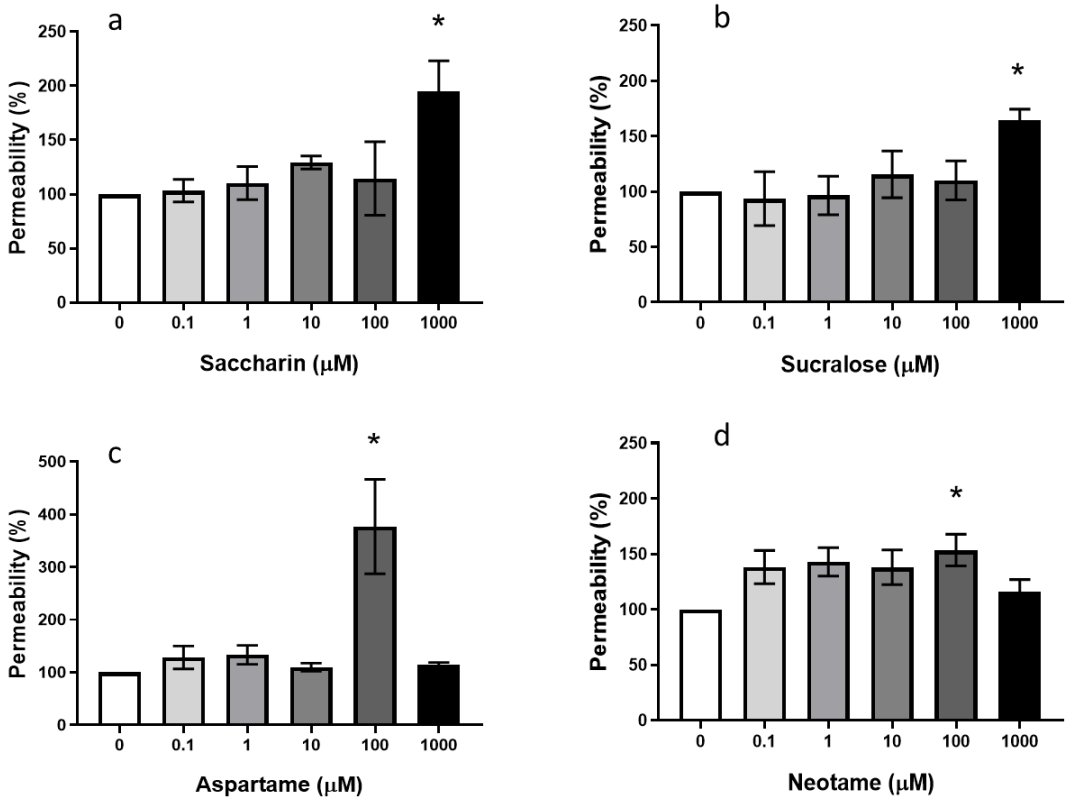

Figure 2.3.30: Effect of artificial sweeteners on the Caco-2 cell monolayer permeability.

Caco-2 cells ($2x10^4$) were exposed to different concentrations of the sweeteners or vehicle for 24 hours. FITC-Dextran 4000 protein (FD4) could pass for 180 seconds and samples were collected into 96-well plate from both upper and lower compartment. Plates were read at excitation and emission wavelengths of 485-535 nm using PerkinElmer (Victor X3). Data shows percentage of ratio (base/insert), normalised with the control as 100%. Data were analysed using ordinary one-way ANOVA with Dunnett's multiple comparisons test and are presented as the mean ± S.E.M., n=7. *p<0.05 versus 0 µM of AS.

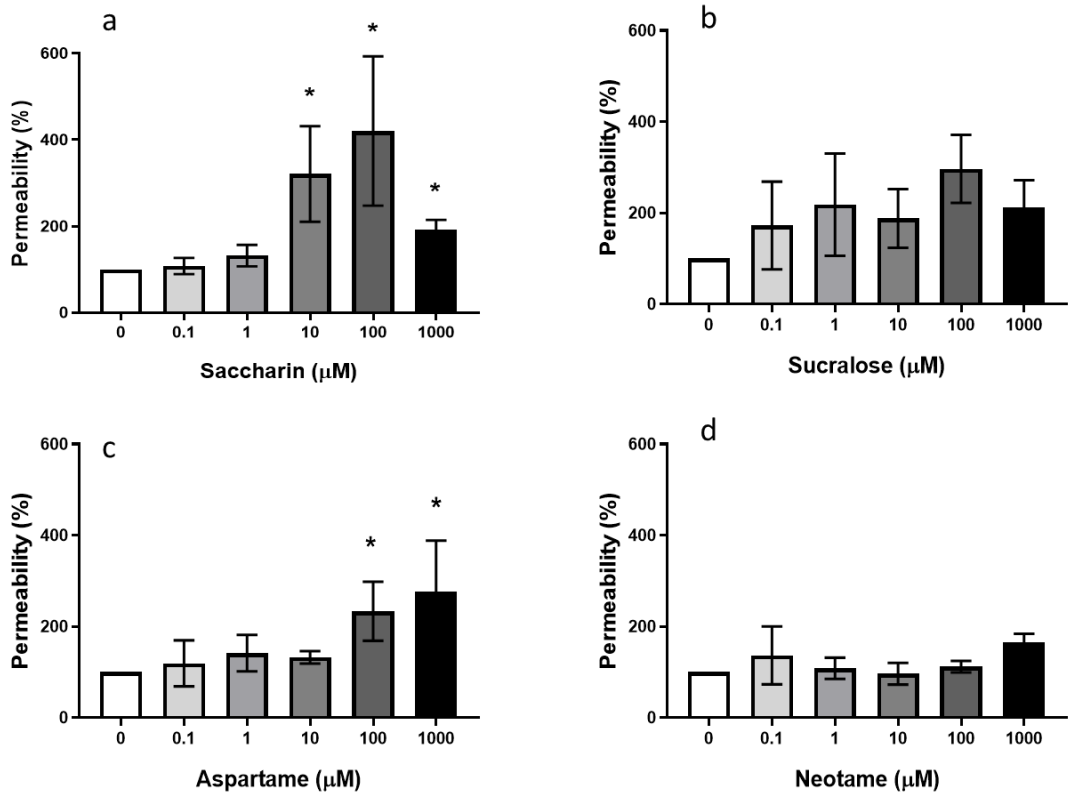

Figure 2.3.31: Effect of artificial sweeteners on the Caco-2 cell monolayer permeability at 360 seconds.

Caco-2 cells were seeded in the upper compartment of transwell plate at $2x10^4$ cells/well. Cells were incubated for 24 hours and exposed to different concentrations of the AS or vehicle for 24 hours. Fluorescein isothiocyanate-Dextran protein 4000 (FD4) could pass the cell monolayer for 360 seconds, samples were collected from both insert and base compartments into 96-well plates and read at 485-535 nm using PerkinElmer (Victor X3). Data shows percentage of ratio (base/insert), normalised with the control as 100%. Data are analysed using one-way ANOVA with uncorrected Dunn's test and are presented as the mean ± S.E.M., n=7. *p<0.05 versus 0 μM of AS.

2.3.3.3 Effect of LPS and AS on cell monolayer permeability

LPS increases Caco-2 cell monolayer permeability (Guo et al., 2013). In the gut environment, LPS is the most prominent endotoxin (Moreira et al., 2012), it is likely that IECs are exposed to AS in conjunction with LPS. So, the next set of FITC-Dextran permeability was assessed for Caco-2 cell monolayer exposed to both AS and LPS.

Exposing cells to AS in presence of LPS (1 μg/ml) caused cell monolayer leak at lower concentrations in comparison with the baseline AS effect (fig.2.3.33 and 2.3.34). At 180 seconds, saccharin caused leak of FD4 at 1 μM (fig.2.3.33.a) while sucralose caused leak at 0.1 μM in presence of LPS (fig.2.3.33.b). The transport of FD4 across the monolayer was also increased for all the used concentrations of aspartame (except 1 mM) and neotame when exposed with LPS (fig.2.3.33.c and d, respectively).

Saccharin caused leak at concentrations 1 and 100 μM at 360 seconds in presence of LPS (fig.2.3.34.a), whereas no significance was observed for any concentrations of the

sucralose (fig.2.3.34.b). Moreover, both aspartame (fig.2.3.34.c) and neotame (fig.2.3.34.d) increased leak at 1 and 10 µM at 360-second permeation time.

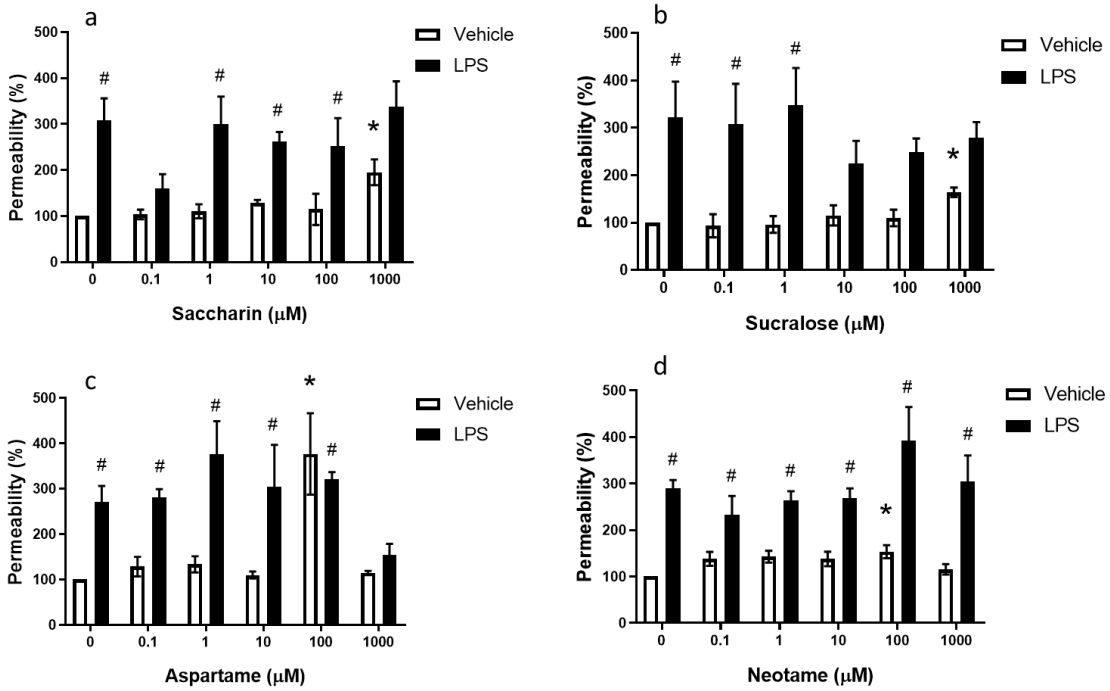

Figure 2.3.32: Effect of AS with LPS on Caco-2 cell monolayer permeability.

Cells were grown to monolayer on the insert of transwell plate and treated with AS with/out LPS (1 µg/ml) or vehicle. Permeation of FITC-dextran through cell monolayer was allowed for 180 second at room temperature and samples were collected in 96-well plate from both insert and base compartments. Absorbance was measured using excitation and emission wavelengths of 485 – 535 nm using PerkinElmer (Victor X3). Permeability was measured as normalised (with vehicle) percentage of the ratio of insert/base. Data were analysed using two-way ANOVA with Tukey's multiple comparisons test, and presented as the mean ± S.E.M., n=7. *p<0.05 versus 0 µM of AS, #p<0.05 versus 1 µg/ml of LPS.

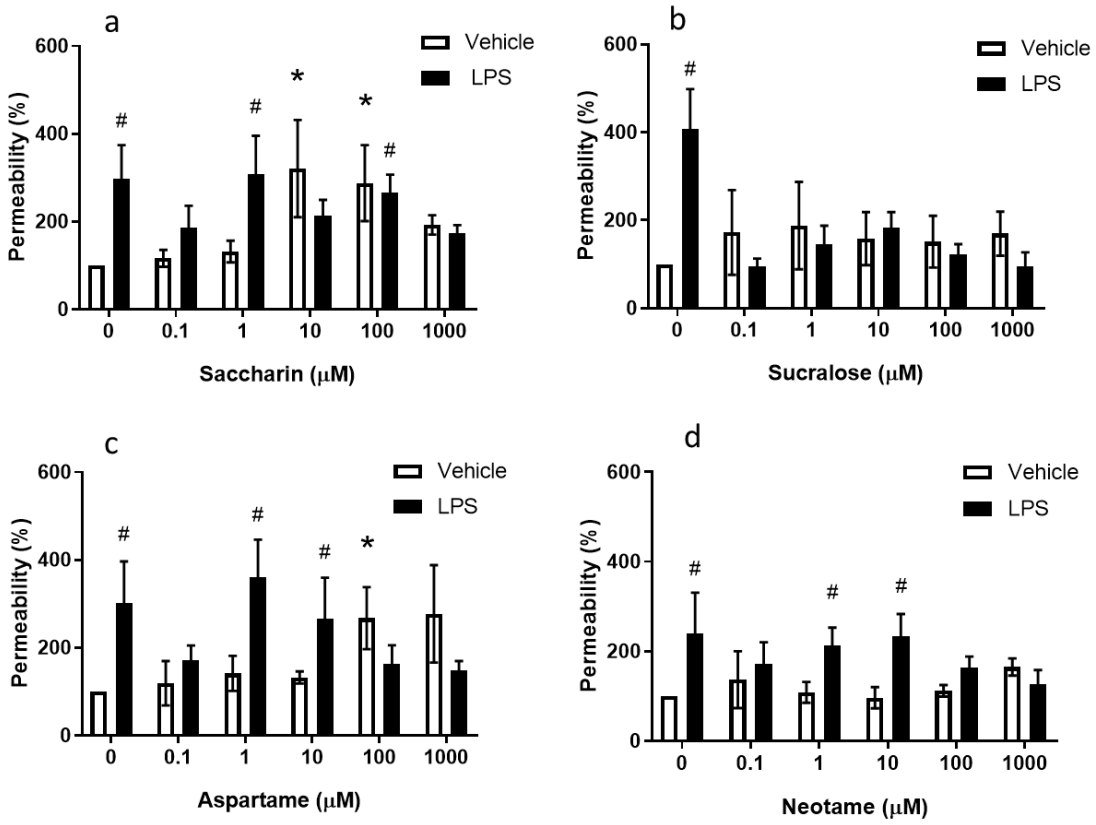

Figure 2.3.33: Effect of AS and LPS on Caco-2 cell monolayer permeability at 360 seconds.

Cells were grown on the inserts of transwell plate and treated with AS with/out 1 μg/ml of LPS or vehicle. FITC-dextran was added in inserts and samples were collected in 96-well plate at 360 seconds from both insert and base compartments. Absorbance was measured using excitation and emission wavelengths of 485 – 535 nm (PerkinElmer, Victor X3). Permeability was measured as normalised (with vehicle) percentage of the ratio of insert/base. Data were analysed using two-way ANOVA with Uncorrected Fisher's LSD test, and presented as the mean ± S.E.M., n=7. *$p<0.05$ versus 0 μM of AS, $^{\#}p<0.05$ versus 1 μg/ml of LPS.

Taken together, the above findings suggest that the AS causes Caco-2 cell monolayer permeability and the leak exacerbates due to combined effect of AS and LPS. The permeability is linked to F-actin cytoskeletal arrangements (Banan et al., 2001). Therefore, the effect of AS on the stress fibre formation (actin stress fibres) was observed in the next step.

2.3.4 Stress fibre formation

The epithelial barrier properties are regulated by specialized plasma membrane structures called apical junctions (Mooseker, 1985). These membrane structures are composed of different adhesive and scaffolding proteins that are anchored into different cytoskeletal structures including the actin filaments (Ivanov et al., 2010). Increasing research showed the pivotal role of actin cytoskeleton in regulating junctional integrity under physiological states. Reorganizations of F-actin cytoskeleton (disassembly and instability of the actin fibres) during inflammation drive disruption of epithelial barriers leading to permeability (Ivanov et al., 2010; Banan et al., 2001). Since AS exposure caused cell viability reduction

and monolayer permeability, therefore, it is likely that they enhance F-actin cytoskeleton disruption, hence, the effect of AS on the F-actin was assessed.

Stress fibre formation was investigated after AS-exposure using phalloidin stain, as illustrated in figures 2.3.35 to 2.3.37. The control cells have fine, long and uniform distribution of actin fibres, captured only in the edges of cell islands (fig.2.3.35.a). The LPS exposed cells demonstrated localized dense spots of F-actin accumulation and prominent bead-like appearance with marked rounding of the cell cytoskeleton (fig.2.3.35.b). Saccharin caused some actin accumulation (fig.2.3.36.c), however, sucralose-exposed cells (fig.2.3.36.d) showed similar response of LPS. Aspartame- (fig.2.3.37.e) and neotame- (fig.2.3.37.f) treated cells developed different patterns of F-actin alteration, with much prominent changes in neotame-exposed cells. Other than the localized F-actin accumulation, neotame caused large translucent zones, marked rounding with conserved punctuated appearance in the centre of the cells (fig.2.3.37.f).

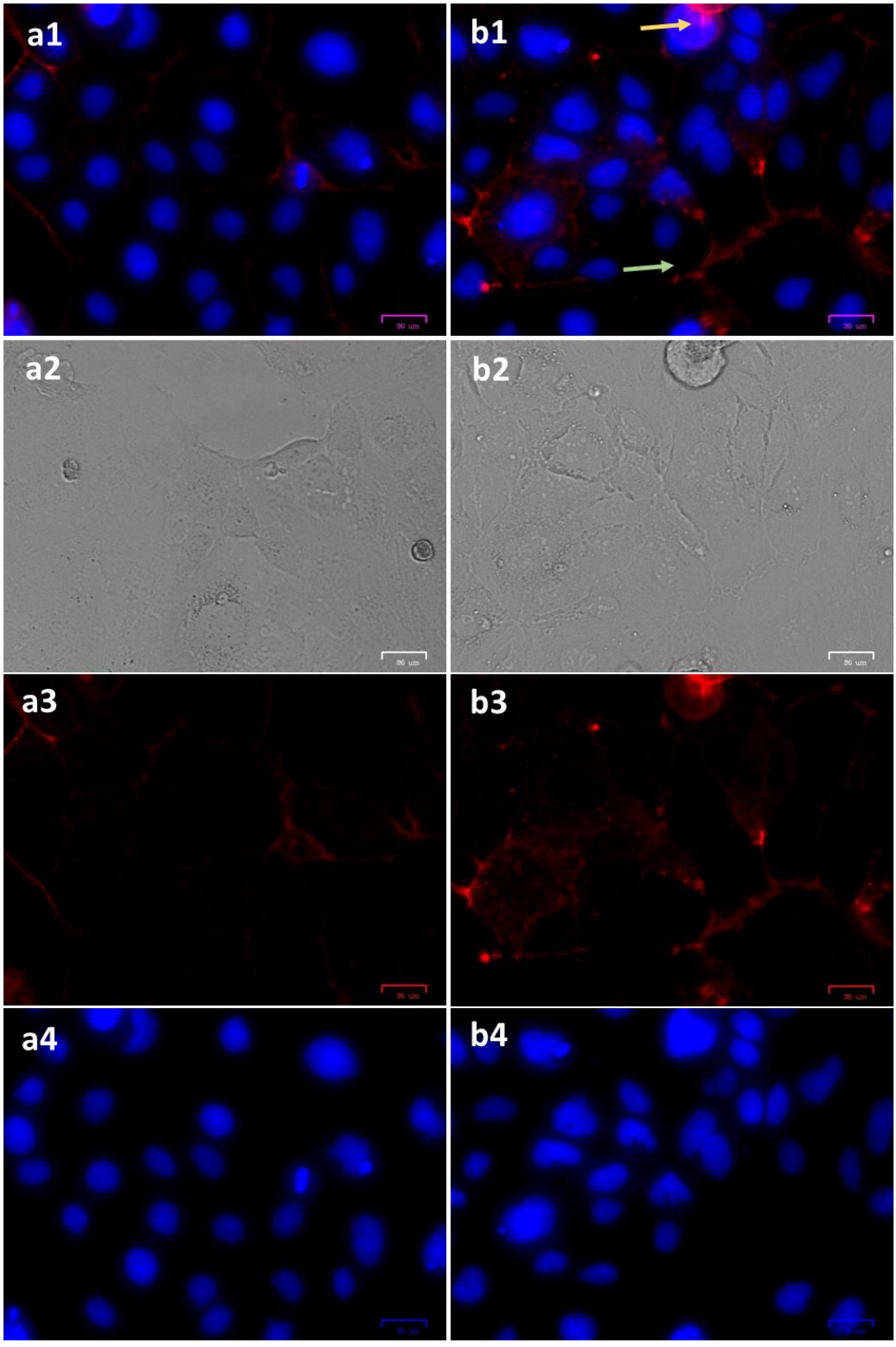

Figure 2.3.34: Stress fibre formation of Caco-2 cells following LPS exposure.

Caco-2 cells were grown on 24-well plate, treated with 100 µg/ml of LPS or vehicle for 24 hours, and stress fibres and nuclei were visualized by staining for 20 minutes with phalloidin-iFluorTM594 Conjugate and Prolong® Gold-DAPI, respectively. Panel a and b represent the control and LPS-treated cells, respectively. 1, 2, 3 and 4 indicates merge, brightfield, phalloidin and DAPI, respectively. The microscopic exposure was gain (16, 34, 16), exposure (320, 360, 300), LED (28, 50, 10), and contrast (17, 13, 46) for the brightfield, red and blue fluorescent lights, respectively. Scale = 30 µm.

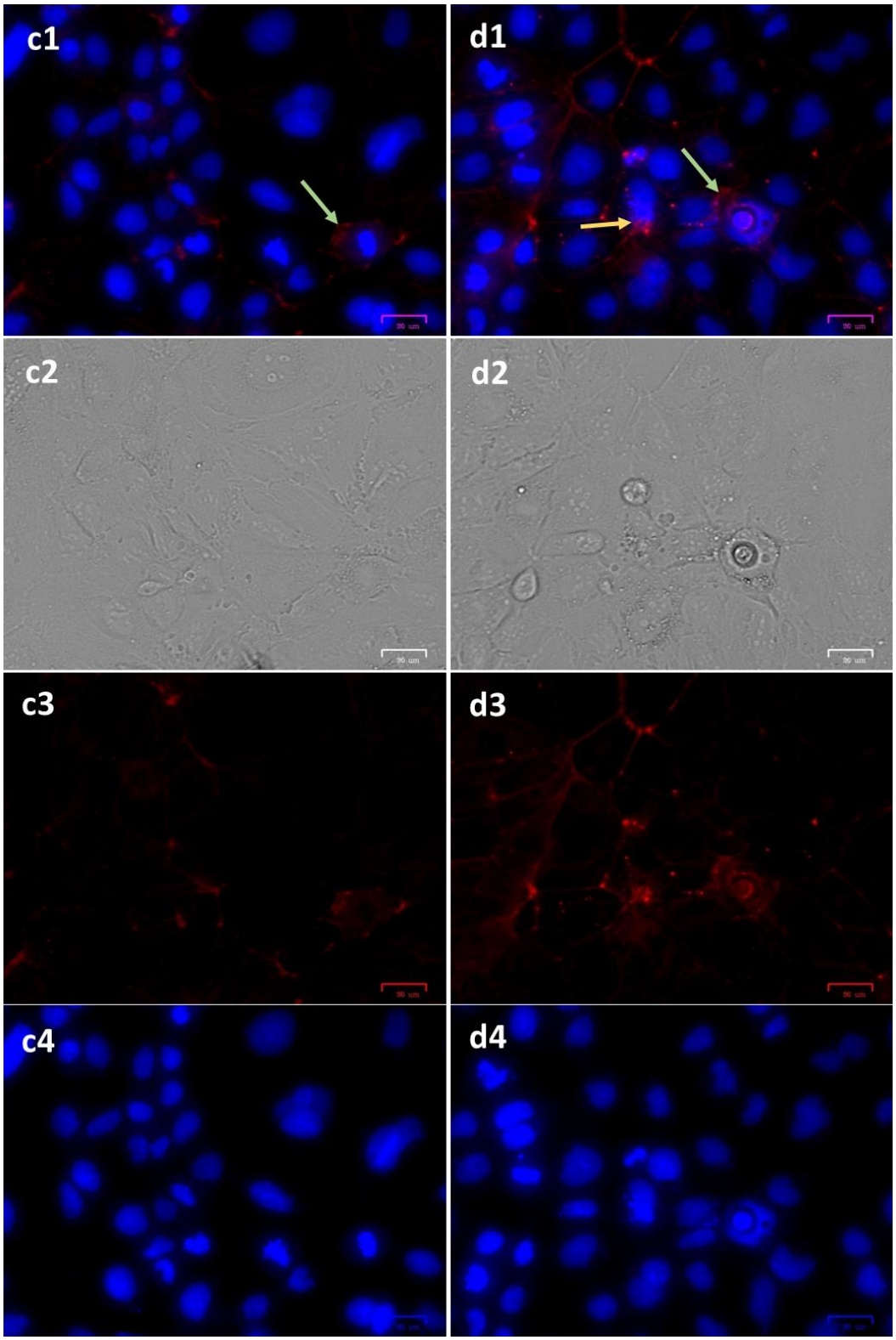

Figure 2.3.35: Effect of saccharin and sucralose on the stress fibre network of Caco-2 cells.

Cells were grown on 24-well plate for 24 hours and exposed to saccharin (c) and sucralose (d) for 24 hours at 37°C. Under panels c and d; 1, 2, 3 and 4 indicates merge, brightfield, phalloidin and DAPI, respectively. Fixed and permeabilized cells were stained with phalloidin-iFluorTM594 Conjugate and Prolong® Gold-DAPI to visualize stress fibre and nuclei, respectively. The microscopic exposure conditions were gain (16, 34, 16), exposure (320, 360, 300), LED (28, 50, 10), and contrast (17, 13, 46) for the brightfield, red and blue fluorescent lights, respectively. In comparison to the control (fig.3.35a), prominent bordering (green arrow) were visible in both saccharin- and sucralose-exposed cells while stress fibre accumulation (yellow arrow) was present in the latter one.

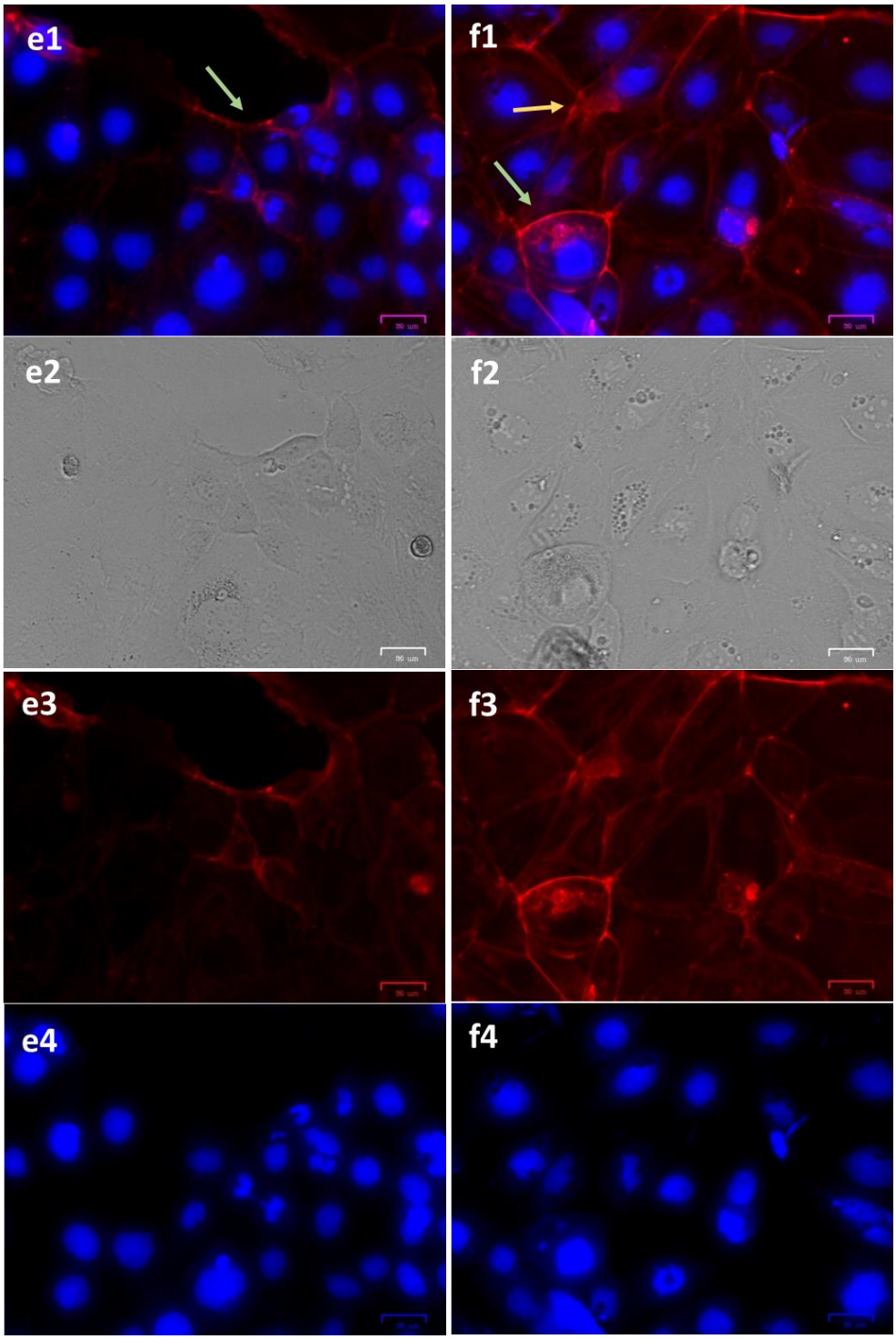

Figure 2.3.36: Effect of Aspartame and neotame on the stress fibre of Caco-2 cells.

Cell monolayers were maintained in EMEM for 24 hours and exposed to aspartame and neotame for 24 hours at 37°C. Fixed (4% paraformaldehyde) and permeabilized (0.1% Triton X-100) cells were labelled with phalloidin-iFluorTM594 Conjugate and Prolong® Gold-DAPI to visualize stress fibre and nuclei, respectively. Cells treated with aspartame (e) and neotame (f) developed different patterns of stress fibre distribution compared to control (fig.3.35a). Images 1, 2, 3, and 4 indicates merge, brightfield, phalloidin and DAPI, respectively. The microscopic exposure conditions were gain (16, 34, 16), exposure (320, 360, 300), LED (28, 50, 10), and contrast (17, 13, 46) for the brightfield, red and blue fluorescent lights, respectively. The stress fibres are prominent in the borders (green arrow) in both aspartame and neotame treated cells. Also, fibre accumulation was common in neotame-exposed cells (f1) (yellow arrow). Neotame promoted disorganisation of the stress fibre distribution, showing more prominent fibres around cell cytoskeleton than control, having more condensed and fragmenting nucleus.

2.3.5 Determination of sweet taste receptor protein level

AS stimulates the STRs to stimulate the mechanism of sweet taste perception (Shirazi-Beechey et al., 2014); T1R2/T1R3 dimer or a 'standalone' T1R3 are the only receptors responsible for this mechanism (Zhao et al., 2003). The Caco-2 cells have the mRNA for T1R3 (O'Brien and Corpe, 2016), therefore, T1R3 protein level in response to AS were tested.

Method evaluation was performed using LPS, followed by measuring the T1R3 protein level in Caco-2 cells upon AS-exposure using indirect whole cell ELISA.

No significant expression of the STR, T1R3 (both extracellular and intracellular) was observed after exposure to lipopolysaccharide (fig.2.3.38) and the AS saccharin, sucralose, aspartame and neotame. The findings for T1R3 protein level for saccharin and sucralose were presented in fig.2.3.39 and for aspartame and neotame were shown in fig.2.3.40.

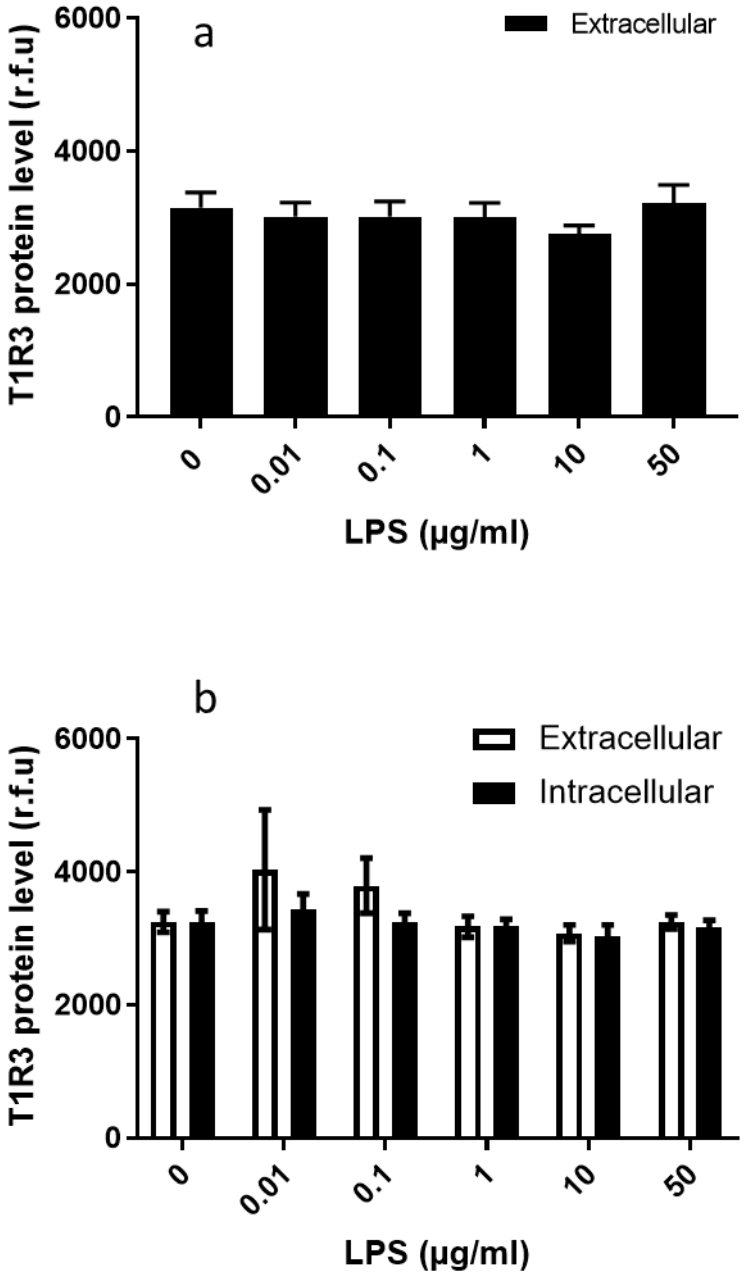

Figure 2.3.37: Sweet taste receptor protein level in response to lipopolysaccharide.

Caco-2 cells were (1×10^4 cells/well) were maintained in 96-well plate for 24 hours and exposed to different concentrations of LPS for 24 hours. An indirect whole cell ELISA was performed on non-permeabilized (a) and permeabilized cells (b) and T1R3 primary antibody for extracellular domain (a) and both extracellular and intracellular domain (b) were used. FITC-conjugated secondary antibody was used to detect the primary antibody and T1R3 protein level was measured as fluorescence at 485–535 nm. Data were analysed using Kruskal-Wallis test followed by Dunn's test (a), and Two-way ANOVA with Sidak's multiple comparison test (b), and presented as the mean ± S.E.M., n=6.

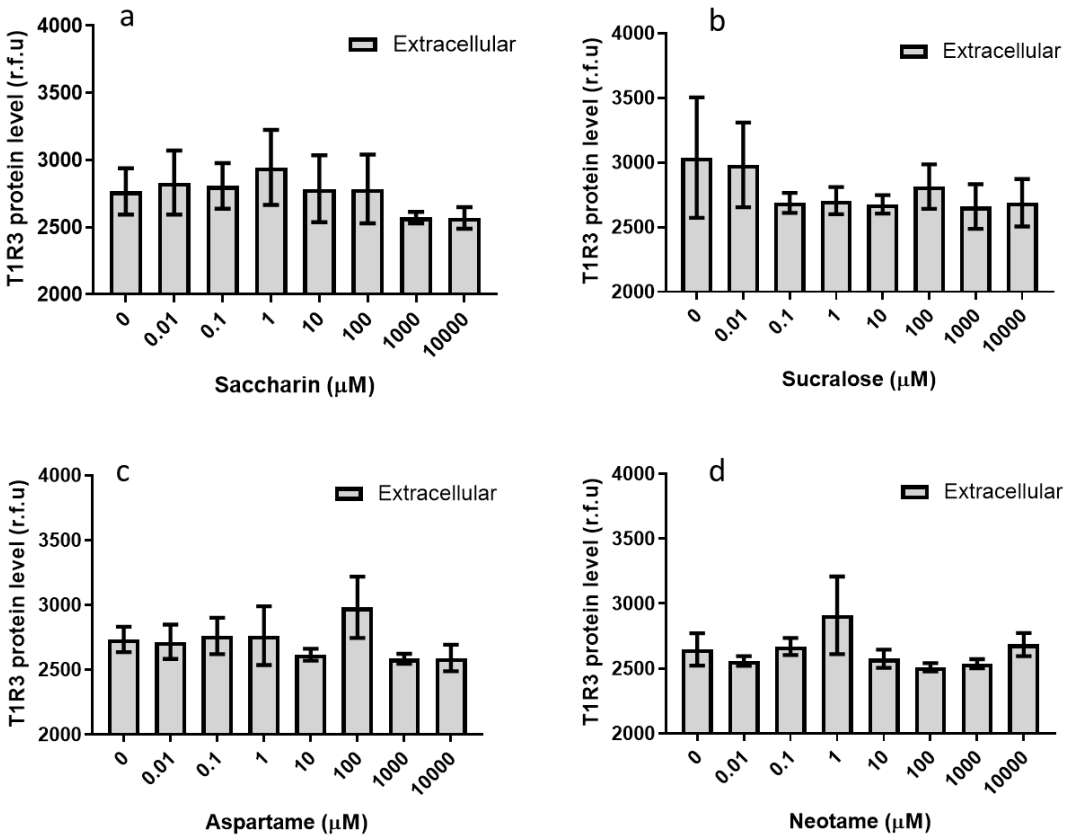

Figure 2.3.38: Effect of AS on sweet taste receptor protein level in the extracellular domain.

Caco-2 cells were seeded at 1×10^4 cells/well in 96-well plate and maintained for 24 hours. The cells were exposed to different concentrations of AS for 24 hours and indirect whole cell ELISA was performed on non-permeabilized cells to measure the T1R3 protein level. Protein level was measured as fluorescence at 485 – 535 nm (PerkinElmer). Panel shows effect of saccharin (a), sucralose (b), aspartame (c), and neotame (d) concentrations. Data were analysed using Kruskal-Wallis test followed by Dunn's test and presented as the mean ± S.E.M., n=6.

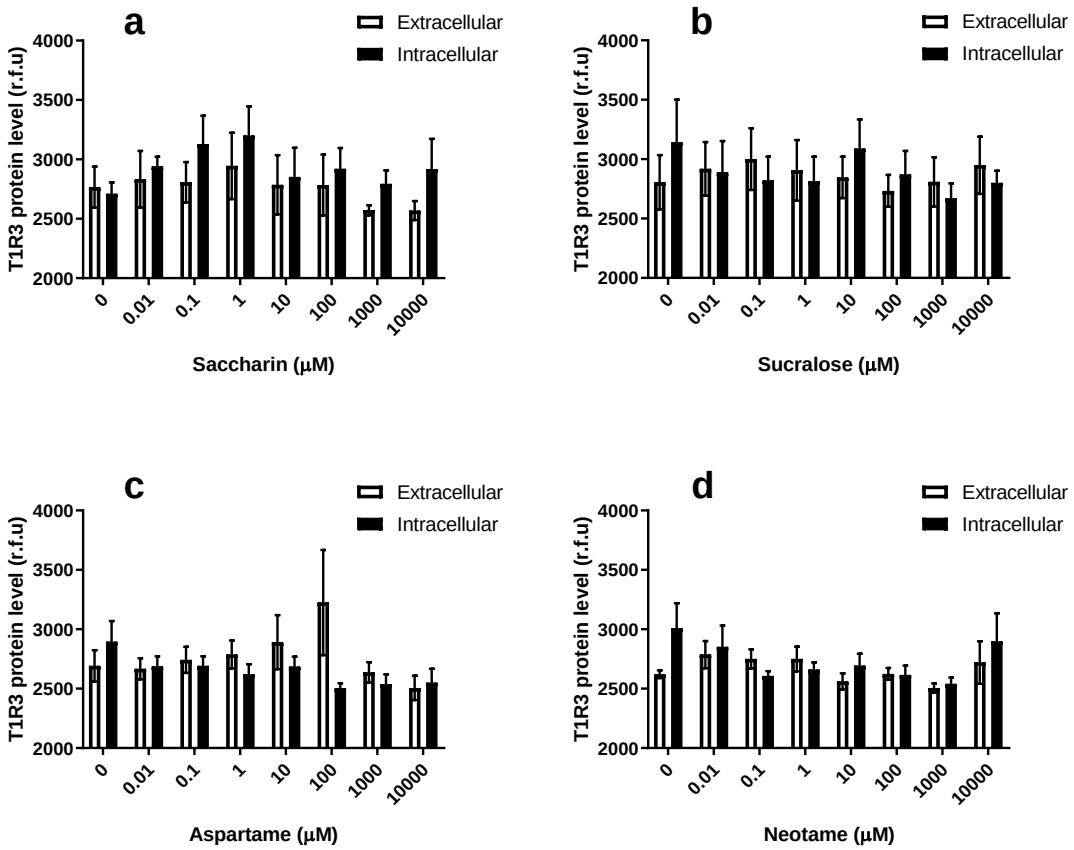

Figure 2.3.39: Effect of AS on sweet taste receptor protein level.

Caco-2 cells were seeded at 1×10^4 cells/well in 96-well plate and maintained for 24 hour and exposed to different concentrations of AS for 24 hours. Cells were fixed and permeabilized with 0.1% Triton X-100. Indirect whole cell ELISA was performed with both extracellular and intracellular primary antibodies, FITC-conjugated secondary antibody was used to detect the primary antibody, T1R3 protein level was measured as fluorescence at 485 – 535 nm (PerkinElmer). Data were analysed using Two-way ANOVA with Sidak's multiple comparison test and presented as the mean ± S.E.M., n=6.

2.4 Discussion

The purpose of the study was to determine the effect of AS on the IEC function, with an emphasis on barrier function and an *in vitro* model (Caco-2 cell line) was used to mimic the IECs. Fogh *et al*. (1977) have established the Caco-2 cell line from a human colon adenocarcinoma. Initially the Caco-2 cell line was used for studying the resistance mechanisms and cytotoxic effect of antitumor drugs but later was recognised as a promising model for studying IEC functions (Lea, 2015). The cell line was demonstrated as a rational model for transepithelial and paracellular transport studies (Fonti et al., 1994). So, this intestinal enterocyte-like Caco-2 cell line was chosen for this study.

The histological analysis of Caco-2 cell architecture resembles that of human colon epithelia. Caco-2 cells have many characters like typical intestinal enterocytes which can form an adherent monolayer, express general digestive enzymes, membrane peptidases and disaccharidases, and actively transport nutrients and ions. They also express the intercellular TJ proteins such as occuldin, ZO-1, ZO-2 (Lea, 2015; Lei et al., 2014; Ulluwishewa et al., 2011), limiting the barrier for the solute movement through the paracellular route, and therefore are an appropriate mimic of the intestinal epithelium. In addition, Caco-2 cells express most of the receptors similar to normal intestinal cells, including T1R3 for the sweet taste perception which increased their suitability for the current study on whether AS affect cell function via sweet taste sensing and whether inhibiting the receptor can help. Since Caco-2 cell line holds these morphological and functional qualities, therefore, they are a valid *in vitro* model for studying the effect of AS on IEC functions in this study.

The single layer of the IECs maintains the barrier function and absorbance of essential molecules in the gut, therefore, any changes in these cells would affect the homeostatic condition. In this study, changes in cell morphology, viability, apoptosis, monolayer permeability, and T1R3 protein level were assessed after AS exposure. The rationale is that any change in these features would eventually influence the other resulting an impact on the barrier function, and impaired intestinal permeability is linked to conditions related to MD. The STR expression has an alleviating effect on the barrier permeability in endothelial cells (Harrington et al., 2017), therefore, studying the T1R3 protein level is justified.

The intensely sweet AS molecules are present in many foods and beverages these days, leading to high and steady consumption by the people. The relevant literature mentions the association of AS-consumption and metabolic disease development, however, the mechanism remained unclear, suggesting further investigations are needed to understand the effects of AS on the IEC function.

Four sweeteners were used in the present study considering their sweetness level (table-1.1.1) and use. Saccharin, sucralose and aspartame are mid-range AS among which

aspartame is the lowest in sweetness level. Saccharin is the oldest sweetener while sucralose is very close to sucrose in terms of sweet taste, quality and time-intensity profile, and neotame is one of the newest and the sweetest sweetener than the others (Chattopadhyay et al., 2014). All these sweeteners are used in various foods and pharmaceuticals and often in conjunction with each other to compensate their weakness. Saccharin and sucralose are mostly used as tabletop sweetener and aspartame is most common in diet cola. In addition, saccharin, sucralose and neotame are non-caloric, while aspartame contributes few calories. Moreover, sucralose and neotame demonstrate excellent stability, whereas saccharin and aspartame show decreasing stability with increasing temperature. Since the current study focuses on how AS affect the IBF, therefore, the selected sweeteners having diverse characteristics better represent the family and studying them are reasonable.

IECs have specific morphological features to serve their functional requirements, therefore, changes in the structure can affect their behaviour. They usually demonstrate the typical morphologic appearance of epithelioid cells in culture, having a large, centrally located nucleus, and grow as tightly packed colonies of polygonal cells (Quaroni and May, 1980). The morphological changes such as flatter cells, not well defined appearance, stretched edges, more floating cells were observed for 1 mM of saccharin and neotame, although similar morphological changes were observed in Caco-2 cells at >10 mM concentration of saccharin, sucralose and aspartame by van Eyk (2014). Also, 10 mM of all AS caused all the above-mentioned changes, along with increased gaps among cell islands with an extended cell adherence loss at 10 mM of saccharin and neotame. The viability data and cell necrosis from the apoptosis assay supports these morphological features at 10 mM concentration, as the cell death was found highest for all AS. Also, gaps among cell islands could have link to increased permeability.

In addition, DAPI staining demonstrates the changes in the nuclei such as irregular bordering, lobules in the nucleus, blebbing, and condensation which can represent the state whether the cells are going to the apoptosis stage. LPS-exposed cells showed nuclear condensation and lobules in the nucleus (fig.2.3.27). Also, small vacuoles are present in the cytoplasm which might be autophagic vesicles. Similar nuclear condensation was also observed in the saccharin- and aspartame-treated cells, along with irregular bordering of the nucleus (fig.2.3.28.a and 2.3.29.a, respectively). Fragmentation, irregular bordering and lobules in the nucleus are obvious in the neotame-exposed cells (fig.2.3.29.b). Also, the number of small vacuoles in the cytoplasm are greater in the neotame-treated cells than any other AS.

Moreover, Phalloidin stain incorporates with the F-actin facilitating the visualisation of stretching of the cells including irregular cellular edges. Components that interact with the cell cytoskeletal actin filaments have been shown to induce a simultaneous increase in the

paracellular leak. Therefore, F-actin have direct or indirect association with TJ protein complexes (Madara, 1987), and changes in their distribution can have impact on the barrier permeability. The stress fibres were prominent only at the edges of Caco-2 cell islands in the LPS-treated cells, however, they are not conspicuous inside the cell cluster (fig.2.3.15.b). Sucralose did not cause Caco-2 cell stress fibre formation among cells in a cell island, although there were fibre lining in the edges like the controls (fig.2.3.16.d). However, saccharin and aspartame caused some fibre formation around cells (fig.2.3.16.c and 2.3.17.e) and more conspicuous fibres in the edges. The highest amount of stress fibre formation was observed in the neotame-exposed cells, both around the cells and in the edges of the cell islands (fig.2.3.17.f).

The cells were stained with Phalloidin for only 20 minutes at RT, therefore, there is possibility that the probe attached with regions having high concentration of F-actin only. This justifies the vehicle-exposed cells having almost no fluorescence (fig.2.3.15.a), may be the actin cytoskeleton is properly spread, and there is no actin accumulation other than the edges. Nevertheless, with the probe used, sometimes it become highly concentrated at actin intact structures, whereas, when it is spread, the fluorescence is displaced. So, the images were presented without quantification.

Furthermore, being the bioenergetics and metabolic centre of the eukaryotic cells, changes in mitochondria, e.g., enlarged or reduced in size, mitochondria with disorganised crests, mitochondrial hypertrophy demonstrates the cells with stress. Survival and appropriate functioning of the cells largely depend on a healthy mitochondrial network. However, mitochondrial component's structural integrity constantly faces environmental and metabolic stresses in the cellular environment. The normal cycles of fission and fusion takes place that help mitochondria to cope with the stresses (Dorn, 2015; Friedman and Nunnari, 2014; Archer, 2013; Youle and van der Bliek, 2012).

Mitochondrial morphology is an important determinant of mitochondrial function (McBride et al., 2006). Mitochondrial dynamics are regulated by the balance between fusion and fission processes that occur in normal condition. Cells with greater fusion than fission causes longer and fewer mitochondria. Fission has important role in physiological functions like apoptosis (Youle and Karbowski, 2005). The increase of fission leads to mitochondrial fragmentation which is important for apoptotic cell death programmes. Since mitochondria play an important role in integration and transmission of cell death signals due to stress, therefore, mitochondrial observation after AS-exposure was reasonable.

DiOC6 staining helps visualisation of mitochondria, thereby facilitating the comparison of the AS-treated cells with the control. The most frequent abnormalities of mitochondria in response to apoptosis-inducing factors are reduction in size and a hyperdensity of their matrix which is referred to as 'mitochondrial pyknosis' (Desagher and Martinou, 2000). They have demonstrated the morphological changes and redistribution of mitochondria in HeLa

cells that overexpressing Bax. Bax-untreated cells showed worm-like mitochondria, while cells overexpressing Bax represented either punctiform mitochondria dispersed throughout the cells or mitochondria that have disappeared from the cell periphery to form aggregates around the nucleus (Desagher and Martinou, 2000). The later characteristic of mitochondria is prominent in the neotame-exposed cells, where many cells have disorganised mitochondria with lots of small vacuoles inside (fig.2.3.32.f). LPS-exposure caused stretching of the mitochondria with small vesicles, and diffused pattern is visible in few cells (fig.2.3.30.b). LPS may cause oxidative stress and may be that is why the DiOC6 is attached more. Saccharin and aspartame exposure also caused diffused pattern of cell mitochondria although vacuoles are not prominent (fig.2.3.31.c and 2.3.32.c, respectively). The disorganised cytoskeleton, small and large vacuoles, fragmented nucleus of the AS-exposed cells demonstrate the characteristics of apoptosis and supports the cell viability findings. Physiological stress or physical injury could also be the reason of morphological changes observed in the AS-exposed cells. Phosphatidyl Serine (PS) probe could also be used to assess these further.

Sweeteners affected the viability of Caco-2 cells at high concentrations only, and the effect was highest with neotame. The EC_{50} for neotame was found 2.2 mM whereas for sucralose it was >50 mM (fig.2.3.7). This might be because sucralose is much closer to sucrose in terms of taste and time intensity but neotame is extremely sweeter than sucrose (Chattopadhyay et al., 2014). On the other hand, saccharin, sucralose and aspartame were demonstrated to have no cytotoxic effect on the Caco-2 cell at 10 mM concentration (Santos et al., 2018). However, the AS-exposure duration was only 3.5 h in comparison to 24 h of the present study. In addition, Santos *et al.* (2018) have used 1×10^5 cells per well of the 96-well plate for the MTT assay while this study has used 2×10^4 cells and performed the CCK-8 assay. Nevertheless, both MTT and CCK-8 assays relies on the same biochemical mechanism.

The observed morphological changes partially agree with van Eyk (2014) who found Caco-2 cell morphology as similar size and shape as untreated control up to a concentration of approximately 10 mM of saccharin, sucralose and aspartame. The cells became flatter and the border was less well-defined although they remained attach to the flask at concentration >10 mM. However, the incubation time was 48 to 72 hour which is different from the current study period of 24 h, also the concentration was 10 mM. Furthermore, sucralose-exposure increased Caco-2 cell viability at lower concentrations (fig.2.3.4) which agrees with previous findings where similar viability increase was observed for Caco-2 and HT29 cells in response to lower concentrations of saccharin, sucralose and aspartame (van Eyk, 2014).

Zinc at high concentrations have toxic effect on eukaryotic cells which negatively affect cell morphology and can enhance cell apoptosis (d'Heureuse, 2000). Zinc oxide (ZnO) was reported to significantly reduce epithelial cell viability (IEC-6) at concentrations 0.2 and 1

mM (Medeiros et al., 2013). Although at 1 mM, $ZnSO_4$ did not affect Caco-2 cells, but significant reduction was observed at 10 mM (25%) and 50 mM (22%). Effect of $ZnSO_4$ as a sweet taste inhibitor was assessed for the co-culture studies.

Lactisole alone affected cell viability at only 1 mM dose which is below the documented IC_{50} for the inhibitor by Jiang *et al*. (2005). At high concentration, the additive effect of sweeteners (10 mM) and Lactisole (3 mM) showed significant reduction of cell viability. However, the 0.1 mM concentration of Lactisole represented higher absorbance level than 100 µM of all sweeteners except saccharin. But when applied in combination (100 µM AS + 0.1 mM Lactisole), saccharin and neotame showed significance in cell viability reduction although sucralose and aspartame did not. The additive effect of the sweeteners and Lactisole determined that the 100 µM dose of sweetener and 0.1 µM of Lactisole can be used for the further experimentation. However, whether this Lactisole concentration is enough to inhibit the sweet taste sensing remained unresolved. Also, Lactisole is a human-specific sweet taste inhibitor (Jiang et al., 2005), however, it does not dissolve in water (Brayton, 1986). The vehicles, ethanol and DMSO, both have a toxic effect on mammalian cells (Tong et al., 2013; Nasrallah et al., 2008). Therefore, the use of siRNA or T1R3 knockdown cell lines could be other choices for sweet taste receptor investigation.

In healthy condition, a balance between cell proliferation and cell death is maintained. Since Caco-2 cell viability is affected due to AS-exposure at high concentration, there may occur cell injury leading to cell death via necrosis and apoptosis. Also, cell morphology demonstrated characteristic apoptosis-related changes, therefore, apoptosis assay facilitated understanding whether cell death was via apoptotic pathway or not. Zoe imager showed irregular shape cells with numerous small vacuoles. In response to the apoptosis inducer, 0.8 mM H_2O_2, after 24-hour incubation the cells have lost their adherence (fig.2.3.15, right) and became clots of cells. Flow cytometric analysis represented about 98% cells death after H_2O_2 exposure.

Increased levels of inflammatory cytokines regulate the corresponding signalling pathways and lead to IEC apoptosis in human and mouse (Yan and Polk, 2002). They have purified novel proteins (MW 75 and 40 KDa) from *Lactobacillus rhamnosus* and demonstrated their role in inhibiting cytokine-induced cell apoptosis thereby preventing IEC loss. These proteins showed concentration-dependent Akt activation whilst inhibition of the cytokine-induced apoptosis, suggesting the novel role of microbial products in intestinal cell survival (Yan et al., 2007).

The cell continuously faces multiple opposing signals of death and survival and cells decide depending on the internal and external regulating factors (Van Engeland et al., 1998). There are some known factors that triggers apoptosis, such as, lack of growth factors, any kind of

DNA damage, Fas ligand binding, action of chemotherapeutic agents (Berke, 1995; Collins et al., 1994), however still lot of these apoptosis signalling and controlling remains to understand. Also, the lag time length between triggering the initiator of the apoptosis cascade and final cell death as well as morphological signs of apoptosis varies hugely depending on the cell type, growth conditions, type of triggers (Van Engeland et al., 1998). Therefore, morphological and flow-cytometric analysis in the study was essential.

Surface exposure of the phosphatidylserine challenges the plasma membrane structure leading to apoptosis. The phospholipid binding protein, AV has high affinity for the PS and binds with the externalised PS. The FITC-labelled AV was measured using flow-cytometry thereby detecting the amount of exposed PS. Discrimination of the dead cells and apoptotic cells were maintained by using the membrane impermeable DNA stain PI. So, detection of live, apoptotic and dead cells by double staining with AV and PI and analyzing them using flow-cytometry was appropriate method for the apoptosis assay.

The viability assay showed that high concentration AS-exposure caused significant cell death, so the apoptosis assay aimed to determine whether the death was via apoptosis. PS are located facing the cytoplasm in healthy normal viable cells, cells possess the ability to maintain the plasma membrane lipid asymmetry and translocation of PS to outer leaflet. PS exposition is the early stage phenomena of apoptosis which last until the late execution phase of breaking up cells into apoptotic bodies (Verhoven et al., 1999). AV specifically binds to PS in presence of calcium, labelling of AV using biotin- or FITC- labels facilitates the measurement of the exposed PS. AV cannot penetrate the phospholipid bilayer, therefore unable to bind to PS of inner leaflet, however, dead cells lose their plasma membrane integrity and allow the binding in the inner leaflet.

In the current studies, a concentration dependent increase of Caco-2 cell death for AS exposure was observed (fig.2.3.24). For the apoptotic cells, the correlation was not well defined, which might be because the cells followed pathways other than apoptosis or the AS-exposure duration was longer. By the time apoptosis was measured, the cells had already undergone apoptosis and reached the death phase. Induced cell death can impair the IBF via reduced absorption and increased permeability, leading to inflammatory responses (Cox et al., 2017).

Epithelial barrier impairment is an important factor of gastric permeability systemically linked with the inflammatory response that is related to MD (Lei et al., 2014). Previous studies represented a relationship between artificial sweetener intake and barrier function impairment via dysbiosis and sweet taste sensing (Suez et al., 2015; Suez et al., 2014). Lipopolysaccharide was also found to increase barrier permeability when secretes at high concentration (Wang et al., 2015; Lei et al., 2014). LPS makes up almost 80% of the Gram-negative bacterial endotoxin and is prominent in the gut environment because of the

presence of trillions of microbes, and this major endotoxin can be released into lumen by shedding or lysis of bacteria (Guo et al., 2013). However, in healthy balanced condition, LPS cannot penetrate the intestinal barrier although impaired TJ allows paracellular permeation of endotoxins and luminal antigens (Guo et al., 2013). Previous studies on Caco-2 cells with LPS (0.1 to 100 µg/ml) demonstrated no effect on cell viability (Lei et al., 2014; Guo et al., 2013) which agrees with the present findings. Obviously, the decrease of cell viability at high concentration (100 µg/ml) did not cause 50% cell death.

Literature showed the important role of LPS in barrier permeability, so determining the effect of LPS on Caco-2 cell monolayer permeability was important. Lei *et al*. (2014) demonstrated that LPS impairs intestinal barrier integrity through the breakdown of occludin and ZO-1 in Caco-2 cell. Exposure of Caco-2 cells to increasing LPS concentrations showed a concentration-dependent decrease in TJ protein expression. LPS stimulation was also reported to induce barrier dysfunction in Caco-2 cell monolayer by interfering with the expression and distribution of occludin and ZO-1. In addition, LPS was reported to activate the ERK-MAPK pathway which induces TJ breakdown (Lei et al., 2014).

The decrease in cell viability or increase in cell death as observed in the cell viability and apoptosis assays, can lead to impaired permeability. In addition, changes in the morphology such as cell appearance, nucleus, and mitochondria can interfere with its function. Moreover, the formation of stress fibre or disorganisation of the F-actin can directly affect the intestinal barrier permeability via changes in cell cytoskeleton. Furthermore, negative changes in F-actin directly interferes with the TJ protein expression and distribution, thereby affecting the paracellular permeability. Therefore, studying the effect of AS on the Caco-2 cell monolayer permeability is reasonable.

TJ permeability can be measured *in vitro* by different methods. TEER is measuring the ionic permeability of the cell monolayer. Also, paracellular passage of non-absorbable and non-metabolized extracellular markers (e.g. FITC-Dextran proteins) of different sizes by the cell monolayer can be used. Although TEER is a useful indicator of early perturbations of the ionic permeability, however, it does not distinguish between membrane and paracellular conductance of the cell monolayer. On the other hand, paracellular marker passage is a more suitable way to describe time-dependent variations in the TJ-mediated permeability to molecules (McEwan et al., 1993). Therefore, FITC-Dextran permeability method was utilized in the present study to assess the effects of AS on Caco-2 cells.

Assessing the permeability of Caco-2 cell monolayers in response to AS and LPS exposure requires the determination of the right experimental condition including cell number, appropriate FITC-Dextran protein, and incubation duration. If AS-exposure affects cell viability, it will eventually cause permeability. So, initial assessment of Caco-2 cell viability and apoptosis in response to AS and LPS concentrations were justified from the viability and apoptosis assay. These findings helped to determine the appropriate concentration of

AS to measure permeability without affecting cell viability. Likewise, Lactisole was found to reduce cell viability, at concentrations lower than the IC50 ≈4 mmol/l demonstrated in MIN6 cells (Hamano et al., 2015) therefore the use of siRNA to inhibit the STR could be investigated further.

Epithelial barrier functions are extremely important for nutrient absorption, ion transport and the influx of pathogens (König et al., 2016). Imbalanced gut permeability may cause pathogenic bacteria to go across the blood stream causing conditions leading to MD (Lei et al., 2014). LPS was demonstrated to have an enormous effect on epithelial barrier dysfunction in model cells from human and other animals (Lei et al., 2014; Guo et al., 2013). The effect of LPS on the Caco-2 cell monolayer was determined with significant findings at 1 µg/ml concentration at both 60 and 180 second in case of FD4. The LPS-induced permeability was significant for the FD20 at 60- and 360 seconds and at concentration as low as 0.1 µg/ml. For the 5×10^4 cells, there observed FD4 leak at 0.01 µg/ml at 60 second, whereas, FD20 leaked at 0.01 and 0.1 concentrations at 360 second. Barrier integrity was higher at other concentrations which are theoretically incorrect, since lower concentrations caused leak, the higher concentrations had more probability to cause leak. On the other hand, no significance was found in 1×10^5 cells for both FD proteins. The cell density was high, and the marker proteins could pass through for an hour, therefore, either the cells were overlapped and was impermeable or most of the FD proteins passed through by the one-hour time. These findings were considered for setting the FITC-Dextran permeability experiment to investigate the effect of AS on the Caco-2 monolayer permeability.

Considering the findings from the three different cell numbers seeded, three time points allowed for FD protein permeation, the molecular weight of the FD protein, 2×10^4 cells were found reasonable to use with FD4 protein to be allowed to permeate for 180 and 360 seconds (fig.2.3.33). Permeability was significant for FD4 protein at concentrations 1, 10 and 50 µg/ml at different time points (fig.2.3.33.a). On the other hand, FD20 permeation was found significant at concentrations 0.1 µg/ml at 60- and 360-seconds (fig.2.3.33.b). FD20 is bigger molecule than FD4 and may be stuck into the paracellular junctions or may be struggled to pass through the leak in the monolayer or the number of Caco-2 cells maintained are higher for their permeation, which is why the significance in concentrations and timepoints was inconsistent.

60-second is very short time allowed for FD4 permeation, also, if FD protein passes at 60 second timepoint, that will be in the insert at 180 seconds as well. Again, same time were allowed for the next sampling at 360 seconds giving an opportunity to compare. Therefore, considering the timepoints, 180 and 360 seconds for the conducted permeability assay was reasonable.

In addition, although 5×10^4 cells/well is the standard seeding density for the 24-well plate (ThermoFisher Scientific), no significant change was observed for the seeding density in

the present study, and the fluorescence was low. Besides, cells were seeded only on the insert of the transwell plates, so these number of cells might become too confluent to overlap. In addition, the cells were maintained for 48 hours and exposed to AS for 24 hours before adding the FD protein. This might allow cells to grow on top of each other forming a multilayer rather than a monolayer and therefore FD protein could not pass through in the given amount of time.

In 1×10^5 cells, the FD protein permeation was allowed for an hour, resulting approximately same level of fluorescence for all the concentrations and there was no significance. The FD proteins might have permeated the barrier within this time and made the concentration effect insignificant. Similar protocol for 1×10^5 Caco-2 cells were also used by Lei *et al*. (2014) and they have demonstrated significant increase in permeability of cell monolayer at 100 µg/ml LPS. Since the CCK-8 assay in the present study showed cell death at this concentration, so this concentration was not considered for the permeability assay. Guo *et al*. (2013) however determined that 0.3 ng/ml or above concentrations of LPS can increase Caco-2 cell permeability via TJ integrity dysfunction which agrees with the current study. Considering all these facts, 2×10^4 cells were found appropriate to assess the effect of AS and AS ± LPS on the IEC permeability.

Many conditions that interferes with the permeability of the intestinal epithelial barrier also cause changes in the expression and distribution of the TJ proteins and actin cytoskeleton (Ranaldi et al., 2002; Madara, 1987). Therefore, increase in the monolayer permeability in the present study corresponded with the morphological changes in F-actin (fig.2.3.37).

All the AS caused Caco-2 cell monolayer permeability varying from concentration 1 mM for saccharin and sucralose to 0.1 mM for aspartame and neotame (fig.2.3.34). The cells showed increased leak at lower concentrations when exposed to AS with LPS (fig.2.3.36). Santos *et al.* (2018) showed that saccharin induced Caco-2 cell monolayer permeability at 10 mM concentration. However, they have considered only one concentration and the FD4 permeation was allowed for 1.5 hour which differs from the present study. They have also mentioned that the barrier permeability is not related to cytotoxicity. However, saccharin was found to reduce viability and increase permeability at 1 mM, considering the findings of Santos *et al.* (2018), there might have other mechanism than viability-related pathway affecting permeability.

Although barrier impairment is linked to conditions leading to MD, however, regulated permeability might have positive use. Regulation of solute permeation across the epithelial barrier might represent a potential mean of improving bioavailability of orally administered bioactive solutes. Therefore, the AS induced permeability might have positive applications, provided that appropriate regulators are in place to overcome the harmful effects.

T1R2/T1R3, the heterodimeric STR stimulation by AS was reported to have a link with metabolic consequences (Suez et al., 2015; Pepino, 2015). Also, an opposite link in STR

expression was shown in endothelial barrier permeability (Harrington et al., 2017), although how AS affect the epithelial barrier via sweet sensing is not clarified. Brown *et al*. (2010) also mentioned AS to be active in the GI tract affecting the intestinal STRs which might eventually lead to increased insulin secretion, thereby influencing weight, appetite and glycaemia. Therefore, detection of the STR protein level in response to AS exposure in the enteroendocrine cell model in this study was performed. Hence background research showed that amplicon for T1R2 was not detected in Caco-2 cells (O'Brien and Corpe, 2016) and Zhao *et al*. (2003) also described T1R3 as potential sweet taste transduction receptor in the human, so only T1R3 protein level was measured. Additionally, quantitative real-time PCR was performed to quantify the STR, T1R2/T1R3 expression by Swartz *et al.*, 2011 who reported a significant increase of this receptor in intestinal cells in the germ-free mice in contrast with the conventional mice. They have demonstrated that germ-free mice have more affinity to sucrose solutions although both mice category have a similar preference to saccharin solutions, and germ-free mice did not exert significant differences in sweet taste sensitivity which was inferred as an adaptive change in intestinal STR due to lacking intestinal microflora.

No significant expression of the STR protein, neither intracellular nor extracellular, was observed in the present study. This might happen because the primary antibody used could not attach to the receptor, or unrecognised technical reasons. Moreover, Caco-2 cell have T1R3 receptor only (O'Brien and Corpe, 2016), whereas all these AS have binding recognition site at the Venus Flytrap domain of the T1R2 monomer of the STR (DuBois, 2016). The insignificant expression of the T1R3 in the present study might have link with this. However, T1R3 protein forms dimer and is a 'stand-alone' receptor for the sweet taste perception (Zhao et al., 2003), which does not support the previous indication. Therefore, further studies are important to understand the AS-mediated sweet taste sensing in the Caco-2 cells.

No positive control was found for the incomplete whole cell ELISA and therefore the experiment did not have the positive control. The positive allosteric modulators, SE-2 and SE-3 which specifically interacts with human T1R2/T1R3 and enhances sweet taste perception (Zhang et al., 2010) could be an alternative which could be considered in future studies. Neither LPS (fig.3.38) nor the AS (fig.2.3.39 and fig.2.3.40) showed significance in T1R3 expression in this study. So, immunofluorescence assay or quantitative real-time PCR for T1R3 detection might be better option for future studies.

2.5 Conclusion

Low-calorie AS consumption is believed to have association with avoiding obesity and dental caries, leading to healthy way of life. However, the present research findings suggest that AS have negative impact on cell viability and monolayer permeability. Therefore, further studies are necessary to investigate how these intensely sweet molecules affects the IEC function.

3 An investigation into the effect of artificial sweeteners on two model gut bacteria

3.1 Introduction

3.1.1 Gut Microbiota

GM refers to all the microorganisms (mostly bacteria but also viruses, fungi and protozoa) harboured by the human GI tract (Sekirov et al., 2010). This flora has co-evolved over time with the host epithelium to develop an intricate and favourable mutual existence (Thursby and Juge, 2017). There are more than 100 trillion microbes in the gut which outnumber, more than tenfold, the total number of human somatic and germ cells (fig.3.1.1) (O'Hara and Shanahan, 2006). A continuing concert of studies, such as the Human Microbiome Project and Metagenomics of the Human Intestinal Tract, have recognised the contribution of the microbiome in providing unique protein coding genes as 360 times greater than their host (Qin et al., 2010; Consortium, 2012).

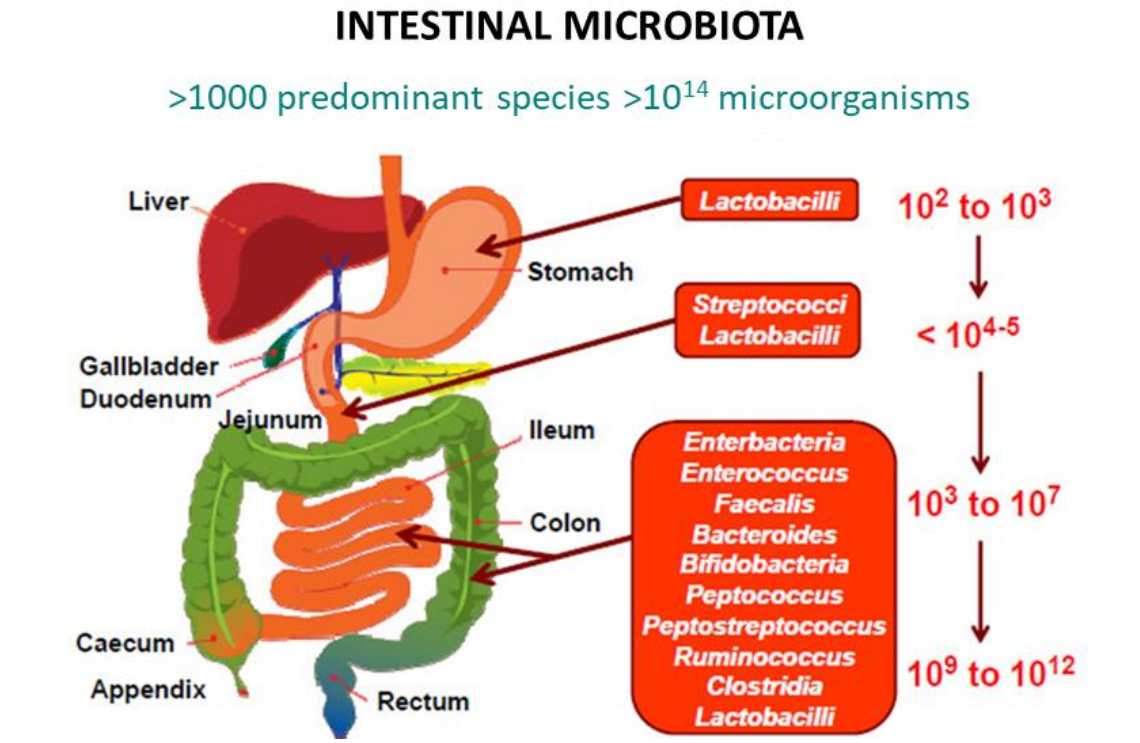

Figure 3.1.1: Spatial and longitudinal variations in microbial numbers and composition across the length of the gastrointestinal tract.

The human microbiota contains as many as 10^{14} bacterial cells, which is more than 10 times greater than the number of human cells present in the body. The number of bacterial cells present in the mammalian gut shows a continuum that goes from 10^2 to 10^3 bacteria per gram of contents in the stomach and duodenum, progressing to 10^4 to 10^7 bacteria per gram in the jejunum and ileum, and culminating in 10^9 to 10^{12} cells per gram in the colon. Figure taken from Konturek *et al*., (2015).

The microbiome encodes more than three million genes and the combined microbial genome is 100 times greater than the human genome (Gill et al., 2006, Valdes et al., 2018). The development of microflora generally begins from birth with rapid colonisation in the GI

tract occurring during the first year, and by around 3 years of age, microbiota composition, diversity and functional capabilities resemble the adults (Rodriguez et al., 2015; Koenig et al., 2011). The microbiota is therefore a vital component of the gut ecosystem and human health.

The human GI tract is a highly complex organ comprising of both the host and the resident microbial genetic power, encoding a large number of mechanisms regulating food digestion, absorption and metabolism (Payne et al., 2012; Qin et al., 2010). The intricate relationship between the gut flora and metabolism of components of the hosts' diet aids several processes such as vitamin production and energy homeostasis (fig.3.1.2) (Nicholson et al., 2012; Flint et al., 2008; Turnbaugh et al., 2006). In addition, the microflora-host gut relationship contributes to immune system development, enteric nervous system regulation, as well as the synthesis, protection and metabolism of drugs and toxins (Bian et al., 2017; Lopetuso et al., 2015; Hooper et al., 2012; Diaz Heijtz et al., 2011; Mazmanian et al., 2005). Collectively, the level of dietary metabolism performed by the GM is equal to that of the stomach (Bocci, 1992). There are therefore a significant number of studies to address this host-microbiota relationship and its impact on health and wellbeing.

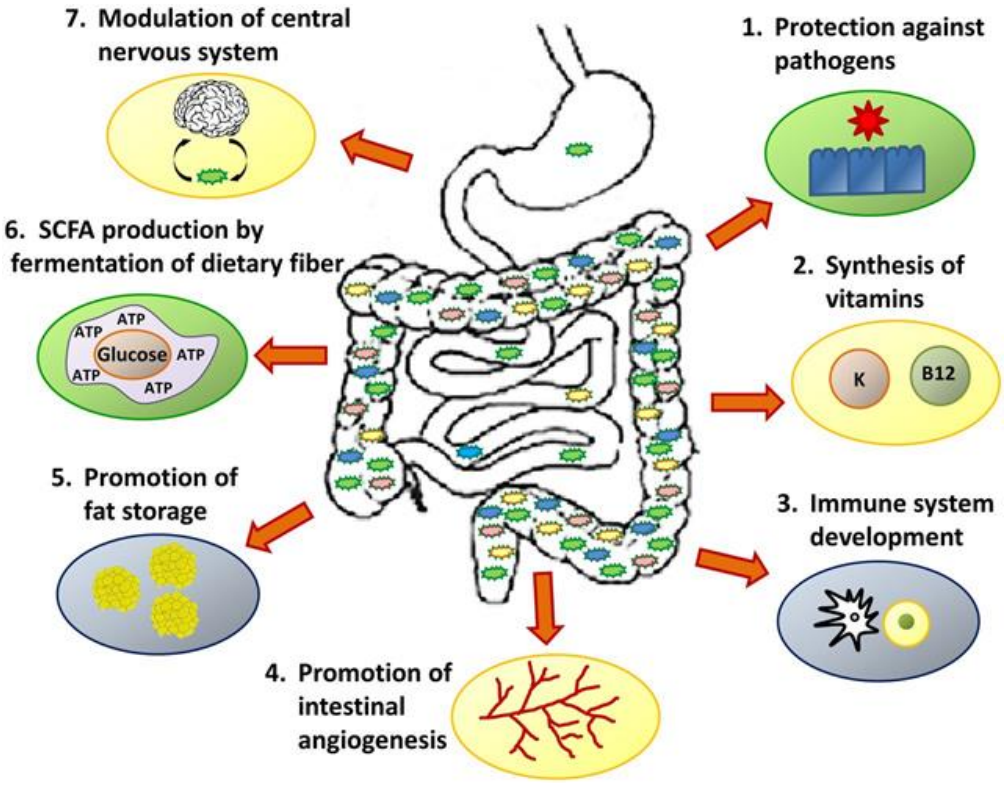

Figure 3.1.2: Role of gut bacteria in host physiology.

Other than breaking down the foods and synthesizing vitamins, gut bacteria play an enormous role in other physiological mechanisms including resistance to infection and protection against autoimmunity, and regulation of intestinal architecture and barrier permeability. SCFA, short-chain fatty acid. Figure taken from Amon and Sanderson, 2017.

3.1.2 Factors affecting intestinal microbiota

A delicate balance in GM composition is crucial in preserving host immunity and homeostasis, perturbation of the microbial balance could lead to devastating pathophysiological consequences (Bian et al., 2017; Yang et al., 2015). An imbalance in GM is commonly referred to as dysbiosis (Sekirov et al., 2010). Although depiction of a healthy microflora remains at its early stages (Turnbaugh et al., 2009), an imbalance commonly suggests alterations in the microbiota community such as changes in the ratio of Firmicutes and Bacteroidetes (Mariat et al., 2009), decrease in microbial richness, diversity and evenness (Yang et al., 2015), depletion of beneficial non-pathogenic gut bacteria (i.e., probionts) and increase of pathogenic inflammatory bacteria (i.e., pathobionts) (Kigerl et al., 2016). Multiple factors regulate the development and maintenance of GM such as host geographical location, diet, lifestyle, bacterial infections, use of antibiotics, and exposure to heavy metals (fig.3.1.3) (Bian et al., 2017; Rodriguez et al., 2015; Tenaillon et al., 2010). These factors alone, or in combination, can change the ecological balance of the GM resulting in dysbiosis (Lopetuso et al., 2015).

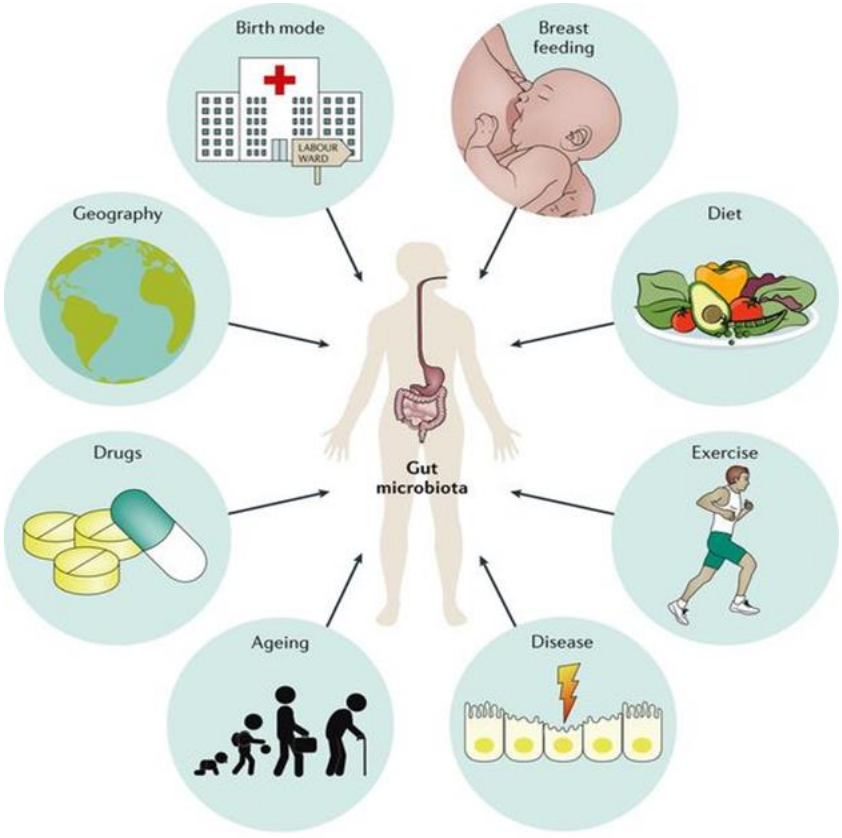

Figure 3.1.3: Factors influencing the composition and function of human gut microflora.

Numerous factors have an influence on the gut microbiota. Clockwise from top left: methods of delivery at childbirth; whether breast or bottle fed; diet; exercise and other personal habits; presence of disease (e.g. intestinal inflammation); ageing; medications (especially antibiotics but also acid suppressants and metformin); geography. Figure taken from Quigley, 2017.

Dysbiosis make the host prone to a variety of MD including obesity, insulin resistance, cardiovascular diseases and diabetes (Nettleton et al., 2016; Fukuda and Ohno, 2014; Muegge et al, 2011). Bian *et al*., (2017) showed that Acesulfame-potassium (Ace-K) consumption for 4 weeks can significantly change the gut metabolic profiles in CD1 mice. In female mice, Ace-K treatment decreased the bacterial metabolism-related metabolites, such as lactic acid and succinic acid. Also, 2-Oleoylglycerol was also largely decreased in females. On the other hand, Ace-K significantly increased the concentration of pyruvic acid in the male mice in comparison with the controls. Hence pyruvic acid is a central metabolite of energy metabolism, this may have important role in host energy homeostasis. Also, Ace-K exposure increased cholic acid while decreased deoxycholic acid in the feces of male mice (Bian et al., 2017). Moreover, Ace-K consumption increased the abundance of one bacterial toxin synthesis gene, thiol-activated cytolysin in both male and female mice (Bian et al, 2017). In particular, the consumption of AS in the diet has been linked with dysbiosis (Suez et al, 2014) however, the effect of AS on the pathogenicity of gut bacteria is not known. Despite this understanding, further studies are needed to establish the mechanism of how AS exposure changes the commensals into pathogens.

3.1.3 Gut bacteria and artificial sweeteners

Since AS are cheap, easily available and enhance food flavour, they have been incorporated into many food products such as baked goods, canned foods, desserts, and beverages such as soda, juice, coffee and tea, as well as pharmaceutical products. Several epidemiological studies have evidenced their beneficial role on weight loss and on people suffering from glucose intolerance and T2D (Gardner et al., 2012), however, there are studies which indicate opposing results (Bian et al., 2017). AS paradoxically increase calorie consumption and may also negatively impact the biological mechanisms such as T1R2/T1R3 receptor mediated downstream signalling, resting metabolic rate, as well as GM activity, as discussed in section-2.1.9. In addition to weight management, using animal and human studies, AS consumption has been linked with conditions leading to MD development (Suez et al, 2014), as mentioned in chapter 2 (section-2.1.10).

Study on male rats showed that, consumption of Splenda, a plant-originated natural sweetener, containing sucralose (1.1%) for a 12-week period significantly decreased the number of beneficial faecal microflora (Abou-Donia et al., 2008). Sucralose intake decreased total anaerobes, bifdobacteria, *Bacteroides,* lactobacilli, Clostridia and the total aerobic bacteria in gut. Also, the tested sucralose concentrations (1.1 – 11 mg/kg) increased the stool pH and raised the expression of membrane efflux transporter P-glycoprotein and the cytochrome P-450, which indicates that the US FDA approved daily intake of sucralose (5 mg/kg) can adversely affect the beneficial faecal microflora (Abou-Donia et al., 2008).

Suez *et al.* (2014) demonstrated that saccharin consumption enhanced several biochemical pathways in mice including the glycan degradation pathways, sphingolipid metabolism and lipopolysaccharide biosynthesis. They have mentioned the importance of these altered biochemical pathways in energy harvest system and developing MD like diabetes mellitus and obesity.

Similarly, Bian *et al* (2017) demonstrated that numerous pro-inflammatory mediators (such as LPS synthesis) were potentially produced by gut bacteria, which is associated with other metabolic disease conditions like diabetes and obesity, indicating the link between AS-mediated dysbiosis and chronic inflammation. They have investigated the changes in the composition and functional genes of GM that contribute to inflammation. They showed that Ace-K enhanced the genes related to LPS synthesis in mice, with a distinct difference between male and female mice. In female, Ace-K increased the LPS synthesis-related genes, LPS-export genes, and an LPS-assembly protein. Similarly, two genes participating in LPS biosynthesis, glycosyltransferase and UDP-perosamine 4-acetyltransferase were up-regulated in the Ace-K-consuming male mice. Ace-K also increased multiple genes encoding flagella components in the female mice (Bian et al, 2017).

Frankenfeld *et al.* (2015) also employed Ace-K on 31 healthy human adults and assessed the effect of AS consumption on GM using faecal samples. The subjects consumed aspartame (n=7) or Ace-K (n=7) or both (n=3) or other natural sweeteners. No difference in the bacterial median percentage or gene abundance between AS consumers and non-consumers but overall bacterial diversity was different across the subjects (Frankenfeld et al., 2015). The aspartame consumption was 5.3- to 112 mg/day, with a mean of 62.7 (SD:40.2) and Ace-K intake ranged from 1.7- to 33.2 mg/day. The study period was, however, too short to conclude concrete findings. Taken together, these studies indicate that AS consumption exert a negative impact on metabolism by changing bacterial diversity and potentially pathogenicity, with/out affecting GM composition which can influence host health. There are, however, limited studies which focus on the negative impact of AS on bacterial pathogenicity.

3.1.4 The taste receptor in gut bacteria

Although it was traditionally believed that the ability of bacteria to coordinate neighbourhood perception and behaviour occurred indirectly, sophisticated communication systems have been identified over the past few decades. Bacterial biological activities, such as growth and virulence factors (e.g., production of haemolysin/ cytolysin, aggregation substances, gelatinase, biofilm formation) (Franz et al., 2001), are therefore coordinated by the production and response of biochemical molecules, a process called quorum sensing (Miller and Bassler, 2001). These sensing are the key virulence regulators in bacteria and could

be a novel target for bacterial infection prevention and treatment (Sifri, 2008). Recent studies have demonstrated the crosstalk between bacteria and host, they are able to produce and detect chemical signals (e.g., N>-acylhomoserine signalling, quinolone signalling in Gram-negative bacteria, and modified oligopeptides called autoinducing peptides in Gram-positive bacteria) and react accordingly (Miller and Bassler, 2001; Hughes et al., 2008; Sifri, 2008).

The Gram-negative bacteria demonstrates several quorum-sensing systems including the lux-type (such as elastase and rhamnolipid production) and synthesising quinolone compounds (4-hydroxy-2-alkylquinolines) (Sifri, 2008). Quorum sensing is the regulation of gene expression depending on the changes in bacterial cell density. It relies upon the interaction of a diffusible signal molecule with a transcriptional activator protein to link gene expression with cell population density. Quorum-sensing bacteria produce, release, and react to a small, pheromone-like biochemical signal molecules (commonly called autoinducers), which accumulate in the external environment as the cell population grows (Sifri, 2008; Surette et al., 1999). Autoinducers (e.g., N-Acylhomoserine lactones, AHLs) are produced by many gram-negative bacteria to maintain intercellular signals thereby facilitating the quorum sensing. These signal molecules, AHLs, differ in the structure of their N-acyl side chains (McClean et al., 1997). These allows a bacterial species to monitor its population density and activate specific sets of genes at sufficiently high cell numbers (Fuqua et al., 1996).

Enteric *E. coli* produces and detects certain auto-inducers such as autoinducer 2 (furanosyl borate diester), autoinducer 3 (unidentified); these auto-inducers have the functional capability to activate gene (such as *LuxS*) necessary for bacterial adhesion and invasion, thereby facilitating intestinal colonisation and intrusion (Sifri, 2008). On the other hand, the domesticated non-pathogenic laboratory strain *E. coli* DH5α neither produce nor degrade autoinducer 2 (Surette and Bassler, 1998). Autoinducer 3 synthesis in enterohaemorrhagic *E. coli* depends on the presence of LuxS gene and can be stimulated by the epinephrine and norepinephrine host signalling system (Sifri, 2008; Sperandio et al., 2003), implying a potential cross-communication between bacterial quorum sensing and host signalling systems. Since AS consumption is involved with host sweet taste signalling and gut bacteria dysbiosis, there might have potential quorum sensing in bacteria via direct exposure to AS or from host signalling. However, there are no literature that can indicate these mechanisms.

There is no considerable research on taste receptors or sensors in bacteria. In the lungs, studies showed the response and contribution of bacterial products in triggering host STR (T1R2/3) and suppressing bitter taste receptors (T2R) to play a role in the respiratory defence system. These studies do not, however, demonstrate the presence of bacterial

receptor proteins. The study showed that *Staphylococcus* species isolated from the respiratory samples secrete D-amino acids such as D-isoleucine, D-phenylalanine, and D-leucine. These amino acids can activate the T1R2/3, whilst inhibiting the T2R-mediated signalling and defensin secretion (Lee et al., 2017). In the respiratory epithelium, Lee *et al.* (2017) have demonstrated that STR activation is linked to the inhibition of innate immune defence response. The secreted D-amino acids (D-phenylalanine and D-leucine) stimulate T1R2/3 and enhances epithelial cell death by suppressing the activation of the T2R-mediated protective bitter taste signalling. Similar observations were made on sweet and bitter receptors of specialized sinonasal solitary chemosensory cells, as well as on T2R38 in sinonasal ciliated cells, showing these receptors cause host susceptibility to upper airway infections, such as chronic rhinosinusitis (Carey and Lee, 2019).These findings suggest that STR activation in the airways triggers the epithelial cell vulnerability to infections, indicating a possibility whether AS-mediated sweet-sensing in the IECs also exerts a similar effect.
Lactisole is a STR antagonist for the mammalian GPCR only (Fernstrom et al., 2012), therefore is not applicable for prokaryotes. Alternatively, zinc ions have a higher affinity to chemical groups like thio- and hydroxyl. Once exposed, they readily bind with protein, peptides and amino acids; this ability enabled zinc to interfere with sweet taste perception. Zinc readily binds to the STR protein and causes structural changes in the configuration (Keast et al., 2004). Therefore, the receptor-binding site of T1R2/3 is altered, and it cannot respond to sweet taste stimulants.

3.1.5 Gut bacteria models

The GI tract harbours between 1000 and 1150 predominant bacterial species belonging to above 50 microbial phyla (Payne et al., 2012). The diversity of GM varies in regions of the GI tract (fig.3.1.4), their importance has been mentioned in section-1.3.

Among the diverse range of GM of mammals, enterococci are Gram-positive bacteria under the phylum Firmicutes that are also ubiquitously present in soil, environment and in many food products (Semedo et al., 2003). Enterococci are gaining increasing interest in research as inhabitants of the GI tract because of their potential role as both ‘good’ and ‘harmful’ bacteria.

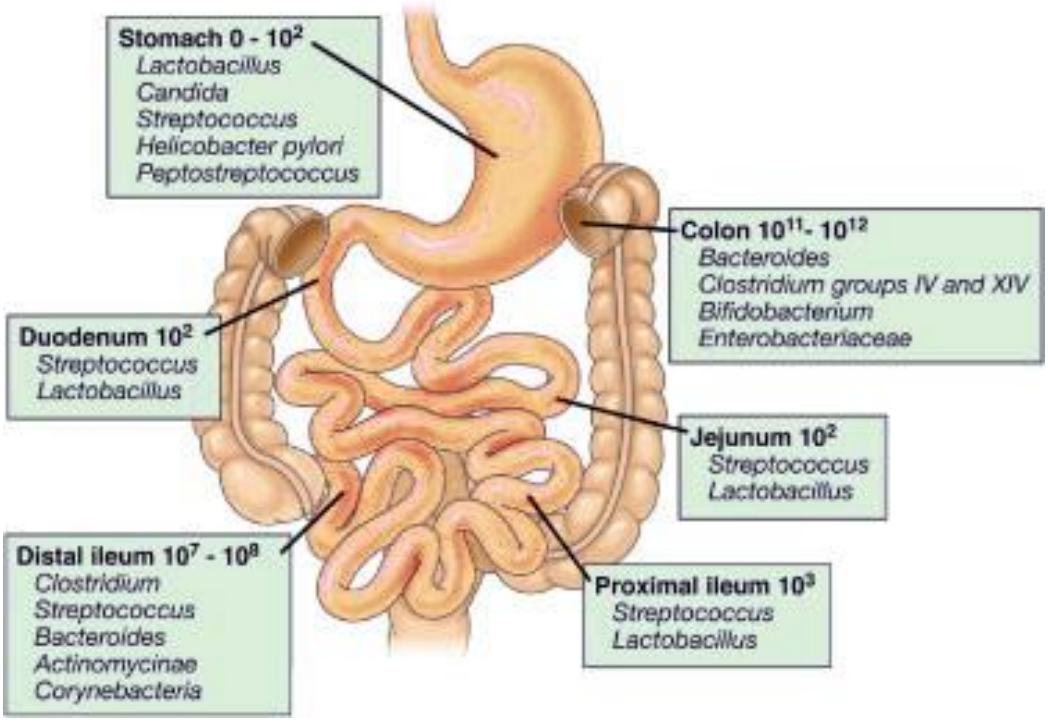

Figure 3.1.4: Distribution and abundance of bacteria in human gastrointestinal tract.

The gut microbiota contains an extraordinarily complex variety of metabolically active bacteria and other organisms. However, their diversity is limited in comparison to their number in the gut. Figure taken from Sartor, 2008.

On the positive side, bacteriocinogenic enterococci inhibit the growth and development of certain pathogenic and spoilage microorganisms, thus play potential protective roles (Gomes et al., 2008). Some enterococci such as *E. casseliflavus* and *E. gallinarum* can produce bile salt hydrolases indicating prospective probiotic properties (Gomes et al., 2008). They showed that among the 299 food enterococci isolates, 67.7% was found to present bile salt hydrolases activity, however, *E. faecalis* and *E. faecium* demonstrated either inactivity or presented low bile salt hydrolase activity. Still, strains of *E. faecium* and *E. faecalis* species have been applied as probiotic supplements in human (Moreno et al., 2006; Eaton and Gasson, 2001), and *E. faecalis* strains have also been widely used as veterinary feed supplements (Moreno et al., 2006). Also, some species have potential roles in food preservation because of their capacity of performing proteolysis, lipolysis, citrate breakdown, and production of bacteriocins (Moreno et al., 2006). Conversely, they have the innate ability to acquire and incorporate extrachromosomal genetic elements, allowing expression of virulence characteristics or antibiotic resistance, and they are capable of interspecies transferring of the traits (Palmer et al., 2010; Eaton and Gasson, 2001; Franz et al., 2001; Cetinkaya et al., 2000).

Enterococcus faecalis (*E. faecalis*), is a regular inhabitant of the human GI tract and solely responsible for about 80-90% of enterococcal infections in humans (Mohamed and Huang, 2007; Semedo et al., 2003; Jett et al., 1994). They are non-sporulating, facultatively

anaerobic cocci that can tolerate extreme environments, including temperature (5–65 °C), pH (4.5−10.0) and a high sodium chloride concentration (6.5%) (Fisher and Phillips, 2009).

E. faecalis is one of the bacteria that colonizes at the beginning of life and remains as a predominant commensal flora with a density of about 10^7–10^8 colony forming units (CFU) per gram in the GI tract (Huycke et al., 1998). Whilst remaining as a major bacteria, their detrimental characteristics such as antibiotic resistance, virulence, ability to integrate external genetic element, response to environmental changes and dietary components indicate their potential conversion into the evidently safe ('good') and unsafe ('harmful') *E. faecalis* and therefore increase their importance as a model organism for the current study.

Enterobacteriaceae is another important family under the class γ-Proteobacteria (phylum Proteobacteria), which includes both beneficial and harmful symbionts (Lupp et al., 2007). *Escherichia coli*, one of the most characterized bacteria, is a prototypic example of the Enterobacteriaceae (Winter et al., 2013). It is a Gram-negative, non-sporulating facultative anaerobe and has been identified in mammalian GM (Gordon and Couling, 2003). *E. coli* receives a nutrient supply and protection from human host, in turn it induces colonization resistance to reduce attachment of external pathogens to the epithelium (Vollaard and Clasener, 1994; Hudault et al., 2001). The number of anaerobic bacteria in the GI tract is more than 100 times higher than *E. coli* numbers, however, the latter is a predominant aerobic organism in the intestine (Tenaillon et al., 2010). In the large intestine, specifically in the caecum and colon, this commensal *E. coli* population resides in the mucous layer, however they shed into the intestinal lumen along with the degraded mucous elements, and eventually excrete/egest in the faeces (Poulsen et al., 1994). *E. coli* is not only well-distributed in the intestine of vertebrates but also a versatile pathogen responsible for various intestinal diseases in over two million people per year (Tenaillon et al., 2010). Since this study aims to investigate how enteric bacteria is altered due to AS exposure, more specifically, how the commensal bacteria turn into pathogenic bacteria, therefore, *E. coli* represents a perfect candidate for assessment.

Both MGB, *E. coli* and *E. faecalis*, colonize at the very early stages of life and were isolated from the earliest faeces of normal healthy neonates (Jimenez et al., 2008). *E. coli* reaches very high density of colonization (>10^9 cfu/g of faeces) before other anaerobic microbes extend their colonization. After 2.5 years of age, when the gut flora resembles that in the adult (Koenig et al., 2011), *E. coli* density stabilizes (≈10^8 cfu/g of faeces) and remains the same during adulthood, although it gradually decreases in the elderly (Ouwehand et al., 1999).

Both bacteria have pro-carcinogenic features, and both produce DNA-damaging compounds (Boleij and Tjalsma, 2012). *E. faecalis* cause DNA damage in IECs by excreting extracellular superoxide. This superoxide converts into H_2O_2 that has potential DNA-

damaging features (Huycke et al., 2002; Wang and Huycke, 2007). Similarly, some *E. coli* strains in the gut harbour the polyketide synthetase site, a gene encoding colibactin (a genotoxin), causing DNA damage or genetic mutation. Colibactin induces breaks in DNA single strands, enhancing the activation of DNA-damage induced signalling pathway, thereby increasing the mutation rate of attacked cells (Cuevas-Ramos et al., 2010; Nougayrède et al. 2006). Therefore, considering the commensal distribution, behaviour, sensitivity and pathogenic potential, selection of the MGB is rational for the present study.

3.1.6 Importance of bacterial metabolism in host physiology

The role of intestinal microbial metabolism is becoming increasingly important due to their close relation with hosts and the host's health and wellbeing is equally dependent on host/microflora interactions (Wong et al., 2016). For example, the host's predisposition to various MD is influenced by the array of harbouring microbiota (fig.3.1.2). Since microbes are exposed to AS in the gut environment, investigating their metabolism after AS-exposure is important in defining bacterial dysbiosis. The specific effect of AS on the intestinal bacterial metabolism remained elusive. GM function (e.g., SCFA production) and host metabolisms are intricately intertwined (Koh et al., 2016). Minor changes in the bacterial metabolism may result in huge alterations in the metabolic homeostasis of the host (Makki et al 2018). AS can directly impact intestinal bacteria, also bacterial metabolites after AS exposure can affect IEC function (Bian et al., 2017). In addition, the receptors in the intestine that sense these bacterial metabolites can influence gut physiology. Moreover, the signalling pathways involved either directly with AS metabolism or AS-mediated bacterial metabolites, play roles in manipulating host metabolism and host-microbiome interactions (Wong et al., 2016). Therefore, AS can directly impact gut bacteria, or bacterial metabolites can be changed after AS exposure.

Claus *et al.* (2016) reviewed the extensive ability of GI microbiota in metabolising a range of environmental pollutants, xenobiotics and AS. They have described the breakdown of cyclamate, the carcinogenic effects of the component cyclohexamine and these studies have resulted in the banning of this sweetener in the UK and the US. The researchers also noted that Ace-K has no growth-promoting or -inhibiting effect on bacteria. Moreover, they have discussed the growing research on other AS, including saccharin, sucralose and aspartame, and urged the necessity of reassessment in appropriate gut microbial ecosystems. Since GI microbiota have the potential to metabolise unusual substances and can alter their metabolic activity due to long-term exposure, the authors emphasised that exposure of microbiota to chemical pollutants, especially during perinatal period and early childhood, may have critical impact on microbial development and host physiological

functions (Claus et al., 2016). Thus, it is important to study pathogenic factors of the GM stimulated due to AS-exposure.

3.1.7 Bacterial pathogenic factors

Whilst predominant *E. coli* and *E. faecalis* strains in the normal colon promote and maintain the stability of the intestinal microbial flora, their pathogenic states possess distinct virulence properties (Kaper et al., 2004). Among the virulent features of GM (fig.3.1.5), the most studied ones for *E. coli* are enterotoxin production, tissue invasion and adherence to enterocytes (Levine, 1987). *E. faecalis* are recognised as opportunistic pathogens and are responsible for various infections including intra-abdominal infections (Mohamed and Huang, 2007).

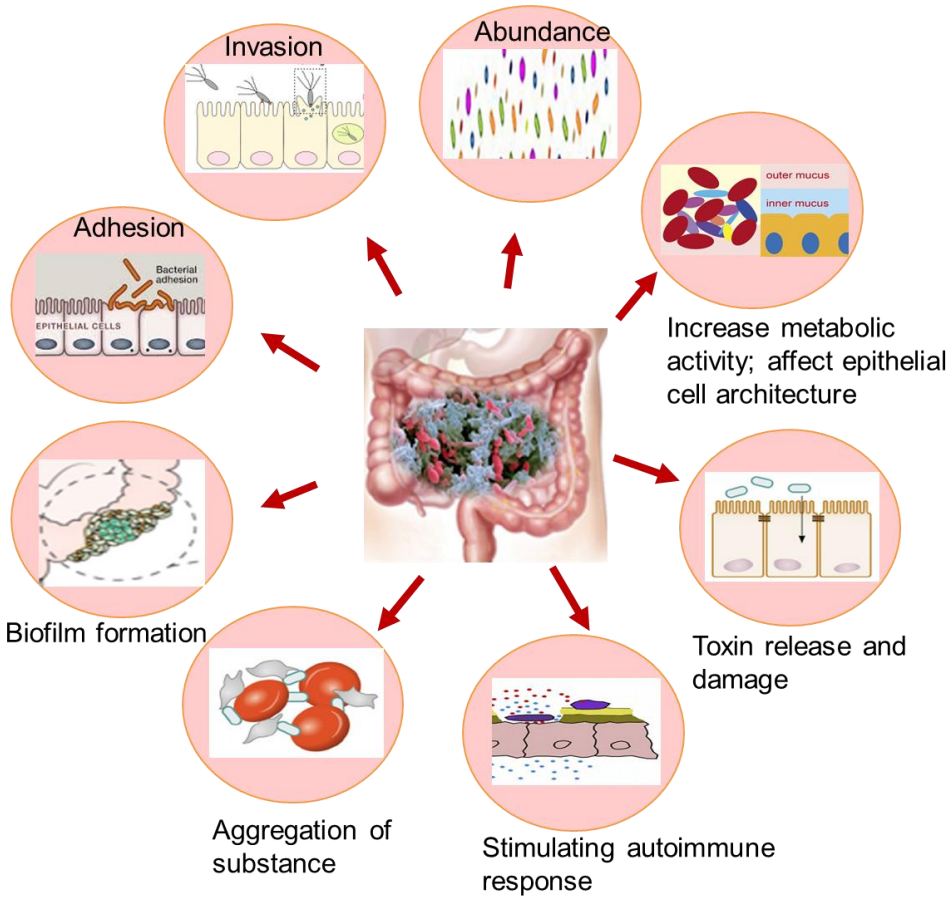

Figure 3.1.5: Schematic diagram representing potential pathogenic factors in gut bacteria.

Bacterial metabolism can directly affect intestinal epithelial cell function or can release substances harmful to cells. Also, they can increase number, and can influence the bacteria-intestinal epithelial cell interactions. Figure made using online images following Amon and Sanderson, 2017.

Enterococcal infections have become a frequent concern in the last few decades in relation to a wide range of human infections, such as cystic fibrosis, bacterial endocarditis, abdomen, biliary tract, nosocomial infections, and those affecting the central nervous system (Tendolkar et al., 2004; Jett et al., 1994). The virulence of *E. faecalis* cannot only be explained by their antibiotic resistance; other virulence factors may stimulate or enhance their pathogenicity (Toledo-Arana et al., 2001). Several virulence factors have been demonstrated in *E. faecalis* in different studies, including cytolysin, aggregation substances, surface carbohydrates, extracellular superoxide and surface proteins such as Ace, Efa A and Esp, however, these factors are highly dependent on the strains and environmental conditions (Toledo-Arana et al., 2001). In addition, a number of possible pathogenic activities of *E. faecalis* exist, including their ability of haemolysis and biofilm formation (Coburn and Gilmore, 2003, Kristich et al., 2004; Furumura et al., 2006). It is normally γ-haemolytic but turns into β-haemolytic when virulent (Shankar et al., 2002). Since physiological factors such as diet have influence on the above-mentioned pathogenic factors in *E. faecalis*, and these pathogenic factors are important for host health, therefore, it is sensible to investigate the effect of AS on the growth, haemolysin and biofilm formation of this microorganism.

Haemolysin production is frequently observed in pathogenic *E. coli* strains isolated from disease processes. For example, strains from urinary tract infection (UTI), peritonitis and appendicitis could produce haemolysin (Giaffer et al., 1992). Study on faecal samples of patients with UTI, *E. coli* strains were found to possess more haemolytic capacity than those from healthy individuals (Cooke and Ewins, 1975). The haemolytic *E. coli* strains were also associated with necrotoxin production and cytotoxicity (Cooke and Ewins, 1975). Similar studies demonstrated that the diffusible haemolysin production of *E. coli* has close correlation with cytotoxicity in chick embryo cell cultures. However, the same strain had no cytotoxic effect on monkey kidney and mouse embryo cell cultures (Chaturvedi et al., 1969). In addition, haemolytic *E. coli* strains were isolated from patients suffering with IBD along with either Crohn's disease or ulcerative colitis. The research indicated equal distribution of the haemolytic strains in both diseases without differing according to disease activity (Giaffer et al., 1992). Therefore, whether bacteria produce haemolysin after AS-exposure needs to be investigated since this feature has link to other diseases.

Communities of microorganisms adhered to an abiotic or a biotic surface and protected in a matrix composed of bacterial secretions, is called biofilms (O'Toole et al., 2000). Some genetic factors such as *E. faecalis* regulator (fsr), enterococcal surface protein (esp), autolysin (atn) etcetera genes have contribution in *E. faecalis* biofilm formation (Mohamed and Huang, 2007). Similarly, *E. coli* contains specific genes that promote biofilm formation upon stimulation from environmental conditions. Some cell surface components such as

flagella, type I fimbrae, outer membrane proteins, colonic acid, poly (β-1,6-GlcNAc) in *E. coli* K-12 have contribution in biofilm formation during static growth conditions (Reisner et al., 2006). Therefore, biofilm formation may occur due to the genetic factors or response of bacteria to environmental changes and has significant phenomenon in studying the microbial development (Mohamed and Huang, 2007; O'Toole et al., 2000).

Biofilm development is an important pathogenic phenotype associated with several chronic infections (Reisner et al., 2006; Mohamed and Huang, 2007). Biofilms form through a complex series of mechanisms (Tendolkar et al., 2004). Beside the genetic factors, nutrient availability and physical conditions such as available CO_2, osmotic pressure, pH, and temperature influence biofilm formation (Mohamed and Huang, 2007). Evaluation of these factors in different studies on *E. faecalis* suggested that this organism monitors the milieu and modulates biofilm development (Kristich et al., 2004). Besides, being a non-pathogenic member of the GI tract, *E. coli* causes diarrhoea and a variety of other infections indicating their ability to form biofilm under appropriate environmental conditions (Reisner et al., 2006), however biofilm formation in response to AS has not been previously studied.

Pathogenic bacteria produce different cytolytic toxins which have important virulence features. In both commensal and pathogenic states of *E. coli*, three different pore-forming cytolysins were identified so far; HlyA, EHEC HlyA, and ClyA stands for α-, enterohaemorrhagic *E. coli*– haemolysin and cytolysin A, respectively (Burgos and Beutin, 2010; Ludwig et al., 2004). α-haemolysin is the most predominant cytolysin in the Gram-negative pathogenic bacteria, *E. coli* strains exhibiting the phenomenon of haemolysis usually harbour a homologous gene clusters for the production, activation and secretion of α- and EHEC- haemolysin (Ludwig et al., 1999). ClyA is released in small amounts in the external medium and can cause complete haemolysis of erythrocytes (Ludwig et al., 2004). Influence of dietary carbohydrates on ClyA release was confirmed in recombinant *E. coli* DH5α; dextran (30 mM) but not sucrose (30 mM) demonstrated a protective role in ClyA-mediated haemolysis (Ludwig et al., 1999). Moreover, Gomes *et al*. (2008) studied enterococci isolated from Brazilian foodstuff and reported that 72.4% of the *E. faecalis* developed biofilm while 13.8% showed adherence to Caco-2 cells and 12% caused β-haemolysis. The study also described higher frequency of antibiotic resistance genes and traits in *E. faecalis* than other enterococci such as *E. faecium* (Gomes et al., 2008). There might have a connection among the biofilm formation, haemolysin production and antibiotic resistance in *E. faecalis* indicating their adherence to IECs can interact in a variety of ways.

Food components have been determined to have enormous impact on the structure and behaviour of the microflora (section-1.3.2). AS came under focus as they exert unusual implications on gut bacteria (section-1.4.3). Background research has already indicated that

AS cause gut bacteria dysbiosis (Suez et al., 2014), however, there are no clear studies on how AS changes the commensal bacteria and how that potential might elicit pathogenic response in the intestine.

Rationale for chapter 3

The changes in growth and pathogenicity of one organism may have influence on the response of others and the interactions among gut flora. The alterations can be attributed to either the effects of AS on mammalian cells, or the effect of AS on bacteria, or a combination of both. Research into this area will help our understanding on the effect of AS consumption on the bacterial metabolism and whether this food component can be used to regulate the bacterial pathogenicity.

Both *E. coli* and *E. faecalis* are commensal as well as pathogens and are good representative of corresponding phyla. From a technical perspective, both species can be isolated easily, grown and maintained in laboratory and are frequently used as potential human faecal indicators (Wheeler et al., 2002). Considering the aim of the present study, investigating how the normal commensal bacteria could potentially become pathogenic in response to AS consumption in the gut environment, these organisms represent good models to study.

Aims and hypothesis

The hypothesis for the present chapter is that **artificial sweeteners alter the model gut bacterial metabolism and increase pathogenicity.**

To address this hypothesis, the specific aims for the chapter are:

- To determine the role of AS on metabolism of models of gut bacteria.
- To assess whether exposure to AS increase model gut bacterial pathogenicity factors.

3.2 Material and methods

3.2.1 Materials

Bacterial culture plates and universal tubes were purchased from ThermoScientific (USA), the glassware and micropipette tips were from Fisherbrand (UK), and the micropipettes were from Eppendorf (UK). Bacteria *Escherichia coli* DH5α and *Escherichia coli* NCTC 10418 were obtained from the Microbiology laboratory, Anglia Ruskin University. *Enterococcus faecalis* was bought from ATCC (ATCC® 19433™, USA). 2YT solid and liquid media were from Sigma. All other bacterial media, and carbohydrates glucose, fructose, and sucrose were purchased from Oxoid (UK). $ZnSO_4$ and the antibiotics were purchased from Sigma-Aldrich (USA). Sterile, flat-bottom, polystyrene 96-well plates were purchased from CytoOne (USA).

AS in the diet can easily reach to 100 µM. This sub-physiological concentration did not affect Caco-2 cell viability, while bacterial growth remained unchanged for a range of concentrations of the AS. Considering the co-culture assays in chapter 4, and the findings from growth data, 100 µM was found appropriate for the further assays with bacteria. Also, if there is an effect at sub-physiological concentration, it is likely that higher concentrations would also have the effect, so 100 µM concentration was used for the other assays (table-3.2.1). Zinc sulphate, glucose, sucrose, and fructose concentrations used in the study were less than or equal to the concentrations previously used by Keast *et al.* (2003).

Table 3.2.1: AS and sweet taste inhibitor ($ZnSO_4$) concentrations used in different experiments.

The bacterial growth conditions were determined using model bacteria *E. coli* DH5α, and further experiments was performed on the model gut bacteria *E. coli* NCTC 10418 and *E. faecalis* ATCC 19433.

Assay performed	Chemical name	Cell type exposed to AS	Concentration(s) (μM)
Growth measurement	AS (saccharin, sucralose, aspartame, neotame)	*E. coli* DH5α	0, 0.01, 0.1, 1, 10, 100, 1000, 10000
	Glucose, fructose and sucrose		0, 0.2, 2, 20, 200, 2000, 20000, 200000
	$ZnSO_4$		0, 1, 10, 50, 100, 500, 1000, 10000
Growth measurement	AS (saccharin, sucralose, aspartame, neotame)	*E. coli* *E. faecalis*	0, 0.1, 1, 10, 100, 1000
	$ZnSO_4$		100
Biofilm Assay	AS	*E. coli*	100
	$ZnSO_4$	*E. faecalis*	100
Haemolysis Assay	AS (saccharin, sucralose, aspartame, neotame), Sucrose	*E. coli* *E. faecalis*	100 AS, 73 mM Sucrose
	$ZnSO_4$		100

3.2.2. Bacterial cell culture

Bacteria were grown at 37 ˚C either on solid media without shaking (LMS Cooled incubator, UK) for single colonies, or in liquid media with shaking (New Brunswick Scientific Co. Inc., G25, USA) at 150 revolutions per minute (rpm). Aseptic techniques were followed for all the bacterial and cell works.

3.2.3 Bacterial growth determination

3.2.3.1. Method evaluation

Measuring pH of the chemical solutions

The stock solutions for the natural carbohydrates, AS, and $ZnSO_4$ were prepared in water and pH was measured (Jenway, Model 3510, Bibby Scientific ltd, UK). The working solutions were prepared in 2YT for the model bacteria *E. coli* DH5α, and in NB and BHI for the MGB, *E. coli* NCTC 10418 and *E. faecalis* ATCC 19433, respectively. The pH of the stock solution and the working solutions are presented in Appendix B (table-B8.1).

Determination of the culture conditions

E. coli DH5α was used to determine the conditions such as inoculum concentration and shaking for bacterial growth. From the stock culture, a loopful bacteria was spread on 2YT plate and incubated overnight. A single colony from the overnight culture was inoculated into 10 ml of 2YT liquid medium (pH 6.72) and incubated overnight at 37 °C with shaking at 150 rpm. The optical density of the culture was measured at 600 nm against 2YT media (blank) and was used as base culture for further dilutions. Different dilutions (1:50, 1:100, 1:500, 1:1000, 1:5000, 1:10000) of the base *E. coli* DH5α culture were re-suspended in 200 µl of the fresh 2YT liquid media in 96-well plates and plates were incubated with or without shaking. Bacterial growth was measured as absorbance at 600 nm using PerkinElmer (Victor X3) from 0 to 96 hour at interval of 0.5 hour.

Effect of carbohydrates, AS, and $ZnSO_4$ on model bacterial growth

Once the bacterial concentration and growth condition was determined, the effect of different concentrations of the AS, natural carbohydrates glucose, sucrose, and fructose, and the sweet taste inhibitor, $ZnSO_4$ was determined on the growth of *E. coli* DH5α.

3.2.3.2 Determination of the model gut bacterial growth

The model gut bacterial growth was assessed using the same protocol described above. Brain Heart infusion (BHI) medium was suggested by the supplier for the *Enterococcus faecalis* ATCC 19433 (*E. faecalis*) growth and maintenance. *Escherichia coli* NCTC 10418 (*E. coli*) was grown in several liquid medium such as NB, BHI, Iso-sensitest broth, 2YT and Luria-Bertani to determine the appropriate medium for the study. Optical density (OD600) was measured using spectrophotometer (Eppendorf BioPhotometer Plus, Germany) and NB was selected for the *E. coli* growth. A single bacterial colony of *E. coli* or *E. faecalis* was

transferred from NA or BHI agar plates, respectively, into corresponding liquid media using aseptic techniques. Growth was measured as absorbance at 600 nm using spectrophotometers, cuvette photometer (Eppendorf BioPhotometer) or the multiplate reader (PerkinElmer, Victor X3).

OD600 is the measurement of absorbance or optical density (OD) of bacterial growth. The bacterial scattering of the light provides a measurement of turbidity. Simply, the more turbid the sample, more bacteria are present to scatter the light, so less amount of light will pass through the sample. Use of multiplate reader (PerkinElmer) is easier and less amount of sample and time are needed. The machine uses fast absorbance measurement method to provide bacterial density. In contrast, the cuvette photometer (Eppendorf) requires more sample and longer time to read. It measures OD600 for calculating the bacteria density through measuring turbidity. The basic idea of measurement for both cuvette photometer and the PerkinElmer are same, other than the mode of measurement. For the convenience to differ cuvette and multiplate read in the study, the former is denoted as OD600 and the latter as A_{600}.

Determination of absorbance to bacterial count

OD600 measurement differs for different bacteria due to their size, so an initial assessment was done to estimate the number of bacteria in relation to absorbance. The MGB were cultured overnight in NB and BHI, respectively and OD600 was measured. Also, CFU/ml of the bacterial culture was assessed using standard plate count method.

In addition, to determine the number of bacteria in different growth cultures, the CFU for a range of absorbance was measured using simplification of the protocol maintained for the McFarland standards (Lahuerta Zamora and Pérez-Gracia, 2012) with the standard plate counting method. A serial dilution (up to 10^{-10}) of the diluted base culture (table-B8.2) of the MGB was performed, and A_{600} of 100 µl of bacterial suspension was measured in 96-well plate. The diluted sample (100 µl) was plated for overnight at 37 ˚C for CFU. Absorbance index were developed by accounting the relative absorbance and the CFU unit.

3.2.4 Effect of AS on model gut bacterial growth

The MGB were cultured in the respective liquid medium supplemented with different concentrations of the AS saccharin, sucralose, aspartame and neotame (table-3.2.1) to assess the effect of AS on their growth. For each assay, the bacteria were grown between one and four days to measure the changes until complete stationary phase, and growth was recorded as A_{600} (fig.3.2.1).

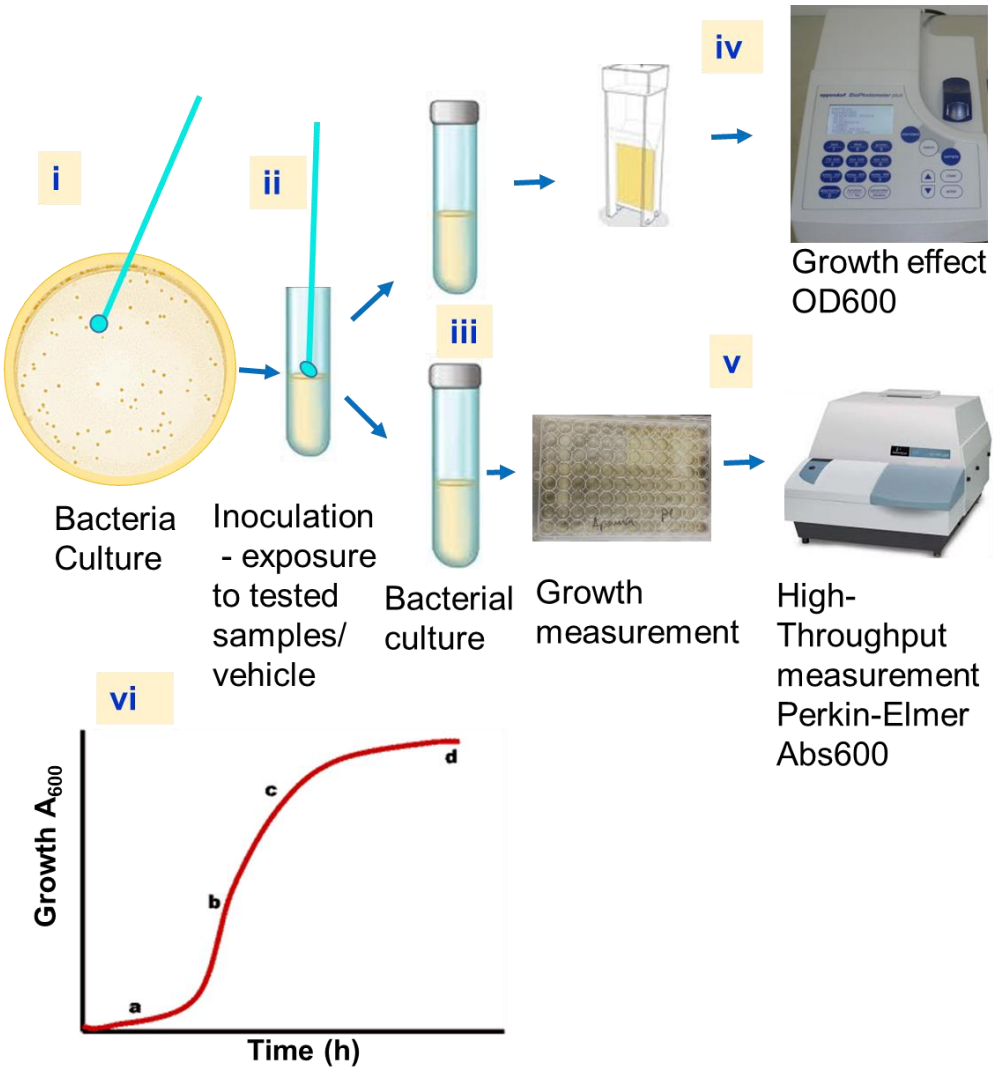

Figure 3.2.1: Experimental process for bacterial growth measurement.

(i) bacterial strain was streaked on solid media; (ii) single colony was inoculated into liquid media with/out AS; (iii) overnight culture – growth was measured and continued incubation; (iv,v) sample was measured in cuvette using spectrophotometer and/or 96-well plate using Perkin-Elmer (Victor™ X3); (vi) representative feature of a growth curve having lag phase, exponential phase, transitional or diminishing growth phase and plateau or stationary phase denoted by a, b, c and d, respectively.

3.2.5 Biofilm formation Assay

Biofilm formation of *E. coli* and *E. faecalis* was measured after exposure to different AS (fig.3.2.2) at 100 µM concentration (table-3.2.1). A single bacterial colony was inoculated into 10 ml of the respective liquid media supplemented with AS, 73 mM sucrose or vehicle, and allowed to grow overnight. The base cultures were diluted 1:200 with fresh liquid media with/out treatments for continuous- or pre-exposure, respectively. In addition, $ZnSO_4$ was used with AS to inhibit the sweet sensing and biofilm formation was assessed for continuous exposure at 37 ˚C. Equal distribution of the bacterial cell number into each of the wells was confirmed by A_{600} measurement (fig.3.2.2).

Aliquots of 200 µl of bacterial cultures were dispensed in triplicate into wells of a sterile 96-well flat-bottom plastic tissue culture plate. The sides of wells under consideration were filled with equal amount of distilled water to prevent evaporation or drying. The cultures were grown aerobically for 48 hours at RT or 37 °C without shaking. Comparable bacterial growth in each well was confirmed by measuring the A_{600}. The supernatant was removed, and the wells were washed once with 200 µl of double distilled water (ddH_2O). The adherent cells were stained with 150 µl of 0.1% Gram crystal violet (CV) for 20 minutes at RT to facilitate CV absorption by the biofilm-forming bacteria. The wells were washed (200 µl ddH_2O, X3) to remove the unbound or loosely adhered CV and 30% acetic acid in water (200 µl) was employed to release retained CV. Plates were incubated at 37 °C for 5 minutes to facilitate CV release. A_{600} of the wells was again measured using the same protocol to assess the biofilm forming bacteria as a measurement of the CV retained.

The biofilm forming unit was calculated (fig.3.2.2.vii) and were normalised to the control (100%) to eradicate normal growth influence on the treatment and presented as % biofilm formations.

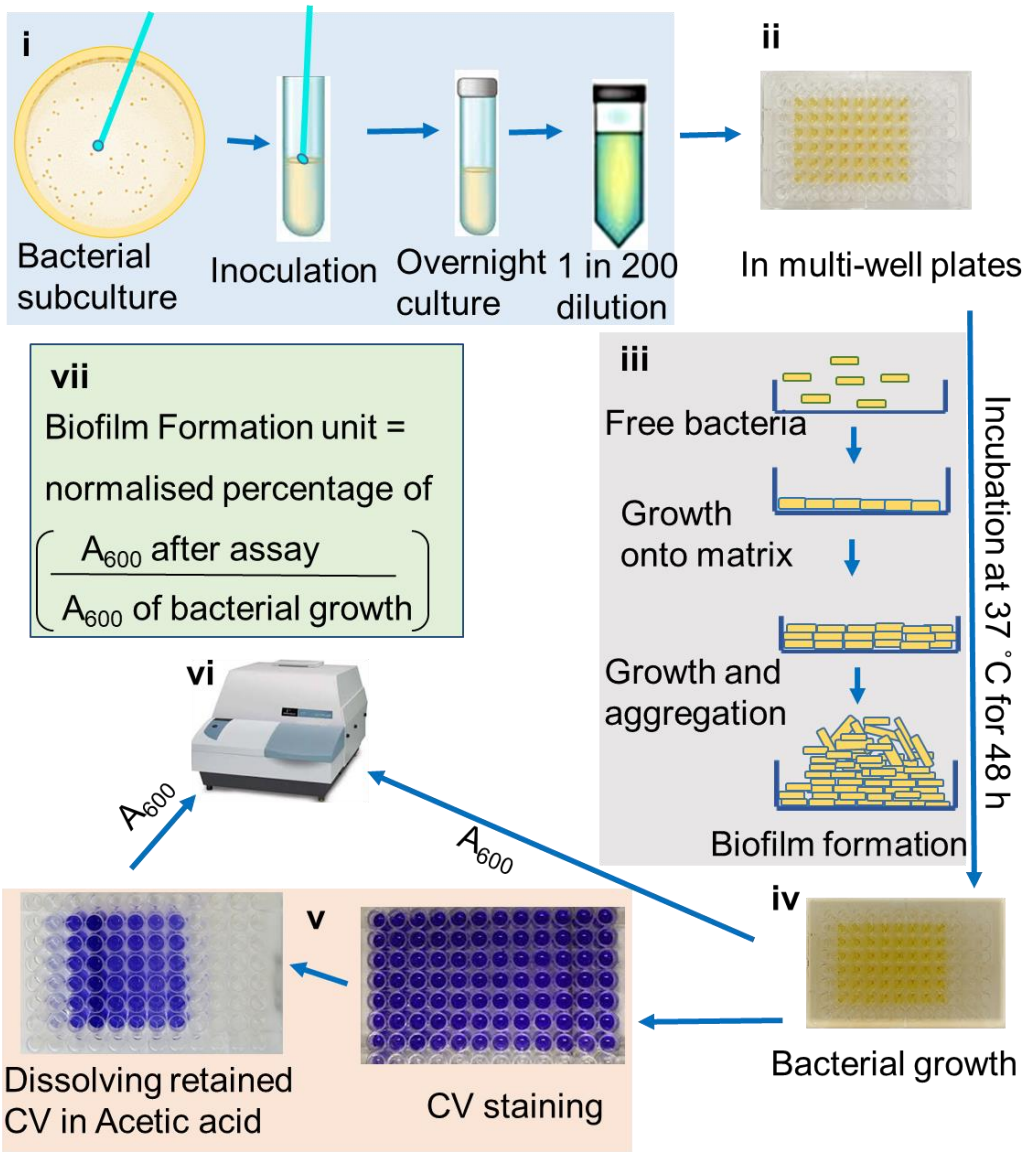

Figure 3.2.2: Schematic diagram of the crystal violet biofilm formation assay in plastic microtiter plates.

(i) bacterial inoculum preparation; (ii) 200 µl of inoculum into the 96-well plate for biofilm development; (iii) steps of biofilm formation; (iv) bacterial culture after 48 hour incubation; (v) staining with Crystal violet (CV) staining assay; (vi) measuring absorbance at 600 nm (A_{600}) using Perkin-Elmer (Victor™ X3) of total bacterial growth and retained CV by biofilms; and (vii) method used to calculate biofilm formation.

3.2.6 Hemolysis Assay

Blood Agar Base with 7% Horse Blood (Thermo Scientific Oxoid) was used to investigate the haemolytic properties of *E. coli* and *E. faecalis* after exposure to 100 µM of the AS or sucrose (73 mM) or vehicle (fig.3.2.3).

A single colony of MGB was grown in 10 ml of liquid media supplemented with the AS or sucrose or vehicle, in the presence or absence of $ZnSO_4$. After 24-hour incubation at 37 °C with shaking at 150 rpm, A_{600} was measured. A cotton swab soaked with bacterial culture was spotted and dragged on Blood Agar Plates with and plates were incubated at 37 °C. Hemolysis was assessed after 24-, 48-, and 72-hours of incubation. *Staphylococcus aureus* was used as positive control for the assay (Wiseman, 1975). Images of the plates were taken (UVI-Tec imager, Cambridge, UK) and qualitative data was collected.

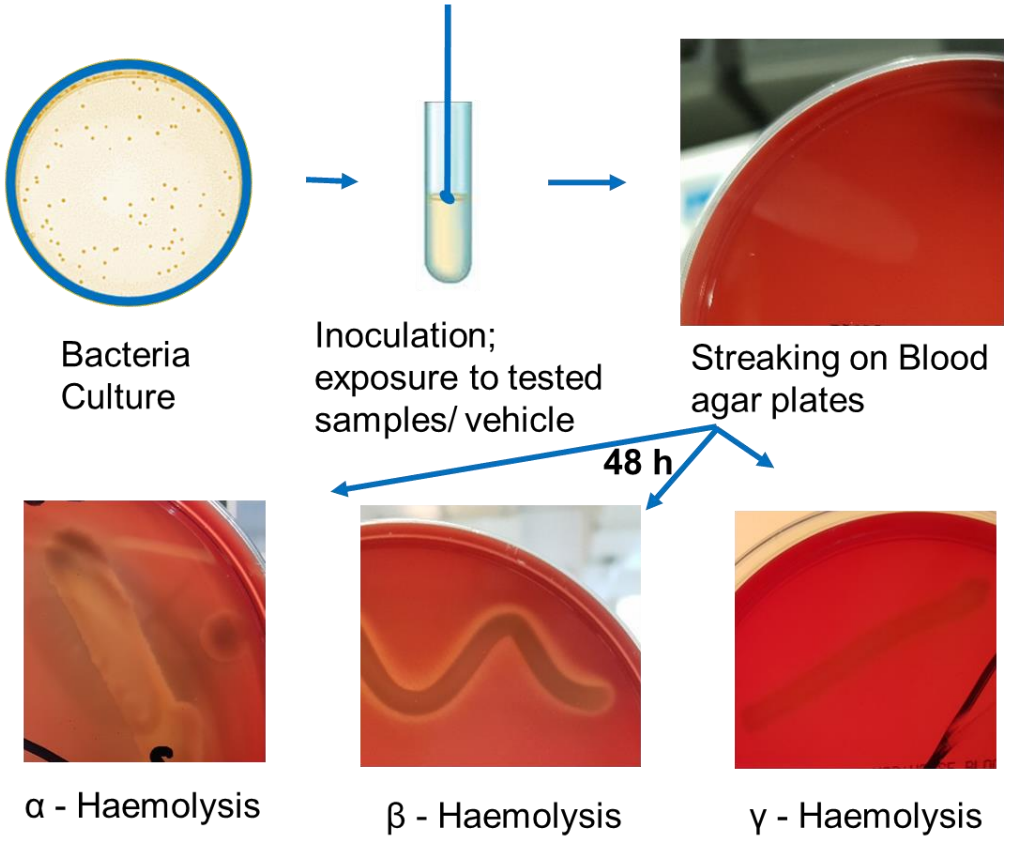

Figure 3.2.3: Haemolysis assay on blood agar plate.

A single colony was inoculated into liquid media containing AS or sucrose or vehicle with/out $ZnSO_4$ for 24 hours. Cotton swab soaked with overnight bacterial culture was streaked on blood agar plates and incubated at 37 °C for 24- to 72-hours. The plates were observed for the clearing of erythrocytes due to haemolysin production. Panels show three different types of haemolysis bacteria can cause.

3.2.7 Data analysis

Differences among the means were tested for significance in all experiments by ANOVA with least significance difference test, one-way ANOVA with Holm-Sidak multiple comparison test, ordinary one-way ANOVA with Kruskal-Wallis test, unpaired t-test and non-parametric test. Significance was reached when $p<0.05$.

3.3. Results

3.3.1 Protocol determination

3.3.1.1 *Escherichia coli* DH5α growth

E. coli DH5α were cultured at different dilutions and grown with or without shaking to determine the inoculum concentration and growth condition for further experiments. The initial lag phase and subsequent exponential growth phase lasted for 8-10 hours with shaking condition, followed by an extended period of late exponential phase of slow growth before stationary phase (fig.3.3.1). The effect of the increasing dilution on growth was observed in the growth curves (fig.3.3.1). The growth curve varied with different concentrations of bacteria as well as with shaking (fig.3.3.1.a) and without shaking (fig.3.3.1.b).

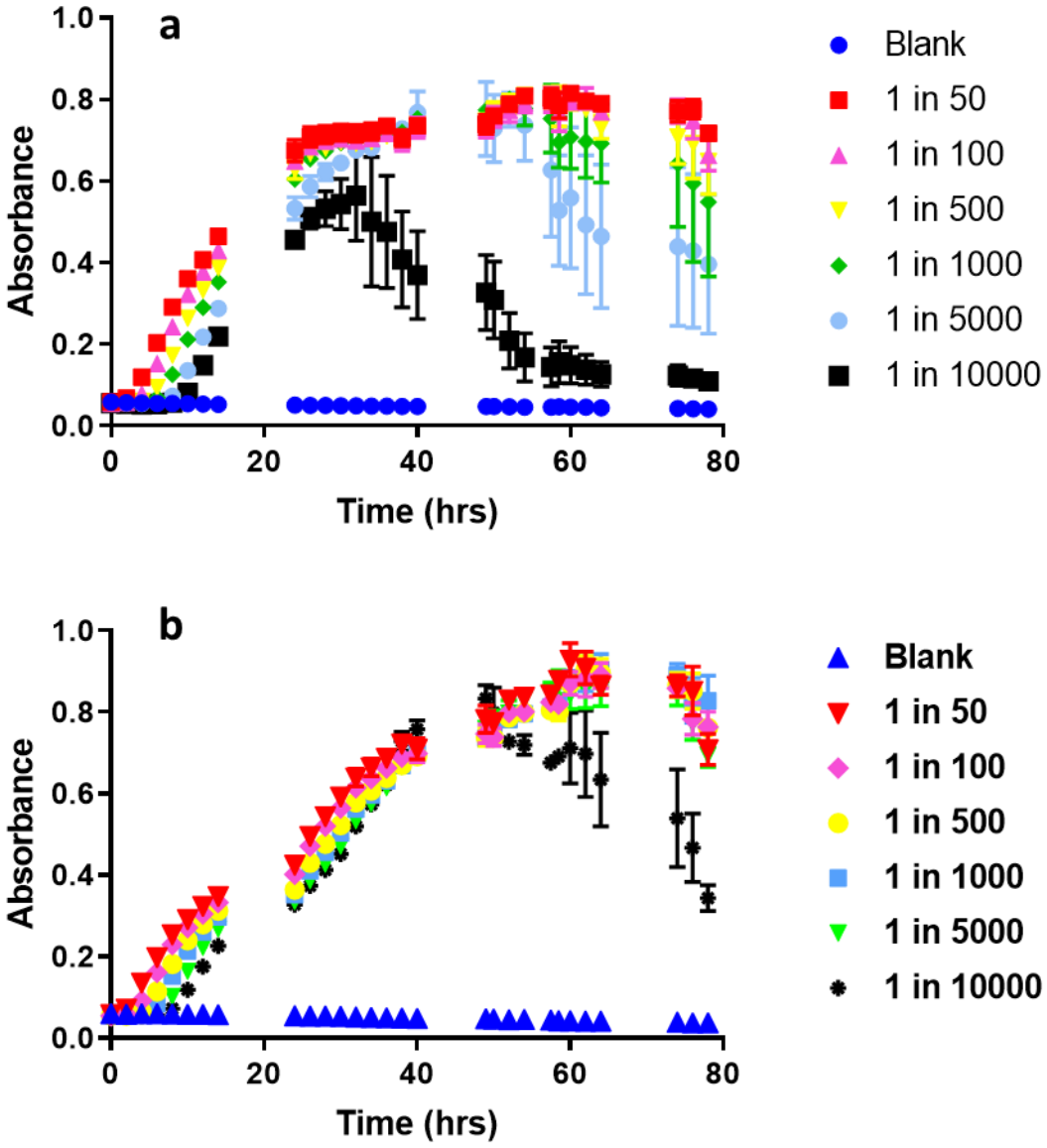

Figure 3.3.1: Growth curve of *E. coli* DH5α.

Different dilutions of overnight grown base culture were plated in 96-well plates with 200 µl of 2YT liquid media (pH 7.2). The plates were incubated at 37 °C with shaking at 150 rpm (a) and without shaking (b), and absorbance was measured at 600 nm at 30-minute intervals (except for near 20 and 40 hours, for about 10 h). Data are presented as the mean ± S.E.M., n=3.

The initial lag phase lasted for about 2-4 hours, followed by an extended exponential phase for about 14-18 h (fig.3.3.1.b). The late exponential phase was longer (25 – 40 hour) with lower growth rate after which bacteria reached the stationary phase.

The 1:50 dilution bacterial culture incubated with shaking showed very short (approximately 1.5 hour) lag phase followed by about 16–18 hour log phase after which it has reached to a long stationary phase (fig.3.3.1.a). The dilution 1:500 represented almost similar growth pattern like 1:50 but showed a long late exponential phase. The 1 in 1000 dilution reached near 0.8 (a.u.) but the lag phase was longer (approximately 8 hour). Also, the curve started

to decline after 48 hours (fig.3.3.1). A similar decline was observed in 1:5000 dilution and the lag phase were prolonged (10 hour). The lowest absorbance (near 0.6) peak was recorded for the 1:10000 dilution with shaking incubation where the lag phase was extended for about 10 hour followed by an exponential phase of approximately 16 hour (fig.3.3.1.a).

Without shaking, a similar trend of growth was observed however the growth rate was slow and the duration of each phase was extended (fig.3.3.1.b) than shaking. The highest absorbance was 0.9 for all the less diluted bacterial suspensions (1:50 to 1:1000) at 60 hours. The less diluted cultures showed shorter lag phase while the more diluted bacterial suspensions undergone prolonged lag phase. On the other hand, the higher bacterial number presented a long stationary phase (about 10 hours for 1:50 dilution) whereas the lowest bacterial dilution (1:10000) started to decline just after reaching its peak.

Taken together these findings show that bacterial concentration (1:500) and shaking technical approaches provide an appropriate growth curve with phases as expected and found feasible for the project. Also, the microvilli mediated continuous mixing and movement due to peristalsis represent shaking as more physiological condition. Further studies with MGB will therefore use this approach to grow bacteria in liquid media.

3.3.1.2 The effect of natural sugars

The effect of sweeteners on gut bacteria metabolism is important to determine the exact mechanism of how they change bacterial diversity and/or alter/drive bacteria to be pathogenic (Nettleton et al., 2016). In addition, effect of the carbohydrates such as glucose, fructose and sucrose, need to be assessed since they may have an effect on host metabolism and absorbance (Payne et al., 2012), also, the changes due to AS exposure can be compared to the natural carbohydrates. *E. coli* DH5α is a non-pathogenic laboratory strain that shows sensitivity to growth conditions (Phue et al., 2008). Therefore, the next set of experiments were performed with *E. coli* DH5α as a model organism to assess the role of glucose, fructose, sucrose, and AS on the bacterial growth.

The pH of the solutions containing bacterial growth media and sweeteners, which the bacteria were exposed to, was measured (Jenway, Model 3510, Bibby Scientific ltd, UK) to keep the pH of the solutions consistent. The stock solutions (1M) for the natural carbohydrates, AS, and $ZnSO_4$ were prepared in water and the working solutions were prepared in 2YT for the model bacteria *E. coli* DH5α, and in NB and BHI for the MGB *E. coli* and *E. faecalis*, respectively. The pH of the working solution concentrations was close to the vehicle and there was no statistically significant difference (appendix B, table-B8.1).

The carbohydrates showed differential effect on the model bacteria, *E. coli* DH5α growth and the shaking condition has distinct impact, as expected. All without shake data were

presented in appendix B. Glucose and fructose marginally increased *E. coli* DH5α growth at lower concentrations (0.2 – 20 μM) while the higher concentrations (2 – 200 mM) reduced bacterial growth below the control (fig.3.2.a,b). In contrast, sucrose had no effect other than a marginal reduction for the highest concentration, 200 mM (fig.3.3.2.c). However, the shaking condition gave a growth curve like the vehicle (fig.3.3.2.c) while a 24-hour lag phase was observed without shake condition (fig.B8.1). A similar difference in the growth peak was also observed for glucose and fructose due to shaking, as anticipated. The growth reached at stationary phase for shaking condition after 36 hours (fig.3.3.2.a,b), whilst at 60-hour for without shake condition (fig.B8.1.a,b).

The higher concentrations (20 and 200 mM) of glucose and fructose had inhibitory effect on *E. coli* DH5α growth at both conditions (fig.3.3.2 and B8.1.a and b). Similar inhibition was also observed for the 2 mM at with shake condition until 24 hours (fig.3.3.2.a,b), although this was not distinct in without shake (fig.B8.1.a,b).

These studies suggest that shaking is better for model bacterial growth as expected. Also, glucose and fructose have an initial inhibitory effect on *E. coli* DH5α growth, but sucrose has no effect.

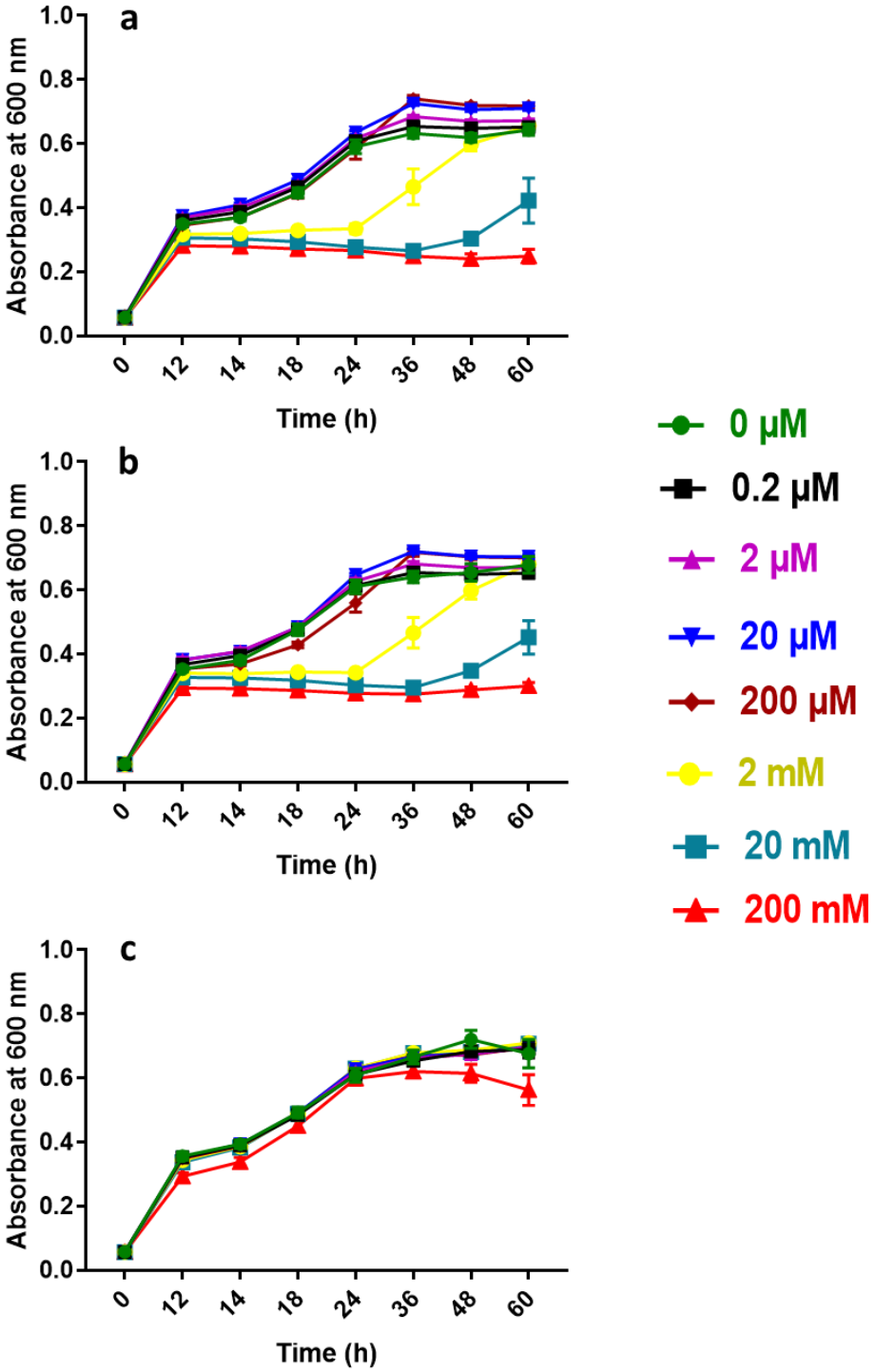

Figure 3.3.2: Effect of natural carbohydrates on *E. coli* DH5α growth.

Overnight culture was inoculated into liquid media (1:500) at planktonic condition and incubated at 37 °C with shaking at 150 rpm. Plates were read at 12-hour intervals at 600 nm using PerkinElmer (Victor X3). All cultures plateau to a degree after 12 hours, the cultures with higher added sugar concentrations 20, 200 mM) of glucose (a) and fructose (b) took longer to re-enter exponential phase. Sucrose (c) growth curves were same for all the tested concentrations. Data are presented as the mean ± S.E.M., n=3, each with two replications.

3.3.1.3 Effect of AS

AS did not have effect on *E. coli* DH5α growth (fig.3.3.3), except for the highest concentration (10 mM) of saccharin (fig.3.3.3.a) and neotame (fig.3.3.3.d) that reduced growth marginally. In addition, fig.3.3.3 and fig.B8.2 represent that shaking caused a difference in the growth of the bacteria.

The AS at different concentrations presented an exponential growth for 24 hours, then a long late exponential growth phase with the very slow increase in absorbance (fig.3.3.3). The model bacteria showed its optimum growth for 100 µM of saccharin and neotame (≈0.72) at approximately 48 hours, whereas, for 10 mM of sucralose and aspartame (≥0.72) at around 60 hours. The sucralose and aspartame at all concentrations gave nearly same level of growth (fig.3.3.3.b,c). In without shake condition, there was no distinguishable differences in the growth curves for the different concentrations, neither for the different AS (fig.B8.2).

These findings suggest that shaking is important for the model bacterial growth in liquid media in the planktonic condition. Also, AS do not have effect on *E. coli* DH5α growth.

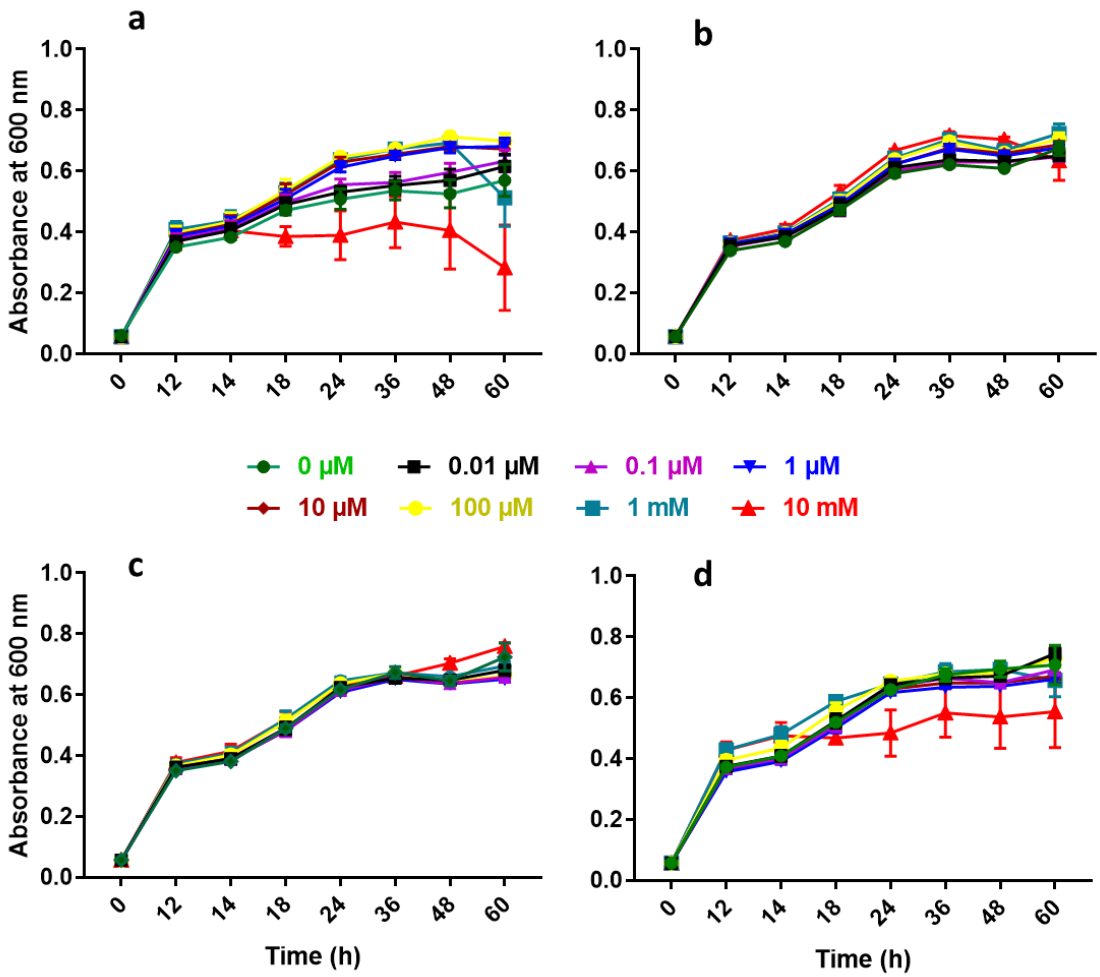

Figure 3.3.3: Effect of artificial sweetener on *E. coli* DH5α growth.

E. coli DH5α was inoculated in 200 µl of 2YT liquid media containing different doses of artificial sweetener saccharin, sucralose, aspartame and neotame and were incubated at 37 °C with and without shaking. Figure demonstrates the effect of a. saccharin, b. sucralose, c. aspartame and d. neotame. Data presented as the mean ± S.E.M., n=3, each with two replications.

3.3.1.4 Effect of sweet taste inhibitor

There was no literature found with indications on the STR in bacteria. $ZnSO_4$ non-specifically inhibits the sweet taste sensing (Keast, 2003), therefore, its effect on model bacterial growth was measured so that it can be used a pan-inhibitor of sweet sensing. $ZnSO_4$ marginally increased *E. coli* DH5α growth up to 24 hours in shaking condition, except for the highest concentration (10 mM) (fig.3.3.4). Absorbance reached a peak at 60 hour and showed a concentration-dependent response in growth; (absorbance 0.57 at 0 dose, 0.60 at 1 µM, 0.62 at 10 µM, 0.64 at 50 µM, 0.66 at 100 µM, 0.67 at 500 µM and 0.69 at 1 mM) for the shaking condition (fig.3.3.4). An almost similar response was observed in the without shaking condition, except for the 10 mM concentration (fig.B8.3).

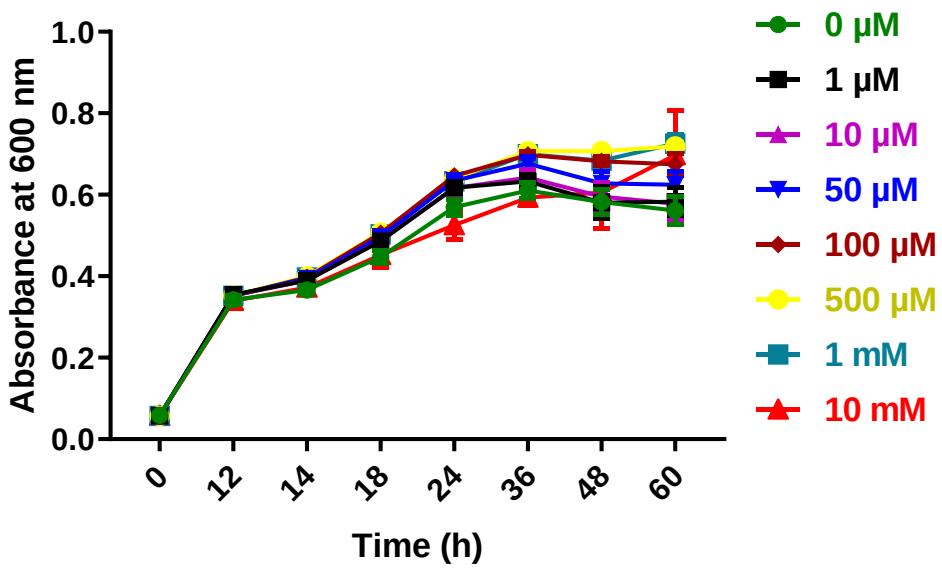

Figure 3.3.4: Effect of $ZnSO_4$ on bacterial growth.

E. coli DH5α was inoculated in 200 µl of 2YT liquid media containing different concentrations of $ZnSO_4$ and was incubated at 37 °C with and without shaking. Data are presented as the mean ± S.E.M., n=3, each with two replications.

Taken together, the above findings on the model bacteria, *E. coli* DH5α, show that 1:500 base culture concentration is appropriate inoculum and growing bacteria with shaking is better option (fig.3.3.1). Also, the natural carbohydrates, AS and the sweet taste inhibitor do not have effect on the model bacterial growth at physiologically achievable concentrations. Glucose and fructose but not sucrose have an initial inhibition on growth at concentrations ≥2 mM (fig.3.3.2). In addition, saccharin and neotame reduce model bacterial growth at 10 mM (fig.3.3.3). Besides, *E. coli* DH5α is a non-pathogenic laboratory strain (Chart et al., 2000), therefore, this model bacteria was used to determine the culture conditions only, the further studies on the changes in the pathogenic potential was performed on the MGB.

3.3.2 Determination of the model gut bacterial growth

3.3.2.1 Establishing protocols

3.3.2.1.1 Growth of *E. coli* NCTC 10418 in different liquid media

E. coli was grown in several broths to determine the appropriate media for the study, and NB was selected. Table-B8.3 (appendix B) represent the growth of *E. coli* (OD600) in different liquid media at 24 hours. The bacteria showed growth in all the liquid media and growth in NB was in the mid-level (OD600, 1.5).

To first assess the correct conditions, the MGB *E. coli* and *E. faecalis*, were grown in NB and BHI medium, respectively for 12 to 96 hours at 37 ˚C with shaking (150 rpm) and the growth was measured as absorbance at 600 nm. These growth curves (fig.3.3.5) also demonstrate the difference in measurement for the two machines.

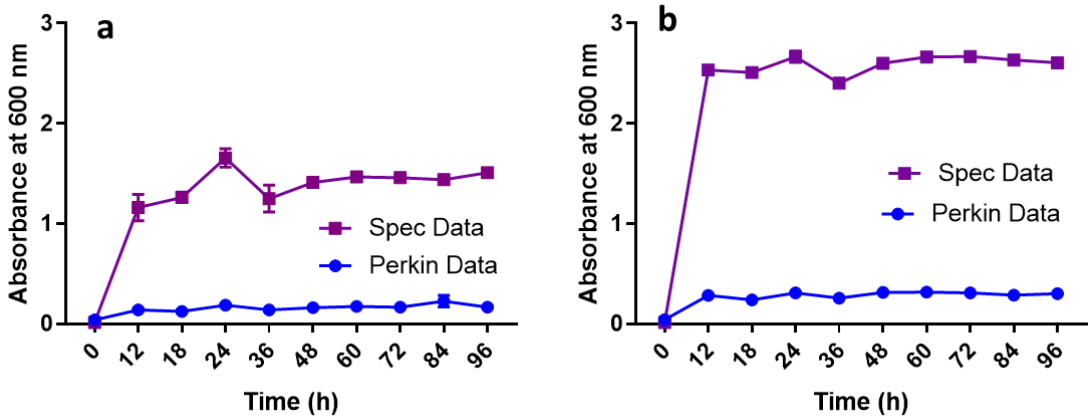

Figure 3.3.5: Growth curve of *E. coli* NCTC 10418 (a) and *E. faecalis* ATCC 19433 (b).

A single bacterial colony was inoculated into 10 ml of the Nutrient broth and Brain Heart infusion liquid media, respectively, and incubated at 37 ˚C with shaking at 150 rpm for four days. 1 ml of the sample was taken into cuvette and optical density (OD600) was measured against appropriate blank using spectrophotometer (EppendorfBioPhotometer). On the other side, 100 µl of the same sample was taken into 96-well plate and absorbance was measured at 600 nm using PerkinElmer (Victor X3). Growth was recorded at different time points and represent the difference of reads between spectrophotometers used. Data are presented as the mean ± S.E.M., n=4 (a), 3 (b).

3.3.2.1.2 Determination of the absorbance to CFU

To determine the number of bacteria in culture, a serial dilution of the base culture was performed, and the standard plate count method was used. The model gut bacterial absorbance and the number of CFU at 24-hour growth was presented in table-3.3.1. *E. faecalis* showed higher absorbance than *E. coli*, however, both MGB demonstrated absorbance-dependent increase in CFU/ml. Therefore, overnight culture of the MGB represented average growth of 10^{10} CFU/ml (OD600, 1.587) for the *E. coli* and 10^{12} CFU/ml (OD600, 2.169) for the *E. faecalis*.

Table 3.3.1: Absorbance related CFU of model bacteria.

Optical density of the overnight bacterial culture was measured using spectrophotometry (EppendorfBioPhotometer) and the standard plate count method was used to assess the CFU/ml.

Bacteria	***OD600 (Spectrophotometry)**	**#CFU (per ml)**
E. coli NCTC 10418	1.502	5×10^{10}
	1.589	2.8×10^{10}
	1.599	6.2×10^{10}
	1.656	6.4×10^{11}
E. faecalis ATCC 19433	1.496	1×10^{12}
	2.134	3×10^{12}
	2.382	3.6×10^{12}
	2.664	4.7×10^{12}

*OD600 = optical density at 600 nm, #CFU = colony-forming units

In addition, CFU was measured for a range of absorbance (A_{600}) following McFarland standards to determine the bacterial concentration in each suspension (table-3.3.2). *E. faecalis* showed higher absorbance and CFU number than *E. coli*.

Table 3.3.2: Absorbance to CFU of the model gut bacteria following the McFarland standards.

Overnight bacterial culture was diluted (according to table-B8.2) and absorbance at 600 nm was measured using spectrophotometry (PerkinElmer, Victor X3). The standard plate count method was used to assess the number of CFU/ml of the corresponding bacterial suspension and absorbance index was prepared.

E. faecalis ATCC19433		*E. coli* NCTC10418	
*A_{600}	#**CFU**	**A_{600}**	**CFU**
0.539	2.48×10^{12}	0.292	2.9×10^{12}
0.507	1.65×10^{12}	0.275	1.8×10^{12}
0.467	1.37×10^{12}	0.266	1.44×10^{12}
0.438	9.2×10^{11}	0.249	1.25×10^{12}
0.401	8.8×10^{11}	0.228	1.46×10^{11}
0.380	5.7×10^{11}	0.197	4.7×10^{10}
0.316	3.4×10^{11}	0.168	1.85×10^{10}
0.272	3.5×10^{10}	0.152	1.45×10^{10}
0.240	2.8×10^{9}	0.142	1.38×10^{10}

* Absorbance at 600 nm ** Colony Forming Unit.

3.3.2.2 The effect of AS on model gut bacterial growth

The effect of AS on the MGB (*E. coli* and *E. faecalis*) growth was measured as A_{600}. Growth in planktonic culture was measured every 12-hour after exposure to a range of concentrations of saccharin, sucralose, aspartame and neotame for 4 days.

3.3.2.2.1 Effect of AS on *E. coli* NCTC 10418 growth

None of the four AS affected *E. coli* growth at any of the tested concentrations and duration in comparison to control (fig.3.3.6). Only 1 mM saccharin inhibited *E. coli* growth until 18 hours, after which it started to grow in the same manner as the vehicle (fig.3.3.6.a). There is a marginal increase in growth at 1 mM of sucralose from 36 to 84 hour in comparison to the control (fig.3.3.6.b), while a slight decrease was observed for neotame 1 mM (fig.3.3.6.d), however, the changes are not significant.

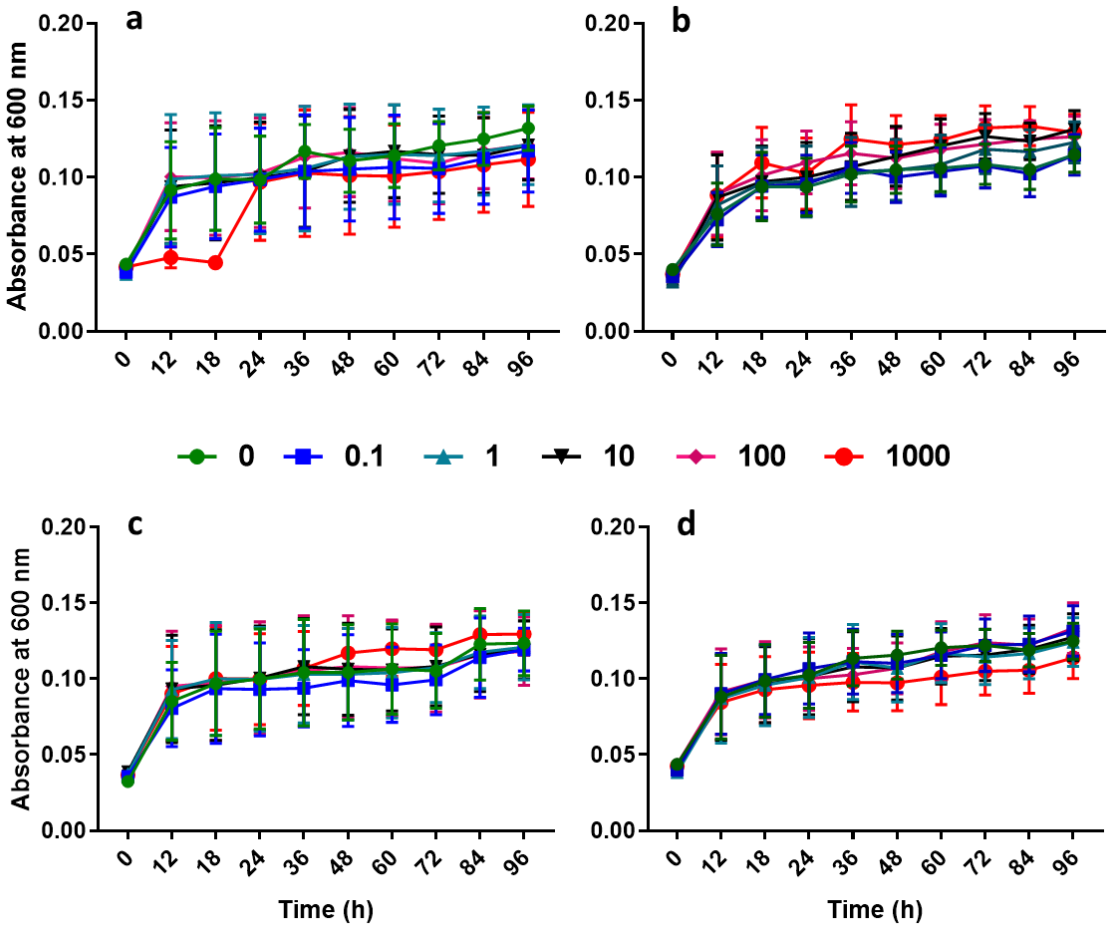

Figure 3.3.6: Effect of artificial sweeteners on *E. coli* NCTC 10418 growth.

A single colony was inoculated into liquid media and was incubated for 12 to 96 hours at 37 °C with shaking at 150 rpm. Growth was measured as absorbance at 600 nm using PerkinElmer (Victor X3) at 12-hour intervals. Graphs represent effect of different concentrations (μM) of AS saccharin (a), sucralose (b), aspartame (c), and neotame (d). Data are presented as the mean ± S.E.M., n=3-5.

3.3.2.2.2 Effect of AS on *E. faecalis* ATCC 19433 growth

The AS did not exert any significant effect compared to control on *E. faecalis* growth at the given concentrations and the duration of exposure (fig.3.3.7). Sucralose and neotame showed a marginal increase at all the concentrations (fig.3.3.7.b and fig.3.3.7.d, respectively). Saccharin demonstrated a low inhibition at 1 mM (fig.3.3.7.a), while aspartame did not (fig.3.3.7.c).

Therefore, the AS have no significant effect at any concentration on the MGB, *E. coli* and *E. faecalis*, growth.

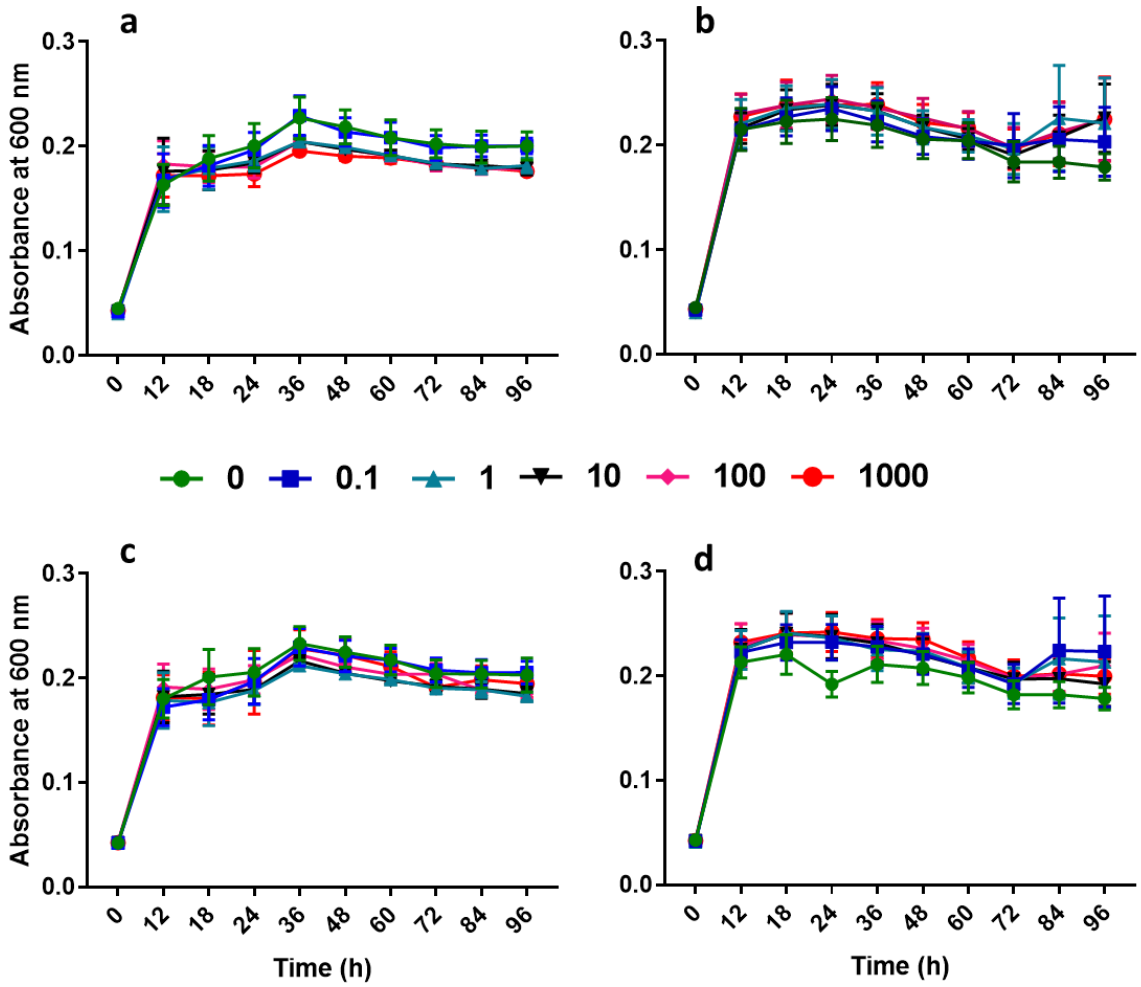

Figure 3.3.7: Effect of artificial sweeteners on *E. faecalis* ATCC 19433 growth.

A single colony was inoculated into liquid Brain Heart infusion media and was incubated for 12 to 96 hours at 37 °C with shaking at 150 rpm. Samples were read at 12-hour intervals using PerkinElmer (Victor X3). Graphs represent effect of different concentrations (μM) of AS saccharin (a), sucralose (b), aspartame (c), and neotame (d) on *E. faecalis* growth. Data are presented as the mean ± S.E.M., n=3-5.

There was no significant change in bacterial growth for *E. coli* (fig.3.3.8.a) or *E. faecalis* (fig.3.3.8.b) after AS (100 μM) exposure for 24 hours. Likewise, sweet taste inhibitor, $ZnSO_4$ and natural sugar, sucrose (73 mM), had no significant effect on the MGB growth.

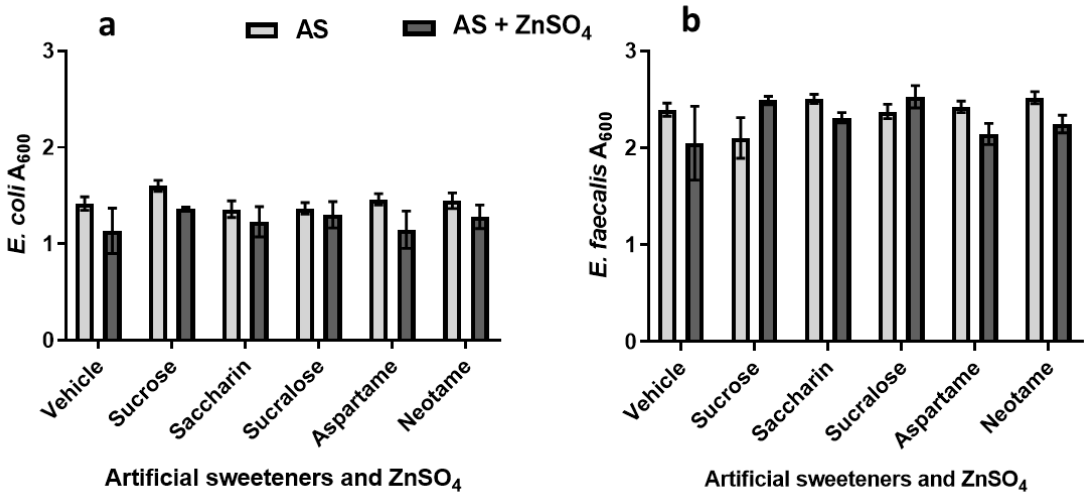

Figure 3.3.8: The effect of artificial sweeteners on model gut bacterial growth.

Bacteria were exposed to 100 µM of AS saccharin, sucralose, aspartame and neotame or vehicle with/out $ZnSO_4$ and growth was measured as optical density at 600 nm at 24 hours. a) represents *E. coli* and b) represents *E. faecalis* growth curve. Data were analyzed using Dunn's multiple comparisons test and are presented as the mean ± S.E.M., n=8.

3.3.3 AS enhanced bacterial biofilm formation

The *in vitro* biofilm assay was performed to evaluate the influence of AS on the ability of MGB to form a biofilm on polystyrene plates in planktonic culture condition. Absorbance was measured for biofilm quantification after dissolution of biofilm-bound CV stain. Two model gut organisms were tested for AS with/out $ZnSO_4$. Sucrose was used as a test substance to compare the effect of AS with natural carbohydrate.

E. coli exposed to sucrose formed a biofilm at RT; short-term exposure (pre-exposure for 24 h) caused 144% biofilm formation in comparison with vehicle while continuous exposure caused 630% (fig.3.3.9.a,c). However, no biofilm formation was recorded for either case when incubated at 37 ˚C (fig.3.3.9.b,d). Saccharin caused significant biofilm formation only when *E. coli* was continuously exposed at 37 ˚C (fig.3.3.9.d). On the other hand, sucralose caused *E. coli* biofilm formation at 37 ˚C for both the pre- and continuous exposure (fig.3.3.9.b,d), however, continuous sucralose exposure but not pre-exposure caused significant *E. coli* biofilm formation (360%) at RT (fig.3.3.9.a,c). Oppositely, aspartame exposure enhanced *E. coli* biofilm formation for all the given conditions, except for the pre-exposure and at 37 ˚C (139%). Exposing *E. coli* to neotame for overnight or continuously and irrespective of the temperatures showed significant biofilm development (fig.3.3.9). Overall, *E. coli* showed higher biofilm percentage at RT than 37 ˚C, except for saccharin.

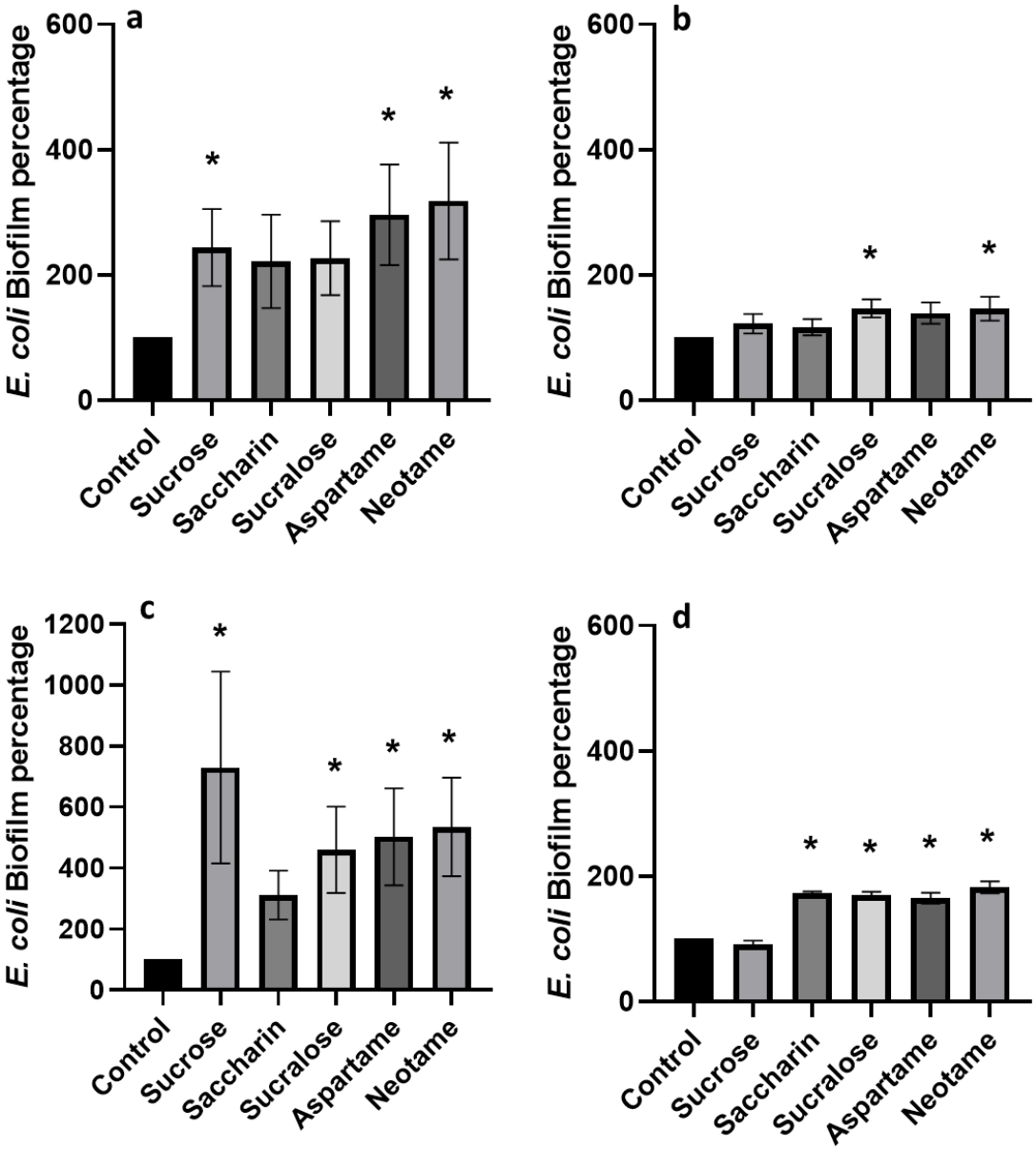

Figure 3.3.9: Effect of AS on *E. coli* biofilm formation.

Bacteria exposed to AS for 24 hours and the culture was diluted (1:200) and sub-cultured in nutrient broth supplemented with (c,d) or without (a,b) AS. Biofilms were grown on polystyrene plates for 48 hours incubating at different environmental condition, either at RT (a,c) or 37 °C (b,d). Retained crystal violet absorbance was measured at 600 nm using PerkinElmer (Victor X3). Data were analysed using one-way ANOVA with uncorrected Dunn's test and presented as the mean ± S.E.M., n= 3-5. *p<0.05 versus vehicle.

Analysing *E. faecalis* biofilm properties showed no effect of the AS on biofilm development for short-term or continuous exposure at the tested temperatures, other than a marginal increase (43%) in continuous aspartame exposure at 37 ˚C (fig.3.3.10). Effect of sucrose on *E. faecalis* biofilm formation varied largely depending on exposure duration and incubation temperature. Significant biofilm was observed at RT; short-term exposure

showed an increase of 276% (fig.3.3.10.a), whereas 141% higher biofilm formation than control was recorded for continuous exposure (fig.3.3.10.c). On the other hand, incubation at 37 ˚C decreased biofilm formation by 42% than control for the continuous exposure (sucrose-containing) (fig.3.3.10.d) while remaining almost unchanged for the pre-exposure (fig.3.3.10.b).

Taken together, these studies represent that AS-exposure duration and temperature influence the model gut bacterial biofilm formation ability *in vitro*. *E. coli* is more capable to form biofilm because of AS-exposure than the other MGB, *E. faecalis*.

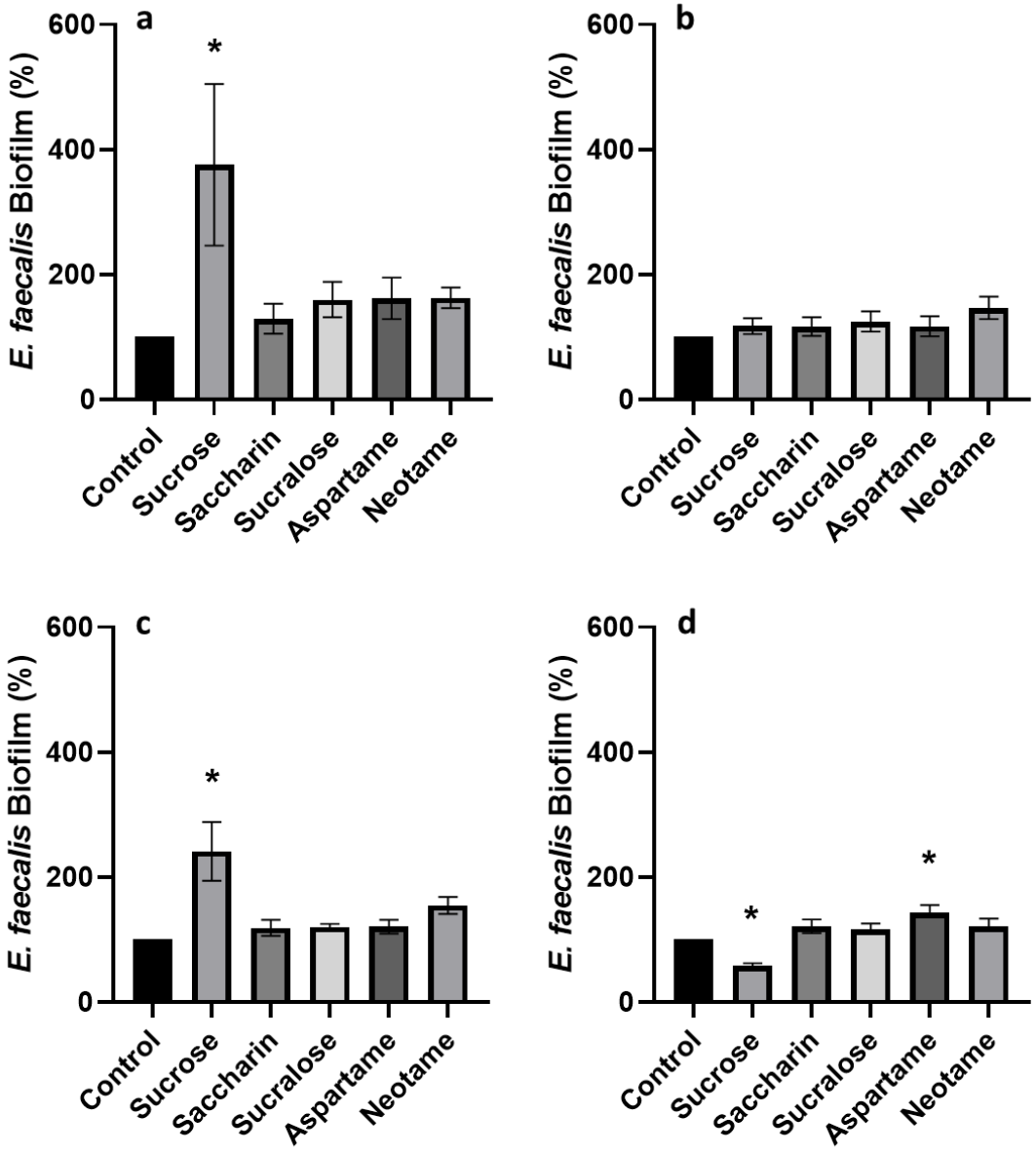

Figure 3.3.10: Quantification of biofilm development by *E. faecalis* after AS exposure.

AS-exposed *E. faecalis* overnight culture was diluted (1:200), sub-cultured in BHI with/out AS and incubated at RT or 37 °C. Biofilm assay was performed at 48 hours and retained crystal violet absorbance was measured at 600 nm using PerkinElmer (Victor X3). Panel a and b shows pre-exposure data at RT and 37 ˚C, respectively and panel c and d, represents the continuous exposure data at RT and 37 ˚C, respectively. Data are analysed using Ordinary one-way ANOVA with Dunnett's multiple comparison test and presented as the mean ± S.E.M., n=3-5. *p<0.05 versus vehicle.

All the four AS significantly increased *E. coli* biofilm formation (fig.3.3.11.a) when exposed to the sweeteners continuously at 37 ˚C. Conversely, only aspartame significantly increased *E. faecalis* biofilm formation (fig.3.3.11.b). $ZnSO_4$ reduced the biofilm percentage for all AS

to *E. coli*, however, aspartame and neotame effect remained significant. $ZnSO_4$ did not show any effect on *E. faecalis* biofilm formation.

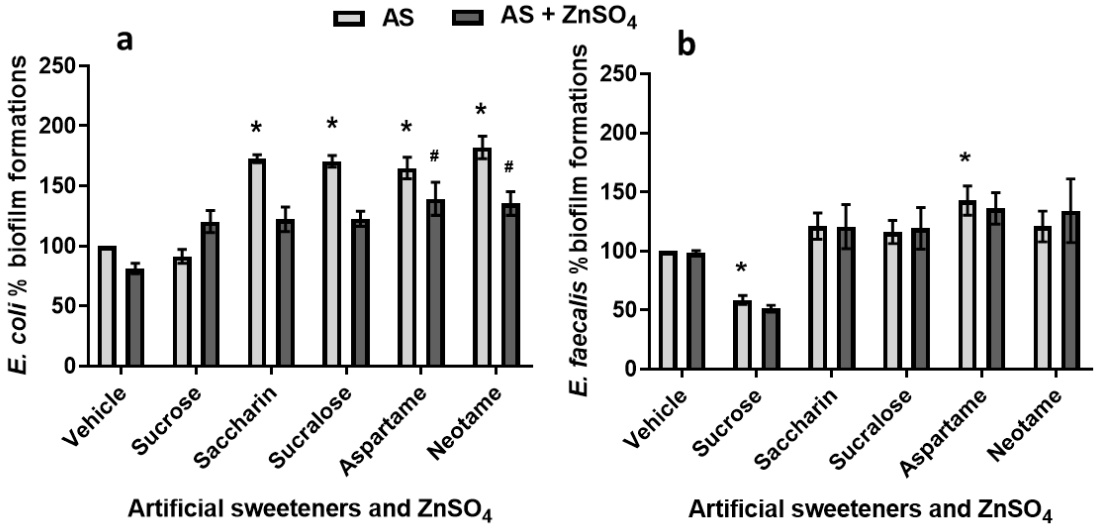

Figure 3.3.11: Effect of AS and $ZnSO_4$ on a) *E. coli* and b) *E. faecalis* biofilm formation.

Bacteria were treated with 100 µM of sucrose or AS or AS+$ZnSO_4$ or vehicle for 24 hours, 200 µl of fresh media with same treatments were aliquot with 1/200 of overnight bacterial culture on 96-well plate and incubated at 37 °C for 48 hours. The biofilm assay was performed using crystal violet (CV) staining and absorbance at 600 nm was measured. The biofilm formation was calculated by dividing the absorbance of retained CV with the absorbance of the total bacterial growth. Data are normalized with control as 100%, analysed using ordinary one-way ANOVA with Holm-Sidak multiple comparison test and presented as the mean ± S.E.M., n=5. *p<0.05 versus vehicle, 0 µM/ml AS and #p<0.05 versus $ZnSO_4$.

3.3.4 AS did not affect haemolytic activity

The *in vitro* haemolysis assay was performed on blood agar plates to study the effect of AS on haemolytic ability of the two MGB. Exposure to each AS overnight did not affect the haemolysis activity (fig.3.3.12–3.3.15). *E. coli* treated with higher concentrations of saccharin (1 and 10 mM) was observed to produce α-haemolysis compared to the positive control *S. aureus* which produced β-haemolysis on the blood agar plate (fig.3.3.12). Similar concentrations of saccharin also did not affect the MGB, *E. faecalis* haemolytic feature (fig.3.3.13). Treating the MGB with AS (100 µM) or sugar in presence and absence of $ZnSO_4$ did not bring any changes in comparison with the controls, as expected. *E. coli* formed characteristic α-haemolysis and *E. faecalis* showed γ-haemolysis, and none of the treatments affected the outcomes.

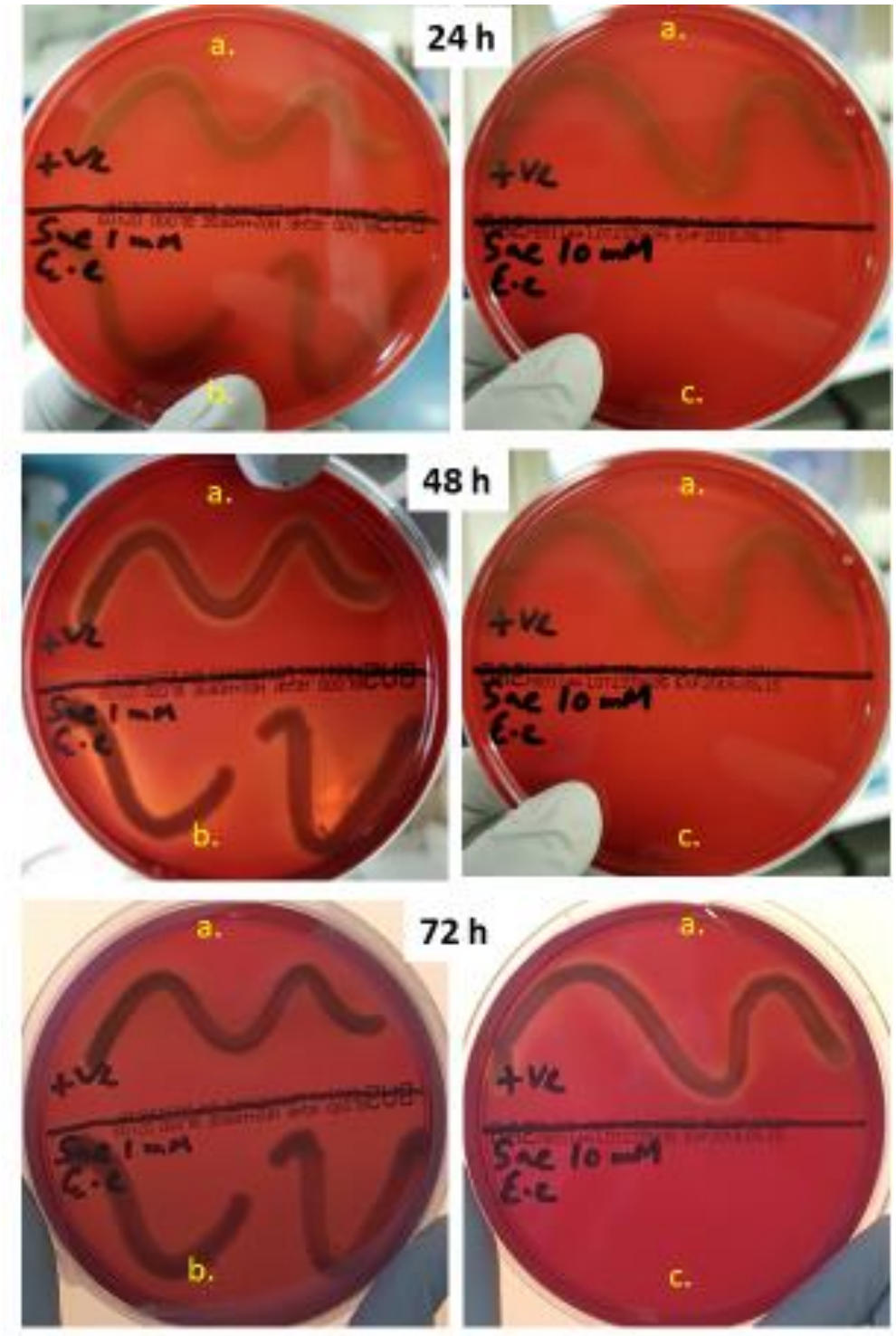

Figure 3.3.12: Effect of 1 and 10 mM of saccharin on haemolysin production of *E. coli*.

Single colony of the bacteria was exposed to 1 mM (b.) and 10 mM (c.) of saccharin for 24 hours and bacterial culture was streaked on blood agar plates using cotton swab. Growth was observed for haemolysis at 24 to 72 hours. *E. coli* produced α-haemolysis whilst the positive control *S. aureus* (a.) produced characteristic β-haemolysis. At 10 mM, *E. coli* growth was inhibited and did not form any colony on blood agar plates.

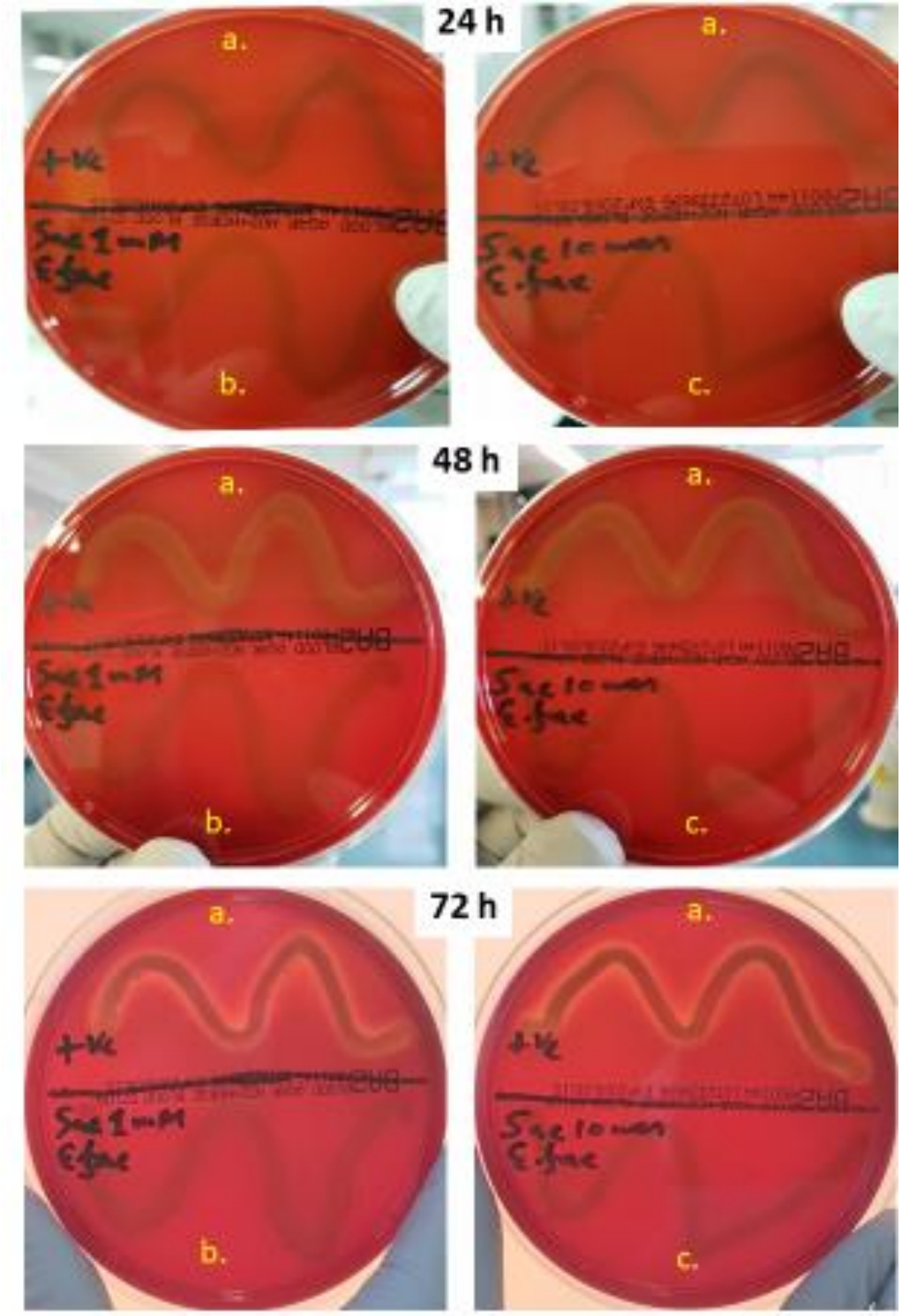

Figure 3.3.13: Effect of saccharin on *E. faecalis* haemolytic property.

E. faecalis was exposed to 1 mM (b.) and 10 mM (c.) of saccharin for 24 hours and bacterial culture was streaked on blood agar plate using cotton swab. Plates were incubated at 37 °C for 24 to 72 hours and were observed every 24 h interval for any clearing of the red blood cells. *E. faecalis* (b. and c.) represented γ-haemolysis whilst the positive control, *S. aureus* (a.) showed β-haemolysis.

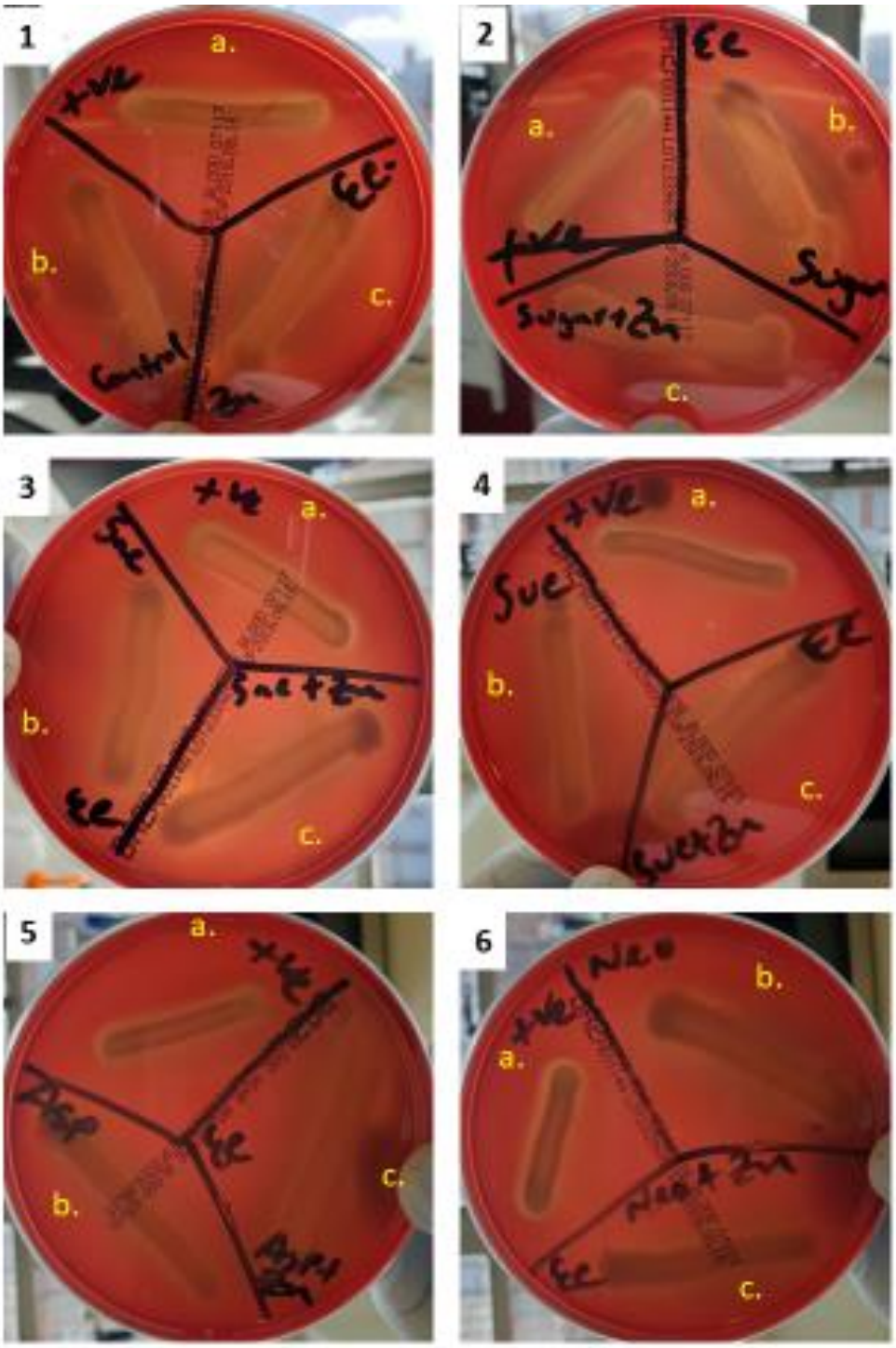

Figure 3.3.14: Effect of AS on *E. coli* haemolysis.

Bacteria were exposed to vehicle (1) or 73 mM of sucrose (2) or 100 µM of saccharin (3) or sucralose (4) or aspartame (5) or neotame (6) in presence or absence of the sweet taste inhibitor, $ZnSO_4$ for 24 hours. A loopful of the overnight culture was streaked on blood agar plate and incubated for 24 to 72 hours. Results from 48-hour incubation were presented. *S. aureus* which represent β-haemolysis was used as positive control. The used strain showed α-haemolysis irrespective of AS- exposure. In each plate, a. represents the positive control, b. represents only treatment effect and c. represents treatment plus $ZnSO_4$ results.

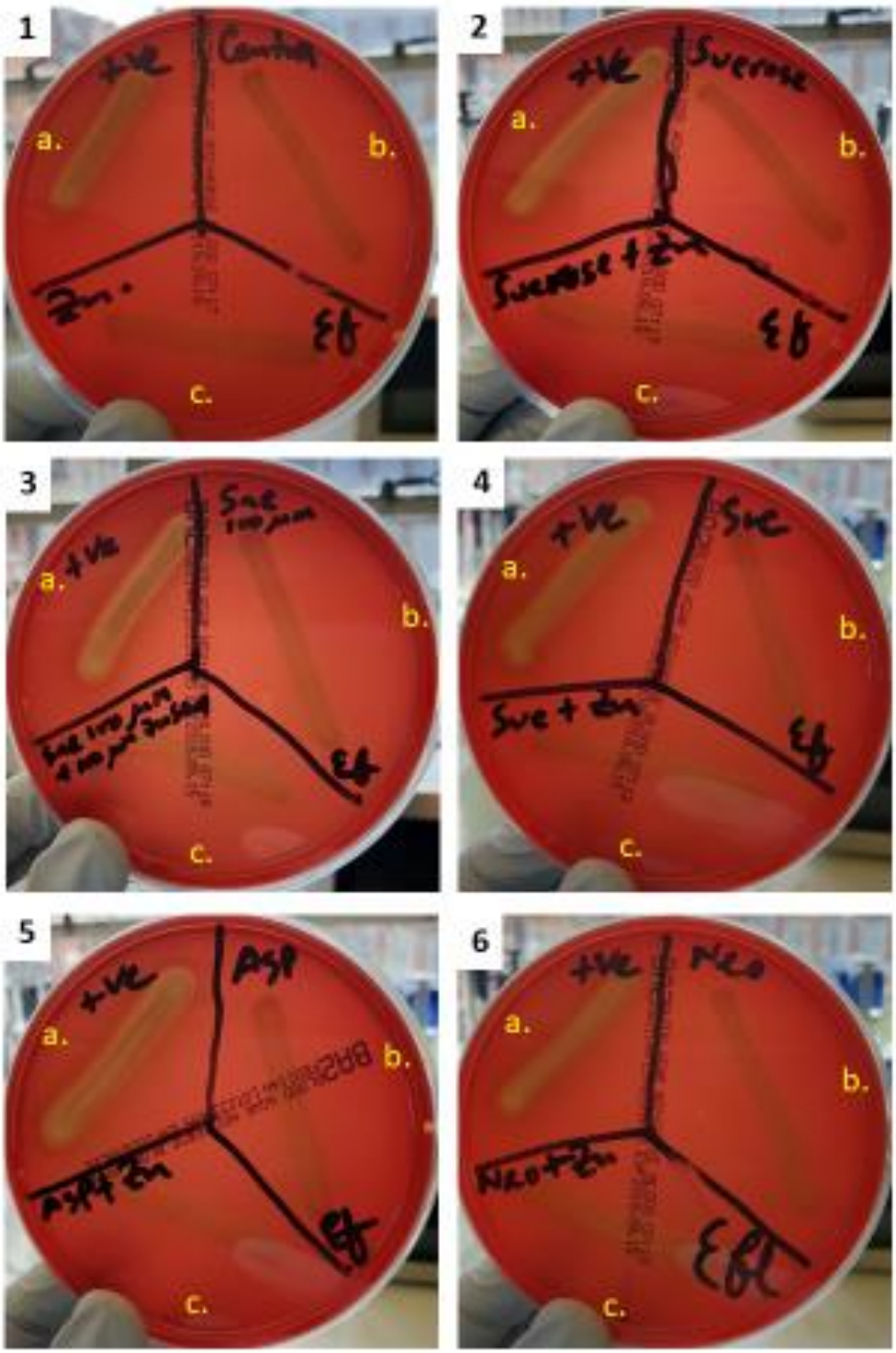

Figure 3.3.15: Effect of AS on *E. faecalis* haemolysis.

A single colony of *E. faecalis* was exposed to vehicle (1) or 73 mM of sucrose (2) or 100 µM of saccharin (3) or sucralose (4) or aspartame (5) or neotame (6) in presence or absence of $ZnSO_4$ for 24 hours. Single dip of cotton swab into the overnight culture was streaked on blood agar plate and incubated for 24 to 72 hours. At the tested concentration of AS, the organism did not show any haemolytic activity for the tested duration. Results from 48-hour incubation were presented. *S. aureus* which represent β-haemolysis was used as positive control. In each panel, a. represents the positive control, b. represents AS or vehicle effect and c. represent treatment plus $ZnSO_4$ results.

3.4 Discussion

The pivotal role of microbiota in host health and wellbeing is gaining increased interest as microflora are now denoted as an ‘organ’ and more studies are being conducted to investigate the alteration of this organ in disease states (Kau et al., 2011). Changes in the composition and function of gut bacteria has been linked to various MD (Cani, 2018). However, AS-mediated metabolic dysfunction remains largely undefined, and therefore this study focused on AS-mediated changes in microbiota elucidating the effect of AS on microbial metabolism and pathogenic factors.

Aim II of the study was to investigate the effect of AS on the metabolism and pathogenicity of two MGB. The role of the GM in food processing and physiological balance is well-established, but whether they modulate STR and transporters to alter food consumption in the host epithelium is not known, and little information is available on the metabolic machinery of GM to process natural sugars and AS (Payne et al., 2012). Swartz *et al*. (2011) reported that absence of GM alters STR expression in the small intestine which has the association with increased intake of nutritive sweet solutions. They investigated the preference of sucrose/saccharin in germ-free and conventional mice and found no difference for saccharin, but germ-free mice consumed 8% more sucrose solution than conventional mice. In another study, 8-week aspartame exposure perturbed the GM in rats resulting in higher fasting glucose level and disturbed insulin tolerance (Palmnäs et al., 2014). Therefore, the gut bacteria are negatively influenced by the sweet molecules, however, the mechanism of microflora perturbation needs further investigations.

Considering that GM consists of trillions of bacteria and other microorganisms (fig.3.1.1) (Lozupone et al., 2012), although dominated by four major phyla (Consortium, 2012), it was difficult to work on large number of bacteria in the study period. Therefore, with consideration of the available laboratory support and purpose of the study, two MGB were taken under consideration. These findings will provide an indication on the effect of AS on gut bacteria, offering a base for further studies. *E. coli* is one of the most common bacteria available in the gut (Koenig et al., 2011), readily changes from commensal to pathogenic state depending on external factors (Tenaillon et al., 2010), and safe to work on, so it was listed. In addition, *E. faecalis* was marked considering its facultative anaerobic nature, it is one of the signature organisms from the healthy microbiome found by metagenomics studies, colonise at the beginning of life (Huycke et al., 1998) and have both commensal and pathogenic state (Consortium 2012). So, the MGB were appropriate representative to conduct the study.

3.4.1 Determination of the culture conditions

In microbiology lab settings, measuring OD is a widely accepted approach to assess bacterial growth (McBirney et al., 2016). OD measurement is relatively simple, faster, reliable and reproducible method (Biesta-Peters et al., 2010). The lag phase is the initial period of slow growth when cells enlarge and synthesize critical proteins and metabolites. Therefore, measuring OD for an extended time period was reasonable to assess the AS-mediated changes in the bacterial population.

In the growth experiment, different dilutions and conditions were used initially to optimise the protocol by growing *E. coli* DH5α (fig.3.3.1). For the growth experiment with natural sweeteners, AS and $ZnSO_4$, 1:500 dilution of the overnight bacterial culture was considered, and absorbance was measured using PerkinElmer (Victor X3). The 1:50 and 1:100 dilutions showed fast lag phase and higher variability in the late exponential slow growing phase and therefore were not considered for the later experiments. The lowest dilution, 1:10000, conversely, represented prolonged lag phase, a fast-exponential phase and then fall quickly after 24- and 48 hours in with and without shake conditions, respectively. So, 1:500 and 1:1000 bacterial concentrations were considered from which 1 in 500 dilution was used for the experiment with sweeteners and $ZnSO_4$.

Identical bacterial number was confirmed by using same absorbance of base culture. As the CFU was calculated for the corresponding absorbance (table-3.3.1) and for a range of absorbance (table-3.3.2), the number of bacteria used can also be calculated. Also, same growth phase was taken for all experiments considering the variation of bacterial cell size of the different physiological state of growth.

The natural carbohydrates showed nearly similar effect on bacterial growth and the results varied a little bit depending on shaking condition (fig.3.3.2), may be because shaking made the nutrients more available to organisms in comparison to without shaking (fig.B8.1). However, the general trend of the graphs showed slightly less growth, absorbance 0.80 and 0.91 for with and without shake (fig.3.3.1), respectively in the 1:500 dilution whereas absorbance was below 0.8 for all the treatments in the later experiments.

Glucose at lower concentrations marginally increased the bacterial growth under shaking from the beginning (fig.3.3.2.a) and for without shaking after 18 hours (fig.B8.1.a). This might be because most of the organisms use glucose as primary energy source although the media do not contain glucose as main carbon source. But the high concentrations of glucose (20 mM and 200 mm) negatively affected cell growth (0.2 a.u.) which demonstrates that very high concentration of glucose has inhibitory effect on *E. coli* DH5α growth. This data agrees with the previous findings of Boyd and Lichstein (1951) who demonstrated that glucose presence in media inhibits bacterial growth; it affects the deaminases either by

preventing the coenzyme formation or by destroying the enzymes. Earlier work of Epps and Gale (1942) also found the negative effect of increased glucose concentration on cell growth. They showed that the formation of several deaminases is somehow inhibited or produced in a very low concentration in presence of glucose. Similarly, Phue *et al*. (2008) showed that *E. coli* DH5α growth and production was much slower when they have used glucose as a carbon source.

Fructose, although is a direct dietary energy source and have a potential downstream effect, but it is one of the most poorly absorbed carbohydrates in human. Malabsorption of fructose in human was reported to be a result of microbial fructose fermentation (Gibson et al., 2007), meaning microbes utilise fructose which was indicated as an inherent genetic propensity of the intestinal microflora (Payne et al., 2012). In the present study, fig.3.3.2 and fig.B8.1.b shows that fructose (up to 200 µM) enhanced bacterial growth both in with/out shake condition and the higher concentrations (2 mM and 20 mM) also started to rise after prolonged incubation period which might be supported by the above-mentioned finding.

Saccharin and sucralose enhanced *E. coli* DH5α growth in a concentration-dependent manner in shaking condition although the difference was very low, and the highest concentration (10 mM) showed an inhibitory effect for saccharin and neotame (fig.3.3.3). Overall growth for all the AS displayed an end of exponential phase after 24 hours with shake although this phase was prolonged for without shake (fig.B8.2). Saccharin metabolism has increased the relative number of intestinal aerobic bacteria in human (Payne et al., 2012), which might support the obtained results. They also demonstrated alteration (aerobic to anaerobic) of the faecal bacteria in male rats fed on 7.5% saccharin for ten days.

Since zinc inhibits the sweet sensing stimulated by diverse sweetener molecules in different organisms (Keast et al., 2004) and also because there was no available literature on bacterial STR, therefore, $ZnSO_4$ was selected to investigate whether it inhibit changes in bacterial metabolism induced by AS. So, the effect of $ZnSO_4$ on *E. coli* DH5α was determined initially. $ZnSO_4$ at high concentration (10 mM) showed an insignificant decrease in the bacterial growth at 24 hours but sharp increase after 48 hours (fig.3.3.4). However, the lower concentrations enhanced bacterial growth at 24 hour for without shaking condition (fig.B8.3). Although $ZnSO_4$ inhibits enteric pathogens at 1.2 – 1.8 mg/ml including *E. coli* (Surjawidjaja et al., 2004) but such inhibition was not observed in the present study. This might be because the used *E. coli* DH5α was not pathogenic and, the bacteria might have adjusted with $ZnSO_4$ after an initial inhibition.

3.4.2 Importance of Bacterial metabolism

The MGB *E. coli* showed growth in all the liquid media (table-3.3.1). NB is a general-purpose medium and *E. coli* does not have exact nutritional requirements. *E. coli* growth in NB was ≈1.5 (OD600), whilst ≥2 in 2YT and Luria-Bertani (LB) (table-B8.3). Both 2YT and LB are nutrient-rich media containing yeast extract and peptone, which facilitates bacterial growth.

The variations among the pH values of medium were statistically insignificant ($p>0.9999$) (appendix B, table-B8.1). Also *E. coli* was shown to grow maintaining similar level of cell number (10^7) for a range of pH between 5.5 and 7.2 (Wilks and Slonczewski, 2007). *E. faecalis*, are also able to grow in range of pH 4.5 to 10 (Fisher and Phillips, 2009). Additionally, the gut bacteria must have the ability to grow between pH 4.5 and 9 in order to colonize in the gastrointestinal tract (De Jonge et al., 2003). The effect of AS was compared to vehicle in the study; therefore, pH did not have influence on the findings.

Bacterial growth in the respective liquid media showed different readings for the two spectrophotometers used. Readings of the same sample from the PerkinElmer were lower than the cuvette photometer (fig.3.3.5). This difference might be due to the sample size taken for the measurement (PerkinElmer, 100 µl/ Cuvette photometer, 1 ml), or other technical matters related to measurement process. However, the growth curves generated using data from both spectrophotometers showed the same trend for both MGB. Also, the effect of treatments was counted as the relative changes with control, therefore, the absorbance readings from both spectrophotometers are appropriate. Moreover, the CFU counts of the overnight culture (table-3.3.1) represent the bacterial concentration in the corresponding samples.

Furthermore, the absorbance to CFU count following McFarland standards provide a reference for bacterial concentrations (table-3.3.2). It represents the probable number of bacteria in a range of absorbance. Although the McFarland standards was not exactly maintained, however, the absorbance to CFU standardization provides information on the approximate number of bacteria in the further experiments. Nonetheless, the McFarland standards have frequent use in the antimicrobial studies (Lahuerta Zamora and Pérez-Gracia, 2012). Also, the outcomes vary for conditions such as bacterial strains, growth medium, physical parameters including the absorbance reader (Lahuerta Zamora and Pérez-Gracia, 2012). The growth medium and physical conditions in the study was consistent for all experiments. Therefore, the absorbance to CFU data were appropriate and the approximate number of CFU/ml can be estimated from the absorbance measurements (table-3.3.2).

Once conditions were optimised, effect of AS on model gut bacterial growth and virulence factors was investigated *in vitro*. Using bacteria individually provided less-complex and more-tractable models to study the effect of AS on bacterial metabolism.

The tested sweeteners and inhibitor did not affect growth of the MGB (fig.3.3.8), although there was minor insignificant increase of *E. coli* growth (fig.3.3.6.a) for saccharin and neotame. Similar response was observed in *E. faecalis* growth (fig.3.3.7). The relative number of intestinal aerobic bacteria in human was reported to increase due to saccharin metabolism (Payne et al., 2012). Saccharin and neotame at 1 mM slightly reduced *E. coli* growth (fig.3.3.6), almost no change was observed for same concentration of saccharin on *E. faecalis* growth although 10 mM of neotame slightly increased growth (fig.3.3.8). At high concentration of 10 mM, saccharin and neotame also reduced *E. coli* DH5α growth (fig.3.3.3.a,d). There were two phases in some of the growth curves (fig.3.3.2, fig.3.3.7), showing an initial exponential phase and plateau, then a second exponential phase and plateau. This might be due to the bacteria using an easy-to-access carbon source first, which then runs out, and they must switch to a less accessible carbon source.
Saccharin consumption was demonstrated to alter (aerobic to anaerobic) the faecal bacteria in male rats fed on 7.5% saccharin for ten days. Although intestinal colon region should be densely colonized by obligate anaerobic bacteria, but these rats due to saccharin exposure represented a reduction in the number of anaerobic faecal bacteria whilst an increase in the aerobic bacteria (Anderson and Kirkland, 1980). Sucralose did not affect the MGB growth (fig.3.3.6, fig.3.3.7, fig.3.3.8), although 1.1% sucralose was demonstrated to impair rat gut bacterial growth (Abou-Donia et al., 2008). In the 12-week study, they found sucralose to suppress (≥70%) beneficial anaerobes such as Bifidobacteria, lactobacilli, and Bacteroides, whilst less inhibition on the harmful strains like enterobacteria. In contrast, 15 mg/kg BW sucralose intake (8-weeks) brought no change in the relative amounts of total faecal bacteria in male and female mice, although sucralose exposure decreased the relative amount of *Clostridium cluster XIVa* in a dose-dependent manner (Uebanso et al., 2017).

In the study, AS was supplemented in the growth medium, so the organisms have all the required nutrients for growth. In diet, AS are used as sucrose substitute which is the source of energy. Similarly, substituting bacterial carbohydrate source with AS might give different metabolic outcomes. Young and Bowen (1990) substituted glucose with sucralose in agar medium and observed complete growth inhibition of ten oral bacterial strains. Opposite results were demonstrated where sucralose induced but saccharin inhibited growth in gut bacterial model, *E. coli* TV1061 (Harpaz et al., 2018). However, similar to the current study, Harpaz *et al.* (2018) did not replace the carbon source, therefore similar bias remains.
Wang *et al*., (2018) also used *E. coli* as a gut bacteria model, and investigated the effect of saccharin, sucralose and acesulfame K on growth. *E. coli* HB101 was grown in LB liquid

and solid media supplemented with the above-mentioned sweeteners and significant reduction in growth was observed. Sucralose in 1.25% and 2.5% reduced growth by 17% and 66%, respectively in liquid culture whilst 22% and 66% in plates. These findings partially support the present study as *E. coli* DH5α growth was reduced after exposure to 10 mM of saccharin (fig.3.3.3.a). Also, overnight culture of *E. coli* to 10 mM of saccharin did not grow on Blood agar plates representing complete growth inhibition (fig.3.3.12). Bacteriostatic effect of AS might be employed through suppression of metabolic enzymes or by inhibiting nutrient transportation or by limiting the other processes essential for bacterial growth (Wang et al., 2018; Anderson and Kirkland, 1980). However, this is not clear in the present study and further studies are needed to answer this properly. Sucrose did not affect *E. coli* growth, however, slightly reduced *E. faecalis* growth 0.4 (a.u.) (fig.3.3.8). Whilst there are not many studies in the literature dedicated on AS and bacterial growth, studies with other food substances show that diet does not impact on bacteria growth. The findings in the present study is therefore not surprising.

Zinc is an essential micronutrient at low concentrations but has antibacterial potential at high concentrations (Medeiros et al., 2013). $ZnSO_4$ have inhibitory effect on the enteric bacterial growth (Faiz et al., 2011), however, the growth curve represents that the given concentrations of the $ZnSO_4$ had no effect on MGB growth (fig.3.3.8). In combination with the AS, 0.1 mM of $ZnSO_4$ slightly reduced bacterial growth except sucrose (73 mM) and sucralose (0.1 mM) for *E. faecalis* (fig.3.3.8.b). Zinc may have some effect in these two cases of growth enhancement whilst slight reduction for all other cases, however, none of these effects are significant on bacterial growth.

ZnO was reported to partially inhibit enteroaggregative *E. coli* growth at 0.1 mM, whereas complete growth inhibition was recorded at 1 mM and 10 mM (Medeiros et al., 2013). They have mentioned similar observations for zinc acetate and $ZnSO_4$ and suggested that to inhibit the human disease-associated *E. coli* strain 042, appropriate physiological concentration of ZnO is ≤0.05 mM. *E. coli* DH5α did not show growth inhibition at 1 mM and 10 mM in the present study (fig.3.3.4). Also, their findings do not match with the results for the MGB, their growth was not inhibited at 0.1 mM concentration of the $ZnSO_4$ (fig.3.3.8).

3.4.3 Pathogenic factor – biofilm formation

Competitive survival and growth of bacteria depends on their ability of adaptation in a densely populated environment or in limited nutrient diffusion condition. Biofilm formation starts with bacterial transition from planktonic lifestyle to firmly attached state on biotic or abiotic supports. This decision depends on many factors including genetics, nutritional availability and environmental factors (Mohamed and Huang, 2007; Reisner et al., 2006;

O'Toole and Kolter, 1998). Depending on the surroundings, bacteria communicate through biochemical signalling called quorum sensing.

Considering the closeness of bacteria to molecules that can diffuse into the biofilm only limitedly indicates that quorum sensing may have crucial role in biofilm development. Cotter and Stibitz (2007) identified a small-molecule signalling system that control the conversion of *P. aeruginosa* from planktonic to biofilm growth. Bis-(3'-5')–cyclic dimeric guanosine monophosphate, an intracellular second messenger, is the basis of this signalling mechanism. Quorum sensing was mentioned to have positive influence on biofilm formation with specific findings in *P. aeruginosa* and some other bacteria (Sifri, 2008). In a study on chronic bacterial infection, Hentzer and Givskov (2003) showed that molecules that have negative effect on bacterial quorum sensing also hinder biofilm formation in *P. aeruginosa*. However, quorum sensing does not have any influence on biofilm development by staphylococci (Vuong et al., 2003).

Measuring the retained CV absorbance to quantify the biofilm-formation of the tested bacteria ensured the identical condition for all the wells. CV biofilm assay is biofilm biomass assay based on matrix staining (fig.3.2.2). This is an indirect biofilm quantification method that counts both living and dead cells. However, normalisation of the data with corresponding control removed any possibility of errors in the results. Also, the blank well absorbance was deducted from all the samples to guarantee the absorbance only for the retained CV by biofilms. Besides, the use of ddH_2O in the side wells of the wells under consideration removed the possibility of drying or evaporation from the wells in the edge.

As discussed earlier, diet influence the characteristics of microbiome (fig.3.1.3). Maltodextrin, a polysaccharide derived from starch hydrolysis, was demonstrated to enhance biofilm formation of *E. coli* associated with Crohn's disease (Nickerson and McDonald, 2012). Commercially available aspartame and sucralose, containing maltodextrin as a bulking agent, significantly increased the *E. coli* biofilm formation in comparison with the glucose supplemented medium in their experiment. But when maltodextrin was removed, only aspartame and sucralose did not enhance biofilm formation, neither increased the level of biofilm when added to only maltodextrin ones. These do not agree with the current study as the *E. coli* biofilm development was increased after exposure to the sweeteners (fig.3.3.9). However, the models differ from the Crohn's disease-associated strain and therefore may behaved differently.

Besides, sucrose was found to significantly enhance biofilm development in *E. coli* when incubated at RT but not 37 °C in the present study (fig.3.3.9). Nickerson and McDonald (2012) demonstrated no effect of sucrose on biofilm development of the *E. coli* strain. In addition to the variation in source of organism, they have incubated the bacteria in M9 medium at 30 °C for 24 hours for biofilm formation which might influenced the findings.

Regular consumption of AS-containing foods indicates a continuous exposure. Besides, the gut physiological temperature is approximately 37 ˚C, and previous studies showed that *E. coli* strains isolated from the gut expresses most of their virulence factors at 37 ˚C that are needed indeed for colonization (reviewed by Rossi et al., 2018). In addition, findings from the initial biofilm formation (fig.3.3.9, fig.3.3.10) represent continuous AS-exposure (37 ˚C) as the appropriate conditions. Therefore, the further studies with AS and $ZnSO_4$ were conducted under those conditions.

Although *E. coli* growth was unchanged, biofilm formation was significantly increased for AS exposure (fig.3.3.9) and addition of $ZnSO_4$ reduced the effect for all AS (fig.3.3.11.a). Sucrose did not affect *E. coli* biofilm formation at 37 °C and $ZnSO_4$ merely increased (10%) the biofilm (fig.3.3.11.a). Instead, sucrose reduced *E. faecalis* biofilm formation about 50% and $ZnSO_4$ had no effect (fig.3.3.11.b). AS exposure did not increase *E. faecalis* biofilm formation except aspartame, and $ZnSO_4$ reduced the effect (fig.3.3.11.b). Similar findings were demonstrated in enteroaggregative *E. coli* where bacterial growth was not affected by ≤0.05 mM of ZnO, however, biofilm formation was significantly reduced (Medeiros et al., 2013).

Oppositely, *E. faecalis* biofilm formation index was reported to be just double than *E. coli* in a mixed-microbial populations study, although they did not develop any biofilm when cultured together (Teh et al., 2010). They have maintained 20 different strains in Mueller-Hinton broth and screened their biofilm formation capacity in individual and combination culture. Considering the biofilm formation index, *E. faecalis* was indicated as one of the organisms having strong biofilm forming ability whereas *E. coli* was the opposite (Teh et al., 2010). These findings are different from the present study as the *E. coli* was found to develop biofilm significantly at 37 °C with continuous exposure to the AS (fig.3.3.9) while *E. faecalis* did not (fig.3.3.10). Besides, combination culture was not performed as this study aimed to investigate individual bacterial response to AS.

E. faecalis forms biofilm more frequently than other enterococci. However, this pathogenesis depends on genetic material as well as environmental factors (Mohamed and Huang, 2007). The culture media plays an immense role for the biofilm formation. For example, *E. faecalis* was exposed to different media; while the biofilm formation was inhibited due to media osmolarity, the growth of the bacteria remained unaffected (Kristich et al., 2004). In the present study, BHI was used for *E. faecalis* growth, and no significant biofilm formation agrees with the findings of Kristich *et al*. (2004), where they demonstrated that this media abruptly stops the biofilm growth of *E. faecalis* after 4 hours and further incubation decreases the density of the emerged biofilm.

3.4.4 Pathogenic factor – Haemolysing red blood cells

The model bacteria, *E. coli* and *E. faecalis* are α- and γ-haemolytic, respectively in normal condition, however, they can turn into β-haemolytic when pathogenic (Giaffer et al., 1992; Shankar et al., 2002). The haemolysis assay was performed to check whether AS exposure impact haemolysin production. The MGB did not show haemolytic activity upon exposure to AS (100 µM) for 24 hours.

Pathogenic *E. faecalis* from clinical samples were found to be β-haemolytic (Shankar et al., 2002). Also, *E. faecalis* from foods can have haemolytic property; 52.5% of the food samples showed Enterococci contamination and *E. faecalis* was the second highest contributor (38.7%) with β-haemolysis (Gomes et al., 2008). As a dietary component, AS might have influence on bacterial conversion form non-haemolytic to haemolytic state. The model *E. faecalis* was not haemolytic in the study conditions, however, since it is able to incorporate external genes (Toledo-Arana et al., 2001), it may behave differently in a co-culture condition like gut environment.

E. coli showed α-haemolysis with no changes for $ZnSO_4$ co-exposure (fig.3.3.14), however, visual observation was made only. Further investigations are needed to assess whether this haemolysis is caused by α-, EHEC- or ClyA- haemolysin, and to characterise the haemolysin protein. Besides, sucrose was non-protective to ClyA-mediated haemolysis in *E. coli* DH5α (Ludwig et al., 1999), which supports the present findings and also indicates a similarity in behaviour of tested AS, however, use of osmotic protectants like dextran 8 could clarify this further (Ludwig et al., 1999). In addition, *E. coli* strains isolated from patients suffering from MD like IBD, Crohn's disease and ulcerative colitis, irrespective of disease activity, were found to be haemolytic (Giaffer et al., 1992), and AS consumption was linked to MD development (Suez et al., 2014), therefore, there may have underlying mechanisms of haemolysis and disease activity. Besides, bacteria were exposed to AS for 24 hours only in the present study, long-term AS exposure may change bacterial response as the GM were reported to have extensive ability of metabolising xenobiotics, including AS (Claus et al., 2016).

Recent study investigated the aspartame-linked metabolic disorders and found that aspartame yields β-sheet-rich nanofibrils under mimicked physiological conditions that have cytotoxic effects. These aspartame fibrils induce haemolysis and cause DNA damage that leads to cell death via both apoptosis and necrosis. The investigators also mentioned that aspartame shows self-assembly which can cause protein aggregation and cell death (Anand et al., 2019).

Blood agar plates were used which directly represent the haemolysis of red blood cells. Also, plates were incubated for 24 to 72 hours to note the influence of incubation duration. The blood agar plates do not have AS, bacteria were exposed to AS for 24 hours, so only

the long-lasting response was recorded. It is easier for bacteria to recover any effect when they are not continuously exposed. In the biofilm formation, initial exposure to saccharin and aspartame did not affect the *E. coli* biofilm whilst continuous exposure caused significant biofilm formation (fig.3.3.9). Besides, in the diet, there is daily intake of sweeteners making it more likely to be a continuous exposure. So, it is possible that AS might have a temporary effect which may switch on and off quickly, and do not have a long-lasting response. Further studies are required to investigate the bacterial haemolytic activity.

3.5 Conclusion

The changes in growth and pathogenicity at species level ultimately affects the structural and functional stability of the whole gut ecosystem. There were no significant changes observed in the growth of the MGB, neither on their haemolytic behaviour. However, AS-exposure enhanced model gut bacterial pathogenic factor (biofilm development) and inhibiting the sweet sensing reduced the effect. The study forms the basis for further research to characterize how AS modulate gut bacteria dysbiosis. Further studies using *in vivo* or artificial gut system with a range of AS might extend our knowledge in this field.

4 Effect of artificial sweeteners on gut microflora and epithelial cell co-culture model

4.1 Introduction

4.1.1 Mutual existence in gut

The human intestinal epithelium is one of the densest microbial niches and represents a critical interface of continuous microbial exposure (Valdes et al., 2018). Human host and residing microbiota have a variable relationship, that can have a beneficial or detrimental impact (Bian et al., 2017; Lopetuso et al., 2015). The physiological and immunological importance of the microflora was mentioned (section-3.1.1). The residing bacteria initially protect the host from exogenous pathogenic invasion by prior colonisation and by increasing competition for nutrients. Pathogens must out-compete the commensals to initiate colonisation on the intestinal epithelium (Schuijt et al., 2013). This colonisation usually follows three distinguishable steps initiating with migration of pathogen to the IEC surface, followed by navigation through the commensal microbial layer, adhesion, and finally, invasion of epithelial cells (Kaper et al., 2004).

The gut bacterial profile can indicate the host disease state or vulnerability to certain diseases. Compared to healthy subjects, patients with IBD harbour fewer bacteria of the phyla Bacteroidetes and Firmicutes, whilst more from the phyla Actinobacteria and Proteobacteria (Frank et al., 2007). Patients with T2D have a higher ratio of Bacteroidetes but reduced proportion of Firmicutes (Larsen et al., 2010). Also, microbiota from infants with necrotizing enterocolitis was composed of bacteria from the phyla Proteobacteria and Firmicutes, while the healthy subject's contain species from all the four dominant phyla (Wang et al., 2009). Similar studies on stool samples from human patients with colorectal carcinoma demonstrated that Fusobacter level could indicate colorectal cancer or risk of developing cancer (Meyerson and Kostic, 2014). Therefore, changes in the gut bacteria can be linked to whether a host is suffering or susceptible to certain diseases.

The IEC layer is constantly exposed to various antigenic substances, including GM metabolites and dietary components (Kim and Jobin, 2005). Studies performed in the 1980s under *in vitro* conditions demonstrated the close associations between AS intake and changes in bacterial dynamics and behaviour (Abou-Donia et al., 2008; Palmnas et al., 2014), suggestive that AS might interact with gut microbes and exert negative impacts. However, detailed studies with appropriate subjects and controls have not been performed to provide concrete evidence of the effects of AS on human GM (Daly et al., 2016).

The pivotal contribution of the commensal microbiota to health and disease is gaining more appreciation. Approximately 4000 papers were published (2013–2017) emphasising different aspects of GM, which is 80% greater than the total publications in this area over the last 40 years (1977–2017) (Cani, 2018). This high volume of research highlights the

importance and potential of the microflora and suggests further investigations to provide a full understanding of the related mechanisms. Understanding the effect of AS is pivotal for its contribution to dysbiosis.

In the gut, shifts in bacterial species or colonies can trigger specific disease-inducing or disease-protective activity. Studies on microbiome transplantation from diseased animal into a germ-free healthy subject have represented several disease phenotypes. The microbiota grafting could transfer diseases such as obesity (Turnbaugh et al., 2009), metabolic syndrome (Vijay-Kumar et al., 2010), ulcerative colitis (Garrett et al., 2007), which are characteristics of metabolic disorders and are influenced by the host's genetics and gut environmental factors (Spor et al., 2011). Similarly, exposure of beneficial microbiota from healthy subjects showed a positive effect on host-microbial communities (Spor et al., 2011). In addition, the human host and GM symbiosis can trigger both local and systematic biological responses, which can be influenced by factors like AS in the diet. According to Wen *et al*. (2008), specific pathogen-free non-obese diabetic mice that lack an adaptor namely MyD88 for multiple immune receptors, do not acquire T1D. This MyD88 protein recognises microbial stimuli and MyD88-negative mice harbouring human-like gut bacteria phyla attenuated T1D. They also found that deficiency of MyD88 alters the composition of the distal GM and exposure of the germ-free non-obese diabetic recipients to the microbiota of specific pathogen-free MyD88-lacking mice attenuates T1D in the former. They concluded that the interaction of the microbiota with the innate immune system is a vital epigenetic factor that alters predisposition to T1D (Wen et al., 2008). This shows only one component can determine a disease state. Since AS intake has already been linked to conditions to diabetes (Suez et al., 2014), studying changes in microbial metabolism and their interactions with epithelium are important.

4.1.2 Cytotoxic effect of AS-mediated bacterial products on IEC

Beside the positive roles in host health, the microbiota can produce potentially dangerous chemicals in response to dietary components. In chapter 1, AS negatively affected the intestinal epithelium via reduction of cell viability (fig.2.3.7 and fig.2.3.21), which can cause intestinal epithelial dysfunction (Patterson and Watson, 2017). In chapter 2 AS enhanced model gut bacterial pathogenic feature (fig.3.3.11), which can negatively impact the intestinal epithelium (Nickerson and McDonald, 2012; Sifri, 2008). So, determination of the cytotoxic effect of the AS-mediated bacterial metabolites on IEC is an effective method of measuring the virulence. Lazar *et al*., (2010) have investigated the cytotoxic effect of adherent opportunistic enterobacterial strains on Caco-2 cell monolayer. They isolated bacterial strains from different sources, pre-tested their ability to adhere and invade mammalian cells and determined cytotoxic effect. Both qualitative and quantitative

measurements were performed using Transmission Electron Microscopy (TEM) and MTT assay, respectively. They found that a *Citrobacter freundii* strain (strain 93), isolated from stool culture, caused the highest level of cytotoxic effect whilst *E. coli* (strain 115) isolated from patients with acute diarrhoea, caused about 68% cytotoxicity. The investigators concluded that pathogenic potential of organisms is through their ability to produce and release cytotoxic factors into the adjacent extracellular environment and that these also represent pathogen's virulence potential. The authors also highlighted the responsibility of the organisms in the etiology of acute infections and food-borne diseases (Lazar et al., 2010).

Any cellular response elicited by the interaction between gut microbes and IECs might have a contribution to the virulent activity of other pathogens in the gut milieu. These responses are related to the binding of bacterial relevant structures and/or metabolites to host cell receptors together with signalling pathways (Cotter and Stibitz, 2007). Attacking the host intestinal epithelial barrier cell cytoskeleton is the key mechanism by which pathogenic bacteria cause structural and functional changes (Pizarro-Cerdá and Cossart, 2006). The intervention of cytoskeleton organisation, signal transduction machinery, and affecting the cell membrane can be facilitated by enzymatic alteration by soluble toxins (Boquet et al., 1998). This interference can also take place through the recruitment of signal transduction molecules related to decay acceleration and disassembly of actin network by direct prokaryote-eucaryote interactions (Guignot et al., 2000; Bernet-Camard et al., 1996). For example, adherence to human embryonic intestinal cell line (INT 407) by diffusely-adhered *E. coli* C1845 (clinical isolate) can provoke dramatic F-actin rearrangements without causing cell injury. The alterations in the F-actin distribution has been linked to intestinal permeability in chapter 2. The pathogen takes the authority of host regulatory mechanisms to express the cell membrane-associated decay-acceleration factors glycosylphosphatidylinositol, leading to alterations in the cell cytoskeleton (Peiffer et al., 1998). Therefore, AS might stimulate the bacterial pathogenic factors directly or bacteria might produce metabolites that have a connection with host cell damage.

Like the nervous system, enteric microbiota can modulate intestinal mobility and control diseases. Prominent human symbionts like *Bifidobacteria fragilis* was demonstrated to inhibit the pathogenic potential of another commensal bacterium, *Helicobacter hepaticus* in experimental colitis (Mazmanian et al., 2008). The former symbiont produces a beneficial molecule, polysaccharide A, which resists the pathogenicity of other bacteria. In addition, *Bifidobacteria bifidum* and *Lactobacillus acidophilus* can boost mobility, whereas, *Escherichia* species do the opposite (Rhee et al., 2009). Intestinal bacterial metabolic products like short-chain fatty acids or other chemotactic peptides (such as N-formylmethionyl-leucine-phenylalanine) affect the rate of gut transit and can stimulate the

enteric nervous system (Barbara et al., 2005; Rhee et al., 2009). Gut bacteria imbalance can lead host to altered gut motility and secretions resulting in diarrhoea or constipation. In return, these changes influence the enteric microbiota balance (Rhee et al., 2009).

Previous studies with different cell lines or animal models with varying measuring techniques have reliably and consistently demonstrated that AS affects gut bacterial characteristics. Qu *et al.* (2017) have shown that pre-treatment of *E. coli* BW25113 with sucralose increased their resistance against several antibiotics such as oxolinic acid or moxifloxacin and rifampicin. In addition to antibiotic resistance, sucralose elevated the bacterial mutation rate in a dose-dependent manner. Sucralose (62.5 mg/ml) significantly increased mutation frequency at 24 hours and about 50-fold at 72 hours (Qu et al., 2017). Since cytotoxic factors have important virulence potential (Lazar et al., 2010), it is important to investigate whether AS-exposure stimulates gut bacteria to exert a cytotoxic effect on IECs.

4.1.3 Bacterial adhesion and invasion

Bacterial adherence to the IECs is an essential prerequisite for microbial colonisation, biofilm formation and virulence manifestation (Falkow et al., 1992). In fact, the first step of infection is the formation of a close association between bacteria and IEC (Bernet et al., 1994; Levine, 1987; Scaletsky et al., 2002; Lee et al., 2003). *E. coli* have been identified to demonstrate different patterns of adherence such as localized adherence, diffuse adherence or aggregative adherence, depending on their pathogenicity factor (Scaletsky et al., 2002). *E. coli* also shows localised adherence like (LAL) patterns of bacterial adhesion. Caco-2 cells were mentioned to be suitable for adhesion studies as the monolayers exhibit appropriate characteristic of mature enterocytes in the microvilli (chapter 1; section-2.1.7). In addition, irrespective of the adhesion and invasion factors of the bacteria (Kaper et al., 2004), Caco-2 cell line was demonstrated to represent adhesion characteristics close to those acquired *in vitro* adhesion assay with human enterocytes (Darfeuille-Michaud et al., 1990). The Caco-2 cell surface is irregular with naturally formed domes which bacteria will preferentially adhere to (Darfeuille-Michaud et al., 1990).

Attachment of bacteria to Caco-2 cells is regulated by complex signalling, and specific to bacteria and IEC. Coconnier *et al*. (1993) demonstrated the adhesion and invasion potential of four enterovirulent organisms, *Salmonella typhimurium*, *Escherichia coli*, *Yersinia pseudotuberculosis* and *Listeria monocytogenes*. All these strains invaded Caco-2 cells; however, their adherence patterns were different. The study showed that *S. typhimurium* and enteropathogenic *E. coli* adhered to the brush border of differentiated Caco-2 cells *in vitro* whereas the other two strains displayed adherence to peripheral region of undifferentiated cells. They also demonstrated the concentration-dependent inhibitory

action of the *Lactobacillus acidophillus* strain LB which could hinder the steric human enterocytic pathogen receptor, thereby preventing both adhesion and invasion of these enterovirulent organisms to Caco-2 cells (Coconnier et al., 1993). Therefore, the adhesion and invasion mechanisms are not only complex but also species specific.

IECs are the primary route of enteric pathogen invasion in the host. In response to bacterial intrusion, these cells upregulate the inflammatory gene regulation and expression within 1-2 hours (Kim et al., 1998). This upregulation includes the expression of cytokines, interleukins (Jung et al., 1995), and an array of proinflammatory chemokines (Yang et al., 1997; Jung et al., 1995; Eckmann et al., 1993). Additionally, bacterial invasion activates the expression and production of NO synthase (iNOS) and NO in human colon epithelial cells (Witthöft et al., 1998), these chemicals are linked to IBF (section-2.1.4.2). All these inflammatory mediators can induce apoptosis in IEC (Kim et al., 1998; Abreu Martin et al., 1995; Sandoval et al., 1995) which may contribute to barrier permeability, leading to increased sepsis (Rajan et al., 2008; Coopersmith et al., 2002).

The co-evolved, co-existence of prokaryotic and eukaryotic organisms are of great interest because human health and wellbeing are largely dependent on harbouring microflora. GM is now termed as the second brain and the impact of this intimate contact is of physiological relevance (Cani, 2018). Co-culture studies for understanding host-microbe interactions have been performed for only several decades, understanding of the complete relationship of GM and host remained in early stage urging more research (Neish, 2002). This chapter aimed to focus on the contact between MGB and IECs; and whether AS alters bacterial metabolites and influence bacterial ability of adhesion and invasion to the mammalian cell. At the point of contact, i.e., IEC lining in the lumen, both mammalian cell and commensal bacteria employ efforts to keep a normal symbiotic relationship (Neish, 2002). AS modulated GM composition (Suez et al., 2014) and these microbial changes affected human metabolic activity and immune functions (Dethlefsen et al., 2007). Although there are studies demonstrating the increase or decrease of some strains or phyla of bacteria due to AS intake, with indications of MD development, but the mechanisms through which microbiota affects the intestinal lining leading to diseases remained veiled.

Rationale of chapter 4

Following consumption of AS-containing foods, both IEC and GM would be exposed to various concentrations of AS in the gut. Studies from chapter 1 demonstrate a cytotoxic and leak effect of sweeteners on the intestinal epithelium. Studies from chapter 2 demonstrate an increase in pathogenic factor such as biofilm formation, but not growth/haemolytic effect. However, the gut includes both cells in proximity, so co-cultivation to mimic gut physiology is important to understand the true effect. Assessing the effect of AS on the bacteria-epithelial cell axis is therefore important. Moreover, use of established enterocytic cell model Caco-2 to assess the safety of AS is of great interest. Therefore, the study aimed to assess the cytotoxic effect caused by AS-mediated gut bacterial metabolites on the IEC. Also, adhesion and invasion assays were performed to evaluate the AS-mediated pathogenic factors affecting the gut bacteria-IEC interactions, which could help to explain the mechanism of bacterial pathogenicity upon AS exposure.

Aims and objectives

To advance our understanding of the role of AS on intestinal microbiota and resulting impact on function of the intestinal epithelium, the present study aimed to employ co-culture studies using model gut bacteria and intestinal epithelial cell.

The hypothesis for the chapter is **"Artificial sweeteners negatively affect the bacterial functions (metabolites and pathogenicity) leading to disrupted bacteria-epithelium interactions".**

To address this hypothesis, the specific aims for the chapter are:

- To assess the effect of AS mediated model gut bacterial metabolites on the IEC.
- To investigate whether exposure to AS enhances model gut bacterial adhesion ability to intestinal epithelium.
- To assess the effect of AS on invasiveness of model gut bacteria to the IEC.

4.2 Materials and methods

4.2.1 Cytotoxicity assay

The cytotoxicity assay was performed to assess the effect of AS-mediated bacterial metabolites on IEC following the protocol described by Furumura *et. al.* (2006) with modifications (fig.4.2.1). Caco-2 cells were grown on 96-well plates (1×10^4 cells/well) and incubated for 48 hours. Simultaneously, *E. coli* or *E. faecalis* was grown in 10 ml liquid media (fig.3.2.1, chapter 2) supplemented with 100 µM of AS (saccharin, sucralose, aspartame, and neotame) with/out 100 µM $ZnSO_4$ or vehicle (H_2O) for 18 hours. The cultures were centrifuged at 4000 rpm for 15 minutes at 4 ˚C (accuSpin^{TM} 1R, Fisher Scientific) and supernatant was collected, filter-sterilized (0.22 µM membranes; Millipore, USA). 50 µl supernatant and 50 µl EMEM without antibiotics was added on the PBS washed Caco-2 cell monolayer and incubated for 18 hours.

CCK-8 assay (section-2.2.3) and microscopic observations (section-2.2.4) were performed to assess viability and morphological changes, respectively.

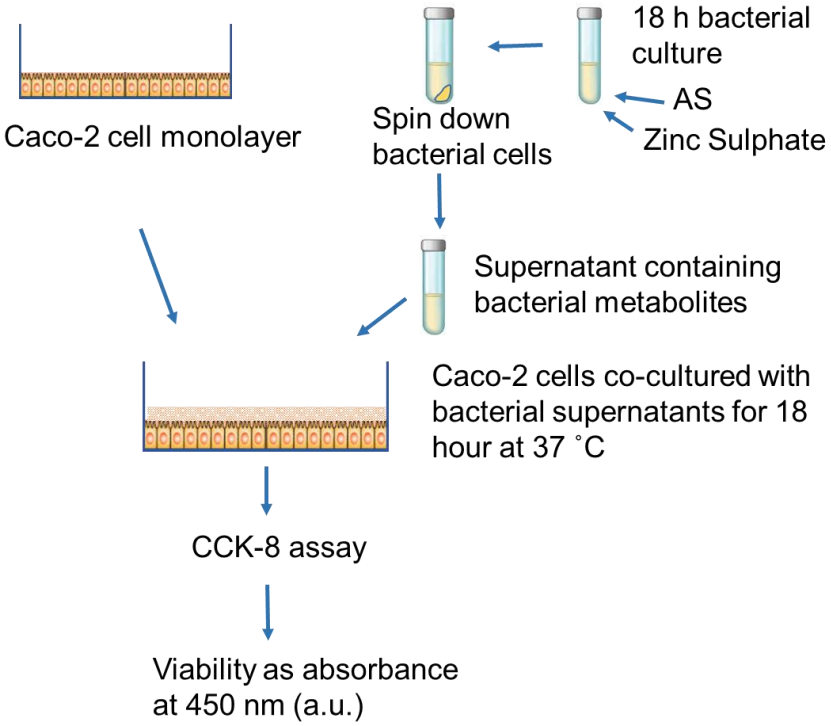

Figure 4.2.1: Cytotoxic effect of AS-exposed bacterial metabolites on Caco-2 cell viability.

Cells were seeded at 1×10^4 cells/well and grew for 48 hours at 37 ˚C in humidified condition. On the other side, a single bacterial colony was inoculated into 10 ml of the liquid media containing AS±$ZnSO_4$ or vehicle and grown for 18 hours at 37 ˚C with shaking at 150 rpm. Bacterial supernatant containing excreted metabolites was collected after centrifugation and cell monolayer was exposed to it for 18 hours. Cell viability was performed using CCK-8 assay and absorbance was measured at 450 nm.

4.2.2 Adhesion and invasion assay

An adhesion/invasion assay was performed to determine the effect of AS on the model gut bacterial adherence to and invasion into IEC following the previous procedure of Darfeuille-Michaud *et al*. (1990) with modifications (fig.4.2.2). AS-exposed *E. faecalis* and *E. coli* were assessed for their ability to adhere to Caco-2 cells. The Caco-2 cells were seeded on 24-well plates (7.5×10^4 cells/well) and incubated at 37 °C and 5% CO_2 for 48 hours. Cells were exposed to concentrations of AS for 24 hours under the same conditions mentioned above. On the bacterial side, a single colony was inoculated into 10 ml of media supplemented with the AS in presence or absence of $ZnSO_4$, or vehicle and incubated overnight at 37 °C with shaking at 150 rpm. Bacteria washed twice with serum-free DMEM and re-suspended in EMEM without antibiotics.

Caco-2 cell monolayers were washed (500 µl PBS, X2) and EMEM (490 µl) without antibiotics was added to each well. The total number of adherent Caco-2 cells were measured by performing a cell count. Caco-2 cells were co-cultured with untreated or treated bacteria at multiplicity of infection (number of bacteria per mammalian cell, MOI 1:300) (calculation shown in appendix C, 8.3.1) with an infection incubation time of 1 hour.

After the infection period, cells were washed (PBS, X2) to remove non-attached bacteria. For the adhesion assay, cells were detached at this stage. For the invasion assay, cell monolayer was incubated with EMEM supplemented with antibiotics and incubated at 37 °C for 30 minutes to kill the external adhered bacteria followed by washing (PBS, X2). The cell detachment was performed using TX-100 (500 µl, 0.5%) with mixing by pipetting up and down. This concentration of TX-100 had no effect on bacterial viability for more than 30 minutes. To count the viable bacteria, the spread plate method was used after serial dilutions (1/10 to 1/10,000) of the cell suspensions.

Caco-2 cells were exposed to AS in all cases, except controls, the bacteria were either untreated or treated with AS with/out $ZnSO_4$. In the initial adhesion and invasion assays, the Caco-2 cells were exposed to a range of AS concentrations and infection was allowed with untreated bacteria; these findings were used to determine the concentrations of AS for the further assays with AS-exposed bacteria (table 4.2.1). Bacterial adhesion and invasion were expressed as the percentage of total bacteria attached per Caco-2 cells (fig.4.2.2).
Initially, the effect of a range of antibiotic concentrations and incubation durations on bacterial growth were tested for the invasion assay. *E. coli* were tested for gentamicin to confirm that the used concentration kills the adhered bacteria in given time (Altenhoefer et al., 2004). *E. faecalis* was exposed to three antibiotics (gentamicin, ampicillin, and meropenem) individually and in combination (gentamicin plus ampicillin and gentamicin plus meropenem).

Caco-2 cells were also exposed to concentrations of same antibiotics and viability was measured using CCK-8 assay. This was to confirm that the antibiotics do not interfere bacterial invasiveness via cell viability.

Table 4.2.1: The concentrations of AS, Caco-2 cells were exposed to, for the adhesion and invasion assay.

Initial adhesion and invasion assay were performed with AS concentrations ranging from 0.1 to 1000 µM, and bacteria were untreated. In the later experiments, both bacteria and Caco-2 cells were exposed AS. Only one concentration of each AS for Caco-2 cells, as mentioned below, was determined at this point using the findings from the initial experiments.

AS (µM)	Adhesion assay		Invasion assay	
	E. coli	*E. faecalis*	*E. coli*	*E. faecalis*
Saccharin	100	100	10	0.1
Sucralose	10	10	0.1	0.1
Aspartame	10	100	10	10
Neotame	1	1	10	1000

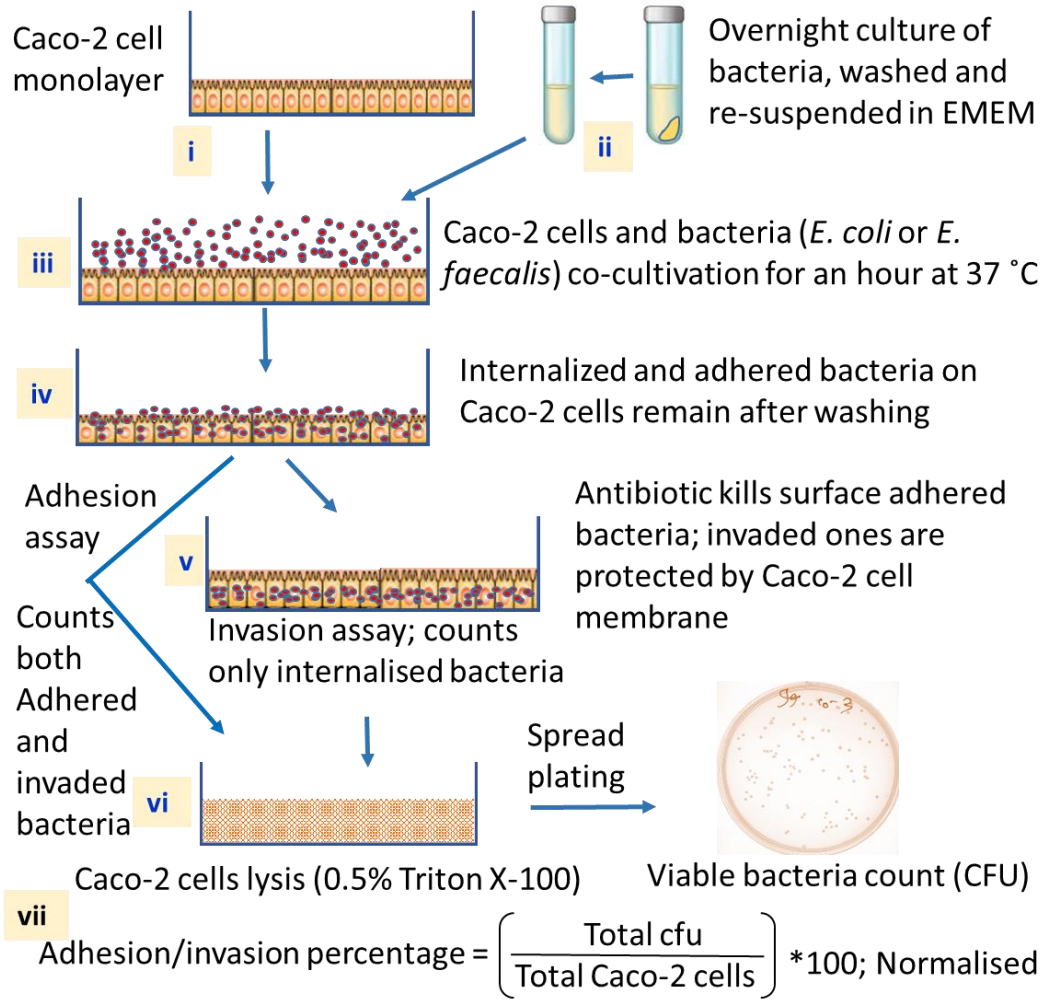

Figure 4.2.2: Schematic diagram of the adhesion and invasion assay.

(i) Caco-2 cells were grown on 24-well plates (7.5×10^4 cells/well) in EMEM with 10% FBS for 48 hours; (ii) single bacterial colony was inoculated into liquid media with/out AS for 18 hours, measured OD, washed (PBS×2) by centrifuging at 4000 rpm for 10 minutes and re-suspended in EMEM; (iii) Bacteria and Caco-2 cells were co-cultivated (MOI 1:300) for an hour; (iv) gentle wash (PBS×2) removed non-adhered or loosely adhered bacteria; (v) antibiotic action killed the adhered bacteria in the invasion assay; (vi) cells were lysed with 0.5% Triton X-100, homogeneously mixed, diluted and spread on solid media and incubated overnight at 37 °C to count colony forming units; (vii) calculation of the adhesion/invasion percentage.

4.2.4 Data analysis

Data for the cytotoxic effect was calculated as for the cell viability data (chapter 1). Adhesion and invasion assay data calculation were mentioned in each section. For two groups, the variance in data sets was analysed using the non-parametric test followed by the Mann Whitney test. For three or more groups, variance was assessed by using ordinary one-way ANOVA followed by uncorrected Dunn's test, Holm-Sidak's multiple comparison test, and Fisher's LSD test. Significance was reached when $p<0.05$. The replication number was mentioned in the legend.

4.3 Results

4.3.1 Cytotoxic effect of AS-mediated gut bacterial metabolites

4.3.1.1 Method validation

The cytotoxicity assay was performed to investigate the effect of AS-exposed bacterial metabolites on mammalian cell function. The Caco-2 cells were exposed to bacterial secretions and changes in cell morphology and viability were measured. Observation of the morphological changes (Zoe imager), assessed changes in cell nuclei, mitochondria, and stress fibre formation. Additionally, the CCK-8 assay was performed to measure the viability upon exposure to bacterial metabolites.

Exposure to *E. coli* metabolites did not cause significant changes in cell morphology as observed in the brightfield images (fig.4.3.1), however, few tiny vesicles were found scattered throughout the Caco-2 cell culture exposed to *E. coli* and *E. faecalis* metabolites. *E. faecalis* metabolites increased the frequency of vesicles along with characteristic small, round, grey features throughout the microscopic field (fig.4.3.1.c).

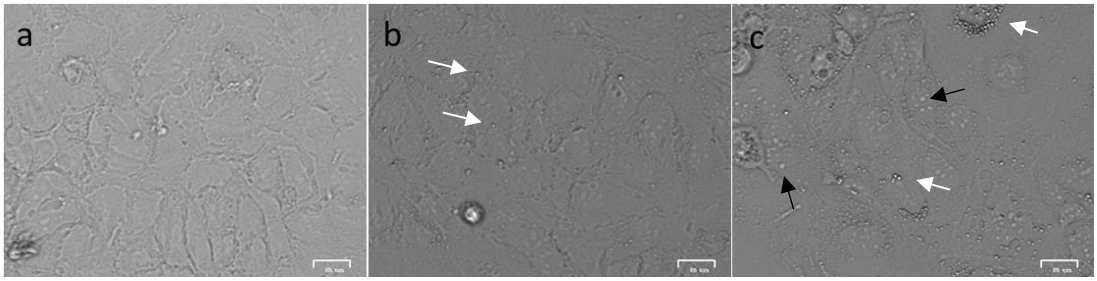

Figure 4.3.1: Intestinal epithelial cell morphology after exposure to gut bacterial metabolites.

Caco-2 cells were exposed to *E. coli* and *E. faecalis* metabolites for 24 hours and morphological changes were observed microscopically (Zoe imager). Panel a represents vehicle-treated, and panels b and c represent untreated *E. coli* and *E. faecalis* metabolite exposed cells, respectively. White arrows show the vesicles on the panel b, and c, and the black arrows (c) show the small round features in the *E. faecalis* metabolites-exposed Caco-2 cells. The images were taken with gain, 16; exposure, 320; LED intensity, 28; and contrast, 17, scale bar = 25 µM.

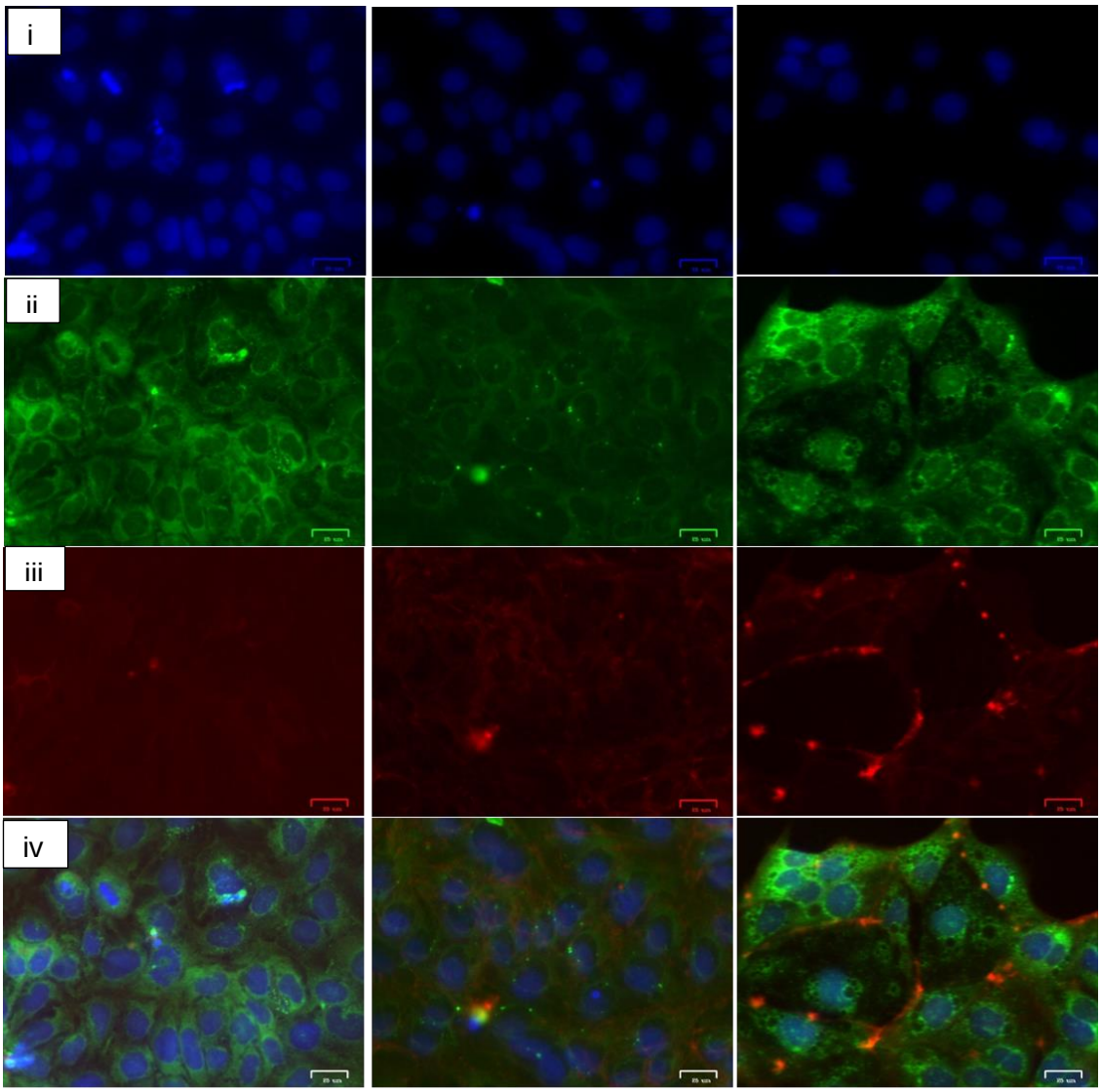

Figure 4.3.2: Caco-2 cell morphology after exposure to vehicle-treated model bacterial metabolites.

Caco-2 cells were exposed to *E. coli* and *E. faecalis* metabolites for 18 hours and changes in the (i) nuclei (blue), (ii) mitochondria (green) and (iii) stress fibre formation (red) were observed using the Zoe imager. Panel (iv) a, b and c present merge of images. Panels represent vehicle-treated Caco-2 cells (a), and panels b and c represent *E. coli* and *E. faecalis* metabolite exposed cells. The conditions for the images were gain (16, 8, 34), exposure (300, 280, 360), LED intensity (10, 28, 50), and contrast (46, 21, 13) for the blue, green, and red fluorescence, respectively; scale bar = 25 µM.

Following exposure to bacterial metabolites, Caco-2 cells remained adhered to the plate surface without demonstrating cell rounding or monolayer disruption (fig.4.3.1.b and 4.3.1.c). No conspicuous changes in the nuclei were observed. The mitochondria of the *E. coli* metabolites-treated cells showed some bright green spots (fig.4.3.2.b.ii), while numerous small vacuoles were found in *E. faecalis* metabolite-treated cells (fig.4.3.2.c.ii). In addition, no changes in the stress fibre were observed in the *E. coli* metabolite-treated cells in comparison to the vehicle-exposed cells (fig.4.3.2.c.iii). However, stress fibres were more prominent with uneven fused appearance of fibres in cells exposed to *E. faecalis* metabolites (fig.4.3.2.c.iii).

IEC were exposed to AS-treated model gut bacterial supernatant and cytotoxic effect was assessed by CCK-8 assay. Model gut bacterial secretions did not decrease cell viability, in fact, media from *E. coli* significantly increased (241%; <0.0001) absorbance of CCK-8 compared to the vehicle. In contrast, there was no change in viability following exposure to media from *E. faecalis* (fig.4.3.3).

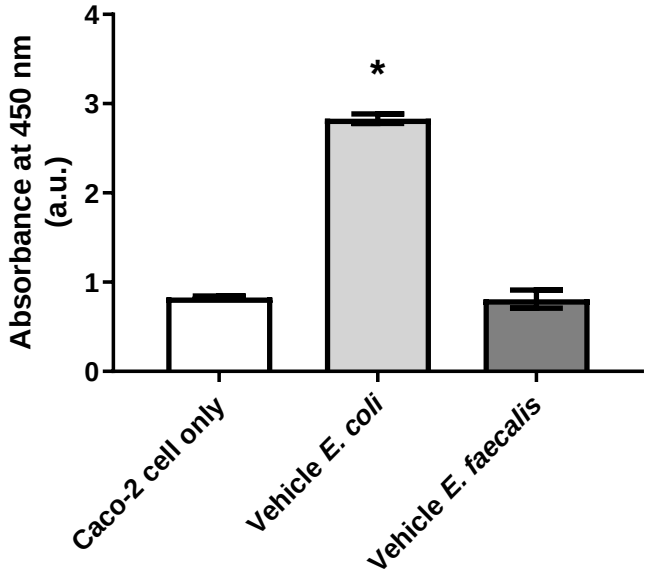

Figure 4.3.3: Effect of bacterial metabolites on intestinal epithelial cell viability.

Caco-2 cells were maintained on 96-well plates in EMEM supplemented with 10% FBS and 1% antibiotics. Model gut bacteria, *E. coli* and *E. faecalis*, were grown overnight in the respective liquid media and centrifuged to remove bacteria. Washed Caco-2 cell monolayer was exposed to 50 µl of bacterial supernatant in the presence of 50 µl of the complete EMEM media without antibiotics for 18 hours. CCK-8 assay was performed, and the absorbance was measured at 450 nm (Tecan Sunrise™). Data were analysed using Ordinary one-way ANOVA with Holm-Sidak's multiple comparisons test and are presented as the mean ± S.E.M., n=3. *p<0.05 versus Caco-2 cell only.

Considering the assessment procedure, measuring the viability was found as a better method to assess cytotoxicity in further experiments as it gave a more sensitive and quantitative output.

4.3.1.2 AS-mediated gut bacterial metabolites differentially affected IEC viability

To evaluate cytotoxic effect of AS-mediated bacterial metabolites on intestinal epithelium, Caco-2 cells were exposed to AS-treated model gut bacterial metabolites and viability was measured. Saccharin- and sucralose-treated *E. coli* metabolites, in culture supernatant, reduced Caco-2 cell viability (21.5 ± 0.42% and 20 ± 3.1%, respectively), however, neither aspartame nor neotame caused any change (fig.4.3.4.a).

E. faecalis metabolites did not cause any significant change in cell viability, although both sucralose and aspartame demonstrated a trend of decrease (fig.4.3.4.b). Saccharin-exposed *E. faecalis* metabolites increased (10%) viability. Conversely, sucralose and aspartame reduced cell viability 35- and 40%, respectively. However, neotame treated *E. faecalis* excretions did not change viability at the given conditions (fig.4.3.4.b).

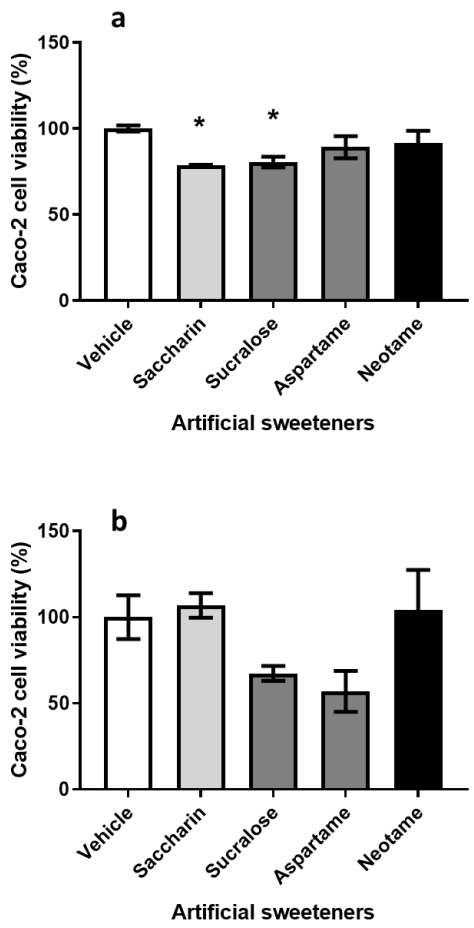

Figure 4.3.4: Effect of AS-exposed bacterial supernatant on Caco-2 cell viability.

Bacteria were exposed to 100 µM of saccharin, sucralose, aspartame, or neotame or vehicle with/out $ZnSO_4$. Caco-2 ($1x10^4$ cells/well) were maintained in EMEM for 48 hours, exposed to the bacterial supernatant for 18 hour, and CCK-8 assay was performed. The cell viability was measured as absorbance 450 nm (PerkinElmer). Panel represent results of (a) *E. coli* and b) *E. faecalis* supernatant. Data were analyzed using ordinary one-way ANOVA with Holm-Sidak's test and are presented as the mean ± S.E.M., n=3. *$p<0.05$ versus 0 µM of AS.

The images from different microscopic views of the wells could be considered to get quantitative data, however, these still do not represent the reaction of every cell in the wells. Conversely, the CCK-8 assay measures absorption and quantitative data represent the response of all living cells. This assay relies on the biochemical activity of cells and the absorbance directly represent the number of living cells.

4.3.2 Effect of AS on bacterial adhesion

4.3.2.1 Method validation

Many factors are likely to influence the adhesion of gut bacteria to IECs. Some of these factors, such as buffer composition, incubation period and growth medium are related to the culture *in vitro* (Edwards and Massey, 2011). These factors were determined using

references (Dogan et al., 2006; Furumura et al., 2006) with modifications and were consistent for all the experiments. Bacterial concentration is another important determinant for adherence as expected; higher the bacterial concentration, increased the level of bacterial adherence (Tuomola and Salminen, 1998). The concentration of bacteria was tested for the study on an absorbance to CFU count. Bacterial absorbance was adjusted to 1 (OD_{600}) which is equivalent to 8×10^8 CFU/ml for *E. coli* (fig.4.3.5.i) and 0.5×10^8 CFU/ml for *E. faecalis* (fig.4.3.5.ii). The used MOI was 1:300 for both MGB.

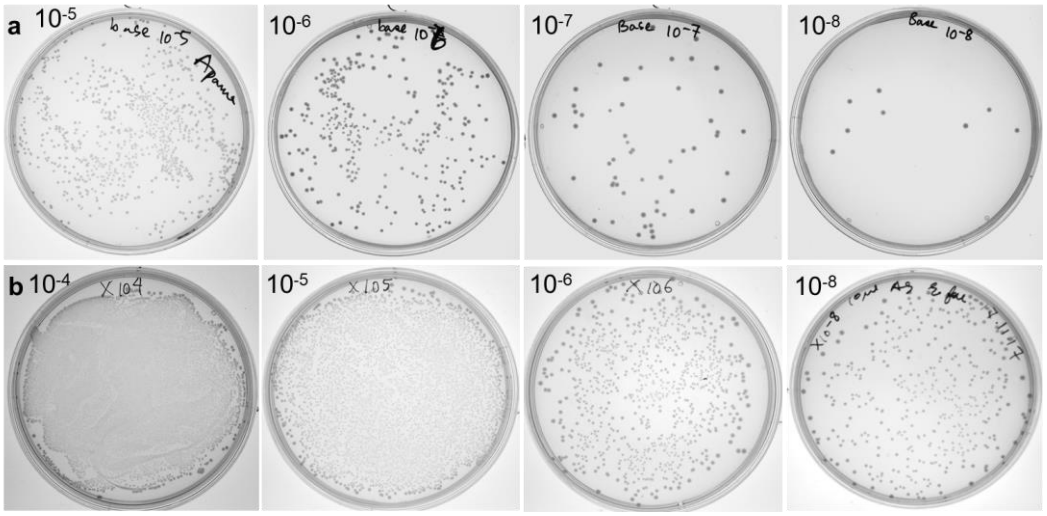

Figure 4.3.5: Determination of the bacterial number using standard colony count method.

The base bacterial culture was serially diluted and 100 µl was plated for colony forming units (CFU). Panel a shows *E. coli* CFU for the dilutions 10^{-5} to 10^{-8}, the number of bacteria from 10^{-7} was considered as the CFU was in the range of the bacterial standard count. Panel b represent the *E. faecalis* CFU for dilutions 10^{-4} to 10^{-6} and 10^{-8}, the 10^{-8} dilution was considered for the further bacterial count.

After the adhesion assay was performed, the number of CFU in the 10 µl cell lysate was too numerous to count (fig.4.3.6.a) for both *E. coli* and *E. faecalis*. So, a serial dilution of the cell lysate containing bacteria was performed and the dilution was determined using standard plate count method (representative fig.4.3.6). For both MGB, 10^{-4} dilution was found appropriate and was used for the further adhesion studies with AS.

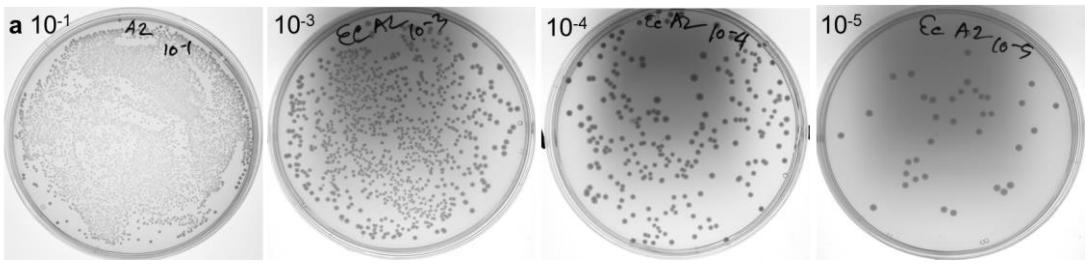

Figure 4.3.6: Representative plates for the bacterial colony count after serial dilution.

Panel a represents colony formation of *E. coli* from the serially diluted Caco-2 cell suspension containing bacteria.

4.3.2.2 Adhesion of untreated gut bacterial adherence to AS-treated Caco-2 cells

Once the adherence study was optimised, the next experiment was to assess the effect of the AS on IEC sensitivity for model gut bacterial adhesion. Exposure of Caco-2 cells to saccharin significantly increased the adhesion ability of *E. coli* at all concentrations from 0.1 µM to 1 mM however significance was only achieved at 1 and 100 µM (fig.4.3.7.a). Sucralose exposure demonstrated a dose-dependent increase in *E. coli* adherence up to 10 µm (fig.4.3.7.b), although a significant increase was only observed at 10 µm and 1 mM. Both aspartame and neotame exposure increased *E. coli* adhesion at 0.1 µM (fig.4.3.7.c, and d, respectively); with aspartame at 0.1 and 10 µM concentrations caused similar adhesion on Caco-2 cells. Neotame exposure also caused significant increase in *E. coli* adhesion to Caco-2 cells at concentrations 1 µM and 1 mM however no significance was observed for 10 and 100 µM.

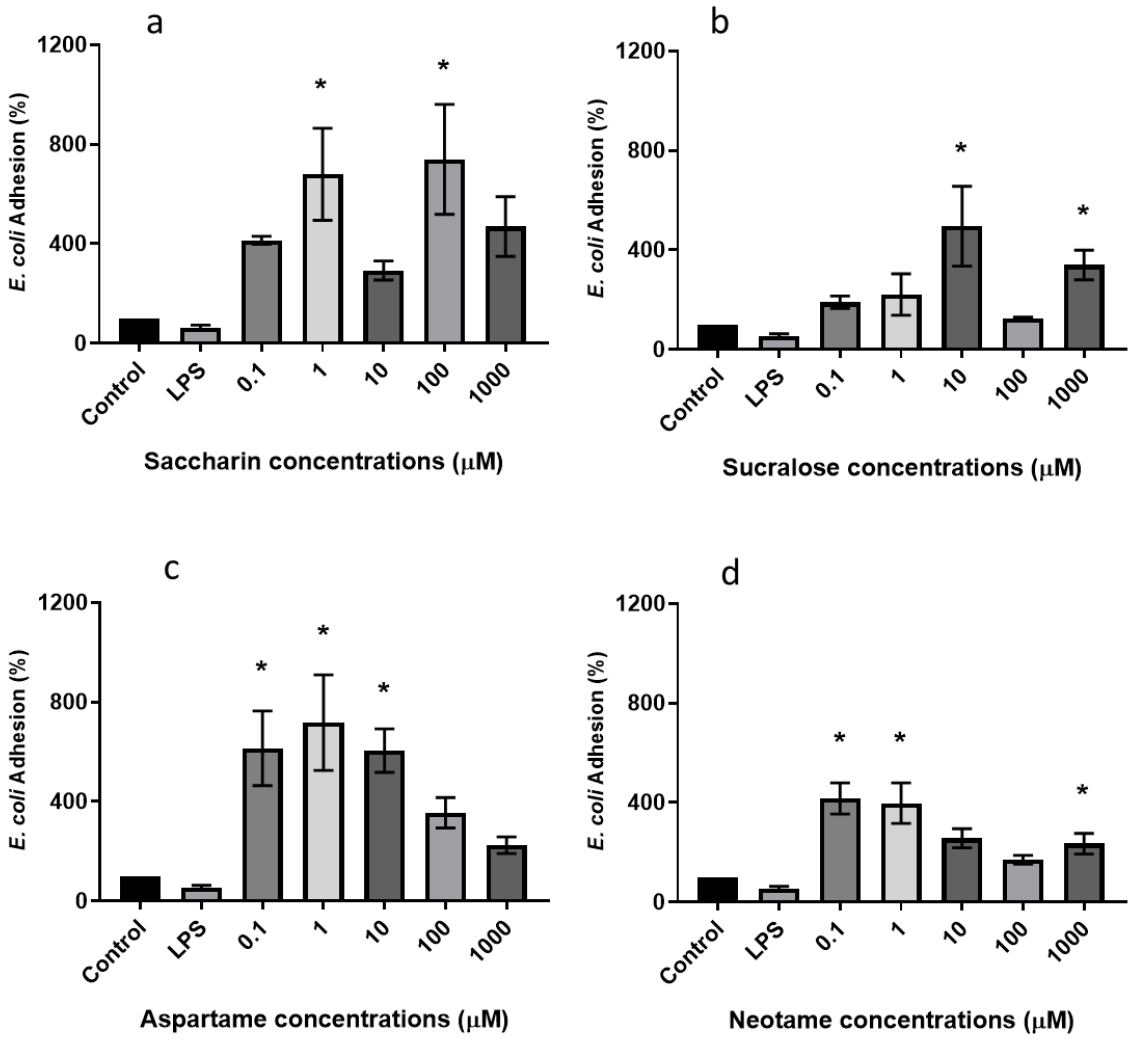

Figure 4.3.7: Effect of AS on the adherence of *E. coli* to Caco-2 cells.

The adherence of *E. coli* to Caco-2 cells was assessed for saccharin (a), sucralose (b), aspartame (c), and neotame (d). Mammalian cells were grown up to 60% confluence and treated with sweetener concentrations for 24 hours. Cells were exposed to the bacteria (MOI 1:300) and infection was allowed for an hour. Non-adhered bacteria were washed away, and cell lysate was diluted 4 times before plating to count the bacterial colonies. Bacterial CFU was divided by Caco-2 cell number to measure the bacteria per cell and was normalised with control as 100%. Data are analysed using ordinary one-way ANOVA with uncorrected Dunn's test and presented as the mean ± S.E.M., n=4. *p<0.05 versus vehicle.

E. faecalis adherence on AS-exposed Caco-2 cells was significantly increased for saccharin (fig.4.3.8.a) and aspartame (fig.4.3.8.c) concentrations of 10 µM, 100 µM and 1 mM. Sucralose exposure significantly increased *E. faecalis* adherence to Caco-2 cells at concentrations as low as 0.1 µM, continued until 100 µM, although insignificant at 1 mM (fig.4.3.8.b). In addition, exposure to neotame increased *E. faecalis* adherence for all the concentrations, the percentage of adhesion increased from 0.1 µM (161%) to the highest at 10 µM (688%) compared to vehicle. The percentage of adhesion reduced to 567% at the highest concentration, 1 mM, of neotame (fig.4.3.8.d).

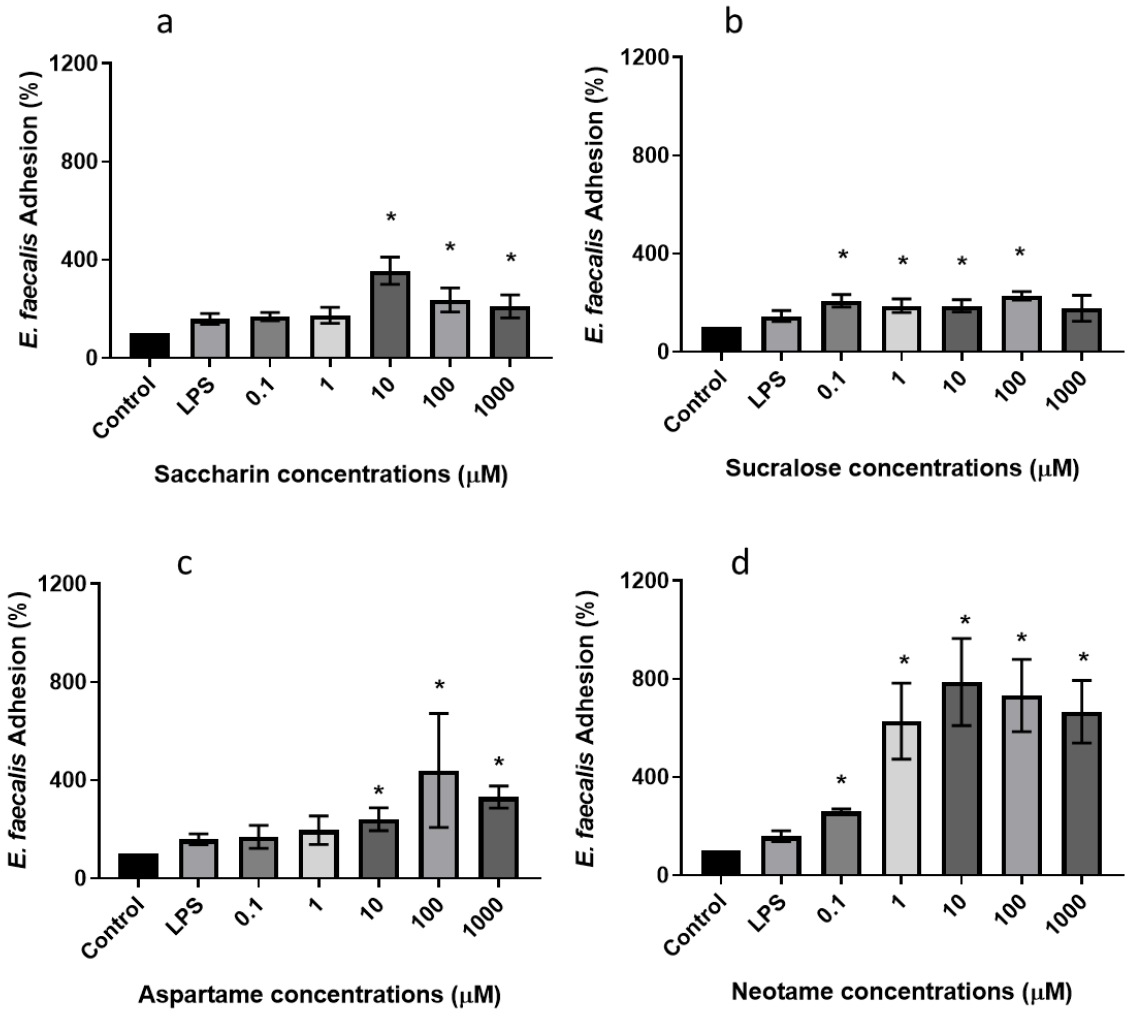

Figure 4.3.8: Effect of AS on the adherence of *E. faecalis* to Caco-2 cells.

Mammalian cells were treated with different concentrations of AS, saccharin (a), sucralose (b), aspartame (c), and neotame (d). Assays were prepared in 24-well plates, a confluent epithelial cell was inoculated with *E. faecalis* suspensions (MOI 1:300) for an hour. The supernatant with non-adherent bacteria was removed after an hour. After washing with PBS, adherent and invaded cells were brought into solution by lysing Caco-2 cells with 0.1% Triton X-100. Bacteria were plated and total bacteria per cell was counted. Data are normalised with the control as 100% and analysed using ordinary one-way ANOVA with uncorrected Dunn's test. Data are presented as the mean ± S.E.M., n=4. *p<0.05 versus vehicle.

4.3.2.3 Adhesion of AS-treated bacteria to AS-treated Caco-2 cells

Adhesion interaction of the MGB and IECs after exposure to the AS was assessed using the co-culture method. AS-treated MGB were exposed to AS-treated Caco-2 cells and bacterial adherence to the epithelium was measured. Except for neotame, all AS significantly increased *E. coli* adhesion (fig.4.3.9). Sucralose increased adherence 105%, followed by saccharin (126%), and the highest adherence was caused by aspartame (186.4%).

The adhesion pattern of the MGB on the Caco-2 cell monolayers was observed using bright-field microscopy (representative figures in appendix C). There was no distinguishable change in adhesion pattern of both bacteria for AS exposure (fig.C8.1-fig.C8.4). Untreated *E. faecalis* (fig.C8.3) did not adhere prominently, although some *E. coli* has adhered (fig.C8.1). AS-treated *E. coli* demonstrated similarities to localized adherence like pattern as observed using Zoe imager (fig.C8.2.b,c). In addition, *E. coli* showed clusters near cell-cell contact areas of Caco-2 islands (fig.C8.2.c) and dispersed throughout without any characteristic pattern. AS-exposed *E. faecalis* showed clusters, small chains and scattered bacteria throughout the microscopic field (fig.C8.4). The number of isolated *E. faecalis* was higher near the edge of cell islands although no specific pattern was observed.

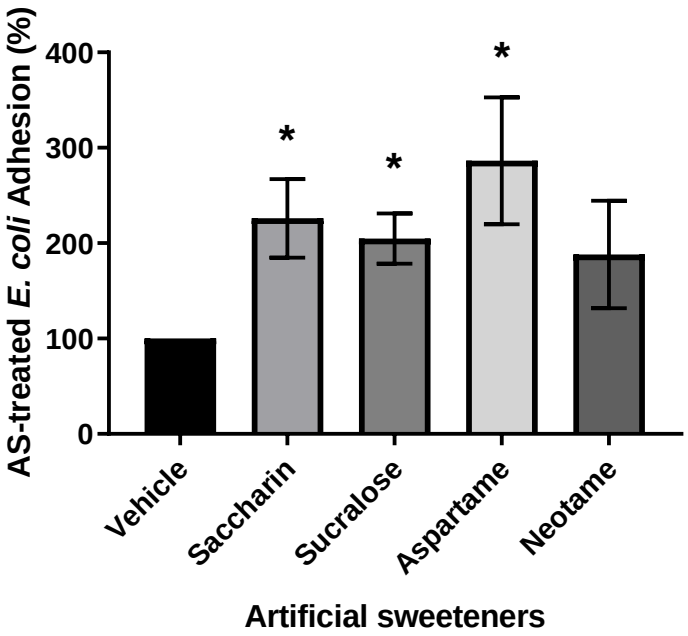

Figure 4.3.9: Effect of AS on *E. coli* adherence to Caco-2 cells.

E. coli was treated with AS (100 μM) for 24 hours and co-cultivated for an hour (MOI 1:300) with Caco-2 cells pre-exposed to AS or vehicle (24 hours). Non-adhered bacteria were washed away with PBS and Caco-2 cells were lysed with 0.5% Triton X-100. The diluted cell lysate was plated to count the colony-forming units. Data were normalised as bacteria per Caco-2 cells with control (100%). Data are analysed using ordinary one-way ANOVA with uncorrected Dunn's test and presented as the mean ± S.E.M., n=4. *p<0.05 versus vehicle.

Nevertheless, all AS caused significant adherence when both *E. faecalis* and Caco-2 cells were treated (fig.4.3.10). Neotame caused adhesion increase by 708%, followed by aspartame (546%), saccharin (449%) and sucralose increased (407%) (fig.4.3.10). Therefore, exposure to AS might increase the bacterial adhesion (pathogenic potential) to the mammalian cells.

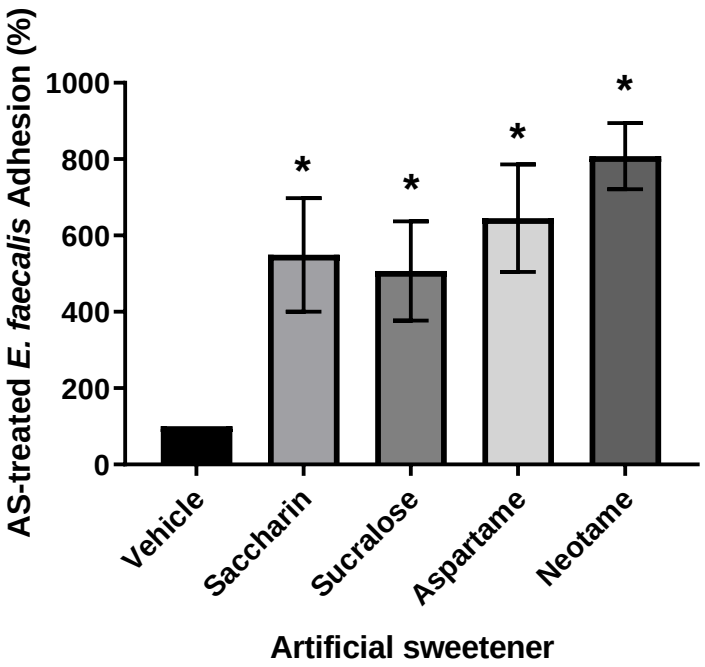

Figure 4.3.10: Adhesion level of *E. faecalis* to intestinal epithelial cells.

Caco-2 cells treated with different concentrations of saccharin, sucralose, aspartame, and neotame or vehicle were co-cultured with 100 µM of AS-treated bacteria at the same multiplicity of infection (MOI 1:300) and infections were performed for an hour. Mammalian cells were washed twice to remove non-adhered bacteria and lysed with 0.5% Triton X-100. Colony-forming units (CFU) were measured using standard plate count method. Adhesion was calculated as the percentage (normalised with control, 100%) of CFU/cell and presented as the mean ± S.E.M., n=4. Data were analysed using Ordinary one-way ANOVA with Holm-Sidak multiple comparisons test. *p<0.05 versus vehicle.

4.3.3 Effect of AS on model gut bacterial invasiveness

4.3.3.1 Method validation

Since Caco-2 cells and bacteria were co-cultured in presence of the antibiotic, the antibiotic concentrations were tested to confirm bacterial extermination without affecting cell viability. The bacterial concentration and dilution factor for cell lysate were determined prior to the invasion assay with AS, to ensure the assay was effective and sensitive.

4.3.3.1.1 Effect of antibiotics on Caco-2 cell viability

To ensure the antibiotics used do not impact Caco-2 cell function, the cell viability assay was performed first. None of the antibiotics, Gentamicin (fig.4.3.11.a), ampicillin and meropenem (fig.4.3.11.b), affected cell viability, as observed from the CCK-8 assay. Similar results were observed for the combination of gentamicin and ampicillin (fig.4.3.11.c). Although the combination of gentamicin and meropenem reduced viability marginally (100

µg/ml gentamicin and 100 µg/ml meropenem), however, there was no significant differences in the viability of Caco-2 cells (fig.4.3.11.c).

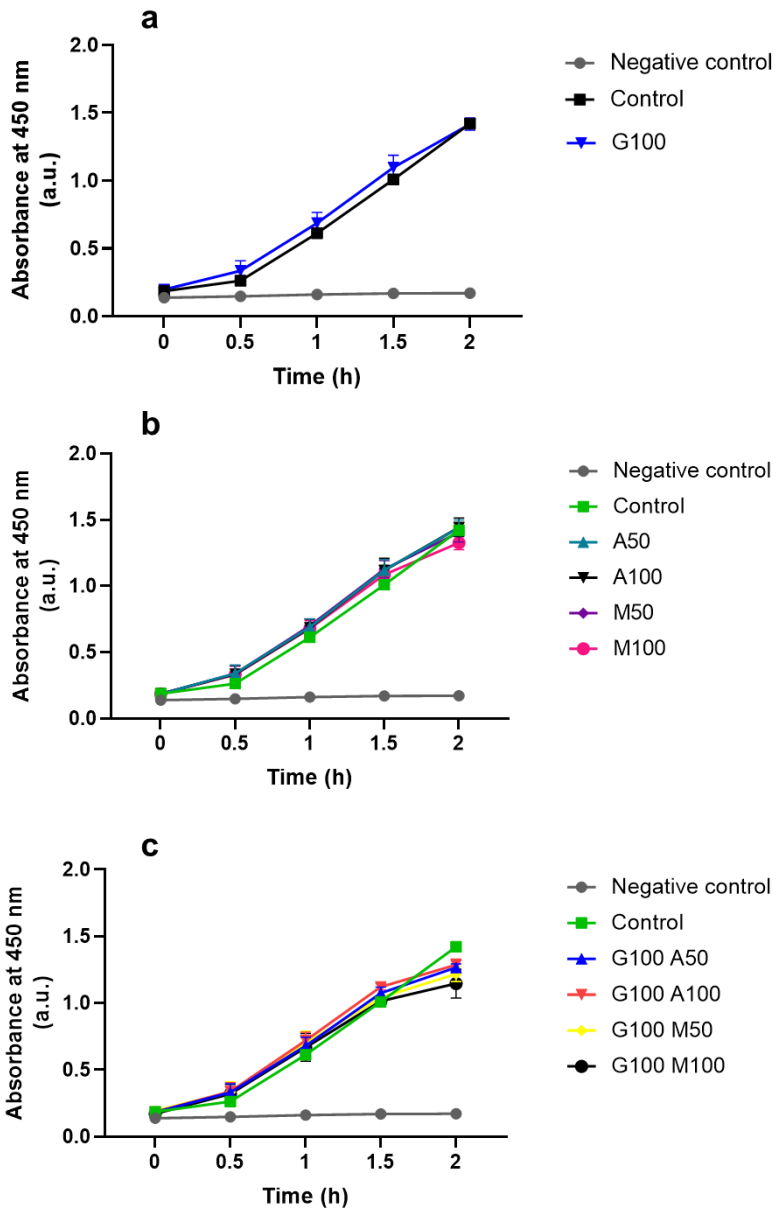

Figure 4.3.11: Effect of different antibiotics and their concentrations on Caco-2 cell viability.

Caco-2 cells (1×10^4 cells/well) were plated on 96-well plate for 48 hours and was exposed to different concentrations of the antibiotics gentamicin (a), ampicillin (b) and meropenem (b). In addition, cells were exposed to combination of antibiotics (c), gentamicin plus ampicillin, and gentamicin plus meropenem for 0.5 h to 2 hours at 37 ºC with 5% CO_2. The antibiotics were mentioned with the first letter of the name and the concentration was in µg/ml. CCK-8 reagent was added and incubated at the same incubation condition. Plates were read at different time points for absorbance at 450 nm. Cell viability remained unaffected for antibiotic concentrations and exposure duration. Data presented as the mean, n=2-3.

4.3.3.1.2 Model bacterial sensitivity to the antibiotics

MGB *E. coli* was sensitive to gentamicin, and the *E. faecalis* was sensitive to the combination of gentamicin and ampicillin. Gentamicin completely inhibited *E. coli* growth (fig.4.3.12), therefore, at 1 hour the control without antibiotic started to show growth but antibiotic-exposed bacterial absorbance remained like blank.

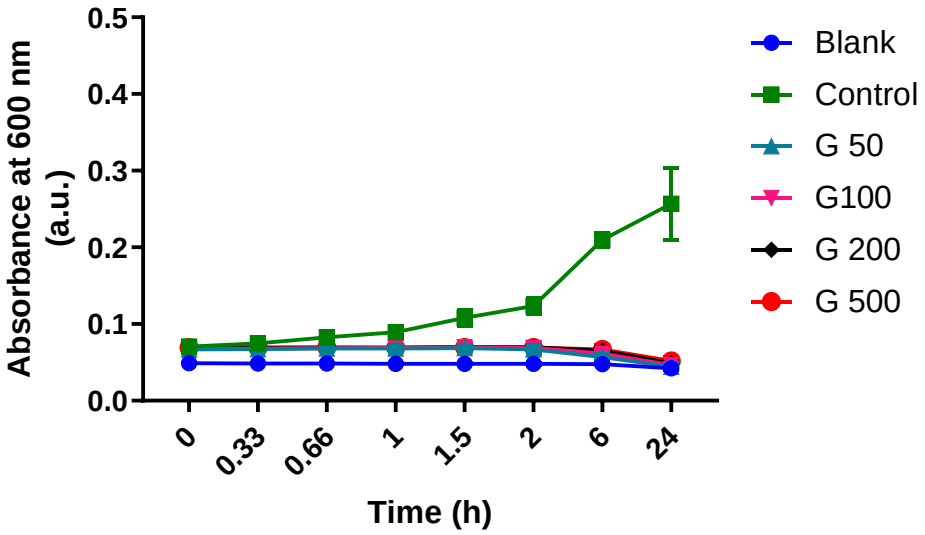

Figure 4.3.12: Effect of gentamicin on *E. coli* growth.

All the concentrations of gentamicin inhibited *E. coli* growth. After 1 hour, the control started to grow and a difference between gentamicin treatments and the vehicle was observed at 1.5 hour. *E. coli* was grown in 96-well plate in 100 µl of Nutrient broth with gentamicin or vehicle. Growth was measured as absorbance at 600 nm using PerkinElmer (Victor X3). Data are presented as the mean ± S.E.M., n=2.

Conversely, *E. faecalis* strain demonstrated resistance to aminoglycoside antibiotic gentamicin for concentrations as high as 500 µg/ml. A dose-dependent inhibition was observed, and the highest concentration of 1000 µg/ml completely killed bacteria at 24 hours (fig.4.3.13). 100 µg/ml gentamicin reduced bacterial growth (0.1 a.u., A_{600}) at 6 hours.

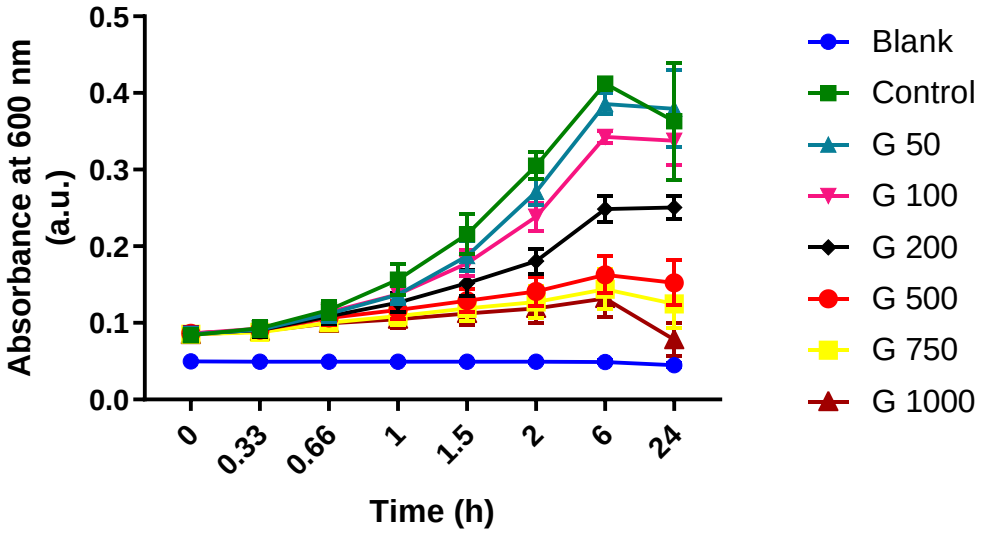

Figure 4.3. 13: *In vitro* activity of gentamicin against *E. faecalis* ATCC 19433.

Gentamicin concentrations are expressed in µg/ml. A concentration-dependent inhibition was observed although complete inhibition was found for the highest concentration (1000 µg/ml) at 24 hours. *E. faecalis* was grown in 96-well plate in 100 µl of Brain Heart Infusion supplemented with a range of gentamicin concentrations or vehicle. Growth was measured as absorbance at 600 nm using PerkinElmer (Victor X3). Data are presented as the mean ± S.E.M., n=3.

Ampicillin, the first 'broad-spectrum' penicillin inhibited *E. faecalis* growth at all concentrations, although marginal increase was found for 50 µg/ml at 1.5 hour (fig.4.3.14.a). Likewise, the carbapenem antibiotic meropenem also completely inhibited *E. faecalis* growth (fig.4.3.14.b). The combination of gentamicin and ampicillin/meropenem showed similar results like meropenem for all the concentrations (Fig.4.3.14.c,d).

Depending on findings from MIC tests, gentamicin (100 µg/ml) was chosen for *E. coli*, and combination of gentamicin (100 µg/ml) and ampicillin (50 µg/ml) was chosen for *E. faecalis* for the invasion assay. Previous study with human epithelial cell also used a combination of ampicillin (200 ug/ml) and gentamicin (300 ug/ml) for invasion assay (Inaba et al., 2019).

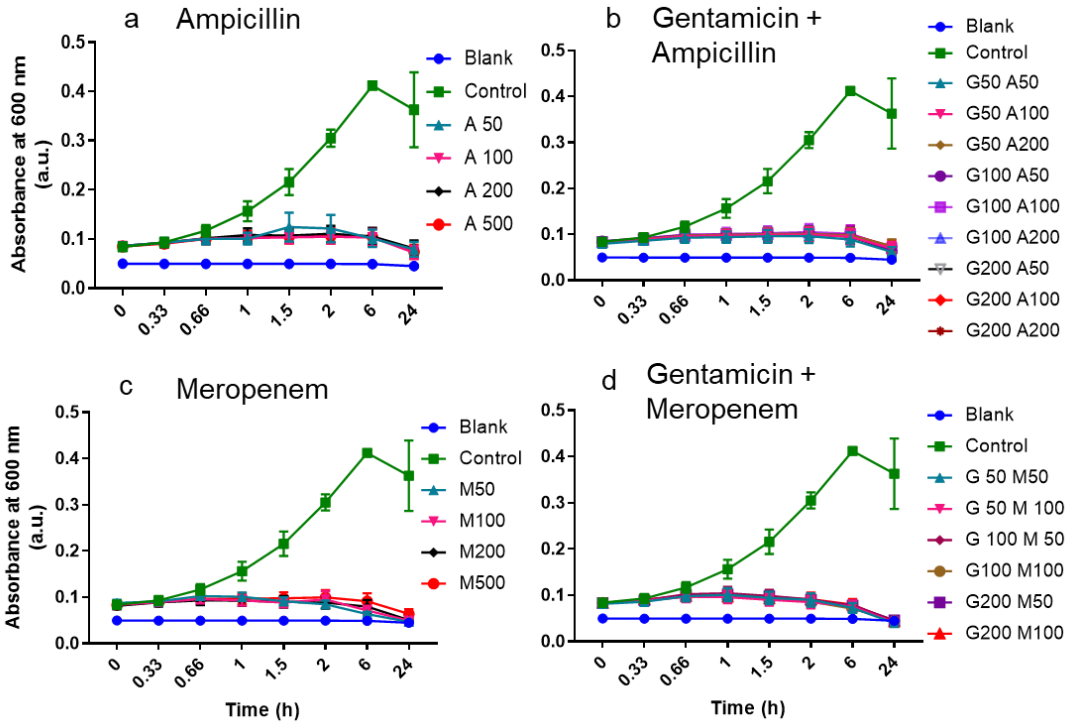

Figure 4.3.14: Antibiotic activity against *E. faecalis* ATCC 19433 in Brain Heart Infusion.

All antibiotics are expressed as the first letter of their names, and concentrations are in µg/ml. Both ampicillin (a) and meropenem (c) inhibited bacterial growth individually and in combination of gentamicin plus ampicillin (b), and gentamicin plus meropenem (d). Growth was measured as absorbance at 600 nm (PerkinElmer, Victor X3). Data are presented as the mean ± S.E.M., n=2, each containing 3 replications.

4.3.3.2 Effect of AS on model gut bacterial invasion into Caco-2 cell

4.3.3.2.1 Untreated bacterial invasion to AS-exposed Caco-2 cells

Effect of AS on gut bacterial invasion into the IECs was quantified by employing antibiotic protection assay, invasion percentage are presented for *E. coli* (fig.4.3.15) and *E. faecalis* (fig.4.3.16).

Both saccharin and sucralose significantly increased *E. coli* invasion in AS-treated Caco-2 cells at 1 µM (fig.4.3.15. a and b, respectively), whereas aspartame and neotame increased at the lowest concentration of 0.1 µM (fig.4.3.15. c and d, respectively). Aspartame also increased invasion at 100 µM concentration, however, none of the other concentrations of neotame caused significant *E. coli* invasion to Caco-2 cells.

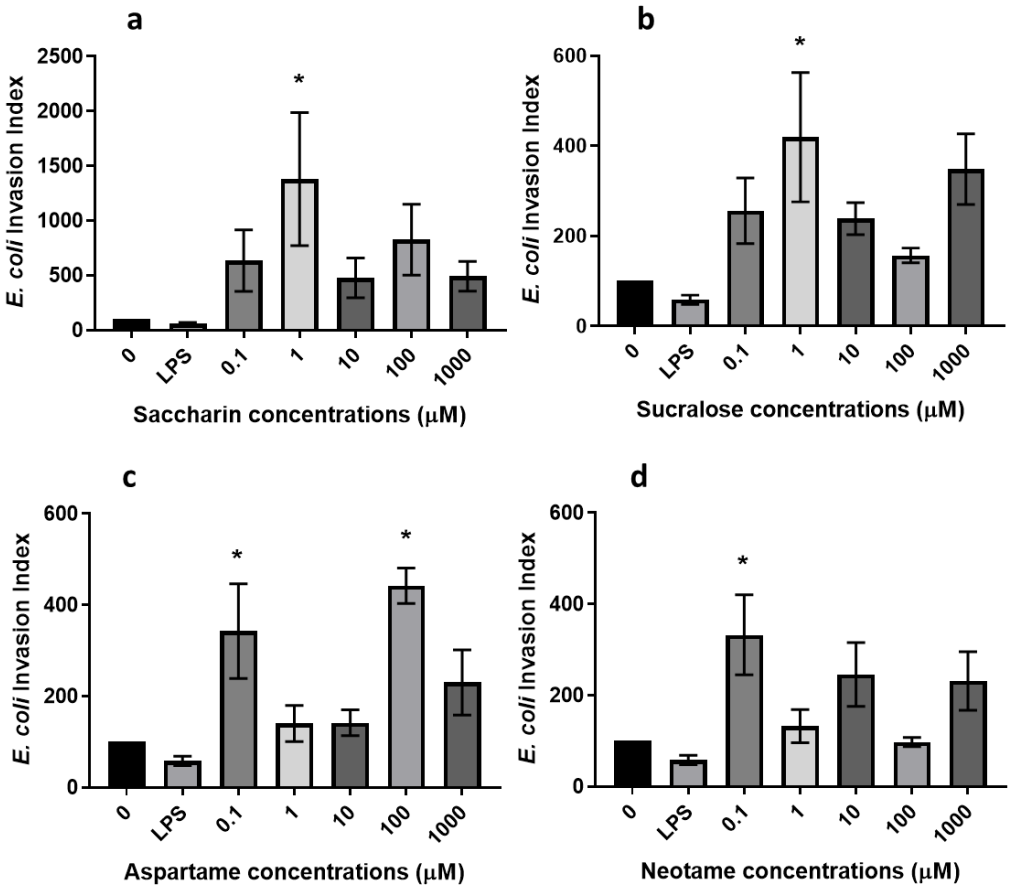

Figure 4.3.15: Effect of AS on *E. coli* invasion to intestinal epithelial cells.

Caco-2 cells were exposed to different concentrations of saccharin(a), sucralose(b), aspartame(c), neotame(d) or vehicle and co-cultivated with bacteria at multiplicity of infection (MOI 1:300) for an hour. Washing removed non-adhered and gentamicin (100 µg/ml) killed adhered bacteria. Cells were lysed (0.5% Triton X-100) and colony-forming units (CFU) were measured using standard plate count method. Invasion was calculated as percent CFU/cell and normalised with control (100%). Panel a has higher percentage value and the 'y' axis has higher value than other panels. Data were analysed using ordinary one-way ANOVA with Holm-Sidak multiple comparisons test and presented as the mean ± S.E.M. n=4. *p<0.05 versus vehicle.

Untreated *E. faecalis* did not demonstrate invasion ability to a large extent (fig.4.3.16). Treating Caco-2 cells with saccharin and neotame did not cause *E. faecalis* invasion at concentrations ranging from 0.1 µM to 1 mM (fig.4.3.16. a and c, respectively). Sucralose increased invasion approximately 100% at 0.1 µm concentration (fig.4.3.16.b) and aspartame at 100 µm (fig.4.3.16.c), none of the other concentrations of sucralose and aspartame affected the model gut bacterial invasiveness.

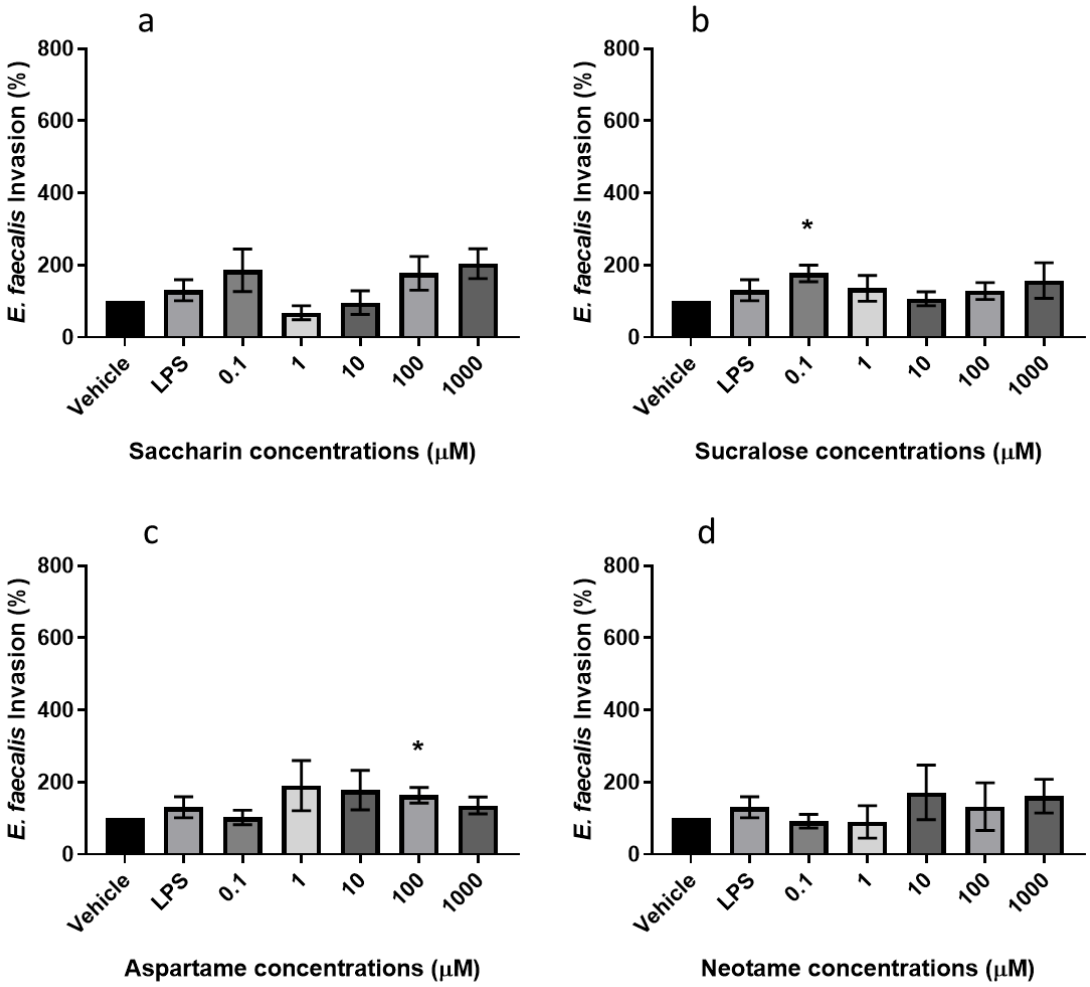

Figure 4.3. 16: Effect of AS on *E. faecalis* invasion to intestinal epithelial cells.

Caco-2 cells were treated with different concentrations of the artificial sweeteners saccharin (a), sucralose (b), aspartame (c) and neotame (d) or vehicle and were co-cultured with *E. faecalis* (MOI 1:300) for an hour. Mammalian cells were washed twice to remove non-adhered bacteria and 100 µg/ml gentamicin was used to kill surface adhered bacteria. Caco-2 cells were lysed with 0.5% Triton X-100 and the standard plate count method was performed to measure the colony-forming units (CFU). Invasion percentage of CFU/cell was measured, and data were normalised with control as 100%. Data are analysed using ordinary one-way ANOVA followed by uncorrected Fisher's LSD test and presented as the mean ± S.E.M., n=4. *p<0.05 versus vehicle.

4.3.3.2.2 AS-exposed bacterial invasion to AS-exposed Caco-2 cells

Mimicking the gut milieu, both bacteria and IEC were exposed to AS prior co-cultivation to assess their effect on bacterial invasion ability (fig.4.3.17 and fig.4.3.18). Saccharin exposure did not cause *E. coli* invasion to Caco-2 cells, other AS significantly increased (close to 150%) *E. coli* invasion to AS-exposed Caco-2 cells compared to vehicle (fig.4.3.17.a).

The IEC-GM interactions were observed microscopically to understand the invasion pattern (representative images shown in appendix C). Control *E. coli* (fig.C8.5) and *E. faecalis* (fig.C8.7) did not show invasion, AS-treated *E. coli* and *E. faecalis* invasion patterns were

also indistinctive (fig.C8.6 and fig.C.8.8, respectively). The AS-exposed bacteria showed more invaded bacteria in comparison to the control, *E. coli* represented higher invasion ability than *E. faecalis* and the former was diffusely accumulated on the Caco-2 cells (fig.C8.6.b,c). Like adhesion, the rod-shaped invaded *E. coli* was dispersed into cell islands avoiding the large vacuoles and inter-island spaces. AS-treated *E. faecalis* demonstrated small clusters; the cocci also formed characteristic short-chains or pairs (diplococci) or remained isolated and scattered (fig.C8.8).

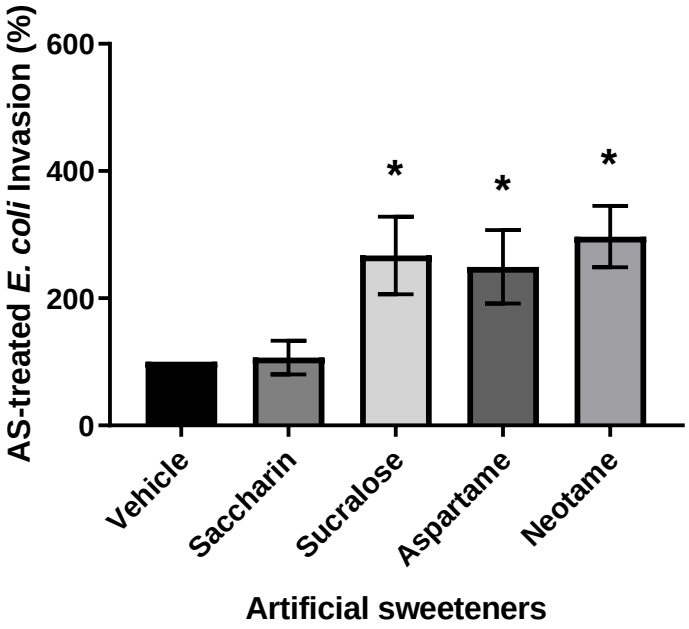

Figure 4.3.17: Invasion of *E. coli* to intestinal epithelial cells in co-infection experiments.

AS-treated Caco-2 cells were co-cultivated with AS-treated (100 μM) or vehicle-treated *E. coli* at multiplicity of infection (MOI), 1:300 for an hour. Surface bacteria were killed using antibiotic treatment for 0.5 hour, and invaded bacteria were released through lysis (0.5% Triton X-100). The standard plate count method was performed to measure colony-forming units (CFU). Invasions are expressed as percentage of CFU/cell. Data were normalised with control (100%), analysed using ordinary one-way ANOVA with Uncorrected Fisher's LSD test and presented as the mean ± S.E.M., n=4. *p<0.05 versus vehicle.

All AS significantly increased treated *E. faecalis* invasion into Caco-2 cells (fig.4.3.18). Neotame caused the highest invasion (398%), nearly double of other three. Saccharin increased invasion (163%) followed by aspartame (127%) and sucralose (121%) (fig.4.3.18).

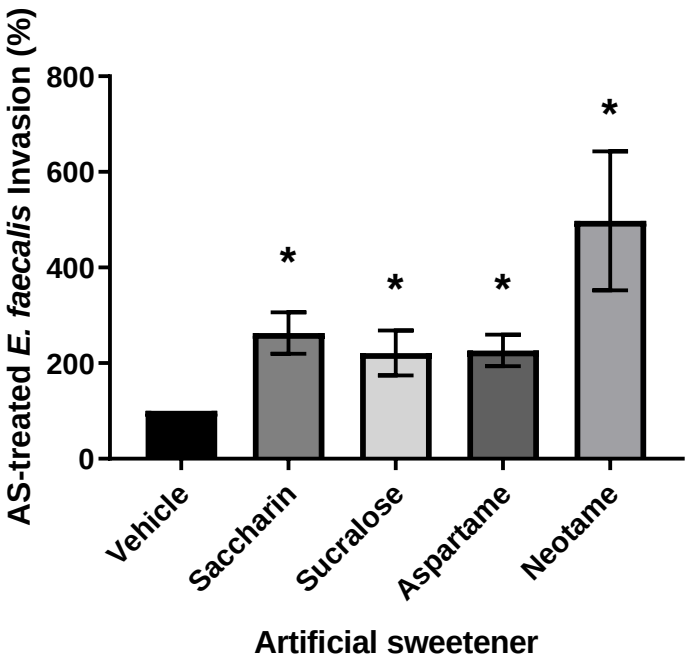

Figure 4.3.18: Effect of AS on the *E. faecalis* invasion ability to Caco-2 cells.

AS- or vehicle-treated Caco-2 cells were co-cultivated for an hour (MOI 1:300) with *E. faecalis* treated with AS. Gentamicin was used to get rid of adhered *E. faecalis*, total CFU/cell were counted and data were normalised with control (100%). Data are analysed using ordinary one-way ANOVA followed by uncorrected Dunn's test and presented as the mean ± S.E.M. n=6. *p<0.05 versus vehicle.

4.3.4 Effect of sweet taste inhibitor on bacterial pathogenic factors

$ZnSO_4$ was used as a pan-inhibitor of sweet sensing to assess whether it can prevent model gut bacterial pathogenic effect on IECs. The effect of inhibition was assessed on bacterial cytotoxicity, adhesion, and invasion to Caco-2 cells.

4.3.4.1 Cytotoxic effect of bacterial metabolites

4.3.4.1.1 $ZnSO_4$ concentrations did not affect cell viability

Effect of $ZnSO_4$ on Caco-2 cell viability and model gut bacterial growth was determined to confirm that effect is not via cytotoxicity. Cell viability was unaffected at concentrations ranging from 0.1 to 500 µM; absorbance was above 0.93 (a.u.) for all concentrations (fig.4.3.19).

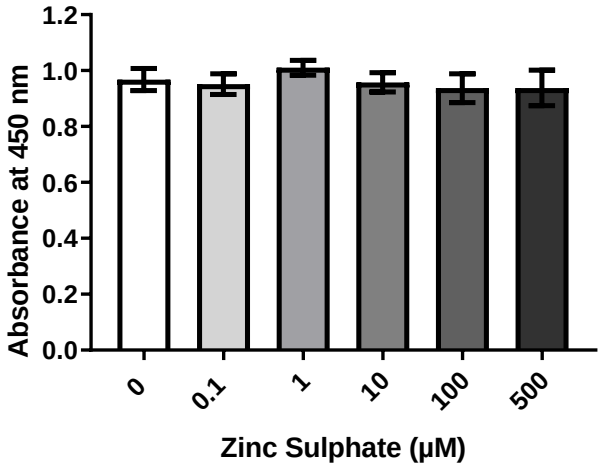

Figure 4.3.19: Effect of $ZnSO_4$ on Caco-2 cell viability.

Cells were seeded on 96-well plates (1×10^4 cells/well) and maintained for 48 hours at standard tissue culture conditions. The used media was replaced with EMEM supplemented with ZnSO4 concentrations and incubated for 24 hours. CCK-8 assay was performed, and viability was measured as absorbance at 450 nm (Tecan Sunrise™). Data were analysed using Uncorrected Dunn's test and presented as mean and S.E.M., n=6.

$ZnSO_4$ decreased *E. coli* and *E. faecalis* growth marginally in comparison to the vehicle (fig.4.3.20). No significant inhibition was found and difference between medians of *E. coli* results was 0.0595 (p=0.9546) and *E. faecalis* was 0.0825 (p=0.6009).

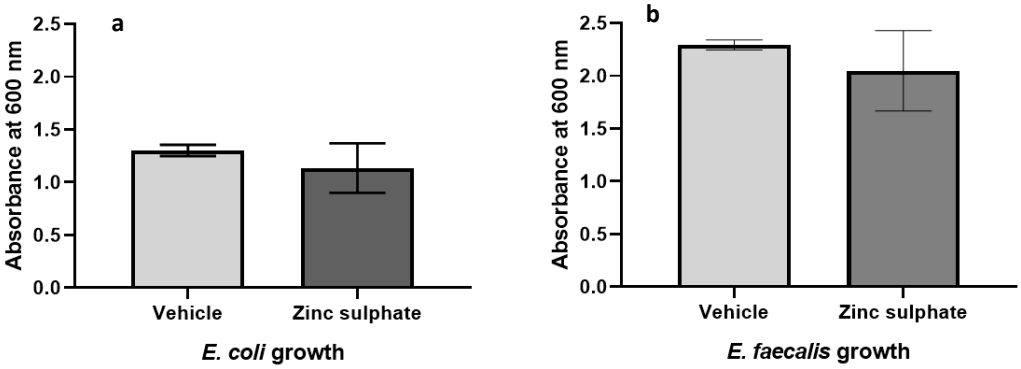

Figure 4.3.20: Effect $ZnSO_4$ on model gut bacterial growth.

A single *E. coli* (a) or *E. faecalis* (b) colony was inoculated into 10 ml of Nutrient broth or Brain Heart infusion, respectively containing $ZnSO_4$ (100 μM) or vehicle and incubated for 24 hours. The optical density was measured by spectrophotometry (EppendorfBioPhotometer). Data were analysed using the nonparametric test followed by Mann Whitney test and presented as mean and S.E.M, n=6.

4.3.4.1.2 Effect of sweet taste inhibition on AS-mediated changes in bacterial metabolites

To evaluate whether STR is involved in the cytotoxic effect of AS-mediated bacterial metabolites on mammalian cells, gut bacteria was exposed to AS in presence of $ZnSO_4$, and IEC monolayer was exposed to the resultant bacterial metabolites (fig.4.3.21 and

fig.4.3.22). Previous studies revealed that the $ZnSO_4$ concentration was non-toxic to Caco-2 cells and MGB.

$ZnSO_4$-treated *E. coli* metabolites significantly reduced Caco-2 cell viability compared to control (without $ZnSO_4$). As appeared in fig.4.3.21, almost no changes in viability occurred for *E. coli* metabolites for $ZnSO_4$ co-exposure with saccharin and sucralose. Aspartame and neotame with $ZnSO_4$ reduced cell viability by 18% and 15.3%, respectively. However, viability was increased by 12.5% (aspartame) and 15.1% (neotame) compared to the vehicle (with $ZnSO_4$) (fig.4.3.21).

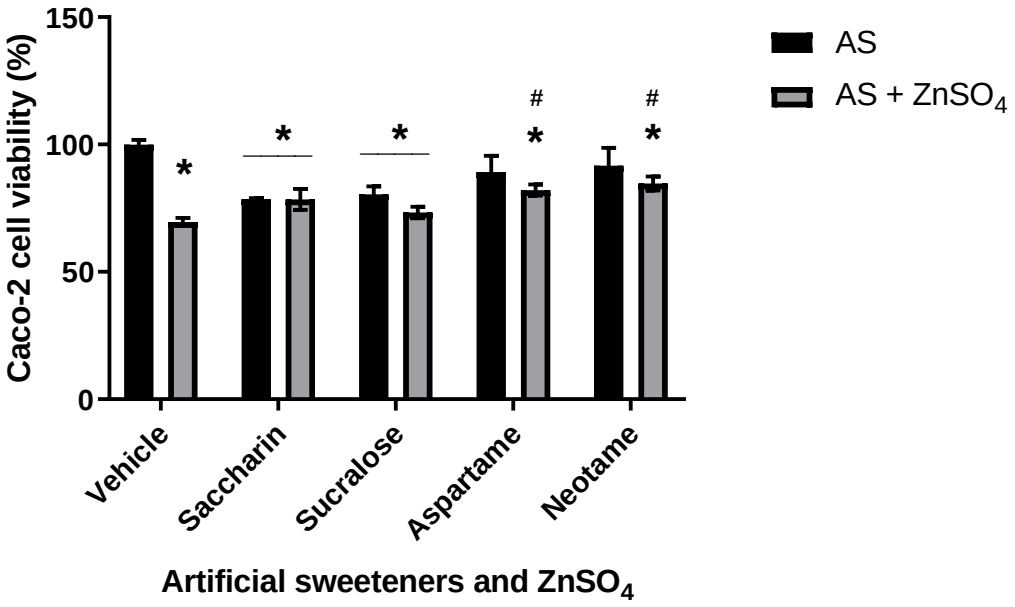

Figure 4.3.21: Effect of $ZnSO_4$ on AS-mediated changes in *E. coli* affecting Caco-2 cell viability.

E. coli was exposed to AS with $ZnSO_4$ or vehicle for 24 hours. Cells were seeded in 96-well plate (1×10^4 cells/well) and maintained for 48 hours. Cells were exposed to the bacterial culture supernatant for 18 hours. CCK-8 assay was performed, and viability was measured as absorbance at 450 nm (PerkinElmer). Data were analysed using ordinary one-way ANOVA with Holm-Sidak's multiple comparisons test and presented as the mean ± S.E.M., n=3. *p<0.05 versus control and #p<0.05 versus vehicle.

AS and $ZnSO_4$ exposed *E. faecalis* metabolites showed a differential effect on Caco-2 cell viability (fig.4.3.22). The vehicle (with $ZnSO_4$) marginally (11.5%) increased viability. A similar outcome was found for sucralose and $ZnSO_4$, viability increased by 19% compared to only sucralose-exposed metabolites. Other three AS-exposed *E. faecalis* metabolites, with $ZnSO_4$ reduced cell viability, the highest reduction was observed for saccharin (37.5%), followed by neotame (36%), and minor reduction for aspartame (9%). However, *E. faecalis* metabolites mediated changes of Caco-2 cell viability that were insignificant for all AS compared to control or the vehicle (fig.4.3.22).

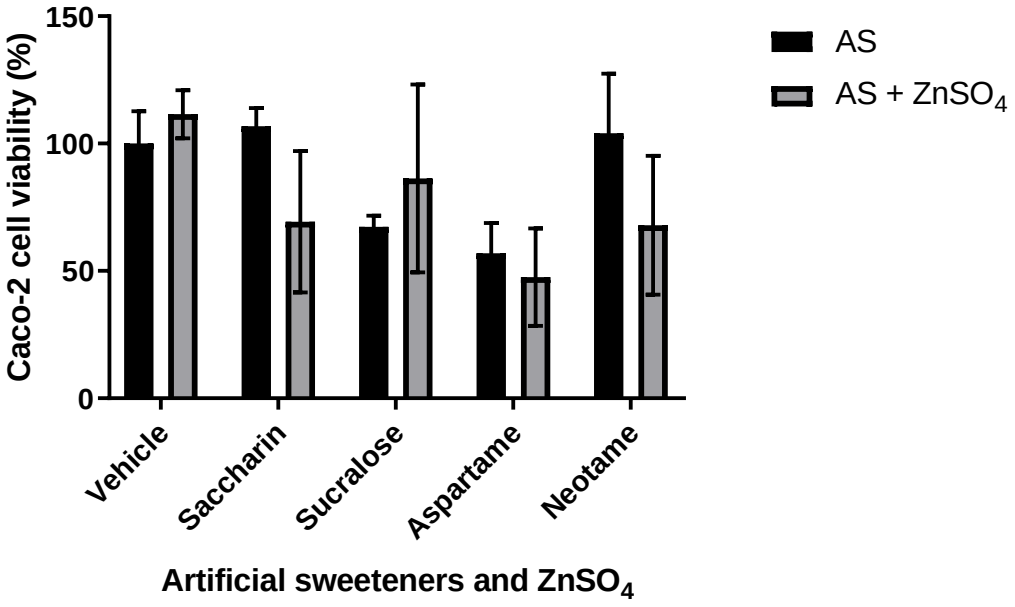

Figure 4.3.22: Viability of Caco-2 cells exposed to AS ± $ZnSO_4$-treated *E. faecalis* metabolites.

Bacteria were exposed to vehicle or AS with/out $ZnSO_4$ for 24 hours and culture supernatant was collected. Simultaneously maintained Caco-2 cell monolayer was exposed to the bacterial supernatant for 18 hour and CCK-8 assay was performed. Cell viability was measured as absorbance at 450 nm (PerkinElmer) and viability was normalised with control (100%). Data were analysed using ordinary one-way ANOVA with Holm-Sidak's multiple comparisons test and presented as the mean ± S.E.M., n=3.

4.3.4.2 $ZnSO_4$ decreased model gut bacterial adhesion

$ZnSO_4$ inhibits the sweet sensing of many sweet molecules including the AS (Keast, 2003). Because AS-exposure increased model gut bacterial adherence to the IECs, $ZnSO_4$ was employed to investigate whether this can reduce bacterial pathogenicity, implying the involvement of sweet sensing with gut bacterial adherence. $ZnSO_4$ vehicle did not change *E. coli* and *E. faecalis* adherence to Caco-2 cell compared to control (fig.4.3.23 and fig.4.3.24, respectively).

Saccharin, sucralose and aspartame, all significantly increased *E. coli* adherence to Caco-2 cells, however, $ZnSO_4$ co-exposure reduced the effect. Also, neotame itself insignificantly increased *E. coli* adherence by 88%, and $ZnSO_4$ co-exposure condensed the effect by 77.5% (fig.4.3.23).

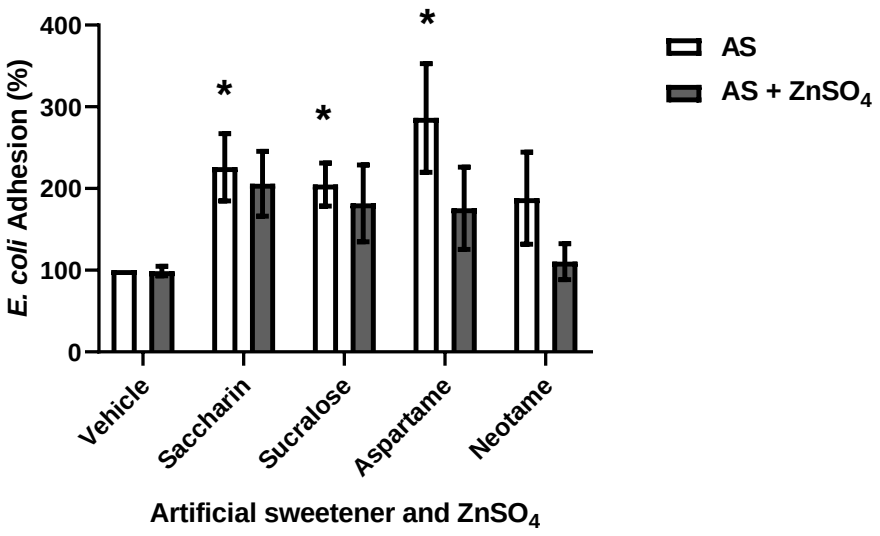

Figure 4.3.23: Effect of $ZnSO_4$ on AS-mediated *E. coli* adherence to Caco-2 cells.

E. coli was treated with 100 µM of AS ± $ZnSO_4$ or vehicle and co-cultivated (MOI 1:300) with AS-treated Caco-2 cells for an hour. Non-adhered bacteria were washed away with PBS and cells were lysed with 0.5% Triton X-100. The diluted cell lysate was plated to count colony-forming units. Invasion percent (CFU/Caco-2) was calculated and normalised with control (100%). Data were analysed using Holm-Sidak's multiple comparison test, presented as the mean ± S.E.M., n=4. *p<0.05 versus vehicle.

AS significantly increased *E. faecalis* adherence to Caco-2 cells and neotame caused the highest adherence. $ZnSO_4$ co-exposure reduced the AS-mediated *E. faecalis* pathogenic factor/s related to adhesion, it has abridged the adherence for the AS (fig.4.3.24).

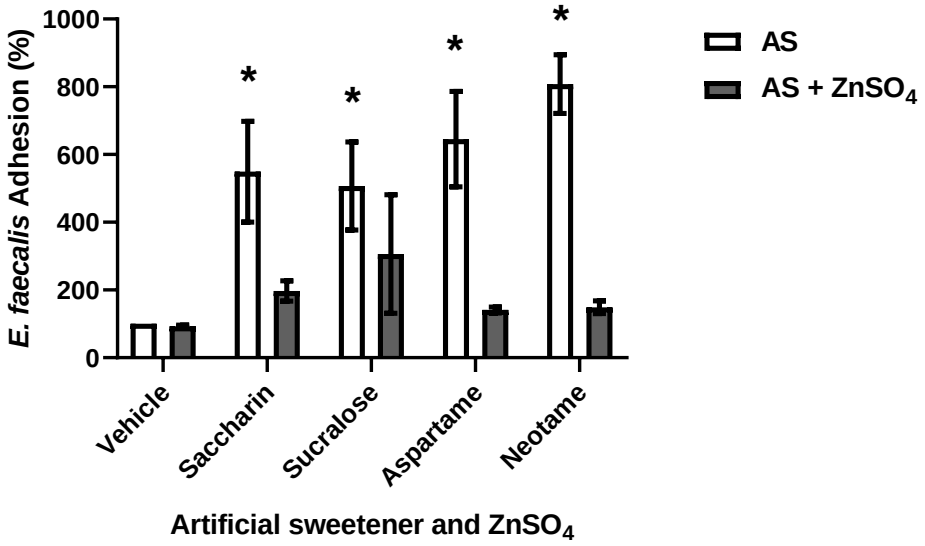

Figure 4.3.24: $ZnSO_4$ inhibition of the AS-mediated *E. faecalis* adherence to Caco-2 cells.

AS-treated Caco-2 cells were co-cultivated for an hour with AS±$ZnSO_4$-treated *E. faecalis* (MOI, 1:300). Non-adhered bacteria were washed away, and both adhered and internalized bacteria were counted, and normalised with 100% of control. Data were analysed using ordinary one-way ANOVA followed by Holm-Sidak's multiple comparison test and presented as the mean ± S.E.M., n=6(AS), 3(AS+$ZnSO_4$). *p<0.05 versus vehicle.

4.3.4.3 $ZnSO_4$ co-exposure inhibited AS-mediated bacterial invasion

Since AS-exposure significantly increased gut bacterial ability to invade IECs, the hypothesis whether inhibiting the sweet sensing interfere with invasiveness was tested. For that purpose, the invasion efficiency of MGB upon exposure to AS with $ZnSO_4$ was determined using the antibiotic protection assays. Results of these clearly demonstrated an inhibitory effect of $ZnSO_4$ on the invasiveness of the MGB *E. coli* (fig.4.3.25) and *E. faecalis* (fig.4.3.25).

$ZnSO_4$ co-exposure reduced *E. coli* invasion by 120% for neotame, followed by 84% and 40% for aspartame and sucralose, respectively. Conversely, saccharin increased *E. coli* invasiveness by 63% in presence of $ZnSO_4$ (fig.4.3.25).

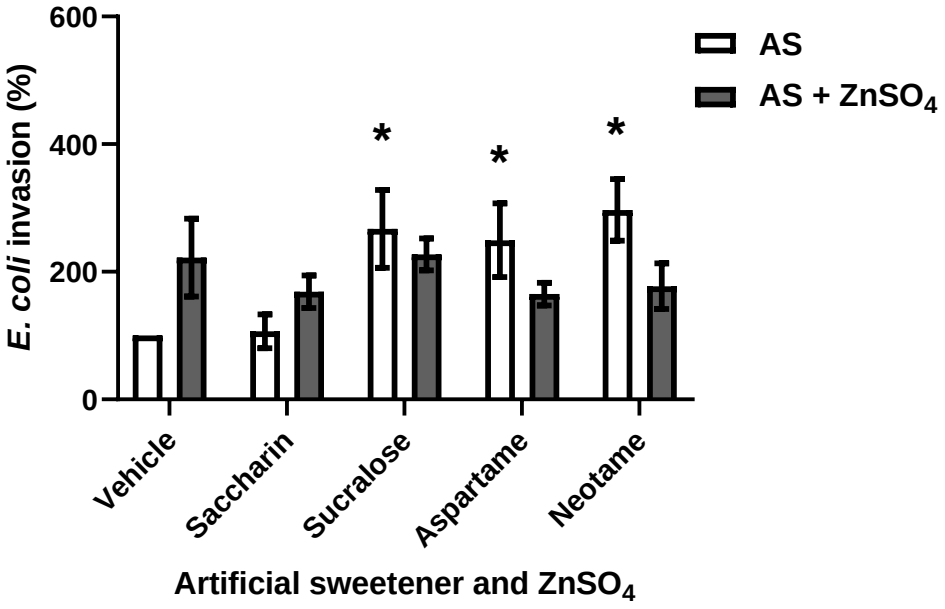

Figure 4.3.25: Effect of AS and $ZnSO_4$ on the invasion level of *E. coli* to Caco-2 cells.

Mammalian cells were treated with AS or vehicle, and *E. coli* was treated with AS ± $ZnSO_4$ or vehicle, and co-culture was performed for an hour (MOI, 1:300). Adhered cells were killed using gentamicin and total CFU per cell was counted using standard plate count. Data were normalised with 100% of control. Data analysed using ordinary one-way ANOVA followed by Holm-Sidak's multiple comparison test and are presented as the mean ± S.E.M., n=5. *p<0.05 versus vehicle.

In the co-culture experiment of gentamicin and ampicillin protection assay for *E. faecalis*, the invasiveness of the bacteria was determined in the presence and absence of $ZnSO_4$ with AS (fig.4.3.26). The invasion percentage of *E. faecalis* into Caco-2 cells were reduced by 404% (neotame) and 64% (sucralose) in presence of $ZnSO_4$. However, inhibition of *E. faecalis* invasion by $ZnSO_4$ for the AS was insignificant (p=0.3-0.5, *E. coli*; and p=0.2-0.4, *E. faecalis*; multiple t-tests with Holm-Sidak's test).

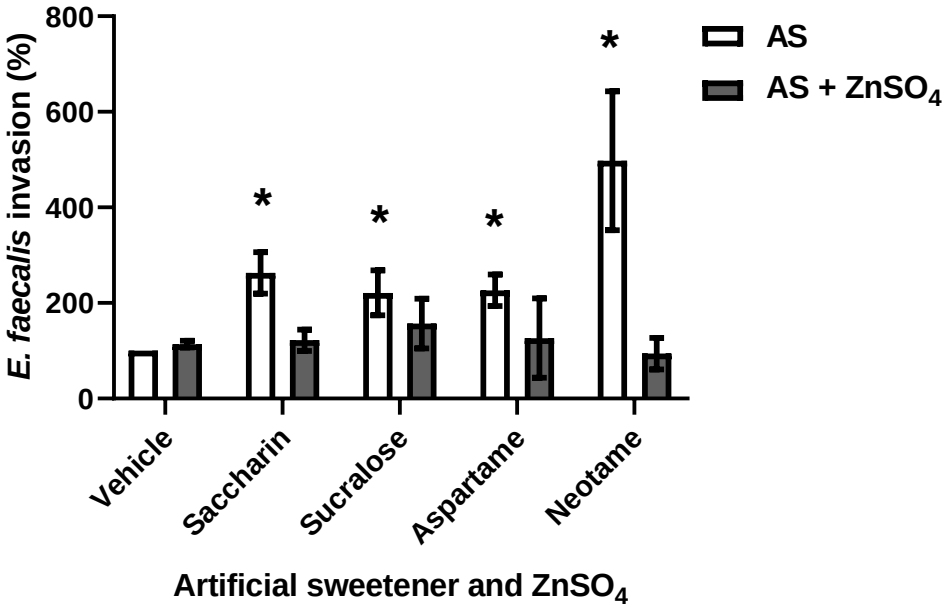

Figure 4.3.26: Effect of AS and $ZnSO_4$ on the *E. faecalis* invasion ability into Caco-2 cells.

AS- or vehicle-treated Caco-2 cells were co-cultivated for an hour (MOI 1:300) with *E. faecalis* treated with AS ± $ZnSO_4$ or vehicle. Treating bacteria with AS significantly increased their ability to invade Caco-2 cells, however, the use of $ZnSO_4$ reduced invasion. Combination of gentamicin (100 µg/ml) and ampicillin (50 µg/ml) was used to get rid of adhered *E. faecalis*, total CFU/cell were counted, and normalised with control (100%). Data were analysed using ordinary one-way ANOVA followed by uncorrected Dunn's test and presented as the mean ± S.E.M. n=3. *p<0.05 versus vehicle.

4.4 Discussion

AS perturbs the homeostatic GM and interferes with bacteria-intestinal epithelium interaction leading to MD development (Suez et al., 2014). Therefore, AS might have the capacity to alter good bacteria to pathogen by stimulating virulence factors although the mechanisms remained unclear. This chapter aims to investigate AS- mediated changes in gut bacteria-enterocytes interactions.

Interaction with the IECs is a major element of the virulent activity of the intestinal pathogens. AS comes in direct contact with the gut bacteria, therefore, any influence on bacterial quorum sensing and/or metabolism might have a cytotoxic effect on the IECs. In addition, adhesion of gut bacteria on the intestinal enterocytes prevents their elimination by the clearing mechanism of the intestine. AS can stimulate gut microbial adherence or increase enterocytes' susceptibility to microbes. Besides, adhered bacteria can trigger other biological responses in host cell by inducing surface receptor-associated signalling pathways. A further hallmark of pathogenicity is the ability of intrusion of virulent gut microbes into non-phagocytic host cells. Many pathogens cause intense changes in host cell anatomy and function through a series of mechanisms mediated by exocellular factors and/or direct interactions between prokaryotic-eukaryotic cells (Minnaard et al., 2004; Sears and Kaper, 1996). So, studying pathogenic responses in gut bacteria-intestinal enterocytes interactions upon AS exposure is justified.

Most intestinal microflora studies have used rodents as models or used faecal samples of the human host. These are easier to perform compared to humans, however, the extrapolated data from rodents have misleading interpretations for the physiological and metabolic differences between humans and rodents (Daly et al., 2016). Also, most published human microbiome studies have used faecal specimens since this is easier to collect. However, faecal samples are inappropriate representatives of non-pathogenic microflora of the oesophagus region. Similarly, it is a poor representative of proximal gastrointestinal tract and the mucosa-inhabited microflora (Hollister et al., 2014).

Despite some limitations of the single lineage monoculture systems to represent the complex biological processes occur *in vivo*, *in vitro* models based on single cell types provide key information on a cell type's reaction to certain treatment/microbe. In addition, such monocultures provide an efficient and economical way of avoiding a wide range of experimental variables. Therefore, considering the available technical supports, a well-established IEC model was used for the co-culture studies.

The intestinal epithelium has continuously renewing cell system, the cells differentiate as they migrate along the crypt-villus axis (Van Der Flier and Clevers, 2009). The differentiation of the enterocytes regulates the cell accessibility of receptors for bacterial adhesins and

invasins (Kerneis et al., 1992; Isberg and Leong, 1990). The confluent monolayers demonstrate both phenotypically and functionally the property of typical enterocytic differentiation due to the formation of TJs (Lea, 2015; Coconnier et al., 1994). In addition, invasion of atypical enteropathogenic *E. coli* into the HeLa cells was dependent on the actin filaments (Yamamoto et al., 2009). Also, disruption of TJ in the T84 cells enhanced the bacterial invasion efficiency (Yamamoto et al., 2009). The plasma membrane segregates into apical and basolateral domains, these changes mimic the IECs (Lea, 2015). So, it is already accepted that the enterocyte differentiation regulates the availability of cell receptors for bacterial adhesion and invasion (Yamamoto et al., 2009; Rosa et al., 2001). Therefore, using the enterocyte cell model Caco-2 for these experiments, which demonstrate the biological responses in bacteria-intestinal epithelium contact is reasonable.

Despite their intensity and diversity, most gut bacterial species cannot be cultured *in vitro*, and co-culturing gut bacteria and human cells is even more challenging (Allen-Vercoe, 2013). The major complication in a host-microbiome co-culture system is that above 90% of the gut bacteria are obligate anaerobes, while human cells depend on oxygen, the bacteria die rapidly on exposure to atmospheric conditions (21% O_2). Maintaining both the eukaryotic and bacterial cell co-culture simultaneously is difficult as the growth rate of bacteria is much faster than that of eukaryotic cells (Kim et al., 2010). However, different co-culture methods were established meanwhile (Sadabad et al., 2015) to investigate the host-microbe interactions or the effect of compounds and drugs. Since the present study investigated the changes in morphology and viability of the eukaryotic cells in response to the bacterial secretions, therefore, the co-culture methods were different from Kim *et al*., (2010) who have used it as a screening tool for identifying the beneficial bacterial signal in the GI tract.

Assessing morphological changes are a common way of investigating the cytotoxic effect; the changes in Caco-2 cell morphology co-cultivated with vehicle-exposed model gut bacterial metabolites were observed (fig.4.3.1 and fig.4.3.2). *E. faecalis* metabolites caused small vacuoles in the cell while there were prominent nods in the stress fibres in contrast with control (fig.4.3.2.c). The nuclei structure was similar for both *E. coli* and *E. faecalis* metabolite-treated Caco-2 cells in comparison to the control. However, morphology observation demonstrates physical damage of the cells, while the viability assay represents the effect on the cellular biochemical activity. Also, measuring the cell viability directly represents the number of living cells, which is a more straightforward, precise and better method to measure the cytotoxic effect. Therefore, the effect of AS-mediated bacterial metabolites was studied using the CCK-8 viability assay.

The viability measurement found from cytotoxicity assay could not be compared as no relevant literature was found. The background was maintained using 1:1 of mammalian cell culture media and bacterial media, which is reasonable, however, the control also contained untreated bacterial supernatant. The cytotoxic effect on cell viability could also be measured by FITC-AV apoptosis assay followed by flow cytometric analysis, which might represent exact number of viable, apoptotic and necrotic cells. However, findings from present study provide an idea on cytotoxic effect of AS-mediated metabolites.

Interestingly, saccharin- and sucralose-exposed *E. coli* supernatant decreased Caco-2 cell viability and $ZnSO_4$ addition reduced the effect (fig.4.3.21). On the other hand, *E. faecalis* supernatant did not significantly affect cell viability. Although $ZnSO_4$ increased viability only 11%, however, $ZnSO_4$ with saccharin, aspartame and neotame slightly reduced viability (fig.4.3.22).

Likewise, Rettig *et al*. (2014) also investigated the effect of an AS on metabolic activity of several gut flora of the phyla Bacteroides (*B. fragilis, B. uniformis*) and Firmicutes (*E. faecalis*, *Clostridium sordelli*). They have shown that sucralose caused metabolic inhibition on Bacteroides in a concentration-dependent manner (1.1, 3.3, 5.5, and 11 mg/kg/day), however, it had no significant effect compared to control group on the metabolic activity of the *E. faecalis* at any tested concentrations. These findings support the current results on the cytotoxic effect of *E. faecalis* metabolites on Caco-2 cells (fig.4.3.4.b). Oppositely, sucralose-mediated *E. coli* metabolites reduced Caco-2 cell viability in the present study. Previous findings from Boudeau *et al*. (2003) demonstrated that even though *E. coli* Nissle 1917 bacteria showed a high level of adherence ($p<0.001$) to the IEC (Intestine-407), they did not induce any cytotoxic effect. The *E. coli* Nissle 1917 were non-pathogenic like *E. coli* NCTC 10418, which implies the AS-exposed bacterial metabolites might be responsible for the viability reduction (fig.4.3.4.a).

Although AS-mediated bacterial metabolites did not affect viability, but AS differentially enhanced bacterial adherence to Caco-2 cells. This effect can take place in two ways; Caco-2 cells can generate positive signals for gut bacterial adherence, or bacteria can be stimulated from AS exposure. Bacterial adherence, Caco-2 cell-associated bacteria (adhering and invading), were determined using the plate count method. This could also be measured using Real-Time PCR (Candela et al., 2005), however, another study using both techniques demonstrated no significant statistical difference between the methods (Nawaz et al., 2011).

Bacterial adherence to IECs is the primary step for pathogenic colonisation of pathogens and eventual invasion. This ability also facilitates efficient toxin release on the cell milieu or its entrance into the target cells (Pizarro-Cerdá and Cossart, 2006; Cossart and Sansonetti, 2004). A comparison between adhesion and invasion percentages does not represent

correlation of the pathogenic features. This indicates adhesion and invasion process might have different specific nature. Invasion seems to rely more on specialized receptor molecules, distinct from the receptors responsible for the adherence. Also, adhesion and invasion processes do not show much correlation with concentrations of the AS.

Aspartame caused Caco-2 cell susceptibility to *E. coli* adherence at only 0.1 μM, although saccharin and sucralose caused at 1 and 10 μM, respectively. There might have an opposite connection of the sweet sensing and *E. coli* adherence, aspartame is the lowest in sweetness level, followed by saccharin and sucralose (table-1.1.1). Nonetheless, the response to neotame (6000) does not support this (fig.4.1.9), the intense sweetness might remain unrecognised by the cells for *E. coli* response. Likewise, the exposure of both Caco-2 cells and *E. coli* to neotame did not cause any significant adherence of bacteria, which might have relevance with the previous statement about sweetness level. These findings could not be compared with other studies for limitations of literature.

Opposite to *E. coli*, all concentrations of neotame significantly increased *E. faecalis* adherence to Caco-2 cells. Sucralose also caused adherence at the lowest concentration (0.1 μM), although the percentage is low for all concentrations. The comparatively low sweet molecules, saccharin and aspartame, both caused Caco-2 cell susceptibility at >10 μM concentrations. Other than sweet taste perception, the enterocytes might have different receptors for MGB which therefore differentially influence their adherence in response to the same AS concentrations.

Potential adherence factors that mediate enterococcal virulence include cell surface carbohydrates, cell surface adhesins or their homologs, which share features with cell surface proteins of other Gram-positive bacteria (Lowe et al., 1995), these can act as a collagen adhesion or an aggregation substance (Furumura et al., 2006). However, detailed information on the adhesion promoting factors of *E. faecalis* remain unknown (Archimbaud et al., 2002). Besides, two different glycoproteins, β1 integrins and E-cadherin were already identified in the Caco-2 cells that act as receptors for bacterial entry into enterocytes (Mengaud et al., 1996; Isberg and Leong, 1990). Furumura *et al.* (2006) studied *E. faecalis* adhesion to human epithelial cell lines suggesting 50% and 40.6% adhesion of the studied clinical isolates to the HeLa and Hep-2 cells, respectively. This clearly indicates that adhesion to the epithelial cells is related to pathogenicity.

Both *E. coli* and *E. faecalis* adhesion was significantly increased when Caco-2 cells were treated with different concentrations of the tested AS (fig.4.3.7 and fig.4.3.8, respectively), which remained same when both Caco-2 cells and bacteria were treated with the sweeteners (fig.4.3.9 and fig.4.3.10, respectively), except neotame-treated *E. coli*. However, treating bacteria with AS and $ZnSO_4$ decreased both bacterial adhesion; *E. faecalis* adhesion (fig.4.3.24) was more reduced than *E. coli* adhesion (fig.4.3.23). Only

$ZnSO_4$ did not affect any of the bacterial adherence and the percentage was like the vehicle (fig.4.3.23, fig.4.3.24). Since adherence to IECs is an important prerequisite for pathogenic gut bacterial colonisation and pathogenesis development, inhibition of their adherence ability decreases intestinal colonisation thereby preventing their invasion and subsequent pathogenicity.

Nickerson and Mcdonald (2012) found Crohn's disease-associated *E. coli* strain to be more adhesive to IECs when exposed to the polysaccharide, maltodextrin. This food additive enhanced bacterial adherence to IEC monolayer at both 3- and 6-hour time points, but *E. coli* invasion remained unaffected after maltodextrin exposure. Other than the difference in the bacterial source, they have used HT29 cell line whereas the present study was performed on Caco-2 cells, however, the study might support current findings.

Adhesion of *E. coli* to Caco-2 cells closely resembles the localized adherence like pattern whereas the *E. faecalis* showed small clusters and pairs without any specific patterns as revealed from the images (fig.C8.1 to fig.C8.4) (Scaletsky et al., 2002; Darfeuille-Michaud et al., 1990). Both *E. coli* and *E. faecalis* demonstrated differences in bacterial number and distribution compared to control in the adhesion and invasion assays, however, the effect of different AS was not distinct.

E. coli was dispersed on the cells, and some areas had higher number (fig.C8.2, fig.C8.5), this might occur for different maturation process of the Caco-2 cells and the resulting density of bacterial adherence receptors (Darfeuille-Michaud et al., 1990). On the other hand, adhered *E. faecalis* formed clusters or short-chains or pairs irrespective of the cellular area, with no specific pattern (fig.C8.4). Further studies with the adherence-related DNA probes (Scaletsky et al., 2002) or staining Caco-2 cells and bacteria (Nishikawa et al., 1994), and observation using transmission electron microscopy might give a better idea on the adhesion pattern of *E. coli* and *E. faecalis* to Caco-2 cells.

Beside the pathogenic effect, the ability of the MGB to adhere to IEC after AS exposure could have a positive effect. Since adherence is one of the most important characters for probiotics (FAO, WHO, 2001), the potential effect of AS might be exploited for further research. The current data could serve as a preliminary base for screening potential factors that leads to adhesion, thereby opening a window of probiotic research using AS.

Similar to adhesion, AS differentially affected model gut bacterial invasion ability into IEC. Bacterial attachment to IECs requires incorporation of bacteria-host receptors. This attachment might result in several outcomes, such as cell distortion, colonisation, bacterial internalization, interference with cell regulatory mechanisms and intracellular proliferation (Coconnier et al., 1993). Bacterial invasion in adjacent epithelial barrier induces an inflammatory reaction in the nearby intestinal mucosa (Jung et al., 1995). The bacteria

invade the epithelial cell membrane, increase their number and leads to host cell death. Exfoliation of these cells result in decreased mucosal surface and the presence of a greater number of immature enterocytes. Reduced or damaged mucosa surface therefore negatively affects the capacity of ion transport and nutrient digestive-absorptive functions (Coconnier et al., 1993).

In the current study, the total co-culture time was an hour, allowing little or no chance for the bacteria to internally multiply. The percentage of bacterial invasion into mammalian cells was measured using gentamicin, hence antibiotic action kills non-internalized bacteria whilst intracellular ones are protected. A significant statistical difference was observed between vehicle-treated and AS-treated bacterial invasion (fig.4.3.15, fig.4.3.16). Sweetener with $ZnSO_4$ reduced the invasiveness for all cases of both bacteria, and like adhesion, *E. faecalis* invasion (fig.4.3.26) was decreased more than *E. coli* (fig.4.3.25) due to $ZnSO_4$ action. This indicates sweet sensing-mediated prokaryote-eukaryote interactions, which could be a matter of further studies.

Antibiotic protection assay is used widely to study bacterial invasion to host cells. The assay relies on the inability of the antibiotics to kill intracellular bacteria thereby allowing a count of invaded bacteria only. Since gentamicin cannot diffuse into the apical domain of Caco-2 cells (Bernet et al., 1994), so adhered bacteria to the Caco-2 cells are killed by the antibiotic action whilst invaded bacteria remain alive.

E. coli is sensitive to gentamicin and the gentamicin protection assay is well-established to study *E. coli* invasion. The MIC (minimum inhibitory concentration) findings support this and 100 µg/ml gentamicin concentration is widely used for *E. coli* invasion studies (Dogan et al., 2006; Altenhoefer et al., 2004; Boudeau et al., 2003). Although some studies used lower concentrations of gentamicin (50 µg/ml) for *E. coli* (Ghosal et al., 2013; Roselli et al., 2003; Kim et al., 1998), however, the incubation duration with antibiotics was different.

Conversely, some *E. faecalis* strains show less sensitivity to the aminoglycoside antibiotic, gentamicin (Wells et al., 1992; Huycke et al., 1991) and a concentration-dependent inhibition was observed in the MIC test (fig.4.3.13). Some of the *E. faecalis* strains were found to be insensitive to ampicillin (Ono et al., 2005; Cercenado et al., 1996; Inoue et al., 1992), therefore, using the combination of antibiotics is better option (Fernández-Hidalgo et al., 2013; Gavaldà et al., 2003; Gavalda et al., 1996). However, the model gut bacterial strain showed sensitivity to penicillin-like antibiotic, ampicillin and the carbapenem antibiotic, meropenem. Also, the bacteria were sensitive to the combinations of gentamicin and the broad-spectrum antibiotics ampicillin or meropenem; MIC test demonstrates that the extracellular bacteria must be killed by the used antibiotics (fig.4.3.14). Since meropenem is less stable in stock solution (Mendez et al., 2008; Mendez et al., 2003), so

gentamicin and ampicillin combination was considered for the *E. faecalis* for the convenience of experiments.

Besides, the temperature and duration of antibiotic exposure were determined earlier, The MOI was 1:300 for the final adhesion and invasion assays. Use of higher MOI was avoided to reduce risk of mammalian cell damage and to ensure a precise assessment of the bacterial ability to invade (Edwards et al., 2010). The number of bound bacteria is dependent not only on the number of bacteria added, but also on the binding capacity of IEC (Tuomola and Salminen, 1998), however, the number of bacteria added was kept constant in order to compare the effect. Some studies used lower MOI (1:100, 1:200), they might have employed techniques such as shaking, centrifugation or extended incubation time to facilitate invasion (Cordeiro et al., 2013; Donnenberg et al., 1989), none of these were employed in the current study. Also, the co-culture time is also important which was longer for those studies (1-4 and 3 hour/s, respectively), and was an hour in this study.

Furthermore, the bacteria were washed prior to exposure to mammalian cells. This minimizes the risk of any toxin exposure limiting Caco-2 cell damage. However, bacterial invasion can induce apoptosis leading to interference into normal cellular functions resulting in cell damage. This can allow the permeation of antibiotics into the Caco-2 cells (Kim et al., 1998), so bacteria could be killed giving an inappropriate impression about the invasion. Sucralose pre-exposure was demonstrated to increase *E. coli* BW25113 resistance to several antibiotics as well as their mutation frequency (Qu et al., 2017), however, both bacterial strain and the antibiotics are different in the current study. Nonetheless, the bacterial inocula were insufficient to cause physical damage, the exposure duration was short (1 hour), and more importantly the cytotoxic effect on viability does not show cell death.

Also, the composition of the medium in co-culture can have a significant effect on invasion (Edwards and Massey, 2011). However, the bacteria were washed stepwise with the used media and the data were normalised with the vehicle, which justifies that the findings are unbiased. Finally, a lower concentration of the TX-100 was used, and the handling time was fast which delimits lysis related interference. Besides, the used concentration of TX-100 does not affect *E. coli* and *E. faecalis* viability for at least 30 minutes (Vieira et al., 2008), therefore, the invaded bacteria remained unaffected in the given amount of time. In addition, the serial dilution of the cell lysate was performed in the respective liquid medium instead of ddH_2O or PBS. Bacteria was already in PBS containing TX-100, diluting them in liquid media reduced undue stress. Nevertheless, the steps of serial dilution and plating were quick (took maximum of two minutes), so the duration was too short for bacteria to increase their number. Nonetheless, all possible factors that can play a role in the invasion assay were considered and the findings were appropriate.

$ZnSO_4$ is a potential sweet taste inhibitor (Keast et al., 2004), but can inhibit enteric bacterial growth (Faiz et al., 2011). However, the growth curve data represents that MGB growth was unchanged at the used $ZnSO_4$ concentration in this study (fig.4.3.19), therefore, the reduced bacterial CFU in the $ZnSO_4$ treated adhesion and invasion is not through growth suppression. These divalent metal cations form complexes with amino acids and interact through sweet taste chemosensory mechanisms (Keast et al., 2004). There may be a connection between sweet molecules and bacterial signalling that mediates the pathogenic potential. Because no studies were found on the sweet sensing in bacteria, more specifically on taste receptor and chemosensory activity, therefore, the current study could not determine whether the adhesion and invasion reduction were via any taste receptor inhibition.

Medeiros *et al*. (2013) also demonstrated the inhibitory effect of zinc on the adherence property of enteroaggregative *E. coli* strain 042 to IEC-6 epithelial cells. ZnO at ≤0.05 mM did not affect the bacterial growth or epithelial cell proliferation; however, it significantly inhibited the adherence of *E. coli* strain to the IECs. These observations support the current findings where 0.1 mM of $ZnSO_4$ affected neither epithelial cell viability (fig.4.3.19) nor model bacterial growth (fig.4.3.20), however, it reduced both *E. coli* and *E. faecalis* adherence to Caco-2 cells (fig.4.3.23 and 4.3.24, respectively). The inhibitory effect of zinc on enterotoxigenic *E. coli* strain's ability to adhere and invade to IECs was also demonstrated by Roselli *et al*. (2003). Rather than antibacterial activity, ZnO prevented the increase of TJ mediated permeability and modulated the cytokine gene expression on the Caco-2 cell surface, thereby limiting the space for bacterial adherence on the cells and internalisation. AS increased model bacterial adherence when both Caco-2 cells and bacteria were treated, the adherence increased, whether this increase is through taste receptor or quorum sensing or any other mechanism, remains veiled. Exposing bacteria in presence of $ZnSO_4$ reduced the effect, this might be because zinc reduced cell permeability for bacteria (Roselli et al., 2003), or because zinc altered important pathogenic properties of the bacteria required for adherence (Medeiros et al., 2013), or through quorum sensing, however, the process needs further investigation. As the untreated bacteria showed adherence to AS-treated Caco-2 cells, the STR may have a role in epithelial cell susceptibility to bacterial adhesion and invasion ability. However, Caco-2 cells were not exposed to $ZnSO_4$, therefore, it is unclear whether T1R3 played a role in this occasion.

The percentage of the invaded cells was lower than the adhered cells. Caco-2 cells were exposed to the same number of bacteria for adhesion and invasion. Since adhesion assay counts both adhered and invaded bacteria, so the number of CFU is higher in adhesion. However, CFU/ml was calculated, and data were normalised with the corresponding control converted into 100% for both the adhesion and the invasion assay. Therefore, the presented

data express relative changes in adhesion and invasion in response to AS exposure with control.

Fascinatingly, AS increased *E. faecalis* adherence (fig.4.3.10) and invasion (fig.4.3.18), but it did not induce bacteria to secrete metabolites affecting cell viability (fig.4.4b). Nonetheless, untreated *E. faecalis* demonstrated significant adhesion for all AS in different concentrations (fig.4.3.8), however, it did not represent much invasion ability to AS-exposed Caco-2 cells at those concentrations (fig.4.3.16). On the other hand, saccharin exposed *E. coli* metabolites significantly reduced Caco-2 cell viability (fig.4.3.4.a), increased their adherence (fig.4.3.9), but had no effect on invasion (fig.4.3.25). This demonstrates that invasion is not a must for all cases of adhesion. $ZnSO_4$ co-exposure did not improve cell viability reduction (fig.4.3.21) although decreased adherence (≈20%) (fig.4.3.23) while increasing invasion by about 62% (fig.4.3.25). These indicate that adhesion and invasion might follow different pathways.

Interestingly, neotame exposed Caco-2 cells were prone to untreated *E. coli* adherence (fig.4.3.7), but neotame exposure prevented its adhesion ability (fig.4.3.9). More remarkably, neotame caused significant invasiveness of *E. coli* irrespective of the bacterial exposure to the AS (fig.4.3.15, 4.3.17). These findings also suggest that adhesion and invasion might not always follow the same signalling system, also invasion is not always adhesion dependent. There might be other mechanisms or receptors that facilitate invasion, for example, apoptosis or cellular damage (Kim et al., 1998). However, the neotame exposed cell-free *E. coli* excretions did not affect Caco-2 cell viability (fig.4.3.4.a), suggesting there is less chance of apoptosis facilitated invasion although it is different from exposure to bacteria. In addition, neotame caused changes in the cell morphology (fig.2.3.17.f, chapter 1), although the concentration used for the invasion assay is very low (0.1 μM) in comparison to the concentration causing cellular damage (10 mM). So, there might be other strategies involved that triggered direct or indirect interactions between model bacteria and IEC receptors enabling invasion which need further investigations.

Since long-term diet (intake of AS) play an important role in GM transformation leading to metabolic disease development, alternatively, it might have a huge possibility of fighting against these gut disease/GM modulations via designed diet intervention to combat these diseases.

4.5 Conclusion

To address Aim III (assessing the effect of AS and sweet taste inhibitor on microflora and IEC co-culture model), mammalian and bacterial cells were co-cultured to develop a physiological model of the gut. Adhesion and invasion assays were performed with exposure of IEC to AS-treated or -untreated MGB. These studies established changes in the pathogenic potential of bacteria and how that impacts mammalian cells. Studies also used $ZnSO_4$ to assess whether sweet taste inhibition can rescue the pathogenic effect of sweeteners.

Taken together, the results from this study suggest that AS triggers model gut bacterial pathogenic properties involved with adhesion and invasion to host cells. Also, different AS differentially affect bacterial metabolism following triggered pathogenicity (*E. coli*) or no effect (*E. faecalis*). Inhibition of the sweet sensing reduced the pathogenic effect for most cases indicating sweet taste perception might have a link with gut bacterial virulence. However, further studies are needed to investigate the AS effect on other virulence properties to clarify the pathogenicity. Also, inhibiting the sweet sensing might help reducing pathogenicity which needs further investigations.

5 General Discussion

This PhD project used various in vitro approaches to investigate the effects of AS on the gut to understand whether the consumption of non-nutritive sweeteners had a negative impact on gut health. Specifically, the studies emphasised establishing the effect of AS on IEC function, MGB metabolism and pathogenicity, and intestinal epithelium-gut bacteria interactions. Diet is one of the most important modulators of the intestinal environment and the gut microflora composition and function (Suez et al., 2014). The consumption of AS in food and beverages is common and the use is increasing, although controversy remains regarding their physiological effects and safety (Payne et al., 2012). Whilst it is known that IECs are in direct contact with AS, research in this area is very limited. Previous findings indicate that AS cause gut microbial dysbiosis (Fukui, 2016), however, there are no studies that demonstrate the direct effect of AS exposure on bacterial metabolism or pathogenic features. Also, whether AS consumption stimulates or enhances bacterial pathogenicity to IEC remains unknown. Therefore, it is timely to investigate the role of AS on gut health and understand whether AS consumption is safe.

The studies in the thesis used experiments on IEC, MGB, and co-culture models to determine whether AS exert negative effects on IEC function via interfering with viability and monolayer permeability, increase MGB pathogenicity, and negatively impact IEC-MGB interactions (table 5.1) which are associated with inflammation and metabolic diseases. At first, this study investigated the effects of a range of physiologically achievable concentrations of four common AS on IEC to understand the potential cytotoxic effect of AS at the cellular level. Overall, the public can consume AS in the diet at varying concentrations; for example, 0.01 µM in chewing gum to 2 mM in diet soda (Gardner et al., 2012). Yet, there is limited information on the amount of AS in the diet as well as on how much AS intestinal epithelial cells can see. Also, the FDA and EFSA recommended daily intake of AS is very high and the amount varies considerably (table 1.1.1). So, a range of concentrations was chosen to use from very low (0.01 µM) to sub-physiological (100 µM) concentrations, covering people who consume low amount, to higher concentrations (10 and 50 mM), maybe mimicking people who consume AS high in the diet. Previous studies also used similar or higher concentrations of saccharin, sucralose, and aspartame than the range used in the current study (van Eyk, 2014; reviewed in Brown and Rother, 2012). So, the AS concentration range were well representative of the available limit in the diet to study their effects on IEB function.

Table 5.1: Summary of the key findings in the study.

Aims	Name of experiment		Artificial sweeteners response			
			Saccharin	Sucralose	Aspartame	Neotame
Effect of AS on intestinal epithelial cells (IEC)	Viability		↓	↓	↓	↓
	Apoptosis (dead %)		↑	↑	↑	↑
	Morphological changes		√	√	√	√
	Monolayer Permeability	AS	↑	↑	↑	↑
		AS + LPS	↑	↑	↑	↑
	Stress fibre formation		−	√	√	√
	T1R3 receptor expression		−	−	−	−
Effect of AS on gut bacteria	Metabolism (growth measurement)	*E. coli*	−	−	−	−
		E. faecalis	-	-	-	-
	Biofilm formation	*E. coli*	+	+	+	+
		E. faecalis	-	-	+	-
	Haemolysin production	*E. coli*	−	−	−	−
		E. faecalis	−	−	−	−
Effect of AS on co-culture of IEC and model gut bacteria	Cytotoxicity	*E. coli*	+	+	−	−
		E. faecalis	-	-	-	-
	Untreated bacterial adhesion	*E. coli*	+	+	+	+
		E. faecalis	+	+	+	+
	AS-treated bacterial adhesion	*E. coli*	+	+	+	-
		E. faecalis	+	+	+	+
	Untreated bacteria invasion	*E. coli*	+	+	+	+
		E. faecalis	-	+	+	-
	AS-treated bacterial invasion	*E. coli*	-	+	+	+
		E. faecalis	+	+	+	+

At the higher concentrations, saccharin, aspartame and neotame increased cell death in the IEC model (fig.2.3.7), may be through the apoptotic pathway (fig.2.3.21), which can directly impact barrier integrity. Viability loss can open the barrier to harmful antigenic substances causing inflammation leading to MD development (König et al., 2016). Previous study with a dietary factor, acrolein, also demonstrated Caco-2 cell viability reduction by apoptosis, which ultimately contributed to intestinal barrier dysfunction and permeability (Chen et al., 2017). Opposite to current findings, Santos *et al.* (2018) did not see viability reduction in Caco-2 cell upon exposure to 10 mM of saccharin, sucralose, aspartame, and Ace-K. The contradiction with Santos *et al*. (2018) findings might be for the experimental conditions. Oppositely, another study on Caco-2 cell found similar viability decrease at >10 mM concentration of saccharin, sucralose and aspartame (van Eyk, 2014) which agrees with present findings except for sucralose. Increased epithelial cell loss or decreased regenerative capacity causes epithelial layer dysfunction leading to an increase in the intestinal barrier permeability, promoting the leakage of potentially hazardous substances and microorganisms into the body (reviewed by Delgado et al., 2016). So, higher

concentrations of AS in the diet interfere with IEC viability and enhance disease state by causing barrier dysfunction.

Morphological alterations, for example in mitochondria, AS might affect the mitochondrial membrane permeability resulting in the activation of the apoptotic proteins (table 2.1.1). Also, the AS might have caused DNA damage, since the previous study on Caco-2, HT-29, and HEK-293 cell lines demonstrated DNA damage after exposure to the AS (van Eyk, 2014). The study showed that sodium saccharin and sucralose caused highest level of DNA damage in all types of cells, suggesting that it could trigger the intrinsic apoptotic pathway resulting in apoptosis-mediated cell viability loss (van Eyk, 2014). Delgado *et al.* (2016) also reviewed the mitochondrial pathway of apoptosis triggered by DNA damage or genotoxic stress. These stimulants promote stress signals to converge at the mitochondrial membranes by promoting the formation of pores. These pores eventually cause the permeabilization of the mitochondrial outer membrane and the release of proteins from the intermembrane space to the cytosol with lethal consequences for the cell (reviewed by Delgado et al., 2016). Also, Grabinger *et al.* (2014) noted that DNA-damage-induced apoptosis mostly occurs in the intestinal crypts. Although proliferative intestinal stem and progenitor cells are more vulnerable to such apoptosis, mature, terminally differentiated epithelial cells in the villus can also face it (Grabinger et al., 2014). Therefore, AS cause morphological changes of the IEC which might have relation to the apoptosis mediated viability reduction, which ultimately impact the intestinal barrier funciton.

Besides all AS are not physiologically inert (Wal et al., 2019), they or their derivative compounds might have lethal factors that trigger the extrinsic pathway of apoptosis, leading to activation of the procaspase-8 (Muzio et al., 1996; Boldin et al., 1996). Nonetheless, both extrinsic and intrinsic pathways ultimately activate the downstream effector caspases, subsequently causing cell death (Muzio et al., 1996). The study could not clarify the apoptosis pathway, however, further studies using specific apoptosis triggers such as caspase assay would be able to clarify this. Also, the cells were exposed for 24 hours, which might have missed the point of apoptosis, shorter exposure period imaging might help to detect the apoptotic cells. Additionally, the morphological features studied represent some characteristics of the apoptosis, similar morphological alterations of Caco-2 cells were also reported previously by van Eyk (2014). AS caused loss of cell adherence, and observations were performed on cells remained on the culture plate, but not the actual representative of the number of cells, implying only morphological studies might misinterpret the findings. So, observations could be made at different time points or through continuous imaging to detect

morphological signs of apoptosis. However, quantitative methods, along with morphological studies, would be a better representative of the effects.

While that is relevant to people who consume a large amount of AS, the vast majority of the population will consume a lower amount (Logue et al., 2017; Gardner et al., 2012). The study shows that lower concentration is still causing damage to the epithelium via a leak. A similar increase in barrier permeability of FD4 across Caco-2 cell monolayer was demonstrated upon exposure to a dietary component, acrolein (Chen et al., 2017). In agreement with the FD4 permeation, Chen *et al*. (2017) also found decreased TEER and downregulation and delocalization of key TJ proteins, which indicate that present *in vitro* studies could have similar outcomes. More importantly, their study found intestinal barrier permeability in mice after oral intake of the acrolein, which resulted in increased translocation of bacterial endotoxin/LPS into the blood (Chen et al., 2017). Additionally, the presence of LPS significantly increased the leak (fig.2.3.33), implying in the gut environment where the endotoxin is common, the AS mediated leak could be exacerbated for the presence of LPS. Previous study showed that LPS at physiologically relevant concentration increased Caco-2 cell monolayer permeability through the TJ-mediated pathway in a time-dependent manner, and a similar increase was observed *in vivo* (Guo et al., 2013). Another study with saccharin showed increased paracellular transport via decreasing claudin-1 expression in Caco-2 cells (Santos et al., 2018). Nonetheless, their study showed no significant leak for 10 mM of sucralose and aspartame, which contradict with the findings showing sucralose at 1 mM and aspartame at 0.1 mM caused a leak (fig.2.3.31. b, c). The leak was not for cell viability reduction, as viability was unaffected at these concentrations (fig.2.3.7). This finding agrees with Santos *et al*. (2018), who also observed a similar effect of saccharin, causing permeability without affecting viability. However, aspartame did not cause a significant leak at 1 mM in this study, which might indicate aspartame cause leak at lower concentrations only and might explain Santos *et al*. (2018) findings. Therefore, the barrier integrity impairment was not through viability reduction; other pathways such as TJ-mediated or sweet taste receptor modulation might have interactions. Altered expression and redistribution of the TJs increase the intestine's paracellular permeability (König et al., 2016; Ulluwishewa et al., 2011). It strongly suggests that the permeability caused by the dietary component, AS, can subsequently affect gut physiological homeostasis. Epithelial barrier dysfunction is one of the significant contributors in chronic inflammation (Fukui, 2016). It can also facilitate the permeation of endotoxins and bacterial antigens into the circulation (Mendrick et al., 2017; Moreira et al., 2012; Ukleja et al., 2010). Permeability eventually increases inflammation, which triggers insulin resistance and adipose tissue plasticity leading to metabolic diseases (Fukui, 2016; Serino et al., 2009). This pathophysiological cascade has also been linked to the development of other MD, including

T2D (Clemente et al., 2012; Serino et al., 2009). So, people consuming lower amount of AS in the diet are still at risk of having intestinal leak which have negative impact on health.

Whilst the monolayer permeability was independent of cell death, it is likely to be through TJ-mediated pathway. The advantage of paracellular permeability is that TJ proteins can be annealed, so there should be a short-term leak. Higher concentrations caused cell death and that will take longer to recover because the epithelium needs to grow, and the epithelial cell turnover time is 5-6 days (Van Der Flier and Clevers, 2009). On the other hand, claudins express in epithelia and form paracellular barriers and pores that determine TJ permeability (Günzel and Yu, 2013). Using pulse-chase-pulse analysis Van Itallie *et al.* (2017) demonstrated that claudins preferentially incorporate with newly synthesized claudins into break sites to reanneal. Another study showed that paracellular leaks are followed by temporary local activation of RhoA, or Rho flares, which concentrate TJ proteins locally through Rho kinase-mediated contraction of the junction (Stephenson et al., 2019). Leak happens and this reverse kind of a regular basis, gut will see leak at various substances' regular basis. So, irrespective of lower or higher concentration consumption, there will be an impact on gastric permeability. Though the TJ permeability has a greater chance to seal promptly, however, this will need to be studied further over time.

Adjacent to the intestinal epithelium, the GM is the core part which is also exposed to the AS in a greater degree than IEC. So, the effect of AS on GM metabolism and their interactions with IEC is crucial to understand the overall impact of AS consumption. It is difficult to determine the real magnitude of host exposure to intestinal pathogens; the development of infectious diseases barely happens due to pathogen-epithelium confrontation in homeostatic conditions (Neish, 2002; Adlerberth et al., 2000). Also, assessing the exact role of AS is challenging in such an environment as the organisms are intricately interdependent for their existence and metabolism (Cani, 2018). Other studies showed dysbiosis (Suez et al., 2014), but this study focussed on the possibilities of GM pathogenicity because increased pathogenesis of set bacteria is linked to MD (Chen and Devaraj, 2018; Sartor and Wu, 2017). The study focussed on two MGB, which are prevalent. Interestingly, there was no effect on growth and haemolysin production other than increased biofilm formation (fig.3.3.9). Although a previous study used much higher concentrations showed that high concentrations (12.5 and 25 mg/ml) saccharin, sucralose and Ace-K have a strong inhibitory effect on *E. coli* growth (Wang et al., 2018). Interestingly, Mahmud *et al*. (2019) demonstrated a concertation-dependent increase of *E. coli* growth upon Ace-K exposure up to 15 mg/ml, and similar to previous studies, they found inhibited growth at high concentration of 25 mg/ml. They also found aspartame (1 mg/ml) to stimulate *E. coli*

growth insignificantly like present study (fig.3.3.6.c), although they observed growth inhibition at concentrations ≥3 mg/ml (Mahmud et al., 2019).

The host epithelial defence mechanisms ensure host protection; however, managing the inflammatory reactivity is a pivotal requirement to conserve the intestinal barrier integrity (Nagai et al., 2016). While commensals do not trigger epithelial defensive response, they influence the host's immune modulation (Petersson et al., 2010). Pathogenic bacterial colonization may cause host cell damage, thereby stimulating the host's response to resist the antigen, raising an inflammatory response (Vijay-Kumar et al., 2010). There are several features of the GM which can be linked to pathogenesis such as haemagglutination, cytolysin production, induction of proinflammatory cytokine production (reviewed by Rossi et al., 2018). These findings cannot be compared because there is no literature to link bacterial pathogenicity and AS consumption. However, biofilm formation, which is frequent in the gut (Rossi et al., 2018) and is often linked to pathogenic activity (Hold and Allen-Vercoe, 2019), was increased after AS exposure (table 5.1). Therefore, AS consumption can increase the pathogenic factor of GM, although further studies are needed to understand the mechanisms.

Intestinal pathogenic *E. coli* can acquire different abilities to form a biofilm, although how nutrient provisions in the gut affects biofilm formation is mostly unknown (reviewed by Rossi et al., 2018). Quorum sensing may play a role via autoinducer-1 in *E. coli* biofilm formation in the gut, but it is still elusive how autoinducer-1 is stimulated (reviewed by Rossi et al., 2018). Nonetheless, Mahmud *et al*. (2019) indicated that aspartame and Ace-K might influence *E. coli* K-12 biofilm formation in the gut. They showed that Ace-K and aspartame upregulated several genes such as 6-phosphofructokinase I and II (*pfk*A and *pfk*B, respectively), Pyruvate dehydrogenase (*ace*), and Lipoamide dehydrogenase (*lpd*). These genes are essential for glucose metabolic pathways in *E. coli* (Mahmud et al., 2019), whilst mutations in sugar pathways affected colonization by *E. coli* MG1655 (Chang et al., 2004). Because the gut bacteria model (*E. coli* MG1655) use gluconate as a major carbon source to colonize in mouse intestine, defected pathway negatively impacts on both the initiation and maintenance stages of biofilm development (Chang et al., 2004). Besides, Thymidylate synthetase (*thy*A) and Thymidylate kinase (*tmk*) genes which are important for *de novo* synthesis of pyrimidine (*Thy*A and *Tmk*) in *E. coli*, were also overexpressed upon aspartame and Ace-K exposure (Mahmud et al., 2019). Previous study suggested that *de novo* pyrimidine synthesis is essential for *Salmonella typhimurium* biofilm establishment in the chicks (Yang et al., 2017). One bacterial biofilm might facilitate colonization of other bacteria or delimit the proximity of essential commensals. Therefore, AS exposure in the present study might have enhanced expression of certain genes in MGB or increased the metabolic

activity, which facilitated the increased biofilm development; however, further investigations are important to ascertain this.

In addition to biofilm, saccharin- and sucralose-treated *E. coli* metabolites decreased Caco-2 cell viability in the co-culture model (fig.4.3.4.a). In the gut milieu, the production of one metabolite may have a combined effect on the conversion of the product into other compounds or stimulation or suppression of other organisms (Sartor and Wu, 2017). For example, colonization of the *Enterococcus faecium* in the small intestine of the pigs was shown to have an inhibitory effect on the colonization of *E. coli* (Ushe and Nagy, 1985). Sucralose- and aspartame-mediated *E. faecalis* metabolites reduced Caco-2 cell viability (fig.4.3.4.b). Although the reduction was insignificant, this may induce unplanned apoptosis, which can affect the barrier function (Elmore, 2007). Studying the bacterial proteins using western blotting or mass spectrometry might answer whether exposure of Caco-2 cells to AS-mediated bacterial metabolites alter intestinal epithelial cells protein profile.

Also, AS negatively affected the intestinal epithelium-gut bacteria interactions by increasing the adhesion and invasion of the MGB to the Caco-2 cells. Overall, AS caused an increase in the bacterial adhesion except for neotame. Previous study showed that type 1 fimbrial adhesin is an *E. coli* adhesion protein present on the tips of fimbriae of enterotoxigenic strains (Kukkonen et al., 1993). AS, have stimulated Caco-2 cell receptors for the bacterial adhesion, as untreated bacteria adhered to the AS-exposed Caco-2 cells (fig.4.3.7–4.3.8). Nonetheless, it is not clear whether the adhesion was mediated by mammalian cell-bacteria receptors, or by the release of adhesins or other means. Further investigations with adhesion target inhibition might clarify the AS-mediated bacterial adhesion.

Notably, the decreased adhesion of neotame-exposed *E. coli* (fig.4.3.9) in comparison to untreated bacteria (fig.4.3.7.d) indicates that there might have mismatched receptor interactions. In contrast, neotame exposed Caco-2 cells showed significant adherence to untreated *E. faecalis* (fig.4.3.8.d); and exposure of both Caco-2 cells and *E. faecalis* to neotame increased the adhesion percentage by 179% (fig.4.3.10). Importantly, these findings indicate that AS can enhance enteric bacterial adhesion to intestinal epithelium without affecting their growth. In addition to facilitating invasion, this phenomenon could assist other pathogenic features such as biofilm formation (Fons et al., 2000). Also, adhesion of one species may influence others, i.e., mice harbouring a relatively high density of *E. coli* population in the intestine were shown to be more susceptible to *Salmonella enterotica* induced gut inflammation (Stecher et al., 2010). Consumption of Ace-K has increased the risk of chronic inflammation in the host via gut microflora perturbation. Ace-K increased the abundance of a bacterial toxin secreting gene, thiol-activated cytolysin, as

well as enriched the LPS synthesis-related genes, eventually upsurge the risk of inflammations (Bian et al., 2017). Therefore, it may be predicted that AS not only cause bacterial adhesion to intestinal epithelium but also could indirectly stimulate other pathogenic bacterial colonization in the intestinal epithelium, which can make host prone to various diseases.

AS differentially increased model gut bacterial invasiveness into Caco-2 cells (fig.4.3.15 and fig.4.3.16). Invading the epithelial lining by the enteric pathogens to establish an infection involves enzymes and toxins (Altenhoefer et al., 2004). Pathogens can invade and enter the bloodstream, thereby disseminating in the body through the blood flow and cause inflammation (König et al., 2016). Also, AS-exposure significantly increased *E. faecalis* invasion into AS-treated Caco-2 cells (fig.4.3.18) in comparison to untreated bacteria (fig.4.3.16). It indicates the involvement of more than one pathway in the AS-mediated invasion mechanism. Although cell death could open the barrier for bacteria to pass, which can take place as observed in the viability reduction, that is not applicable in this *in vitro* assay results. Because, if there were dead cells, that would have been removed in the washing steps as death cause loss of adherence. It indicates more possibilities of receptor-mediated bacterial invasion; however, further investigations are necessary to establish the AS-mediated bacterial invasion pathway.

Bacteria may also use the host cellular apparatus for invasion (Coconnier et al., 1993). Pathogens use many inducers of the inflammatory cascade, which may exacerbate the inflammation (Burgos and Beutin, 2010). Upon invasion, the inflammatory response persists for the recruitment of leukocytes (Santos and Broz, 2018). Infection with pathogenic bacteria results in the expression and upregulation of a specific array of inflammatory mediators (Heimesaat et al., 2016; Jung et al., 1995). Therefore, perpetuated inflammation leads to conditions leading to metabolic disease development.

The STR in the mammalian cells has been shown to express (Shirazi-Beechey et al., 2014; Moran et al., 2010) but not shown in bacteria (Lee et al., 2017). The study has shown that STR is expressed in the epithelial cells, although only T1R3 in Caco-2 cells (O'Brien and Corpe, 2016). Whilst current study does not show the presence of STR in the gut bacteria, it indicates the presence of a sweet taste sensor, because of the zinc sulphate work. These raise question whether there are GPCRs in gut bacteria. Also, there might have quorum sensing linked to sweet taste, which needs further investigations. Sweet sensing in the lung were shown to have negative correlation with the epithelial cell viability (Lee et al., 2017; Carey and Lee, 2019). Although the studies did not show any GPCR or quorum sensing,

however, established a link between sweet taste mediated bacterial secretions and epithelial cell death signalling.

The study is not purely driven by STR. AS that was more able to bind a receptor, e.g., neotame, it could have the worst effect and gradually less effect for saccharin, sucralose and aspartame. However, findings from the present study do not support this. If this was taste receptor driven, then the data should show that the less sweet AS would have a less effect, but this is not the case. For some of them, that was the case, but for most of them, there was no link with the sweetness perception level. The reason behind this, maybe they all do not bind to the STR in the same way (Fernstrom et al., 2012; Assadi-Porter et al., 2010).

There is no known literature to explain the presence of a taste receptor or such signalling in bacteria, AS might not bind all sweet receptors either. In addition, all AS are structurally quite different; they might bind differently or may bind partially (DuBois, 2016). Besides, there could be an indirect effect of the AS, e.g., in the gut, we do not undoubtedly know whether the AS are broken down (Wal et al., 2019). Moreover, does the gut bacteria metabolise AS or their components is unknown. The initial concept of these chemically derived intense sweet molecules was questioned as all of them are not physiologically inert (Wal et al., 2019), which indicates that sweeteners have different metabolic activities. Also, they or their derivatives may cause physical injury to the cells (van Eyk, 2014).

The barrier permeability was not related to the sweetness perception level either (table-1.1.1), because saccharin is half the sweetness perception of sucralose, but both caused leak at 1 mM. Instead, aspartame was the lowest in sweetness perception level, while neotame was the highest of the tested AS, but both caused leak at 0.1 mM (fig.2.3.31). Additionally, the permeability findings did not represent concentration dependence. Sucralose caused a leak at concentrations 0.1 and 1 µM when exposed with LPS, but not at other concentrations of more than 10 µM (fig.2.3.33). Likewise, neotame with LPS increased permeability for all the concentrations (fig.2.3.33). The cell monolayer permeability was neither correlated with the sweetness perception level, nor the concentration of the AS.

While there was no correlation between sweetness perception and paracellular transport of FD4, the appearance of stress fibre showed the opposite, except aspartame (fig.2.3.35 – 2.3.37). Saccharin caused almost no prominent stress fibres in the Caco-2 cells (fig.2.3.36.c), whereas sucralose-exposed cells represented a similar level of stress fibre like LPS (fig.2.3.36.d). Moreover, neotame exposed cells demonstrated the highest level of stress fibres compared to others (fig.3.3.37.f). Disorganisation and disassembly of F-actins

lead to disruption of the epithelial barrier, causing a leak (Madara, 1987). There is no literature demonstrating AS-mediated stress fibre alteration; hence the findings of the study could not be critically analysed. The stress fibres in the present study produced a basic idea on the effect of AS. Further studies with quantification or measurement of the actin fibres would generate more specific information in this regard.

Although the study presented here shows negative impact of AS on IEC function and GM pathogenicity, which are new information, still, there are some limitations. These experiments used an *in vitro* approach, which is relatively simple and easily tractable, but limitations remain over *in vivo* studies. Also, Caco-2 cell line represents only primary enterocytes. Although above 80% of cells of the intestinal epithelium is the enterocytes (Van der Flier and Clevers, 2009), but the response of other intestinal epithelial cells was not included. Whilst studies on the effect of AS on human is important, the use of artificial gut system could be the next step of the investigation. Like the epithelial cell model, the MGB represents individual response, which might be different *in vivo*. Future studies with other MGB or their combination, more preferably whole gut microflora would represent a better understanding of the effect of AS.

Besides, food and drink often contain more than one AS, but the present study investigated individual AS effect, although the individual findings can indicate the combined effect. Also, consumption of AS is commonly based on dietary information only. In contrast, consumers may be unaware when intake AS in many other products like toothpaste, mouthwash, sauces, and frozen set foods containing AS (Pearlman et al., 2017). Whilst saccharin, sucralose and aspartame are ubiquitously used in food and beverages in the UK, neotame is not commercially used in the food products. Nevertheless, use of neotame is common in countries in North America, South America, Africa, Asia, and Australia (Das and Chakraborty, 2016).

Despite these limits, the findings raised some exciting inquiries. The effect of AS on viability or permeability was not via T1R3 signalling, therefore what mechanisms underlie in the AS-mediated effect on IEC remained unclear and would be interesting to study in future. Also, zinc sulphate inhibition of pathogenicity of the MGB indicates some sweet sensor, but no T1R3 homology was invented in bacteria yet. So, the study opened a window whether bacteria have sweet taste receptor homology or sweet sense mediated quorum sensing or other signalling mechanism.

Also, the findings are important for public health to understand the safety of AS consumption. The increase in diabetes and the obesity epidemic has led more and more

people to consume AS as a healthy alternative (Pearlman et al., 2017; Payne et al., 2012). The availability and naming as ‘diet’ options could influence people to select AS containing products too (Gardner et al., 2012). Also, the ubiquitous use of AS in food and beverages might passively drive people to consume AS (Pearlman et al., 2017). Besides, the food processors and manufacturers are liable to express the ingredient AS names, except saccharin, but not the amount of AS used (Mattes and Popkin, 2008). Also, there is a good percentage (73%) of people who prefer AS consumption to reduce calorie intake (Gardner et al., 2012). The number of people consuming AS-containing foods has increased from 3.2% to 5.8% between 1989 and 2004 (Mattes and Popkin, 2008). Consumption of AS as a healthy option by people already having chronic inflammation or T2D could, therefore, exacerbate their conditions.

In addition, the increased sugar tax may motivate people to choose AS since it is cheap and require less amount. Besides, to keep the food taste as before with reformulation of the sugar content, the food companies might be encouraged to rely on AS to avoid tax (Vandevijvere and Vanderlee, 2019). However, AS do not exactly taste like sucrose (Steinert et al., 2011). In six months of implementing the sugar tax in 2018, GBP 150 million in revenue was collected from the tax, which was twice as expected (Vandevijvere and Vanderlee, 2019). Although the initial idea of a sugar tax was to reduce sugar in products by 20% by 2020 (Buttriss, 2018), but the achievement of half of the target reduction in the average sugar content in the UK beverages was reported (Hashem et al., 2017). The companies might partially replace sugar or employ combinations of AS to achieve their goal, indicating more dependence on controversial food additive.

When the UK government increased dietary awareness and made companies put labels about calorie content and sugar content on food (EU FIC, 2011), many companies felt pressure to reduce the numbers of calorie by replacing some sugar with AS to make their product appear healthier. The companies do not present the AS name on the front labelling, rather keep it in the ingredient list without mentioning the concentration (Mattes and Popkin, 2008). Consumers might follow the front of package calorie information only, thereby consuming AS without knowledge. Since the controversy of the safety of AS remained (Harpaz et al., 2018), and we are still waiting for concrete findings, it would be worth adding AS names and concentration in the food packaging like calorie. It would help consumers to make their decision on intaking AS or not. In addition, in future, the FDA should test food additives more thoroughly before sending them to the market.

In the current beverage industry, specially diet-cola, AS almost replaced sugar (Gardner et al., 2012). The rising health awareness resulted in expanded demand for low-to-zero-calorie foods in the packaged food sector, indicating a greater need for AS (Praveena et al., 2019; Whitehouse et al., 2008). So, considering the continually increasing AS market, further research should introduce safer AS and could find ways to overcome the negative impact

of the existing ones. The current study provides knowledge on the metabolic and health effect of four common AS and indicates a rescuing possibility. Further research could expand this knowledge to improve AS-mediated physiological impact and find an ideal AS. Nonetheless, the study suggests that consumption of AS could have potentially harmful effects on human health. They are sugar substitutes; however, sugar could be burnt but, dysbiosis of the gut microflora might have worse effects. AS are great in theory, but research needs to develop one that triggers sweet taste perception without inducing factors that can provoke inflammation. Therefore, everyone related to healthcare should educate people about this. The concentration of the AS in the products should be closely monitored before any concrete decision comes about AS use. Moreover, the AS approval process might have evaluations and regulations similar to pharmaceutical drugs.

6 Conclusion

A large number of the population consume AS in the diet, either to reduce calorie intake or to reduce blood glucose levels. However, there is significant controversy around the safety of AS consumption which, to date, remains unresolved. The aim of the present work was therefore to study the effect of commonly available AS (saccharin, sucralose, aspartame, and neotame) on intestinal health. These studies were performed using *in vitro* models of the gut epithelium (Caco-2 cells) and the MGB (*E. coli* and *E. faecalis*). Studies in the thesis show that AS, at physiological concentrations, decreases intestinal epithelial cell viability, which is associated with increased intestinal barrier leak, as measured using a FITC-dextran model. This increased leak can lead to antigenic substances entering the circulation which causes systemic inflammatory responses and metabolic diseases. In MGB, AS exposure increased pathogenicity (biofilm formation, adhesion and invasion to the epithelium) but not metabolic capacity, which is indicative of further inflammatory responses in those who consume AS in the diet. The results of these studies demonstrate that AS negatively impact the intestinal epithelium and perturbs epithelium-gut bacteria interactions. Further studies are, however, needed to develop a thorough understanding of how these physiological effects of AS can be attenuated to improve gut health.

7 References

Abou-Donia, M.B., El-Masry, E.M., Abdel-Rahman, A.A., McLendon, R.E. and Schiffman, S.S., 2008. Splenda alters gut microflora and increases intestinal p-glycoprotein and cytochrome p-450 in male rats. *Journal of Toxicology and Environmental Health*, Part A, [e-journal] 71 (21), pp.1415-1429. Available through: google.

Abreu-Martin, M.T., Vidrich, A., Lynch, D.H. and Targan, S.R., 1995. Divergent induction of apoptosis and IL-8 secretion in HT-29 cells in response to TNF-alpha and ligation of Fas antigen. *Journal of immunology* (Baltimore, Md.: 1950), [e-journal] 155 (9), pp.4147-4154.

Adlerberth, I., Cerquetti, M., Poilane, I., Wold, A. and Collignon, A., 2000. Mechanisms of colonisation and colonisation resistance of the digestive tract. *Microb.Ecol.Health Dis*, [e-journal] 11, pp.223-239. Available through: google.

Alican, I. and Kubes, P., 1996. A critical role for nitric oxide in intestinal barrier function and dysfunction. *American Journal of Physiology-Gastrointestinal and Liver Physiology*, [e-journal] 270 (2), pp.G225-G237. Available through: google.

Allen-Vercoe, E., 2013. Bringing the gut microbiota into focus through microbial culture: recent progress and future perspective. *Current opinion in microbiology,* [e-journal] 16 (5), pp.625-629. Available through: google.

Altenhoefer, A., Oswald, S., Sonnenborn, U., Enders, C., Schulze, J., Hacker, J. and Oelschlaeger, T.A., 2004. The probiotic *Escherichia coli* strain Nissle 1917 interferes with invasion of human intestinal epithelial cells by different enteroinvasive bacterial pathogens. *FEMS Immunology & Medical Microbiology*, [e-journal] 40 (3), pp.223-229. Available through: google.

Amon, P. and Sanderson, I., 2017. What is the microbiome? *Archives of disease in childhood. Education and practice edition,* [e-journal] 102 (5), pp.257-260. 10.1136/archdischild-2016-311643 [doi].

Anand, B.G., Prajapati, K.P., Dubey, K., Ahamad, N., Shekhawat, D.S., Rath, P.C., Joseph, G.K. and Kar, K., 2019. Self-Assembly of Artificial Sweetener Aspartame Yields Amyloid-Like Cytotoxic Nanostructures. *ACS nano*, [e-journal] Available through: google.

Anderson, R. and Kirkland, J., 1980. The effect of sodium saccharin in the diet on caecal microflora. *Food and cosmetics toxicology,* [e-journal] 18 (4), pp.353-355. Available through: google.

Anton, S.D., Martin, C.K., Han, H., Coulon, S., Cefalu, W.T., Geiselman, P. and Williamson, D.A., 2010. Effects of stevia, aspartame, and sucrose on food intake, satiety, and postprandial glucose and insulin levels. *Appetite*, [e-journal] 55 (1), pp.37-43. Available through: google.

Archer, S.L., 2013. Mitochondrial dynamics—mitochondrial fission and fusion in human diseases. *New England Journal of Medicine,* [e-journal] 369 (23), pp.2236-2251. Available through: google.

Archimbaud, C., Shankar, N., Forestier, C., Baghdayan, A., Gilmore, M.S., Charbonné, F. and Joly, B., 2002. *In vitro* adhesive properties and virulence factors of *Enterococcus faecalis* strains. *Research in microbiology*, [e-journal] 153 (2), pp.75-80. Available through: google.

Armstrong, S.M., Khajoee, V., Wang, C., Wang, T., Tigdi, J., Yin, J., Kuebler, W.M., Gillrie, M., Davis, S.P. and Ho, M., 2012. Co-regulation of transcellular and paracellular leak across microvascular endothelium by dynamin and Rac. *The American journal of pathology,* [e-journal] 180 (3), pp.1308-1323. Available through: google.

Assadi-Porter, F.M., Tonelli, M., Maillet, E.L., Markley, J.L. & Max, M. 2010, "Interactions between

the human sweet-sensing T1R2–T1R3 receptor and sweeteners detected by saturation transfer difference NMR spectroscopy", *Biochimica et Biophysica Acta (BBA)-Biomembranes,* vol. 1798, no. 2, pp. 82-86.

Banan, A., Fitzpatrick, L., Zhang, Y. and Keshavarzian, A., 2001. OPC-compounds prevent oxidant-induced carbonylation and depolymerization of the F-actin cytoskeleton and intestinal barrier hyperpermeability. *Free Radical Biology and Medicine*, [e-journal] 30 (3), pp.287-298. Available through: google.

Barbara, G., Stanghellini, V., Brandi, G., Cremon, C., Di Nardo, G., De Giorgio, R. and Corinaldesi, R., 2005. Interactions between commensal bacteria and gut sensorimotor function in health and disease. *The American Journal of Gastroenterology*, [e-journal] 100 (11), pp.2560. Available through: google.

Bates, J.M., Akerlund, J., Mittge, E. and Guillemin, K., 2007. Intestinal alkaline phosphatase detoxifies lipopolysaccharide and prevents inflammation in zebrafish in response to the gut microbiota. *Cell host & microbe,* [e-journal] 2 (6), pp.371-382. Available through: google.

Berg, R.D., 1996. The indigenous gastrointestinal microflora. *Trends in microbiology*, [e-journal] 4 (11), pp.430-435. Available through: google.

Berke, G., 1995. The CTL's kiss of death. *Cell,* [e-journal] 81 (1), pp.9-12. Available through: google.

Bernet, M.F., Brassart, D., Neeser, J.R. and Servin, A.L., 1994. *Lactobacillus acidophilus* LA 1 binds to cultured human intestinal cell lines and inhibits cell attachment and cell invasion by enterovirulent bacteria. *Gut*, [e-journal] 35 (4), pp.483-489.

Bernet-Camard, M.F., Coconnier, M.H., Hudault, S. and Servin, A.L., 1996. Pathogenicity of the diffusely adhering strain *Escherichia coli* C1845: F1845 adhesin-decay accelerating factor interaction, brush border microvillus injury, and actin disassembly in cultured human intestinal epithelial cells. *Infection and immunity*, [e-journal] 64 (6), pp.1918-1928.

Berova, N., Di Bari, L. and Pescitelli, G., 2007. Application of electronic circular dichroism in configurational and conformational analysis of organic compounds. *Chemical Society Reviews*, [e-journal] 36 (6), pp.914-931. Available through: google.

Beutler, B. and Rietschel, E.T., 2003. Innate immune sensing and its roots: the story of endotoxin. *Nature Reviews Immunology,* [e-journal] 3 (2), pp.169. Available through: google.

Biagi, E., Nylund, L., Candela, M., Ostan, R., Bucci, L., Pini, E., Nikkïla, J., Monti, D., Satokari, R. and Franceschi, C., 2010. Through ageing, and beyond: gut microbiota and inflammatory status in seniors and centenarians. *PloS one,* [e-journal] 5 (5), pp.e10667. Available through: google.

Bian, X., Chi, L., Gao, B., Tu, P., Ru, H. and Lu, K., 2017. The artificial sweetener acesulfame potassium affects the gut microbiome and body weight gain in CD-1 mice. *PloS one*, [e-journal] 12 (6), pp.e0178426. Available through: google.

Biesta-Peters, E.G., Reij, M.W., Joosten, H., Gorris, L.G. and Zwietering, M.H., 2010. Comparison of two optical-density-based methods and a plate count method for estimation of growth parameters of *Bacillus cereus*. *Applied and Environmental Microbiology*, [e-journal] 76 (5), pp.1399-1405. 10.1128/AEM.02336-09 [doi].

Binder, H.J., Rajendran, V., Sadasivan, V. and Geibel, J.P., 2005. Bicarbonate secretion: a neglected aspect of colonic ion transport. *Journal of clinical gastroenterology,* [e-journal] 39 (4), pp.S53-S58. Available through: google.

Bischoff, S.C., Barbara, G., Buurman, W., Ockhuizen, T., Schulzke, J., Serino, M., Tilg, H.,

Watson, A. and Wells, J.M., 2014. Intestinal permeability–a new target for disease prevention and therapy. *BMC gastroenterology*, [e-journal] 14 (1), pp.189. Available through: google.

Bocci, V., 1992. The neglected organ: bacterial flora has a crucial immunostimulatory role. *Perspectives in biology and medicine,* [e-journal] 35 (2), pp.251-260. Available through: google.

Boldin, M.P., Goncharov, T.M., Goltseve, Y.V. and Wallach, D., 1996. Involvement of MACH, a novel MORT1/FADD-interacting protease, in Fas/APO-1-and TNF receptor–induced cell death. *Cell*, [e-journal] 85 (6), pp.803-815. Available through: google.

Boleij, A. and Tjalsma, H., 2012. Gut bacteria in health and disease: a survey on the interface between intestinal microbiology and colorectal cancer. *Biological Reviews,* [e-journal] 87 (3), pp.701-730. Available through: google.

Boquet, P., Munro, P., Fiorentini, C. and Just, I., 1998. Toxins from anaerobic bacteria: specificity and molecular mechanisms of action. *Current opinion in microbiology*, [e-journal] 1 (1), pp.66-74. Available through: google.

Boudeau, J., Glasser, A., Julien, S., Colombel, J. and Darfeuille-Michaud, A., 2003. Inhibitory effect of probiotic *Escherichia coli* strain Nissle 1917 on adhesion to and invasion of intestinal epithelial cells by adherent–invasive *E. coli* strains isolated from patients with Crohn's disease. *Alimentary Pharmacology & Therapeutics*, [e-journal] 18 (1), pp.45-56. Available through: google.

Boyd, W.L. and Lichstein, H.C., 1951. The inhibitory effect of glucose on certain amino acid deaminases. *Journal of Bacteriology*, [e-journal] 62 (6), pp.711-715.

Brandtzaeg, P., 2011. The gut as communicator between environment and host: immunological consequences. *European journal of pharmacology*, [e-journal] 668, pp.S16-S32. Available through: google.

Brayton, C.F., 1986. Dimethyl sulfoxide (DMSO): a review. *The Cornell veterinarian*, [e-journal] 76 (1), pp.61-90.

Brown, R.J. & Rother, K.I. 2012, "Non-nutritive sweeteners and their role in the gastrointestinal tract", *The Journal of Clinical Endocrinology & Metabolism,* vol. 97, no. 8, pp. 2597-2605.

Brown, R.J., De Banate, M.A. and Rother, K.I., 2010. Artificial sweeteners: a systematic review of metabolic effects in youth. *International Journal of Pediatric Obesity,* [e-journal] 5 (4), pp.305-312. Available through: google.

Brubaker, P. and Drucker, D., 2002. Structure-function of the glucagon receptor family of G protein-coupled receptors: the glucagon, GIP, GLP-1, and GLP-2 receptors. *Receptors and Channels*, [e-journal] 8 (3-4), pp.179-188. Available through: google.

Brubaker, P. and Drucker, D., 2004. Minireview: glucagon-like peptides regulate cell proliferation and apoptosis in the pancreas, gut, and central nervous system. *Endocrinology,* [e-journal] 145 (6), pp.2653-2659. Available through: google.

Burgos, Y. and Beutin, L., 2010. Common origin of plasmid encoded alpha-hemolysin genes in *Escherichia coli*. *BMC microbiology*, [e-journal] 10 (1), pp.193. Available through: google.

Buteau, J., 2008. GLP-1 receptor signaling: effects on pancreatic β-cell proliferation and survival. *Diabetes & metabolism*, [e-journal] 34, pp.S73-S77. Available through: google.

Buttriss, J., 2018. Calorie reduction programme launched. *Nutrition Bulletin*, [e-journal] 43 (2), pp.106-111. Available through: google.

Candela, M., Seibold, G., Vitali, B., Lachenmaier, S., Eikmanns, B.J. and Brigidi, P., 2005. Real-time PCR quantification of bacterial adhesion to Caco-2 cells: competition between bifidobacteria and enteropathogens. *Research in microbiology*, [e-journal] 156 (8), pp.887-895. Available through: google.

Cani, P.D., 2018. Human gut microbiome: hopes, threats and promises. *Gut,* [e-journal] 67 (9), pp.1716-1725. Available through: google.

Cani, P.D., Possemiers, S., Van de Wiele, T., Guiot, Y., Everard, A., Rottier, O., Geurts, L., Naslain, D., Neyrinck, A., Lambert, D.M., Muccioli, G.G. and Delzenne, N.M., 2008. Changes in gut microbiota control inflammation in obese mice through a mechanism involving GLP-2-driven improvement of gut permeability. *Gut,* [e-journal] 58 (8), pp.1091-1103. 10.1136/gut.2008.165886 [doi].

Carey, R.M. and Lee, R.J., 2019. Taste receptors in upper airway innate immunity. *Nutrients*, [e-journal] 11 (9), pp.2017. Available through: google.

Carrière, F., Renou, C., Lopez, V., De Caro, J., Ferrato, F., Lengsfeld, H., De Caro, A., Laugier, R. and Verger, R., 2000. The specific activities of human digestive lipases measured from the *in vivo* and *in vitro* lipolysis of test meals. *Gastroenterology*, [e-journal] 119 (4), pp.949-960. Available through: google.

Cercenado, E., Vicente, M.F., Diaz, M.D., Sanchez-Carrillo, C. and Sanchez-Rubiales, M., 1996. Characterization of clinical isolates of beta-lactamase-negative, highly ampicillin-resistant *Enterococcus faecalis*. *Antimicrobial Agents and Chemotherapy*, [e-journal] 40 (10), pp.2420-2422.

Cetinkaya, Y., Falk, P. and Mayhall, C.G., 2000. Vancomycin-resistant enterococci. *Clinical microbiology reviews,* [e-journal] 13 (4), pp.686-707. Available through: google.

Chang, D.E., Smalley, D.J., Tucker, D.L., Leatham, M.P., Norris, W.E., Stevenson, S.J., Anderson, A.B., Grissom, J.E., Laux, D.C., Cohen, P.S. and Conway, T., 2004. Carbon nutrition of *Escherichia coli* in the mouse intestine. Proceedings of the National Academy of Sciences of the United States of America, [e-journal] 101 (19), pp.7427-7432. 10.1073/pnas.0307888101 [doi].

Chassaing, B., Koren, O., Goodrich, J.K., Poole, A.C., Srinivasan, S., Ley, R.E. and Gewirtz, A.T., 2015. Dietary emulsifiers impact the mouse gut microbiota promoting colitis and metabolic syndrome. *Nature,* [e-journal] 519 (7541), pp.92. Available through: google.

Chassaing, B., Van de Wiele, T., De Bodt, J., Marzorati, M. and Gewirtz, A.T., 2017. Dietary emulsifiers directly alter human microbiota composition and gene expression *ex vivo* potentiating intestinal inflammation. *Gut,* [e-journal] 66 (8), pp.1414-1427. Available through: google.

Chattopadhyay, S., Raychaudhuri, U. & Chakraborty, R. 2014, "Artificial sweeteners–a review", *Journal of food science and technology,* vol. 51, no. 4, pp. 611-621.

Chaturvedi, U., Mathur, A., Khan, A. and Mehrotra, R., 1969. Cytotoxicity of filtrates of haemolytic *Escherichia coli*. *Journal of medical microbiology,* [e-journal] 2 (3), pp.211-218. Available through: google.

Chelakkot, C., Ghim, J. and Ryu, S.H., 2018. Mechanisms regulating intestinal barrier integrity and its pathological implications. *Experimental & molecular medicine*, [e-journal] 50 (8), pp.1-9. Available through: google.

Chen, W., Zhang, J., Barve, S., McClain, C. and Joshi-Barve, S., 2017. Intestinal epithelial barrier function is disrupted by acrolein, an environmental/dietary pollutant and lipid metabolite. *The FASEB Journal*, [e-journal] 31 (1_supplement), pp.1067.9-1067.9. Available through: google.

Chen, X. and Devaraj, S., 2018. Gut microbiome in obesity, metabolic syndrome, and diabetes. *Current diabetes reports*, [e-journal] 18 (12), pp.129. Available through: google.

Chi, L., Bian, X., Gao, B., Tu, P., Lai, Y., Ru, H. and Lu, K., 2018. Effects of the artificial sweetener neotame on the gut microbiome and fecal metabolites in mice. *Molecules*, [e-journal] 23 (2), pp.367. Available through: google.

Claus, S.P., Guillou, H. and Ellero-Simatos, S., 2016. The gut microbiota: a major player in the toxicity of environmental pollutants? *Npj biofilms and microbiomes,* [e-journal] 2, pp.16003. Available through: google.

Clemente, J.C., Ursell, L.K., Parfrey, L.W. and Knight, R., 2012. The impact of the gut microbiota on human health: an integrative view. *Cell*, [e-journal] 148 (6), pp.1258-1270. Available through: google.

Coates, M.E. and Walker, R., 1992. Interrelationships between the gastrointestinal microflora and non-nutrient components of the diet. *Nutrition research reviews,* [e-journal] 5 (1), pp.85-96. Available through: google.

Coburn, P.S. and Gilmore, M.S., 2003. The *Enterococcus faecalis* cytolysin: a novel toxin active againsteukaryotic and prokaryotic cells. *Cellular microbiology,* [e-journal] 5 (10), pp.661-669. Available through: google.

Coconnier, M., Bernet, M., Kernéis, S., Chauvière, G., Fourniat, J. and Servin, A.L., 1993. Inhibition of adhesion of enteroinvasive pathogens to human intestinal Caco-2 cells by *Lactobacillus acidophilus* strain LB decreases bacterial invasion. *FEMS microbiology letters*, [e-journal] 110 (3), pp.299-305. Available through: google.

Coconnier, M., Bernet-Camard, M. and Servin, A.L., 1994. How intestinal epithelial cell differentiation inhibits the cell-entry of *Yersinia pseudotuberculosis* in colon carcinoma Caco-2 cell line in culture. *Differentiation,* [e-journal] 58 (1), pp.87-94. Available through: google.

Coleman, M.L., Sahai, E.A., Yeo, M., Bosch, M., Dewar, A. and Olson, M.F., 2001. Membrane blebbing during apoptosis results from caspase-mediated activation of ROCK I. *Nature cell biology,* [e-journal] 3 (4), pp.339. Available through: google.

Collins, M.K., Perkins, G.R., Rodriguez-Tarduchy, G., Nieto, M.A. and López-Rivas, A., 1994. Growth factors as survival factors: regulation of apoptosis. *Bioessays,* [e-journal] 16 (2), pp.133-138. Available through: google.

Cooke, E.M. and Ewins, S.P., 1975. Properties of strains of *Escherichia coli* isolated from a variety of sources. *Journal of medical microbiology,* [e-journal] 8 (1), pp.107-111. 10.1099/00222615-8-1-107 [doi].

Coopersmith, C.M., Stromberg, P.E., Dunne, W.M., Davis, C.G., Amiot II, D.M., Buchman, T.G., Karl, I.E. and Hotchkiss, R.S., 2002. Inhibition of intestinal epithelial apoptosis and survival in a murine model of pneumonia-induced sepsis. *Jama*, [e-journal] 287 (13), pp.1716-1721. Available through: google.

Cordain, L., Eaton, S.B., Sebastian, A., Mann, N., Lindeberg, S., Watkins, B.A., O'Keefe, J.H. and Brand-Miller, J., 2005. Origins and evolution of the Western diet: health implications for the 21st century. *The American Journal of Clinical Nutrition*, [e-journal] 81 (2), pp.341-354. Available through: google.

Cordeiro, F., da Silva, Rita Ifuoe K, Vargas-Stampe, T.L., Cerqueira, A.M. and Andrade, J.R., 2013. Cell invasion and survival of Shiga toxin-producing *Escherichia coli* within cultured human intestinal epithelial cells. *Microbiology*, [e-journal] 159 (8), pp.1683-1694. Available through: google.

Cornier, M., Dabelea, D., Hernandez, T.L., Lindstrom, R.C., Steig, A.J., Stob, N.R., Van Pelt, R.E., Wang, H. and Eckel, R.H., 2008. The metabolic syndrome*. Endocrine reviews*, [e-journal] 29 (7), pp.777-822. Available through: google.

Cossart, P. and Sansonetti, P.J., 2004. Bacterial invasion: the paradigms of enteroinvasive pathogens. *Science* (New York, N.Y.), [e-journal] 304 (5668), pp.242-248. 10.1126/science.1090124 [doi].

Cotter, P.A. and Stibitz, S., 2007. c-di-GMP-mediated regulation of virulence and biofilm formation. *Current opinion in microbiology*, [e-journal] 10 (1), pp.17-23. Available through: google.

Cox, A., Zhang, P., Bowden, D., Devereaux, B., Davoren, P., Cripps, A. and West, N., 2017. Increased intestinal permeability as a risk factor for type 2 diabetes. *Diabetes & metabolism*, [e-journal] 43 (2), pp.163-166. Available through: google.

Csáki, K.F., 2011. Synthetic surfactant food additives can cause intestinal barrier dysfunction. *Medical hypotheses*, [e-journal] 76 (5), pp.676-681. Available through: google.

Cuevas-Ramos, G., Petit, C.R., Marcq, I., Boury, M., Oswald, E. and Nougayrède, J., 2010. *Escherichia coli* induces DNA damage *in vivo* and triggers genomic instability in mammalian cells. *Proceedings of the National Academy of Sciences,* [e-journal] 107 (25), pp.11537-11542. Available through: google.

Cummings, D.E. & Overduin, J. 2007, "Gastrointestinal regulation of food intake", *The Journal of clinical investigation,* vol. 117, no. 1, pp. 13-23.

Daly, K., Darby, A.C. and Shirazi-Beechey, S.P., 2016. Low calorie sweeteners and gut microbiota. *Physiology & Behavior*, [e-journal] 164, pp.494-500. Available through: google.

Damak, S., Rong, M., Yasumatsu, K., Kokrashvili, Z., Varadarajan, V., Zou, S., Jiang, P., Ninomiya, Y. and Margolskee, R.F., 2003. Detection of sweet and umami taste in the absence of taste receptor T1r3. *Science* (New York, N.Y.), [e-journal] 301 (5634), pp.850-853. 10.1126/science.1087155 [doi].

Damci, T., Nuhoglu, I., Devranoglu, G., Osar, Z., Demir, M., & Ilkova, H. (2003). Increased intestinal permeability as a cause of fluctuating postprandial blood glucose levels in type 1 diabetic patients. *European Journal of Clinical Investigation, 33*(5), 397-401.

Darfeuille-Michaud, A., Aubel, D., Chauviere, G., Rich, C., Bourges, M., Servin, A. and Joly, B., 1990. Adhesion of enterotoxigenic *Escherichia coli* to the human colon carcinoma cell line Caco-2 in culture. *Infection and immunity*, [e-journal] 58 (4), pp.893-902.

Das, A. and Chakraborty, R., 2016. Sweeteners: Classification, Sensory and Health Effects. In Encyclopedia of Food and Health, pp.234-240 [e-journal] Available through: google.

David, L.A., Maurice, C.F., Carmody, R.N., Gootenberg, D.B., Button, J.E., Wolfe, B.E., Ling, A.V., Devlin, A.S., Varma, Y. and Fischbach, M.A., 2014. Diet rapidly and reproducibly alters the human gut microbiome. *Nature*, [e-journal] 505 (7484), pp.559-563. Available through: google.

Davidson, L.A., Jiang, Y., Derr, J.N., Aukema, H.M., Lupton, J.R. & Chapkin, R.S. 1994, "Protein kinase C isoforms in human and rat colonic mucosa", *Archives of Biochemistry and Biophysics*, vol. 312, no. 2, pp. 547-553.

De Filippis, F., Pellegrini, N., Vannini, L., Jeffery, I.B., La Storia, A., Laghi, L., Serrazanetti, D.I., Di Cagno, R., Ferrocino, I., Lazzi, C., Turroni, S., Cocolin, L., Brigidi, P., Neviani, E., Gobbetti, M., O'Toole, P.W. and Ercolini, D., 2016. High-level adherence to a Mediterranean diet beneficially impacts the gut microbiota and associated metabolome. *Gut,* [e-journal] 65 (11), pp.1812-1821. 10.1136/gutjnl-2015-309957 [doi].

De Filippo, C., Cavalieri, D., Di Paola, M., Ramazzotti, M., Poullet, J.B., Massart, S., Collini, S., Pieraccini, G. and Lionetti, P., 2010. Impact of diet in shaping gut microbiota revealed by a comparative study in children from Europe and rural Africa. *Proceedings of the National Academy of Sciences of the United States of America,* [e-journal] 107 (33), pp.14691-14696. 10.1073/pnas.1005963107 [doi].

De Jonge, R., Takumi, K., Ritmeester, W. and Van Leusden, F., 2003. The adaptive response of *Escherichia coli* O157 in an environment with changing pH. *Journal of applied microbiology,* [e-journal] 94 (4), pp.555-560. Available through: google.

de La Peña, C., 2010. Artificial sweetener as a historical window to culturally situated health. *Annals of the New York Academy of Sciences*, [e-journal] 1190 (1), pp.159-165. Available through: google.

de Queiroz Pane, D., Dias, C.B., Meinhart, A.D., Ballus, C.A. and Godoy, H.T., 2015. Evaluation of the sweetener content in diet/light/zero foods and drinks by HPLC-DAD. *Journal of Food Science and Technology*, [e-journal] 52 (11), pp.6900-6913. Available through: google.

Deitch, E.A., Xu, D., Naruhn, M.B., Deitch, D.C., Lu, Q. and Marino, A.A., 1995. Elemental diet and IV-TPN-induced bacterial translocation is associated with loss of intestinal mucosal barrier function against bacteria. *Annals of Surgery*, [e-journal] 221 (3), pp.299-307. 10.1097/00000658-199503000-00013 [doi].

Delgado, M.E., Grabinger, T. and Brunner, T., 2016. Cell death at the intestinal epithelial front line. *The FEBS journal*, [e-journal] 283 (14), pp.2701-2719. Available through: google.

Desagher, S. and Martinou, J., 2000. Mitochondria as the central control point of apoptosis. *Trends in cell biology,* [e-journal] 10 (9), pp.369-377. Available through: google.

Dethlefsen, L., McFall-Ngai, M. and Relman, D.A., 2007. An ecological and evolutionary perspective on human–microbe mutualism and disease. *Nature,* [e-journal] 449 (7164), pp.811. Available through: google.

d'Heureuse, H., 2000. Effects of exogenous zinc supplementation on intestinal epithelial repair *in vitro*. *European journal of clinical investigation*, [e-journal] 30 (5), pp.419-428. Available through: google.

Diabetes UK. https://www.diabetes.co.uk/diabetes-history.html, posted on 15 January 2019, accessed on 14 December 2019.

Diaz Heijtz, R., Wang, S., Anuar, F., Qian, Y., Bjorkholm, B., Samuelsson, A., Hibberd, M.L., Forssberg, H. and Pettersson, S., 2011. Normal gut microbiota modulates brain development and behavior. *Proceedings of the National Academy of Sciences of the United States of America,* [e-journal] 108 (7), pp.3047-3052. 10.1073/pnas.1010529108 [doi].

Dogan, B., Klaessig, S., Rishniw, M., Almeida, R., Oliver, S., Simpson, K. and Schukken, Y., 2006. Adherent and invasive *Escherichia coli* are associated with persistent bovine mastitis. *Veterinary microbiology*, [e-journal] 116 (4), pp.270-282. Available through: google.

Donnenberg, M.S., Donohue-Rolfe, A. and Keusch, G.T., 1989. Epithelial cell invasion: an overlooked property of enteropathogenic *Escherichia coli* (EPEC) associated with the EPEC adherence factor. *Journal of Infectious Diseases*, [e-journal] 160 (3), pp.452-459. Available through: google.

Dorn, G.W., 2015. Mitochondrial dynamism and heart disease: changing shape and shaping change. *EMBO molecular medicine,* [e-journal] 7 (7), pp.865-877. Available through: google.

Drago, S., El Asmar, R., Di Pierro, M., Grazia Clemente, M., Sapone, A.T.A., Thakar, M., Iacono, G., Carroccio, A., D'Agate, C. and Not, T., 2006. Gliadin, zonulin and gut permeability: Effects

on celiac and non-celiac intestinal mucosa and intestinal cell lines. *Scandinavian Journal of Gastroenterology,* [e-journal] 41 (4), pp.408-419. Available through: google.

Drucker, D.J., 2003. Glucagon-like peptides: regulators of cell proliferation, differentiation, and apoptosis. *Molecular endocrinology*, [e-journal] 17 (2), pp.161-171. Available through: google.

Dublin, May 28, 2019 (GLOBE NEWSWIRE) -- The "Artificial Sweeteners Market, Consumption & Forecast, By Products, Regions, Applications, Company Analysis" report has been added to ResearchAndMarkets.com's offering. https://www.globenewswire.com/news-release/2019/05/28/1853082/0/en/Global-Artificial-Sweeteners-Aspartame-Sucralose-Saccharin-Neotame-Acesulfame-Potassium-ACE-K-Stevia-and-Cyclamate-Market-Report-2019-2025.html. Accessed on 14 December 2019.

DuBois, G.E., 2016. Molecular mechanism of sweetness sensation. *Physiology & Behavior*, [e-journal] 164, pp.453-463. Available through: google.

Duffy, V.B. and Anderson, G.H., 1998. Position of the American Dietetic Association: use of nutritive and nonnutritive sweeteners. *Journal of the American Dietetic Association*, [e-journal] 98 (5), pp.580-587. Available through: google.

Eaton, T.J. and Gasson, M.J., 2001. Molecular screening of *Enterococcus* virulence determinants and potential for genetic exchange between food and medical isolates. *Applied and Environmental Microbiology,* [e-journal] 67 (4), pp.1628-1635. 10.1128/AEM.67.4.1628-1635.2001 [doi].

Eckel, R.H., Alberti, K.G., Grundy, S.M. and Zimmet, P.Z., 2010. The metabolic syndrome. *Lancet* (London, England), [e-journal] 375 (9710), pp.181-183. 10.1016/S0140-6736(09)61794-3 [doi].

Eckmann, L., Kagnoff, M.F. and Fierer, J., 1993. Epithelial cells secrete the chemokine interleukin-8 in response to bacterial entry. *Infection and immunity*, [e-journal] 61 (11), pp.4569-4574.

Edwards, A.M. and Massey, R.C., 2011. Invasion of human cells by a bacterial pathogen. *JoVE* (*Journal of Visualized Experiments*), [e-journal] (49), pp.e2693. Available through: google.

Edwards, A.M., Potts, J.R., Josefsson, E. and Massey, R.C., 2010. *Staphylococcus aureus* host cell invasion and virulence in sepsis is facilitated by the multiple repeats within FnBPA. *PLoS pathogens*, [e-journal] 6 (6), pp.e1000964. Available through: google.

Elliott, R.A., Kapoor, S. & Tincello, D.G. 2011, "Expression and distribution of the sweet taste receptor isoforms T1R2 and T1R3 in human and rat bladders", *The Journal of urology*, vol. 186, no. 6, pp. 2455-2462.

Elmore, S., 2007. Apoptosis: a review of programmed cell death. *Toxicologic pathology*, [e-journal] 35 (4), pp.495-516. Available through: google.

Epps, H.M. & Gale, E.F. 1942, "The influence of the presence of glucose during growth on the enzymic activities of *Escherichia coli*: comparison of the effect with that produced by fermentation acids", *The Biochemical journal*, vol. 36, no. 7-9, pp. 619-623.

Esposito, K. and Giugliano, D., 2004. The metabolic syndrome and inflammation: association or causation? [e-journal] Available through: google.

European Food Safety Authority (EFSA), accessed on 14 December 2019 for aspartame; https://efsa.onlinelibrary.wiley.com/doi/epdf/10.2903/j.efsa.2006.356

European Food Safety Authority (EFSA), accessed on 14 December 2019 for neotame; https://efsa.onlinelibrary.wiley.com/doi/epdf/10.2903/j.efsa.2007.581

European Food Safety Authority (EFSA), accessed on 14 December 2019 for saccharin; https://efsa.onlinelibrary.wiley.com/doi/epdf/10.2903/j.efsa.2012.2640

European Food Safety Authority (EFSA), accessed on 14 December 2019 for sucralose; https://efsa.onlinelibrary.wiley.com/doi/epdf/10.2903/j.efsa.2016.4361

Faiz, U., Butt, T., Satti, L., Hussain, W. and Hanif, F., 2011. Efficacy of zinc as an antibacterial agent against enteric bacterial pathogens. *Journal of Ayub Medical College Abbottabad,* [e-journal] 23 (2), pp.18-21. Available through: google.

Falkow, S., Isberg, R. and Portnoy, D., 1992. The interaction of bacteria with mammalian cells. *Annual Review of Cell Biology,* [e-journal] 8 (1), pp.333-363. Available through: google.

Fang, X., Neyrinck, A.P., Matthay, M.A. and Lee, J.W., 2010. Allogeneic human mesenchymal stem cells restore epithelial protein permeability in cultured human alveolar type II cells by secretion of angiopoietin-1. *The Journal of biological chemistry,* [e-journal] 285 (34), pp.26211-26222. 10.1074/jbc.M110.119917 [doi].

FAO *Food and nutrition paper 85*, 2001. Probiotics in food, health and nutritional properties and guidelines for evaluation. Report of a joint FAO/WHO expert consultation on evaluation of health and nutritional properties of prebiotics in food including milk with live Lactic acid bacteria. http://www.fao.org/3/a-a0512e.pdf

Farhadi, A., Banan, A., Fields, J. and Keshavarzian, A., 2003. Intestinal barrier: an interface between health and disease. *Journal of gastroenterology and hepatology,* [e-journal] 18 (5), pp.479-497. Available through: google.

Farhadi, A., Keshavarzian, A., Ranjbaran, Z., Fields, J.Z. & Banan, A. 2006, "The role of protein kinase C isoforms in modulating injury and repair of the intestinal barrier", *The Journal of pharmacology and experimental therapeutics,* vol. 316, no. 1, pp. 1-7.

Fasano, A., Fiorentini, C., Donelli, G., Uzzau, S., Kaper, J.B., Margaretten, K., Ding, X., Guandalini, S., Comstock, L. & Goldblum, S.E. 1995, "Zonula occludens toxin modulates tight junctions through protein kinase C-dependent actin reorganization, *in vitro*", *The Journal of clinical investigation,* vol. 96, no. 2, pp. 710-720.

FDA. High-intensity sweeteners. 2014. Available from: FDA. https://www.fda.gov/food/food-additives-petitions/additional-information-about-high-intensity-sweeteners-permitted-use-food-united-states, accessed on 14 December 2019.

Fernández-Hidalgo, N., Almirante, B., Gavaldà, J., Gurgui, M., Peña, C., De Alarcón, A., Ruiz, J., Vilacosta, I., Montejo, M. and Vallejo, N., 2013. Ampicillin plus ceftriaxone is as effective as ampicillin plus gentamicin for treating *Enterococcus faecalis* infective endocarditis. *Clinical infectious diseases,* [e-journal] 56 (9), pp.1261-1268. Available through: google.

Fernstrom, J.D., Munger, S.D., Sclafani, A., de Araujo, I.E., Roberts, A. & Molinary, S. 2012, "Mechanisms for sweetness", *The Journal of nutrition,* vol. 142, no. 6, pp. 1134S-41S.

Finamore, A., Massimi, M., Conti Devirgiliis, L. & Mengheri, E. 2008, "Zinc deficiency induces membrane barrier damage and increases neutrophil transmigration in Caco-2 cells", *The Journal of nutrition,* vol. 138, no. 9, pp. 1664-1670.

Findley, M. K., & Koval, M. (2009). Regulation and roles for claudin-family tight junction proteins. *IUBMB Life, 61*(4), 431-437.

Fisher, K. and Phillips, C., 2009. The ecology, epidemiology and virulence of *Enterococcus*. *Microbiology*, [e-journal] 155 (6), pp.1749-1757. Available through: google.

Fletcher, S.J., Iqbal, M., Jabbari, S., Stekel, D. & Rappoport, J.Z. 2014, "Analysis of Occludin

Trafficking, Demonstrating Continuous Endocytosis, Degradation, Recycling and Biosynthetic Secretory Trafficking", *PloS one*, vol. 9, no. 11, pp. e111176.

Flint, H.J., Bayer, E.A., Rincon, M.T., Lamed, R. and White, B.A., 2008. Polysaccharide utilization by gut bacteria: potential for new insights from genomic analysis. *Nature Reviews Microbiology*, [e-journal] 6 (2), pp.121. Available through: google.

Fogh, J., Fogh, J.M. and Orfeo, T., 1977. One hundred and twenty-seven cultured human tumor cell lines producing tumors in nude mice. *Journal of the National Cancer Institute,* [e-journal] 59 (1), pp.221-226. Available through: google.

Fons, Ana Gomez, Tuomo Karjalainen, Michel, 2000. Mechanisms of colonisation and colonisation resistance of the digestive tract part 2: bacteria/bacteria interactions. *Microbial Ecology in Health and Disease*, [e-journal] 12 (2), pp.240-246. Available through: google.

Fonti, R., Latella, G., Bises, G., Magliocca, F., Nobili, F., Caprilli, R. and Sambuy, Y., 1994. Human colonocytes in primary culture: a model to study epithelial growth, metabolism and differentiation. *International journal of colorectal disease,* [e-journal] 9 (1), pp.13-22. Available through: google.

Forsythe, R.M., Xu, D., Lu, Q. and Deitch, E.A., 2002. Lipopolysaccharide-induced enterocyte-derived nitric oxide induces intestinal monolayer permeability in an autocrine fashion. *Shock*, [e-journal] 17 (3), pp.180-184. Available through: google.

Frank, D.N., St Amand, A.L., Feldman, R.A., Boedeker, E.C., Harpaz, N. and Pace, N.R., 2007. Molecular-phylogenetic characterization of microbial community imbalances in human inflammatory bowel diseases. *Proceedings of the National Academy of Sciences of the United States of America*, [e-journal] 104 (34), pp.13780-13785. 0706625104 [pii].

Frank, L.L., 1957. Diabetes mellitus in the texts of old Hindu medicine (Charaka, Susruta, Vagbhata). *The American Journal of Gastroenterology*, [e-journal] 27 (1), pp.76-95.

Frankenfeld, C.L., Sikaroodi, M., Lamb, E., Shoemaker, S. and Gillevet, P.M., 2015. High-intensity sweetener consumption and gut microbiome content and predicted gene function in a cross-sectional study of adults in the United States. *Annals of Epidemiology,* [e-journal] 25 (10), pp.736-742. e4. Available through: google.

Franz, C.M., Muscholl-Silberhorn, A.B., Yousif, N.M., Vancanneyt, M., Swings, J. and Holzapfel, W.H., 2001. Incidence of virulence factors and antibiotic resistance among enterococci isolated from food. *Applied and Environmental Microbiology,* [e-journal] 67 (9), pp.4385-4389. Available through: google.

Franz, M., 2010, “Diet soft drinks: how safe are they?” *Diabetes Self Manag*. 27(2):8, 11-13.

Frazier, T.H., Dibaise, J.K. and Mcclain, C.J., 2011. Gut microbiota, intestinal permeability, obesity-induced inflammation, and liver injury. *Journal of Parenteral and Enteral Nutrition*, 35(5_suppl), pp. 20S.

Fredriksson, K., Van Itallie, C.M., Aponte, A., Gucek, M., Tietgens, A.J. & Anderson, J.M. 2015, "Proteomic analysis of proteins surrounding occludin and claudin-4 reveals their proximity to signaling and trafficking networks", *PloS one*, vol. 10, no. 3, pp. e0117074.

Friedman, J.R. and Nunnari, J., 2014. Mitochondrial form and function. *Nature,* [e-journal] 505 (7483), pp.335-343. Available through: google.

Frisch, S., 2016. Artificial Sweeteners and Weight Gain: Fighting or Feeding the Obesity Epidemic? *The Science Journal of the Lander College of Arts and Sciences*, [e-journal] 9 (2), pp.9. Available through: google.

Fritz, J.V., Desai, M.S., Shah, P., Schneider, J.G. and Wilmes, P., 2013. From meta-omics to causality: experimental models for human microbiome research. *Microbiome*, [e-journal] 1 (1), pp.14. Available through: google.

Fukuda, S. & Ohno, H. 2014, "Gut microbiome and metabolic diseases", Seminars in immunopathology. Springer, pp. 103.

Fukui, H., 2016. The gut impacts diabetic management tomorrow: the recent messages from intestine and microbiota. *J.Clin.Nutr.Dietetics*, [e-journal] 2, pp.2472-1921.100027. Available through: google.

Fuqua, C., Winans, S.C. and Greenberg, E.P., 1996. Census and consensus in bacterial ecosystems: the LuxR-LuxI family of quorum-sensing transcriptional regulators. *Annual Review of Microbiology,* [e-journal] 50 (1), pp.727-751. Available through: google.

Furumura, M.T., Figueiredo, P., Carbonell, G.V., Darini, Ana Lucia da Costa and Yano, T., 2006. Virulence-associated characteristics of *Enterococcus faecalis* strains isolated from clinical sources. *Brazilian Journal of Microbiology,* [e-journal] 37 (3), pp.230-236. Available through: google.

Furuse, M. 2010, "Molecular basis of the core structure of tight junctions", Cold Spring Harbor perspectives in biology, vol. 2, no. 1, pp. a002907.

Garcia-Lafuente, A., Antolin, M., Guarner, F., Crespo, E. and Malagelada, J.R., 2001. Modulation of colonic barrier function by the composition of the commensal flora in the rat. *Gut*, [e-journal] 48 (4), pp.503-507. Available through: google.

Gardner, C., Wylie-Rosett, J., Gidding, S.S., Steffen, L.M., Johnson, R.K., Reader, D. and Lichtenstein, A.H., 2012. Nonnutritive sweeteners: current use and health perspectives: a scientific statement from the American Heart Association and the American Diabetes Association. *Circulation*, [e-journal] 126 (4), pp.509-519. Available through: google.

Garrett, W.S., Lord, G.M., Punit, S., Lugo-Villarino, G., Mazmanian, S.K., Ito, S., Glickman, J.N. and Glimcher, L.H., 2007. Communicable ulcerative colitis induced by T-bet deficiency in the innate immune system. *Cell*, [e-journal] 131 (1), pp.33-45. Available through: google.

Gavalda, J., Cardona, P.J., Almirante, B., Capdevila, J.A., Laguarda, M., Pou, L., Crespo, E., Pigrau, C. and Pahissa, A., 1996. Treatment of experimental endocarditis due to *Enterococcus faecalis* using once-daily dosing regimen of gentamicin plus simulated profiles of ampicillin in human serum. *Antimicrobial Agents and Chemotherapy,* [e-journal] 40 (1), pp.173-178.

Gavaldà, J., Onrubia, P.L., Gómez, M.T.M., Gomis, X., Ramírez, J.L., Len, O., Rodríguez, D., Crespo, M., Ruíz, I. and Pahissa, A., 2003. Efficacy of ampicillin combined with ceftriaxone and gentamicin in the treatment of experimental endocarditis due to *Enterococcus faecalis* with no high-level resistance to aminoglycosides. *Journal of Antimicrobial Chemotherapy,* [e-journal] 52 (3), pp.514-517. Available through: google.

Geibel, J.P., 2005. Secretion and absorption by colonic crypts. *Annu.Rev.Physiol.,* [e-journal] 67, pp.471-490. Available through: google.

Ghosal, A., Chatterjee, N.S., Chou, T. and Said, H.M., 2013. Enterotoxigenic *Escherichia coli* infection and intestinal thiamin uptake: studies with intestinal epithelial Caco-2 monolayers. *American Journal of Physiology-Cell Physiology*, [e-journal] 305 (11), pp.C1185-C1191. Available through: google.

Ghosh, T.S., Rampelli, S., Jeffery, I.B., Santoro, A., Neto, M., Capri, M., Giampieri, E., Jennings, A., Candela, M., Turroni, S., Zoetendal, E.G., Hermes, G.D.A., Elodie, C., Meunier, N., Brugere, C.M., Pujos-Guillot, E., Berendsen, A.M., De Groot, L.C.P.G.M., Feskins, E.J.M.,

Kaluza, J., Pietruszka, B., Bielak, M.J., Comte, B., Maijo-Ferre, M., Nicoletti, C., De Vos, W.M., Fairweather-Tait, S., Cassidy, A., Brigidi, P., Franceschi, C. and O'Toole, P.W., 2020. Mediterranean diet intervention alters the gut microbiome in older people reducing frailty and improving health status: the NU-AGE 1-year dietary intervention across five European countries. *Gut*, [e-journal] gutjnl-2019-319654 [pii].

Giaffer, M.H., Holdsworth, C.D. and Duerden, B.I., 1992. Virulence properties of *Escherichia coli* strains isolated from patients with inflammatory bowel disease. *Gut,* [e-journal] 33 (5), pp.646-650. 10.1136/gut.33.5.646 [doi].

Gibson, P., Newnham, E., Barrett, J., Shepherd, S. & Muir, J. 2007, "Review article: fructose malabsorption and the bigger picture", *Alimentary Pharmacology & Therapeutics,* vol. 25, no. 4, pp. 349-363.

Gill, S.R., Pop, M., DeBoy, R.T., Eckburg, P.B., Turnbaugh, P.J., Samuel, B.S., Gordon, J.I., Relman, D.A., Fraser-Liggett, C.M. and Nelson, K.E., 2006. Metagenomic analysis of the human distal gut microbiome. *Science,* [e-journal] 312 (5778), pp.1355-1359. Available through: google.

Glick-Bauer, M. and Yeh, M., 2014. The health advantage of a vegan diet: exploring the gut microbiota connection. *Nutrients,* [e-journal] 6 (11), pp.4822-4838. Available through: google.

Goldberg, R.B. and Mather, K., 2012. Targeting the consequences of the metabolic syndrome in the Diabetes Prevention Program. *Arteriosclerosis, Thrombosis, and Vascular Biology*, [e-journal] 32 (9), pp.2077-2090. Available through: google.

Gomes, B.C., Esteves, C.T., Palazzo, I.C., Darini, A.L.C., Felis, G.E., Sechi, L.A., Franco, B.D. and De Martinis, E.C., 2008. Prevalence and characterization of *Enterococcus* spp. isolated from Brazilian foods. *Food Microbiology*, [e-journal] 25 (5), pp.668-675. Available through: google.

Gonzalez-Mariscal, L., Tapia, R. and Chamorro, D., 2008. Crosstalk of tight junction components with signaling pathways. *Biochimica et Biophysica Acta (BBA)-Biomembranes,* [e-journal] 1778 (3), pp.729-756. Available through: google.

Gordon, D.M. and Cowling, A., 2003. The distribution and genetic structure of *Escherichia coli* in Australian vertebrates: host and geographic effects. *Microbiology,* [e-journal] 149 (12), pp.3575-3586. Available through: google.

Grabinger, T., Luks, L., Kostadinova, F., Zimberlin, C., Medema, J.P., Leist, M. and Brunner, T., 2014. Ex vivo culture of intestinal crypt organoids as a model system for assessing cell death induction in intestinal epithelial cells and enteropathy. *Cell death & disease*, [e-journal] 5 (5), pp.e1228-e1228. Available through: google.

Groschwitz, K.R. and Hogan, S.P., 2009. Intestinal barrier function: molecular regulation and disease pathogenesis. *Journal of allergy and clinical immunology*, [e-journal] 124 (1), pp.3-20. Available through: google.

Guignot, J., Peiffer, I., Bernet-Camard, M.F., Lublin, D.M., Carnoy, C., Moseley, S.L. and Servin, A.L., 2000. Recruitment of CD55 and CD66e brush border-associated glycosylphosphatidylinositol-anchored proteins by members of the Afa/Dr diffusely adhering family of *Escherichia coli* that infect the human polarized intestinal Caco-2/TC7 cells. *Infection and immunity*, [e-journal] 68 (6), pp.3554-3563. 10.1128/iai.68.6.3554-3563.2000 [doi].

Gunther, C., Neumann, H., Neurath, M.F. and Becker, C., 2013. Apoptosis, necrosis and necroptosis: cell death regulation in the intestinal epithelium. *Gut*, [e-journal] 62 (7), pp.1062-1071. 10.1136/gutjnl-2011-301364 [doi].

Günzel, D. and Yu, A.S., 2013. Claudins and the modulation of tight junction permeability. *Physiological Reviews*, [e-journal] 93 (2), pp.525-569. Available through: google.

Guo, S., Al-Sadi, R., Said, H.M. & Ma, T.Y. 2013, "Lipopolysaccharide causes an increase in intestinal tight junction permeability *in vitro* and *in vivo* by inducing enterocyte membrane expression and localization of TLR-4 and CD14", *The American journal of pathology*, vol. 182, no. 2, pp. 375-387.

Halter, J.B. and Porte JR, D., 1978. Mechanisms of impaired acute insulin release in adult onset diabetes: studies with isoproterenol and secretin. *The Journal of Clinical Endocrinology & Metabolism*, [e-journal] 46 (6), pp.952-960. Available through: google.

Hamano, K., Nakagawa, Y., Ohtsu, Y., Li, L., Medina, J., Tanaka, Y., Masuda, K., Komatsu, M. & Kojima, I. 2015, "Lactisole inhibits the glucose-sensing receptor T1R3 expressed in mouse pancreatic beta-cells", *The Journal of endocrinology,* vol. 226, no. 1, pp. 57-66.

Hamilton, I., Fairris, G., Rothwell, J., Cunliffe, W., Dixon, M. and Axon, A., 1985. Small intestinal permeability in dermatological disease. *QJM: An International Journal of Medicine,* [e-journal] 56 (3-4), pp.559-567. Available through: google.

Hamilton, M.K., Boudry, G., Lemay, D.G. and Raybould, H.E., 2015. Changes in intestinal barrier function and gut microbiota in high-fat diet-fed rats are dynamic and region dependent. *American Journal of Physiology-Gastrointestinal and Liver Physiology*, [e-journal] 308 (10), pp.G840-G851. Available through: google.

Harhaj, N.S. & Antonetti, D.A. 2004, "Regulation of tight junctions and loss of barrier function in pathophysiology", *The international journal of biochemistry & cell biology,* vol. 36, no. 7, pp. 1206-1237.

Harpaz, D., Yeo, L., Cecchini, F., Koon, T., Kushmaro, A., Tok, A., Marks, R. and Eltzov, E., 2018. Measuring artificial sweeteners toxicity using a bioluminescent bacterial panel. *Molecules,* [e-journal] 23 (10), pp.2454. Available through: google.

Harrington, E.O., Vang, A., Braza, J., Shil, A. and Chichger, H., 2018. Activation of the sweet taste receptor, T1R3, by the artificial sweetener sucralose regulates the pulmonary endothelium. *American Journal of Physiology-Lung Cellular and Molecular Physiology*, [e-journal] 314 (1), pp.L165-L176. Available through: google.

Harrison, A., Erlwanger, K., Elbrønd, V., Andersen, N. and Unmack, M., 2004. Gastrointestinal-tract models and techniques for use in safety pharmacology. *Journal of pharmacological and toxicological methods*, [e-journal] 49 (3), pp.187-199. Available through: google.

Hashem, K.M., He, F.J. and MacGregor, G.A., 2017. Cross-sectional surveys of the amount of sugar, energy and caffeine in sugar-sweetened drinks marketed and consumed as energy drinks in the UK between 2015 and 2017: monitoring reformulation progress. *BMJ open*, [e-journal] 7 (12), pp.e018136-2017-018136. 10.1136/bmjopen-2017-018136 [doi].

Heimesaat, M.M., Alter, T., Bereswill, S. and Gölz, G., 2016. Intestinal expression of genes encoding inflammatory mediators and gelatinases during Arcobacter butzleri infection of gnotobiotic IL-10 deficient mice. *European Journal of Microbiology and Immunology*, [e-journal] 6 (1), pp.56-66. Available through: google.

Held, P., 2009. An absorbance-based cytotoxicity assay using high absorptivity, water-soluble tetrazolium salts. Application Note. BioTek Instruments, INC., Winooski, *Vermont*, [e-journal] 5404 Available through: google.

Helliwell, P.A., Rumsby, M.G. and Kellett, G.L., 2003. Intestinal sugar absorption is regulated by phosphorylation and turnover of protein kinase C betaII mediated by phosphatidylinositol 3-kinase- and mammalian target of rapamycin-dependent pathways. *The Journal of biological chemistry,* [e-journal] 278 (31), pp.28644-28650. 10.1074/jbc.M301479200 [doi].

Hengartner, M.O., 2000. The biochemistry of apoptosis. *Nature,* [e-journal] 407 (6805), pp.770. Available through: google.

Henry, C.M., Hollville, E. and Martin, S.J., 2013. Measuring apoptosis by microscopy and flow cytometry. *Methods,* [e-journal] 61 (2), pp.90-97. Available through: google.

Hentzer, M. and Givskov, M., 2003. Pharmacological inhibition of quorum sensing for the treatment of chronic bacterial infections. *The Journal of clinical investigation*, [e-journal] 112 (9), pp.1300-1307. Available through: google.

Herder, C., Schneitler, S., Rathmann, W., Haastert, B., Schneitler, H., Winkler, H., Bredahl, R., Hahnloser, E. and Martin, S., 2007. Low-grade inflammation, obesity, and insulin resistance in adolescents. *The Journal of Clinical Endocrinology & Metabolism*, [e-journal] 92 (12), pp.4569-4574. Available through: google.

Himsworth, H.P., 1936. Diabetes mellitus. Its differentiation into insulin-sensitive and insulin-insensitive types. *Lancet*, [e-journal] 230, pp.127-130. Available through: google.

Hockenbery, D., 1995. Defining apoptosis. *The American journal of pathology,* [e-journal] 146 (1), pp.16-19.

Hold, G.L. and Allen-Vercoe, E., 2019. Gut microbial biofilm composition and organisation holds the key to CRC. Nature Reviews Gastroenterology & Hepatology, [e-journal] 16 (6), pp.329-330. Available through: google.

Hollander, D. 1999, "Intestinal permeability, leaky gut, and intestinal disorders", *Current gastroenterology reports,* vol. 1, no. 5, pp. 410-416.

Hollister, E.B., Gao, C. and Versalovic, J., 2014. Compositional and functional features of the gastrointestinal microbiome and their effects on human health. *Gastroenterology,* [e-journal] 146 (6), pp.1449-1458. Available through: google.

Hooper, L. V., Littman, D. R., & Macpherson, A. J. (2012). Interactions between the microbiota and the immune system. *Science (New York, N.Y.), 336*(6086), 1268-1273. doi:10.1126/science.1223490 [doi]

Horio, Y., Sun, Y., Liu, C., Saito, T. and Kurasaki, M., 2014. Aspartame-induced apoptosis in PC12 cells. *Environmental toxicology and pharmacology,* [e-journal] 37 (1), pp.158-165. Available through: google.

https://assets.publishing.service.gov.uk/government/uploads/system/uploads/attachment_data/file/566251/FoP_Nutrition_labelling_UK_guidance.pdf REGULATION (EU) No 1169/2011 OF THE EUROPEAN PARLIAMENT AND OF THE COUNCIL of 25 October 2011 on the provision of food information to consumers, amending Regulations (EC) No 1924/2006 and (EC) No 1925/2006 of the European Parliament and of the Council, and repealing Commission Directive 87/250/EEC, Council Directive 90/496/EEC, Commission Directive 1999/10/EC, Directive 2000/13/EC of the European Parliament and of the Council, Commission Directives 2002/67/EC and 2008/5/EC and Commission Regulation (EC) No 608/2004. Appendix-4, p 23.

https://issuu.com/surajtaur/docs/low_calorie_sweeteners_market_pdf, accessed on 14 December 2019.

https://www.fda.gov/food/food-additives-petitions/high-intensity-sweeteners, Accessed May 2020.

https://www.globenewswire.com/news-release/2019/05/28/1853082/0/en/Global-Artificial-Sweeteners-Aspartame-Sucralose-Saccharin-Neotame-Acesulfame-Potassium-ACE-K-Stevia-and-Cyclamate-Market-Report-2019-2025.html

https://www.marketwatch.com/press-release/low-calorie-sweeteners-market-global-research-2019-size-share-demand-competitor-strategy-industry-trend-and-forecast-to-2023-2019-02-27, accessed on 14 December 2019.

Hudault, S., Guignot, J. and Servin, A.L., 2001. *Escherichia coli* strains colonising the gastrointestinal tract protect germfree mice against *Salmonella typhimurium* infection. *Gut,* [e-journal] 49 (1), pp.47-55. Available through: google.

Huet, C., Sahuquillo-Merino, C., Coudrier, E. and Louvard, D., 1987. Absorptive and mucus-secreting subclones isolated from a multipotent intestinal cell line (HT-29) provide new models for cell polarity and terminal differentiation. *The Journal of cell biology,* [e-journal] 105 (1), pp.345-357. 10.1083/jcb.105.1.345 [doi].

Hughes, D.T. and Sperandio, V., 2008. Inter-kingdom signalling: communication between bacteria and their hosts. *Nature Reviews Microbiology,* [e-journal] 6 (2), pp.111. Available through: google.

Human Microbiome Project Consortium 2012, "Structure, function and diversity of the healthy human microbiome", *Nature,* vol. 486, no. 7402, pp. 207-214.

Humphries, P., Pretorius, E. and Naude, H., 2008. Direct and indirect cellular effects of aspartame on the brain. *European journal of clinical nutrition*, [e-journal] 62 (4), pp.451. Available through: google.

Huycke, M.M., Abrams, V. and Moore, D.R., 2002. *Enterococcus faecalis* produces extracellular superoxide and hydrogen peroxide that damages colonic epithelial cell DNA. *Carcinogenesis,* [e-journal] 23 (3), pp.529-536. Available through: google.

Huycke, M.M., Sahm, D.F. and Gilmore, M.S., 1998. Multiple-drug resistant enterococci: the nature of the problem and an agenda for the future. *Emerging infectious diseases,* [e-journal] 4 (2), pp.239. Available through: google.

Huycke, M.M., Spiegel, C.A. and Gilmore, M.S., 1991. Bacteremia caused by hemolytic, high-level gentamicin-resistant *Enterococcus faecalis*. *Antimicrobial Agents and Chemotherapy,* [e-journal] 35 (8), pp.1626-1634. Available through: google.

IDF 6th atlas (2014)

Inaba, H., Nomura, R., Kato, Y., Takeuchi, H., Amano, A., Asai, F., Nakano, K., Lamont, R.J. and Matsumoto-Nakano, M., 2019. Adhesion and invasion of gingival epithelial cells by *Porphyromonas gulae*. *PloS one*, [e-journal] 14 (3), pp.e0213309. 10.1371/journal.pone.0213309 [doi].

Inoue, M., Okamoto, R., Okubo, T., Inoue, K. and Mitsuhashi, S., 1992. Comparative in-vitro activity of RP 59500 against clinical bacterial isolates. *Journal of Antimicrobial Chemotherapy*, [e-journal] 30 (suppl_A), pp.45-51. Available through: google.

Isberg, R.R. and Leong, J.M., 1990. Multiple β1 chain integrins are receptors for invasin, a protein that promotes bacterial penetration into mammalian cells. *Cell*, [e-journal] 60 (5), pp.861-871. Available through: google.

Ivanov, A.I., Parkos, C.A. and Nusrat, A., 2010. Cytoskeletal regulation of epithelial barrier function during inflammation. *The American journal of pathology*, [e-journal] 177 (2), pp.512-524. Available through: google.

Iwasaki, K. & Sato, M. 1986, "Inhibition of taste nerve responses to sugars and amino acids by cupric and zinc ions in mice", *Chemical senses,* vol. 11, no. 1, pp. 79-88.

J.F.Lawrence. 2003. SACCHARIN. In *Encyclopedia of Food Sciences and Nutrition* (Second Edition). Pages 5033-5035.

James N. BeMiller, 2018. Carbohydrate and Noncarbohydrate Sweeteners. In *Carbohydrate Chemistry for Food Scientists* (Third Edition), pp 371 – 399. [e-book] Elsevier. Available through: google.

Jang, H.J., Kokrashvili, Z., Theodorakis, M.J., Carlson, O.D., Kim, B.J., Zhou, J., Kim, H.H., Xu, X., Chan, S.L., Juhaszova, M., Bernier, M., Mosinger, B., Margolskee, R.F. and Egan, J.M., 2007. Gut-expressed gustducin and taste receptors regulate secretion of glucagon-like peptide-1. *Proceedings of the National Academy of Sciences of the United States of America*, [e-journal] 104 (38), pp.15069-15074. 0706890104 [pii].

Jett, B.D., Huycke, M.M. and Gilmore, M.S., 1994. Virulence of enterococci. *Clinical microbiology reviews*, [e-journal] 7 (4), pp.462-478. Available through: google.

Jiang, P., Cui, M., Zhao, B., Liu, Z., Snyder, L.A., Benard, L.M., Osman, R., Margolskee, R.F. & Max, M. 2005, "Lactisole interacts with the transmembrane domains of human T1R3 to inhibit sweet taste", *The Journal of biological chemistry,* vol. 280, no. 15, pp. 15238-15246.

Jiménez, E., Marín, M.L., Martín, R., Odriozola, J.M., Olivares, M., Xaus, J., Fernández, L. and Rodríguez, J.M., 2008. Is meconium from healthy newborns actually sterile? *Research in microbiology,* [e-journal] 159 (3), pp.187-193. Available through: google.

Johnston, C.A., Stevens, B. and Foreyt, J.P., 2013. The Role of Low-calorie Sweeteners in Diabetes. *European endocrinology*, [e-journal] 9 (2), pp.96-98. 10.17925/EE.2013.09.02.96 [doi].

Jung, H.C., Eckmann, L., Yang, S., Panja, A., Fierer, J., Morzycka-Wroblewska, E. and Kagnoff, M.F., 1995. A distinct array of pro-inflammatory cytokines is expressed in human colon epithelial cells in response to bacterial invasion. *The Journal of clinical investigation,* [e-journal] 95 (1), pp.55-65. Available through: google.

Kaper, J.B., Nataro, J.P. and Mobley, H.L., 2004. Pathogenic *Escherichia coli*. *Nature reviews microbiology*, [e-journal] 2 (2), pp.123. Available through: google.

Karbowski, M. and Youle, R., 2003. Dynamics of mitochondrial morphology in healthy cells and during apoptosis. *Cell death and differentiation*, [e-journal] 10 (8), pp.870. Available through: google.

Kau, A.L., Ahern, P.P., Griffin, N.W., Goodman, A.L. and Gordon, J.I., 2011. Human nutrition, the gut microbiome and the immune system. *Nature,* [e-journal] 474 (7351), pp.327. Available through: google.

Kay O'Donnell, 2006. Aspartame and Neotame. In *Sweeteners and sugar alternatives in food technology*. Edited by Helen Mitchell. Blackwell publishers, pp 86-100.

Keast, R.S., 2003. The effect of zinc on human taste perception. *Journal of Food Science,* [e-journal] 68 (5), pp.1871-1877. Available through: google.

Keast, R.S., Canty, T.M. and Breslin, P.A., 2004. Oral zinc sulfate solutions inhibit sweet taste perception. *Chemical senses*, [e-journal] 29 (6), pp.513-521. Available through: google.

Kerneis, S., Chauviere, G., Darfeuille-Michaud, A., Aubel, D., Coconnier, M.H., Joly, B. and Servin, A.L., 1992. Expression of receptors for enterotoxigenic *Escherichia coli* during enterocytic differentiation of human polarized intestinal epithelial cells in culture. *Infection and immunity,* [e-journal] 60 (7), pp.2572-2580.

Kerr, J.F., Wyllie, A.H. and Currie, A.R., 1972. Apoptosis: a basic biological phenomenon with

wide ranging implications in tissue kinetics. *British journal of cancer*, [e-journal] 26 (4), pp.239. Available through: google.

Kigerl, K.A., Hall, J.C., Wang, L., Mo, X., Yu, Z. and Popovich, P.G., 2016. Gut dysbiosis impairs recovery after spinal cord injury. *Journal of Experimental Medicine,* [e-journal] 213 (12), pp.2603-2620. Available through: google.

Kim, J., Hegde, M. and Jayaraman, A., 2010. Co-culture of epithelial cells and bacteria for investigating host and pathogen interactions. *Lab on a Chip*, [e-journal] 10 (1), pp.43-50. Available through: google.

Kim, J.M., Eckmann, L., Savidge, T.C., Lowe, D.C., Witthoft, T. and Kagnoff, M.F., 1998. Apoptosis of human intestinal epithelial cells after bacterial invasion. *The Journal of clinical investigation*, [e-journal] 102 (10), pp.1815-1823. 10.1172/JCI2466 [doi].

Kim, J.S. and Jobin, C., 2005. The flavonoid luteolin prevents lipopolysaccharide-induced NF-κB signalling and gene expression by blocking IκB kinase activity in intestinal epithelial cells and bone-marrow derived dendritic cells. *Immunology*, [e-journal] 115 (3), pp.375-387. Available through: google.

Kim, M., Hwang, S., Park, E. and Bae, J., 2013. Strict vegetarian diet improves the risk factors associated with metabolic diseases by modulating gut microbiota and reducing intestinal inflammation. *Environmental microbiology reports,* [e-journal] 5 (5), pp.765-775. Available through: google.

Kimmich, G., Randles, J. and Anderson, R., 1988. Inhibition of the serosal sugar carrier in isolated intestinal epithelial cells by saccharin. *Food and chemical toxicology*, [e-journal] 26 (11-12), pp.927-934. Available through: google.

Kimmich, G., Randles, J. and Anderson, R., 1989. Effect of saccharin on the ATP-induced increase in Na permeability in isolated chicken intestinal epithelial cells. *Food and chemical toxicology*, [e-journal] 27 (3), pp.143-149. Available through: google.

Kischkel, F., Hellbardt, S., Behrmann, I., Germer, M., Pawlita, M., Krammer, P.H. and Peter, M., 1995. Cytotoxicity-dependent APO-1 (Fas/CD95)-associated proteins form a death-inducing signaling complex (DISC) with the receptor. *The EMBO journal*, [e-journal] 14 (22), pp.5579-5588. Available through: google.

Koenig, J.E., Spor, A., Scalfone, N., Fricker, A.D., Stombaugh, J., Knight, R., Angenent, L.T. and Ley, R.E., 2011. Succession of microbial consortia in the developing infant gut microbiome. *Proceedings of the National Academy of Sciences of the United States of America,* [e-journal] 108 Suppl 1, pp.4578-4585. 10.1073/pnas.1000081107 [doi].

Koh, A., De Vadder, F., Kovatcheva-Datchary, P. and Bäckhed, F., 2016. From dietary fiber to host physiology: short-chain fatty acids as key bacterial metabolites. *Cell*, [e-journal] 165 (6), pp.1332-1345. Available through: google.

Kong, S., Zhang, Y.H. and Zhang, W., 2018. Regulation of intestinal epithelial cells properties and functions by amino acids. *BioMed research international*, [e-journal] 2018 Available through: google.

König, J., Wells, J., Cani, P.D., García-Ródenas, C.L., MacDonald, T., Mercenier, A., Whyte, J., Troost, F. & Brummer, R. 2016, "Human Intestinal Barrier Function in Health and Disease", *Clinical and Translational Gastroenterology*, vol. 7, no. 10, pp. e196.

Konishi, Y., 2003. Modulations of food-derived substances on intestinal permeability in Caco-2 cell monolayers. *Bioscience, biotechnology, and biochemistry,* [e-journal] 67 (10), pp.2297-2299. Available through: google.

Konturek, P.C., Haziri, D., Brzozowski, T., Hess, T., Heyman, S., Kwiecien, S., Konturek, S.J. and Koziel, J., 2015. Emerging role of fecal microbiota therapy in the treatment of gastrointestinal and extra-gastrointestinal diseases. *Journal of physiology and pharmacology: an official journal of the Polish Physiological Society,* [e-journal] 66 (4), pp.483-491.

Korem, T., Zeevi, D., Suez, J., Weinberger, A., Avnit-Sagi, T., Pompan-Lotan, M., Matot, E., Jona, G., Harmelin, A., Cohen, N., Sirota-Madi, A., Thaiss, C.A., Pevsner-Fischer, M., Sorek, R., Xavier, R., Elinav, E. and Segal, E., 2015. Growth dynamics of gut microbiota in health and disease inferred from single metagenomic samples. *Science* (New York, N.Y.), [e-journal] 349 (6252), pp.1101-1106. 10.1126/science.aac4812 [doi].

Krammer, P.H., Behrmann, I., Daniel, P., Dhein, J. and Debatin, K., 1994. Regulation of apoptosis in the immune system. *Current opinion in immunology,* [e-journal] 6 (2), pp.279-289. Available through: google.

Kristich, C.J., Li, Y., Cvitkovitch, D.G. and Dunny, G.M., 2004. Esp-independent biofilm formation by *Enterococcus faecalis*. *Journal of Bacteriology,* [e-journal] 186 (1), pp.154-163. Available through: google.

Kubica, P., Namieśnik, J. and Wasik, A., 2015. Determination of eight artificial sweeteners and common *Stevia rebaudiana* glycosides in non-alcoholic and alcoholic beverages by reversed-phase liquid chromatography coupled with tandem mass spectrometry. *Analytical and bioanalytical chemistry,* [e-journal] 407 (5), pp.1505-1512. Available through: google.

Kukkonen, M., Raunio, T., Virkola, R., Lähteenmäki, K., Mäkelä, P.H., Klemm, P., Clegg, S. and Korhonen, T.K., 1993. Basement membrane carbohydrate as a target for bacterial adhesion: binding of type I fimbriae of *Salmonella enterica* and *Escherichia coli* to laminin. *Molecular microbiology*, [e-journal] 7 (2), pp.229-237. Available through: google.

Lahuerta Zamora, L. and Pérez-Gracia, M., 2012. Using digital photography to implement the McFarland method. *Journal of The Royal Society Interface,* [e-journal] 9 (73), pp.1892-1897. Available through: google.

Lai, M., Chandrasekera, P.C. & Barnard, N.D. 2014, "You are what you eat, or are you & quest; the challenges of translating high-fat-fed rodents to human obesity and diabetes", *Nutrition & diabetes*, vol. 4, no. 9, pp. e135.

Larsen, N., Vogensen, F.K., Van Den Berg, Frans WJ, Nielsen, D.S., Andreasen, A.S., Pedersen, B.K., Al-Soud, W.A., Sørensen, S.J., Hansen, L.H. and Jakobsen, M., 2010. Gut microbiota in human adults with type 2 diabetes differs from non-diabetic adults. *PloS one*, [e-journal] 5 (2), pp.e9085. Available through: google.

Lavrik, I.N., Golks, A. and Krammer, P.H., 2005. Caspases: pharmacological manipulation of cell death. *The Journal of clinical investigation,* [e-journal] 115 (10), pp.2665-2672. 10.1172/JCI26252 [doi].

Lazar, V., Chifiriuc, M.C., Steward-Tull, D.E., Bleotu, C., Candlich, D. and Wardlaw, A.C., 2010. Investigation of the cytotoxic capacity of some adherent opportunistic enterobacterial strains by the MTT assay and transmission electron microscopy. *Roumanian archives of microbiology and immunology*, [e-journal] 69 (1), pp.35-40.

Lea, T. 2015, 'Caco-2 cell line', P. Cotter, I. López-Expósito, C. Kleiveland, A. Mackie, T. Requena, D. Swiatecka, H. Wichers (Eds.), in The Impact of Food Bio-actives on Gut Health: *In Vitro* and *Ex Vivo* Models, *SpringerOpen*. pp. 103 – 111.

Lee, H.C., Yin, P.H., Lu, C.Y., Chi, C.W. and Wei, Y.H., 2000. Increase of mitochondria and mitochondrial DNA in response to oxidative stress in human cells. *The Biochemical journal,* [e-journal] 348 Pt 2, pp.425-432.

Lee, R.J., Hariri, B.M., McMahon, D.B., Chen, B., Doghramji, L., Adappa, N.D., Palmer, J.N., Kennedy, D.W., Jiang, P., Margolskee, R.F. and Cohen, N.A., 2017. Bacterial d-amino acids suppress sinonasal innate immunity through sweet taste receptors in solitary chemosensory cells. *Science signaling,* [e-journal] 10 (495), pp.10.1126/scisignal.aam7703. eaam7703 [pii].

Lee, Y., Puong, K., Ouwehand, A.C. and Salminen, S., 2003. Displacement of bacterial pathogens from mucus and Caco-2 cell surface by lactobacilli. *Journal of medical microbiology*, [e-journal] 52 (10), pp.925-930. Available through: google.

Lei, S., Cheng, T., Guo, Y., Li, C., Zhang, W. & Zhi, F. 2014, "Somatostatin ameliorates lipopolysaccharide-induced tight junction damage via the ERK–MAPK pathway in Caco2 cells", *European journal of cell biology*, vol. 93, no. 7, pp. 299-307.

Lerner, A. and Matthias, T., 2015. Changes in intestinal tight junction permeability associated with industrial food additives explain the rising incidence of autoimmune disease. *Autoimmunity reviews,* [e-journal] 14 (6), pp.479-489. Available through: google.

Levine, M.M., 1987. *Escherichia coli* that cause diarrhea: enterotoxigenic, enteropathogenic, enteroinvasive, enterohemorrhagic, and enteroadherent*,* [e-journal] Available through: google.

Lewis, J.D., Chen, E.Z., Baldassano, R.N., Otley, A.R., Griffiths, A.M., Lee, D., Bittinger, K., Bailey, A., Friedman, E.S. and Hoffmann, C., 2015. Inflammation, antibiotics, and diet as environmental stressors of the gut microbiome in pediatric Crohn's disease. *Cell host & microbe,* [e-journal] 18 (4), pp.489-500. Available through: google.

Ley, R.E., Peterson, D.A. & Gordon, J.I. 2006, "Ecological and evolutionary forces shaping microbial diversity in the human intestine", *Cell*, vol. 124, no. 4, pp. 837-848.

Li, X., 2009. T1R receptors mediate mammalian sweet and umami taste. The American *Journal of Clinical Nutrition*, [e-journal] 90 (3), pp.733S-737S. Available through: google.

Li, X., Staszewski, L., Xu, H., Durick, K., Zoller, M. and Adler, E., 2002. Human receptors for sweet and umami taste. *Proceedings of the National Academy of Sciences of the United States of America*, [e-journal] 99 (7), pp.4692-4696. 10.1073/pnas.072090199 [doi].

Li, Y., Hansotia, T., Yusta, B., Ris, F., Halban, P.A. and Drucker, D.J., 2003. Glucagon-like peptide-1 receptor signaling modulates beta cell apoptosis. *The Journal of biological chemistry*, [e-journal] 278 (1), pp.471-478. 10.1074/jbc.M209423200 [doi].

Lin, F., Hsu, J., Chou, C., Wu, W., Chang, C. and Liu, H., 2011. Activation of p38 MAPK by damnacanthal mediates apoptosis in SKHep 1 cells through the DR5/TRAIL and TNFR1/TNF-α and p53 pathways. *European journal of pharmacology*, [e-journal] 650 (1), pp.120-129. Available through: google.

Liu, D., Morris-Natschke, S.L., Kucera, L.S., Ishaq, K.S. and Thakker, D.R., 1999. Structure—activity relationships for enhancement of paracellular permeability by 2-alkoxy-3-alkylamidopropylphosphocholines across Caco-2 cell monolayers. *Journal of pharmaceutical sciences*, [e-journal] 88 (11), pp.1169-1174. Available through: google.

Liu, S., Song, Y., Ford, E.S., Manson, J.E., Buring, J.E. & Ridker, P.M. 2005, "Dietary calcium, vitamin D, and the prevalence of metabolic syndrome in middle-aged and older U.S. women", *Diabetes care*, vol. 28, no. 12, pp. 2926-2932.

Liu, Z., Li, N. and Neu, J., 2007. Tight junctions, leaky intestines, and pediatric diseases. *Acta paediatrica,* [e-journal] 94 (4), pp.386-393. Available through: google.

Locke, A.E., Kahali, B., Berndt, S.I., Justice, A.E., Pers, T.H., Day, F.R., Powell, C., Vedantam, S., Buchkovich, M.L. and Yang, J., 2015. Genetic studies of body mass index yield new insights for obesity biology. *Nature*, [e-journal] 518 (7538), pp.197. Available through: google.

Logue, C., Dowey, L.R.C., Strain, J., Verhagen, H., McClean, S. and Gallagher, A.M., 2017. Application of liquid chromatography–tandem mass spectrometry to determine urinary concentrations of five commonly used low-calorie sweeteners: a novel biomarker approach for assessing recent intakes? *Journal of Agricultural and Food Chemistry*, [e-journal] 65 (22), pp.4516-4525. Available through: google.

Lopetuso, L. R., Scaldaferri, F., Bruno, G., Petito, V., Franceschi, F., & Gasbarrini, A. (2015). The therapeutic management of gut barrier leaking: The emerging role for mucosal barrier protectors. *Eur Rev Med Pharmacol Sci*, 19(6), 1068-1076.

Louis, K.S. and Siegel, A.C., 2011. Cell viability analysis using trypan blue: manual and automated methods. [e-book] 2011. *Mammalian cell viability*. Springer. pp.7-12. Available through: google.

Lowe, A.M., Lambert, P.A. and Smith, A.W., 1995. Cloning of an *Enterococcus faecalis* endocarditis antigen: homology with adhesins from some oral streptococci. *Infection and immunity*, [e-journal] 63 (2), pp.703-706.

Lozupone, C.A., Stombaugh, J.I., Gordon, J.I., Jansson, J.K. & Knight, R. 2012, "Diversity, stability and resilience of the human gut microbiota", *Nature*, vol. 489, no. 7415, pp. 220-230.

Ludwig, A., Bauer, S., Benz, R., Bergmann, B. and Goebel, W., 1999. Analysis of the SlyA-controlled expression, subcellular localization and pore-forming activity of a 34 kDa haemolysin (ClyA) from *Escherichia coli* K-12. *Molecular microbiology,* [e-journal] 31 (2), pp.557-567. Available through: google.

Ludwig, A., von Rhein, C., Bauer, S., Huttinger, C. and Goebel, W., 2004. Molecular analysis of cytolysin A (ClyA) in pathogenic Escherichia coli strains. *Journal of Bacteriology*, [e-journal] 186 (16), pp.5311-5320. 10.1128/JB.186.16.5311-5320.2004 [doi].

Lupp, C., Robertson, M.L., Wickham, M.E., Sekirov, I., Champion, O.L., Gaynor, E.C. and Finlay, B.B., 2007. Host-mediated inflammation disrupts the intestinal microbiota and promotes the overgrowth of Enterobacteriaceae. *Cell host & microbe,* [e-journal] 2 (2), pp.119-129. Available through: google.

Ma, T.Y., Nguyen, D., Bui, V., Nguyen, H. and Hoa, N., 1999. Ethanol modulation of intestinal epithelial tight junction barrier. *American Journal of Physiology-Gastrointestinal and Liver Physiology*, [e-journal] 276 (4), pp.G965-G974. Available through: google.

Ma, X., X. Fan, P., Li, L., Qiao, S., Zhang, G. and Li, D., 2012. Butyrate promotes the recovering of intestinal wound healing through its positive effect on the tight junctions. *Journal of animal science*, [e-journal] 90 (suppl_4), pp.266-268. Available through: google.

Mace, O.J., Affleck, J., Patel, N. and Kellett, G.L., 2007. Sweet taste receptors in rat small intestine stimulate glucose absorption through apical GLUT2. *The Journal of physiology,* [e-journal] 582 (1), pp.379-392. Available through: google.

Madara, J. & Pappenheimer, J. 1987, "Structural basis for physiological regulation of paracellular pathways in intestinal epithelia", *The Journal of membrane biology*, vol. 100, no. 1, pp. 149-164.

Madara, J.L., 1987. Intestinal absorptive cell tight junctions are linked to cytoskeleton. *American Journal of Physiology-Cell Physiology*, [e-journal] 253 (1), pp.C175. Available through: google.

Mahler, G.J., Shuler, M.L. and Glahn, R.P., 2009. Characterization of Caco-2 and HT29-MTX cocultures in an *in vitro* digestion/cell culture model used to predict iron bioavailability. *The Journal of nutritional biochemistry*, [e-journal] 20 (7), pp.494-502. Available through: google.

Mahmud, R., Shehreen, S., Shahriar, S., Rahman, M.S., Akhteruzzaman, S. and Sajib, A.A., 2019. Non-Caloric Artificial Sweeteners Modulate the Expression of Key Metabolic Genes in the Omnipresent Gut Microbe *Escherichia coli*. *Journal of Molecular Microbiology and Biotechnology*, [e-journal] , pp.1-14. 10.1159/000504511 [doi].

Makki, K., Deehan, E.C., Walter, J. and Bäckhed, F., 2018. The impact of dietary fiber on gut microbiota in host health and disease. *Cell host & microbe*, [e-journal] 23 (6), pp.705-715. Available through: google.

Marí, M., Morales, A., Colell, A., García-Ruiz, C., Kaplowitz, N. and Fernández-Checa, J.C., 2013. Mitochondrial glutathione: features, regulation and role in disease. *Biochimica et Biophysica Acta (BBA)-General Subjects*, [e-journal] 1830 (5), pp.3317-3328. Available through: google.

Mariat, D., Firmesse, O., Levenez, F., Guimarăes, V.D., Sokol, H., Doré, J., Corthier, G. and Furet, J.P., 2009. The Firmicutes/Bacteroidetes ratio of the human microbiota changes with age. *BMC microbiology,* [e-journal] 9 (1), pp.123. Available through: google.

Martin, S.J., Henry, C.M. and Cullen, S.P., 2012. A perspective on mammalian caspases as positive and negative regulators of inflammation. *Molecular cell,* [e-journal] 46 (4), pp.387-397. Available through: google.

Marzorati, M., Vanhoecke, B., De Ryck, T., Sadabad, M.S., Pinheiro, I., Possemiers, S., Van den Abbeele, P., Derycke, L., Bracke, M. and Pieters, J., 2014. The HMI™ module: a new tool to study the Host-Microbiota Interaction in the human gastrointestinal tract *in vitro*. *BMC microbiology*, [e-journal] 14 (1), pp.133. Available through: google.

Mathan, V.I., Penny, G.R., Mathan, M.M. and Rowley, D., 1988. Bacterial lipopolysaccharide-induced intestinal microvascular lesions leading to acute diarrhea. *The Journal of clinical investigation*, [e-journal] 82 (5), pp.1714-1721. 10.1172/JCI113785 [doi].

Mathur, K., Agrawal, R.K., Nagpure, S. and Deshpande, D., 2020. Effect of artificial sweeteners on insulin resistance among type-2 diabetes mellitus patients. *Journal of Family Medicine and Primary Care*, [e-journal] 9 (1), pp.69. Available through: google.

Mattes, R.D. and Popkin, B.M., 2008. Nonnutritive sweetener consumption in humans: effects on appetite and food intake and their putative mechanisms. *The American Journal of Clinical Nutrition*, [e-journal] 89 (1), pp.1-14. Available through: google.

Mazmanian, S.K., Liu, C.H., Tzianabos, A.O. and Kasper, D.L., 2005. An immunomodulatory molecule of symbiotic bacteria directs maturation of the host immune system. *Cell,* [e-journal] 122 (1), pp.107-118. Available through: google.

Mazmanian, S.K., Round, J.L. and Kasper, D.L., 2008. A microbial symbiosis factor prevents intestinal inflammatory disease. *Nature*, [e-journal] 453 (7195), pp.620. Available through: google.

McBirney, S.E., Trinh, K., Wong-Beringer, A. and Armani, A.M., 2016. Wavelength-normalized spectroscopic analysis of *Staphylococcus aureus* and *Pseudomonas aeruginosa* growth rates. *Biomedical optics express*, [e-journal] 7 (10), pp.4034-4042. Available through: google.

McBride, H.M., Neuspiel, M. and Wasiak, S., 2006. Mitochondria: more than just a powerhouse. *Current biology,* [e-journal] 16 (14), pp.R551-R560. Available through: google.

McClean, K.H., Winson, M.K., Fish, L., Taylor, A., Chhabra, S.R., Camara, M., Daykin, M., Lamb, J.H., Swift, S. and Bycroft, B.W., 1997. Quorum sensing and *Chromobacterium violaceum*:

exploitation of violacein production and inhibition for the detection of N-acylhomoserine lactones. *Microbiology,* [e-journal] 143 (12), pp.3703-3711. Available through: google.

McEwan, G.T., Jepson, M.A., Hirst, B.H. and Simmons, N.L., 1993. Polycation-induced enhancement of epithelial paracellular permeability is independent of tight junctional characteristics. *Biochimica et Biophysica Acta (BBA)-Biomembranes,* [e-journal] 1148 (1), pp.51-60. Available through: google.

Meddings, J., Jarand, J., Urbanski, S., Hardin, J. and Gall, D., 1999. Increased gastrointestinal permeability is an early lesion in the spontaneously diabetic BB rat. *American Journal of Physiology-Gastrointestinal and Liver Physiology*, [e-journal] 276 (4), pp.G951-G957. Available through: google.

Medeiros, P., Bolick, D.T., Roche, J.K., Noronha, F., Pinheiro, C., Kolling, G.L., Lima, A. and Guerrant, R.L., 2013. The micronutrient zinc inhibits EAEC strain 042 adherence, biofilm formation, virulence gene expression, and epithelial cytokine responses benefiting the infected host. *Virulence,* [e-journal] 4 (7), pp.624-633. Available through: google.

Mendez, A., Chagastelles, P., Palma, E., Nardi, N. and Schapoval, E., 2008. Thermal and alkaline stability of meropenem: degradation products and cytotoxicity. *International journal of pharmaceutics*, [e-journal] 350 (1-2), pp.95-102. Available through: google.

Mendez, A.S., Steppe, M. and Schapoval, E.E., 2003. Validation of HPLC and UV spectrophotometric methods for the determination of meropenem in pharmaceutical dosage form. *Journal of pharmaceutical and biomedical analysis*, [e-journal] 33 (5), pp.947-954. Available through: google.

Mendrick, D.L., Diehl, A.M., Topor, L.S., Dietert, R.R., Will, Y., La Merrill, M.A., Bouret, S., Varma, V., Hastings, K.L. and Schug, T.T., 2017. Metabolic syndrome and associated diseases: from the bench to the clinic. *Toxicological Sciences*, [e-journal] 162 (1), pp.36-42. Available through: google.

Mengaud, J., Ohayon, H., Gounon, P., Mège, R. and Cossart, P., 1996. E-cadherin is the receptor for internalin, a surface protein required for entry of L. monocytogenes into epithelial cells. *Cell*, [e-journal] 84 (6), pp.923-932. Available through: google.

Meunier, V., Bourrie, M., Berger, Y. and Fabre, G., 1995. The human intestinal epithelial cell line Caco-2; pharmacological and pharmacokinetic applications. *Cell biology and toxicology*, [e-journal] 11 (3-4), pp.187-194. Available through: google.

Meyer-Gerspach, A.C., Häfliger, S., Meili, J., Doody, A., Rehfeld, J.F., Drewe, J., Beglinger, C. and Wölnerhanssen, B., 2016. Effect of L-tryptophan and L-leucine on gut hormone secretion, appetite feelings and gastric emptying rates in lean and non-diabetic obese participants: a randomized, double-blind, parallel-group trial. *PloS one,* [e-journal] 11 (11), pp.e0166758. Available through: google.

Meyerson, M. and Kostic, A., 2014. Bacterial etiology of colorectal cancer, [e-journal] Available through: google.

Miele, L., Valenza, V., La Torre, G., Montalto, M., Cammarota, G., Ricci, R., Masciana, R., Forgione, A., Gabrieli, M.L. and Perotti, G., 2009. Increased intestinal permeability and tight junction alterations in nonalcoholic fatty liver disease. *Hepatology*, [e-journal] 49 (6), pp.1877-1887. Available through: google.

Miller, M.B. and Bassler, B.L., 2001. Quorum sensing in bacteria. *Annual Reviews in Microbiology,* [e-journal] 55 (1), pp.165-199. Available through: google.

Mine, Y. and Zhang, J.W., 2003. Surfactants enhance the tight-junction permeability of food allergens in human intestinal epithelial Caco-2 cells. *International archives of allergy and immunology*, [e-journal] 130 (2), pp.135-142. Available through: google.

Minnaard, J., Lievin-Le Moal, V., Coconnier, M.H., Servin, A.L. and Perez, P.F., 2004. Disassembly of F-actin cytoskeleton after interaction of *Bacillus cereus* with fully differentiated human intestinal Caco-2 cells. *Infection and immunity,* [e-journal] 72 (6), pp.3106-3112. 10.1128/IAI.72.6.3106-3112.2004 [doi].

Mitic, L.L., Van Itallie, C.M. & Anderson, J.M. 2000, "Molecular physiology and pathophysiology of tight junctions I. Tight junction structure and function: lessons from mutant animals and proteins", *American journal of physiology. Gastrointestinal and liver physiology,* vol. 279, no. 2, pp. G250-254.

Mohamed, J.A. and Huang, D.B., 2007. Biofilm formation by enterococci. *Journal of medical microbiology*, [e-journal] 56 (12), pp.1581-1588. Available through: google.

Monaghan-Benson, E. and Wittchen, E.S., 2011. *In vitro* analyses of endothelial cell permeability. [e-book] 2011. *Permeability Barrier*. Springer., pp.281-290. Available through: google.

Mooseker, M.S., 1985. Organization, chemistry, and assembly of the cytoskeletal apparatus of the intestinal brush border. *Annual Review of Cell Biology*, [e-journal] 1 (1), pp.209-241. Available through: google.

Moran, A.W., Al-Rammahi, M.A., Arora, D.K., Batchelor, D.J., Coulter, E.A., Daly, K., Ionescu, C., Bravo, D. and Shirazi-Beechey, S.P., 2010. Expression of Na /glucose co-transporter 1 (SGLT1) is enhanced by supplementation of the diet of weaning piglets with artificial sweeteners. *British Journal of Nutrition*, [e-journal] 104 (5), pp.637-646. Available through: google.

Moreira, A.P.B., Texeira, T.F.S., Ferreira, A.B., Peluzio, Maria do Carmo Gouveia and Alfenas, Rita de Cássia Gonçalves, 2012. Influence of a high-fat diet on gut microbiota, intestinal permeability and metabolic endotoxaemia. *British Journal of Nutrition*, [e-journal] 108 (5), pp.801-809. Available through: google.

Moreno, M.F., Sarantinopoulos, P., Tsakalidou, E. and De Vuyst, L., 2006. The role and application of enterococci in food and health. *International journal of food microbiology*, [e-journal] 106 (1), pp.1-24. Available through: google.

Muegge, B.D., Kuczynski, J., Knights, D., Clemente, J.C., Gonzalez, A., Fontana, L., Henrissat, B., Knight, R. & Gordon, J.I. 2011, "Diet drives convergence in gut microbiome functions across mammalian phylogeny and within humans", *Science* (New York, N.Y.), vol. 332, no. 6032, pp. 970-974.

Muzio, M., Chinnaiyan, A.M., Kischkel, F.C., O'Rourke, K., Shevchenko, A., Ni, J., Scaffidi, C., Bretz, J.D., Zhang, M. and Gentz, R., 1996. FLICE, a novel FADD-homologous ICE/CED-3–like protease, is recruited to the CD95 (Fas/APO-1) death-inducing signaling complex. *Cell*, [e-journal] 85 (6), pp.817-827. Available through: google.

Myhrvold, C., Kotula, J.W., Hicks, W.M., Conway, N.J. and Silver, P.A., 2015. A distributed cell division counter reveals growth dynamics in the gut microbiota. *Nature communications*, [e-journal] 6, pp.10039. Available through: google.

Nagai, M., Obata, Y., Takahashi, D. and Hase, K., 2016. Fine-tuning of the mucosal barrier and metabolic systems using the diet-microbial metabolite axis. *International immunopharmacology,* [e-journal] 37, pp.79-86. Available through: google.

Nair, A.B. and Jacob, S., 2016. A simple practice guide for dose conversion between animals and human. *Journal of basic and clinical pharmacy*, [e-journal] 7 (2), pp.27-31. 10.4103/0976-0105.177703 [doi].

Nakagawa, Y., Nagasawa, M., Yamada, S., Hara, A., Mogami, H., Nikolaev, V.O., Lohse, M.J., Shigemura, N., Ninomiya, Y. & Kojima, I. 2009, "Sweet taste receptor expressed in pancreatic β-cells activates the calcium and cyclic AMP signaling systems and stimulates insulin secretion", *PloS one,* vol. 4, no. 4, pp. e5106.

Nandi, N., Sen, A., Banerjee, R., Kumar, S., Kumar, V., Ghosh, A.N. and Das, P., 2010. Hydrogen peroxide induces apoptosis-like death in *Entamoeba histolytica* trophozoites. *Microbiology,* [e-journal] 156 (7), pp.1926-1941. Available through: google.

Narai, A., Arai, S. and Shimizu, M., 1997. Rapid decrease in transepithelial electrical resistance of human intestinal Caco-2 cell monolayers by cytotoxic membrane perturbents. *Toxicology in vitro*, [e-journal] 11 (4), pp.347-354. Available through: google.

Nasrallah, F.A., Garner, B., Ball, G.E. and Rae, C., 2008. Modulation of brain metabolism by very low concentrations of the commonly used drug delivery vehicle dimethyl sulfoxide (DMSO). *Journal of neuroscience research*, [e-journal] 86 (1), pp.208-214. Available through: google.

National Center for Biotechnology Information. PubChem Database. Neotame, CID=9810996, https://pubchem.ncbi.nlm.nih.gov/compound/Neotame (accessed on Dec. 4, 2019)

Nawaz, M., Wang, J., Zhou, A., Ma, C., Wu, X. and Xu, J., 2011. Screening and characterization of new potentially probiotic lactobacilli from breast-fed healthy babies in Pakistan. *African Journal of Microbiology Research,* [e-journal] 5 (12), pp.1428-1436. Available through: google.

Neish, A.S., 2002. The gut microflora and intestinal epithelial cells: a continuing dialogue. *Microbes and Infection*, [e-journal] 4 (3), pp.309-317. Available through: google.

Nettleton, J.E., Reimer, R.A. & Shearer, J. 2016, "Reshaping the gut microbiota: Impact of low calorie sweeteners and the link to insulin resistance?" *Physiology & Behavior,* vol. 164, pp. 488-493.

NHS, UK. https://www.nhs.uk/live-well/eat-well/what-does-100-calories-look-like/, accessed on 13 December 2019.

Nicholson, J. K., Holmes, E., Kinross, J., Burcelin, R., Gibson, G., Jia, W., et al. (2012). Host-gut microbiota metabolic interactions. *Science (New York, N.Y.), 336*(6086), 1262-1267. doi:10.1126/science.1223813 [doi]

Nickerson, K.P. and McDonald, C., 2012. Crohn's disease-associated adherent-invasive *Escherichia coli* adhesion is enhanced by exposure to the ubiquitous dietary polysaccharide maltodextrin. *PloS one*, [e-journal] 7 (12), pp.e52132. Available through: google.

Nishikawa, Y., Hase, A., Ogawasara, J., Scotland, S., Smith, H. and Kimura, T., 1994. Adhesion to and invasion of human colon carcinoma Caco-2 cells by *Aeromonas* strains. *Journal of medical microbiology*, [e-journal] 40 (1), pp.55-61. Available through: google.

Nougayrède, J., Homburg, S., Taieb, F., Boury, M., Brzuszkiewicz, E., Gottschalk, G., Buchrieser, C., Hacker, J., Dobrindt, U. and Oswald, E., 2006. *Escherichia coli* induces DNA double-strand breaks in eukaryotic cells. *Science,* [e-journal] 313 (5788), pp.848-851. 313/5788/848 [pii]. Available through: google.

O'Brien, P. & Corpe, C.P. 2016, "Acute Effects of Sugars and Artificial Sweeteners on Small Intestinal Sugar Transport: A Study Using CaCo-2 Cells as an *in Vitro* Model of the Human Enterocyte", *PloS one*, vol. 11, no. 12, pp. e0167785.

O'Hara, A.M. and Shanahan, F., 2006. The gut flora as a forgotten organ. *EMBO reports,* [e-journal] 7 (7), pp.688-693. Available through: google.

Ono, S., Muratani, T. and Matsumoto, T., 2005. Mechanisms of resistance to imipenem and ampicillin in *Enterococcus faecalis*. *Antimicrobial Agents and Chemotherapy*, [e-journal] 49 (7), pp.2954-2958. 49/7/2954 [pii].

O'Toole, G., Kaplan, H.B. and Kolter, R., 2000. Biofilm formation as microbial development. *Annual Reviews in Microbiology*, [e-journal] 54 (1), pp.49-79. Available through: google.

O'Toole, G.A. and Kolter, R., 1998. Initiation of biofilm formation in Pseudomonas fluorescens WCS365 proceeds via multiple, convergent signalling pathways: a genetic analysis. *Molecular microbiology,* [e-journal] 28 (3), pp.449-461. Available through: google.

Ouwehand, A., Kirjavainen, P., Grönlund, M., Isolauri, E. and Salminen, S., 1999. Adhesion of probiotic micro-organisms to intestinal mucus. *International Dairy Journal,* [e-journal] 9 (9), pp.623-630. Available through: google.

Pahwa, R., Singh, A. and Jialal, I., 2019. Chronic Inflammation. [e-book] 2019. *StatPearls.* Treasure Island (FL):StatPearls Publishing LLC. Available through: .

Palmer, K.L., Kos, V.N. and Gilmore, M.S., 2010. Horizontal gene transfer and the genomics of enterococcal antibiotic resistance. *Current opinion in microbiology,* [e-journal] 13 (5), pp.632-639. Available through: google.

Palmnäs, M.S., Cowan, T.E., Bomhof, M.R., Su, J., Reimer, R.A., Vogel, H.J., Hittel, D.S. & Shearer, J. 2014, "Low-dose aspartame consumption differentially affects gut microbiota-host metabolic interactions in the diet-induced obese rat", *PloS one,* vol. 9, no. 10, pp. e109841.

Patterson, A.M. and Watson, A.J., 2017. Deciphering the complex signaling systems that regulate intestinal epithelial cell death processes and shedding. *Frontiers in immunology,* [e-journal] 8, pp.841. Available through: google.

Payne, A., Chassard, C. & Lacroix, C. 2012, "Gut microbial adaptation to dietary consumption of fructose, artificial sweeteners and sugar alcohols: implications for host–microbe interactions contributing to obesity", *obesity reviews*, vol. 13, no. 9, pp. 799-809.

Pearlman, M., Obert, J. and Casey, L., 2017. The association between artificial sweeteners and obesity. *Current gastroenterology reports*, [e-journal] 19 (12), pp.64. Available through: google.

Peiffer, I., Servin, A.L. and Bernet-Camard, M.F., 1998. Piracy of decay-accelerating factor (CD55) signal transduction by the diffusely adhering strain *Escherichia coli* C1845 promotes cytoskeletal F-actin rearrangements in cultured human intestinal INT407 cells. *Infection and immunity,* [e-journal] 66 (9), pp.4036-4042.

Peltonen, R., Nenonen, M., Helve, T., Hanninen, O., Toivanen, P. and Eerola, E., 1997. Faecal microbial flora and disease activity in rheumatoid arthritis during a vegan diet. *British journal of rheumatology,* [e-journal] 36 (1), pp.64-68. 10.1093/rheumatology/36.1.64 [doi].

Peng, L., He, Z., Chen, W., Holzman, I.R. and Lin, J., 2007. Effects of butyrate on intestinal barrier function in a Caco-2 cell monolayer model of intestinal barrier. *Pediatric research,* [e-journal] 61 (1), pp.37. Available through: google.

Pepino, M.Y. 2015, "Metabolic effects of non-nutritive sweeteners", *Physiology & Behavior,* vol. 152, pp. 450-455.

Petersson, J., Schreiber, O., Hansson, G.C., Gendler, S.J., Velcich, A., Lundberg, J.O., Roos, S., Holm, L. and Phillipson, M., 2010. Importance and regulation of the colonic mucus barrier in

a mouse model of colitis. *American Journal of Physiology-Gastrointestinal and Liver Physiology,* [e-journal] 300 (2), pp.G327-G333. Available through: google.

Phue, J., Lee, S.J., Trinh, L. and Shiloach, J., 2008. Modified *Escherichia coli* B (BL21), a superior producer of plasmid DNA compared with *Escherichia coli* K (DH5α). *Biotechnology and bioengineering,* [e-journal] 101 (4), pp.831-836. Available through: google.

Pijls, K.E., Jonkers, D.M., Elamin, E.E., Masclee, A.A. and Koek, G.H., 2013 (a). Intestinal epithelial barrier function in liver cirrhosis: an extensive review of the literature. *Liver international*, [e-journal] 33 (10), pp.1457-1469. Available through: google.

Pijls, K.E., Koek, G.H., Elamin, E.E., de Vries, H., Masclee, A.A. and Jonkers, D.M., 2013 (b). Large intestine permeability is increased in patients with compensated liver cirrhosis. *American Journal of Physiology-Gastrointestinal and Liver Physiology*, [e-journal] 306 (2), pp.G147-G153. Available through: google.

Pizarro-Cerdá, J. and Cossart, P., 2006. Bacterial adhesion and entry into host cells. *Cell*, [e-journal] 124 (4), pp.715-727. Available through: google.

Porikos, K., Booth, G. and Van Itallie, T., 1977. Effect of covert nutritive dilution on the spontaneous food intake of obese individuals: a pilot study. *The American Journal of Clinical Nutrition*, [e-journal] 30 (10), pp.1638-1644. Available through: google.

Potten, C.S., 1992. The significance of spontaneous and induced apoptosis in the gastrointestinal tract of mice. *Cancer and metastasis reviews,* [e-journal] 11 (2), pp.179-195. Available through: google.

Poulsen, L.K., Lan, F., Kristensen, C.S., Hobolth, P., Molin, S. and Krogfelt, K.A., 1994. Spatial distribution of *Escherichia coli* in the mouse large intestine inferred from rRNA in situ hybridization. *Infection and immunity,* [e-journal] 62 (11), pp.5191-5194. Available through: google.

Prakash, I., Bishay, I. and Schroeder, S., 1999. Neotame: Synthesis, stereochemistry and sweetness. *Synthetic Communications*, [e-journal] 29 (24), pp.4461-4467. Available through: google.

Praveena, S.M., Cheema, M.S. and Guo, H., 2019. Non-nutritive artificial sweeteners as an emerging contaminant in environment: A global review and risks perspectives. *Ecotoxicology and environmental safety*, [e-journal] 170, pp.699-707. Available through: google.

Price, J.M., Biava, C.G., Oser, B.L., Vogin, E.E., Steinfeld, J. and Ley, H.L., 1970. Bladder tumors in rats fed cyclohexylamine or high doses of a mixture of cyclamate and saccharin. *Science (New York, N.Y.),* [e-journal] 167 (3921), pp.1131-1132. 10.1126/science.167.3921.1131 [doi].

PubChem Database. National Center for Biotechnology Information. Aspartame, CID=134601, https://pubchem.ncbi.nlm.nih.gov/compound/Aspartame (accessed on Dec. 4, 2019)

PubChem Database. National Center for Biotechnology Information. Sucrose, CID=5988, https://pubchem.ncbi.nlm.nih.gov/compound/Sucrose (accessed on Dec. 4, 2019)

PubChem Database. National Center for Biotechnology Information. Sucralose, CID=71485, https://pubchem.ncbi.nlm.nih.gov/compound/Sucralose (accessed on Dec. 4, 2019)

PubChem Database. National Center for Biotechnology Information. Saccharin, CID=5143, https://pubchem.ncbi.nlm.nih.gov/compound/Saccharin (accessed on Dec. 4, 2019)

Qin, J., Li, R., Raes, J., Arumugam, M., Burgdorf, K.S., Manichanh, C., Nielsen, T., Pons, N., Levenez, F. and Yamada, T., 2010. A human gut microbial gene catalogue established by metagenomic sequencing. *Nature,* [e-journal] 464 (7285), pp.59. Available through: google.

Qu, Y., Li, R., Jiang, M. and Wang, X., 2017. Sucralose increases antimicrobial resistance and stimulates recovery of *Escherichia coli* mutants. *Current microbiology*, [e-journal] 74 (7), pp.885-888. Available through: google.

Quaroni, A. and May, R.J., 1980. Establishment and characterization of intestinal epithelial cell cultures. In Methods in cell biology. *Elsevier*, pp. 403-427.

Quigley, E.M., 2017. Gut microbiome as a clinical tool in gastrointestinal disease management: are we there yet? *Nature Reviews Gastroenterology & Hepatology,* [e-journal] 14 (5), pp.315. Available through: google.

Rajan, S., Vyas, D., Clark, A.T., Woolsey, C.A., Clark, J.A., Hotchkiss, R.S., Buchman, T.G. and Coopersmith, C.M., 2008. Intestine-specific overexpression of IL-10 improves survival in polymicrobial sepsis. *Shock* (Augusta, Ga.), [e-journal] 29 (4), pp.483-489. 10.1097/shk.0b013e31815bbb26 [doi].

Ranaldi, G., Marigliano, I., Vespignani, I., Perozzi, G. and Sambuy, Y., 2002. The effect of chitosan and other polycations on tight junction permeability in the human intestinal Caco-2 cell line. *The Journal of nutritional biochemistry,* [e-journal] 13 (3), pp.157-167. Available through: google.

Rasouli, Z. and Akbari-Adergani, B., 2016. Assessment of aspartame exposure due to consumption of some imported chewing gums by microwave digestion and high-performance liquid chromatography analysis. *Oriental Journal of Chemistry*, [e-journal] 32 (3), pp.1649-1658. Available through: google.

Reisner, A., Krogfelt, K.A., Klein, B.M., Zechner, E.L. and Molin, S., 2006. *In vitro* biofilm formation of commensal and pathogenic *Escherichia coli* strains: impact of environmental and genetic factors. *Journal of Bacteriology*, [e-journal] 188 (10), pp.3572-3581. 188/10/3572 [pii].

Renwick, A., 1985. The fate of intense sweeteners in the body. *Food Chemistry,* [e-journal] 16 (3-4), pp.281-301. Available through: google.

Rettig, S., Tenewitz, J., Ahearn, G. and Coughlin, C., 2014. Sucralose causes a concentration dependent metabolic inhibition of the gut flora Bacteroides, *B. fragilis* and *B. uniformis* not observed in the Firmicutes, E. faecalis and C. sordellii (1118.1). *The FASEB Journal*, [e-journal] 28 (1_supplement), pp.1118.1. Available through: google.

Rhee, S.H., Pothoulakis, C. and Mayer, E.A., 2009. Principles and clinical implications of the brain–gut–enteric microbiota axis. *Nature reviews Gastroenterology & hepatology*, [e-journal] 6 (5), pp.306. Available through: google.

Roberts, A., Renwick, A.G., Sims, J. and Snodin, D.J., 2000. Sucralose metabolism and pharmacokinetics in man. *Food and chemical toxicology*, [e-journal] 38, pp.31-41. Available through: google.

Rodríguez, J.M., Murphy, K., Stanton, C., Ross, R.P., Kober, O.I., Juge, N., Avershina, E., Rudi, K., Narbad, A. and Jenmalm, M.C., 2015. The composition of the gut microbiota throughout life, with an emphasis on early life. *Microbial Ecology in Health and Disease,* [e-journal] 26 (1), pp.26050. Available through: google.

Rodríguez, J.M., Murphy, K., Stanton, C., Ross, R.P., Kober, O.I., Juge, N., Avershina, E., Rudi, K., Narbad, A. and Jenmalm, M.C., 2015. The composition of the gut microbiota throughout life, with an emphasis on early life. *Microbial Ecology in Health and Disease,* [e-journal] 26 (1), pp.26050. Available through: google.

Rogers, P.J., 2018. The role of low-calorie sweeteners in the prevention and management of overweight and obesity: Evidence v. conjecture. Proceedings of the Nutrition Society, [e-journal] 77 (3), pp.230-238. Available through: google.

Rolfes, S. R., Pinna, K., & Whitney, E. (2014). *Understanding normal and clinical nutrition*. Chapter 4, page – 114.

Rosa, A.C., Vieira, M.A., Tibana, A., Gomes, T.A. and Andrade, J.R., 2001. Interactions of *Escherichia coli* strains of non-EPEC serogroups that carry eae and lack the EAF and stx gene sequences with undifferentiated and differentiated intestinal human Caco-2 cells. *FEMS microbiology letters*, [e-journal] 200 (1), pp.117-122. Available through: google.

Roselli, M., Finamore, A., Garaguso, I., Britti, M.S. and Mengheri, E., 2003. Zinc oxide protects cultured enterocytes from the damage induced by *Escherichia coli*. *The Journal of nutrition,* [e-journal] 133 (12), pp.4077-4082. Available through: google.

Rossi, E., Cimdins, A., Lüthje, P., Brauner, A., Sjöling, Å., Landini, P. and Römling, U., 2018. "It'sa gut feeling"–Escherichia coli biofilm formation in the gastrointestinal tract environment. *Critical reviews in microbiology*, [e-journal] 44 (1), pp.1-30. Available through: google.

Ruiz-Ojeda, F.J., Plaza-Díaz, J., Sáez-Lara, M.J. and Gil, A., 2019. Effects of sweeteners on the gut microbiota: a review of experimental studies and clinical trials. *Advances in Nutrition*, [e-journal] 10 (suppl_1), pp.S31-S48. Available through: google.

Rutili, G. and Arfors, K., 1976. Fluorescein-labelled dextran measurement in interstitial fluid in studies of macromolecular permeability. *Microvascular research,* [e-journal] 12 (2), pp.221-230. Available through: google.

Rysavy, N.M., Shimoda, L.M., Dixon, A.M., Speck, M., Stokes, A.J., Turner, H. and Umemoto, E.Y., 2014. Beyond apoptosis: the mechanism and function of phosphatidylserine asymmetry in the membrane of activating mast cells. *BioArchitecture,* [e-journal] 4 (4-5), pp.127-137. Available through: google.

Sadabad, M.S., Von Martels, J.Z., Khan, M.T., Blokzijl, T., Paglia, G., Dijkstra, G., Harmsen, H.J. and Faber, K.N., 2015. A simple coculture system shows mutualism between anaerobic faecalibacteria and epithelial Caco-2 cells. *Scientific reports,* [e-journal] 5, pp.17906. Available through: google.

Sanderson, I.R., Boulton, P., Menzies, I. and Walker-Smith, J.A., 1987b. Improvement of abnormal lactulose/rhamnose permeability in active Crohn's disease of the small bowel by an elemental diet. *Gut*, [e-journal] 28 (9), pp.1073-1076. 10.1136/gut.28.9.1073 [doi].

Sanderson, I.R., Udeen, S., Davies, P.S., Savage, M.O. and Walker-Smith, J.A., 1987a. Remission induced by an elemental diet in small bowel Crohn's disease. *Archives of Disease in Childhood*, [e-journal] 62 (2), pp.123-127. 10.1136/adc.62.2.123 [doi].

Sandoval, M., Liu, X., Oliver, P.D., Zhang, X.J., Clark, D.A. and Miller, M.J., 1995. Nitric oxide induces apoptosis in a human colonic epithelial cell line, T84. *Mediators of inflammation*, [e-journal] 4 (4), pp.248-250. 10.1155/S0962935195000391 [doi].

Santos, J., Yang, P.C., Söderholm, J.D., Benjamin, M. and Perdue, M.H., 2001a. Role of mast cells in chronic stress induced colonic epithelial barrier dysfunction in the rat. *Gut*, [e-journal] 48 (5), pp.630-636. Available through: google.

Santos, J., Yang, P.C., Söderholm, J.D., Benjamin, M. and Perdue, M.H., 2001b. Role of mast cells in chronic stress induced colonic epithelial barrier dysfunction in the rat. *Gut*, [e-journal] 48 (5), pp.630-636. Available through: google.

Santos, J.C. and Broz, P., 2018. Sensing of invading pathogens by GBPs: At the crossroads

between cellâ€• autonomous and innate immunity. *Journal of leukocyte biology*, [e-journal] 104 (4), pp.729-735. Available through: google.

Santos, P., Caria, C., Gotardo, E., Ribeiro, M., Pedrazzoli, J. and Gambero, A., 2018. Artificial sweetener saccharin disrupts intestinal epithelial cells' barrier function *in vitro*. *Food & function,* [e-journal] 9 (7), pp.3815-3822. Available through: google.

Sanz, A.B., Santamaria, B., Ruiz-Ortega, M., Egido, J. and Ortiz, A., 2008. Mechanisms of renal apoptosis in health and disease. *Journal of the American Society of Nephrology*: *JASN*, [e-journal] 19 (9), pp.1634-1642. 10.1681/ASN.2007121336 [doi].

Sarafidis, P.A. and Nilsson, P.M., 2006. The metabolic syndrome: a glance at its history. *Journal of hypertension*, [e-journal] 24 (4), pp.621-626. 10.1097/01.hjh.0000217840.26971.b6 [doi].

Sartor, R.B. and Wu, G.D., 2017. Roles for intestinal bacteria, viruses, and fungi in pathogenesis of inflammatory bowel diseases and therapeutic approaches. *Gastroenterology*, [e-journal] 152 (2), pp.327-339. e4. Available through: google.

Sartor, R.B., 2008. Microbial influences in inflammatory bowel diseases. *Gastroenterology,* [e-journal] 134 (2), pp.577-594. Available through: google.

Sawai, T., Lampman, R., Hua, Y., Segura, B., Drongowski, R.A., Coran, A.G. & Harmon, C.M. 2002, "Lysophosphatidylcholine alters enterocyte monolayer permeability via a protein kinase C/Ca 2 mechanism", *Pediatric surgery international,* vol. 18, no. 7, pp. 591-594.

Scaletsky, I.C., Fabbricotti, S.H., Aranda, K.R., Morais, M.B. and Fagundes-Neto, U., 2002. Comparison of DNA hybridization and PCR assays for detection of putative pathogenic enteroadherent *Escherichia coli*. *Journal of clinical microbiology,* [e-journal] 40 (4), pp.1254-1258. Available through: google.

Scheurer, M., Brauch, H. and Lange, F.T., 2009. Analysis and occurrence of seven artificial sweeteners in German waste water and surface water and in soil aquifer treatment (SAT). *Analytical and Bioanalytical Chemistry*, [e-journal] 394 (6), pp.1585-1594. Available through: google.

Schiffman, S.S., Booth, B.J., Sattely-Miller, E.A., Graham, B.G. and Gibes, K.M., 1999. Selective inhibition of sweetness by the sodium salt of±2-(4-methoxyphenoxy) propanoic acid. *Chemical senses*, [e-journal] 24 (4), pp.439-447. Available through: google.

Schuijt, T.J., van der Poll, T., de Vos, W.M. & Wiersinga, W.J. 2013, "The intestinal microbiota and host immune interactions in the critically ill", *Trends in microbiology,* vol. 21, no. 5, pp. 221-229.

Schulze-Osthoff, K., Walczak, H., Droge, W. and Krammer, P.H., 1994. Cell nucleus and DNA fragmentation are not required for apoptosis. *The Journal of cell biology*, [e-journal] 127 (1), pp.15-20. 10.1083/jcb.127.1.15 [doi].

Schuster, D.P., 2010. Obesity and the development of type 2 diabetes: the effects of fatty tissue inflammation. *Diabetes, metabolic syndrome and obesity: targets and therapy*, [e-journal] 3, pp.253-262. 10.2147/dmsott.s7354 [doi].

Sears, C. L. (2005). A dynamic partnership: Celebrating our gut flora. *Anaerobe, 11*(5), 247-251.

Sears, C.L. and Kaper, J.B., 1996. Enteric bacterial toxins: mechanisms of action and linkage to intestinal secretion. *Microbiological reviews*, [e-journal] 60 (1), pp.167-215.

Sebaugh, J., 2011. Guidelines for accurate EC50/IC50 estimation. *Pharmaceutical statistics*, [e-journal] 10 (2), pp.128-134. Available through: google.

Sekirov, I., Russell, S.L., Antunes, L.C.M. and Finlay, B.B., 2010. Gut microbiota in health and disease. *Physiological Reviews*, [e-journal] 90 (3), pp.859-904. Available through: google.

Semedo, T., Santos, M.A., Lopes, M.F., Marques, J.J.F., Crespo, M.T. and Tenreiro, R., 2003. Virulence factors in food, clinical and reference enterococci: a common trait in the genus? *Systematic and applied microbiology,* [e-journal] 26 (1), pp.13-22. Available through: google.

Serino, M., Luche, E., Chabo, C., Amar, J. and Burcelin, R., 2009. Intestinal microflora and metabolic diseases. *Diabetes & metabolism*, [e-journal] 35 (4), pp.262-272. Available through: google.

Shankar, N., Baghdayan, A.S. and Gilmore, M.S., 2002. Modulation of virulence within a pathogenicity island in vancomycin-resistant *Enterococcus faecalis*. *Nature,* [e-journal] 417 (6890), pp.746. Available through: google.

Sheth, P., Seth, A., Atkinson, K.J., Gheyi, T., Kale, G., Giorgianni, F., Desiderio, D.M., Li, C., Naren, A. and Rao, R., 2007. Acetaldehyde dissociates the PTP1B–E-cadherin–β-catenin complex in Caco-2 cell monolayers by a phosphorylation-dependent mechanism. *Biochemical Journal*, [e-journal] 402 (2), pp.291-300. Available through: google.

Shirazi-Beechey, S.P., Daly, K., Al-Rammahi, M., Moran, A.W. and Bravo, D., 2014. Role of nutrient-sensing taste 1 receptor (T1R) family members in gastrointestinal chemosensing. *British Journal of Nutrition,* [e-journal] 111 (S1), pp.S8-S15. Available through: google.

Sifri, C.D., 2008. Quorum sensing: bacteria talk sense. *Clinical infectious diseases,* [e-journal] 47 (8), pp.1070-1076. Available through: google.

Singh, S.K., Binder, H.J., Boron, W.F. and Geibel, J.P., 1995. Fluid absorption in isolated perfused colonic crypts. *The Journal of clinical investigation,* [e-journal] 96 (5), pp.2373-2379. 10.1172/JCI118294 [doi].

Song, J.C., Hanson, C.M., Tsai, V., Farokhzad, O.C., Lotz, M. & Matthews, J.B. 2001, "Regulation of epithelial transport and barrier function by distinct protein kinase C isoforms", *American journal of physiology.Cell physiology,* vol. 281, no. 2, pp. C649-61.

Sonnenburg, J.L. and Bäckhed, F., 2016. Diet–microbiota interactions as moderators of human metabolism. *Nature*, [e-journal] 535 (7610), pp.56-64. Available through: google.

Sperandio, V., Torres, A.G., Jarvis, B., Nataro, J.P. and Kaper, J.B., 2003. Bacteria-host communication: the language of hormones. *Proceedings of the National Academy of Sciences of the United States of America,* [e-journal] 100 (15), pp.8951-8956. 10.1073/pnas.1537100100 [doi].

Spor, A., Koren, O. and Ley, R., 2011. Unravelling the effects of the environment and host genotype on the gut microbiome. *Nature Reviews Microbiology*, [e-journal] 9 (4), pp.279. Available through: google.

Stecher, B., Chaffron, S., Käppeli, R., Hapfelmeier, S., Freedrich, S., Weber, T.C., Kirundi, J., Suar, M., McCoy, K.D. and von Mering, C., 2010. Like will to like: abundances of closely related species can predict susceptibility to intestinal colonization by pathogenic and commensal bacteria. *PLoS pathogens*, [e-journal] 6 (1), pp.e1000711. Available through: google.

Steinert, R. E., Frey, F., Töpfer, A., Drewe, J. and Beglinger, C. (2011) “Effects of carbohydrate sugars and artificial sweeteners on appetite and the secretion of gastrointestinal satiety peptides,” *British Journal of Nutrition*. Cambridge University Press, 105(9), pp. 1320–1328. doi: 10.1017/S000711451000512X.

Stenman, L.K., Holma, R., Eggert, A. & Korpela, R. 2013, "A novel mechanism for gut barrier dysfunction by dietary fat: epithelial disruption by hydrophobic bile acids", *American journal of physiology*. *Gastrointestinal and liver physiology*, vol. 304, no. 3, pp. G227-34.

Stephenson, R.E., Higashi, T., Erofeev, I.S., Arnold, T.R., Leda, M., Goryachev, A.B. and Miller, A.L., 2019. Rho flares repair local tight junction leaks. *Developmental cell*, [e-journal] 48 (4), pp.445-459. e5. Available through: google.

Stice, E., Spoor, S., Bohon, C., Veldhuizen, M.G. and Small, D.M., 2008. Relation of reward from food intake and anticipated food intake to obesity: a functional magnetic resonance imaging study. *Journal of abnormal psychology*, [e-journal] 117 (4), pp.924. Available through: google.

Strasser, A., O'Connor, L. and Dixit, V.M., 2000. Apoptosis signaling. *Annual Review of Biochemistry,* [e-journal] 69 (1), pp.217-245. Available through: google.

Stuart, R.O. & Nigam, S.K. 1995, "Regulated assembly of tight junctions by protein kinase C", *Proceedings of the National Academy of Sciences of the United States of America,* vol. 92, no. 13, pp. 6072-6076.

Suenaert, P., Bulteel, V., Lemmens, L., Noman, M., Geypens, B., Van Assche, G., Geboes, K., Ceuppens, J.L. and Rutgeerts, P., 2002. Anti-tumor necrosis factor treatment restores the gut barrier in Crohn's disease. *The American Journal of Gastroenterology,* [e-journal] 97 (8), pp.2000. Available through: google.

Suez, J., Korem, T., Zeevi, D., Zilberman-Schapira, G., Thaiss, C.A., Maza, O., Israeli, D., Zmora, N., Gilad, S. & Weinberger, A. 2015, "Artificial Sweeteners Induce Glucose Intolerance by Altering the Gut Microbiota", *Obstetrical & gynaecological survey*, vol. 70, no. 1, pp. 31-32.

Suez, J., Korem, T., Zeevi, D., Zilberman-Schapira, G., Thaiss, C.A., Maza, O., Israeli, D., Zmora, N., Gilad, S. & Weinberger, A. 2014, "Artificial sweeteners induce glucose intolerance by altering the gut microbiota", *Nature*, vol. 514, no. 7521, pp. 181-186.

Surette, M.G. and Bassler, B.L., 1998. Quorum sensing in *Escherichia coli* and *Salmonella typhimurium*. *Proceedings of the National Academy of Sciences of the United States of America,* [e-journal] 95 (12), pp.7046-7050. 10.1073/pnas.95.12.7046 [doi].

Surette, M.G., Miller, M.B. and Bassler, B.L., 1999. Quorum sensing in *Escherichia coli*, *Salmonella typhimurium*, and *Vibrio harveyi*: a new family of genes responsible for autoinducer production. *Proceedings of the National Academy of Sciences of the United States of America,* [e-journal] 96 (4), pp.1639-1644. 10.1073/pnas.96.4.1639 [doi].

Surjawidjaja, J.E., Hidayat, A. & Lesmana, M. 2004, "Growth inhibition of enteric pathogens by zinc sulfate: an *in vitro* study", *Medical principles and practice: international journal of the Kuwait University, Health Science Centre*, vol. 13, no. 5, pp. 286-289.

Suzuki, T. 2013, "Regulation of intestinal epithelial permeability by tight junctions", *Cellular and molecular life sciences,* vol. 70, no. 4, pp. 631-659.

Svensjö, E., Arfors, K., Arturson, G. and Rutili, G., 1978. The hamster cheek pouch preparation as a model for studies of macromolecular permeability of the microvasculature. *Upsala journal of medical sciences,* [e-journal] 83 (1), pp.71-79. Available through: google.

Swartz, T.D., Duca, F., De Wouters, T., Sakar, Y. & Covasa, M. 2011, "Up-regulation of intestinal type 1 taste receptor 3 and sodium glucose luminal transporter-1 expression and increased sucrose intake in mice lacking gut microbiota", *British Journal of Nutrition*, vol. 107, no. 05, pp. 621-630.

Swithers, S.E., 2013. Artificial sweeteners produce the counterintuitive effect of inducing metabolic derangements. *Trends in Endocrinology & Metabolism*, [e-journal] 24 (9), pp.431-441. Available through: google.

Swithers, S.E., 2015. Not so sweet revenge: unanticipated consequences of high-intensity sweeteners. *The Behavior Analyst*, [e-journal] 38 (1), pp.1-17. Available through: google.

T. Lea, 2015, 'Caco-2 cell line', P. Cotter, I. López-Expósito, C. Kleiveland, A. Mackie, T. Requena, D. Swiatecka, H. Wichers (Eds.), *in* The Impact of Food Bio-actives on Gut Health: *In Vitro* and *Ex Vivo* Models, *SpringerOpen*. pp. 103 – 111.

Taylor, R.C., Cullen, S.P. and Martin, S.J., 2008. Apoptosis: controlled demolition at the cellular level. *Nature reviews Molecular cell biology,* [e-journal] 9 (3), pp.231. Available through: google.

Teh, K.H., Flint, S. and French, N., 2010. Biofilm formation by *Campylobacter jejuni* in controlled mixed-microbial populations. *International journal of food microbiology*, [e-journal] 143 (3), pp.118-124. Available through: google.

Tenaillon, O., Skurnik, D., Picard, B. and Denamur, E., 2010. The population genetics of commensal *Escherichia coli*. *Nature Reviews Microbiology,* [e-journal] 8 (3), pp.207. Available through: google.

Tendolkar, P.M., Baghdayan, A.S., Gilmore, M.S. and Shankar, N., 2004. Enterococcal surface protein, Esp, enhances biofilm formation by *Enterococcus faecalis*. *Infection and immunity*, [e-journal] 72 (10), pp.6032-6039. 10.1128/IAI.72.10.6032-6039.2004 [doi].

Tey, S., Salleh, N., Henry, J. and Forde, C., 2017. Effects of aspartame-, monk fruit-, stevia-and sucrose-sweetened beverages on postprandial glucose, insulin and energy intake. *International journal of obesity*, [e-journal] 41 (3), pp.450. Available through: google.

Thompson, C.B., 1995. Apoptosis in the pathogenesis and treatment of disease. *Science (New York, N.Y.),* [e-journal] 267 (5203), pp.1456-1462. 10.1126/science.7878464 [doi].

Thursby, E. and Juge, N., 2017. Introduction to the human gut microbiota. *The Biochemical journal*, [e-journal] 474 (11), pp.1823-1836. 10.1042/BCJ20160510 [doi].

Toledo-Arana, A., Valle, J., Solano, C., Arrizubieta, M.J., Cucarella, C., Lamata, M., Amorena, B., Leiva, J., Penadés, J.R. and Lasa, I., 2001. The enterococcal surface protein, Esp, is involved in *Enterococcus faecalis* biofilm formation. *Applied and Environmental Microbiology,* [e-journal] 67 (10), pp.4538-4545. Available through: google.

Tomasello, G., Mazzola, M., Leone, A., Sinagra, E., Zummo, G., Farina, F., Damiani, P., Cappello, F., Gerges Geagea, A., Jurjus, A., Bou Assi, T., Messina, M. and Carini, F., 2016. Nutrition, oxidative stress and intestinal dysbiosis: Influence of diet on gut microbiota in inflammatory bowel diseases. Biomedical papers of the Medical Faculty of the University Palacky, Olomouc, Czechoslovakia, [e-journal] 160 (4), pp.461-466. 10.5507/bp.2016.052 [doi].

Tong, J., Wang, Y., Chang, B., Zhang, D. and Wang, B., 2013. Evidence for the involvement of RhoA signaling in the ethanol-induced increase in intestinal epithelial barrier permeability. *International journal of molecular sciences*, [e-journal] 14 (2), pp.3946-3960. Available through: google.

Toubal, A., Treuter, E., Clément, K. and Venteclef, N., 2013. Genomic and epigenomic regulation of adipose tissue inflammation in obesity. *Trends in Endocrinology & Metabolism*, [e-journal] 24 (12), pp.625-634. Available through: google.

Trier, J.S., 1963. Studies on Small Intestinal Crypt Epithelium. I. the Fine Structure of the Crypt Epithelium of the Proximal Small Intestine of Fasting Humans. *The Journal of cell biology*, [e-journal] 18, pp.599-620. 10.1083/jcb.18.3.599 [doi].

Tuomola, E.M. and Salminen, S.J., 1998. Adhesion of some probiotic and dairy *Lactobacillus* strains to Caco-2 cell cultures. *International journal of food microbiology*, [e-journal] 41 (1), pp.45-51. Available through: google.

Turnbaugh, P.J. and Gordon, J.I., 2009. The core gut microbiome, energy balance and obesity. *The Journal of physiology*, [e-journal] 587 (17), pp.4153-4158. Available through: google.

Turnbaugh, P.J., Ley, R.E., Mahowald, M.A., Magrini, V., Mardis, E.R. and Gordon, J.I., 2006. An obesity-associated gut microbiome with increased capacity for energy harvest. *Nature*, [e-journal] 444 (7122), pp.1027. Available through: google.

Turner, J.R., 2009. Intestinal mucosal barrier function in health and disease. *Nature reviews immunology,* [e-journal] 9 (11), pp.799. Available through: google.

Uebanso, T., Ohnishi, A., Kitayama, R., Yoshimoto, A., Nakahashi, M., Shimohata, T., Mawatari, K. and Takahashi, A., 2017. Effects of low-dose non-caloric sweetener consumption on gut microbiota in mice. *Nutrients,* [e-journal] 9 (6), pp.560. Available through: google.

Ukleja, A., Freeman, K.L., Gilbert, K., Kochevar, M., Kraft, M.D., Russell, M.K., Shuster, M.H. and Task Force on Standards for Nutrition Support: Adult Hospitalized Patients, and the American Society for Parenteral and Enteral Nutrition Board of Directors, 2010. Standards for nutrition support: adult hospitalized patients. *Nutrition in Clinical Practice*, [e-journal] 25 (4), pp.403-414. Available through: google.

Ulluwishewa, D., Anderson, R.C., McNabb, W.C., Moughan, P.J., Wells, J.M. & Roy, N.C. 2011, "Regulation of tight junction permeability by intestinal bacteria and dietary components", *The Journal of nutrition,* vol. 141, no. 5, pp. 769-776.

Ushe, T.C. and Nagy, B., 1985. Inhibition of small intestinal colonization of enterotoxigenic *Escherichia coli* by *Streptococcus faecium* M74 in pigs. *Zentralblatt fur Bakteriologie, Mikrobiologie und Hygiene.1.Abt.Originale B, Hygiene*, [e-journal] 181 (3-5), pp.374-382.

Valdes, A.M., Walter, J., Segal, E. and Spector, T.D., 2018. Role of the gut microbiota in nutrition and health. *BMJ,* [e-journal] 361, pp.k2179. Available through: google.

Van Der Flier, Laurens G and Clevers, H., 2009. Stem cells, self-renewal, and differentiation in the intestinal epithelium. *Annual Review of Physiology*, [e-journal] 71, pp.241-260. Available through: google.

Van Engeland, M., Nieland, L.J., Ramaekers, F.C., Schutte, B. and Reutelingsperger, C.P., 1998. Annexin V-affinity assay: a review on an apoptosis detection system based on phosphatidylserine exposure. *Cytometry: The Journal of the International Society for Analytical Cytology,* [e-journal] 31 (1), pp.1-9. Available through: google.

van Eyk, A.D., 2014. The effect of five artificial sweeteners on Caco-2, HT-29 and HEK-293 cells. *Drug and chemical toxicology,* [e-journal] 38 (3), pp.318-327. Available through: google.

Van Itallie, C.M., Tietgens, A.J. and Anderson, J.M., 2017. Visualizing the dynamic coupling of claudin strands to the actin cytoskeleton through ZO-1. *Molecular biology of the cell*, [e-journal] 28 (4), pp.524-534. Available through: google.

Vandevijvere, S. and Vanderlee, L., 2019. Effect of formulation, labelling, and taxation policies on the nutritional quality of the food supply. *Current nutrition reports*, [e-journal] 8 (3), pp.240-249. Available through: google.

Venkatasubramanian, J., Rao, M.C. & Sellin, J.H. 2015. Intestinal electrolyte absorption and secretion. In *Gastroenterology and Hepatology*. p.1675.

Verhoven, B., Krahling, S., Schlegel, R.A. and Williamson, P., 1999. Regulation of phosphatidylserine exposure and phagocytosis of apoptotic T lymphocytes. *Cell death and differentiation,* [e-journal] 6 (3), pp.262. Available through: google.

Vieira, O.V., Hartmann, D.O., Cardoso, C.M., Oberdoerfer, D., Baptista, M., Santos, M.A., Almeida, L., Ramalho-Santos, J. and Vaz, W.L., 2008. Surfactants as microbicides and contraceptive agents: a systematic *in vitro* study. *PLoS One*, [e-journal] 3 (8), pp.e2913. Available through: google.

Vijay-Kumar, M., Carvalho, F.A., Aitken, J.D., Fifadara, N.H. and Gewirtz, A.T., 2010. TLR5 or NLRC4 is necessary and sufficient for promotion of humoral immunity by flagellin. *European journal of immunology,* [e-journal] 40 (12), pp.3528-3534. Available through: google.

Vogelsang, H., Schwarzenhofer, M. and Oberhuber, G., 1998. Changes in gastrointestinal permeability in celiac disease. *Digestive diseases (Basel, Switzerland),* [e-journal] 16 (6), pp.333-336. 16886 [pii].

Vollaard, E.J. and Clasener, H.A., 1994. Colonization resistance. *Antimicrobial Agents and Chemotherapy,* [e-journal] 38 (3), pp.409. Available through: google.

Vors, C., Capolino, P., Guérin, C., Meugnier, E., Pesenti, S., Chauvin, M., Monteil, J., Peretti, N., Cansell, M. and Carrière, F., 2012. Coupling in vitro gastrointestinal lipolysis and Caco-2 cell cultures for testing the absorption of different food emulsions. *Food & function*, [e-journal] 3 (5), pp.537-546. Available through: google.

Vuong, C., Gerke, C., Somerville, G.A., Fischer, E.R. and Otto, M., 2003. Quorum-sensing control of biofilm factors in *Staphylococcus epidermidis*. *The Journal of infectious diseases*, [e-journal] 188 (5), pp.706-718. Available through: google.

Wal, P., Pal, R.S. and Wal, A., 2019. A review on the sugar alternates. *IJPSR*; Vol. 10(4): 1595-1604. [e-journal] Available through: google.

Wang, F., Meng, W., Wang, B. and Qiao, L., 2014. *Helicobacter pylori*-induced gastric inflammation and gastric cancer. *Cancer letters*, [e-journal] 345 (2), pp.196-202. Available through: google.

Wang, Q., Browman, D., Herzog, H. and Neely, G.G., 2018. Non-nutritive sweeteners possess a bacteriostatic effect and alter gut microbiota in mice. *PloS one,* [e-journal] 13 (7), pp.e0199080. Available through: google.

Wang, Q.P., Browman, D., Herzog, H. and Neely, G.G., 2018. Non-nutritive sweeteners possess a bacteriostatic effect and alter gut microbiota in mice. *PloS one*, [e-journal] 13 (7), pp.e0199080. 10.1371/journal.pone.0199080 [doi].

Wang, W., Xia, T. and Yu, X., 2015. Wogonin suppresses inflammatory response and maintains intestinal barrier function via TLR4-MyD88-TAK1-mediated NF-κB pathway *in vitro*. *Inflammation Research*, [e-journal] 64 (6), pp.423-431. Available through: google.

Wang, X. and Huycke, M.M., 2007. Extracellular superoxide production by *Enterococcus faecalis* promotes chromosomal instability in mammalian cells. *Gastroenterology,* [e-journal] 132 (2), pp.551-561. Available through: google.

Wang, Y., Hoenig, J.D., Malin, K.J., Qamar, S., Petrof, E.O., Sun, J., Antonopoulos, D.A., Chang, E.B. and Claud, E.C., 2009. 16S rRNA gene-based analysis of fecal microbiota from preterm infants with and without necrotizing enterocolitis. *The ISME journal*, [e-journal] 3 (8), pp.944. Available through: google.

Washburn, C. and Christensen, N., 2012. Sugar substitutes: artificial sweeteners and sugar alcohols. [e-journal] Available through: google. All Current Publications. Paper 204. https://digitalcommons.usu.edu/extension_curall/204

Watts, T., Berti, I., Sapone, A., Gerarduzzi, T., Not, T., Zielke, R. & Fasano, A. 2005, "Role of the intestinal tight junction modulator zonulin in the pathogenesis of type I diabetes in BB diabetic-prone rats", *Proceedings of the National Academy of Sciences of the United States of America*, vol. 102, no. 8, pp. 2916-2921.

Wauson, E.M., Zaganjor, E., Lee, A., Guerra, M.L., Ghosh, A.B., Bookout, A.L., Chambers, C.P., Jivan, A., McGlynn, K. and Hutchison, M.R., 2012. The G protein-coupled taste receptor T1R1/T1R3 regulates mTORC1 and autophagy. *Molecular cell*, [e-journal] 47 (6), pp.851-862. Available through: google.

Weiser, M.M., 1973. Intestinal epithelial cell surface membrane glycoprotein synthesis. I. An indicator of cellular differentiation. *The Journal of biological chemistry*, [e-journal] 248 (7), pp.2536-2541.

Weiss, K.M., Ferrell, R.F. and Hanis, C.L., 1984. A new world syndrome of metabolic diseases with a genetic and evolutionary basis. *American Journal of Physical Anthropology*, [e-journal] 27 (S5), pp.153-178. Available through: google.

Wells, J. M., Rossi, O., Meijerink, M., & van Baarlen, P. (2011). Epithelial crosstalk at the microbiota-mucosal interface. *Proceedings of the National Academy of Sciences of the United States of America, 108 Suppl 1*, 4607-4614. doi:10.1073/pnas.1000092107 [doi]

Wells, V.D., Wong, E.S., Murray, B.E., Coudron, P.E., Williams, D.S. and Markowitz, S.M., 1992. Infections due to beta-lactamase-producing, high-level gentamicin-resistant *Enterococcus faecalis*. *Annals of Internal Medicine,* [e-journal] 116 (4), pp.285-292. Available through: google.

Wen, L., Ley, R.E., Volchkov, P.Y., Stranges, P.B., Avanesyan, L., Stonebraker, A.C., Hu, C., Wong, F.S., Szot, G.L. and Bluestone, J.A., 2008. Innate immunity and intestinal microbiota in the development of Type 1 diabetes. *Nature*, [e-journal] 455 (7216), pp.1109. Available through: google.

Wheeler, A.L., Hartel, P.G., Godfrey, D.G., Hill, J.L. and Segars, W.I., 2002. Potential of *Enterococcus faecalis* as a human fecal indicator for microbial source tracking. *Journal of environmental quality,* [e-journal] 31 (4), pp.1286-1293. Available through: google.

Whitehouse, C.R., Boullata, J. and McCauley, L.A., 2008. The potential toxicity of artificial sweeteners. *AAOHN Journal*, [e-journal] 56 (6), pp.251-261. Available through: google.

Wilks, J.C. and Slonczewski, J.L., 2007. pH of the cytoplasm and periplasm of *Escherichia coli*: rapid measurement by green fluorescent protein fluorimetry. *Journal of Bacteriology,* [e-journal] 189 (15), pp.5601-5607. JB.00615-07 [pii].

Winter, S.E., Winter, M.G., Xavier, M.N., Thiennimitr, P., Poon, V., Keestra, A.M., Laughlin, R.C., Gomez, G., Wu, J. and Lawhon, S.D., 2013. Host-derived nitrate boosts growth of *E. coli* in the inflamed gut. *Science,* [e-journal] 339 (6120), pp.708-711. Available through: google.

Wiseman, G.M., 1975. The hemolysins of *Staphylococcus aureus*. *Bacteriological Reviews,* [e-journal] 39 (4), pp.317-344.

Witthöft, T., Eckmann, L., Kim, J.M. and Kagnoff, M.F., 1998. Enteroinvasive bacteria directly activate expression of iNOS and NO production in human colon epithelial cells. *American Journal of Physiology-Gastrointestinal and Liver Physiology*, [e-journal] 275 (3), pp.G564-G571. Available through: google.

Wong, A.C., Vanhove, A.S. and Watnick, P.I., 2016. The interplay between intestinal bacteria and host metabolism in health and disease: lessons from *Drosophila melanogaster*. *Disease models & mechanisms,* [e-journal] 9 (3), pp.271-281. 10.1242/dmm.023408 [doi].

Wu, G.D., Chen, J., Hoffmann, C., Bittinger, K., Chen, Y.Y., Keilbaugh, S.A., Bewtra, M., Knights, D., Walters, W.A., Knight, R., Sinha, R., Gilroy, E., Gupta, K., Baldassano, R., Nessel, L., Li, H., Bushman, F.D. and Lewis, J.D., 2011. Linking long-term dietary patterns with gut microbial enterotypes. *Science (New York, N.Y.),* [e-journal] 334 (6052), pp.105-108. 10.1126/science.1208344 [doi].

Wu, G.D., Compher, C., Chen, E.Z., Smith, S.A., Shah, R.D., Bittinger, K., Chehoud, C., Albenberg, L.G., Nessel, L., Gilroy, E., Star, J., Weljie, A.M., Flint, H.J., Metz, D.C., Bennett, M.J., Li, H., Bushman, F.D. and Lewis, J.D., 2016. Comparative metabolomics in vegans and omnivores reveal constraints on diet-dependent gut microbiota metabolite production. *Gut,* [e-journal] 65 (1), pp.63-72. 10.1136/gutjnl-2014-308209 [doi].

Xiang, J., Wan, C., Guo, R. and Guo, D., 2016. Is hydrogen peroxide a suitable apoptosis inducer for all cell types? *BioMed research international*, [e-journal] 2016 Available through: google.

Xiao, K., Allison, D.F., Buckley, K.M., Kottke, M.D., Vincent, P.A., Faundez, V. and Kowalczyk, A.P., 2003. Cellular levels of p120 catenin function as a set point for cadherin expression levels in microvascular endothelial cells. *The Journal of cell biology*, [e-journal] 163 (3), pp.535-545. Available through: google.

Xu, H., Staszewski, L., Tang, H., Adler, E., Zoller, M. & Li, X. 2004, "Different functional roles of T1R subunits in the heteromeric taste receptors", *Proceedings of the National Academy of Sciences of the United States of America,* vol. 101, no. 39, pp. 14258-14263.

Yamamoto, D., Hernandes, R.T., Blanco, M., Greune, L., Schmidt, M.A., Carneiro, S.M., Dahbi, G., Blanco, J.E., Mora, A. and Blanco, J., 2009. Invasiveness as a putative additional virulence mechanism of some atypical Enteropathogenic *Escherichia coli* strains with different uncommon intimin types. *BMC microbiology,* [e-journal] 9 (1), pp.146. Available through: google.

Yan, F. and Polk, D.B., 2002. Probiotic bacterium prevents cytokine-induced apoptosis in intestinal epithelial cells. *The Journal of biological chemistry,* [e-journal] 277 (52), pp.50959-50965. 10.1074/jbc.M207050200 [doi].

Yan, F., Cao, H., Cover, T.L., Whitehead, R., Washington, M.K. and Polk, D.B., 2007. Soluble proteins produced by probiotic bacteria regulate intestinal epithelial cell survival and growth. *Gastroenterology,* [e-journal] 132 (2), pp.562-575. Available through: google.

Yang, H.J., Bogomolnaya, L., McClelland, M. and Andrews-Polymenis, H., 2017. De novo pyrimidine synthesis is necessary for intestinal colonization of *Salmonella Typhimurium* in chicks. *PloS one*, [e-journal] 12 (10), pp.e0183751. 10.1371/journal.pone.0183751 [doi].

Yang, S., Eckmann, L., Panja, A. and Kagnoff, M.F., 1997. Differential and regulated expression of CXC, CC, and C-chemokines by human colon epithelial cells. *Gastroenterology*, [e-journal] 113 (4), pp.1214-1223. Available through: google.

Yang, T., Santisteban, M.M., Rodriguez, V., Li, E., Ahmari, N., Carvajal, J.M., Zadeh, M., Gong, M., Qi, Y. and Zubcevic, J., 2015. Gut dysbiosis is linked to hypertension. *Hypertension,* [e-journal] 65 (6), pp.1331-1340. Available through: google.

Yatsunenko, T., Rey, F.E., Manary, M.J., Trehan, I., Dominguez-Bello, M.G., Contreras, M., Magris, M., Hidalgo, G., Baldassano, R.N. & Anokhin, A.P. 2012, "Human gut microbiome viewed across age and geography", *Nature,* vol. 486, no. 7402, pp. 222-227.

Yen, T. and Wright, N.A., 2006. The gastrointestinal tract stem cell niche. *Stem cell reviews*, [e-journal] 2 (3), pp.203-212. Available through: google.

Youle, R.J. and Karbowski, M., 2005. Mitochondrial fission in apoptosis. *Nature reviews Molecular cell biology,* [e-journal] 6 (8), pp.657. Available through: google.

Youle, R.J. and van der Bliek, A.M., 2012. Mitochondrial fission, fusion, and stress. *Science (New York, N.Y.),* [e-journal] 337 (6098), pp.1062-1065. 10.1126/science.1219855 [doi].

Young, D. and Bowen, W., 1990. The influence of sucralose on bacterial metabolism. *Journal of dental research,* [e-journal] 69 (8), pp.1480-1484. Available through: google.

Yu, Q., Wang, Z., Li, P. and Yang, Q., 2013. The effect of various absorption enhancers on tight junction in the human intestinal Caco-2 cell line. *Drug development and industrial pharmacy*, [e-journal] 39 (4), pp.587-592. Available through: google.

Zhang, F., Klebansky, B., Fine, R.M., Liu, H., Xu, H., Servant, G., Zoller, M., Tachdjian, C. & Li, X. 2010, "Molecular mechanism of the sweet taste enhancers", *Proceedings of the National Academy of Sciences of the United States of America,* vol. 107, no. 10, pp. 4752-4757.

Zhao, G.Q., Zhang, Y., Hoon, M.A., Chandrashekar, J., Erlenbach, I., Ryba, N.J. and Zuker, C.S., 2003. The receptors for mammalian sweet and umami taste. *Cell*, [e-journal] 115 (3), pp.255-266. Available through: google.

Zhu, L., Wang, G., Dong, B., Peng, C., Tian, Y. and Gong, L., 2016. Effects of sweetener neotame on diet preference, performance and hematological and biochemical parameters of weaned piglets. *Animal Feed Science and Technology*, [e-journal] 214, pp.86-94. Available through: google.

Ziegler, U. and Groscurth, P., 2004. Morphological features of cell death. *Physiology,* [e-journal] 19 (3), pp.124-128. Available through: google.

8 Appendices

8.1 Appendix A - data for chapter 2

8.1.1 Growth of Caco-2 cells in different tissue culture medium

Caco-2 cells were grown in three different media to assess their growth performance up to three days. The cells have grown in all three media with fine differences as observed using the inverted microscope. Approximately 75% confluence was observed at day 3 in DMEM, followed by about 85% confluence in RPMI, and complete monolayer in EMEM medium. In addition, cell adherence was found faster in EMEM as observed at day 1 compared to RPMI, and cell remained mostly round in DMEM at that time point. Growth of the Caco-2 cells were found better in EMEM, which agrees with the supplier's suggestion (ATCC® 30-2003) and used for the rest of the study.

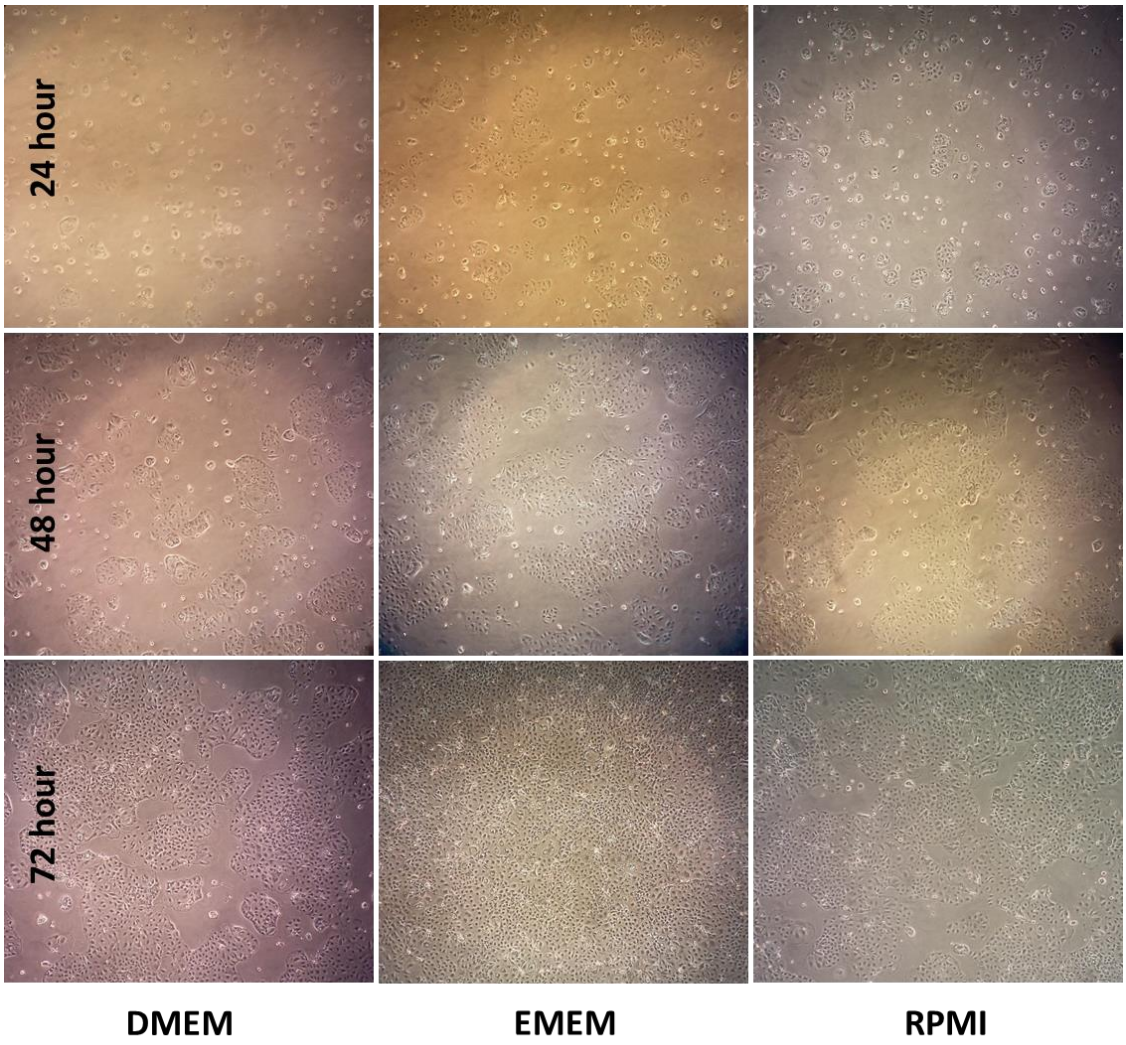

Figure A8. 1: Growth of Caco-2 cells in different tissue culture medium.

Cells were seeded at same concentration into T75 flasks with DMEM (Dulbecco's Modified Eagle Medium; Gibco, ThermoFisher Scientific) or EMEM (Eagle's Minimal Essential medium; American Type Culture Collection 30-2003) or RPMI (Roswell Park Memorial Institute 1640 Medium; ThermoFisher Scientific). The media were supplemented with 10 % FBS, 1% antibiotics, and 1% L-glutamine. The flasks were observed using inverted microscope and images were taken using Samsung grand prime mobile phone. Magnification was X40.

8.1.2 Maintenance of Caco-2 cells

8.1.2.1 Cell passaging

Cells were fed by replacing the used medium with the pre-warmed (37 ˚C) fresh medium. Once grown to confluence (70 – 80 %), cells were split 1:3 or 1:6 depending on necessity of the experiments (fig.A8.2). Used culture media was discarded, and cells were washed gently with PBS. Cells were then exposed to Trypsin-EDTA, incubated at 37 ˚C for 2 – 5 minutes (depending on flask size) with intermittent microscopic monitoring for cell detachment. Cell layer dispersion was facilitated by gentle tapping. Fresh medium was

added to stop Trypsin action, and cells were dissociated by pipetting up and down gently. Appropriate amount of cell suspensions (depending on split and vessel size) were transferred to new cell culture vessels. For cell culture the amount of chemicals used for tissue culture vessels were given in table-A8.1.

Table A8. 1: Volume of different solutions used for different cell culture vessels.

Flask size	Surface area (cm^2)	Volume of media (ml)	Volume of trypsin (ml)	Volume of DPBS (ml)
T-25	25	6	1	5
T-75	75	12	2	10
T-175	175	25	5	20

8.1.2.2 Freezing and thawing cells

Cells were frozen down before reaching 70% confluence (fig.2.2.1). Cells were brought in suspension similar to cell passaging protocol and cell counting was performed using Haemocytometer. The cell suspension was centrifuged at 1000 rpm for 5 min, and supernatant was discarded. Cell pellet was resuspended in freezing medium (90 % complete EMEM and 10 % DMSO) by gently pipetting up and down. Volume of cryopreservation medium was calculated based on the cell count; approximately 1×10^6 cells / ml was frozen. 1 ml of the cell suspension was dispensed into freezing vials which was immediately immersed into the Isopropanol solution of the freezing container (Nalgene® Mr. Frosty™, Cat no 5100), and it was transferred into the – 80 ˚C freezer. After about 24 h, the freezing vials were placed into liquid nitrogen (-196 ˚C; Taylor-Wharton, USA).

The thawing of the cells was quick (1 – 2 min) to improve cell recovery. The freezing vial from the liquid nitrogen was warmed into a water bath at 37 ˚C. The partially defrosted cell solution was pipetted dropwise into a universal tube containing warm (37 ˚C) medium. After gently resuspending cells by pipetting up and down, cell suspension was centrifuged at 1000 rpm for 5 minutes. The cells pellet was resuspended into 2 ml of medium and transferred into a T75 flask containing 10 ml of the medium and kept beforehand at standard cell culture condition. The flask was observed using inverted microscope and placed in the incubator.

8.1.2.3 Cell counting

Caco-2 cell count was performed using haemocytometer. 10 µl of the thoroughly mixed cell suspension was gently placed to the edge of the counting chamber and it was drawn in by capillary action. Cells in each of the four quadrants were counted under inverted microscope and the calculation was done as below.

Cell density (cells / ml) = average cell counts of four quadrants [(q1 + q2 + q3 + q4)] × 10,000 (capacity of the four quadrants is 10^4 / ml)

Total cells 'p' ml of cell suspension = cell density × p (p = amount of total cell suspension in a flask).

Therefore, total number of cell count was performed for individual flasks and the required number of cells were used for each experiment.

8.1.3 Calculation for the Caco-2 cell number using serial dilution

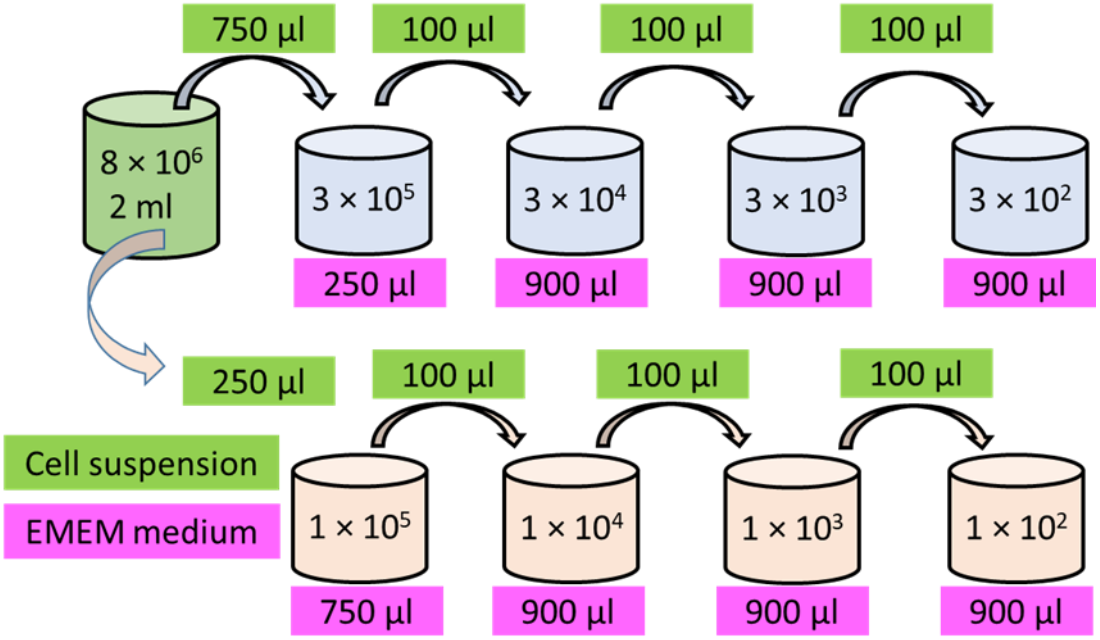

Figure A8. 2: Example of cell number calculation for the CCK-8 viability assay.

For example, 8×10^6 Caco-2 cells were harvested from a T175 flask (above 80% confluent), and cell pellet was re-suspended into 2 ml of fresh medium. 1 ml of cell suspension was prepared for each cell concentrations. 750 µl of stock cell suspension was added to 250 µl of fresh medium to get the desired cell concentrations 3×10^5, and serial dilution was performed to get lower cell concentrations to 3×10^2. Similarly, 250 µl of the stock cell suspension was added to 750 µl to get 1 ml of 1×10^5 cell concentration, and the lower concentrations was prepared using serial dilution method.

8.1.4 Treatments and concentrations

8.1.4.1 Lipopolysaccharide

LPS stock solution (5 mg/ml) was prepared in ddH_2O, and filter-sterilized following supplier's instructions. The following calculation was used to prepare the concentrations 0 to 100 µg/ml of LPS. The preparation for 10 ml of the concentrations are listed in table-A8.2, the lower concentrations were prepared using serial dilution method (fig.A8.2).

Table A8. 2: Calculation of the LPS concentrations.

Equation, $C_1V_1 = C_2V_2$ i.e., $V_1 = (C_2V_2) / C_1$ So, V_1 = (100µg/ml×10000 µl)/5000 µg/ml V_1 = 200 µl	C_1 = conc. of stock solution 5 mg/ml V_1 = required volume of stock solution C_2 = conc. of desired solution (100 µg/ml) V_2 = volume to be prepared (10 ml)

Desired conc. (µg/ml)	Stock solution (µg/ml)	Volume of stock solution (ml)	Volume of vehicle (water) (µl)	Volume of media (ml)
100	5000	0.2	0	9.8
50	100	5	100	4.9
10	100	1	180	8.820
5	50	1	180	8.820
1	10	1	180	8.820
0.5	5	1	180	8.820
0.1	1	1	180	8.820
0	-	-	200	9.8

8.1.4.2 Artificial Sweeteners

The employed concentrations of the saccharin, sucralose, aspartame and neotame were 0 µM, 0.01 µM, 0.1 µM, 1 µM, 10 µM, 100 µM, 1 mM, 10 mM and 50 mM. The highest concentration 50 mM was prepared (vehicle EMEM medium) using equation mentioned in table-A8.3, which was used as stock solution for the 10 mM. The other concentrations were

prepared using serial dilution method (fig.A8.2). The stock solutions of the AS were prepared using the calculation given in table-A8.3. The required amount of the AS were weighed and solutions were prepared using the medium as a solvent and the solutions were sterile-filtered. Caco-2 cells were seeded at 1 x 10^4 cells/well in 96-well plates with 100 µl EMEM supplemented with 10 % FBS and 1 % penicillin/streptomycin and incubated for 48 hours at 37 ˚C in the presence of 5% CO_2. The used medium was replaced with AS doses (100 µl) and again incubated for 24 hours at the same conditions. To adjust reagent concentration (1:10) while minimising cell stress, 10 µl of the used medium was aspirated and CCK-8 reagent (10 µl) was added to the wells. Plates were incubated for 2 hours and viability was measured as absorbance at 450 nm using a Tecan Sunrise™ microplate reader.

Table A8. 3: Calculation of the required AS for the concentrations.

Each AS has different molecular weight (MW; g/mol), and the example calculation was used to determine the required amount of dried AS. Required amount of AS to prepare 1 ml of 50 mM concentration for other AS are mentioned as well.

<table>
<tr><th>AS details</th><th>Calculation of concentration</th></tr>
<tr><td>Saccharin

MW 183.18; Purity ≥99%</td><td rowspan="4">1 Molar = 1 mole/litre (1 M × 1L)

Required dried form of the AS, denotes as S

Required concentration, denoted as C_1

Therefore, S = [(MW) X C_1] / (1 M × 1L)

The actual required amount was calculated using the purity percentage.</td></tr>
<tr><td>Sucralose

MW 397.63; Purity ≥98%

0.02029 g</td></tr>
<tr><td>Aspartame

MW 294; Purity 99%

0.01485 g</td></tr>
<tr><td>Neotame

MW 378.46; Purity ≥98%

0.01931 g</td></tr>
<tr><td></td><td>For example, to prepare 1 ml of 50 mM saccharin, the calculation is –

S = [(183.18g) X (50mM)] / [(1000ml) X (1000mM)]

So, S = 0.009159 g

The purity is 99%, so, actual amount required is,

S = [(100g) X (0.009159g)] / (99g)

Therefore, to prepare 1 ml of 50 mM saccharin solution, 0.009252 g saccharin power was dissolved in 1 ml vehicle.</td></tr>
</table>

The following control experiments were run in parallel with the CCK-8 study. 90 µl of the AS concentrations and 10 µl of CCK-8 reagent was incubated in 96-well plates under standard incubation condition for 2 hours to assess any nonspecific binding. The absorbance of the without cell control was also measured at 450 nm (Tecan Sunrise^{TM}).

The without cell absorbance was deducted from the with cell absorbance to calculate the effect of AS on Caco-2 cell viability.

8.1.4.3 Sweet taste inhibitor

Zinc Sulphate

The CCK-8 assay was also performed to assess the cytotoxic effect of the sweet taste inhibitor, zinc sulphate. The concentrations used were 0, 0.1 µM, 1 µM, 10 µM, 100 µM, 500 µM, 1 mM, 10 mM and 50 mM, and the vehicle was distilled de-ionized water. Zinc sulphate stock solution (1M) was prepared in ddH_2O and filter sterilized. Calculation for the different concentrations were shown in table-A8.4., gradually decreasing solutions were prepared using serial dilution method (fig.A8.2). The CCK-8 viability assay was performed as described above.

Table A8. 4: Preparation of the zinc sulphate concentrations.

The highest concentration 50 mM was prepared, and the other concentrations were prepared from it. Calculation was shown for 10 ml of each of the concentrations.

Zinc sulphate MW = 287.56; Purity ≥ 99.5%; 1 M stock solution was prepared using the calculation shown in table 8.3. The other concentrations were prepared as below			
$C_1V_1 = C_2V_2$ i.e., $V_1 = (C_2V_2) / C_1$ So, V_1 = (50 mM × 10 ml) / 1000 mM V_1 = 0.5 ml		C_1 = conc. of stock solution 1M V_1 = required volume of stock solution C_2 = conc. of desired solution (50 mM) V_2 = volume to be prepared (10 ml)	
Desired conc. (mM)	Stock solution (mM)	Volume of stock solution (ml) + vehicle (µl)	Volume of media (ml)
50	1000	0.5 + 0	9.5
10	50	2 + 400	7.6
1	10	1 + 450	8.550
0.5	1	5 + 250	4.750
0.1	1	1 + 450	8.550
0.01	0.1	1 + 450	8.550
0.001	0.01	1 + 450	8.550
Vehicle (water)	-	0 + 500	9.5

Lactisole

For the Lactisole, two different vehicles – DMSO (Dimethylsulfoxide) and Ethanol (EtOH, 100%) - were used.

Lactisole was dissolved in DMSO / Ethanol, and sterile-filtered (concentration 50 mM). Different concentrations of Lactisole (0 mM, 0.1 mM, 1 mM, 3 mM, 5 mM and 10 mM) were then prepared (calculation shown in table-A8.5) using complete EMEM media and employed on 24-hour pre-incubated Caco-2 cell monolayer. The Caco-2 cell number, experimental condition and the assay protocol was as mentioned above.

Table A8. 5: Preparation of the Lactisole concentrations.

The stock solution (50 mM) was prepared in DMSO or Ethanol using the calculation shown in the table below; calculation was shown for 10 ml of each of the concentrations.

Lactisole MW = 218.2, purity ≥ 98%; To prepare 1 ml of 50 mM Lactisole solution, required amount = (218.2g X 1 ml X 50mM)/ (1000ml X 1000mM) =0.01091 g Considering the purity percentage, required amount = (100g X 0.01091g) / 98g = 0.011133g Therefore, dissolving 0.011133g of Lactisole powder in 1 ml of vehicle gave 50 mM Lactisole stock solution.				
Desired conc. (mM)	Stock solution (mM)	Volume of stock solution (ml)	Volume of vehicle (ml)	Volume of media (ml)
10	20	2	0	8
5	20	1	1	8
3	20	0.6	1.4	8
1	20	0.2	1.8	8
0.1	20	0.02	1.98	8
vehicle	-	0	2	8

Given the established cytotoxic effect of the vehicle for Lactisole, ethanol (Tong et al., 2013), Lactisole was also studied with a different vehicle. The sweet taste inhibitor was dissolved in ethanol, keeping the same concentrations and all experimental conditions as such, and the CCK-8 assay was performed with Caco-2 cells.

The same experiment was carried out with all the concentrations of Lactisole (in both DMSO and ethanol) using no cells present to observe the effect of the chemicals interacting with

reagents. These ‘without cell’ experimental data were subtracted from the ‘with cell’ experimental data when calculated the absorbance of cell viability.

To determine the additive effect of AS and Lactisole, Caco-2 cells were exposed to different concentrations (100 µM and 10 mM) of AS in combination with Lactisole (0.1 mM and 3 mM) or vehicle (table-A8.6) and CCK-8 assay was performed as above.

Table A8. 6: Calculation of AS and Lactisole combination concentrations.

Water and DMSO were vehicle for Lactisole and AS stock solutions, respectively.

Lactisole (L) stock solution was 50 mM in DMSO.	AS stock solution was 50 mM in EMEM medium.
Preparation of 10 ml intermediate stock solution is shown below	
6 mM Lactisole = 1.2 ml stock solution + 8.8 ml medium 0.2 mM Lactisole = 0.04 ml stock + 1.16 ml vehicle + 8.8 ml medium 0 mM Lactisole = 1.2 ml vehicle + 8.8 ml medium	20 mM AS = 4 ml stock + 6 ml medium 0.2 mM AS = 0.04 ml stock + 9.96 ml medium 0 mM AS = 0 stock + 10 ml medium
The working solutions (10 ml) were prepared using the intermediate stock solutions	
0 AS + 0 L = 5 ml 0 mM AS + 5 ml 0 mM Lactisole 0 AS + 0.1 L = 5 ml 0 mM AS + 5 ml 0.2 mM Lactisole 0 AS + 3 L = 5 ml 0 mM AS + 5 ml 6 mM Lactisole AS + 0 L = 5 ml 0.2 mM AS + 5 ml 0 mM Lactisole AS + 0.1 L = 5 ml 0.2 mM AS + 5 ml 0.2 mM Lactisole AS + 3 L = 5 ml 0.2 mM AS + 5 ml 6 mM Lactisole 10 AS + 0 L = 5 ml 20 mM AS + 5 ml 0 mM Lactisole 10 AS + 0.1 L = 5 ml 20 mM AS + 5 ml 0.2 mM Lactisole 10 AS + 3 L = 5 ml 20 mM AS + 5 ml 6 mM Lactisole	

8.1.4.4 Preparation of FITC-dextran stock solution

FD4 and FD20 (Sigma) were dissolved in 5 ml sterile distilled water to a concentration of 25 mg/ml (following manufacturer’s instructions), aliquoted and stored at -20 °C.

8.1.5 Cell viability assay

The CCK-8 assay relies on the formation of formazan from WST-8 (a water-soluble tetrazolium salt) by dehydrogenases. This enzyme reduces the WST-8 inside cells and gives a yellow to an orange coloured product, the formazan. As formazan is a dye and soluble in the tissue culture medium, the amount produced by the biochemical activity of the living cells is directly proportional to the number of the living cells in respective well (Held, 2009).

8.1.5.1 Effect of AS on Caco-2 cell viability

The relative EC50 values of the AS concentrations for Caco-2 cell were mentioned in table-A8.7.

Table A8. 7: Concentrations of AS reducing Caco-2 cell viability by 50%.

The relative EC50 estimation was performed from the graphs obtained from GraphPad Prism®. The baseline was considered as 0% while the maximum value was considered as 100%.

Artificial sweetener	Concentration causing 50 % cell death
Saccharin	5.4 mM
Sucralose	> 50 mM
Aspartame	15 mM
Neotame	2.2 mM

8.1.5.2 Effect of H_2O_2 on Caco-2 cell viability

Hydrogen peroxide is a known apoptosis inducer (Xiang et al., 2016), therefore, Caco-2 cells were exposed to different concentrations of H_2O_2 to determine the appropriate concentration to use as positive control for the apoptosis assay (fig.A8.3). Cell death was increased significantly at ≥ 0.8 mM of H_2O_2. The number of apoptotic and dead cells were increased while the number of live cells decreased with rising concentration of H_2O_2 in a dose-dependent manner. Number of apoptotic cells were significantly increased at concentrations 0.4 and 0.6 mM (47.5 and 49%, respectively), which implies the use of one of these concentrations as positive control for the study. However, after the pilot experiment with AS, the number of dead cell percentage at 10 mM concentration (fig. 3.21) was found similar or higher than 0.6 mM H_2O_2, therefore, 0.8 mM concentration was used as positive control for the study.

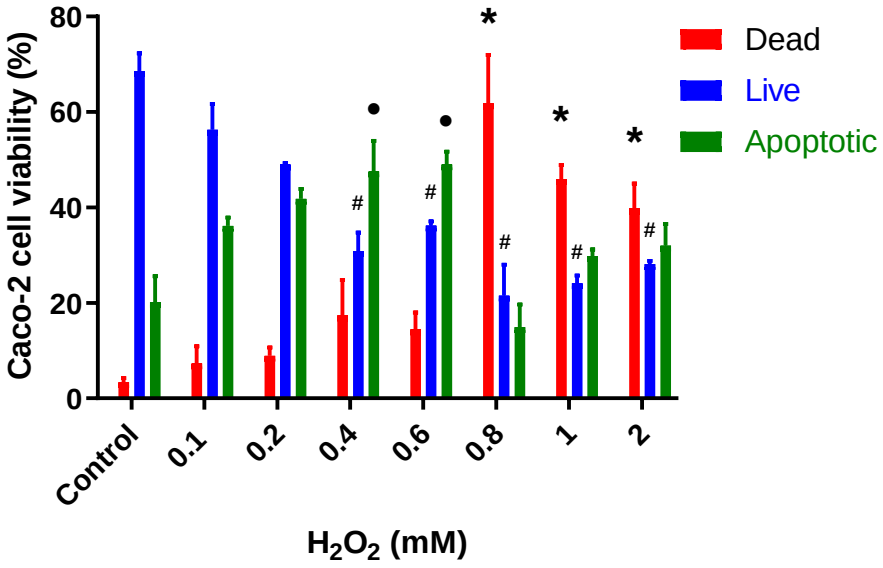

Figure A8. 3: Effect of hydrogen peroxide (H_2O_2) on intestinal epithelial cell apoptosis.

Caco-2 cells ($7.5X10^4$) were maintained in T-25 flasks until about 60% confluence. Cells were exposed to different concentrations of H_2O_2 or vehicle for 24 hour and were stained with FITC Annexin V and Propidium Iodide according to the kit staining protocol (BD Biosciences). Cells were acquired using a BD Accuri C6 flow cytometer using the supplier's kit template and analyzed using BD Accuri C6 software (BD Biosciences). Variation was determined using Two-way ANOVA with Dunnett's multiple comparisons test, and are presented as the mean ± S.E.M., n=2-3. *p<0.05 of dead cells, # p<0.05 of live cells, and •p<0.05 apoptotic cells versus 0 mM H_2O_2.

8.1.5.3 Effect of LPS on Caco-2 cell viability

LPS at high concentrations significantly decreased Caco-2 cell viability (fig.2.3.2), therefore, cells were exposed to different concentrations of LPS to understand whether the effect is via apoptosis (fig. 7.1.3). In addition, this test experiment aimed to pick an appropriate concentration of LPS to use as another control for the later experiment with AS. The number of living cells marginally decreased with increasing concentrations of LPS, however, at 100 µg/ml, the number of apoptotic cell percentage increased significantly indicating apoptosis could be the reason for LPS mediated cell viability reduction. However, the sample number is too low to draw result, however, the purpose of selecting a concentration for the next step was served. 100 µg/ml of LPS was used as one of the controls when performed the apoptosis assay with AS.

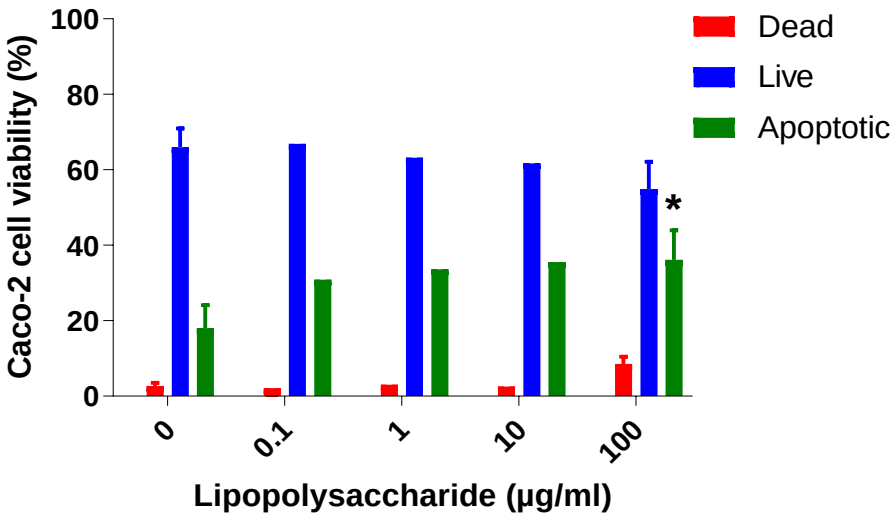

Figure A8. 4: Effect of lipopolysaccharide (LPS) on intestinal epithelial cell apoptosis.

Approximately 60% confluent Caco-2 cells in T-25 flask were exposed to different concentrations of LPS or vehicle for 24 hours. Cells were stained with FITC Annexin V and Propidium Iodide according to the supplier's protocol, acquired using a BD Accuri C6 flow cytometer with the supplier's kit template and analyzed using BD Accuri C6 software (BD Biosciences). Data were analysed using Two-way ANOVA followed by Uncorrected Fisher's LSD test, and are presented as the mean ± S.E.M., n=1-2. *p<0.05 versus 0 µg/ml of LPS.

8.1.6 Fluorescence microscopy – morphological observation

8.1.6.1 Preparation of the stains

DAPI-Prolong Gold was purchased as ready to use. 1 µl of the Phalloidin stock solution (1,000× phalloidin conjugate in DMSO) was diluted into 1 ml of PBS containing 1% BSA (0.01 ng) to prepare the working solution and filter sterilized (0.22 µM Millex® GP;Merck Millipore Ltd, Cork, IRL). The DiOC6 stock solution was 1,000× in PBS, and working solution was prepared as 1:1000 concentration.

8.1.6.2 Observation of stained cells

Prolong Gold-DAPI, DiOC6, and Phalloidin stained nuclei, mitochondria, and stress fibre of AS-exposed Caco-2 cells were observed using Zoe imager. The exposure details of the fluorescence microscopy were mentioned in table-A8.8.

Table A8. 8: Fluorescence microscopy exposure details.

Brightfield, blue, green and red fluorescence were used to observe the brightfield, DAPI, DiOC6, and Phalloidin staining. The criteria were adjusted as such.

Criteria	Brightfield	Blue	Green	Red
Gain	16	16	8	34
Exposure	320	300	280	360
LED intensity	28	10	28	50
Contrast	17	46	21	13

8.1.7 Cell apoptosis

The difference between cell apoptosis and necrosis was first demonstrated in 1972 and cell apoptosis was established as a unique cell death process that time (Xiang et al., 2016; Kerr et al., 1972). During necrosis, cells rapidly lose membrane integrity resulting in cellular content outflow and eventual death (Ziegler and Groscuth, 2004). On the other hand, cells undergoing apoptosis represent structural changes in two distinct stages (Kerr et al., 1972). At the first stage, the cell undergo nuclear and cytoplasmic condensation, alteration in cell volume, disintegration of the cell membrane with blebbing formation and asymmetry (Nandi et al., 2010; Coleman et al., 2001) followed by fragmentation of the cell into a number of membrane-bound, well-preserved blebbing called apoptotic bodies (Kerr et al., 1972).

As such, apoptotic cells display many morphological features that are distinct from the characteristics of cells undergoing death through other pathways such as pathological or necrotic cell death (Hengartner, 2000).
The Extrinsic pathway activates the death receptors while the intrinsic pathway involves the mitochondria, however, both pathways unite to activate the caspases leading to cell death (Muzio et al., 1996; Boldin et al., 1996). Previous studies have mentioned that apoptosis is actively regulated process involving protease enzymes of the caspase family including Caspase-3, -6, -7, -8, and -9 (Taylor et al., 2008; Martin et al., 2012; Henry et al., 2013). The executioner caspase cascade with their proteolytic and DNAse properties, demolish the cell cytoskeleton and organelles. Among the executioner caspases, caspase-3 is a terminally activated protease whose presence usually indicates the late stage of apoptosis (Lavrik et al. 2005).

In the extrinsic pathway, a multiprotein complex called death-inducing signalling complex (DISC) are formed via ligand binding which ultimately activate the procaspase-8 (Kischkel et al., 1995). Activated caspase-8 then triggers the downstream effector caspases (e.g., caspase-3) that subsequently cause cell death (Muzio et al., 1996; Boldin et al., 1996). In addition, p53 upregulated modulator of apoptosis (PUMA) can be transcripted from p53 to initiate the death signals. Furthermore, death receptor mediated (extrinsic) pathway can be

activated by corresponding ligand binding of FAS, TNF or TNF related apoptosis inducing ligands (Lin et al., 2011).

All the stimuli for the intrinsic and extrinsic pathways alters the inner mitochondrial membrane resulting mitochondrial permeability through pore formation. This initiates with the replacement of the anti-apoptotic Bcl family from the outer membrane of mitochondria by the pro-apoptotic proteins such as Bax, Bak, Bid and Bim. All these eventually cause the cytochrome C (cytC) release from the intermediary space of the mitochondrial membrane. CytC binds to Apaf-1, facilitates the activation of pro-caspase-9 and form apoptosome. Caspase-9 activates caspase-3 causing cell death (fig.2.1.6) (Elmore, 2007).

The names of some common proteins involved in apoptosis are listed in table-A8.9.

Table A8. 9: Some proteins involved in the extrinsic and intrinsic apoptotic pathways.

Abbreviations and the protein names are adapted from Elmore, 2007.

Extrinsic pathway		Intrinsic pathway	
Abbreviation	Protein name	Abbreviation	Protein name
TNF-*α*	Tumor necrosis factor alpha	Smac/DIABLO	Second mitochondrial activator of caspases/direct IAP binding protein with low PI
TNFR1	Tumor necrosis factor receptor 1	Apaf-1	Apoptotic protease activating factor
FasL	Fatty acid synthetase ligand	Caspase-9	Cysteinyl aspartic acid-protease-9
FasR	Fatty acid synthetase receptor	AIF	Apoptosis Inducing Factor
Apo3L	Apo3 ligand	CAD	Caspase-Activated DNAse
DR3	Death receptor 3	Bcl-2	B-cell lymphoma protein 2
Apo2L	Apo2 ligand	Bcl-XL	BCL2 related protein, long isoform
DR4	Death receptor 4	Bcl-10	B-cell lymphoma protein 10
DR5	Death receptor 5	BAX	BCL2 associated X protein
FADD	Fas-associated death domain	BAK	BCL2 antagonist killer 1
TRADD	TNF receptor-associated death domain	BID	BH3 interacting domain death agonist
RIP	Receptor-interacting protein	BAD	BCL2 antagonist of cell death
DED	Death effector domain	BIM	BCL2 interacting protein BIM
caspase-8	Cysteinyl aspartic acid-protease 8	BIK	BCL2 interacting killer
c-FLIP	FLICE-inhibitory protein	Puma	BCL2 binding component 3
		Noxa	Phorbol-12-myristate-13-acetate-induced protein 1

8.2 Appendix B - data for chapter 3

8.2.1 Studies on model bacteria *E. coli* DH5α

8.2.1.1 Effect of glucose, fructose and sucrose

Effect of carbohydrates on *E. coli* DH5α at without shake incubation condition (fig.B8.1).

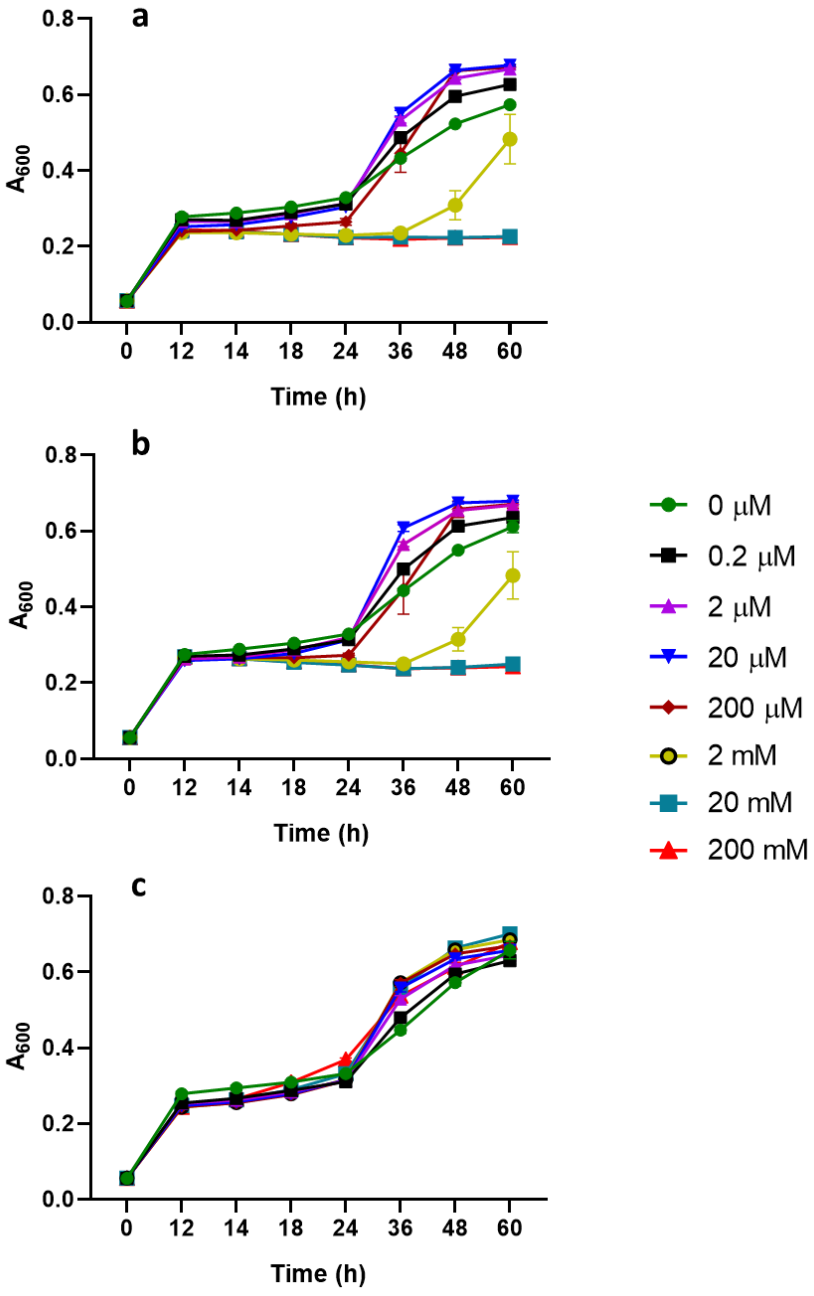

Figure B8. 1: Effect of natural carbohydrates on *E. coli* DH5α growth at 37 °C without shake.

Overnight culture (at dilution 1:500) was inoculated into 200 µl of 2YT liquid media at planktonic condition in 96-well plates and growth was read at 12 h intervals at 600 nm using Perkin Elmer (Victor X3) machine. Panel a, b, and c represent the effect of glucose, fructose, and sucrose, respectively. Data are presented as the mean ± S.E.M., n = 3, each with 2 replicates. Graph shows the effect of glucose (a), fructose (b) and sucrose (c) on *E. coli* DH5α growth.

8.2.1.2 Effect of artificial sweeteners

Effect of AS on *E. coli* DH5α growth at without shake incubation condition (fig.B8.2).

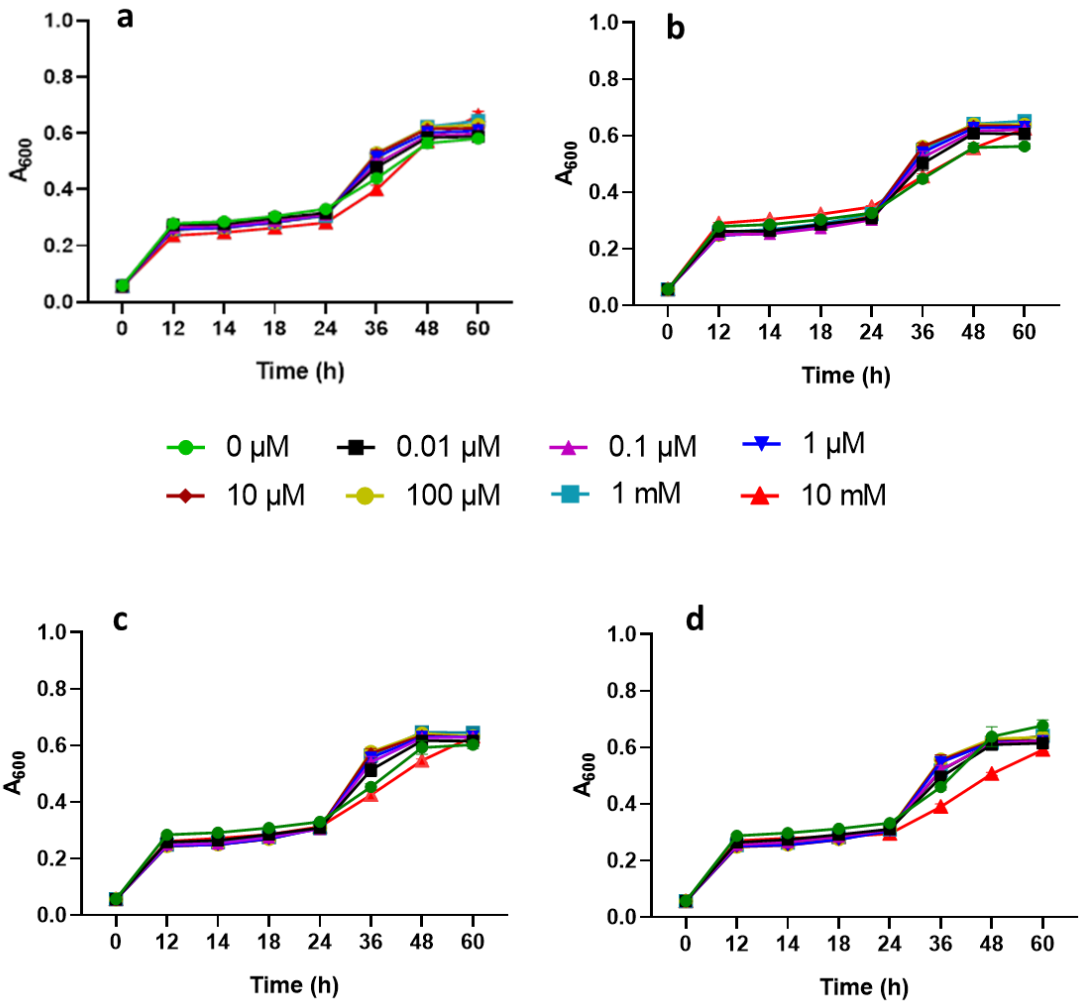

Figure B8. 2: Effect of AS on *E. coli* DH5α growth in without shake condition.

Overnight culture was inoculated (at 1:500 dilution) into 200 µl of fresh 2YT liquid media supplemented with different concentrations of AS. The 96-well plates were incubated at 37 °C without shaking. Growth was measured as absorbance at 600 nm using Perkin Elmer Victor X3. Panel shows growth of *E. coli* DH5α exposed to saccharin (a), sucralose (b), aspartame (c), and neotame (d). Data are presented as the mean ± S.E.M., n = 3, each with 2 replicates.

8.2.1.3 Effect of zinc sulphate

E. coli DH5α growth at without shake incubation condition in presence of zinc sulphate concentrations were shown in fig.B8.3.

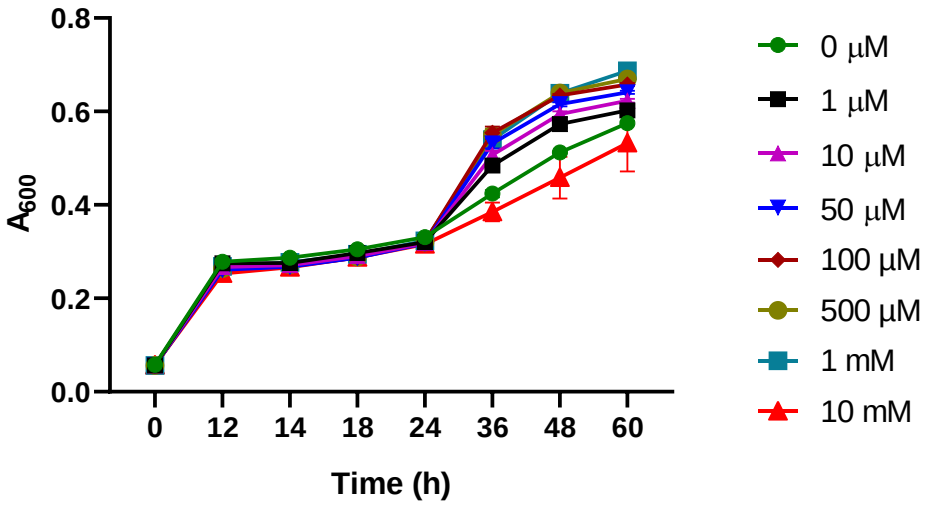

Figure B8. 3: Effect of zinc sulphate on *E. coli* DH5α growth at 37 °C without shake.

Bacteria was exposed to 2YT liquid media supplemented with different concentrations of zinc sulphate in 96-well plates and incubated at 37 °C without shake. Growth was measured as absorbance at 600 nm using Perkin Elmer Victor X3. Data are presented as the mean ± S.E.M., n=3, each with 2 replicates. Graph shows the effect of glucose (a), fructose (b) and sucrose (c) on *E. coli* DH5α.

8.2.2 Data on model gut bacteria *E. coli* NCTC 10418 and *E. faecalis* ATCC 19433

8.2.2.1 Media pH

The pH of the working solutions in the respective media of the MGB ranged between 6.39 ± 0.05 (aspartame) and 6.99 ± 0.09 (neotame) for *E. coli*, and between 6.94 ± 0.05 (sucralose) and 7.10 ± 0.03 (neotame) for the *E. faecalis*. However, the pH of the vehicles was 6.78 ± 0.05 (NB) and 6.93 ± 0.01 (BHI), which were close to the pH range of the working solutions, therefore, it was unlikely that the pH influenced the experiments for the MGB.

Table B8. 1: pH of the carbohydrates, AS and zinc sulphate.

Stock solutions were prepared (1M) in double distilled water and filter sterilised. The working solutions were prepared in the 2YT liquid media for the model bacteria *E. coli* DH5α, in Nutrient broth (NB) and Brain Heart infusion (BHI) for the model gut bacteria, *E. coli* NCTC 10418 and *E. faecalis* ATCC 19433, respectively, and the pH of the solutions were measured (Jenway 3510, UK). Data are analysed using nonparametric Dunn's multiple comparison test (no significance, p>0.9999), and are presented as the mean ± S.E.M., n=2-3.

Chemicals	**Stock solution**	**Working solution**		
		2YT for *E. coli* DH5α	NB for *E. coli* NCTC 10418	BHI for *E. faecalis* ATCC 19433
Media		6.74 ± 0.02	6.87 ± 0.02	6.95 ± 0.01
Vehicle (water)	7.08 ± 0.22	6.75 ± 0.01	6.82 ± 0.05	6.98 ± 0.04
Sucrose	7.393	6.68 ± 0.06	6.99 ± 0.09	7.10 ± 0.03
Glucose	7.125	6.65 ± 0.05	- -	- -
Fructose	6.633	6.53 ± 0.12	- -	- -
Saccharin	1.567	6.78 ± 0.03	6.97 ± 0.06	7.06 ± 0.00
Sucralose	5.823	6.62 ± 0.09	6.65 ± 0.02	7.10 ± 0.00
Aspartame	4.758	6.65 ± 0.02	6.82 ± 0.02	6.94 ± 0.05
Neotame	5.34	6.56 ± 0.08	6.39 ± 0.05	7.10 ± 0.00
Zinc sulphate	3.092	6.7 ± 0.02	6.85 ± 0.03	6.95 ± 0.01

*NB = Nutrient broth ** BHI = Brain Heart Infusion

8.2.2.2 Dilution calculation for absorbance to CFU calculation

Table B8. 2: Dilutions of the base culture for absorbance to CFU determination.

Dilutions	Base culture (µl)	Fresh media (µl)
A	200	1
B	180	20
C	160	40
D	140	60
E	120	80
F	100	100
G	80	120
H	0	200

8.2.2.3 Growth of *E. coli* in different liquid media

Table B8. 3: Growth of *E. coli* NCTC 10418 in different liquid media.

A single bacterial colony was inoculated into 10 ml of the liquid media in universal tubes and growth was allowed for 24 h at 37 ˚C with shaking (150 rpm). The turbidity was measured as optical density at 600 nm (OD600) against corresponding growth medium as blank using spectrophotometer (Eppendorf BioPhotometer Plus, Germany). Data are presented as the Mean ± S.E.M., n=2.

Media	Absorbance (mean ± S.E.M.) *
Nutrient broth	1.5805 ± 0.0028
Brain Heart Infusion	1.497± 0.013
Iso-sensitest™ broth	1.458 ± 0.01376
2YT	1.934 ± 0.2205
Luria Bertani	2.205 ± 0.0065

*Each absorbance presented is the average of two independent experiments each having three replications

8.3 Appendix C - data for chapter 4

8.3.1 Calculation for the multiplicity of infection (MOI):

Calculation for *E. coli*

An OD600 of 1 for *E. coli* have Colony Forming Units (CFU) of 8×10^8 CFU/ml

So, 5 ml of bacterial growth have 4×10^9 bacteria. Bacterial culture was centrifuged at 4000 rpm for 10 minutes at 37 °C, and the pellet was resuspended into 0.5 ml EMEM medium without antibiotics. Therefore, 0.5 ml bacterial suspension contained 4×10^9 *E. coli*, 10 µl was added in each of the wells containing 3×10^5 Caco-2 cells.

10 µl *E. coli* suspension contains [(4×10^9 CFU × 10 µl) / 500 µl] = 8×10^7 CFU

Therefore, MOI = [(number of Caco-2 cells, 3×10^5): (number of *E. coli*, 8×10^7 CFU)] = 1: 300.

Calculation for *E. faecalis*

An OD600 of 1 for *E. faecalis* contain 9×10^9 CFU/ml. Bacterial suspension was centrifuged as above and resuspended in 1 ml complete EMEM medium without antibiotics, 10 µl was added in each of the wells containing 3×10^5 Caco-2 cells.

10 µl *E. faecalis* suspension contains [(9×10^9 CFU × 10 µl) / 1000 µl] = 9×10^7 CFU

Therefore, MOI = [(number of Caco-2 cells, 3×10^5): (number of *E. faecalis*, 9×10^7 CFU)] = 1: 300.

8.3.2 Effect of AS on co-culture models of intestinal epithelial cell and gut bacteria

8.3.2.1 Effect of AS on model bacterial adhesion ability

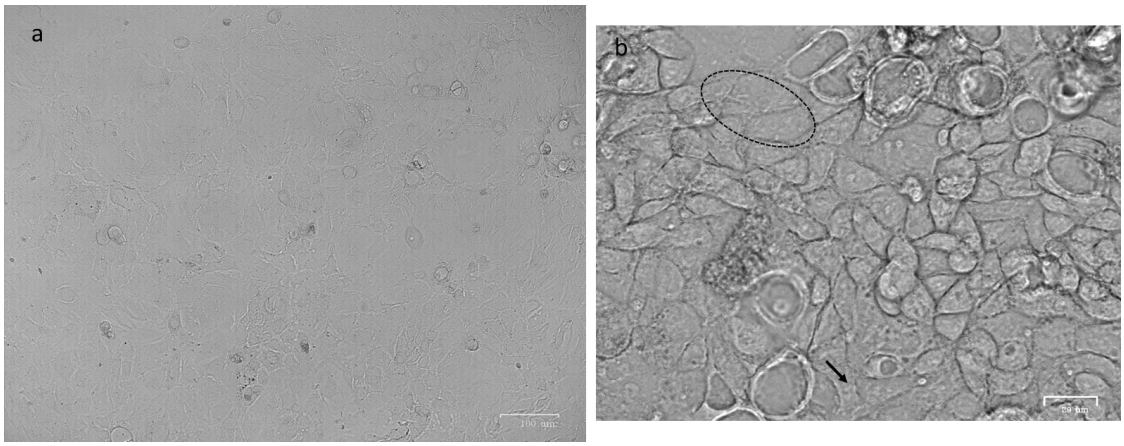

Figure C8. 1: Adhesion of *E. coli* to Caco-2 cell monolayer.

Mammalian cells were incubated with the bacteria (MOI 1:300) for an hour at 37 ˚C. Loosely adhered and non-adhered cells washed away by PBS (×3) and cells were fixed with 4% PFA. The cells were observed using bright field microscopy (Zoe imager). Images were taken with lower (a) and higher (b) magnifications. The black circle (b) shows localized adherence like appearance of the rods. Also, irregular diffuse adhesion (black arrow, c) can be seen on the cells. Bar 100 µm (a) and 25 µm (b).

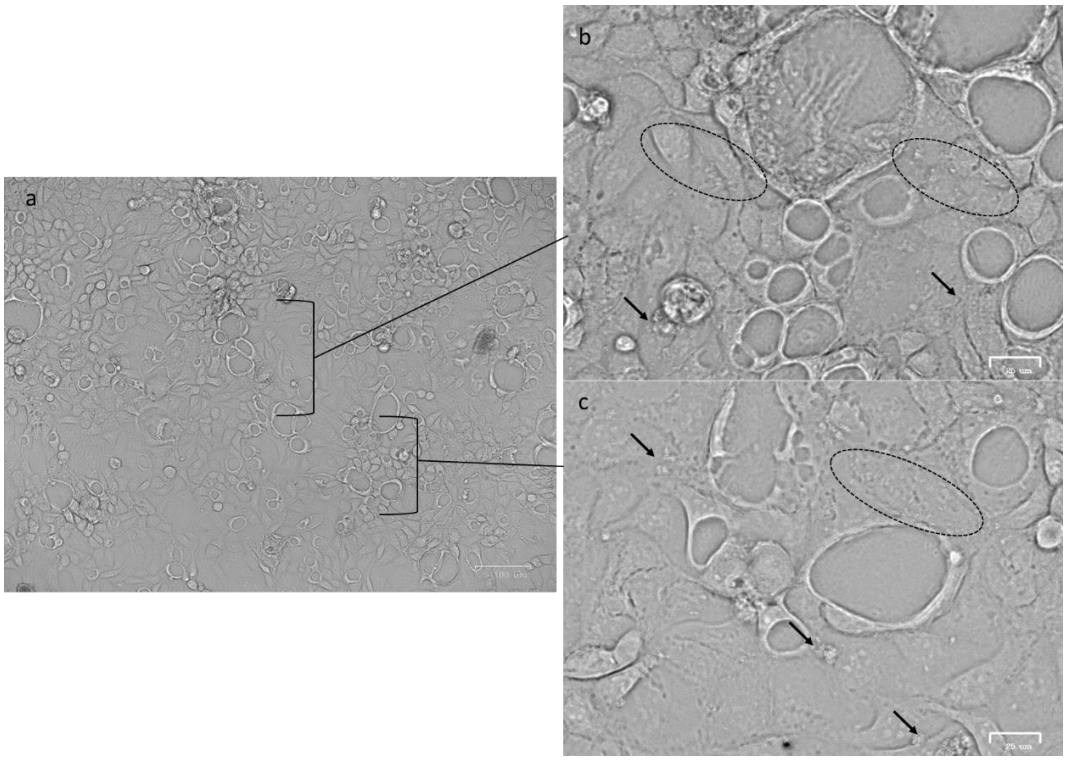

Figure C8. 2: Representative feature of the effect of AS on *E. coli* adhesion to the Caco-2 cell monolayer.

Mammalian cells were grown on 24-well plate for 48 h at standard tissue culture conditions and exposed to AS for 24 h. The bacteria were also exposed to AS (saccharin) for 24 h, washed and co-cultivated with the Caco-2 cells at MOI 1:300 for an hour. Non-adhered cells were washed by PBS washing (×3) and cells were fixed using 4% PFA. Panel represent lower (a) and higher (b and c) magnifications. The *E. coli* shows localised adherence like appearance (black circles, b and c), small clusters of the rods (black arrows) were also observed. Bar 100 µm (a) and 25 µm (b and c).

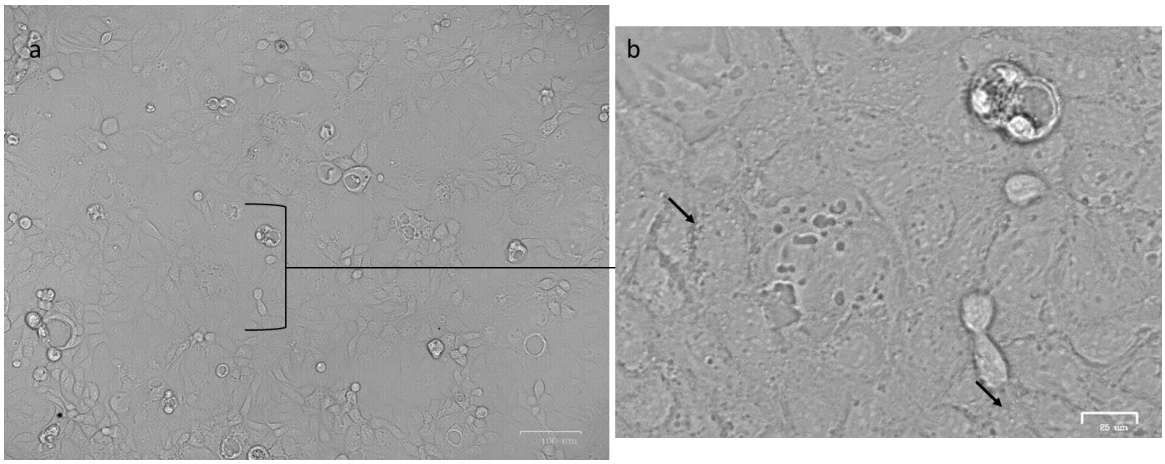

Figure C8. 3: Adhesion of *E. faecalis* to Caco-2 cells.

The bacteria were co-cultivated at MOI 1:300 for an hour and non-adhered or loosely adhered bacteria were washed away with PBS. Cells were observed using Zoe imager. Bar 100 µm (a) and 25 µm (b).

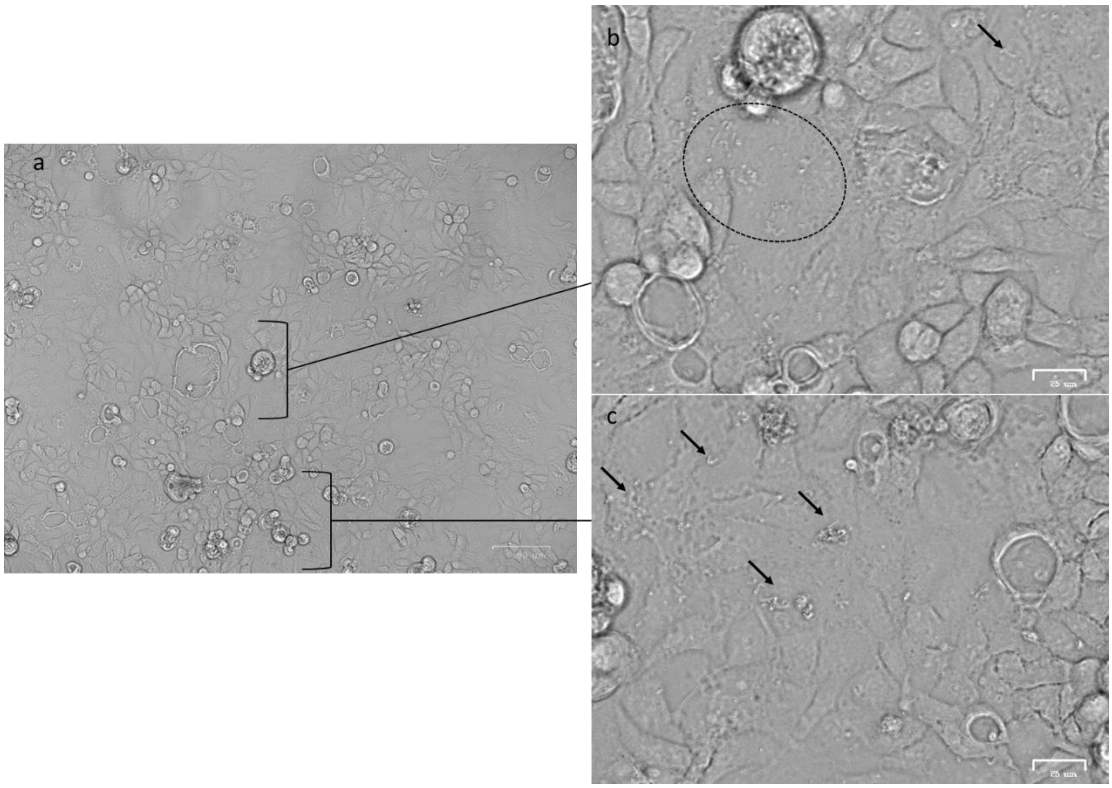

Figure C8. 4: Representative image of adhesion of AS-exposed *E. faecalis* to the AS-exposed Caco-2 cells.

Mammalian cells were grown on 24-well plate, exposed to AS (saccharin) for 24 h and co-cultivation with bacteria were performed for an hour at 37 ˚C. Cells were washed to get rid of unattached bacteria and observed under Zoe imager. Cells and bacteria were observed at lower (a) and higher (b) magnifications. Black arrows represent cluster or chains of the bacteria, and the black circle shows massive irregular adhesion. Bar 100 µm (a) and 25 µm (b and c).

8.3.2.2 Effect of AS on gut bacterial invasiveness

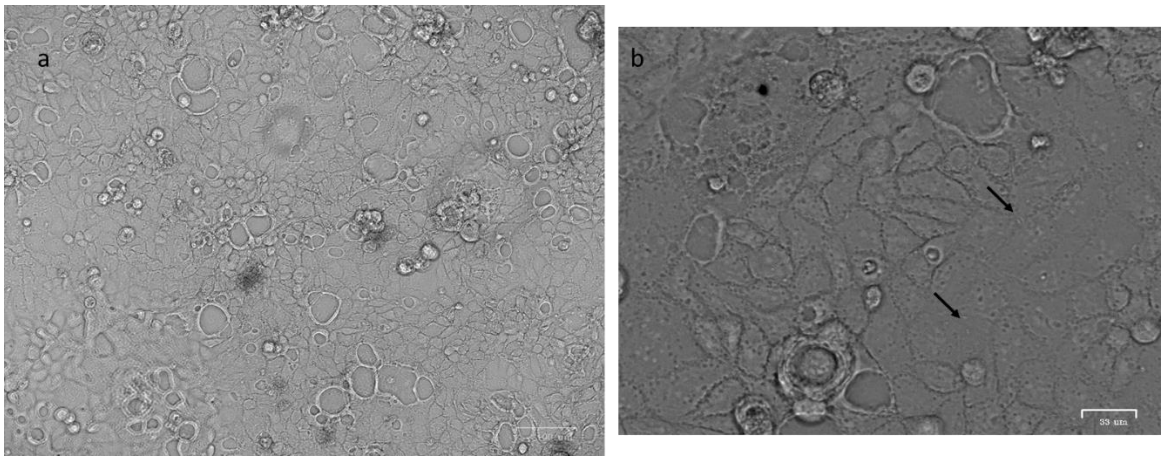

Figure C8. 5: Invasion of *E. coli* NCTC 10418 into the Caco-2 cells at 1 hour co-culture.

Mammalian cell monolayer was infected with the bacteria (MOI 1:300) at 37 ˚C. The adhered *E. coli* was killed by incubating with 100 µg/ml of gentamicin. Cells were washed and fixed and observed using bright field microscopy (Zoe imager). Images were taken with lower (a) and higher (b) magnifications. The black arrows (b) show rod-shaped *E. coli* on the Caco-2 cells. Bar 100 µm (a) and 25 µm (b).

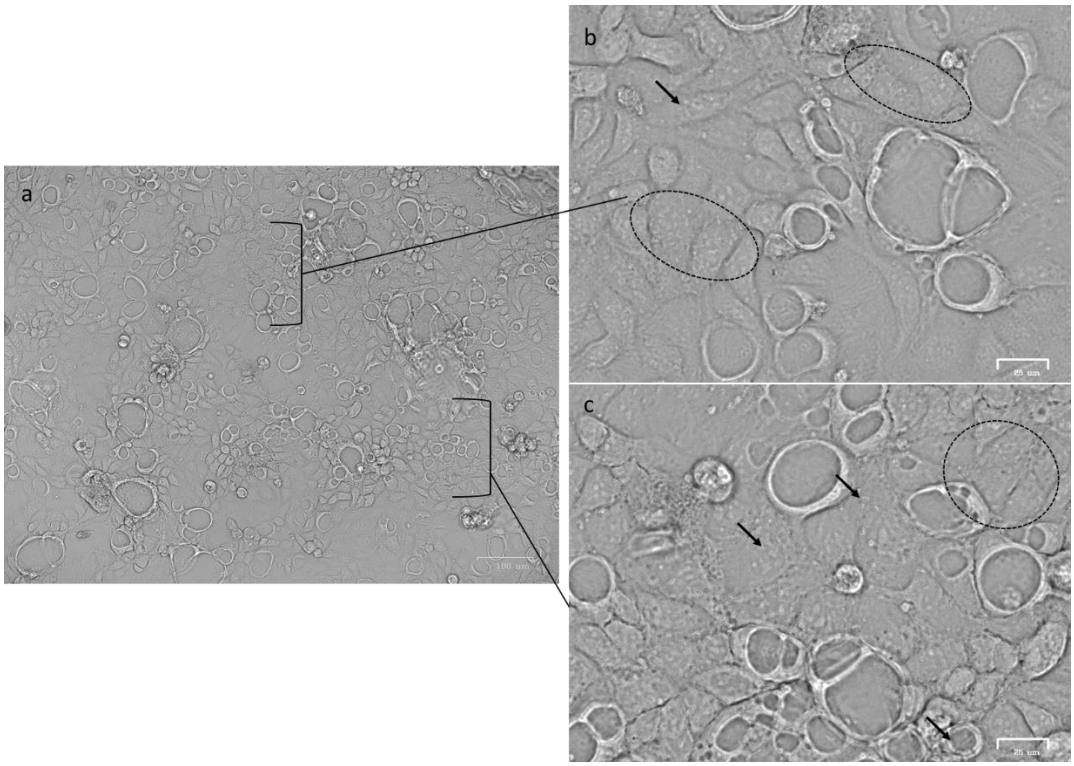

Figure C8. 6: Effect of AS on *E. coli* invasion into the intestinal epithelial cell.

Caco-2 cells were maintained in EMEM for 48 h and exposed to AS (saccharin) for 24 h. Culture media was replaced with fresh media without antibiotic. The AS-exposed *E. coli* was washed and re-suspended in EMEM and infection was allowed for an hour at 37 ˚C. The non-adhered bacteria were removed by washing (PBS ×3) and the adhered bacteria were killed by antibiotic action. The invaded ones were protected by the mammalian cell membrane. Cells were partially lysed with (0.1% Triton X100) for <5 min and fixed using 4% PFA. Cells were observed using bright field microscopy (Zoe imager) with lower (a) and higher (b and c) magnifications. The *E. coli* shows greater numbers in some areas (black circles, b and c), however, individual bacteria and small clusters of the rods (black arrows) were also observed. Bar 100 µm (a) and 25 µm (b and c).

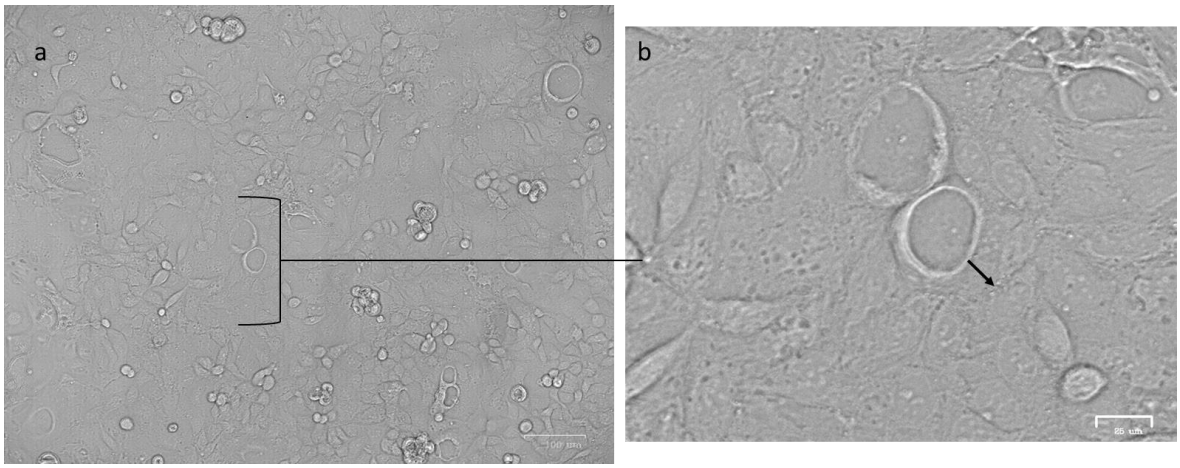

Figure C8. 7: Invasion of *E. faecalis* into Caco-2 cell after co-exposure in vehicle for 1 hour.

Caco-2 cells were maintained in 24-well plate for 24 hours followed by exposure to AS for 24 hours. The washed cells were co-cultured with bacteria and the infection incubation was performed for an hour. The adhered bacteria were killed by gentamicin and ampicillin action while the invaded ones were protected by the Caco-2 cell membrane. The cells were washed and fixed with 4% paraformaldehyde and observed using brightfield microscopy (Zoe imager). Bar 100 µm (a) and 25 µm (b).

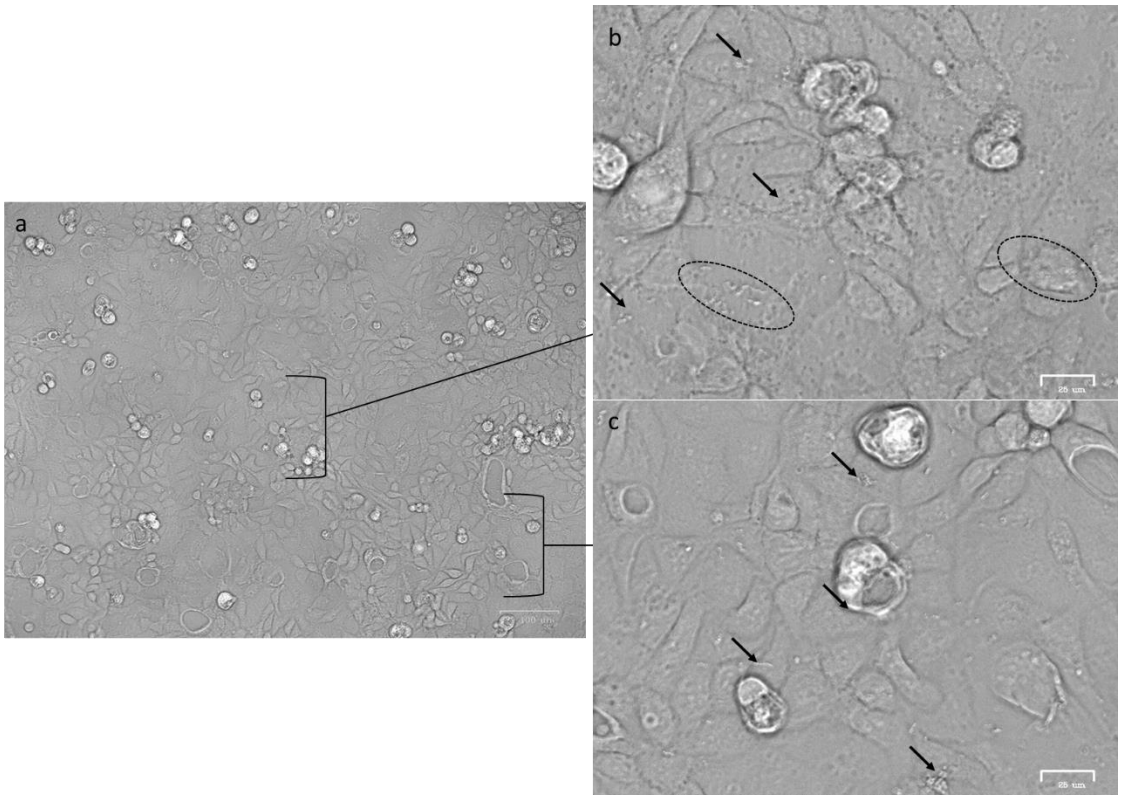

Figure C8. 8: Representative feature of the effect of AS on *E. faecalis* invasion into Caco-2 cell monolayer after 1 hour.

Caco-2 cells were maintained in 24-well plate at standard tissue culture conditions. At 24 hours, cells were exposed to AS for 24 hour and then the co-culture with bacteria were performed for an hour. The adhered bacteria were killed by gentamicin and ampicillin action while the invaded bacteria were protected by the Caco-2 cell membrane. The cell monolayer was washed twice with PBS, fixed and observed using bright field microscopy (Zoe imager). The cocci formed small clusters (black circles, b) without any distinguished appearance. Also, short chains and pairs of *E. faecalis* (black arrows, c) as well as individual bacteria were observed (b, c). Bar 100 µm (a) and 25 µm (b and c).